MAR 14 1991
0830-H-10
0312
NAS 1.55:3103/v.2

NASA Conference Publication 3103, Vol. II

Fourth Annual Workshop on Space Operations Applications and Research (SOAR '90)

Proceedings of a workshop held in
Albuquerque, New Mexico
June 26–28, 1990

NASA

HGW

NASA Conference Publication 3103, Vol. II

Fourth Annual Workshop on Space Operations Applications and Research (SOAR '90)

Robert T. Savely, *Editor*
NASA Lyndon B. Johnson Space Center
Houston, Texas

Proceedings of a workshop sponsored by the
National Aeronautics and Space Administration,
Washington, D.C., the U.S. Air Force, Washington, D.C.,
and cosponsored by the University of New Mexico,
Albuquerque, New Mexico, and held in
Albuquerque, New Mexico
June 26–28, 1990

National Aeronautics and
Space Administration

Office of Management

Scientific and Technical
Information Division

1991

I

PREFACE

The papers presented at the Space Operations, Applications, and Research (SOAR) Symposium, hosted by the Air Force Space Technology Center and held at Albuquerque, New Mexico, on June 26-28, 1990, are documented in this proceeding. Over 150 technical papers were presented at the Symposium which was jointly sponsored by the United States Air Force (USAF) and the NASA/Johnson Space Center. The technical areas included were: Automation and Robotics, Environmental Interactions, Human Factors, Intelligent Systems, and Life Sciences. NASA and USAF programmatic overviews and panel sessions were also held in each technical area. The Symposium proceeding includes papers presented by experts from NASA, the USAF, universities, and industries in various disciplines. These proceedings, along with the comments by technical area coordinators and session chairmen, will be used by the Space Operations Technology Subcommittee (SOTS) of the Air Force Systems Command and NASA Space Technology Interdependency Group (STIG) to assess the status of the technology, as well as the joint projects/activities in various technical areas.

MESSAGE FROM THE GENERAL CHAIR AND ASSISTANT GENERAL CHAIR

The SOAR 90 workshop will bring together Air Force and NASA project/program managers and members of the technical community for an information exchange on space operations. The visibility the SOAR 90 workshop will provide attendees into technology applications will give us a singular opportunity to establish additional cooperative technology development and transition programs.

As you can see, SOAR now represents Space Operations, Applications, and Research. This change reflects the nature of the conference which includes sessions on many areas in addition to automation and robotics. Each session will start with Air Force and NASA programmatic overviews of present efforts which will be followed by technical papers and conclude with panel discussions of problems/ solutions within the topic area.

With your participation, we look forward to an informative and productive workshop.

Col. Paul C. Anderson,
Air Force Space Technology Center

As you noticed, SOAR now stands for Space Operations, Applications and Research, and encompasses the broad scope and excitement felt by the space community as our Nation's revitalized space program gains strength and stability. The planned civil space scenario includes Space Station Freedom, a multitude of science and technology missions, the lunar outpost, and Mars missions/outposts.

The consequences of these space programs will be an infrastructure of space, lunar and Mars surface and ground operations. These operations need to be conducted effectively, efficiently, and with utmost safety. Advanced techniques/ technology are needed to enable future space operations to be carried out with these attributes.

SOAR 90 continues, with amplification, the theme of previous SOAR workshops in the discussion of future techniques/technology and approaches needed for space operations. Also, life sciences was added to the technical areas for the first time this year to reflect the broad scope of the needed research. The benefits to NASA and the Air Force in expanding communications and identifying cooperative programs have made SOAR an invaluable yearly event.

Dr. Kumar Krishen,
NASA Johnson Space Center

CONTENTS

AUTOMATION AND ROBOTICS

SESSION R1: **Manipulation I**
SESSION CHAIR: **Dr. Mark A. Stuart, Lockheed Engineering and Sciences Co.**

Resolved Rate and Torque Control Schemes for Large Scale Space Based Kinematically Redundant Manipulators 2

IVA the Robot: Design Guidelines and Lessons Learned from the First Space Station Laboratory Manipulation System 9

A Novel Design for a Hybrid Space Manipulator 15

Forward and Inverse Kinematics of Double Universal Joint Robot Wrists 23

Performance Capabilities of a JPL Dual-Arm Advanced Teleoperation System 30

SESSION R2: **Manipulation II**
SESSION CHAIR: **Dr. Mark Friedman, Carnegie Mellon University**

SSSFD Manipulator Engineering Using Statistical Experiment Design Techniques 44

Impact of Inertia, Friction and Backlash Upon Force Control in Telemanipulation ... 53

Adaptive Control of Space Based Robot Manipulators 59

The AFIT Gross Motion Control Project 67

SESSION R3: **Automation and Robotics Programmatics**
SESSION CHAIR: **Dr. Mel Montemerlo, NASA**

No papers were presented at this session.

SESSION R4: **Mobility and Exploration Concepts**
SESSION CHAIR: **Prof. M. Shahinpoor, University of New Mexico**

NASA Planetary Rover Program 78

An Architectural Approach to Create Self Organizing Control Systems for Practical Autonomous Robots 84

A Simple 5-DOF Walking Robot for Space Station Application 91

Perception, Planning and Control for Walking on Rugged Terrain 96

SESSION R-5: **Panel Session**
SESSION CHAIR: **Jack Pennington, NASA/Langley AFB**

No papers were presented at this session.

SESSION R-6: **Sensing and Perception**
SESSION CHAIR: **Prof. Neil A. Duffie, University of Wisconsin-Madison**

Comparison of Force and Tactile Feedback for Grasp Force Control in Telemanipulation 104

Autonomous Proximity Operations Using Machine Vision for Trajectory Control and Pose Estimation 113

Berthing Simulator for Space Station and Orbiter 120

Evaluation of Telerobotic Systems Using an Instrumented Task Board 126

SESSION R-7: **Robotic Servicing Systems**
SESSION CHAIR: **Chuck Wooley, NASA/Johnson Space Center**

Operations with the Special Purpose Dexterous Manipulator on Space Station Freedom 134

A Space Servicing Telerobotics Technology Demonstration 143

The Development Test Flight of the Flight Telerobotic Servicer 151

Deployable Robotic Woven Wire Structures and Joints for Space Applications 159

Robotic Applications within the Strategic Defense System 167
(Paper not provided by publication date)

SESSION R-8: **Telerobotics**
SESSION CHAIR: **Dr. Tony Bejczy, Jet Propulsion Laboratory**

Telerobotic Performance Analysis 170
(Paper not provided by publication date)

Tele-Autonomous Control—Theory and Practice 171
(Paper not provided by publication date)

Investigation of Varying Gray Scale Levels for Remote Manipulation 172

Space Station *Freedom* Coupling Tasks: An Evaluation of their Space Operational Compatibility 179

Ground Controlled Robotic Assembly Operations for Space Station Freedom 184

INTELLIGENT SYSTEMS

SESSION R-9: **Trajectory Planning and Safety**
SESSION CHAIR: **Prof. Rui De Figuarito**

A Collision Detection Algorithm for Telerobotic Arms 194

Exact and Explicit Optimal Solutions for Trajectory Planning and Control of Single-Link Flexible-Joint Manipulators 201

Issues Associated with Establishing Control Zones for International Space Operations 207

A Perception and Manipulation System for Collecting Rock Samples 226

SESSION I-1: **Mission Operations**
SESSION CHAIR: **Dr. Mark Stuart, Lockheed Engineering and Sciences Company**

Advanced Automation in Space Shuttle Mission Control 236

SHARP: Automated Monitoring of Spacecraft Health and Status 244

Challenges in Building Intelligent Systems for Space Mission Operations 259

Analyzing Spacecraft Configurations Through Specialization and Default Reasoning 264
(Paper not provided by publication date)

SESSION I-2: **NASA USAF Programmatic Overview**
SESSION CHAIR: **Captain Jim Skinner, Air Force Space Technology Center**
Gregg Swietek, NASA Headquarters

No papers were presented at this session.

SESSION I-3: **Mission Planning and Scheduling**
SESSION CHAIR: **Dr. Barry Smith, MITRE**
Nancy Sliwa, NASA/Ames Research Center

User Interface Issues in Supporting Human-Computer Integrated Scheduling 268

Architecture for Spacecraft Operations Planning 275

The Implementation of COMPASS 279
(Paper not provided by publication date)

The Range Scheduling Aid 280

Request Generation II Mission Planning and Scheduling 285

The Ames-Lockheed Orbiter Processing Scheduling System 290

An Intelligent Value-Driven Scheduling System for Space Station Freedom with Special Emphasis On the Electric Power System 296

SESSION I-4: **Spacecraft Autonomy Panel Session**
SESSION CHAIR: **Dr. George Luger, University of New Mexico**

No papers were presented at this session.

SESSION I-5: **Prelaunch Processing**
SESSION CHAIR: **Captain Doug Tindall, SSD, Wright-Patterson AFB**
Astrid Heard, NASA/Kennedy Space Center

Expert System Decision Support for Low-Cost Launch Vehicle Operations 304

KSC's Work Flow Assistant 317

Intelligent Launch Decision Support System (ILDSS) 323
(Paper not provided by publication date)

EXODUS: Integrating Intelligent Systems for Launch Operations Support 324

An Intelligent Advisory System for Pre-Launch Processing 331

SESSION I-6: **Diagnostics**
SESSION CHAIR: **Bill Baker, WRDC/TXI, Wright-Patterson AFB**
Dave Weeks, NASA/Marshall Space Flight Center

Intelligent Monitoring and Diagnosis Systems for the Space Station Freedom ECLSS 338

Addressing Information Overload in the Monitoring of Complex Physical Systems 344
(Paper not provided by publication date)

The CITS Expert Parameter System (CEPS) 345
(Paper not provided by publication date)

Expert Missile Maintenance Aid (EMMA) 346
(Paper not provided by publication date)

A Failure Management Prototype: DR/Rx 347

Augmentation of the Space Station Module Power Management and Distribution Breadboard 355

SESSION I-7: **Real-Time Systems Control**
SESSION CHAIR: **Spencer Campbell, Aerospace Corporation**
Monte Zweben, NASA/Ames Research Center

The Real-Time Control of Planetary Rovers Through Behavior Modification 362

Qualitative Characterization for Real-Time Control and Monitoring 367
(Paper not provided by publication date)

Reasoning About Real-Time Systems with Temporal Interval Logic Constraints on Multi-State Automata 368

A Framework for Building Real-Time Expert Systems 375

Autonomous Power Expert System Advanced Development 383

SESSION I-8: **Knowledge Acquisition Design Environment**
SESSION CHAIR: **Dr. Kirstie Bellman, Aerospace Corporation**
Chris Culbert, NASA/Johnson Space Center

A Knowledge-Based Approach to Configuration Layout, Justification and Documentation 392

Capturing, Using, and Managing Quality Assurance Knowledge for Shuttle Post-MECO Flight Design 397

Quantitative Knowledge Acquisition for Expert Systems 405

Developing a PROLOG-Based Modeling Environment 414
(Paper not provided by publication date)

Wrapping Mathematical Tools 415
(Paper not provided by publication date)

SESSION I-9: **Intelligent Computer-Aided Training**
SESSION CHAIR: **Dr. Wes Regain, Air Force Human Resources Laboratory, Brooks AFB**
Dr. Bowen Loftin, University of Houston

The Development of Expertise Using an Intelligent Computer-Aided Training System 418

Rule-Based Simulation Models 424

Intelligent Tutoring Systems: Breaking the Price Barrier 429
(Paper not provided by publication date)

Artificial Neural Networks for Intelligent Environments 430
(Paper not provided by publication date)

Rose Garden Promises of Intelligent Tutoring Systems: Blossom or Thorn? 431

SESSION I-10: **Real-Time System Control**
SESSION CHAIR: **Spencer Campbell, Aerospace Corporation**
Monte Zweben, NASA/Ames Research Center

Flexible Wing Aircraft Roll Control Using Fuzzy Logic 440
(Paper not provided by publication date)

Real-Time Fuzzy Logic Based Tuner for PID Control 441
(Paper not provided by publication date)

Assessing Damping Uncertainty in Space Structures with Fuzzy Sets 442

The AI Bus Architecture for Distributed Knowledge-Based Systems 449

SESSION I-11: **Advanced Automation and Software**
SESSION CHAIR: **Robert Savely, NASA/Johnson Space Center**

ART-ADA: An ADA-Based Expert System Tool 456

Advanced CLIPS Capabilities 464

Parallel Processing and Expert Systems 469

The Advanced Software Development Workstation Project 477

P-CLIPS 481
(Paper not provided by publication date)

HUMAN FACTORS

SESSION H-1: **Satellite Monitoring and Control**
SESSION CHAIR: **Captain Al Reinhardt, Air Force Space Technology Center**
Dr. Christine Mitchell, Georgia Institute of Technology

A Human Factors Approach to Range Scheduling for Satellite Control 484

Model-Based Displays for Satellite Ground Control 490

Utilizing Expert Systems for Satellite Monitoring and Control 493

ALLY: An Operator's Associate for Satellite Ground Control Systems 499

SESSION H-2: **Intelligent Interfaces**
SESSION CHAIR: **Dr. Guy Boy, NASA/Ames Research Center**

Cockpit Task Management: A Preliminary, Normative Theory 508

Supervising Unmanned Roving Vehicles Through an Intelligent Interface 521
(Paper not provided by publication date)

OFMspert: An Architecture for an Operator's Associate that Evolves to an Intelligent Tutor 522

Intelligent Tutoring Systems for High-Performance Skills 527
(Paper not provided by publication date)

Automated Acquisition of Information Requirements for an Intelligent Display 528
(Paper not provided by publication date)

Enhancing the Usability of CRT Displays in Test Flight Monitoring 529

SESSION H-3: **AI/Robotics Interfaces**
SESSION CHAIR: **Dr. Michael Shafto, NASA/Ames Research Center**

A Spatial Disorientation Predictor Device to Enhance Pilot Situational Awareness Regarding Aircraft Attitude 536

Evaluation of the Mark III and AX-5 Space Suits Relative to the Shuttle Suit for Robotic Maneuverability 542
(Paper not provided by publication date)

Cognitive Consequences of "Clumsy" Automation on High Workload, High Consequence Human Performance 543

Guidance for Human Interface with Artificial Intelligence Systems 547

SESSION H-4: **Space Human Factors**
SESSION CHAIR: **Dr. Michael Shafto, NASA/Ames Research Center**

Development of Biomedical Models for Human Factors Evaluations 552

Recovery from an Anomalous Thruster Input During a Simulated Docking Maneuver 557

Considerations for Man-Machine Interfacing in Tele-Operations 561

SESSION H-5: **Human Factors Programmatics**
SESSION CHAIR: **Dr. Michael Shafto, NASA/Ames Research Center**
Colonel Donald Spoon, AAMRL

No papers presented at this session.

SESSION H-6: **Human Factors Technology Transfer Panel Session**
SESSION CHAIR: **Dr. Don Monk, Armstrong Medical Research Laboratory**

No papers presented at this session.

SESSION H-7: **Human Computer Interaction**
SESSION CHAIR: **Dr. Tim McKay, Lockheed Engineering and Sciences Company**

The Use of Analytical Models in Human-Computer Interface Design 574

Microgravity Cursor Control Device Evaluation for Space Station Freedom Workstations 582

Developing the Human-Computer Interface for Space Station Freedom 588

Spacecraft Crew Procedures from Paper to Computers 595

NASA/Johnson Space Center Human–Computer Interaction Laboratory 601
(Paper not provided by publication date)

SESSION H-8: **Crew System Dynamics**
SESSION CHAIR: **Dr. Mary Conners, NASA/Ames Research Center**

Crews and Teams in the Future: A Vision of Command and Control 604
(Paper not provided by publication date)

Crew Coordination in Traditional and Automated Cockpits 605
(Paper not provided by publication date)

Electronic Collaboration: Some Effects of Telecommunication Media and Machine Intelligence on Team Performance 606

Issues on Combining Human and Non-Human Intelligence 612

LIFE SCIENCIES

SESSION L-1: **Medical Operations Support**
SESSION CHAIR: **Larry J. Pepper, NASA/Johnson Space Center**

No papers submitted

SESSION L-2: **Environmental Factors**
SESSION CHAIR: **Dane M. Russo, Ph.D., NASA/Johnson Space Center**

No papers submitted

SESSION L-3: **General Biomedical**
SESSION CHAIR: **Charles M. Winget, NASA/Johnson Space Center**

No papers submitted

SESSION L-4: **Programmatic Overview**
SESSION CHAIR: **Dr. Ronald White, NASA Headquarters**

No papers submitted

SESSION L-5: **Decompression Sickness**
SESSION CHAIR: **James A. Waligora, NASA/Johnson Space Center**

Intensity of Exercise and Likelihood of Decompression Sickness 630
(Paper not provided by publication date)

Selection of an Emergency Backup Pressure for an 8.3 psi Space Suit 631
(Paper not provided by publication date)

Analysis of Doppler Ultrasound Bubble Detection Data by Means of the Time/Intensity Integral 632
(Paper not provided by publication date)

Analysis of the Individual Risk of Altitude Decompression Sickness under Repeated Exposures 633

SESSION L-6 **Space Adaptation Syndrome I – Sensory Pathology**
SESSION CHAIR: **Jerry L. Homick, PhD, NASA/Johnson Space Center**

No papers submitted

SESSION L-7 **Space Adaptation Syndrome II – Cardiovascular and Exercise Physiology**
SESSION CHAIR: **John B. Charles, PhD, NASA/Johnson Space Center**

No papers submitted

ENVIRONMENTAL INTERACTIONS

SESSION E-1 **Space Plasma Interactions I**
SESSION CHAIR: **Dale C. Ferguson, NASA/Lewis Research Center**

Spacecraft and Surface Interference 642
(Paper not provided by publication date)

Space Station Freedom and Its Plasma Environment 643
(Paper not provided by publication date)

SSF Solar Array Plasma Tests 644
(Paper not provided by publication date)

Application of Engineering Tools to Spacecraft Polar Aural Charging 645
(Paper not provided by publication date)

Magnetoplasma Sheath Waves on a Conducting Tether in the Ionosphere, with Applications to EMI Propagation on Large Space Structures 646

The Solar Array Module Plasma Interactions Experiment (SAMPIE): A Shuttle-based Plasma Interactions Experiment 655

SESSION E-2 **Space Plasma Interactions II**
SESSION CHAIR: **Dale C. Ferguson, NASA/Lewis Research Center**

Electrostatic Discharges on Spacecraft 664
(Paper not provided by publication date)

Computer Models of Plasma Interactions Between Spacecraft and the Ionosphere 665
(Paper not provided by publication date)

A Fluid Model Approach to Spacecraft Charging 666
(Paper not provided by publication date)

Plasma Effects on the Spacecraft Charging, etc. 667
(Paper not provided by publication date)

ENVIRONET: An Online Environmental Interactions Resource 668

SESSION E-3 **Spacecraft Contamination**
SESSION CHAIR: **Dale C. Ferguson, NASA/Lewis Research Center**

Photometric Analysis of a Space Shuttle Water Venting 676

A Comparison of Shuttle Engine Firings in Space to Code Predictions 681
(Paper not provided by publication date)

Infrared Background Signature Survey: A Review of AF Science Objectives and a Hardware Description 682
(Paper not provided by publication date)

The Shuttle Infrared Test Experiment 683
(Paper not provided by publication date)

The Environment Workbench: A Design Tool for Space Station Freedom 684

Space Environmental Effects Program 688
(Paper not provided by publication date)

Findings of the Joint Workshop on Evaluation of Impacts of Space Station Freedom Ground Configurations 689

SESSION E-4 **Debris**
SESSION CHAIR: **Lieutenant Brian Lillie, Air Force Space Technology Center**

Small Satellite Debris Catalog Maintenance Issues 696

LEO Debris Effects on the Optical Properties of Mirrored Surfaces 705
(Paper not provided by publication date)

The Importance of Momentum Transfer in Collision-Induced Breakups in Low Earth Orbit 706

NAVSPASUR Orbital Processing for Satellite Break-up Events 718

SESSION E-5 **Atomic Oxygen Interaction with Materials**
SESSION CHAIR: **Bruce A. Banks, NASA/Lewis Research Center**

Atomic Oxygen Interaction with Solar Array Blankets at Protective Coating Defect Sites 726

Fast Oxygen Atom Environmental Interactions with LEO Spacecraft 733
(Paper not provided by publication date)

Atomic Oxygen Beam Source for Erosion Simulation 734

Atomic Oxygen and Ultraviolet Radiation Effects on Spacecraft Thermal Control Coatings 742
(Paper not provided by publication date)

Laboratory Investigations of Visible Shuttle Glow Mechanisms 743

Kinematics of Atomic Oxygen-Carbon Reactions 752
(Paper not provided by publication date)

SESSION E-6 **Atomic Interaction with Materials**
SESSION CHAIR: **Bruce A. Banks, NASA/Lewis Research Center**

Atomic Oxygen Resistant Polymer for Space Station Solar Array Applications 754
(Paper not provided by publication date)

The Effect of Atomic Oxygen on Polysiloxane-Polymide for Spacecraft Applications in Low Earth Orbit 755

Preliminary Observations on the LDEF/UTIAS Composite Materials Experiment and Simulator Results on Protective Coatings 763
(Paper not provided by publication date)

Characterization of a 5-eV Neutral Atomic Oxygen Beam Facility 764

Ground and Space Based Optical Analysis of Materials Degradation in Low-Earth-Orbit 772

The Transition of Ground-Based Space Environmental Effects Testing to the Space Environment 778

HUMAN FACTORS

SATELLITE MONITORING AND CONTROL

2

A Human Factors Approach
to
Range Scheduling for Satellite Control

Cameron H.G. Wright and Donald J. Aitken

USAF Space Systems Division
Los Angeles AFB, CA 90009-2960

ABSTRACT

Range scheduling for satellite control presents a classical problem: supervisory control of a large-scale dynamic system, with unwieldy amounts of interrelated data used as inputs to the decision process. Increased automation of the task, with the appropriate human-computer interface, is highly desirable. This paper describes the development and user evaluation of a semi-automated network range scheduling system incorporating a synergistic human-computer interface consisting of a large screen color display, voice input/output, a "sonic pen" pointing device, a touchscreen color CRT, and a standard keyboard. From a human factors standpoint, this development represents the first major improvement in almost 30 years to the satellite control network scheduling task.

1. INTRODUCTION

To maintain today's large number of satellites in their various orbits, it is necessary to schedule regular contacts with them using a global network of satellite tracking and control facilities. During the early days of the military space program, the complexity of the satellite control scheduling task was low enough that a daily schedule of satellite contacts could be easily represented with a paper chart. Data representing satellite/ground station visibility, resource allocation, and conflict resolution could be assimilated by scheduling personnel in an acceptable manner using this method.

However, continued growth in number, size, and complexity of both ground and space assets, combined with the increased dependence on these resources for national defense, has made it necessary to search for a more effective methodology for network scheduling. The Air Force Satellite Control Network (AFSCN) is a large-scale system which provides the essential command, control, and communications (C^3) support to orbital space vehicles using internetted facilities located across the globe. The task of scheduling these network assets effectively is a challenging problem of supervisory control [1]. On any given day, interrelated information depicting nearly 1600 entries of satellite visibility and scheduled network support must be interpreted and used to make decisions that can be critical to the survival of valuable orbital assets [2]. Given an environment which must account for unexpected equipment outages, satellite anomalies, and changing mission priorities, the scheduling task can exceed acceptable workload levels.

While recent attempts to fully automate this task have been less than satisfactory, it is within the state of the art to implement a partially automated system with human-in-the-loop decision making. This system must effectively convey large amounts of interrelated data to the scheduler and allow the scheduler to manipulate this data and to input selected commands at will. These requirements indicate that an optimized human-computer interface (HCI) is a critical design aspect of such a system [3].

This paper describes the development and user evaluation of a semi-automated network scheduling system incorporating a synergistic HCI consisting of a large screen color display, voice input/output, a "sonic pen" pointing device, a touchscreen color CRT, and a standard keyboard.

2. THE PROBLEM DOMAIN

Before we can examine the HCI design, we must first understand the activities involved in satellite control network scheduling. While there are many similarities between scheduling support for civilian satellites [4,5] and for military satellites [2,3], we concentrate here on the latter. Military satellites include many low earth orbiters, which, because of their brief "windows" of satellite/ground station visibility, make the scheduling task more difficult than with the predominantly geosynchronous civilian satellites.

Traditionally, scheduling was performed using a paper acquisition chart. The horizontal axis of the chart represents time, and the vertical axis shows the resources for each ground station of the AFSCN, commonly referred to as Remote Tracking Stations (RTS). A single paper chart encompassing a 24-hour period measures 36" vertically by 144" horizontally, with extremely high information density. Three types of schedules are maintained: a seven day forecast, a 24-hour schedule, and a real-time schedule. The basic scheduling activities are listed below, and a flowchart of a typical real-time response to an RTS outage is shown in Figure 1.

Receive new or modified request for satellite support.
Validate acquisition data and satellite/RTS visibility.
    Compare new data with most recent data from scheduling database.
    Slide supports along time axis of chart to accommodate changes.
Assign or modify satellite support(s).
    Visually scan chart for resource availability.
    Enter support(s) on chart.

- Prepare schedule.
    - Identify time/resource conflicts.
    - Scan chart for alternate support possibilities.
    - Propose alternative solution to Mission Control Center.
    - Reassign supports as approved and notify RTS.
    - Enter new support on chart.
- Update scheduling database to reflect latest chart.

It is important to note how the scheduling chart is central to these activities. It contains a large amount of information relating to the various satellites, RTS resources, and visibilities for the entire world-wide AFSCN by using twenty-nine distinct variations of symbology and annotation style [2]. This graphical representation enables the scheduler to view the "big picture" at a glance, make the necessary RTS assignments, identify conflicts, and resolve them quickly. This is especially critical during real-time scheduling, which is driven by random events (satellite anomalies, RTS equipment outages, changing mission priorities, etc.). The main drawback of the paper chart is that it is a totally manual process, which has become increasingly unmanageable due to the trends identified in Section 1 above. Greater automation of the scheduling task is highly desirable; benefits would include a more acceptable scheduler workload, reduced chance for human error, and greater responsiveness to highly dynamic national security priorities. However, any acceptable design must incorporate into the HCI those positive aspects of the paper acquisition chart outlined above.

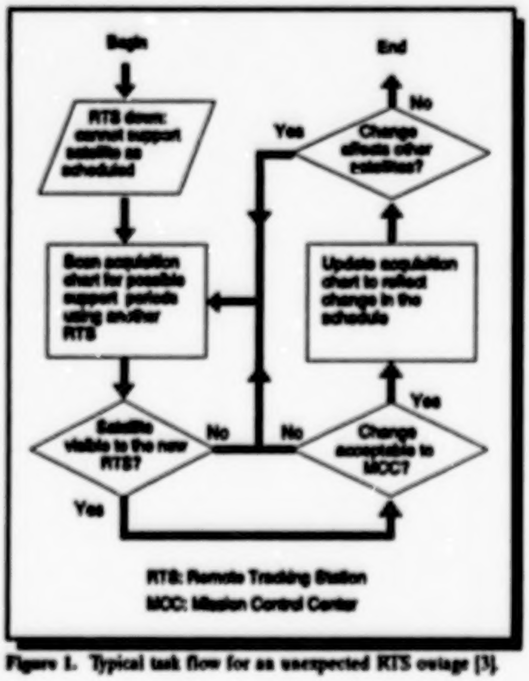
Begin
RTS down: cannot support satellite as scheduled
Scan acquisition chart for possible support periods using another RTS
Satellite visible to the new RTS?
No
Yes
No
Change acceptable to MCC?
Yes
Update acquisition chart to reflect change in the schedule
Change affects other satellites?
Yes
No
End
RTS: Remote Tracking Station
MCC: Mission Control Center

Figure 1. Typical task flow for an unexpected RTS outage [3].

3. ASTRO: A NEW APPROACH

The importance of a well designed HCI has been documented extensively in the literature [6-11]. Recently, significant progress has been made [2-5] in investigating optimal HCIs for various satellite control tasks. The GT-MSOCC simulator at Georgia Tech, for example, has addressed many aspects of NASA satellite operations. However, the Air Force had a pressing need to address the problem of network scheduling for satellite control in an operational military environment.

Initial designs to solve this problem proposed an HCI using standard CRTs, which were limited to displaying only a small subset of the information contained in the paper chart. It was thought that the use of panning, scrolling, zooming, and windowing techniques could overcome this limitation and provide an equivalent capability. However, experienced scheduling personnel evaluated this approach as unacceptable; their stated requirement was to view all the information that the paper chart provided with at least 12 hours of data on a single display. It has been shown [3] that human factors design considerations support this position in that the necessity of accessing multiple sequential displays forces excessive reliance on the short-term memory of the schedulers, resulting in increased error rates. In particular, the error rate increases proportionally with the number of screen accesses required, and with the time required to perform those accesses. By taxing short-term memory, the perceived workload and level of stress experienced by schedulers would actually increase compared to using the paper chart, and scheduling productivity would go down. A new design approach for the HCI was required, and the Automated Scheduling Tools for Range Operations (ASTRO) project was started in October 1987. (*"Range" here denotes the networked RTSs of the AFSCN.*)

In order to satisfy the core requirement of providing 12 hours of scheduling data on one display, a high resolution, large screen color display is required. Analysis indicates that an approximate displayable resolution of 3K vertical points and 4K horizontal points is necessary [2]. (*Note that manufacturer specifications typically cite only **addressable** resolution, which is generally two to four times greater than **displayable** resolution.*) For comfortable viewing of 7×9 format characters, the screen size should be roughly 25" vertically by 42" horizontally [2]. A 12-hour section of the paper chart was photo-reduced to validate these derived estimates. Further requirements include at least 16 colors, ability to mix graphic symbols with characters, imperceptible flicker, low noise level, standard computer interface, standard power and cooling needs, high MTBF, and low MTTR. While these requirements push state-of-the-art display technology, the best match was found to be a continuous projection, laser addressed system using smectic liquid-crystal light valves, produced by Greyhawk Systems [12]. It displays 4096 colors with 2.2K V by 3.4K H displayable resolution on a 22" by 34" screen with excellent clarity and detail, has a contrast ratio of 16:1, a very wide viewing angle, and can be used in normal ambient lighting. A 12 hour acquisition chart representation was found to be quite readable on the Greyhawk display. While the Greyhawk meets the primary display requirement, an effective HCI is a coordinated ensemble; thus we now turn our attention to data entry and manipulation.

Observations have shown that even skilled typists can update a paper chart faster than they can update a computer display using a standard keyboard; alternatives are required [2]. Because the Greyhawk does not produce sync pulses, a light pen is not feasible. A mouse, while usable, would take away too much valuable horizontal workspace. An effective solution for a pointing device was found to be the GP-8 Sonic Pen from Science Accessories, which utilizes audio detectors mounted on two orthogonal edges of the Greyhawk display. The GP-8 controller computes the pen location based on the time-of-arrival of a sonic pulse emitted by the pen when pressed to the screen. The pen is used to both identify specific points on the large screen display, and to select items from standardized pop-up menus via appropriate display interface software [13-15]. While the sonic pen can be used for many tasks, a keyboard would still be required for some alphanumerical entry. Voice-augmented keyboards have been shown to alleviate this potential bottleneck [16]; thus, a Verbex 5060 voice I/O system from Voice Industries was incorporated into the ASTRO HCI design. Using a headset and an intelligent controller, this device supports a continuous speech grammar of up to 600 words; ASTRO required only a 50 word grammar. Initial training of the V-5060 for each speaker required one hour, but resulted in reliable recognition rates of better than 95% for all speakers, and a maximum response time of 0.5 seconds [2]. In addition to the Greyhawk display, a 19" color (VGA) CRT with an Elographics touchscreen overlay was integrated into the HCI to allow operator access to secondary screens and menus, and as a system monitor for the Compaq 386/25 computer that runs the ASTRO software. The sonic pen was also capable of selecting items on the touchscreen CRT, allowing the operator to use the same pointing device for both displays.

The ASTRO HCI is a synergistic combination of a large screen display, a sonic pen, voice I/O, an ancillary touchscreen CRT display, and a standard keyboard, which allows effective manipulation of the schedule data, minimizes the required keyboard entry, and greatly reduces the time required to perform scheduling tasks. See Figure 2 below, and Photo 1 and 2 following the text.

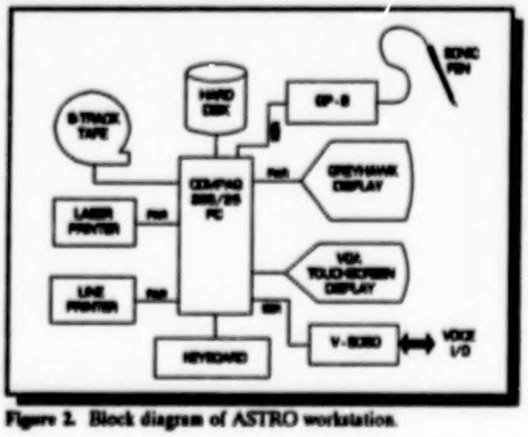

Figure 2. Block diagram of ASTRO workstation.

While ASTRO certainly meets the design goal of improving the methodology for satellite control network scheduling, it also has potential to provide a multi-node, simultaneous scheduling capability never before possible. By connecting multiple units via LAN, WAN, or standard telephone lines, users at different locations could manipulate a shared schedule database, thus improving coordination and wartime survivability.

4. USER EVALUATION

The most effective HCIs result from the user being involved early in the design phase. ASTRO was managed as a prototype project, where instead of copious reports, documentation, and formal design reviews, system demonstrations were given to representative users at frequent intervals during the development. This allowed user feedback to guide the design process. During the initial development period, 40 system demos were given to 320 people with space operations and scheduling backgrounds to solicit their suggestions. Following this, ASTRO prototypes were installed at the two major control nodes of the AFSCN: Falcon Air Force Base (FAFB) in Colorado Springs, CO, and Onizuka Air Force Base (OAFB) in Sunnyvale, CA. An extensive functional evaluation study was conducted from August 7, 1989 to December 8, 1989, and resulted in an extremely favorable final report [17]. Areas and subareas evaluated on a scale of 1 (worst) to 5 (best) were: Functional Requirements (Information Display, Operator Capabilities, Scheduling Functions), Performance Requirements (Display, Functional), Human Factors (Workspace, Displays, Pointing Device, Keyboard, and Voice Input), plus an overall system rating. We concentrate here on a preliminary analysis of the Human Factors area, which rated the HCI. While further statistical analyses will be conducted, Figure 3 depicts the group average ratings given in each subarea, with the overall system rating also shown for comparison.

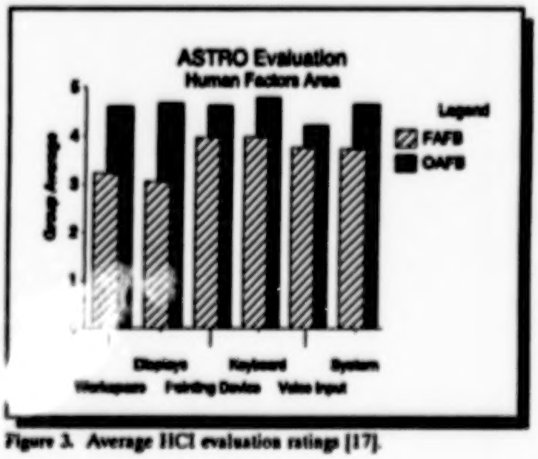

Figure 3. Average HCI evaluation ratings [17].

Note that while the evaluations are very good, the OAFB schedulers consistently rated the ASTRO HCI and the overall system higher than those at FAFB. We feel that this may be due to the fact that while the satellite control and scheduling tasks have been performed at OAFB for 30 years with only recent help from modern tools, FAFB is a new facility with the latest equipment, possibly leading to less appreciation for the advances represented by ASTRO. Further, latent shipping damage to the unit at FAFB resulted in some early reliability problems, which may have biased some of the evaluations. Despite these caveats, ASTRO received enthusiastic response from the schedulers at both nodes.

Following publication of the evaluation final report [17], ASTRO was given two weeks of full operational testing, and performed very well. As a result, Air Force Space Command has submitted formal documents requesting installation of ASTRO at both nodes to support operational scheduling of the AFSCN.

5. CONCLUSIONS

It has been shown that the network scheduling task for satellite control has grown in complexity until the traditional method of using a paper chart representation is insufficient. The desire of the human schedulers to retain the graphical aspects of the paper chart for ASTRO was shown to have a logical basis in human cognitive abilities. The engineering challenge of representing such a data intensive display in a usable format, while allowing efficient supervisory control of the scheduling task, was met by designing an optimized HCI for ASTRO. This interface consists of a large screen color display, a voice input/output subsystem, a sonic pen pointing device which can be used both with the large screen display and the ancillary touchscreen CRT display, and a standard keyboard. Extensive evaluation of the ASTRO system indicated a high level of user satisfaction with ASTRO overall, and its HCI in particular. As a result of this evaluation, Air Force Space Command has recommended that ASTRO be used for full-time scheduling of operational military satellites. Further research is needed to investigate integration of appropriate artificial intelligence technology into the ASTRO design, particularly in the area of automated conflict resolution, and to investigate implementation of networked ASTRO units.

ACKNOWLEDGEMENTS

This material is based upon work supported by the USAF Space Systems Division under contract F04701-86-C-0007. The U.S. Government retains certain rights to this material. The authors would like to express their appreciation to John List and his associates at Unisys for their assistance in preparing this paper. Opinions, conclusions, and recommendations expressed or implied in this paper are solely those of the authors, and do not necessarily represent the views of the United States Air Force, the Department of Defense, or any other Government agency.

The authors may be reached at mail stop SSD/CWO, Los Angeles AFB, CA 90009-2960.

REFERENCES

[1] T. B. Sheridan, "Toward a general model of supervisory control," in *Monitoring Behavior and Supervisory Control*, eds. T. B Sheridan and G. Johannsen, Plenum Press, New York, 1976.

[2] J. L. List et al, "Range Scheduling Via Large-Screen Displays, Phase I-IV," Unisys Corp., Sunnyvale, CA, 1989.

[3] D. E. Egbert et al, "Analysis of Man-Machine Interfaces for the Network Scheduling System," (AFSCF-TR-86-101), Ford Aerospace and Communications Corp., Sunnyvale, CA, 1986.

[4] C. M. Mitchell, "GT-MSOCC: A domain for research on human-computer interaction and supervisory control systems," *IEEE Trans. on Systems, Man, and Cybernetics*, vol. SMC-17, no. 4, pp. 553-572, 1987.

[5] C. M. Mitchell and T. Govindaraj, "A tutor for satellite operators," *Proc. 1989 IEEE Int. Conference on Systems, Man, and Cybernetics* (Cambridge, MA), pp. 766-771, Nov. 1989.

[6] E. J. McCormick and M. S. Sanders, *Human Factors in Engineering and Design*, 5th ed., McGraw-Hill, New York, 1982.

[7] S. K. Card, T. P. Moran, and A. Newell, *The Psychology of Human-Computer Interaction*, Lawrence Earlbaum Associates, Hilsdale, NJ, 1983.

[8] E. Grandjean and E. Vigliani, eds., *Ergonomic Aspects of Visual Display Terminals*, Taylor and Francis, London, 1980.

[9] National Aeronautics and Space Administration, *Bioastronautics Data Book* (NASA SP-3006), U.S. Government Printing Office, Washington, D.C., 1973.

[10] Department of Defense, "Human Engineering Design Criteria for Military Systems, Equipment, and Facilities," (MIL-STD-1472D), U.S. Government Printing Office, Washington, D.C., 1989.

[11] R. A. Olsen, ed., "Handbook for Design and Use of Visual Display Terminals," (Tech. Rep. LMSC 62-91), Lockheed Missiles and Space Company, Sunnyvale, CA, 1982.

[12] F. J. Kahn et al, "A paperless plotter display system using a laser smectic liquid-crystal light valve," *Society for Information Display International Symposium Digest*, paper 14.1, 1987.

[13] S. W. Draper and D. A. Norman, "Software engineering for user interfaces," *IEEE Trans. Software Engineering*, vol. SE-11, pp. 252-258, 1985.

[14] S. L. Smith, "User-System Interface Design for Computer-Based Information Systems," (Tech. Rep. MTR-8464), MITRE Corp., Bedford, MA, 1982.

[15] S. L. Smith et al, "Guidelines for Designing User Interface Software," (ESD-TR-86-278), MITRE Corp., Bedford, MA, 1986.

[16] C. M. Mitchell and M. G. Foren, "Multimodal user input to supervisory control systems: voice-augmented keyboards," *IEEE Trans. on Systems, Man, and Cybernetics*, vol. SMC-17, no. 4, pp. 594-607, 1987.

[17] F. S. Watson et al, "ASTRO Evaluation Final Report," Air Force Space Command (Det 9, 2STG/TA), Falcon AFB, CO, 1990.

PHOTOS

Photo 1. Overall view of the ASTRO workstation.

7

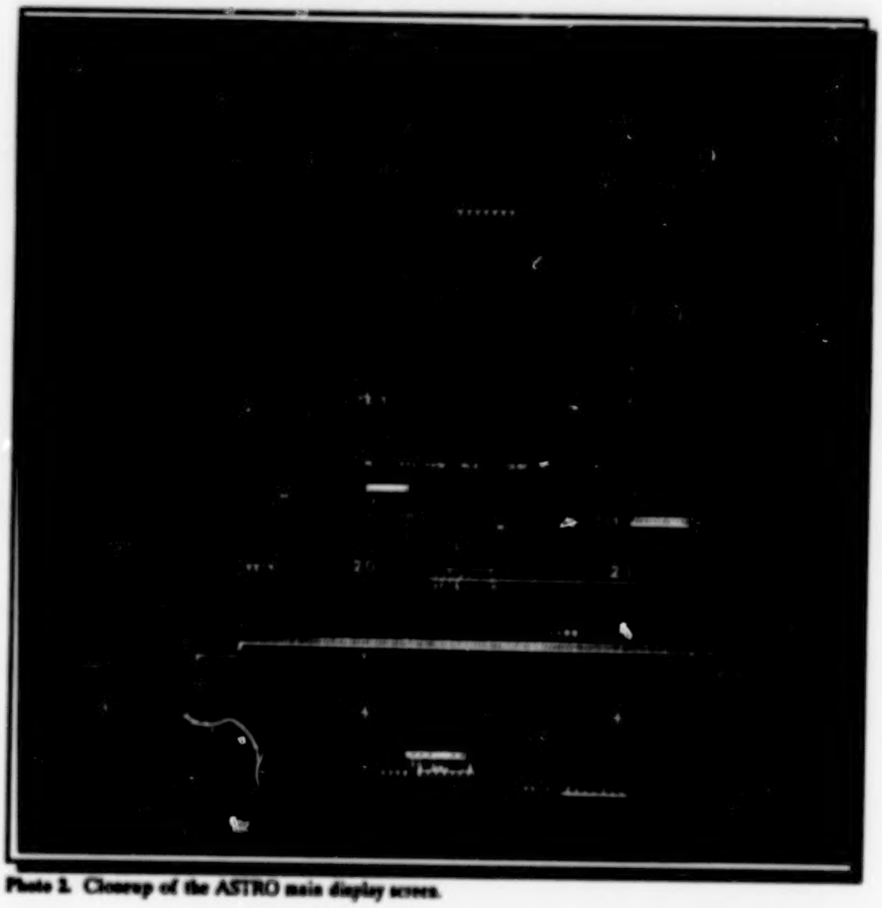

Photo 2. Closeup of the ASTRO main display screen.

Model-Based Displays for Satellite Ground Control[*]

Christine M. Mitchell
Center for Human-Machine Systems Research
School of Industrial and Systems Engineering
Georgia Institute of Technology
Atlanta, GA 30332
(404) 894-4321
cm@chmsr.gatech.edu

With the emergence of new technology for both human-computer interaction and knowledge-based systems, a range of opportunities exists to enhance the effectiveness and efficiency of satellite ground controllers. This presentation illustrates the use of models of operator function to represent operator activity in the context of changing system events and operator functions. Although there are many models, this research used the operator function model (OFM). Figure 1 depicts a generic OFM; Mitchell (1987) gives details about the model structure and the OFM modeling process.

In addition to representing operator activities, the OFM can be used to design 'intelligent' operator displays and, in real time control the displayed information so that the operator has the appropriate information, at the appropriate time, and at the appropriate level of abstraction. The operator function model was demonstrated in the context of a NASA Goddard Space Flight Center satellite ground control system (Figure 2). Figure 3 depicts a portion of the OFM for the Multisatellite Operations Control Center (MSOCC) application.

To evaluate the effectiveness of the model-based workstation, an experiment was conducted to compare system performance with a conventional operator workstation versus the model-based workstation. The conventional workstation consisted of three monitors and showed, in alpha-numeric form, hardware status and equipment and satellite support schedules. The conventional display had more than 150 display pages that the operator could query (Figure 4a).

Two monitors comprised the model-based workstation, one to support monitoring and fault detection, the other to support fault compensation (Figure 4b). The workstation design included qualitative icons and model-based windows. A faucet icon represented hardware status and data flow; the icon was qualitative and depicted the worst case for each equipment network supporting a satellite link. The faucet icon was hierarchical; if the operator wanted more detailed information, a display showing the configuration of the network and status of each equipment was available. The high-level mission icon supported monitoring; the more detailed representation of the equipment network supported fault detection. Fault compensation entailed the selective display of hardware and satellite schedule information. Schedule information was linked to a set of likely operator fault compensation activities derived from the OFM. For each activity the operator could ask for "help" to carry out the function. For example, if component RUP3 failed, the operator could say "Help Replace RUP3", and the model would search the hardware and satellite support schedules to identify a set of possible replacement components that were currently available and not scheduled to support another satellite for the time in question. For both the monitoring/fault detection task and the fault compensation task, the model provided the intelligence to enable the displays to adapt to changing operator and system requirements in real-time.

The experiment comparing the conventional versus model-based workstation demonstrated the effectiveness of the OFM-based design. The model-based workstation enabled operators to effectively handle real-time control with workload that quintupled normal Goddard workload. Figure 5 summarizes the experimental data.

Related Journal Papers

Mitchell, C. M. (1987). GT-MSOCC: A research domain for modeling human-computer interaction and aiding decision making in supervisory control systems. *IEEE Transactions on Systems, Man, and Cybernetics*, SMC-17, 553-570.

Mitchell, C. M. and Saisi, D. S. (1987). Use of model-based qualitative icons and adaptive windows in workstations for supervisory control systems. *IEEE Transactions on Systems, Man, and Cybernetics*, SMC-17, No. 4, 573-593.

Mitchell, C. M. and Forren, M. G. (1987). Effectiveness of multi-modal operator interfaces in supervisory control systems. *IEEE Transactions on Systems, Man, and Cybernetics*, SMC-17, No. 4, 594-607.

Conference Presentations with Proceedings

Forren, M. C. and Mitchell, C. M. (1986) Multi-model interfaces in supervisory control. *Proceedings of the Human Factors Society 30th Annual Meeting*. Dayton, 317-321.

Saisi, D. L. and Mitchell, C. M. (1986). Model-based window display interfaces in real time supervisory control. *Proceedings of the 1986 IEEE International Conference on Systems, Man, and Cybernetics*, 885-889.

Jones, P. M., and Mitchell, C. M. (1987). Operator modeling: Conceptual and methodological distinctions. *Proceedings of the Human Factors Society 31st Annual Meeting*, 31-35.

Jones, P.M. and Mitchell, C. M. (1989). Operator models for supervisory control systems. *Proceedings of the Human Factors Society 33nd Annual Meeting*, 291-295.

This research was supported in part by a Goddard Space Flight Center grant, "Human-Computer Interaction in Distributed Supervisory Control Tasks," NAG 5-1044,Walt Truszkowski, Technical Monitor.

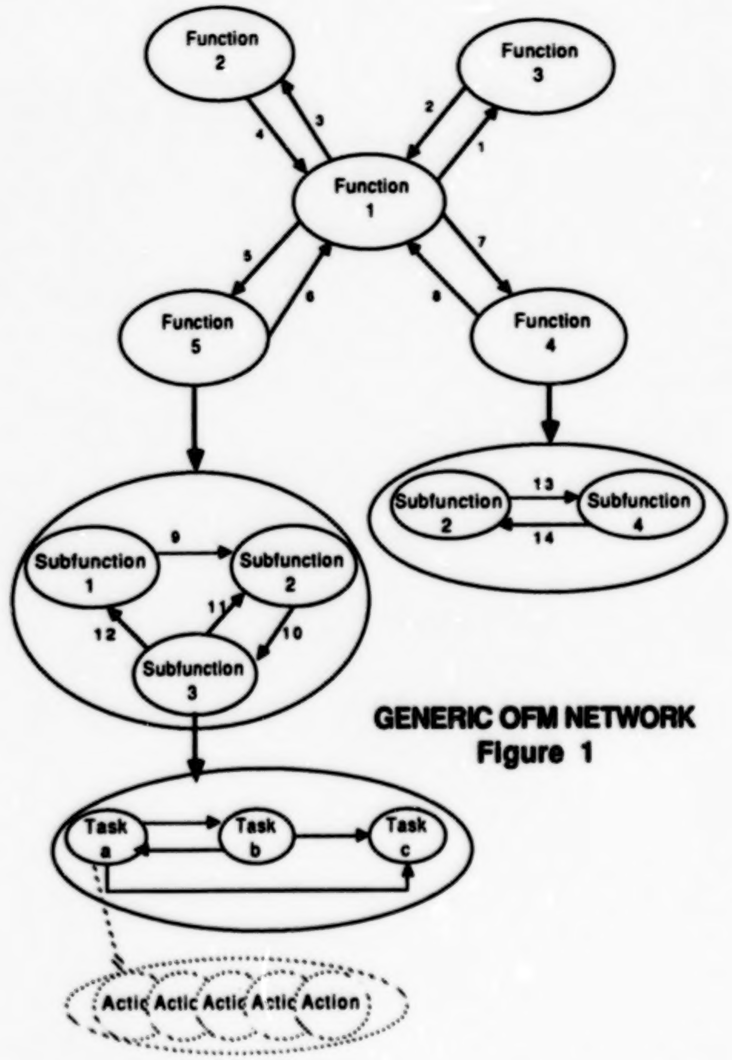
Function 2
Function 3
Function 1
Function 5
Function 4
1
2
3
4
5
6
7
8
Subfunction 1
Subfunction 2
Subfunction 3
9
10
11
12
Subfunction 2
Subfunction 4
13
14
Task a
Task b
Task c
Actic Actic Actic Actic Action

GENERIC OFM NETWORK
Figure 1

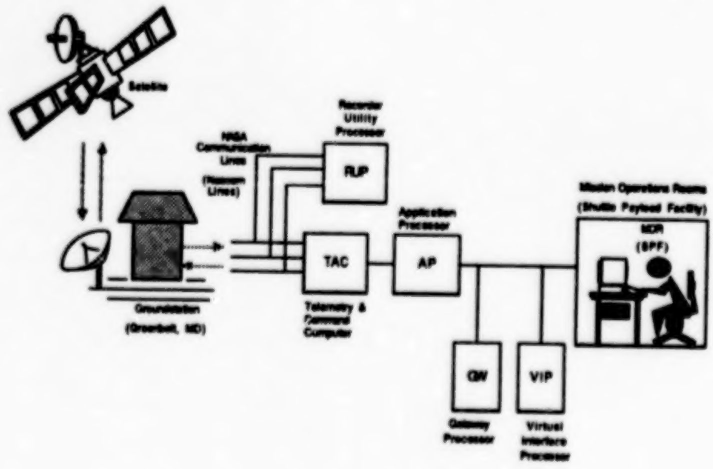
Satellite
Recorder Utility Processor
NASA Communication Lines
(Nascom Lines)
RUP
Application Processor
TAC
AP
Telemetry & Command Computer
Groundstation
(Greenbelt, MD)
Mission Operations Rooms
(Shuttle Payload Facility)
MOR
(SPF)
GW
VIP
Gateway Processor
Virtual Interface Processor

Multisatellite Operations Control Center
Figure 2

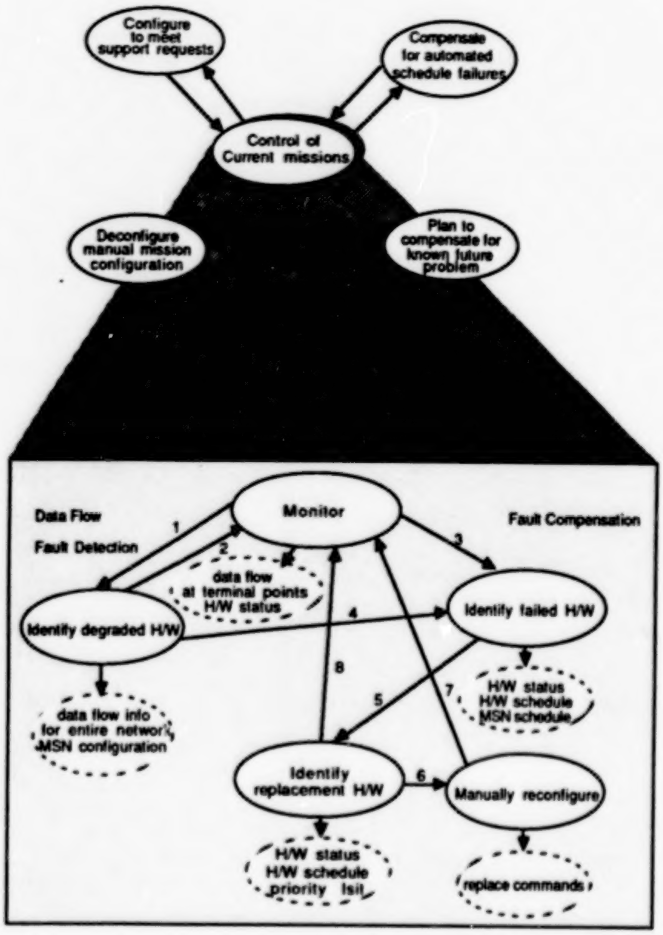
Configure to meet support requests
Compensate for automated schedule failures
Control of Current missions
Deconfigure manual mission configuration
Plan to compensate for known future problem
Data Flow
Fault Detection
Monitor
Fault Compensation
1
2
3
data flow at terminal points H/W status
Identify degraded H/W
4
Identify failed H/W
8
5
7
H/W status H/W schedule MSN schedule
data flow info for entire network MSN configuration
Identify replacement H/W
6
Manually reconfigure
H/W status H/W schedule priority lsit
replace commands

GT-MSOCC OFM
Figure 3

Measures	Model - based	Keyboard	Windows
Time to detect hardware failures	42.5s*	58.4s	68.0s*
Time to detect SW no flow	56.9s*	312.4s	369.4s
Time to detect SW decreased flow	71.2s*	398.9	438.9s
Time to detect high error count	206.0s*	356.7s	391.7s
Time to deconfigure	11.1s*	22.6s	28.0s
Time to compensate for automated schedule problems	46.5s	75.9s	82.9s
Number of operator-caused schedule conflicts	.16*	.70	.93

* indicates significance at $p < 0.01$

Mean Scores Per Session
Figure 5

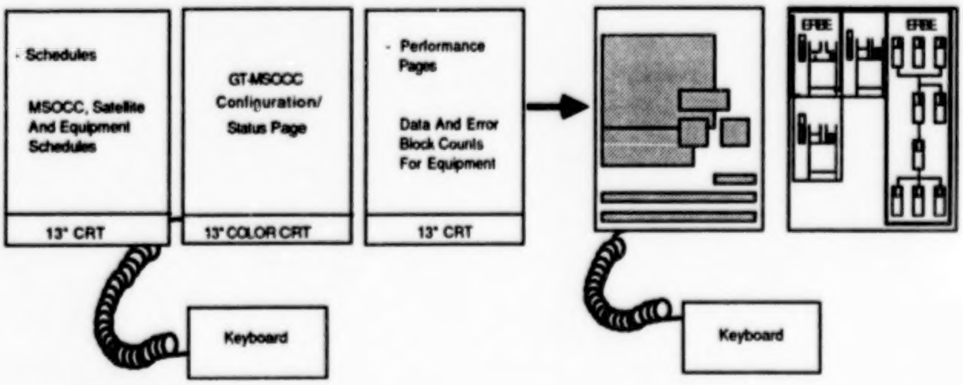
- Schedules
MSOCC, Satellite And Equipment Schedules
13" CRT
GT-MSOCC Configuration/ Status Page
13" COLOR CRT
- Performance Pages
Data And Error Block Counts For Equipment
13" CRT
Keyboard
Keyboard

Conventional Vs. Model-Based(OFM) Workstation
Figure 4

11

Utilizing Expert Systems for Satellite Monitoring and Control

Peter M. Hughes
Software and Automation Systems Branch (Code 522)
NASA Goddard Space Flight Center
Greenbelt, Maryland 20771

Abstract

Spacecraft analysts in the spacecraft control center for the COBE (Cosmic Background Explorer) satellite are currently utilizing a fault-isolation expert system developed to assist them isolate and correct faults in the communications link. This system, named CLEAR (Communications Link Expert Assistance Resource), monitors real-time spacecraft and ground system performance parameters in search of configuration discrepancies and communications link problems. If such a discrepancy or problem is isolated, CLEAR alerts the analyst and provides advice on how to resolve the problem swiftly and effectively. The CLEAR System is the first real-time expert system to be used in the operational environment of a satellite control center at the NASA Goddard Space Flight Center.

CLEAR has not only demonstrated the utility and potential of an expert system in the demanding environment of a satellite control center, it has also revealed many of the pitfalls and deficiencies of the development of expert systems. One of the lessons learned from this and other initial expert system projects is that prototypes can often be developed quite rapidly, but operational expert systems require considerable effort. Development is generally a slow, tedious process that typically requires the special skills of trained programmers.

Due to the success of CLEAR and several other systems in the control center domain, a large number of expert systems will certainly be developed to support control center operations during the early 1990s. To facilitate the development of these systems, a project has been initiated to develop an integrated, domain-specific tool, named GenSAA (Generic Spacecraft Analyst Assistant), that will allow the spacecraft analysts to rapidly create simple expert systems themselves. By providing a highly graphical, point-and-select method of system development, GenSAA allow the analyst to utilize and/or modify previously developed rule bases and system components, thus facilitating software reuse and reducing development time and effort.

Introduction

The Goddard Space Flight Center is responsible for managing the operations of numerous low-earth orbit satellites. These scientific satellites either have a dedicated control center (e.g. LANDSAT and the Hubble Space Telescope) or share computer resources in the Multi-Satellite Operations Control Center (e.g. Cosmic Background Explorer and Earth Radiation Budget Satellite). In either case, highly trained personnel, called flight operations analysts (FOAs), are responsible for the proper command, control, health and safety of the satellite.

The satellite control centers operate round-the-clock throughout the lifetime of the spacecraft. There are typically multiple real-time communications events with each satellite daily. During these real-time communications events, the FOAs must:

- establish and maintain the telecommunications link with the spacecraft,
- monitor the spacecraft's health and safety,
- send commands or command loads to the satellite for on-board execution,
- manage spacecraft resources (including on-board memory, batteries, and tape recorders), and
- oversee the dumping of the scientific data from the on-board tape recorders to ground systems for processing and analysis.

12

To accomplish these activities, the analyst must combine a thorough understanding of the operation of the spacecraft and the ground systems with the current state of operations as indicated by numerous telemetry parameters displayed on the consoles. During an event, the analyst typically monitors hundreds of telemetry parameter values on multiple display pages that may be updating several times per second. The monitoring of the operation of these satellites is a demanding, tedious task that requires well-trained individuals who are quick-thinking and composed under pressure.

As spacecraft become more complex, the task of operating a satellite is becoming increasingly more difficult. The FOAs are reaching a level of saturation as more and more data must be monitored and analyzed during the real-time supports. The need to automate some of these functions is apparent.

The CLEAR System

The Communications Link Expert Assistance Resource (CLEAR) is the first attempt at the Goddard Space Flight Center to utilize an expert system to automate a spacecraft analyst's task. CLEAR is a fault-isolation expert system this is supporting real-time operations in the Payload Operations Control Center (POCC) for the Cosmic Background Explorer (COBE) mission. This system monitors the communications link between COBE and the Tracking and Data Relay Satellite (TDRS), alerts the analyst to any discrepancies or problems, and offers advice on how to correct them. It is the first expert system to become operational in a satellite control center at NASA/Goddard.

CLEAR is a forward chaining, rule-based system that operates in the COBE Mission Operations Room (MOR). It monitors over 100 real-time performance parameters that represent the condition and operation of the spacecraft's communications with the relay satellite. With this information, together with the knowledge of TDRS operations, COBE's on-board communications system and the expected configuration of the scheduled event, CLEAR can accurately portray the status of the communications link.

The CLEAR Expert System is currently supporting the COBE flight operations analysts for fault isolation. It is used routinely and is regarded as the fault-isolation "expert" for the COBE/TDRS telecommunications link.

The user interface for CLEAR utilizes textual and graphical output in a tiled-window format to provide the user with information about the status of the COBE/TDRS/ground communications links. A graphics window displays all of the elements of the communications network from the COBE Spacecraft to the POCC with green lines representing healthy links between elements. If the performance parameters indicate that the communications link or processing system is degrading or down, then the associated icon will turn yellow or red, respectively. This display enables analysts to assess the current status of the communications event in a quick glance.

When CLEAR isolates a problem, a short description of the problem is displayed in the "problems" window. If multiple problems are found, the problem descriptions are ranked and displayed in descending order of criticality. CLEAR suggests actions for the analyst to take in order to correct the problem; however, the system does not take any corrective action itself.

To further assist the analyst and to provide support for its advice, the CLEAR system provides an explanation facility. When the analyst selects a problem displayed in the problems window, CLEAR provides a detailed explanation of why the expert system believes that the problem exists. No backtracking or backward chaining is conducted since the system must continue to monitor the real time data and fire forward chaining rules. CLEAR maintains an event log to record histories and allow offline analysis of problems. The event log has proven to be quite useful for operational support of the mission and continued enhancement of the knowledge base.

The CLEAR System operates on any of the seven PC/AT-type workstations that are used for console operations in the MOR. It is written in the C language and uses the C Language Integrated Production System (CLIPS) and a custom-developed graphics library. It currently has approximately 160 rules. Additional rules may be added to monitor the tape-recorder dumps from the satellite to the Wallops ground station.

CLEAR isolates approximately 70 different problems. The types of problems include: non-reception of data within the control center (system or communication problems, or data reporting not activated); misconfigurations between the COBE MOR and the TDRS ground station (coherency/non-coherency, doppler compensation on/off, power mode, actual TDRS in use; antennae configurations); discrepancies in telemetry rate or format; inactive or non-locked links; and degrading or critical automatic gain control situations (signal strength).

The rule-based method of knowledge representation has proven to be quite powerful for this application. Rules provide a direct method of encoding the fault-isolation knowledge of a spacecraft analyst. The development of CLEAR would have taken much longer using conventional, non-rule-based programming techniques. Perhaps more importantly, the rule-based method of representation has provided the flexibility to easily adapt the knowledge base to unforeseen changes in the operational behavior of the spacecraft. For example, even though the operational nature of COBE was fairly accurately understood by the design engineers and flight operations team before the launch, slight behavioral variations and complications arose once the spacecraft was in orbit. Although the FOAs were able to adjust to such variations rather quickly, ground monitoring software systems required complex modifications. However, the required changes to CLEAR's rule-base were relatively straightforward and quickly implemented. After this modification, CLEAR provided consistent operational assistance. This situation demonstrates one of the advantages of the separation of knowledge and data in rule-based expert systems.

Although CLEAR has demonstrated the utility and potential of an expert system in the demanding environment of a satellite control center, it has also revealed many of the pitfalls and deficiencies of the development of expert systems. One of the lessons learned from this and other initial expert system projects is that prototypes can often be developed quite rapidly, but operational expert systems require considerable effort.

Early in CLEAR's development, the primary concern was the perceived difficulty of the knowledge acquisition effort. However, the knowledge engineering task was found to be relatively straightforward, albeit time-consuming. The development of the rule base was a lengthy process due to the interactive nature of the knowledge acquisition. Basically, the expert would describe a specific piece of knowledge to the "knowledge engineer" who would transcribe it into a rule, pass it back to the expert for validation, test it, and then, finally, release it for operational use. The involvement of various players in this process resulted in long turnaround times from the point at which a piece of knowledge was determined to be important until it was translated into a rule and placed into operation. Later in the project, it was determined that the translation of this type of expertise into rules is quite straightforward and can be easily performed by the expert himself.

The CLEAR development team learned that most of the development time for the system was spent on issues not directly related to the construction of the expert system and its rulebase. A surprising amount of the effort focused on the integration of the expert system with the data source and graphics display system. This required in-depth programming knowledge of the interfacing systems and the ability to trouble shoot problems within them. Tools are needed to simplify the complicated task of integrating expert systems with interfacing systems.

CLEAR is regarded as a successful attempt to automate a control center function using an expert system; several other missions have requested systems similar to it. Although this system is beneficial to the COBE flight operations analysts, additional benefits can be captured through retrospective analysis of the development process and focused application to future systems. The project described below represents the first steps taken that capitalize on a number of the lessons learned from the development of the CLEAR Expert System.

The GenSAA Approach

Partly due to the success of CLEAR, a considerable number of expert systems will be developed to support control center operations in upcoming missions during the early 1990's. To facilitate the development of these systems, a project has been initiated to develop an integrated, domain-specific tool, named GenSAA (Generic Spacecraft Analyst Assistant), that will allow spacecraft analysts to rapidly create simple expert systems without having to directly deal with the complicated details of the systems with which the expert system would have to interface. In addition, this tool will allow the expert system developer to utilize and/or modify previously developed rule bases and system components, thus facilitating software reuse and reducing development time and effort.

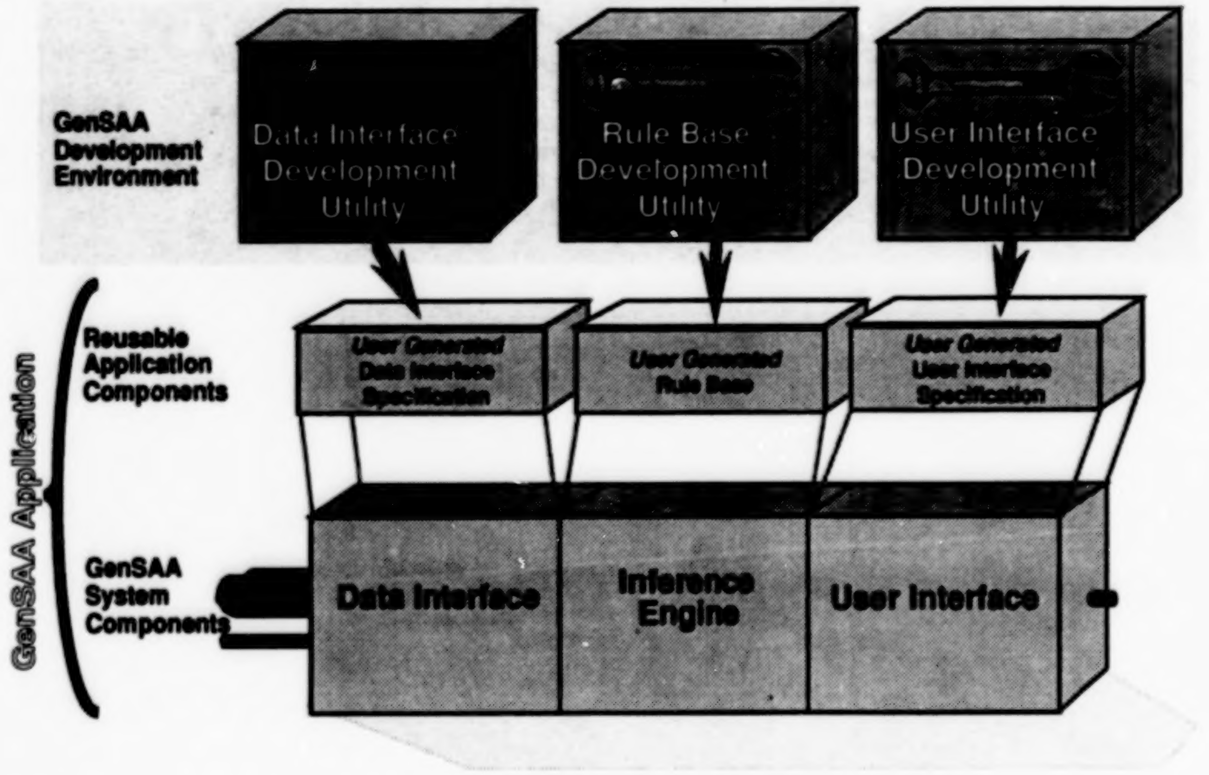
GenSAA Development Environment
Data Interface Development Utility
Rule Base Development Utility
User Interface Development Utility
GenSAA Application
Reusable Application Components
User Generated Data Interface Specification
User Generated Rule Base
User Generated User Interface Specification
GenSAA System Components
Data Interface
Inference Engine
User Interface

Figure 1- Elements of GenSAA

The GenSAA tool will consist of a development environment and system components (figure 1). The system components comprise of:

- the inference engine,
- the display driver, and
- a process that manages the reception of data.

The development environment is composed of three utilities:

- Data Interface Development Utility,
- Rule Base Development Utility, and
- User Interface Development Utility.

Collectively, these utilities will be used to create or modify an instance of an expert system.

The GenSAA development utilities will utilize a highly graphical, point-and-select method of interaction to facilitate use. The expert system developer will use the data interface development utility to select the telemetry parameters to be monitored, the rule base development utility to define the rules which will act on the values of these telemetry parameters, and the user interface development utility to layout a simple graphical representation of the subsystem or process being monitored and where the results of the rule executions will be displayed.

The components generated by the development utilities are called application-specific components. They will be integrated with the GenSAA System Components to create a GenSAA Application. A GenSAA Application is an expert system that will be executed during spacecraft contacts to monitor the selected telemetry parameters and to notify the flight operations analysts of faults inferred from this data.

To demonstrate the advantage of software reuse and to involve the user in the tool definition, the project team decided to initially focus on a class of missions managed by Goddard. A study of upcoming missions was conducted to identify a series of missions that have sufficient commonality to enable reuse of expert system software from mission to mission. The Small Explorer (SMEX) family of missions was determined to be an ideal target group due to the appropriate time frame of this program, the low-cost nature of the missions, the emphasis on system reuse, and the rapid turnaround between missions. All of these factors correlate closely with GenSAA's objectives.

GenSAA is intended to be used by FOAs in a POCC. In an effort to monitor the health and safety of a satellite and its instruments, FOAs monitor real time data looking for combinations of telemetry parameter values, trends, and other indications that may signify a problem or failure. The expert systems created with GenSAA will greatly assist the flight operations analysts with the tedious task of data monitoring thereby allowing them to focus on other, higher-level responsibilities during the real-time contacts with the satellite. This, in turn, will likely result in a more efficient and effective system of operations.

The behavior of a satellite is quite dynamic and often not well understood until the spacecraft is placed in orbit. To quickly create expert systems that can effectively monitor satellites, tools are needed that allow the analysts to formulate the rulebase easily without the intervention or delay of knowledge engineers and programmers. By eliminating these traditional developers, several benefits are expected. The analysts will be able to create rules quickly in response to unforeseen changes in spacecraft behavior or operational procedures. Also, knowledge translation errors will be reduced or, at least, more easily corrected. Knowledge translation errors are errors which are inadvertently introduced during the process of translating a piece of expert knowledge into rule form.

In addition to assisting the FOAs with real-time spacecraft operations, GenSAA will be useful as a training tool in two ways. First, by utilizing the playback utilities provided by the new control center ground system named TPOCC (Transportable Payload Operations Control Center), analysts will be able to replay a previous spacecraft communications event. Thus, a student analyst can observe how the expert system handles a specific problem scenario. Exercises like this will provide a realistic, hands-on environment for training flight operations analysts in a safe, off-line mode. Second, the development of rules used in an expert system is a beneficial mental training exercise for the FOA. Experience from previous expert system projects indicate that the actual formation of rules is a beneficial exercise in itself. By allowing the analysts to create rules themselves, they are forced to consider the alternatives more closely thus promoting a deeper understanding of the problem domain. This may allow the optimal method of fault isolation to be identified.

Another benefit of automating fault-isolation tasks with rule-based systems is that the resulting rulebase serves as accurate documentation of the fault-isolation method. Not only can the rulebase be studied by student analysts to learn about fault-isolation techniques, but, more importantly, mission operations can be better protected against the effects of personnel turnovers. POCC expert systems that capture fault-isolation knowledge preserve expertise from mission to mission and mitigate the impact of the loss of experienced, flight operations analysts.

Conclusion

As satellites become more complex, their operation is becoming increasingly difficult. Flight operations analysts who are responsible for the command, control, health and safety of these spacecraft are rapidly being inundated with the data coming at them at higher and higher rates. Understandably, they are quickly reaching a level of information saturation.

As demonstrated by the CLEAR Expert System, fault-isolation expert systems can help flight operations analysts monitor the flood of data. These systems can accurately monitor hundreds of real-time telemetry parameters, isolating discrepancies and anomalies the instant they can be detected, and alerting the analysts while providing advice on how to correct the problems swiftly and effectively. However, although these expert systems can be quite beneficial, the development of these systems is usually time consuming and costly, and the resulting system often cannot be easily reused by another mission.

Consequently, GenSAA is being developed for use by the flight operations analysts who work in satellite control centers. It is designed to provide quick and easy development of fault-isolation expert systems without the delay or costs of knowledge engineers and programmers. By facilitating the reuse of expert system elements from mission to mission, GenSAA will reduce development costs, preserve expertise between missions and during periods of personnel turnover, and provide a more accurate degree of command and control of our rapidly advancing satellites.

Acknowledgement

The author wishes to thank Mr. Edward Luczak for his dedication and innovative contributions to the GenSAA project and for his insights and suggestions to this paper.

References

1. Hughes, P.M., "CLEAR: Automating Control Centers with Expert System Technology." in Proc. for 1989 SOAR Conference, Houston, TX. 1989.

2. Hughes, P.M., "Integrating Expert Systems into an Operational Environment." in Proc. for Computers in Aerospace VII Conference, Monterey, CA. 1989.

3. Hughes, P.M., and Hull, L.G. "CLEAR: Communications Link Expert Assistance Resource" in Proc. 1987 Goddard Conference on Space Applications of Artificial Intelligence and Robotics, Greenbelt, MD: 1987.

4. Hughes, P.M. and Luczak, E. "Generic Spacecraft Analyst Assistant - Concept Definition." Data Systems Technology Laboratory Document, DSTL-90-008, NASA/Goddard Space Flight Center, Greenbelt, MD: 1990.

ALLY: AN OPERATOR'S ASSOCIATE FOR SATELLITE GROUND CONTROL SYSTEMS

J. B. Bushman*, C. M. Mitchell, P. M. Jones, K. S. Rubin*
Center for Human-Machine
Systems Research School of Industrial and Systems Research
Georgia Institute of Technology
Atlanta, Georgia

Abstract

This paper explores the key characteristics of an intelligent advisory system. A central feature is that human-machine cooperation should be based on a metaphor of human-to-human cooperation. ALLY, a computer-based operator's associate is discussed which is based on a preliminary theory of human-to-human cooperation. ALLY assists the operator in carrying out the supervisory control functions for a simulated NASA ground control system. Experimental evaluation of ALLY indicates that operators using ALLY performed at least as well as they did when using a human associate, and in some cases they performed even better.

INTRODUCTION

Command and control (C2) systems have undergone dramatic changes within the last twenty years. Operators are faced with monitoring and controlling large, complex systems which rely heavily on the use of automaton. Often, the system is too large and complex for a single operator to monitor.

This paper presents the results of a research effort to explore the issues associated with human-machine cooperation in complex, dynamic supervisory control situations and to develop a theory of human-machine cooperation which can be used design the architecture for a computer-based operator's associate. The research focused on the development of a computer-based associate that is cable of cooperating with a human operator in monitoring and controlling a complex, dynamic system.

OPERATOR'S ASSOCIATE

As systems become more automated, the human operator performs fewer tasks on a routine basis. In complex dynamic systems, however, safety requires staffing at a level that can meet the most challenging or threatening abnormal conditions (Wickens, 1984). Normally, these worst-case conditions are well beyond the normal, day-to-day operational conditions. The result is often a team of human operators who are rarely challenged and often underutilized.

The concept of a computer-based operator's associate has been proposed as one method to remedy this situation and to provide intelligent decision aid for operators of complex dynamic systems (Chambers & Nagel, 1985; Rouse, Geddes, & Curry, 1987; Rubin, Jones, & Mitchell, 1988). An operator's associate is a computer-based system that acts as an assistant to the human operator. Functionally, an operator's associate can offer the operator timely advice and reminders, and at the operator's request, assume responsibility for portions of the supervisory control task.

The subordinate role of the operator's associate is a fundamental assumption that characterizes this research effort. The rationale for this assumption is that in complex dynamic systems it is impossible to anticipate and plan for all the contingencies. Thus, a computer system cannot act as the principal or sole "expert" in the system control; a human decision maker will always be present and ultimately responsible for effective and safe system operation. Thus, it is essential to design the system so that the operator is an integral part of the control and decision processes.

The intelligence and utility of the operator's associate rests on its abilities to understand the operator's current intentions and to provide context-sensitive assistance in the form of operator aids (e.g., suggestions, advice, and reminders) or by assuming responsibility for portions of the control task. To ensure generalizability, the operator's associate requires a well-defined knowledge structure. Knowledge concerning the controlled system, operator functions, and operator intentions must be represented (Chambers & Nagel, 1985; Rouse, et. al, 1987; Rubin et. al, 1988; Carroll & McKendree, 1987; Geddes, 1989; Hollangel, 1986; Sime & Coombs, 1983).

The understanding properties of the computer-based associate are based upon the existence of a model that prescribes the operator's interaction with the system (Rouse et. al, 1987; Rubin et. al, 1988; Geddes, 1989). Based on this model of the operator's actions, the automated associate must be able to monitor the operator's actions and model the current status of the decision maker

*Bushman is now with the Training Systems Division, Air Force Human Resources Laboratory, Brooks Air Force Base, Texas, 78235.

*Rubin is now with ParcPlace Systems, 1550 Plymouth St, Mountain View, California, 94043.

18

(i.e., intent inferencing) (Hollangel, 1986).

PRINCIPLES OF COOPERATION

The final property of a computer-based associate is that it should be based on the metaphor of human-to-human cooperation. The computer-based associate should interact with the human operator in a manner similar to the way in which humans interact in a cooperative environment (Carroll & McKendree, 1987; Hollangel, 1986; Fischhoff, 1986; Roth, Bennett & Woods, 1987; Woods, 1986a, 1986b; Woods, Roth & Bennett, 1987). An extensive empirical study was undertaken to investigate the nature of human-to-human cooperation that could serve as the basis for the architecture of an operator's associate.

The general principles of cooperation were derived from two sources. First, an extensive review of the literature was undertaken on cooperative problem solving. Second, extensive data was collected observing a team of experienced operators of the GT-MSOCC system (a typical cooperative supervisory control system) (Mitchell, 1987). The two operators were free to develop a "natural" style of interaction and cooperation. Verbal protocols were collected of the interactions between the operators and data describing their performance were collected. These protocols and data were then analyzed to describe the nature of their cooperative behavior.

A review of the literature indicated that a key principle of cooperation is that operators use multiple mental models to represent their knowledge of the physical system and their functions and to represent their knowledge of the other members of the cooperative team (Athans, 1982; Rasmussen, 1984, 1985; Tenney & Sandell, 1981a, 1981b). These distinct models serve to define and guide the interaction with the system and their interaction among the other operators.

The second feature of cooperation is referred to as cognitive balancing. This term is coined from the cognitive engineering approach to designing human-machine systems (Woods, 1986a, 1986b). Woods argues that the demands of the human and the system need to be considered and supported during the design of a human-machine system. With respect to a cooperative environment, the interacting operators must be aware of the cognitive demands and limitations of the other operators in order for efficient coordination and interaction to occur. One of the objectives of a cooperative team of problem solvers is to attempt to balance the joint cognitive demands of the team, as a whole. This balance is achieved through a mix of communication and delegation.

The final characteristic of cooperation is flexible levels of interaction. Empirical evidence supports the use of Rasmussen's levels of abstraction and aggregation (Rasmussen, 1984, 1985, 1986) to describe the content of the various mental models maintained by the operators and to describe the degree of interaction among the operators. The appropriate level of interaction is dynamic and is determined by the specific cooperation strategy. Interaction among the operators occurs at the levels of abstraction and aggregation common to the operators.

ALLY: A COMPUTER-BASED ASSOCIATE

These properties of a computer based associate and the principles of cooperation form the basis for the development of an architecture for a computer-based associate. The architecture is based on the OFMspert architecture (Rubin et.al, 1988. The architecture incorporates multiple models that represent the system knowledge, procedural knowledge, and operator intentions. The OFMspert architecture uses the operator function modeling (OFM) methodology as the basis for the design of an operator's associate. A key component of an operator's associate is the intent inferencing capability which provides the understanding properties for an intelligent operator's associate. The intent inferencing capability uses a blackboard architecture to understand the operator's current goals. The OFMspert intent inferencing capability was validated in Jones et. al (1989).

ALLY, a computer based associate, is based on an extension of the OFMspert architecture with control capabilities. The architecture provides an interface to the operator that allows the operator to retain complete control over the computer-based associate. The operator can delegate to the associate as many or a few of the tasks as desired.

ALLY was developed to assist an operator in carrying out the supervisory control function for a simulated NASA ground control system, called the Georgia Tech Multisatellite Operations Control Center (GT-MSOCC) (Mitchell 1987; Saisi, 1986). The design was based on a model of the GT-MSOCC operator control functions and attempts to duplicate the capabilities of a human associate. A detailed description of ALLY can be found in (Bushman, 1989).

The operational concept behind ALLY's design is that ALLY is based observations of the relationship that developed between a human operator and a human associate controlling the GT-MSOCC system. The human operator was in complete control of the human associate. The human associate, however, understood the cognitive complexities of the operator functions actively monitored the system for failures, and when necessary, would troubleshoot the system.

ALLY functions in a manner similar to the human associate. The operator has delegate as few or as many of the tasks to ALLY as desired. ALLY also actively monitors and troubleshoots the system on its own.

ALLY was developed in Smalltalk-80TM on a Macintosh II. ALLY interacts with the GT-MSOCC system in a distributed fashion. ALLY acts like another operator of GT-MSOCC system in a distributed fashion. ALLY acts like another operator of GT-MSOCC (see Figure 1). A distributed architecture is consistent with the concept of an assistant that executes autonomously and in its own environment.

Figure 2 provides an example of the ALLY interface to the operator. ALLY performs both delegated and automatic control tasks. The

---

TMSmalltalk-80 is a trademark of ParcPlace Systems, Inc.

operator delegates tasks to ALLY by selecting the corresponding control button. Each control button represents a specific operator control function as described in the GT-MSOCC operator function model (OFM) (Mitchell, 1987). Associated with each control button is a series of tasks that the human operator can delegate to ALLY.

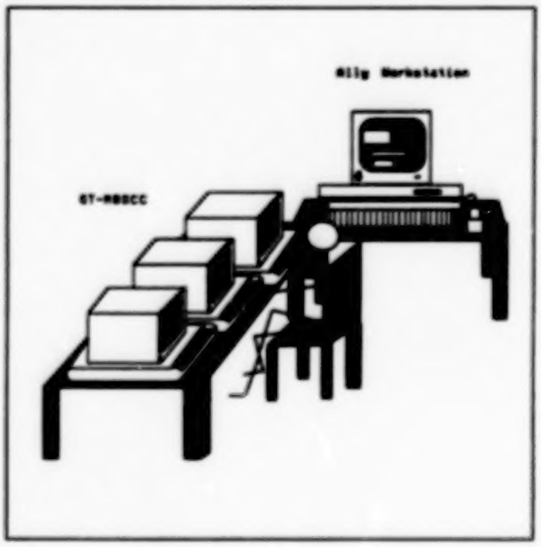

Figure 1. ALLY - GT-MSOCC Workstation

Figure 2. ALLY Basic Windows

The control buttons were designed with specific principles in mind. First, and foremost, the operator is provided the greatest degree of latitude to decide how much or how little support ALLY gives. The operator has complete control over the tasks ALLY performs. If the operator merely wants ALLY to determine the appropriate response and the operator wants to issue the various command, this level of support can be provided. On the other hand, if the operator wants ALLY to perform the entire function, this level of support is also accommodated.

While ALLY only performs the specific task assigned to it, it also understands the nature of the operator control functions. If ALLY knows that the function is still not complete, it offers to complete the task, if it can. It is important to note that this does not remove any of the control flexibility of the operator.

In addition to the delegated tasks, ALLY performs two tasks automatically. ALLY continuously monitors and troubleshoots the equipment networks. ALLY also automatically monitors critical events and offers reminders when it appears the the events might have been missed. This behavior is similar to that observed in a human associate working with the operator to control the GT-MSOCC system.

AN EXPERIMENT

An experiment was conducted to evaluate the effectiveness of ALLY as an operator's associate. The experiment compared the performance of an operator controlling GT-MSOCC working with ALLY as an associate with the performance of an operator working with a human associate.

Experimental Setup

The baseline GT-MSOCC system is a single operator system. In order to conduct the experiment, GT-MSOCC was modified to accommodate two operators. One operator serves as the primary operator and the second operator serves as an associate.

To support the associate position, two additional display screens were added to the baseline configuration. These two screens are functionally equivalent to the left and right screen in the baseline configuration. The center screen showing the GT-MSOCC Configuration and Status page is shared by the operator and associate. Although the physical display terminals are arranged in a different order, the functionality of the screens remain the same.

Each position is capable of issuing any of the GT-MSOCC operator control and information request command. Each position also has a dedicated audible alarm for system alarms. Common alarms indicating system events are sent to both positions, while operator error messages are only sent to the position which originated the error.

Subjects

Ten paid volunteer undergraduate Air Force ROTC cadets from Georgia Institute of Technology participated as subjects for the experiment. The subjects consisted of one female and nine males. The subjects included on junior, one sophomore, and eight freshmen cadets. The subjects were paid six dollars per session.

Experimental Materials

Four sets of written instructions were used in the experiment. The first set consisted of an introduction to the baseline GT-MSOCC system and the operator supervisory control functions. These baseline instructions are found in Saisi (1986). The second set of instructions briefly described the operator-associate operations concept. The third set described the human associate concept and the modified GT-MSOCC workstation for a team of operators. Finally, the last set of instruction described the capabilities of ALLY and the user interface.

Several questionnaires were used during the experiment to collect subjective data. At the end of each data collection session, the subjects were asked to complete a Cooperation Evaluation carrying out the GT-MSOCC supervisory control functions. In addition, the subjects were asked to complete an ALLY Exit Questionnaire and a Human Exit Questionnaire at the end of their last data session with respective associate. The purpose of this these questionnaires was to elicit their opinions about various aspects of the associates. Finally, at the end of the experiment, the subjects were asked to complete a Subjective Comparison Rating questionnaire to compare their opinions about the two associates subjectively.

Overview of Experimental Sessions

The subjects were divided into two groups of five subjects each to control the order in which the subjects received the different associates. One group worked with the human associate first and the other group worked with ALLY first. In addition, to control for the variability of a human associate, a confederate was used in the experiment. The confederate was an expert GT-MSOCC operator and served as the human associate for each subject. The expert was instructed to use the same strategy for carrying out the operator control functions consistently to control the bias that might enter into the experiment from repeatedly seeing the same experimental sessions.

The subjects participated in twenty-four sessions: eight sessions of baseline GT-MSOCC training, three sessions of human associate training, four sessions human associate data collection, five sessions of ALLY training, and four sessions of ALLY data collection. A total of 240 hours of data was collected. The sessions were approximately 45 minutes in length. The sessions were run on consecutive days with typically one session per day. Occasionally, the subjects missed a day and made up the session by running multiple sessions in a single day.

Within each session, three hardware failures and six software failures were scheduled to occur. The failures were scheduled to occur at set times (as determined by the seed of a random number generator) on identical equipment across subjects for a given session. However, since all subjects did not operate the system identically, occasionally failures occurred on different pieces of equipment. In addition, three requests for support of unscheduled spacecraft contacts were also scheduled every session. Again, the sessions were structured such that the requests were identical across subjects for a given session.

Dependent Measures

Eleven baseline dependent measures were developed for GT-MSOCC (Mitchell & Saisi, 1987; Mitchell & Forren, 1987; Saisi, 1986). These measures plus five additional measures to determine how many of the different types of equipment failures were corrected by the subjects were used in the experiment. The performance measures are grouped into four categories: fault compensation, equipment configuration and deconfiguration, operator errors, and percentage of failures corrected.

The fault compensation measures reflect the time to compensate for each of the four types of failures. If the subject failed to compensate for the failure, the measure reflects the total time the failure was present in the system. The next group of performance measures reflect the time to respond to various equipment configuration and deconfiguration requests.

The operator error measures reflect the number of errors committed by the operator. Two types of errors can occur. The first type is when the operator causes a conflict with the automated scheduler. The second type occurs when the operator replaces a component that has not failed.

The last group of performance measures reflect the accuracy of the operator's fault detection strategy. The measure reflects the percentage of errors of a given type that the subject corrected during the session. A separate measure is used for each type of failure. In addition, a separate measure was used to reflect the percentage of total errors corrected.

Analysis

A mixed effect, nested factorial design was used to analyze the data. Because some of the dependent measures did not have a fixed number of repetitions per cell, the design was unbalanced in some cases.

The primary factor of interest is Condition which reflects the type of associate, i.e., human associate or ALLY. The experimental design was a repeated measures design in that each subject was exposed to both of the experimental conditions.

To control for the variability across the subjects, Subject was included as a factor in the experimental design. The Subject effect included 10 levels to reflect the 10 experimental subjects.

In order to account for any variability in the order in which the subjects worked with the two associates, Group was added as a factor in the experimental design. The Group factor includes two levels. The subjects in Group 1 worked with the human associate first, and the subjects in Group 2 worked with ALLY first. Subject, therefore, is a nested factor within Group.

Finally, Session was included as a factor to account for any variability between the sessions. The Session effect included four levels to reflect the four data collection sessions.

Analyses of variances were performed to determine the effect of each of the four independent variables (Condition, Group, Session, and Subject) on each of the sixteen dependent measures. An alpha lower-bar of .10 was used to detect significant effects.

Since the experimental design was a mixed design with random and fixed effects, approximate F statistics were constructed using Satterthwaite's method (Montgomery, 1984). Statistical analyses were performed using the General Linear Model (GLM) procedure of the SAS statistical software package (Spector, Goodnight, Sall, and Sarle, 1985). The GLM procedure computes the expected mean squares which were used to compute Satterthwaite's approximate F-statistic and the adjusted degrees of freedom. These values were then used to compute the significance level of the effects.

In addition to the statistical analysis, the results of the surveys and analysis of audit logs of the subjects' activities were examined to gain additional insight into the individual interaction

Questionnaire to capture subjectively the strategy they used to interact with the associate in strategies used by the subjects. These analyses, in conjunction with the statistical analyses, were used to evaluate the effectiveness of ALLY as an operator's associate and to evaluate the proposed theory of cooperation as it was implemented in ALLY.

DISCUSSION

The experimental results are summarized in Figure 3 and 4. Figure 3 summarizes the means and standard deviations for the two associate conditions across the 16 performance measures. Figure 16 provides a graphical comparison of ALLY's performance compared with the human associate. While these figures indicate that, on the average, ALLY tended to perform better than the human associate, only two of the performance measures yielded significant differences. These were the time to compensate for software type 1 failures (i.e., software failure characterized by termination of data flow) and the number of correct responses to unscheduled support requests. On all other performance measures ALLY performed as well as the human associate. A more exhaustive discussion of the results is found in Bushman (1989).

Dependent Measure	Human Associate		Ally		units
	Mean	Std. Dev	Mean	Std. Dev	
hardware failures	33.4	22.3	26.5	19.3	seconds
software failure 1	113.9	55.9	85.4	49.3	seconds
software failure 2	218.9	104.0	139.1	100.6	seconds
software failure 3	190.4	82.6	102.7	91.4	seconds
schedule conflicts	33.9	30.0	35.8	36.8	seconds
correct responses	2.3	0.7	2.8	0.5	per session
support requests	172.1	156.6	106.0	117.1	seconds
unscheduled contacts	165.3	151.6	120.5	174.6	seconds
deconfigure requests	7.6	5.7	8.7	11.8	seconds
operator error 1	1.2	0.9	0.9	0.8	per session
operator error 2	1.0	0.9	1.3	1.6	per session
% hardware fixed	99.2	5.3	100.0	0.0	percent
% software 1 fixed	83.7	23.7	92.5	18.1	percent
% software 2 fixed	85.0	25.8	93.7	20.2	percent
% software 3 fixed	91.2	16.2	98.7	7.9	percent
% total fixed	90.8	7.5	96.7	6.3	percent

Figure 3. Summary Performance Measures

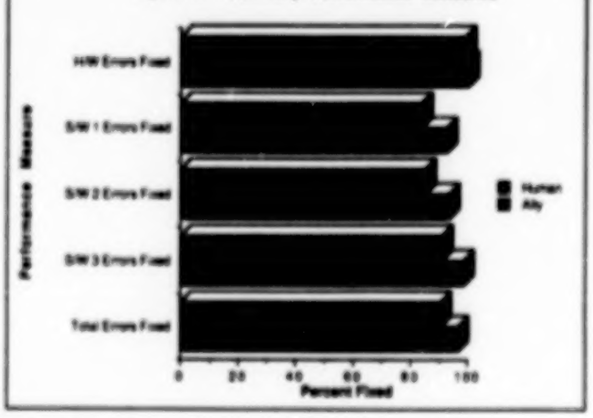

Figure 4c. Mean Performance Measures by Condition

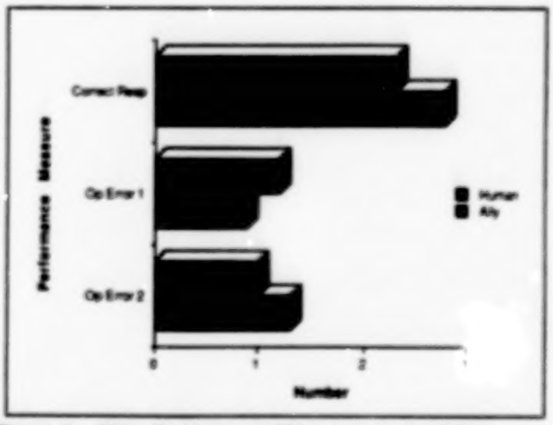

Figure 4b. Mean Performance Measures by Condition

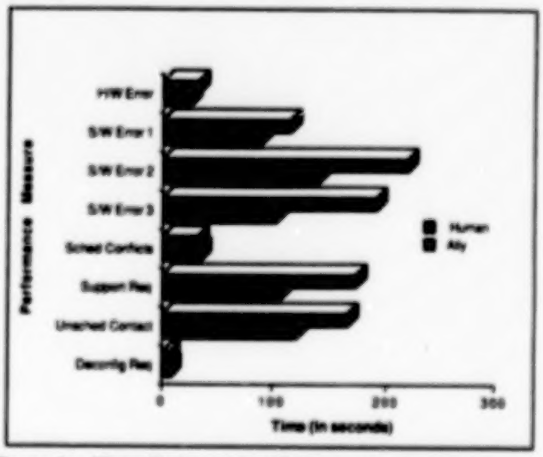

Figure 4a. Mean Performance Measures by Condition

While in only two cases a significant difference was detected between ALLY and the human associate, in most of the performance measures a significant condition by subject interaction was detected. This section presents the results of an in-depth analysis to attempt to explain these results.

Extensive audit records were recorded during each session of the experiment recording the behavior of the system, the behavior of ALLY, and the subject's interaction with both. These audit records were examined to investigate the reason for the significant differences among the subjects. The following sections present a discussion of the results in the four major categories of performance measures: fault compensation, equipment configuration, operator errors, and percentage of errors detected. Finally, the section concludes with a discussion of some of the subjective evaluations of the experiment derived from questionnaires.

Fault Compensation

The first category of performance measures reflects the time to detect and compensate for failures in the system. The analysis indicates that the effect ALLY had on performance depended

COC 22

primarily on the cooperation strategy the subjects used. Subjects that used a more active strategy that takes advantage of ALLY's monitoring and troubleshooting control tasks were able to perform generally better with ALLY than with the human associate. Subjects that used a more passive strategy by relying on ALLY's automatic monitoring and troubleshooting capability, however, performed as well as with the human associate. Overall, the use of ALLY as an associate resulted in performance that was at least as effective as the human associate.

Equipment Configuration

The effectiveness of using ALLY as an associate in response to the various configuration and deconfiguration functions primarily is a factor of the subject's style of interaction. In responding to conflicts with the automated schedule, those subjects that chose to perform these tasks manually performed better than subjects that used ALLY. Lack of planning (ALLY cannot foresee these events) and the need to check ALLY's answers were the contributing factors to ALLY's slower performance.

ALLY performed as well as the human associate in responding to unscheduled support requests. ALLY, however, resulted in fewer incorrect responses than the human associate. No differences were detected with deconfiguration requests because the subjects performed most of these tasks manually, even when they had ALLY as an associate.

Operator Errors

The next category of performance measures relate to operator errors. Two types of errors were recorded. The first type of error relates to operator actions that cause a conflict with the automated schedule. The other type relates to replacing a component that had not failed.

With respect to the first type of errors (schedule conflicts), the analysis indicated that the subjects that used a more cautious strategy tended to generate fewer schedule conflicts. They would regularly check ALLY's replacements and the equipment it identified for support requests. The subjects that gave more responsibility to ALLY to replace components and schedule missions tended to generate more schedule conflicts.

No significant differences were detected with respect to the number of times the operator replaced a component that had not failed. This indicates that ALLY was just as effective as the human associate in correctly identifying equipment failures.

Percentage of Failures Detected

The analysis indicated that the subjects that used a more active fault compensation and detection strategy were able to detect more of the failures than the subjects that used a more passive strategy. The more successful subject consistently used ALLY to identify software failures before ALLY's automatic processing would detect them.

Subjective Evaluations

In addition to the above quantitative analysis, the subjects were asked to provide subjective evaluations of the two associates. Several different types of questionnaires were used to collect this information. This section summarizes the significant findings from these questionnaires.

In summary, the subjects felt that ALLY brought definite strengths to the task. ALLY's speed and accuracy at performing the monitoring tasks were cited as its major strengths. In addition, ALLY could quickly search schedules for free equipment.

On the other hand, they indicated several limitations to the use of ALLY. They had to build their trust in the system. Some of the subjects were able to build the confidence in ALLY and gave it more responsibility. Others, however, needed more experience with the associate before the trust could be established.

At times, ALLY was "resistive" in that it would not change its mind once it found an answer, but the subjects never felt like they were out of control because they had the capability to override ALLY's choices manually.

A common "fault" found with ALLY was that it made the job too easy. Those subjects that actively worked with ALLY to get it to do things, however, felt like they had more control over the situation because they were relieved from the mundane tasks.

Summary

Overall the performance of the subjects using ALLY as an associate was as effective as performance with the human associate. Individual strategies enabled some of the subjects to perform better with ALLY than with the human associate. The primary area that was affected by personal strategies was in detecting and compensating for software failures. Several subjects were able to develop a style of interacting with ALLY that enabled them to detect software failures before either one of them would on their own. This enabled them to detect the failures faster and to correct a larger percentage of the total failures.

Since ALLY does not have the capability to anticipate schedule conflicts, it is not able to plan for these events in advance. The subjects that relied on ALLY's capability to respond to these schedule conflicts could not take advantage of their planning ability. The subjects that performed the best with ALLY did not rely heavily on ALLY, but relied on their own capabilities to anticipate and plan for these events.

An unexpected result was a side-effect associated with the difficulty ALLY has with planning. ALLY performed as well as the human associate in responding to unscheduled support requests. However, because the subjects knew that this was one area in which ALLY can make mistakes, they regularly checked ALLY's answers. As a result, this additional checking resulted in more correct responses to support requests with ALLY.

Conclusions

This experiment demonstrated that a computer-based associate based on a model of the operator's function can perform as well as a human associate. As with any cognitive system (either human or artificial), ALLY brought with it strengths and limitations. The subjects that performed the best with ALLY were able to capitalize on its strengths and compensate for its weaknesses. The result was an overall increase in the system performance.

This research has demonstrated that a computer-based associate founded on the identified principles of human-machine cooperation can achieve performance compatible with a human associate. In addition, this research has provided a "starting-point" from which a finer theory of cooperation can be developed. The significance of this research is that it has provided empirical research concerning the nature of human-machine cooperation.

Quantitative experimental data demonstrated the feasibility of the architecture for a computer-based associate that can perform at least as well as a human associate. Qualitative data, in the form of subjective evaluations, identified some of the varied strategies used by operators to interact with a computer-based associate.

These quantitative and qualitative analyses may form the basis of a more refined theory of human-machine cooperation. Since no theory exists, this exploratory research is essential to develop a more definitive theory of cooperation.

ACKNOWLEDGMENTS

This research was supported in part by NASA Goddard Space Flight Center under contract NAS5-28575 (Walt Truszkowski, technical monitor), and NASA Ames Research Center NAG 2-413 (Everett Palmer, technical monitor).

REFERENCES

Athans, M., "The Expert Team of Experts Approach to Command-and-Control (C2) Organizations", IEEE Control Systems Magazine, Vol. 2, No. 3, 30-38, 1982.

Bushman, J. B., "Identification of an operator's associate model for cooperative supervisory control situations", Doctoral Dissertation, Report No. 89-1, Center for Human-Machine Systems Research, School of Industrial and Systems Engineering, Georgia Institute of Technology, Atlanta, Georgia, 1989.

Carroll, J. M. and J. McKendree, "Interface Design Issues for Advice-Giving Expert Systems", Communications of the ACM, Vol. 30, No. 1, 14-31, January 1987.

Chambers, A. B. and D. C. Nagel, "Pilots of the Future: Human or Computer", Communications of the ACM, Vol. 28, No. 11, 1187-1199, November 1985.

Fischhoff, B., "Decision Making in Complex Systems", in E. Hollnagel, G. Mancini, and D. D. Woods (Eds.), Intelligent Decision Support in Process Environments, 61-85. Berlin: Springer-Verlag, 1986.

Geddes, N. D., 1989, "Understanding Human Operator Intentions is Complex Systems", Unpublished doctoral dissertation, School of Industrial and Systems Engineering, Georgia Institute of Technology, Atlanta, Georgia, June 1989.

Hollnagel, E., "Cognitive System Performance Analysis", in E. Hollnagel, G. Mancini, and D. D. Woods (Eds.), Intelligent Decision Support in Process Environments, 211-226. Berlin: Springer-Verlag, 1986.

Jones, P. M., Mitchell, C. M. and Rubin, K. S., "Validation of intent inferencing by a model-based operator's associate", International Journal of Man-Machine Studies, 1989, in press.

Mitchell, C. M., "GT-MSOCC: A Research Domain for Modelling Human-Computer Interaction and Aiding Decision Making in Supervisory Control Systems", IEEE Transactions on Systems, Man, and Cybernetics, Vol. SMC-17, 553-570, 1987.

Mitchell, C. M. and M. G. Forren, "Multimodal User Input to Supervisory Control Systems: Voice-Augmented Keyboards", IEEE Transactions on Systems, Man, and Cybernetics, Vol. SMC-17, 594-607, 1987.

Mitchell, C. M. and D. L. Saisi, "Use of Model-Based Qualitative Icons and Adaptive Windows in Workstations for Supervisory Control Systems", IEEE Transactions on Systems, Man, and Cybernetics, Vol. SMC-17, 573-593, July 1987.

Montgomery, D. C. Design and Analysis of Experiments. New York: John Wiley & Sons, 1984.

Rasmussen, J., "Strategies for State Identification and Diagnosis in Supervisory Control Tasks, and design of Computer Based Support Systems", in W. B. Rouse (Ed.), Advances in Man-Machine Systems Research, Vol. 1, 139-193. Greenwich, CT: JAI Press, 1984.

Rasmussen, J., "The Role of Hierarchical Knowledge Representation in Decisionmaking and System Management", IEEE Transactions on Systems, Man, and Cybernetics, Vol. SMC-15, No. 2, 234-243, March/April 1985.

Rasmussen, J., Information Processing and Human-Machine Interaction: An Approach to Cognitive Engineering. New York: North-Holland, 1986.

Roth, E. M., K. B. Bennett, and D. D. Woods, "Human Interaction with an Intelligent Machine", International Journal of Man-Machine Studies, Vol. 27, 1-47, 1987.

Rouse, W. B., N. D. Geddes, and R. E. Curry, "An Architecture for Intelligent Interfaces: Outline of an Approach to Supporting Operators of Complex Systems", Human-Computer Interaction, Vol. 3, No. 2, 1987.

Rubin, K. S., P. M. Jones, and C. M. Mitchell, "OFMSPERT: Inference of Operator Intentions in Supervisory Control Using a Blackboard Architecture", IEEE Transactions on Systems, Man, and Cybernetics, Vol. SMC-18, 4, 618-637, 1988.

Saisi, D. L., "The Use of Model-Based, Window Display Interfaces in Real Time Supervisory Control Systems", Masters Thesis, School of Industrial and Systems Engineering, Georgia Institute of Technology, Atlanta, GA, 1986.

Sime, M. E. and K. J. Coombs, "Introduction", in M. E. Sime and M. J. Coombs (Eds.), Designing for Human Computer Communication, 1-20. London: Academic Press, 1983.

Spector, P. C., Goodnight, J. H., Sall J. P., and W. S. Sarle, "The GLM Procedure". SAS User's Guide: Statistics, Version 5 Edition, pp. 433-506. Gary, NC: SAS Institute Inc., 1985.

Tenney, R. R. and N. R. Sandell, "Structures for Distributed Decisionmaking", IEEE Transactions on Systems, Man, and Cybernetics, Vol. SMC-11, No. 8, 517-527, 1981a.

Tenney, R. R. and N. R. Sandell, Strategies for Distributed Decisionmaking", IEEE Transactions on Systems, Man, and Cybernetics, Vol. SMC-11, No. 8, 527-538, 1981b.

Wickens, C. D., Engineering Psychology and Human Performance. Columbus, OH: Charles Merrill, 1984.

Woods, D. D., "Cognitive Technologies: The Design of Joint Human-Machine Cognitive Systems", The AI Magazine, 86-92, 1986a.

Woods, D. D., "Paradigms for Intelligent Decision Support", in E. Hollnagel, G. Mancini, and D. D. Woods (Eds.), Intelligent Decision Support in Process Environments, 255-269. Berlin: Springer-Verlag, 1986b.

Woods, D. D., E. M. Roth, and K. Bennett, "Explorations in Joint Human-Machine Cognitive Systems", in A. Zachary and S. Robertson (Eds.), Cognition, Computing, and Cooperation. Norwood, NJ: Ablex, 1987.

*Bushman is now with the Training Systems Division, Air Force Human Resources Laboratory, Brooks Air Force Base, Texas, 78235.

*Rubin is now with ParcPlace Systems, 1550 Plymouth St, Mountain View, California, 94043.

INTELLIGENT INTERFACES

Cockpit Task Management:
A Preliminary, Normative Theory

Ken Funk

Department of Industrial and Manufacturing Engineering
Oregon State University
Corvallis, OR 97331-2407
(503) 737-2357
funk@guille.ece.orst.edu

Abstract

Cockpit Task Management involves the initiation, monitoring, prioritization, allocation of resources to, and termination of multiple, concurrent tasks. As aircrews have more tasks to attend to, due to reduced crew sizes and the increased complexity of aircraft and of the air transportation system, CTM will become a more critical factor in aviation safety. It is clear that many aviation accidents and incidents can be satisfactorily explained in terms of CTM errors, and it is likely that more accidents induced by poor CTM practivce will occur in the future unless the issue is properly addressed.

Our first step in understanding and facilitating CTM behavior has been the development of a preliminary, normative theory of CTM which identifies several important CTM functions. From this theory some requirements for pilot-vehicle interfaces have been developed which we believe will facilitate CTM. We have developed one prototype PVI which improves CTM performance and are currently engaged in a research program aimed at developing a better understanding of CTM and facilitating CTM performance through better equipment and procedures.

Introduction

Air travel is one of the safest forms of transportation, yet each year hundreds of lives and millions of dollars are lost due to air crashes. Accident investigations reveal that over half of these accidents are attributable to errors by the cockpit crew [Nagel, 1988].

Since crew-induced accidents are rare, the "remedy" has historically been to provide specific fixes for specific causes of specific accidents. For example, ground proximity warning systems were developed in response to a (small) number of controlled flight into terrain accidents. And yaw dampers were installed in response to incidents of Dutch roll, an instability problem characteristic of swept-wing aircraft.

This may have led to what Wiener [1987] calls the "one-box-at-a time" approach to cockpit automation that ignores the need for information and control integration in the cockpit, leaving that integration entirely to the already overburdened aircrew. Responses to specific incidents and problems do not necessarily decrease the liklihood of other incidents and problems. Unless a more general approach to understanding cockpit operations and problems is adopted, it is likely that the trend will continue, perhaps with catastrophic results.

A systems engineering approach to this problem is more desirable than the ad hoc methods now so commonly used. As Sheridan points out [1988], the systems approach provides more precise methods of problem formulation, a basis for simulation and qualitative understanding of systems, a basis for quantitative prediction of system behavior, an accounting framework for design and evaluation, and a language for archival description.

27

Our own application of systems engineering methods to cockpit operations, has led us to a concept we call Cockpit Task Management (CTM). CTM involves the formulation of goals, the definition of tasks to achieve those goals, and the management and execution of those tasks in a dynamic environment until the goals are achieved. The remainder of this paper presents some background definitions, a preliminary, informal version of a normative theory of CTM, some guidelines for the design of pilot-vehicle interfaces to facilitate good CTM, and a summary of our continuing efforts to improve CTM.

Definitions

A dynamic system is an entity which may be described in terms of input, output, and state. Input is matter, energy, or information having a net flow into the system. Output is net flow of matter, energy, or information out of the system. State is a compact representation of the history of the system which makes possible the prediction of future outputs and of state itself [Padulo and Arbib, 1974]. Input, output, and state may each be decomposed into multiple components. For example, an aircraft is a system whose input components include fuel flow, control yoke movements, and radio clearances from air traffic control (ATC). Aircraft outputs include fuel combustion products, heat and noise, and requests for and acknowledgments of ATC clearances. Aircraft state components include position and altitude, flap angles, and radar mode.

Two systems which are connected by inputs and outputs form a more complex system called a supersystem. The supersystem's inputs are the unconnected inputs of the simpler systems. Its outputs are the unconnected outputs. The state of the supersystem is defined by the combined states of the original systems. Through successive system connections, systems of arbitrary scope and complexity may be defined. If a system is formed from simpler systems through input-output connections, the simpler systems are called subsystems. For example, an aircraft system can be defined as a collection of powerplant, electrical, hydraulic, and avionic systems. With respect to the powerplant system, the aircraft may be considered a supersystem. From the perspective of the aircraft system, the powerplant may be considered a subsystem.

The use of the generic terms system, subsystem, and supersystem, rather than terms like equipment and components, permits the examination of domains from many levels of abstraction. Along with this flexibility, though, comes the potential for ambiguity and confusion. For example, a discussion in which the term "system" was applied to that combination of people, machines, policies and procedures called the air traffic control system as well as to a light emitting diode on an aircraft instrument panel would be problematic without further clarification. For any frame of reference, the analyst must clearly identify the levels of abstraction to which the terms "system," "subsystem," and "supersystem" apply.

A system behavior is a (perhaps continuous) series of system input, state, and output values over a time interval. For example, as an airliner flies from Eugene, Oregon to San Francisco, successive values of input components (including the pilot's movement of the control yoke), state components (including position) and output components (including radio transmissions) over the time interval of the flight constitute a behavior of that system. A system exhibits a behavior if observations of the system yield input, state, and output values exactly matching those of the behavior.

An event is a set of system behaviors in which some state component changes in a significant way at the very end of the time interval. For example, **reach 10,000 feet** is an event consisting of a set of aircraft behaviors. In each behavior of this event the aircraft's altitude increases, reaching a value of 10,000 feet at the end of the behavior's time interval. An event occurs if the system exhibits a behavior which is contained in the event set.

A goal for a system is defined by a set of desired behaviors and a state. Each behavior begins with an initiating event and ends with a terminating event. In any behavior of the system, if the initiating event has not occurred, the state of the goal is **latent**. If the initiating event is imminent, the goal is **pending**. If the initiating event has occurred but the terminating event has not occurred and the actual behavior matches the initial portion of some desired behavior, the state of the goal is **active**. If the initiating event has occurred, the terminating event has occurred, and the actual behavior through the time of the terminating event matches one of the goal behaviors, the state of the goal is **achieved**. If the initating event has occurred but the actual behavior does not match any of the goal behaviors, the state of the goal is **violated**.

A goal's initiating event defines the conditions under which the goal is relevant. A typical flight path consists of a series of waypoints which are geographical points along the route that serve as intermediate destinations. So a goal to arrive **at waypoint** 8 is relevant after an **arrive at waypoint** 7 event has occurred. On the other hand, a terminating event may take on more than one meaning, as discussed below.

Formally, only one type of goal is necessary. As a practical matter however, goals may be classified as to intent and interpretation. In an **attainment goal**, the terminating event results in some desired state of the system and the intervening input, state, and output values are unimportant. For example a **gear down and locked** goal could be defined by all possible behaviors terminated with an event resulting in the landing gear being in the down and locked state. In this case, it does not matter how the landing gear is lowered (by motor, gravity, or manual operation). Only the final state is important.

In a **maintenance goal**, it is the portion of the behavior between the initiating and terminating events that is important. For example, a goal to maintain **approach speed until touchdown** might be defined by the collection of all behaviors in which the aircraft's speed was within five knots of the approach speed specified in the aircraft operations manual, until touchdown occurred. Here, the immediate objective of this specific goal is not touchdown on the runway, it is maintaining the proper airspeed until touchdown occurs. Put another way, a maintenance goal reflects a set of constraints on system behavior which are active until some event occurs.

A **constrained attainment** goal is an attainment goal in which the intervening behaviors are important. For example, a goal to arrive **at destination area (via waypoints 1, 2, and 3)** might be defined by a set of behaviors in which the aircraft flies from its origin to waypoint 1, to waypoint 2, to waypoint 3, and ends in the area of the destination airport.

A subgoal of a goal is a set of behaviors consistent with those of the goal, but restricted in time and/or in scope. A goal may be decomposed into a set of subgoals, which are goals consistent with the original goal but restricted in some way. Serial subgoals are defined for the original system, but over distinct time subintervals. Parallel subgoals are defined over the entire time interval, yet are defined for subsystems of the original system. A goal may also be decomposed into a combination of serial and parallel subgoals. For example, a goal to approach the destination airport and arrive **at landing position** (prior to final approach) could be decomposed into serial **cleared to approach waypoint** and **at approach waypoint** subgoals and parallel **approach flaps**, **approach power**, and **approach speed** subgoals.

A goal and all of its subgoals form a hierarchy with the goal at the apex. The topmost goal for a flight mission will be referred to as the mission goal. Part of a simplified goal hierarchy for a flight mission is shown in Figure 1.

Goal priority reflects an ordering of a set of goals and/or subgoals, as determined by the relative importance assigned to them by the aircrew. More important goals have higher priorities. For example, a goal to remain **clear of terrain and other aircraft** established to maintain the safety of the aircraft and its passengers is clearly more important than a goal to maintain **± 20 degrees roll**, established for passenger comfort. The first goal should then have a higher priority than the second.

Performance is how well a system achieves a specific goal. A performance measure is a function that maps a goal and a system behavior to a value set. The simplest performance measure may take on just two values: "satisfactory" if the goal is achieved (or at least not yet violated), and "unsatisfactory" otherwise. More complex performance measures may map to amore complex, ordered set. For example, a goal to maintain **10,000 feet** may be achieved if the aircraft's altitude stays between 9,900 and 10,100 feet. But a behavior in which the maximum deviation was no more than 25 feet might be preferred to a behavior in which the maximum deviation was 75 feet. In this case, we could say that the system performed better when exhibiting the ± 25 foot behavior than when exhibiting the ± 75 foot behavior.

A task is a process completed to cause a system to achieve a goal. A task involves the behaviors of one or more secondary systems or subsystems in order to produce inputs to the primary system to achieve the goal. For example, for the goal to arrive **at waypoint** 7, there must be a **fly to waypoint** 7 task. The pilot, the primary flight controls, the cockpit displays, the electrical system, and the engines are just a few of the secondary systems required to complete the **fly to waypoint** 7 task to achieve the goal for the primary system (the aircraft) to arrive **at waypoint** 7.

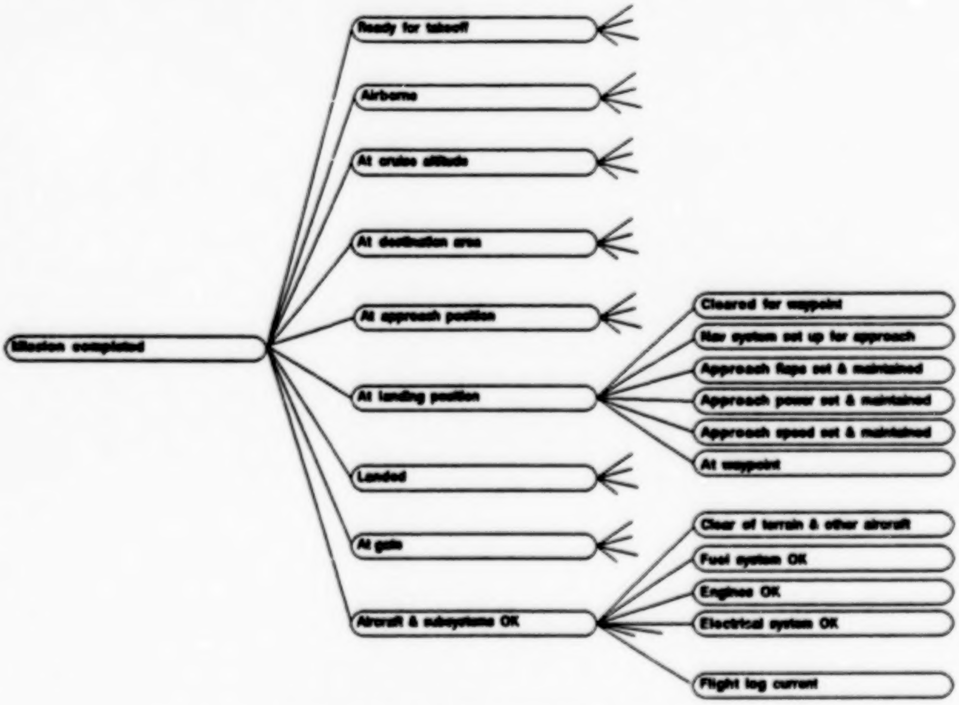
Mission completed
Ready for takeoff
Airborne
At cruise altitude
At destination area
At approach position
At landing position
Landed
At gate
Aircraft & subsystems OK
Cleared for waypoint
Nav system set up for approach
Approach flaps set & maintained
Approach power set & maintained
Approach speed set & maintained
At waypoint
Clear of terrain & other aircraft
Fuel system OK
Engines OK
Electrical system OK
Flight log current

Figure 1: Part of a Simple Goal Hierarchy

Like a goal, a task has state. A task is latent if its goal is latent, pending if its goal is pending, and active if its goal is active. A task is in progress if inputs to the primary system are being applied to achieve the goal. If the task has been in progress but inputs to the primary system to achieve the goal have been suspended, the task is interrupted. A task may be terminated if its goal is achieved, if the goal is not achievable, or if the goal becomes irrelevant. In the case of an unsuccessful termination, the task is considered to be aborted.

The performance of a task is simply the performance of the system with respect to the task's goal while the task is being completed. A pilot keeping the aircraft within 25 feet of a selected altitude is performing a **maintain altitude** task better than one only keeping within 75 feet of the selected altitude.

As we can decompose the goal to approach the airport and arrive **at landing position** into **cleared to approach waypoint** and **at approach waypoint** subgoals, an **approach** task could be decomposed into **get approach clearance** and **fly to approach waypoint** subtasks.

An agenda defines an ordered set of tasks to be completed during a mission. Each task is defined to achieve a specific goal and becomes active when the goal's initiating event occurs. The structure of an agenda follows that of a goal hierarchy but carries additional task information. Figure 2 shows part of an agenda corresponding to the goal hierarchy shown in Figure 1.

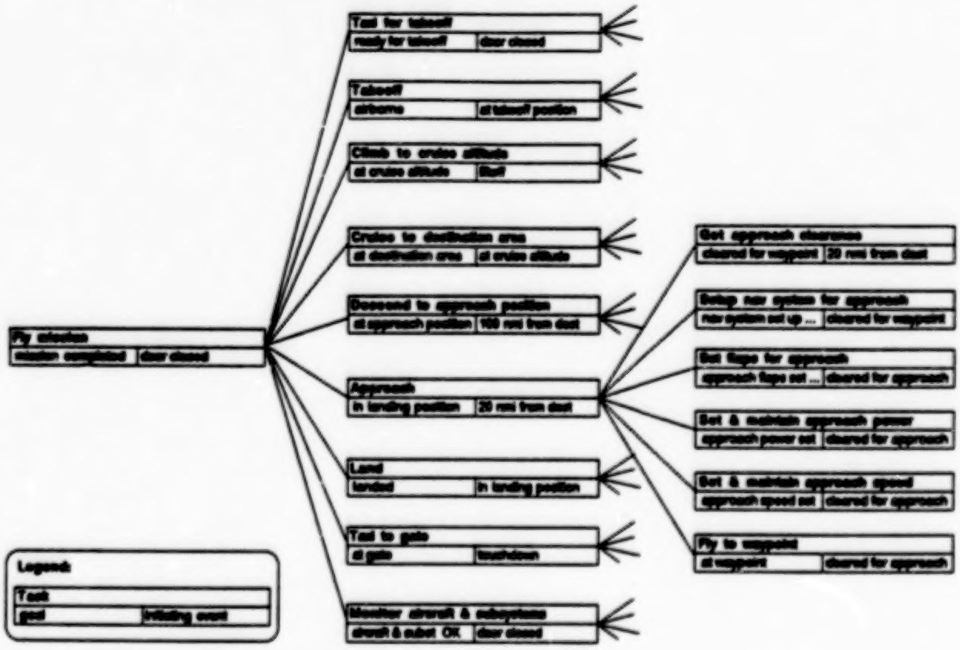
Taxi for takeoff
ready for takeoff
door closed
Takeoff
airborne
at takeoff position
Climb to cruise altitude
at cruise altitude
Staff
Cruise to destination area
at destination area
at cruise altitude
Descend to approach position
at approach position
100 nmi from dest
Fly mission
mission completed
door closed
Approach
in landing position
20 nmi from dest
Land
landed
in landing position
Taxi to gate
at gate
touchdown
Monitor aircraft & subsystems
aircraft & subst OK
door closed
Legend:
Task
goal
initiating event
Get approach clearance
cleared for waypoint
20 nmi from dest
Setup nav system for approach
nav system set up ...
cleared for waypoint
Set flaps for approach
approach flaps set ...
cleared for approach
Set & maintain approach power
approach power set
cleared for approach
Set & maintain approach speed
approach speed set
cleared for approach
Fly to waypoint
at waypoint
cleared for approach

Figure 2: Part of a Simple Agenda

When an initiating event occurs, the corresponding task becomes active. Since two or more tasks may share a common initiating event and since one task may not reach completion before another task becomes active, several tasks may be active at one time. Two or more tasks that are simultaneously active are called concurrent tasks.

Resource-Limited Performance

Executing a task to achieve a system goal, such as to fly an aircraft to a destination, requires that certain inputs be provided to that system over a time interval. These inputs must come from other systems or subsystems, such as pilots, autopilots, and other cockpit equipment. These systems or subsystems are called resources, and resources are required to complete a task. If the resources are not available, that is their outputs cannot be directed to the primary system, the task cannot be completed satisfactorily and the goal cannot be achieved.

A variety of resources are required for cockpit tasks. Equipment resources include autopilots, radios, displays and controls. Human resources include the pilot, first officer, and flight engineer. Some resources are specialized and can only be used for a limited set of tasks. Examples of specialized resources include the landing gear control lever and the altimeter. Other resources are multi-function and can be used for a variety of tasks. Examples of these include multi-function CRT displays and humans.

Since resources are systems, they can be decomposed into simpler subsystems. Of particular interest are the human resources, which can be decomposed into personal sensory, motor, and cognitive resources. Sensory resources include visual, auditory, and other sensory systems which can be used to obtain external system state information necessary for completing a task. Motor resources include hands, feet, voice, and other body systems that can produce inputs to external systems. Cognitive resources are mental subsystems required to perform cognitive tasks, such as those involving pattern recognition, problem solving, and decision making. The resources include the verbal and spatial resources identified and studied by Wickens and his colleagues at the University of Illinois [Wickens 1984; Wickens and Liu, 1988].

Since two concurrent tasks may require the same resources, this poses a potential problem, since resource behavior compatible with achieving one goal may be incompatible with achieving the other goal and the performance of one or more of the tasks may be degraded. That is, task performance is limited by resource availability. With resources like displays or hands and feet, this is obvious. But it is also true for cognitive resources [Navon and Gopher, 1979; Wickens, 1984]. A situation in which task resource requirements exceed resource availability is called a task conflict.

For example, given the agenda in Figure 2, if ATC clearance to an approach waypoint is obtained the **set and maintain approach power** task would become active. Assume that this task requires a multifunction CRT resource on which an engine display format must be shown. Suppose that now a primary electrical system failure event occurs and a subtask to **diagnose and correct electrical system** becomes active. Assume that this subtask requires an electrical system display format on the same CRT resource. If the two display formats cannot be displayed simultaneouly a resource shortage and therefore a task conflict exists.

Even if two CRTs are available to complete both of these tasks simultaneously, there still might be a task conflict due to cognitive resource limitations. Assuming for the purpose of this illustration that no other crewmember is available to assist the pilot in completing these two tasks, he or she may lack sufficient cognitive resources to simultaneously attend to both of them. This might result in errors in completing one or both of the tasks.

Task conflicts like these can be partially resolved through a process of prioritization and resource allocation. In the case outlined above, the pilot can decide that the immediate correction of equipment failure is absolutely essential to the safe continuation of the flight, and temporarily suspend the **set and maintain approach power** task, using all necessary resources to complete the diagnosis and correction subtask.

But if this subtask takes longer than anticipated, flight safety could be endangered, for if the aircraft proceeds at the current altitude longer than the air traffic controller anticipated, the potential exists for collisions with other aircraft travelling at the same altitude. Focussing on one task to the exclusion of others can lead to poor task performance at minimum and disaster at worst.

Given the complex nature of modern aircraft, the speed at which they travel, and the increasing density of air traffic in airspaces, the existence of multiple, concurrent tasks in the cockpit is the norm rather than the exception. Clearly, concurrent tasks must be systematically managed by the aircrew to achieve acceptable levels of system performance.

A Preliminary, Normative Theory of Cockpit Task Management

The process by which the aircrew manages an agenda of cockpit tasks may be called Cockpit Task Management (CTM). Given the requirement to allocate limited resources to tasks in a dynamic environment, some essential functions of CTM are readily apparent. A brief outline of these functions are presented below and a generalized procedure for CTM is shown in Exhibit 1. Please note that the following theory of CTM is a normative one and presents the functions that should be completed. It does not seek, at this point, to explain how they are performed, nor does it explicitly account for errors, which will be discussed later.

```
Procedure: CTM
  create and validate initial agenda
  until mission goal is achieved or unachievable
        activate tasks whose initiation events have occurred
        assess status of active tasks
        terminate tasks with achieved or unachievable goals
        assess task resource requirements
        prioritize active tasks
        allocate resources to tasks in order of priority:
              initiate higher priority tasks not yet in progress
              interrupt lower priority tasks currently in progress
              resume higher priority tasks that were interrupted
        update and validate agenda
  endUntil
End: CTM
```

Exhibit 1: Cockpit Task Management Procedure

Before CTM can begin, an initial planning process must be completed. This planning process yields a set of goals, including a primary mission goal, a hierarchy of subgoals to the mission goal, and perhaps a collection of goals to deal with contingency situations, such as an engine fire or a hydraulic system failure.

Agenda Creation is the first step of CTM and involves the selection and specification of a suitable task to achieve each goal and the definition of the initiating event for each task. The specification of each task includes a list of resources necessary to complete the task, both equipment and human. The creation of the agenda also requires the validation of the goals upon which the agenda is based. It is necessary to make sure that all goals are compatible with the mission goal and with each other.

Once the agenda has been created and validated, true task management begins. This iterative process lasts until the mission goal is achieved or it has been determined that the mission goal is not achievable and no further effort need be expended towards achieving it.

Task Activation is the detection of the initiating event for a task and the recognition that the task should be started. For the initial tasks in a mission, such as the **taxi for takeoff** task, this occurs immediately. For other tasks, such as the **fly to approach waypoint** task, the initiating events and task activation may occur much later in the mission. Some tasks for contingent goals, such as an **extinguish engine fire** task (a subtask of a **monitor aircraft and subsystems** subtask), may never be activated.

Task Status Assessment or task monitoring determines the status of each task, which reflects the achievement of the task's goal. Not only must the current status of the task be assessed, but if the task's goal is not yet achieved, the status of the task must be projected into the future to determine the liklihood that the goal will be achieved.

If the goal is achieved or if the goal has not yet been violated but current trends will likely result in the goal's achievement, the status of the task is **satisfactory**. For example, suppose that **fly to waypoint 7** is an active task. If the aircraft is at waypoint 7 the task's status is satisfactory. If the aircraft is not at waypoint 7, but it is flying in that direction and there is sufficient fuel to reach the waypoint, the task's status is also satisfactory.

If the goal is not yet achieved, not yet violated, but current trends will likely result in a violation of the goal, the status of the task is **marginal**. If **fly to waypoint 7** is active but the aircraft's course is 10 degrees to the right of a heading to waypoint 7, the status of the task is marginal.

If the goal is violated, the status of the task is **critical**. If the aircraft has passed waypoint 7, but has not come within some acceptable range of the waypoint, the **fly to waypoint** 7 task is critical.

The above is a minimal classification scheme for task status. These status values probably should be treated as general categories to be further subdivided to provide more resolution in status assessment.

Task Termination removes tasks from competition for resources. Normal task termination is a result of the achievement of the task's goal. So when the aircraft is airborne, the **takeoff** task may be terminated.

A critical task, one whose goal cannot be achieve or at least probably cannot be achieved, may be aborted, thereby terminating it. Such might be the case if dangerous wind shear conditions are detected during a **land** task. When the possibility of aborting a task exists, the agenda should contain contingent tasks to replace the aborted tasks. For example, an **execute missed approach** task should be included in an agenda to replace an aborted **land** task.

Another reason for terminating a task is because its goal is no longer relevant. For example, if a landing gear fails to operate properly on the first try, a **diagnose/correct landing gear** task might be initiated. If later, through no direct action of the crew, the gear operates properly, the goal to diagnose and fix the landing gear would no longer be relevant and the task could be terminated.

Task Resource Requirements Assessment must be performed to determine what resources are required to complete the active tasks. Each task has minimum resource requirements, but in some cases, task performance can be improved by providing additional resources. For example, the performance of a **diagnose/correct engine problem** task might be improved by allocating two rather than one display resources to it, allowing the simultaneous display of engine parameters on one display surface and an engine diagnosis checklist on the other.

Recognizing the improved performance that additional resources can bring may be especially important in correcting marginal or critical tasks. On the other hand, over-allocating resources to one task may interfere with the performance of another, if those resources are limited.

Task Prioritization is an ordering of tasks by priority. Factors which can influence task priority include the following:

1. the priority of the task's goal.
2. the priorities of the goals of other active tasks.
3. the current and projected status of the task.
4. the current and projected statuses of other active tasks.

Task prioritization can ultimately be defined in terms of a pairwise comparison of tasks based on the above as well as other factors, which results in an ordering of active tasks. For example, suppose that both a **maintain ± 20 degrees roll** task and a **remain clear of terrain and other aircraft** task are active. If the aircrew detects another aircraft on a collision course, they should assign a higher priority to the second task than to the first because the goal to remain **clear of terrain and other aircraft** has greater importance and a higher priority than the goal to maintain ± **20 degrees roll**.

Resource Allocation is the assignment of resources to tasks, with preference given to high priority tasks, so that the tasks may be executed. Resource allocation depends directly on task prioritization, and since that is a dynamic process, resource allocation must be dynamic also.

When a newly activated task has a high enough priority, resources are allocated to it and task initiation occurs. This means that the required resources begin exhibiting behaviors consistent with the achievement of the task's goal. In many cases, task initiation requires a communication of the goal to some of the resources so that they can behave accordingly. For example, if one of the resources required for a task is a human crew member, that crew member must be aware of the goal in order to behave in such a way as to bring about its achievement. This is also true for some equipment resources. For example, to fly automatically to a certain location, the aircraft's navigation computer must be "informed" of the goal by the input of the destination's geographical coordinates.

If a lower priority task is in progress and a higher priority task is initiated which requires those resources, then the resources are allocated to the higher priority task. This is called task interruption, and the lower priority task, while still active, is no longer in progress, or it may said to be suspended.

When a high priority task in progress is terminated, for whatever reason, task resumption of a lower priority, suspended task can occur, in which case resources are reallocated back to the lower priority task and it can continue.

Actually, resource allocation based merely on task priority may be insufficient. In some cases at least, resource reallocation may occur due to the specific status of a task. For example, the autopilot may be allocated to a fly to approach waypoint task, but the autopilot, due to existing conditions, may not be able to adequately control the descent. It may then be necessary to deallocate the autopilot from the task and allocate a human crewmember to it to achieve the goal.

Agenda Updating is necessary since some cockpit tasks may alter the agenda. If bad weather or other contingencies make a planned route infeasible or undesirable, a planning task may be initiated to change the original route. This will, by necessity, change the agenda. The goals and tasks created by this planning task must be integrated into the agenda, perhaps replacing earlier components. Of course, validation of the candidate changes to the agenda must take place to assure that the mission goal is achieved and that no goal conflicts occur.

Cockpit Task Management Failures

The significance of CTM can best be appreciated by using the framework presented above to examine several aviation accidents and incidents which have occurred in the last two decades. The following accounts are summaries from National Transportation Safety Board Aviation Accident Reports.

> On March 21, 1980, at 1949, Eagle Commuter Airlines, Inc. Flight 108, a Piper PA-31-350, with a pilot, a pilot-in-command trainee, and eight passengers on board, crashed on takeoff from runway 22 at William P. Hobby Airport, Houston, Texas. The pilot, the pilot-in-command trainee, and five passengers were killed, and three passengers were injured seriously. The aircraft was destroyed by the crash and the postcrash fire. The National Transportation Safety Board determines that the probable cause of the accident was a power loss in the right engine for undetermined reasons at a critical point in takeoff, the aircraft's marginal single-engine performance capability, and the captain's incorrect emergency response to the engine power loss when he failed to either land immediately on the remaining runway or to configure the aircraft properly for the engine-out condition. [NTSB, 1981]

> An Eastern Airlines Lockheed L-1011 crashed at 2342 eastern standard time, December 29, 1972, 18.7 miles west-northwest of Miami International Airport, Miami, Florida. The aircraft was destroyed. Of the 163 passengers and 13 crewmembers aboard, 94 passengers and 5 crewmembers received fatal injuries. Two survivors died later as a result of their injuries. Following a missed approach because of suspected nose gear malfunction, the aircraft climbed to 2,000 feet mean sea level and proceeded on a westerly heading. The three flight crewmembers and a jumpseat occupant became engrossed in the malfunction. The National Transportation Safety Board determines that the probable cause of the accident was the

> failure of the flightcrew to monitor the flight instruments during the final 4 minutes of flight, and to detect an unexpected descent soon enough to prevent impact with the ground. Preoccupation with a malfunction of the nose landing gear position indicating system distracted the crew's attention from the instruments and allowed the descent to go unnoticed. [NTSB, 1973]

> On June 13, 1984, USAir, Inc. Flight 183, a McDonnell Douglas DC9-31, N964VJ, with 5 crewmembers and 51 passengers aboard, encountered turbulence, hail, and heavy rain as it was making an instrument landing system approach to runway 21R at the Detroit Metropolitan Airport, Detroit, Michigan. The airplane landed on the runway about 2500 feet beyond the threshold of runway 21R before the landing gear was extended fully. The airplane skidded bout 3,800 feet before sliding into the grass on the left side of the runway. The crew and passengers were evacuated with only minor injuries. The airplane was damaged substantially. The National Transportation Safety Board determines that the probable cause of the accident was inadequate cockpit coordination and management which resulted in the captain's inappropriate decision to continue the instrument approach into known thunderstorm activity where the airplane encountered severe wind shear. The failure of air traffic control personnel at the airport to provide additional available weather information deprived the flightcrew of information which may have enhanced their decisionmaking process. [NTSB, 1985]

Each of these accidents or incidents was thoroughly investigated by the NTSB, probable cause was assigned, and contributing factors were identified. In the Eagle Commuter accident the captain "... failed to ... configure the aircraft properly for the engine-out condition." "Preoccupation with a malfunction ... distracted the [Eastern Airlines] crew's attention ..." The USAir captain made an "... inappropriate decision to continue the instrument approach into known thunderstorm activity."

In each case conclusions can be and no doubt were drawn about how the accidents could have been prevented. It is likely that these fixes, were they implemented, would have prevented similar accidents from occurring. But specific explanations of and fixes to specific problems do not necessarily prevent accidents of other types from occurring.

If, on the other hand, we examine these occurrences from the perspective of CTM, we can develop a more comprehensive understanding of cockpit errors and perhaps suggest effective ways of preventing a wider variety of accidents from occurring. With that in mind, consider the following, supplementary explanations of the accidents and incidents, from the perspective of CTM.

Faced with multiple, possibly conflicting tasks, the Eagle Commuter captain failed to initiate an engine-out recovery task. The Eastern Airlines crew failed to monitor the status of the primary flight task, possibly because they assigned too high a priority to the tasks of dealing with the malfunctions. The Eastern crew also overallocated resources to the landing gear diagnosis task (all three crewmembers plus a jump seat occupant became totally absorbed in the diagnosis). The USAir captain failed to terminate the landing task, even though continuation of the task placed the higher priority goal of passenger, crew, and aircraft safety at extreme risk.

Pilot-Vehicle Interface Requirements to Facilitate Cockpit Task Management

The concept of Cockpit Task Management has potential implications for aircrew training and cockpit procedures, and these should be addressed. But our efforts in the past have focussed on cockpit automation, especially the design and development of intelligent pilot-vehicle interfaces (PVIs). Based on the preliminary, normative theory of CTM and the CTM-based analysis of a variety of accidents and incidents, we believe a PVI should perform the following functions to facilitate CTM:

1. Maintain an internal representation of the mission agenda. The PVI should possess knowledge of the agenda for each flight. Once the aircrew has planned a mission, they must be able to create a representation of the mission agenda in the PVI. They must also be able to modify the agenda during the mission as plans change.

2. Display agenda information to the aircrew. The PVI must provide a dynamic agenda display that keeps the aircrew informed about the agenda. It should display information about the state of each goal and the state and status of each task, especially those goals and tasks that are pending or active. The aircrew may not choose to have the agenda display visible at all times, but it must be available and easily accessible to them.

3. Monitor and display aircraft and subsystem states. All PVIs display aircraft and subsystem information, but to facilitate CTM these displays should be controlled by the PVI to emphasize information relevant to pending and active tasks.

4. Monitor task states and inform the aircrew. The PVI should monitor aircraft and subsystem state, note events, and update the agenda. Specifically, the PVI should determine when tasks become pending, active, or terminated. This information should be provided to the aircrew through the agenda display and perhaps through other displays as well, especially when the agenda display is not visible.

5. Determine when tasks are being performed. The PVI must be able to determine when tasks are being performed by the aircrew and by avionics systems. In some cases this may be done implicitly by monitoring aircraft and subsystem states as they change under aircrew and avionics control [Hoshstrasser and Geddes, 1989; Rouse and Hammar, 1990]. In other cases, aircrew intent must be determined by explicit communication from the aircrew that the task is or will soon be underway.

6. Assess task status and inform the aircrew. The PVI should assess task status based on the present or projected status of goals and inform the aircrew through appropriate displays. In the case of marginal or critical tasks, the aircrew should be alerted and perhaps advised so that appropriate and timely action can be taken to maximize the chances of goal achievement.

7. Prioritize tasks and inform the aircrew. Tasks should be prioritized by the PVI and the aircrew should be informed through appropriate displays. Priorities of marginal or critical tasks should be emphasized.

8. Help the aircrew perform specific tasks. Although the major concern here is in facilitating CTM, the functions described above virtually necessitate a PVI architecture that could also support specific task aids, such as planning tools, computational aids, and expert systems for diagnosis and control. The level of support provided by these aids should be selectable by the aircrew and the aids should always remain under aircrew authority. Decisions and control actions provided by the aids should be subject to aircrew authorization, either in real time or by "contractual" arrangement prior to the mission. It is likely that such aids could help improve individual task performance and indirectly improve CTM performance by reducing the cognitive resource demands on the aircrew by the individual tasks.

Steps Toward Better Cockpit Task Management

We have made significant progress in our efforts to understand and facilitate CTM. Our primary accomplishment to date is a prototype PVI and we are currently involved in both theoretical and applied research and development efforts.

The Task Support Subsystem (TSS) is a prototype PVI developed at Oregon State University whose function, in part, is to facilitate CTM [Funk, 1990]. It is a subsystem of an experimental avionics system that runs in a simulated aircraft. Prior to a mission, a mission definition is created which defines the tasks to be accomplished during the flight. During the simulated flight, software modules called Task Agents (TAs) perform the CTM function to see that all tasks are completed satisfactorily.

For each task in the mission there is a TA assigned to it. The TA determines when the task should be started and configures the cockpit for the task. It then monitors the pilot and aircraft subsystems to see that the task is completed correctly and on time. If the pilot fails to act on the task, the TA reminds him via a display and the TA alerts the pilot to actual or anticipated deviations from the task's goal. Most TAs also facilitate task execution by providing procedural prompts and recommendations. Some TAs are capable of completely automating their tasks at the pilot's discretion.

Multiple TAs are coordinated by a high level TA that allocates resources based on priority. A mission display serves to remind the pilot of tasks to be completed and shows the status of each active task.

The TSS, as part of the avionics system, was evaluated by a group of 16 professional pilots in a simulator experiment [Lind et al, 1989]. Each pilot flew two equivalent, simulated missions, one in a baseline cockpit and one with the TSS present. Performance measures involved timing, accuracy and number of errors committed. Statistically significant results favoring the TSS-equipped cockpit were obtained from the data analysis and pilots subjectively rated the TSS-equipped cockpit as superior in terms of situational awareness and workload. Subsequent informal evaluation of the TSS by a variety of pilots and non-pilots have been consistent with the positive results of the experiment.

Our ongoing research involves development of theories of CTM and development of further prototype PVIs to facilitate CTM.

The preliminary, normative theory sketched above is being formalized in the framework of mathematical systems theory [Mesarovic and Takahara, 1975; Funk, 1983]. A simulation model will be developed and validated for internal consistency before finalizing a procedural description of CTM.

The normative theory will serve as the basis for a descriptive theory of CTM which identifies human capabilities and limitations in performing CTM functions. From the descriptive theory will come an error taxonomy, a framework for explaining CTM errors, and a model for predicting CTM performance.

Both theories will be further formalized to create analytic and evaluative methodologies which will be applied to the examination of aviation incidents and accidents from the perspective of CTM and the rating of cockpit equipment and procedures for how they facilitate or impair CTM. We believe that the development and application of these methodologies will also lead to countermeasures to poor CTM, perhaps in the form of general principles as well as specific design guidelines along the lines of those presented above.

From these principles and guidelines we will construct and evaluate further prototype PVIs. Our goal is not just to understand CTM, but to improve it through intelligent engineering research and practice.

We are encouraged by our progress and believe that the CTM concept has significant potential for improving the safety and effectiveness of aerospace systems.

References

Funk, K.H., [1983], "Theories, Models, and Human-Machine Systems," Mathematical Modelling, Vol. 4, pp. 567-587.

Funk, K.H., [1990], "Agent-Based Pilot-Vehicle Interfaces: Concept and Prototype," 1990 TIMS/ORSA Joint National Meeting, Las Vegas, NV, 7-9 May 1990.

Hoshstrasser, B.H. and N.D. Geddes, [1989], "OPAL: Operator Intent Inferencing for Intelligent Operator Support Systems," Proceedings of the IJCAI-89 Workshop on Integrated Human-Machine Intelligence in Aerospace Systems, Detroit, MI, 21 August 1989.

Lind, J.H., C.W. Hutchins, and D.E. Neil, [1990], "The Effect of Knowledge-Based System Assistance on Piloting Performance, Workload, and Satisfaction," IEEE National Aerospace and Electronics Conference, Dayton, OH, 21-25 May 1990.

Mesarovic, M.D. and Y. Takahara, [1975], General Systems Theory: Mathematical Foundations, New York: Academic Press.

Nagel, D.C. [1988] "Human Error in Aviation Operations," in E.L. Wiener and D.C. Nagel (eds.), Human Factors in Aviation, San Diego: Academic Press, Inc., pp. 263-303.

Navon, D. and D. Gopher [1979] "On the Economy of the Human Processing System," Psychological Review, Vol., No. 3, pp. 214-255.

NTSB [1973], Aircraft Accident Report, Eastern Airlines, Inc., L-1011, N310EA, Miami, Florida, December 29, 1972, NTSB-AAR-73-14. Washington, DC: National Transportation Safety Board.

NTSB [1981], Aircraft Accident Report - Eagle Commuter Airlines, Inc., Piper PA-31-350, Navajo Chieftan, N59932, William P. Hobby Airport, Houston, Texas, March 21, 1980, NTSB-AAR-81-4. Washington, DC: National Transportation Safety Board.

NTSB [1985], Aircraft Accident Report - USAir, Inc., Flight 183, McDonnell Douglas DC9-31, N964VJ, Detroit Metropolitan Airport, Detroit, Michigan, June 13, 1984, NTSB/AAR-85/01. Washington, DC: National Transportation Safety Board.

Padulo, L. and M.A. Arbib [1974] System Theory. Washington, DC: Hemisphere.

Rouse, W.B. and J.M. Hammer, [1990], "Computer-Aided Fighter Pilots," IEEE Spectrum, March 1990.

Sheridan, T.B., [1988] "The System Perspective," in E.L. Wiener and D.C. Nagel (eds.), Human Factors in Aviation., San Diego: Academic Press, pp. 27-52.

Wickens, C. D. [1984] "Processing Resources in Attention," in R. Parasuraman and D.A. Davies (eds.), Varieties of Attention. Orlando: Academic Press, pp. 63-102.

Wickens, C.D. and Y. Liu, [1988], "Codes and Modalities in Multiple Resources: A Success and a Qualification," Human Factors, Vol. 30, No. 5, pp. 599-616.

Wiener, E.L. [1987] "Fallible Humans and Vulnerable Systems: Lessons Learned From Aviation," in J.A. Wise and A. Debons (eds.), Information Systems: Failure Analysis, NATO ASI Series, Vol. F32. Berlin: Springer-Verlag, pp. 163-181.

SUPERVISING UNMANNED ROVING VEHICLES THROUGH AN INTELLIGENT INTERFACE

Norman D. Geddes
Search Technology Incorporated

(Paper not provided at publication date)

40

OFMspert: An Architecture for an Operator's Associate that Evolves to an Intelligent Tutor

Christine M. Mitchell
Center for Human-Machine Systems Research
School of Industrial and Systems Engineering
Georgia Institute of Technology
Atlanta, GA 30332
(404) 894-4321
cm@chmsr.gatech.edu

Introduction

With the emergence of new technology for both human-computer interaction and knowledge-based systems, a range of opportunities exist to enhance the effectiveness and efficiency of controllers of high-risk engineering systems. This paper describes the design of an architecture for an operator's associate--a stand-alone model-based system, designed to interact with operators of complex dynamic systems, such as airplanes, manned space systems, and satellite ground control systems, in ways comparable to that of a human assistant. The presentation will have several sections. The first describes the OFMspert architecture. The second describes the design and empirical validation of OFMspert's understanding component. The third describes the design and validation of OFMspert's interactive and control components. The paper concludes with a description of current work in which OFMspert provides the foundation in the development of an intelligent tutor that evolves to an assistant as operator expertise evolves from novice to expert.

OFMspert Architecture

OFMspert--Operator Function Model (OFM) expert system--is a stand-alone knowledge-based system that is intended to function as an assistant to a human expert. This philosophy is different than many knowledge-based systems in which the computer system replaces or operates suggestions. OFMspert is intended to be a subordinate to an experienced operator, possibly replacing a less skilled assistant. As a result, OFMspert includes features such as dynamic allocation of functions between the human and computer controllers, interruption of OFMspert by the human user, and 'repair' of misunderstandings.

OFMspert (Figure 1) has two primary components that enable it to 'understand' operator activity in the control of a complex dynamic system. The first is the operator function model (OFM). The OFM is a representation of operator activity in dynamic systems that represents the interrelations between dynamic system states and operator functions. Each function is hierarchically decomposed down to the level of individual operator actions. The OFM defines the knowledge base that OFMspert uses to hypothesize expectations of operator activities and to infer why a given action was undertaken. Figure 2 depicts a generic OFM

The second major OFMspert component is a blackboard on which OFMspert dynamically constructs expectations of current operator function, subfunctions, tasks and actions. The blackboard, called ACTIN (actions interpreter), keeps track of model-derived expectations and data-derived interpretation of operator actions. ACTIN's hierarchy is a dynamic representation of the operator function model (Figure 3).

ACTIN and the OFM define OFMspert's understanding component. OFMspert's utility and effectiveness depend on its ability to 'understand' accurately.

The Validation of OFMspert's Intent Inferencing (Understanding) Component

In order to evaluate OFMspert's intent inferencing effectiveness two experiments were conducted in the domain of satellite ground control. The first experiment compared OFMspert interpretations of operator activity with a domain expert's interpretations. The second experiment involved verbal protocols in which subjects controlling the system stated the reasons for what they were doing; their reasons were then compared to OFMspert's interpretations. In both cases, OFMspert's understanding was quite impressive. Figure 4a and 4b summarize the empirical results. Areas of mismatch were due primarily to model errors in the OFM (correctable) or long-term planning and browsing--operator functions that the OFM had not represented.

We were very pleased with the intent understanding component. Based on its understanding capabilities, OFMspert was augmented with control properties in order to function as an assistant.

OFMspert as an Assistant

Based on the OFM and Rasmussen's abstraction hierarchy, a user interface to OFMspert was designed. The human operator could request a range of assistance from OFMspert. The types of assistance were identified based on the operator functions and subfunctions defined in the OFM. Each OFMspert function was further decomposed into levels of available assistance so that the user could dynamically choose how much or how little assistance was desired.

An extensive evaluation of OFMspert as an assistant (Figure 5) was conducted, again in the domain of satellite ground control. Trained subjects controlled a simulated satellite ground system using both OFMspert and a well-trained human assistant. Results showed that though the style of use varied, controllers with OFMspert as an assistant controlled the system as effectively as controllers with a human assistant (Figure 6).

This experiment provided strong evidence for the possibility of using knowledge-based technology to augment operator control capabilities. Subject responses indicated that they liked the highly interactive and flexible user interface to OFMspert--and, in fact, would prefer even more capabilities for dialogue and repair of miscommunication. Indeed, for the design of knowledge-based systems for complex domains, the human-human metaphor is an intriguing avenue for further research.

OFMspert as a Tutor that Evolves to an Assistant

Current research at Georgia Tech examines the use of OFMspert as an intelligent tutoring system (ITS) that can evolve to an assistant as the user's skills evolve from novice to expert (Figure 7). With the OFM, OFMspert provides the domain knowledge (static, dynamic, and operational) needed in an ITS. In addition, OFMspert's blackboard, ACTIN, represents expected operator activity, interprets actual activity, and is able to assess the differences. As such it provides the initial definition of the teaching component of an ITS.

Finally, as a tool that is designed to function both as a teacher and as an assistant, OFMspert may be a very viable architecture. With two applications, the assistance function being long term, it is easier to justify the development costs that such systems inevitably incur. From an operations standpoint, novice users may be more likely to spend the time interacting and using a training system that they know will eventually become a tool that they use operationally.

References

Bushman, J. B., Mitchell, C. M. Jones, P. M. and Rubin, K. S., "ALLY: An operator's associate for cooperative supervisory control," submitted for publication.

Bushman, J. B., Mitchell, C. M., Jones, P. M. and Rubin, K. S. Ally: An operator's associate model for cooperative supervisory control situations. *Proceedings of the 1989 IEEE International Conference on Systems, Man, and Cybernetics*, Cambridge, MA, November, 1989, 40-45.

Bushman, J. B. (1989). Identification of an operator's associate model for cooperative supervisory control situations. Ph.D. dissertation, Report 89-1, Center for Human-Machine Systems Research, School of Industrial and Systems Engineering, Georgia Institute of Technology, Atlanta, GA.

Chu, R.W., Mitchell, C. M. and Govindaraj, T. Characteristics of an ITS that evolves from tutor to assistant. *Proceedings of the 1989 IEEE International Conference on Systems, Man, and Cybernetics*, Cambridge, MA, November, 1989, 778-783.

Jones, P. M., Rubin, K. S., and Mitchell, C. M., "Validation of intent inferencing by a model-based operator's associate," *International Journal of Man-Machine Studies*, in press.

Rubin, K.S., Jones, P.M., and Mitchell, C.M., , "OFMspert: inference of operator intentions in supervisory control using a blackboard architecture," *IEEE Transactions on Systems, Man and Cybernetics*, SMC-18, No. 4, 618-637, July/Aug. 1988.

Many people participated in and contributed to this research. They include T. Govindaraj, Richard Robison, Kenny Rubin, Patty Jones, Jim Bushman, and Rose Chu. The research was supported in part by a NASA Ames grant "Operator Function Modeling: An Approach to Cognitive Task Analysis in Supervisory Control Systems," NASA Ames Grant NAG 2-413, Dr. Everett Palmer, Technical Monitor, and NASA Goddard Space Flight Center grant, "Human-Computer Interaction in Distributed Supervisory Control Tasks," NAG 5-1044, Walt Truszkowski, Technical Monitor.

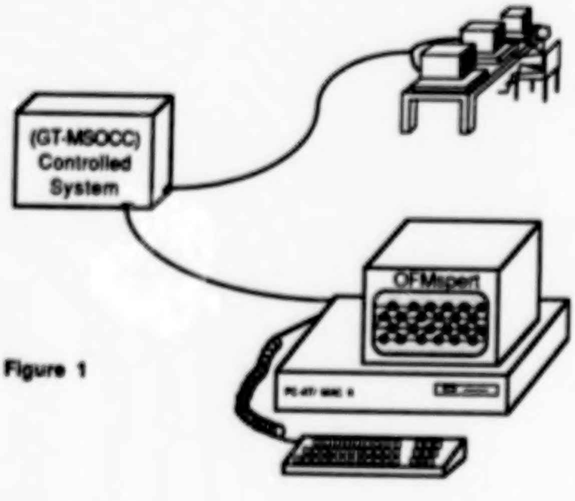

Figure 1

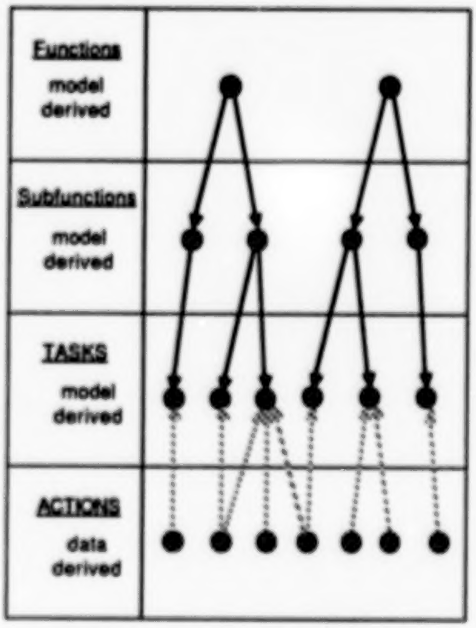

ACTIN's Intent Inferencing Structure
Figure 3

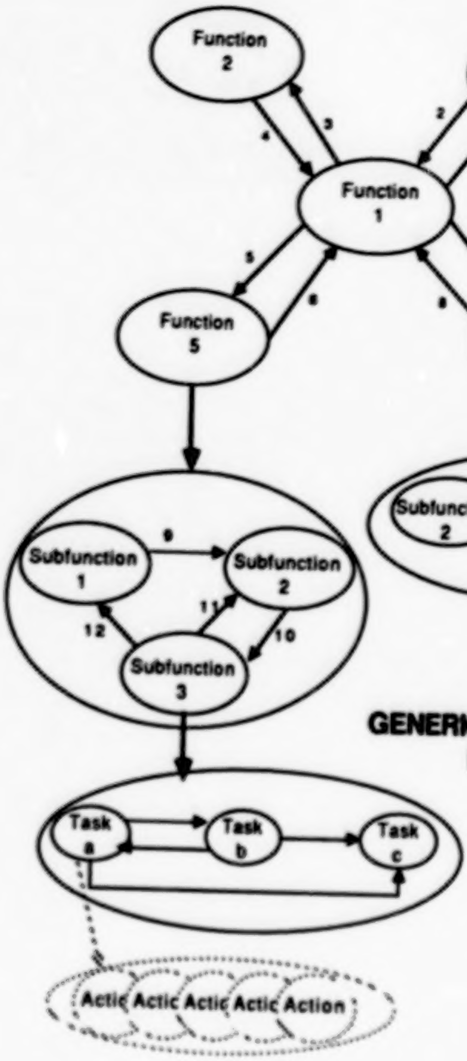
Function 2
Function 3
Function 1
Function 5
Function 4
1
2
3
4
5
6
7
8
Subfunction 1
Subfunction 2
Subfunction 3
9
10
11
12
Subfunction 2
Subfunction 4
13
14
Task a
Task b
Task c
Actic Actic Actic Actic Action

GENERIC OFM NETWORK
Figure 2

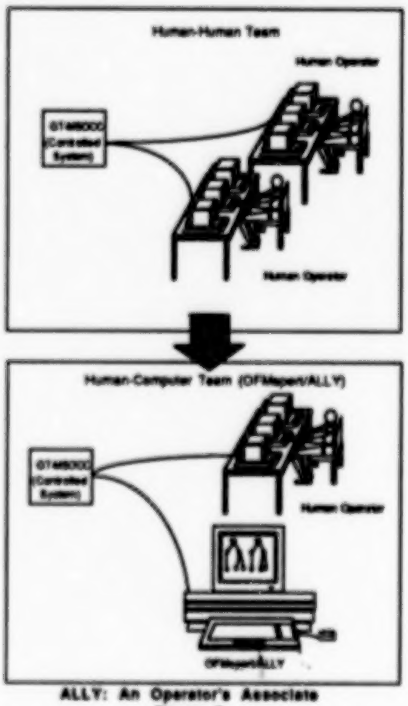
Human-Human Team
Human Operator
GT-MSOCC (Controlled System)
Human Operator
Human-Computer Team (OFMspert/ALLY)
GT-MSOCC (Controlled System)
Human Operator
OFMspert/ALLY

ALLY: An Operator's Associate
Figure 5

43

Experiment 1: Average Percentage of Equivalent Interpretations Between ACTIN and a Human Domain Expert. (Ordered by Rank).

Configure	100 %
Deconfigure	100
Answer	96.2
Replace	94.8
Equipment schedule page requests	90.3
Mission schedule page requests	85.7
Interior telemetry page requests	84.3
Endpoint telemetry page requests	76.5
MSOCC schedule page requests	75.5
Telemetry page requests	70.2
Reconfigure	60.8
Events page request	53.9
Pending page request	33.3

Figure 4a

Experiment 2: Average Percentage Of Equivalent Interpretations Between ACTIN And Verbal Reports. (Ordered By Rank).

Configure	100 %
Endpoint telemetry page requests	100
Deconfigure	97.1
Telemetry page requests	96.3
Answer	91.4
Reconfigure	91.2
Interior telemetry page requests	87.1
Replace	75.3
Mission schedule page requests	66.7
MSOCC schedule page requests	50.3
Equipment schedule page requests	21.8
Events page request	17.7
Pending page request	16.7

Figure 4b

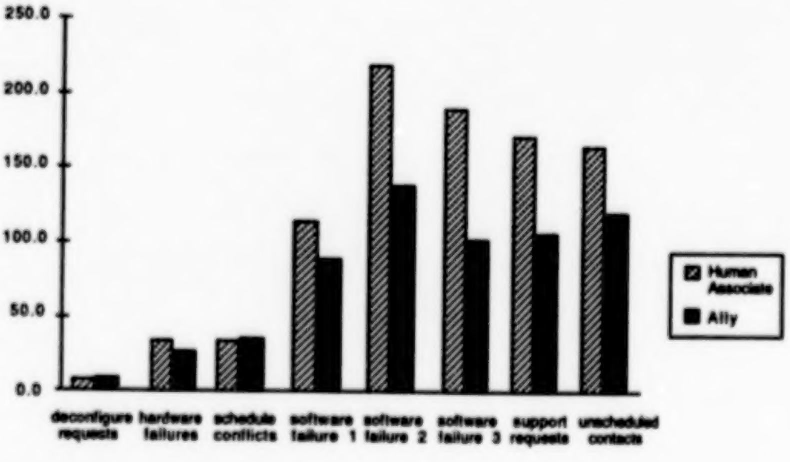

Comparison of Human Associate and Ally

Figure 6

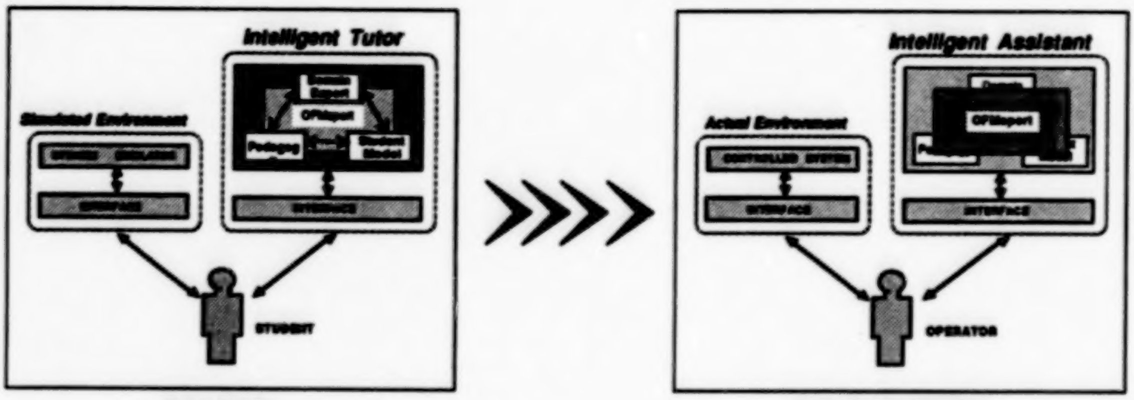
Intelligent Tutor
Simulated Environment
Domain Expert
OFMspert
Pedagog
Student Model
INTERFACE
INTERFACE
STUDENT
Intelligent Assistant
Actual Environment
CONTROLLED SYSTEM
OFMspert
INTERFACE
INTERFACE
OPERATOR

During Training

During On-Line Operations

Architectural evolution of an intelligent tutor to an operator's assistant

Figure 7

INTELLIGENT TUTORING SYSTEMS FOR HIGH-PERFORMANCE SKILLS

J. Wesley Regian
USAF Human Resources Laboratory

(Paper not provided at publication date)

AUTOMATED ACQUISITION OF INFORMATION REQUIREMENTS FOR AN INTELLIGENT DISPLAY

Valerie L. Shalin and Chris A. Miller
Honeywell Systems and Research Center
Norman D. Gedded
Applied Systems Intelligence
Belinda H. Hoshstrasser
Search Technology Incorporated

(Paper not provided at publication date)

47

Enhancing the Usability of CRT Displays
in Test Flight Monitoring

Michael M. Granaas, and Victoria E. Sredinski
Human Factors Laboratory
The University of South Dakota
Vermillion, SD 57069

Enhancing the usability of Mission Control Center (MCC) CRT displays stands to improve the quality, productivity, and safety of flight-test research at the NASA Ames-Dryden Flight Research Facility. The research reported in this paper involves three experiments aimed at improving the usability of the CRT displays in the Ames-Dryden MCCs. The results of this research suggest that much can be done to assist the user, and improve the quality of flight research through the enhancement of current displays. The research reported has applications to a variety of flight data monitoring displays.

Introduction

In the years since World War II, the amount of data collected in flight-test research has increased from a handful of parameters to several hundred parameters (Granaas and Rhea, 1988). Also increasing is the amount of data available to the flight-test researcher in real-time (Moore, 1986). As technology improves, there is every reason to believe that the amount of data available to the researcher will continue to increase.

While this is generally good news for the flight-test researcher, it does not come without some cost. Specifically, increasing amounts of data have lead to cluttered screens and increased mental work load for the user. This in turn reduces the overall effectiveness of flight-test programs.

In order to minimize the negative impact of increasing amounts of data on the flight-test researcher, we have begun a program of research intent on determining appropriate and effective design criteria for CRT flight data displays. This paper reports the preliminary findings from three of these studies.

Experiment 1

Research has shown that reducing screen clutter and increasing information organization can lead to improved task performance (Ramsey and Atwood, 1979). This experiment was done to determine if some of the displays in the Dryden MCC could be reorganized to reduce screen clutter and improve user performance.

During the course of a test flight, MCC users will frequently monitor a set of flight parameters until they match a predetermined set of values that define a test point. Once this match occurs, the user takes some action until the matching ceases to occur. Often the task performed involves making a record of the time at which the aircraft reached the test point so that the data of interest can be retrieved at a later time. Since an aircraft is "on point" for only a few seconds, delays in recognizing that the aircraft is on point can be very costly in terms of the amount and quality of data collected.

This task was chosen because in one form or another, many users monitor one or more parameters. This task should also generalize to a number of tasks outside of the control room setting.

The current screen layout now requires that the user either memorize the three to four target values that define the test point, or scan multiple locations on the screen to determine what those values are. With only three values to monitor this is probably not too mentally taxing for the user. However, as the number parameters to be monitored increases, the mental work load of the user should increase to the point where user performance suffers.

This research utilized a modified display format to test the efficacy of modified displays in the MCC. Target and actual parameter values were placed in adjacent columns to reduce user scanning time. This placement also allowed for the elimination of some redundant parameter labels which helped reduce screen clutter.

Methods

Subjects. Sixty undergraduate students from a small midwestern university were recruited to act as subjects for this study. Subjects received class credit for their participation.

Apparatus. The displays were programmed in Microsoft-C on a CSS 286-A AT compatible computer running at ten megahertz. Displays were presented on a NEC Multisync II monitor in EGA mode. Reaction times were collected via a Microsoft Mouse and software that uses the system hardware timer to measure times with better than millisecond accuracy (Granaas, 1989).

Displays. Two display formats were developed for this study. The first replicated one of the actual alphanumeric displays currently used in the Dryden MCCs. The second was modified so that parameters being monitored appeared in adjacent columns of the display in the upper left quadrant, and redundant labels were eliminated. Each of these displays was tested with subjects monitoring three, five, or seven parameters.

Procedure. After receiving informed consent, subjects were seated at an experimental workstation with the display and mouse. Each subject participated in only one of the six possible display format by number of monitored parameters conditions. The subject was given instructions in both verbal and written form for the condition in which they participated. Subjects were given one practice trial followed by an opportunity to ask questions. After answering any questions, the experimenter left the subject to complete the experiment.

Each subject completed 20 trials as part of the experiment. The first five trials were later treated as practice trials due to the large number of missing data points in those trials.

In each trial subjects were instructed to press the left mouse button when the monitored parameters matched their target values, and again when one or more of the monitored parameters ceased to match its target value. Following each button press one of two tones was presented. One tone indicated a correct response and the other a false alarm. Thus, subjects had feedback to assist them in determining if they had responded correctly.

The computer recorded the reaction times and number of false alarms for both the matching and dematching tasks. So each trial had four data points associated with that trial: Reaction time for the matching task, reaction time for the dematching task, number of false alarms for the matching task and number of false alarms for the dematching task.

Results

For purposes of these preliminary analyses, the only data analyzed was the mean reaction time for each subject on the matching and dematching tasks. Each of these scores was analyzed independently using a 2(display format) by 3(parameters monitored) completely between groups analysis of variance (ANOVA).

Matching Task. The display format by number of parameters monitored interaction was significant ($F(2,54) = 11.53$, $p < .0001$). The main effects for display format and number of parameters were also significant ($F(1,54) = 22.02$, $p < .0001$ and $F(2,54) = 5.08$, $p < .01$).

Table 1

Mean Reaction Times for Matching Task for Old and New Display Formats by Number of Parameters Monitored

Number of Parameters	Format Old	 New
3	1.26 (0.433)	1.21 (0.282)
5	2.87 (1.032)	1.32 (0.437)
7	3.02 (1.394)	1.75 (0.516)

An examination of the means in Table 1 indicates that there is little difference between the two formats when only three parameters are monitored. As the number of parameters increases, reaction times for the unorganized display climbed sharply, while those for the organized display climbed only modestly.

Dematching Task. This analysis found no significant effects.

Discussion

This study shows that display organization is an important component in display design. Reorganizing of poorly organized displays can significantly improve performance. And, reorganization can also reduce the effects of further increases in the difficulty of the task being performed. However, this improvement in performance only occurs when that task is sufficiently difficult that the user cannot effectively compensate for the increased workload.

EXPERIMENT 2

This experiment was designed to look at the effects of different screen colors on task performance. Current guidelines suggest that there are no differences in performance as a function of screen color as long as the foreground/background colors selected are of high contrast (Mitchell, Stewart, Bocast, and Murphy, 1982; NASA, 1989). However, such research is open to the criticism that the tasks performed are relatively simple and of short duration (less than 20 minutes), or do not reflect real tasks. What happens in real task settings over a period of time seems to be unknown.

Methods

Subjects. Fifty-six subjects from the same population as Experiment 1 were recruited to participate in this study. Subjects received course credit for their participation.

Apparatus. The computer hardware used is the same as that used in Experiment 1. The programs from Experiment 1 were modified to meet the needs of this study. The modifications are discussed below.

Displays. The reformatted, seven parameter display was taken from Experiment 1 for use in this study. The programs were modified so that the program would run in one of four foreground/background display modes: White on black, amber on black, green on black, and black on white.

Procedure. The procedure for this study followed that of Experiment 1, except that five practice trials were given, and only 12 trials were used for collecting data. This reduced the number of trials from 20 to 17 total. This task required approximately 50 minutes to complete, and according to subjects from experiment 1, was fairly difficult. Subjects participated in only one of the display mode conditions.

Results

Mean reaction times for the matching and dematching tasks were used in a one-way analysis of variance (ANOVA) to test for differences between the screen color conditions. No significant effects were found for either the matching or dematching tasks.

Discussion

In a relatively difficult task under normal lighting conditions, screen foreground/background color did not affect task performance. Since all color combinations were of relatively high contrast, it can be argued that high contrast between colors is more important than which colors are used.

Since the number of foreground/background combinations used in this study were limited, some caution must be included as part of the recommendation that high contrast is all that is important. The color combinations selected for this study were those that are typically available on commercial CRT displays.

Blue has been suggested as a color to avoid as a character color due to the human eye's inability to focus precisely on wave lengths at either end of the visible spectrum. All of the colors tested can be focused on with a high degree of precision by the human eye. Thus, these results may not be duplicated with a high contrast blue characters on black background display.

EXPERIMENT 3

This experiment was designed to examine the influence of color highlighting on the matching and dematching tasks used in Experiments 1 and 2. To date, the results using color highlighting have been mixed. Many studies show that color highlighting does little or nothing to improve performance. However, a smaller number of studies suggest that under some conditions color highlighting can improve performance (Christ, 1975).

We do know that color highlighting that does not consistently provide useful information does not help, and may actually detract from, user performance (Christ, 1975; Fisher and Tan, 1989). This indicates that color use needs to be consistent if it is to be of any value at all (Schneiderman, 1987).

A limitation of color highlighting, and other highlighting research has been the task difficulty level. Frequently research in this area uses tasks that the subject can already perform with relative ease. Thus, any potential benefits of highlighting are masked due to ceiling effects (Christ, 1977).

In the research reported here, a sufficiently difficult task was used so that any positive effects of highlighting could be detected. In addition, some subjects received an extra task to increase their mental workload. This was done to insure that their mental workload was sufficiently taxing so that the benefits of highlighting could be detected if they exist.

Methods

Subjects. Twenty-four subjects from the same population used in Experiments 1 and 2 were recruited for the current study. Subjects received class credit for their participation.

Apparatus. The computer hardware is the same as used in Experiments 1 and 2. The program used in Experiment 2 was modified to meet the needs of this study. These modifications are described below.

Displays. The base display for this research was the display used in Experiment 2 with white characters on a black background. The program for this display was modified to include different forms of color highlighting to assist the user in the matching and dematching tasks. Four highlighting conditions were used.

The first was a no highlighting condition. In this condition, subjects had to scan the actual and target values for all seven parameters after each screen refresh to determine if all seven matched. Thus the subject was required to make seven comparisons before being able to respond to the matched condition.

The second highlighting condition was labeled individual highlighting. In this condition, each parameter's label, actual, and target values were highlighted in yellow when that parameter matched it's target value. In this condition, the subject was required to make seven yes/no decisions before being able to respond positively to the matched condition.

The third highlighting condition was labeled group highlighting. In this condition, the seven parameter's labels, actual and target values were highlighted in green as a group only when all seven parameters matched their target values. This reduced the matching task to a simple signal detection task. The subject needed to respond only when the highlighting occurred.

The fourth highlighting condition was labeled combined highlighting. This condition combined individual and group highlighting.

Procedure. In a fashion similar to Experiments 1 and 2, subjects received informed consent and general instructions. The highlighting conditions were presented to subjects in one of four presentation orders to balance practice effects. Subjects were presented with five practice trials prior to the first highlighting condition to familiarize them the task and their first highlighting condition. Prior to each subsequent highlighting conditions, subjects received two practice trials to familiarize them with that highlighting condition. Subjects completed a block of ten trials in each highlighting condition.

In addition to the matching and dematching tasks, half of the subjects also performed a safety task. For the safety task subjects were expected to monitor two additional parameters on the upper right portion of the display. When both of these values exceeded predefined limits the subject was to respond by pressing the right mouse button. This condition occurred twice during each block of ten trials and reaction times were recorded.

Results

For each of the highlighting conditions, mean reaction times for the matching task, the dematching task, and, where appropriate, the safety task were calculated for each subject. The matching and dematching reaction times were analyzed using independent 2(number of tasks) by 4(highlighting conditions) split plot ANOVAs where the number of tasks was a between groups factor, and the highlighting conditions were repeated across subjects. The reaction time data for the safety task was analyzed with a repeated measures ANOVA for highlighting conditions.

Matching Task. The data for the matching task showed a significant main effect for highlighting condition ($F(3,66) = 49.92$, $p < .0001$). The difficulty main effect and the difficulty by highlighting condition interaction were not significant.

Table 2

Mean Reaction Times for Matching Task by Highlighting Condition

Type of Highlighting	Mean RT (SD)
none	2.10 (.675)
individual	1.26 (.284)
group	0.93 (.192)
combined	1.05 (.305)

Dematching Task. There were no significant effects for the dematching task.

Safety Task. Highlighting condition failed to have a significant effect on response time for the safety task.

Discussion

These results indicate that color highlighting can provide a display user with information that improves performance in some cases. Taken with the findings for the dematching and safety tasks, this work suggests that the way in which highlighting is used is an important consideration. Highlighting needs to substantially reduce the cognitive workload of the user in order to provide a performance enhancement. An analysis of the matching and dematching tasks suggest an explanation for why highlighting works in one case but not the other. The matching task required confirmation on each of seven items that a match has occurred. The dematching task requires only that one of the seven items has ceased to match. We would expect then that color highlighting would be much more effective in assisting with the more complex task due to the increased mental workload involved in that task.

A further analysis of the task would suggest that group highlighting should have provided a performance advantage over individual highlighting. That these were not different was somewhat surprising. Two explanations for this lack of a significant difference between group and individual highlighting are readily apparent. First, the reduction in cognitive workload may not be great enough to produce a significant difference between these conditions. Second, this study may have lacked the power to reliably detect such a difference if it did exist. These, and other possibilities need to be explored.

That there was no difference in the safety task due to highlighting is not so easily explained. The design of the study may have been flawed. The safety task did not take place very often during the experiment. It also never took place at the same time as the matching task. Thus, subjects may have divided their attention successfully between the two tasks. Again, further research is required.

General Discussion

Taken as a group, these studies indicate two things. First, that laboratory research can be used in the process of display design. While some of the findings of this research are relatively intuitive, others are not. Experiment 2 contradicts those who advocate a particular foreground/background combination for displays under normal lighting conditions. Using the most common foreground/background color combinations available, no performance differences for a relatively involved task were detected.

The second important aspect of this work is that it indicates that there is still a great deal of need for additional basic research in the area of CRT display designs. Experiment 1 demonstrated the usefulness of organizing displays. It did not, however, address the issue of an optimal organization for this or any other display application. Experiment 3 demonstrated that color highlighting can assist the user in task performance under some conditions. This experiment did not, however, explore the full range of when such highlighting is or is not useful.

Acknowledgements

This work was supported in part by NASA Grant NAG2-492 awarded to the first author.

References

Christ, R. E. (1977). Four years of color research for visual displays. Proceedings of the Human Factors Society 21st Annual Meeting. 319-321.

Christ, R. E. (1975). Analysis of Color and Its Effectiveness. Las Cruces, NM., New Mexico State University, NMSU-ONR-FR-75-1.

Fisher, D. L. and Ten, K. C. (1989). Visual displays: The highlighting paradox. Human Factors, 31(1), 17-30.

Granaas, M. M. (1989). TIMEX2: A modified C-language timer for PC-AT class machines. Behavior Research Methods, Instruments, & Computers, 21(6), 619 - 622.

Granaas, M. M. & Rhea, D. C. (1989). Techniques for Optimizing Human-Machine Information Transfer Related to Real-Time Interactive Display Systems. NASA TM 100450.

Mitchell, C. M., Stewart, L. J., Bocast, A. K., & Murphy, E. D. (1982, December). Human Factors Aspects of Control Room Design: Guidelines and Annotated Bibliography. Fairfax, VA. George Mason University, NASA TM 84942.

Moore, A. L. (1986). The Role of a Real-Time Flight Support Facility in Flight Research Programs. NASA TM 86805.

NASA (1988). *Space Station Freedom Program Human-Computer Interface Guidelines.* Houston, TX., Johnson Space Center, NASA USE 1000 V. 2.1.

Ramsey, H. R. & Atwood, M. E. (1979, September). *Human Factors in Computer Systems: A review of the Literature.* Englewood, CO. Sciences Applications, Inc., (NTIS No. AD-A075-679).

Schniderman, B. (1987). *Designing the User Interface.* Massachusetts: Addison-Wesly Publishing Company.

AI/ROBOTICS INTERFACES

A SPATIAL DISORIENTATION PREDICTOR DEVICE TO ENHANCE PILOT SITUATIONAL AWARENESS REGARDING AIRCRAFT ATTITUDE

T.L. Chelette, D.W. Repperger, W. B. Albery
Harry G. Armstrong Aerospace Medical Research Laboratory
Wright Patterson Air Force Base, OH, 45433-6573

Abstract

An effort has been initiated at the AAMRL to investigate the improvement of the situational awareness of a pilot with respect to his aircraft's spatial orientation. This study has as an end product a device to alert a pilot to potentially disorienting situations. Much like a Ground Collision Avoidance System (GCAS) is used in fighter aircraft to alert the pilot to "pull up" when dangerous flight paths are predicted, this device would warn the pilot to put a higher priority on attention to the orientation instruments. A Kalman filter has been developed which estimates the pilot's perceived position and orientation. The input to the Kalman filter consists of two classes of data. The first class of data are the result of passing the aircraft flight trajectory through a set of models including those representing visual, vestibular, kinesthetic, and tactile senses. The second class of data consists of noise parameters (indicating parameter uncertainty), conflict signals (e.g. vestibular and kinesthetic signal disagreement), and some nonlinear effects. The Kalman filter's perceived estimates are now the sum of both Class I data (good information) and Class II data (distorted information). When the estimated perceived position or orientation is significantly different from the actual position or orientation, the pilot will be alerted.

Introduction

When Orville Wright piloted his aircraft for the first time, he flew in a rich sensory environment. He had an excellent field of view, could sense the vibrations, sounds, smells of flying and could feel the wind in his face. Any altitude or attitude changes in the Wright Flyer were sensed immediately, either visually or through some other sensory modality. The modern aircraft pilot flies an immensely more sophisticated machine, but is somewhat at a disadvantage compared to the first aviator. Although the flying machine has become much more agile and responsive, the modern pilot has lost many of the sensory inputs of flying. He or she must interpret digital displays, decipher the numbers, and translate the information to its flight meaning. The modern pilot must operate in a cockpit environment where there are fewer discriminatory cues and there is less time to dwell on them due to the high workload environment (Malcolm, 1987). The pilot cannot hear or feel the wind, cannot (at times) see out-the-window visual cues, and cannot perceive mechanical feedback due to fly-by-wire control systems. Pilots may become disoriented in such environments, lose attitude awareness, and unknowingly pilot $35M aircraft into terrain or water. Spatial disorientation costs the Air Force 8-10 pilots a year and up to $100M a year in lost aircraft and pilot training dollars (Freeman, 1989).

Air Force Experience

Spatial disorientation (SD) is the number one human factors problem facing the Tactical Air Force (DeHart, 1986). SD has been attributed as a contributing factor in 77 Class A mishaps in the Air Force since 1980 (Freeman, 1990). A Class A mishap has been defined as damage to the aircraft over $500,000 or death of the pilot. As of 1990, the value definition has been increased to $1 million (Lyons, 1990). Figure 1 depicts the distribution of SD mishaps over years and across aircraft types.

There has been a high incidence of F-16 Class A mishaps attributed to SD. Of 20 Class A mishaps in the F-16 between 1982 and 1988, 12 were found to have SD as a definite or suspected contributor to the mishap. (McCarthy, 1988)

SD is a silent killer because in many instances, the pilot is never aware that he is disoriented. In many of these Class A mishaps, the pilot has been distracted while flying by a warning light, a missed communication, or changing radio channels. While the pilot is distracted, the aircraft can roll at an imperceptible rate. When the pilot's attention is again directed towards piloting, he or she may discover that the aircraft in an unexpected attitude. If this occurs in total darkness, or in weather where there are no out-the-window visual cues, the pilot can become disoriented. A cross check of the aircraft instruments can correct this situation, but if the pilot's attention is focused out of the cockpit, such as during formation flying or while observing bomb damage over a range, he or she may rely on sensory information to determine spatial orientation.

There are three types of SD recognized by the Air Force Inspection and Safety Center (Marlowe, 1987). Type I is called unrecognized SD. This is the "insidious" type wherein the pilot loses attitude awareness unknowingly. In many cases, the pilot is distracted by a warning light or involved with selecting a radio frequency. While the pilot is distracted with this lower priority task, the aircraft may have rolled or lost altitude.

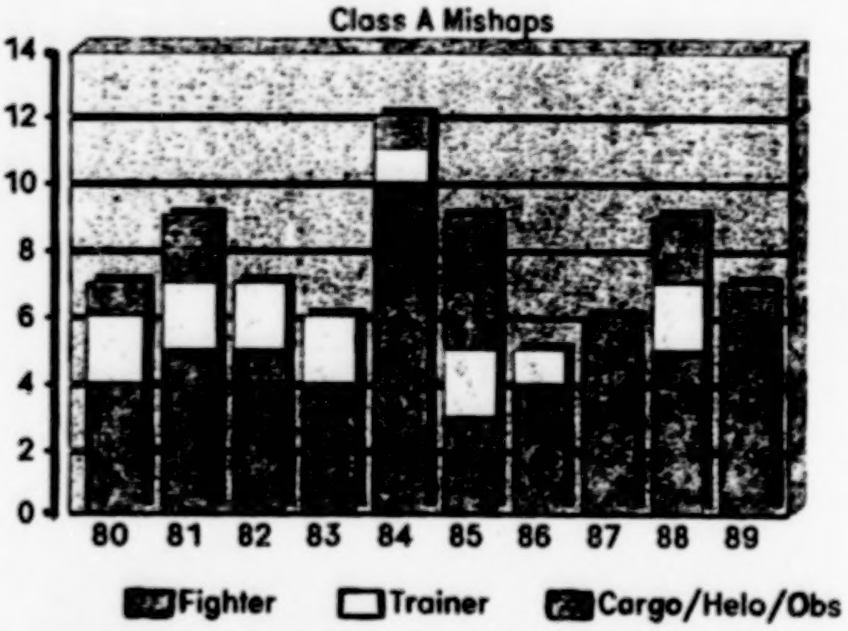

Figure 1: SPATIAL DISORIENTATION MISHAPS. The data above show Class A flight mishaps where the investigating Flight Surgeon found spatial disorientation as a definite or suspected contributor to the mishap. (Freeman, 1990)

At low altitudes, this can result in collision with the ground. Type II disorientation is called classic vertigo. The pilot is disoriented and knows it. He or she realises there is a sensory conflict and becomes aware that they must transition attention to the aircraft instruments. In many instances, the pilot is able to resolve this conflict and provide adequate guidance of the aircraft. Type III is very rare and is an incapacitating SD. In this example, the pilot simply fails to cope with the aircraft condition, such as a violent spin. During high levels of angular acceleration vestibular inputs can cause the eyes to reflexively move uncontrollably, thus making instrument reading impossible.

There are three human factors problems generally associated with spatial disorientation (Marlowe, 1987). First, there is often a distraction source associated with the SD. The pilot tends to focus on a low priority task that absorbs his or her attention, as described in the previous example.

The second human factors problem is that humans are poor time analyzers. Pilots can become distracted while flying and ignore the instrument panel for extended periods of time. If they are not routinely performing the "T cross check" (checking the T-shaped pattern of round dials on the instrument panel), they can miss important attitude and altitude information.

The third human factors problem is the illusion element. When there are no visual cues present, the human tends to transition to somatic (tactile) and vestibular cues. These are not always reliable and frequently may be in conflict with the instruments.

In a 1987 survey conducted by the Air Force Inspection and Safety Center (AFISC), questionnaires were sent to Air Force pilots concerning their experience with spatial disorientation. From the 1500 returned questionnaires, the pilots indicated that they could become disoriented just as likely in daytime as nighttime. Most respondees noted that when they flew in formation, they expected to become disoriented when flying "on the wing". The survey also indicated that Type II disorientation was most likely to occur when pilot attention was focused on attitude changing maneuvers. Regarding SD and the F-16 specifically, seventy percent of the F-16 pilots' responses indicated problems with canopy reflections and human factors problems with head down CRTs on the instrument panel.

Human factors specialists agree that the F-16 head down displays are poorly placed and overly complex to use. In addition, HUD symbology is confusing and difficult to decipher (Taylor, 1987). These difficulties, combined with the high forward seating of the pilot, all contribute to the high incidence of SD mishaps in the F-16 fighter aircraft.

Common Challenges

NASA Space Shuttle pilots and future National Aerospace Plane pilots face similar orientational challenges to those of high performance Air Force pilots. During ascent and re-entry, sustained G forces are experienced that can result in illusions similar to those experienced during takeoff and landing. The important distinction is the potential for extended exposure to zero G while in orbit. This extends the range of consideration to include vestibular and kinesthetic illusions that are unique to a gravity free environment. In addition, consideration must be given to the effects of microgravity adaptation and space motion sickness. Future protective and alarm devices must account for the unique challenges of long term orbital flight trajectories.

Vestibular Function

The vestibular system contains mechanoreceptors specialised to detect changes in both the motion and position of the head. The receptors are part of the ***vestibular apparatus*** which is located in the bony channels of the inner ear, one on each side of the head. The vestibular apparatus is a membranous sac within a bony tunnel in the temporal bone of the skull. It forms three ***semicircular canals*** and a slight bulge for the ***utricle*** and ***saccule*** as shown in Figure 2. (Vander, Sherman, and Luciano, 1975)

The three semicircular canals on each side of the skull are arranged approximately at right angles to each other. The actual receptors of the semicircular canals are hair cells which sit at the ends of the nerve cells. The sensory hairs are closely ensheathed by a gelatinous mass which blocks the channel of the canal at that point.

The receptor system in the semicircular canals works in the following way. Whenever the head is moved, the bony tunnel wall, its enclosed membranous semicircular canal, and the attached bodies of the hair cells, of course, turn with it. The fluid filling the membranous semicircular canal, however, is neither attached to the skull nor necessarily pulled with it. The fluid tends to lag behind. As the bodies of the hair cells move with the skull, the hairs are pulled against the relatively stationary column of fluid and are bent. The speed and magnitude of the movement of the head determine the degree to which the hairs are bent and thus the hair cell stimulation. As the inertia is overcome, the hairs slowly return to their resting position. The hair cells are stimulated only during ***changes*** in rate of motion, i.e. during acceleration of the head. During motion at a constant speed, stimulation of the hair cells ceases.

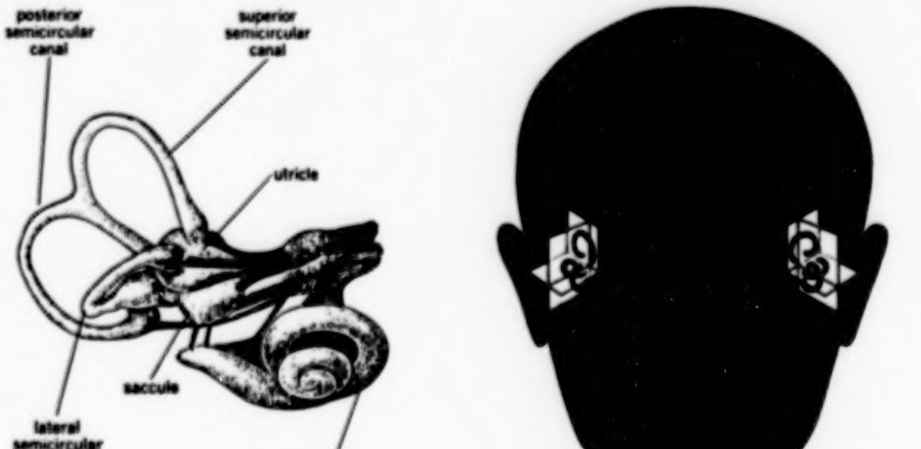
posterior semicircular canal
superior semicircular canal
utricle
saccule
lateral semicircular canal
cochlea
A
B
C
D
direction of movement of head
hair cells in gelatinous mass
direction of force on the hair cells
semicircular canal
utricle
resting activity
stimulation (depolarization)
inhibition (hyperpolarization)
discharge rate of vestibular nerve

Figure 2: A. The vestibular apparatus. B. Relationship of the two sets of semicircular canals. C. Diagram of a semicircular canal. D. Relation between position of hairs and activity in the nerve. (Vander et. al, 1975)

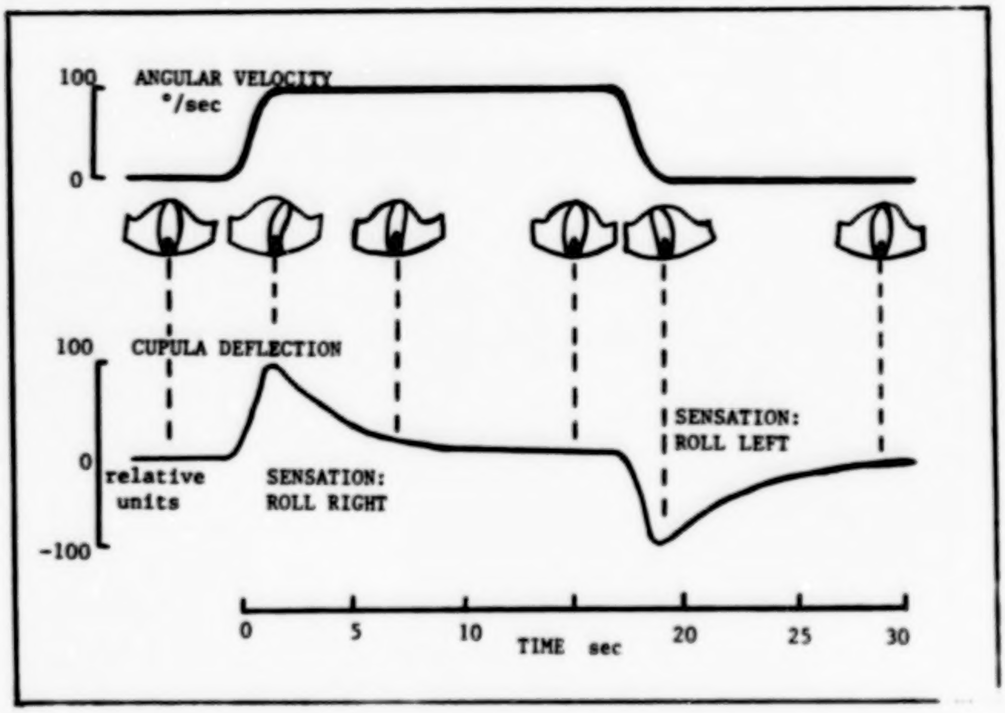

Figure 3: Response of semicircular canal and sensations of turning during and on recovery from sustained rotation. The upper graph shows the speed of rotation; the lower graph shows the deflection of the cupula of a semicircular canal stimulated by angular acceleration in the plane of the canal. (Benson, 1988)

Whereas the semicircular canals signal the rate of change of motion of the head, the otolith organs, the *utricle* and *saccule*, contain the receptors which provide information about the position of the head relative to the direction of gravity. These organs also have mechanoreceptors sensitive to the movement of projecting hairs. The hairs of the hair cells protrude into a gelatinous substance that has calcium carbonate crystals in it, thus making it more dense than the surrounding fluid. When the head is tipped, the heavy gelatinous material slides toward the downward vector and pulls on the hairs. This shearing displacement bends the hair cells and thus stimulates the receptor cells. As the head is tilted further and further, the relative displacement of hair cell body and hair changes. Some hairs may be stimulated while others are inhibited depending on the direction in which the resting hair was biased. This creates a pattern of stimulation across the surface of each organ that can be interpreted and recognized as an amount of tilt relative to gravity.

The information from the vestibular apparatus is used primarily for two purposes. The first is to control the muscles which move the eyes such that the eyes can remain fixed on an object in spite of the head moving. As the head is turned to the left, the balance of input from the vestibular apparatus on each side is altered. Impulses from the vestibular processing centers activate the ocular muscles, which turn the eyes to the right and inhibit their antagonists. Similar responses can be seen for nodding of the head. The second important use of vestibular information is reflex mechanisms for maintaining upright posture and balance. People with a defective vestibular apparatus have a reduced stability while trying to stand or walk with their eyes closed. (Howard, 1986)

Illusions of the Vestibular System

When a pilot's head is moving in a straight line at a constant velocity, the fluid in the semicircular canals remains at rest. When the head is accelerated (i.e. changes speed or direction) the fluid in the canals lags behind the movement of the canal walls due to its non-rigid inertia. After a period of time under constant angular acceleration, the fluid catches up with the walls and there is no longer any stimulus or any sensation of turning. When the head is decelerated, the fluid's inertia will carry it past the walls of the canal creating deflection of the sensing structure in the opposite direction. This causes a sense of rotation in the opposite direction as shown in Figure 3. Upon recovery from a prolonged spin, a pilot can feel as if he or she is spinning in the opposite direction. Attempts to correct for this will put the airplane into a spiral in the direction of the original spin. This is called the somatogyral illusion. (Gillingham & Wolfe, 1986)

Another dangerous illusion of the semicircular canals is known as the Coriolis phenomenon which is the result of head movement while the aircraft is in a prolonged turn. A strong illusion of turning or accelerating in a completely different axis may be created. The pilot may maneuver the aircraft into an inappropriate attitude or may even progress to a onset of dizziness and nausea.

The otolith organs can also give rise to dangerous illusions, especially in the absence of overwhelming visual cues. An abrupt forward acceleration will lead to the illusion of a much steeper climb than is actually the case, known as the somatogravic illusion. This effect has been particularly noted following takeoff, especially when visual reference is inadequate.

The pilot will input a forward motion of the control stick to reduce the aircraft's pitch angle and thereby cause the aircraft to descend. If altitude is low, such as immediately after takeoff, this can be a grave mistake.

While pulling a prolonged coordinated turn, pilots often must look out the cockpit to find another aircraft or survey a target. By tilting the head while under excess gravity, the sensation of head movement is exaggerated and the pilot can sense the aircraft has rolled out of the turn by a few degrees. Upon correction, the aircraft can become overbanked and lose altitude. If the pilot continues to look outside the cockpit at low altitude, the plane can slice downward with fatal speed.

Spatial Disorientation Detector (SDD)

To assist in the study of spatial disorientation, a special tool is being developed at the AAMRL. It consists of a set of electronic elements that will monitor the aircraft's accelerations and predict the possibility that the accelerations have created an illusion for the pilot. This tool consists of a Kalman filter (an unbiased, linear, least squares estimator) that processes the accelerations through a model of the human vestibular and somatic sensory perceptions and estimates the human's perceived attitude and position. If this value does not correlate with the actual attitude and position of the aircraft, the device will activate an audio or visual display to warn the pilot that the potential for spatial disorientation is high. Pilots should then increase their instrument check concentration and vigilance.

The Kalman filter model of the human sensory perception is presently built on an analog computer at the AAMRL as depicted in Figure 4. The six inputs into the device are the three linear acceleration vectors and the three angular acceleration vectors which are the accelerations experienced at a point in the head center coordinate system. One output of the SDD describes the true position and orientation of the aircraft. The second output describes the perceived position and orientation of the pilot. When the error between these two signals becomes large, the device will activate the alarm display to the pilot.

The crucial element of the SDD is the internal model that is used to produce the estimate of perceived orientation. Fortunately, the Kalman filter lends itself to an expanding design where simple vestibular models can be used and then, as more accurate models become available, the system can be enhanced. Many physiological studies have provided data for these models, and there is current research in the aerospace community that will expand the reliability and range of these models. Improved methods are continuously being developed to reduce the false positives of a Kalman filter. (Repperger, 1976, Borah et. al., 1988)

As with any avionics warning system, pilots are concerned about the annoyance of false positive alarms. The consensus among aviators and workload experts is that such a device would routinely be turned off if there is a significant number of false alarms. The Kalman filter approach was selected because of its ability to estimate in spite of signal noise and erroneous sensor information. This rigorous approach has been demonstrated to effectively predict human perception with a low occurrence of false positives or false negatives (Young, Curry, & Albery, 1976, Borah, Albery, & Fiore, 1976, Borah, Young, & Curry, 1988). The SDD would prove to be a valuable lifesaver.

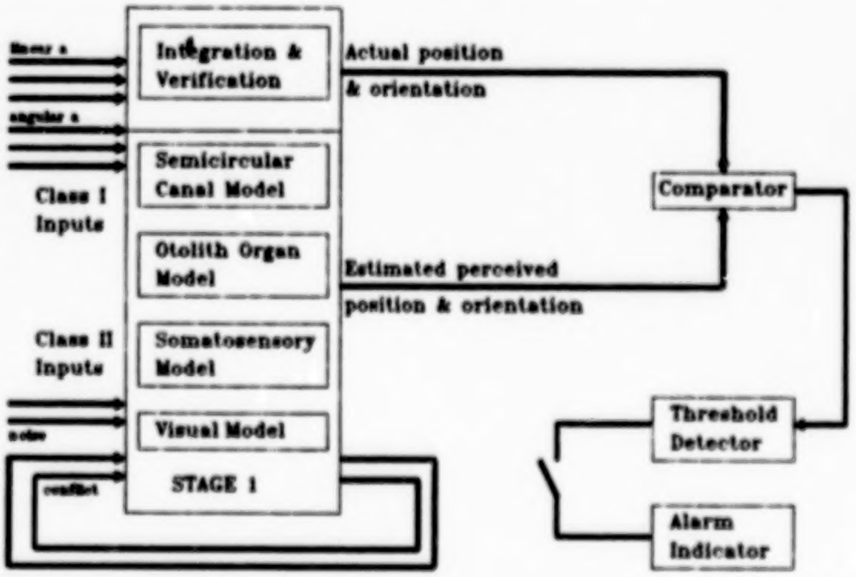

Figure 4: SDD Overview

The Bottom Line

From Flying Safety, IFC Approach, April 1989:

> "Thirty five seconds later, lead called as he passed the IP starting his bomb run. Thirty two second after that, the wingman echoed the call commencing his bomb run. Seventeen seconds later, the wingman impacted the ground in a right 35 to 40 degree bank, with a 3 degree descent, and between 500 and 540 knots."...
>
> "Overwhelming evidence indicates that the crew fell victim to Type I, or unrecognized spatial disorientation, which resulted in this mishap. Relaxed and unaware of their situation, the pilot was intent on keeping the leader in sight during the spacing maneuver, while the Weapons System Officer was preparing for the upcoming bomb run."
>
> " Having flown a completely successful first sortie and almost 20 minutes comfortable at "lead's altitude" when directed to take spacing, the crew expected nothing to change except the distance between aircraft. They did not have any idea the flight environment would be so conducive to illusions, spatial disorientation, or insidious weather conditions."

Although the predictive ability of the Spatial Disorientation Detector may not be perfect, neither is the perceptive power of the human. In the case above, the SDD would most likely have processed the positive acceleration occurring during the bomb run to generate a significant error between its estimate of pilot perception (level coordinated turn) and the actual aircraft attitude (descending turn) and thus alerted the pilot.

References

1. Benson, A.J., "Spatial Disorientation," AVIATION MEDICINE, Second Ed., Butterworths, London, England, 1988, Chaps 20 and 21.

2. Borah J., Albery, W.B., and Fiore, M.D. "Human Motion and Force Sensory Mechanism Modeling," Proceedings of the National Electronics Conference, 1978, Vol 32, pp 204.

3. Borah J., Young L., Curry R. "Optimal Estimator Model for Human Spatial Orientation," Annuals of the New York Academy of Sciences, 1988, Volume 545, New York, NY.

4. DeHart R., 1986. "Human Factors Problems in the Tactical Air Command," Aviation, Space and Environmental Medicine, July 86, 57:725.

5. Freeman J., 1989. Personal letter from Air Force Inspection and Safety Center to W.B. Albery re: Low-altitude Class A Mishaps, dtd 10 Mar 89.

6. Freeman J., 1990. Personal letter from Air Force Inspection and Safety Center to T.L. Chelette re: Spatial Disorientation Mishaps, dtd 11 May 90

7. Gillingham K., Wolfe J., 1986. "Spatial Orientation in Flight," USAFSAM-TR-85-31, School of Aerospace Medicine, Brooks AFB, San Antonio, TX, Dec 86.

8. Howard, I.P., "The Vestibular System," HANDBOOK OF PERCEPTION AND HUMAN PERFORMANCE, John Wiley and Sons, New York, 1986

9. Lyons, T.J., Freeman, J.E., "Spatial Disorientation (SD) Mishaps in the U. S. Air Force - 1988," Presented at the 61st Annual Meeting of the Aerospace Medical Association, May 13th, 1990, New Orleans, La.

10. Malcolm R., 1987. "How the Brain and Perceptual System Work," Presented at the 58th Annual Scientific Meeting of the Aerospace Medicine Association, May 10-14, 1987, Las Vegas, Hilton Hotel.

11. Marlowe B., 1987. "Spatial Disorientation and Loss of Attitude Awareness: Impact on the USAF," Presented at the 58th Annual Scientific Meeting of the Aerospace Medicine Association, May 10-14, 1987, Las Vegas, Hilton Hotel.

12. McCarthy G. W., 1988. "Human Factors in F-16 Aircraft Accidents," Presented at the 59th Annual Scientific Meeting of the Aerospace Medical Association, May 1988, New Orleans, La.

13. Repperger, D.W. "A Study of Identification Methods and Structural Modeling Techniques on Empirical Data From A Motion Study," The 1977 IEEE Conference on Systems, Man, and Cybernetics.

14. Taylor R., 1987. "HUD Pitch Scale Design and Evaluation," Presented at the 58th Annual Scientific Meeting of the Aerospace Medicine Association, May 10-14, 1987, Las Vegas, Hilton Hotel.

15. Vander, A.J., Sherman, J.H., Luciano, D.S., "Coordinated Body Functions," HUMAN PHYSIOLOGY; THE MECHANISMS OF BODY FUNCTION, Second Ed., McGraw Hill Book Co., New York, 1975.

16. Young, L.R., Curry, R.E., Albery, W.B. "A Motion Sensing Model of The Human For Simulator Planning," Proceedings of the 9th. Intec/Industry Conference, Orlando, Florida, November, 1976, pp 149-151.

EVALUATION OF THE MARK III AND AX-5 SPACE SUITS RELATIVE TO THE SHUTTLE SUIT FOR ROBOTIC MANEUVERABILITY

Angele Krishen and Kachroo Pushkin
Rice University

(Paper not provided at publication date)

COGNITIVE CONSEQUENCES OF 'CLUMSY' AUTOMATION ON HIGH WORKLOAD, HIGH CONSEQUENCE HUMAN PERFORMANCE

Richard I. Cook, David D. Woods, Elizabeth McColligan
Cognitive Systems Engineering Laboratory
Department of Industrial Systems and Engineering
The Ohio State University
Columbus, OH 43210

Michael B. Howie
Division of Cardiovascular Anesthesia
Department of Anesthesiology
The Ohio State University Hospitals
Columbus, OH 43210

ABSTRACT

The growth of computational power has fueled attempts to "automate" more of the human role in complex problem solving domains, especially those where system faults have high consequences and where periods of high workload may saturate the performance capacity of human operators. Examples of these domains include flightdecks, space stations, air traffic control, nuclear power operation, ground satellite control rooms, and surgical operating rooms. Automation efforts may have unanticipated effects on human performance, particularly if they increase the workload at peak workload times or change the practitioners' strategies for coping with workload. Smooth and effective changes in automation requires detailed understanding of the cognitive tasks confronting the user -- what has been called *user centered automation*[1]. We have observed the introduction of a new computerized technology in a group of hospital operating rooms used for heart surgery. The study has revealed how automation, especially *clumsy automation*[2,3], effects practitioner work patterns and suggests that clumsy automation constrains users in specific and significant ways. Users tailor both the new system and their tasks in order to accommodate the needs of process and production. The study of this tailoring may prove a powerful tool for exposing previously hidden patterns of user data processing, integration, and decision making which may, in turn, be useful in the design of more effective human-machine systems.

INTRODUCTION

Increasingly sophisticated computers and a sense that human operators need assistance in performing monitoring and control have prompted the development of "automatic" devices, especially in high consequence, semantically rich domains. The purpose of automation in these domains is to release the operator from repetitive control tasks in order to reduce operator workload or to provide the operator more precise or more extensive information about the system under control. These domains already exist and operators already accomplish tasks using skills, rules, and knowledge about the domain and current technology. New automated devices represent a *change* from one way of doing things to another.

Aiding operators, especially highly skilled operators in complex, high risk process control worlds, is itself a complex problem. Operators are facile and sophisticated information users and subtle controllers, whose performance is highly optimized to achieve specific goals or system states. Often overlooked is the fact that most automated devices make certain demands on operators (e.g. setup, device state identification, configuration control, operating sequences), including cognitive demands (e.g. tracking the automated device state, separating display elements, evaluating the automated device's performance). These demands constitute workload for the operator.

Virtually all automated devices are supposed to offset the operator workload increment with some payoff. The devices provide either better control (e.g. automated drip rate controllers instead of hand operated tubing clamps for intravenous solutions), economic value (e.g. flight management systems for commercial aircraft) or better information for control (e.g. nuclear power plant safety parameter displays) or later review (e.g. "automated" anesthesia records). Sometimes these paybacks benefit the operators by reducing their workload (the automated drip rate controller) while others benefit either the larger organization (automated anesthesia records, flight management systems) or society as a whole (safety parameter displays in nuclear plants). In domains where operator performance is critical to safe system function, automated devices are generally supposed to reduce net work, that is, the total operator work with the device is less than without it. But net work (workload integrated over time) is only a poor measure of operator performance. With some automated devices the workload increment occurs during the *peak* workload period and the payback occurs during the workload *trough*, a condition Wiener[2,3] describes as *clumsy automation*.

We have tracked the introduction of a system which has some characteristics of clumsy automation in the domain of cardiac anesthesiology. The study focused on the introduction of a new automated monitoring system, and its immediate and longer term effect on users. The opportunity to see the users adaptations as they occurred provided insight into the user task complexity and information management strategies. These, in turn, point towards specific consequences of certain approaches to automation in this and other high consequence domains.

THE SYSTEM AND THE STUDY

The new system provides monitoring and information management for cardiac surgery. It replaces a multiple discrete monitors with a single device, designed to provide a single source of information about the patient's physiologic condition. In order to accommodate the volume of information displayed, the device automates data presentation and organization. It also computes hemodynamic values from collections of data and keeps track of historical "trends". The device configuration is flexible, to permit users control over the order in which items are displayed on the screen. Virtually all major manufacturers of medical monitoring equipement have developed such devices, which represent the current state of the art in medical monitoring technology. The new device replaces older discrete technology with which the operators were quite familiar. Similar devices may be incorporated into the space station.

We were able to observe the introduction of the device beginning on the first day of use. The devices were purchased specifically for cardiac surgery purposes and are installed in rooms dedicated to thoracic surgery. Coronary artery bypass grafting, the most common cardiac surgery, was observed by a physician observer and the activities of the anesthesiologists recorded. These raw records were coded for protocol analysis and incidents evaluated, paying particular attention to the way the monitoring system was used, who used it, and what the context of the use was. At least two cases per week were recorded, and the observations continued for several months.

RESULTS

The new system replaces discrete monitors using fixed controls and displays with a menu oriented device using a color display showing multiple windows. Menus are displayed one line at a time at the bottom of the screen, and the device automates the recognition of various modules and the management of display formats.

Setup

Device setup is more complicated than with predecessor equipement; operators traverse at least seven major menu branches and enter between twenty and sixty keypresses. Setup occurs as the patient enters the operating room, a time of peak activity for anesthesiologists. For this reason, circulation technologists setup the monitoring equipment and perform configuration. We observed system crashes in mid-case, requiring complete setup during critical periods. Anesthesiologists rely on easily setup backup monitors (ECG, oxygen saturation, end-tidal CO_2) during the initial instrumentation period and also during the case. As time progressed, anesthesiologist users began to connect some new device sensors early (e.g. pulse oximeter) but the reliance on the old ECG was maintained throughout our period of observation.

Data Presentation

Data presented in the default system configuration is highly processed. Default waveform displays, the traditional form of data representation for anesthesiologists, are segregated and unscaled. The presentation segregates each data channel and minimizes the display area occupied by each waveform, maximizing the number of waveforms displayed and eliminating waveform overlap. This *data packing* changes the characteristics of displayed data and reduces information available from the waveform. Users universally and immediately call up a blood pressure graph window for display of blood pressure data and work to maintain it throughout each case.

Another processed data form is the digital representation of waveform characteristics (systolic, diastolic, and mean pressures). Although these representations are highly precise (three significant digits) users relied heavily on waveform presentations. The digital values are averaged; rapid changes in blood pressure appear immediately in the waveform but lag twenty to thirty seconds behind in the digital representations. These rapid pressure fluctuations occur relatively frequently during cardiac procedures and anesthesiologist users rely on waveforms for detecting them.

Determining cardiac output requires calling up a special window. The system automatically removes the blood pressure graph window and replaces it with the segregated traces when the cardiac output window is on the screen. Cognitive task analysis shows that determination of blood pressure and cardiac output occur in parallel during critical periods. Because of the system design, anesthesiologists must manage the display to interleave cardiac output windows with the desired scaled pressure representations. This information management task is new; the discrete monitor predecessors by necessity supported parallel display since cardiac output and blood pressure monitors were separate devices. Early in the study the cardiac output window was left in place on the screen for long periods after cardiac output related activities were complete. Once they were aware of the tradeoffs between windows, anesthesiologist users adapted to this new task of managing serial displays.

In addition, the determination of cardiac output in the new system takes considerably longer than it did in the old one. Multiple cardiac output readings could be obtained in a short period with the old system while the new one has a very slow measurement cycle time.

Screen Organization

The order and color of traces on the screen is flexible. Users may configure trace order in an elaborate menu which specifies relative priority. Fortuitously, when three blood pressures and cardiac output are connected to the system, arranged together, and the pressures placed on the graph window, the blood pressure graph window overlaps exactly these four areas on screen. This means that the blood pressure traces and other traces (end-tidal CO_2, oxygen saturation) are visible when the blood pressure graph window is on the screen. However, when only a single pressure is monitored (for some lung surgery cases), the priority management system places the other traces immediately below the single blood pressure trace. The blood pressure graph window then hides these traces from view. Anesthesiologist and technician users tried various methods of arranging traces so that none would be hidden by the blood pressure graph window. These included complete screen reorganization and sham modules.

In screen reorganization, the other traces were assigned higher priority than the blood pressure traces so they appeared above the pressure traces. When the scaled pressure window is on screen it's top edge begins at the level of the highest priority pressure trace shown on the scale; since the other traces are literally "above" the pressure traces, the scale fills the lower portion of the screen and the other traces are visible. Unfortunately, this scheme destroys the spatial dedication of traces that anesthesiologist and surgeon users expect and interposes unrelated trace groups between two related traces (blood pressure and electrocardiogram). For these reasons, the screen reorganization approach was abandoned.

A clever approach was the use of sham modules. Inserting pressure transducers reserves space for them on the screen, even if they are not connected to the patient. By placing modules in the system, technician users were able to "fool" the system into the desired configuration.

These strategies represent user efforts to tailor the device into a static, spatially dedicated device with fixed data display. Users expend substantial effort to preserve the fixed relationship between data items on the display screen.

DISCUSSION

Operators in high-risk process control settings can and do adapt to technologic change. We observed two broad classes of adaptation, *system tailoring* and *task tailoring*.

System tailoring is the configuration or modification of the new device and related devices to support user cognitive tasks. Most initial tailoring involves trying to make the new system look as much like the old as possible, since this is the easiest way to transfer knowledge about "how things work" from the old system to the new and because the users possess highly refined information processing strategies which depend on features of the old system. The use of redundant monitors is not simply a "backup" technique, but also represents a modification of the new system to maintain characteristics of the old by literally preserving components of the old system in the new. As time goes on users appear to develop confidence in the new components and to gradually get weaned away from the old. System tailoring may also involves exploiting system features in orthodox and unorthodox ways. The orthodox system tailoring is that supported by the device designers, e.g. the trace priority assignment. Unorthodox system tailoring involves approaches not anticipated by designers, e.g. sham modules insertion to preserve trace order. System tailoring actions may go on at any time but are usually heavily weighted to periods of setup.

Task tailoring is the modification or alteration of user activities to accommodate new devices. The goal of task tailoring is to maintain critical functions necessary to achieve the goals of operation. When system tailoring is limited or unsuccessful, users are forced to tailor their tasks. In the most simple form, they add new tasks to their collection. Users learn how to manipulate the serial data display of cardiac output and blood pressure graph windows in order to preserve the flow of high reliability data and they add this device tending task to their activities. These data management tasks occur during critical periods (e.g. coming off bypass) where user cognitive workload is high, a hallmark of clumsy automation. There may also be a more complex task tailoring involving the way users gather and manipulate data; with slower cardiac output determinations and the elimination of scaled pressure waveforms during cardiac output determination, users have an incentive to measure cardiac output less frequently and to develop operating strategies which make less use of output.

System tailoring can usually be developed and refined over a short learning period to achieve a locally optimal arrangement. With devices which can save configuration information, the costs of system tailoring are borne once and, so long as the technical cadre with configuration know how is maintained, can be accomplished with little effort. As time passes, the tailoring gives way to a new routine system. Encoding this collection of details is usually described as 'standard operating procedures' or 'the way we've always done things' and comprises a *ritual*, a collection of actions compiled and performed together but separate from the motivations and purposes which gave rise to them. System tailoring is not limited to automated devices. Anesthesiologists do a great deal of system tailoring to reduce workload, for example drawing up drugs in syringes well before the anesthetic begins. The point is that automated devices constrain system tailoring in specific and complex ways.

Task tailoring, on the other hand, is a continuing operator demand. Added tasks do not, at least in our system, go away, although users become progressively more efficient at accomplishing them. Tailored tasks become permanent fixtures of the work environment. Significantly, the task tailoring we observed was prominent during critical hi-tempo periods. Periods of activity and criticality coincide in this domain, as they do in others, and this tends to concentrate user tasks and task tailoring at these junctions. This may be an intrinsic feature of high consequence, high complexity domains: new technology impacts most directly on crucial periods with high workload which in turn provides the motivation for system and task tailoring by users.

Introducing automation into high reliability environments impacts the work of operators in specific ways, ways related to the tasks of the operators rather than to the technology *per se*. Operators demonstrate sophisticated approaches to tailoring their systems and their tasks for routine operations. They work to accommodate technology smoothly. Paradoxically, the operators' work to tailor the technology may make it appear smooth, hiding the clumsy automation from designers.

Introducing new technology gives rise to system and task tailoring by users. But tailoring, once complete, may be invisible. System tailoring becomes part of 'standard operating procedures'. The tailored and untailored tasks may become indistinguishable as operation of the devices becomes skillful and interwoven with other tasks. Observing task tailoring *as it occurs* can bring into sharp focus user information processing and cognitive strategies. It is this information which is essential to the designers wishing to avoid clumsy automation.

ACKNOWLEDGEMENTS

This research was sponsored in part by the Aerospace Human Factors Division of the NASA Ames Research Center under grant NCC2-592 and by The Ohio State University Department of Anesthesiology. We are grateful to the residents, faculty, and technicians of the Department for their generous assistance and guidance.

REFERENCES

1. Norman, D.A., and Draper, S.W., USER CENTERED SYSTEM DESIGN: NEW PERSPECTIVES ON HUMAN-COMPUTER INTERACTION. Lawrence Erlbaum, Hillsdale, NJ, 1986.

2. Wiener, E.L., "Human Factors of Advanced Technology ("Glass Cockpit") Transport Aircraft", TECHNICAL REPORT 117528, NASA, Washington, D.C., 1989.

3. Wiener, E.L., "Field Studies in Automation", In Norman, S. and Orlady, H.W. Ed.s, FLIGHTDECK AUTOMATION: PROMISES AND REALITIES. NASA Ames Research Center, Moffett Field, CA, 1989.

GUIDANCE FOR HUMAN INTERFACE WITH ARTIFICIAL INTELLIGENCE SYSTEMS

Scott S. Potter and David D. Woods

Cognitive Systems Engineering Laboratory
Department of Industrial and Systems Engineering
The Ohio State University
Columbus, Ohio 43210

Research and experience with artificial intelligence (AI) systems has shown that the interaction of the intelligent system with human users and problem solvers is a critical element in the success and effectiveness of AI system development for real world applications[1]. Performance breakdowns can occur, for example, in situations where the intelligent system interface does not support the problem solving approach of the human operator[2]. Thus, there is a need to integrate human and machine problem solvers into an effective cooperative system[3]. This requires serious consideration of the human interface to AI systems during the design of intelligent systems.

A body of knowledge and guidance about how to integrate intelligent computer power and human practitioners has recently begun to accumulate. Empirical studies of human-human cooperative problem solving[4,5], empirical studies of human-intelligent computer cooperation[6], new research concepts for intelligent support systems[7,8] have contributed to the growth of this body of knowledge. In addition, systems builders and users, who have realize how poor human-intelligent system interfaces can retard cooperative problem solving, are experimenting with new ideas for more sophisticated interfaces to AI systems[9].

More effective AI systems can be developed if we collect, organize, and meaningfully deliver this knowledge to AI system designers[10]. However, there are several obstacles to meeting this objective. First, the state of research on effective human-intelligent computer interaction and cooperation is diffuse. There is a need to gather together, integrate, and assess the research results.

Second, there are cases of intelligent system development where designers and users are trying out new ideas about the human interface to AI systems, especially within NASA. Examining specific cases of both successful and unsuccessful AI system development with respect to human interface capabilities is a critical activity[11]. Collecting and assessing this experience will help expand and clarify the research base on what is effective human-intelligent computer cooperation.

Once integrated, this knowledge base will prove to be immature. There are gaps, ambiguities, and contradictions in the literature and practical experience. Thus, third, there is a need to conduct empirical studies that examine specific concepts about human-intelligent system cooperation related to actual cases of AI system development.

Fourth, one of the fundamental points of research on human-machine cooperative problem solving is that the concepts for how the machine will assist the person can strongly constrain the architecture and design of the machine itself[2]. In the typical design paradigm, one first develops (or independently develops) an autonomous machine problem solver and, only then, one thinks about how the person will use the machine to achieve better performance. Generally, the result has been that the design of the machine has not made allowances for features that turn out to be critical for people to make effective use of the system's capabilities[6]. It is critical, at the design concept stage, to consider how the person will use the machine to achieve better performance so that the inter-constraints between human interface design requirements and intelligent system design requirements can both be satisfied.

This means that a dialogue is needed between researchers in AI (whose research question is how to build better performing machines) and researchers in human-intelligent computer interaction (whose research question is how to use machine power to assist human problem solving). Understanding effective human-intelligent computer interaction is incomplete if it cannot be achieved through practical AI techniques and tools that are available for the development of real world systems which include AI. Consequently, there is a need to consider the interaction between concepts for more effective human-intelligent computer interaction, their implications about aspects of AI systems, and current techniques for building real world AI systems.

Fifth, research results alone do not constitute good advice for designers. The problem of preparing effective guidelines for designers and delivering that guidance in a form that can be used by designers (aiding design) is a substantive problem regardless of the topic of the guidance. One has only to look at existing guideline documents in the area of human-computer interaction to find many examples that have proven less than satisfactory[12,13]. Thus, there is the need to examine how AI systems are designed[14] in order to deliver the right kind of knowledge in a form that designers can really use.

We are beginning a research effort to collect and integrate existing research findings about how to combine computer power and people, including problems and pitfalls as well as desirable features. The goal of this research project is to develop guidance for the design of human interfaces with intelligent systems. Fault management tasks in NASA domains are the focus of the investigation. Research is being conducted to support the development of guidance for designers that will enable them to take human interface considerations into account during the creation of intelligent systems.

The research will examine previous results, NASA cases of AI system development, and conduct new studies of human-intelligent system cooperation focusing on issues such as: (1) how to achieve effective advice, (2) how to create a shared representation of the problem domain, (3) how to provide support for problem solving in situations requiring adaptation to unanticipated events, (4) what are appropriate levels of supervisory control, (5) the need for reasoning strategies consistent with those of the human operator and (6) what kinds and forms of explanation will support human-intelligent system cooperation.

The body of results on what interface and AI system capabilities support effective human-AI system cooperation in fault management tasks will be used to develop guidance for designers. The goal is to help designers take human interface considerations into account during the creation of intelligent systems. The results will provide advice about what kinds of information produced by an intelligent system should be made available to its human partners and advice about how to organize and display the intelligent system's situation assessment and response plan as well as information on the underlying process itself.

References

1. Hollnagel, E., Mancini, G., and Woods, D. (Eds.), INTELLIGENT DECISION SUPPORT IN PROCESS ENVIRONMENTS. Springer-Verlag, New York, 1986.

2. Roth, E. M. and Woods, D. D., "Cognitive task analysis: An approach to knowledge acquisition for intelligent system design", in G. Guida and C. Tasso (Eds.), TOPICS IN EXPERT SYSTEM DESIGN, North Holland, New York, 1989.

3. Woods, D. D. and Roth, E. M., "Cognitive Systems Engineering", In M. Helander (Ed.), HANDBOOK OF HUMAN-COMPUTER INTERACTION, North-Holland, New York, 1988, pp. 1-43.

4. Coombs, M. and Alty, J., "Expert systems: An alternative paradigm", INTERNATIONAL JOURNAL OF MAN-MACHINE STUDIES, 20, 1984, pp. 21-43.

5. Carroll, J. M. and McKendree, J., "Interface design issues for advice-giving expert systems", COMMUNICATIONS OF THE ACM, 30, 1987, pp. 14-31.

6. Roth, E. M., Bennett, K. B., and Woods, D. D., "Human interaction with an 'intelligent' machine", INTERNATIONAL JOURNAL OF MAN-MACHINE STUDIES, 27, 1987, pp. 479-525.

7. Woods, D. D. and Elias, G., "Significance messages: An integral display concept", IN PROCEEDINGS OF THE HUMAN FACTORS SOCIETY, 32ND ANNUAL MEETING, The Human Factors Society, Santa Monica, CA, 1988.

8. Fischer, G., Lemke, A. and Mastaglio, T., "Using critics to empower users", In PROCEEDINGS OF THE CHI'90 HUMAN FACTORS IN COMPUTING SYSTEMS CONFERENCE, Association for Computing Machinery, New York, 1990.

9. Muratore, J. F. et al., "Real time expert system prototype for Shuttle mission control", PROCEEDINGS OF THE 2ND ANNUAL WORKSHOP ON SPACE OPERATIONS, AUTOMATION AND ROBOTICS, NASA, 1988

10. Malin, J. T., "Framework for developing ICAPS (Intelligent Computer-Aided Problem Solving) systems for space operations", AAAI SPRING SYMPOSIUM ON KNOWLEDGE BASED HUMAN-COMPUTER COMMUNICATION, AAAI, 1990.

11. Remington, R. W. and Shafto, M. G. "Building human interfaces to fault diagnostic expert systems: I. Designing the human interface to support cooperative fault diagnosis." Workshop on Human-Computer Interaction in Aerospace Systems, CHI'90 Human Factors in Computing Systems Conference, SIGGRAPH, ACM, 1990.

12. Smith, S. L., "Standards versus guidelines for designing user interface software", In M. Helander (Ed.), HANDBOOK OF HUMAN-COMPUTER INTERACTION, North-Holland, New York, 1988, pp. 877-889.

13. Woods, D. D. and Eastman, M. C., "Integrating principles for human-computer interaction into the design process", In PROCEEDINGS OF THE IEEE INTERNATIONAL CONFERENCE ON SYSTEMS, MAN, AND CYBERNETICS, IEEE, 1989.

14. Malin, J. T. and Lance, N., "Process in construction offailure management expert systems from device design information", IEEE TRANSACTIONS ON SYSTEMS, MAN, AND CYBERNETICS, SMC-17 (11), 1987, pp. 956-967.

68

SPACE HUMAN FACTORS

DEVELOPMENT OF BIOMECHANICAL MODELS FOR HUMAN FACTORS EVALUATIONS

Barbara Woolford
Man-Systems Division
Johnson Space Center
Houston, Texas 77058

Abhilash Pandya
James Maida
Lockheed Engineering and Sciences Company
2400 NASA Road 1 Houston, Texas 77058

ABSTRACT

Previewing human capabilities in a computer-aided engineering mode has assisted greatly in planning well-designed systems without the cost and time involved in mockups and engineering models. To date, the computer models have focused on such variables as field of view, accessibility and fit, and reach envelopes. Program outputs have matured from simple static pictures to animations viewable from any eyepoint. However, while kinematics models are available, there are as yet few biomechanical models available for estimating strength and motion patterns. Those, such as Crew Chief, that are available are based on strength measurements taken in specific positions. Johnson Space Center is pursuing a biomechanical model which will use strength data collected on single joints at two or three velocities to attempt to predict compound motions of several joints simultaneously and the resulting force at the end effector. Two lines of research are coming together to produce this result. One is an attempt to use optimal control theory to predict joint motion in complex motions, and another is the development of graphical representation of human capabilities. This presentation describes the progress to date in this research.

COMPUTER MODELING OF HUMAN MOTION

Computer aided design (CAD) techniques are now well established, and have become the norm in many aspects of aerospace engineering. They enable analytical studies, such as finite element analysis, to be performed to measure performance characteristics of the aircraft or spacecraft long before a physical model is built. However, because of the complexity of human performance, CAD systems for human factors are not in widespread use. The purpose of such a program would be to analyze the performance capability of a crew member given a particular environment and task. This requires the design capabilities to describe the environment's geometry and to describe the task's requirements, which may involve motion and strength. This in turn requires extensive data on human physical performance which can be generalized to many different physical configurations. PLAID is developing into such a program. Begun at Johnson Space Center in 1977, it started out to model only the geometry of the environment. The physical appearance of a human body was generated, and the tool took on a new meaning as fit, access, and reach could be checked. Specification of fields of view soon followed. This allowed PLAID to be used to predict what the Space Shuttle cameras or crew could see from a given point. An illustration of this use is shown in Figures 1a and 1b. Figure 1a was developed well before the mission, to show the planners where the EVA astronaut would stand while restraining a satellite manually, and what the IVA crewmember would be able to see from the window. Figure 1b is the view actually captured by the camera from the window. However, at this stage positioning of the human body was a slow, difficult process as each joint angle had to be specified in degrees.

REACH

The next step in enhancing PLAID's usefulness was to develop a way of positioning bodies by computer simulation, rather than by the engineer's inputs of joint angles. The University of Pennsylvania was contracted to perform this work. Korein (1985) developed an inverse kinematic solution for multijointed bodies. This enabled the engineer to position one "root" of the body (feet in foot restraint, or waist or hips fixed) in a specified location, and then specify what object or point in the workspace was to be touched by other parts of the body (such as place the right hand on a hand controller, and the left on a specific switch). The algorithm then attempted to find a position which would allow this configuration to be achieved. If it was impossible to achieve, due to shortness of arms or position of feet, a message would be presented giving the miss distance. This feedback enabled the engineer to draw conclusions about the suitability of the proposed body position and workspace.While this reach algorithm is extremely useful for body position, it does not enable an analyst to check an entire workspace for accessibility without specifying a large number of "reach to" points. This need has been recently met by a kinematic reach algorithm. The user specifies which joints to exercise. The algorithm then accesses an anthropometry data base giving joint angle limits, positions the proximal joint at its extreme limit, and steps the distal joint through its range of motion in a number of small steps, generating a contour. The proximal joint is moved an increment, and the distal joint swung through its range of motion again. This process continues until the proximal joint reaches its other extreme limit. A three dimensional set of colored contours is thus generated which can be compared to the workstation and conclusions can be drawn. An example of this is shown in Figures 2a and 2b.

In Figure 2a, a fifth percentile female is placed at the proposed foot restraint position intended to provide an eyepoint 20" from the workstation. In this position, her reach envelope falls short of the workstation. Figure 2b shows the same body and reach envelope positioned with a 16" eyepoint, in which case the woman can reach the workstation.

ANIMATION

Human performance is not static. To do useful work, the crewmembers must move their hands at least, and frequently their bodies, their tools, and their equipment. While this can be captured in a sequence of static pictures, animations are much preferred because they show all the intermediate points between the static views. Originally, PLAID animations were created by having the analyst enter every single step individually. This was highly labor intensive, and prohibitive in cost for any but the most essential conditions. However, an animation capability was created that allowed the user to input only "key frames". (A key frame is one where the velocity or direction of motion changes.) The software then smoothly interpolates 20 or 30 intermediate frame scenes, showing the continuous movement. This has many applications for both the Shuttle program and for the Space Station Freedom (SSF) program. For example, in determining where interior handholds were needed, an animation was created showing the process of moving an experiment rack from the logistics module to the laboratory module. Clearances, collisions, and points of change could be identified from the videotape. However, while the tape showed the locations for the handholds, it could not give information as to the loads the handholds would have to bear. Thus a project to model strength was begun.

BIOMECHANICS MODELING

Upper Torso Strength

Using a Loredan, Inc. LIDO dynamometer (Fig.3), single joint strength data was collected for the shoulder, elbow, and wrist of one individual. The data was collected in the form of (velocity, position, strength) triplets. That is, the dynamometer was set to a selected speed, ranging from 30 deg/sec to 240 deg/sec in 30 deg/sec increments. For that speed, the subject moved his joint through its entire range of motion for the specified axis (abduction/adduction, flexion/extension). Data was collected every five degrees and a polynomial regression equation fit to the data for that velocity. The velocity was changed, and the procedure repeated. This resulted in a set of equations giving torque in foot-pounds as a function of velocity and joint angle, for each joint rotation direction. Figure 4 shows shoulder flexion torque over a range of angles, parameterized by velocity. Figure 5 shows the data points and the equation fit for elbow flexion/extension over the range of motion at 90 deg/sec.These regression equations were stored in tables in PLAID. To predict total strength exerted in a given position or during a given motion, the body configuration for the desired position (or sequence of positions) is calculated from the inverse kinematics algorithm. For example, the task used so far in testing is ratchet wrench push/pull. This task is assumed to keep the body fixed, and allow movement only of the arm. (As more strength data is obtained, the tasks can be made more complex.) A starting position or the wrench is established, and the position of the body is set. The angles of the arm joints needed to reach the wrench handle are then calculated. A speed of motion, indicative of the resistance of the bolt, is specified. The tables are searched, and the strength for each joint, for the given velocity, at the calculated angle, is retrieved. The direction of the force vector is calculated from the cross products of the segments, giving a normal to the axis of rotation in the plane of rotation. Once all these force vectors are obtained, they are summed vectorially to calculate the resultant end effector force. Currently the program displays the force for each joint and the resultant end effector force, as illustrated in Figure 6. The ratchet wrench model rotates accordingly for an angular increment. This requires a new configuration of the body, and the calculation is repeated for this new position. A continuous contour line may be generated which shows the end effector force over the entire range of motion by color coding. The model will be validated this summer. A ratchet wrench attachment for a dynamometer has been obtained, and an Ariel Motion Digitizing System will be used to measure the actual joint angles at each point in the pushing and pulling of the wrench. This will provide checks on both the validity of the positioning algorithms and of the force calculations. When this simple model is validated, more complex motions will be investigated. The significance of this model is that it will permit strengths to be calculated from basic data (single joint rotations) rather than requiring that data be collected for each particular motion, as is done in Crew Chief (Easterly, 1989). A synthesis of the reach envelope generating algorithm and the force calculations has been achieved. The analyst can now generate reach contours which are color coded to show the amount of force available at any point within the reach envelope.

Effects of Gravity-Loading on Vision

Human vision is another important parameter being investigated in conjunction with human reach and strength. Empirical data relating maximum vision envelopes vs gravity loading have been collected on several subjects by L. Schafer and E. Saenz. This data will be tabularized in a computer readable form for use in man-modeling. Preliminary software design has begun on a vision model which will utilize this vision data to simulate a period of Space Shuttle launch where gravity loading is a major factor.

This model will be able to dynamically display the vision cone of a particular individual as a function of gravity force and project that cone onto a workstation to determine if all the appropriate gauges/ displays can be seen.

APPLICATIONS

The biomechanical models, combined with geometric and dynamic modeling of the environment, have two major applications. The first is in equipment design. Frequently the strength or force of a crewmember is a key parameter in design specifications. For example, a manually operated trash compactor has recently been built for the Shuttle for extended duration (10-14 days) operations. This is operated by a crew member exerting force on the handle to squeeze the trash, and is seen as an exercise device as well as a trash compactor. The two key specifications needed were: how much force can a relatively weak crewmember exert, so the right amount of mechanical amplification can be built in; and how much force could a very strong crewmember exert, so the machine could be built to withstand those forces. When the biomechanical model is completed, questions such as these can be answered during the design phase with a simulation, rather than requiring extensive testing in the laboratory. In addition, the size of the equipment can be compared visually to the available storage space, and the location of foot restraints relative to the equipment can be determined. Other equipment design applications include determining the specifications for exercise equipment, determining the available strength for opening or closing a hatch or door, and determining the rate at which a given mass could be moved. The second application for a strength model is in mission planning. Particularly during extravehicular activities (EVA), crewmembers need to handle large masses such as satellites or structural elements. A complete dynamics model would enable the mission planners to view the scenes as they would be during actual operations, by simulating the forces which can be exerted and the resulting accelerations of the large mass.

FUTURE PLANS

Currently the only motion modeled is a rotational motion of a wrench using only the arm, not the entire body. One step in developing a useful model is to allow the software already available for animating motion to be used to define any motion and then permit calculation of the strength available, taking the entire body into account. This is a major step to accomplish, because of the many degrees of freedom in the entire human body. Research at the University of Pennsylvania has investigated the use of "comfort models" for predicting path trajectory. Badler, Lee, Phillips, and Otani (1989) have discussed in some detail the effects that varying weights have on trajectories for moving an object from one point to another. Using the Ariel tracking system, this hypotheses can be tested in the lab. In order to consider the entire body in strength analysis, empirical strength data must be collected. The Anthropometry and Biomechanics Lab at Johnson Space Center is beginning work on this project. To date, shoulder and arm strength measurements have been collected on a number of subjects. This data must be made available through the program's data base so that 5th percentile, or median, or 95th percentile strengths can be examined. This will involve another layer of data in the data base. The strength measurements for the entire body, especially torso and legs, are needed. Collecting these strength data for the individual joints at a number of angular positions and angular velocities will be an ongoing project for some time. However, efforts have been made to automate data entry and reduction, which will result in easier data collection. Finally, the most important step is to validate the strength data. An assembly for collecting forces and angles for a ratchet wrench operation is available, and will be used to validate the compound motion of the arm. Movement of the entire body will be validated after the original data is collected, equations fit, and predictions of strength made.

BIBLIOGRAPHY

Badler, N.I., Lee, P., Phillips,C. and Otani, E.M. "The JACK Interactive Human Model". In "Concurrent Engineering of Mechanical Systems, Vol. 1", E.J. Haug, ed. Proceedings of the First Annual Symposium on Mechanical System Design in a Concurrent Engineering Environment, University of Iowa, Oct. 24-25, 1989.

Easterly, J. 'CREW CHIEF: A Model of a Maintenance Technician", AIAA/NASA Symposium on the Maintainability of Aerospace Systems, July 26/27, 1989; Anaheim, CA.

Korein, James U. 'A Geometric Investigation of Reach', MIT Press, Cambridge, MA; 1985.

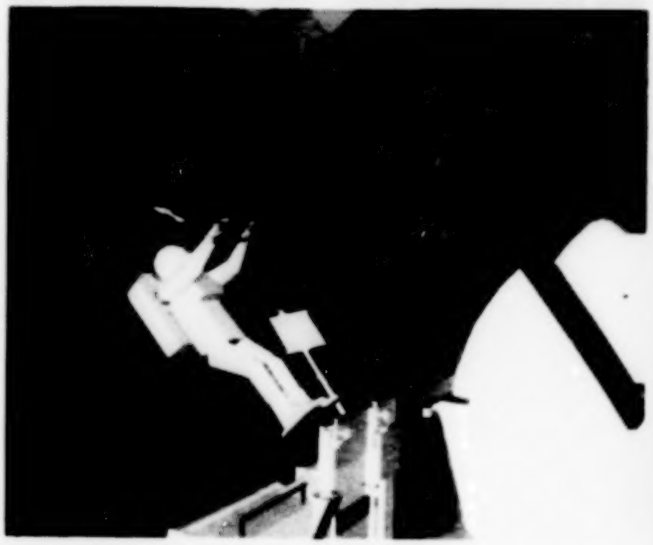

Figure 1a. PLAID rendition of crewmember restraining payload, from pre-mission studies.

Figure 1b. Photo taken during mission from aft crew station.

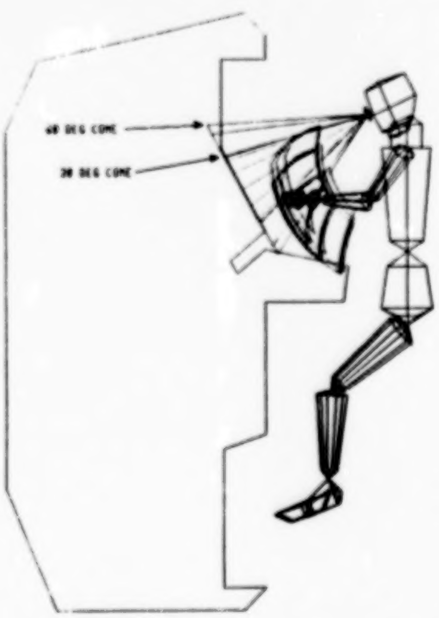

60 DEG CONE
30 DEG CONE
SIDE VIEW

Figure 2a. Fifth percentile female positioned at workspace with 20" eyepoint. Reach contours miss the workstation.

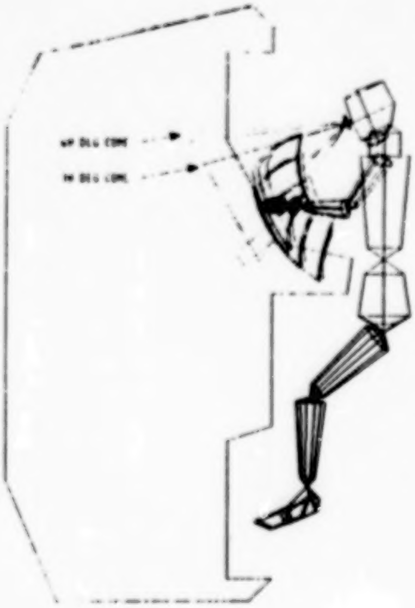

60 DEG CONE
30 DEG CONE
SIDE VIEW

Figure 2b. Fifth percentile female positioned at workspace with 16" eyepoint. Reach contours touch workstation.

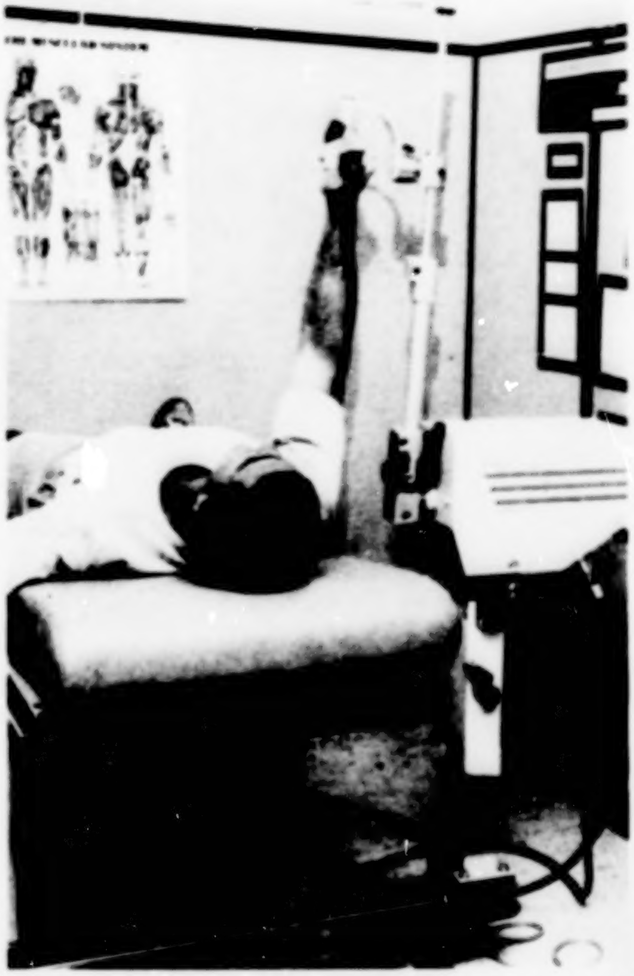

Figure 3. Collecting shoulder strength data with LIDO dynamometer.

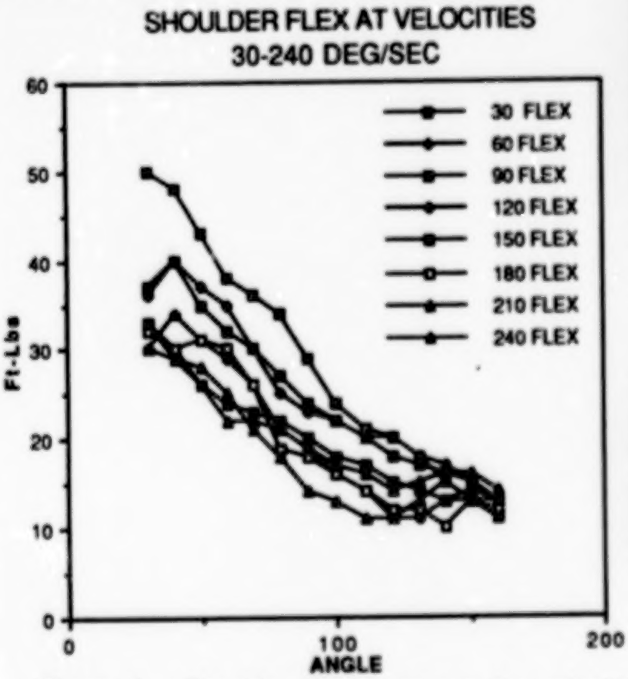

Figure 4. Shoulder flexion torque for velocities ranging from 30^0/sec to 240^0/sec

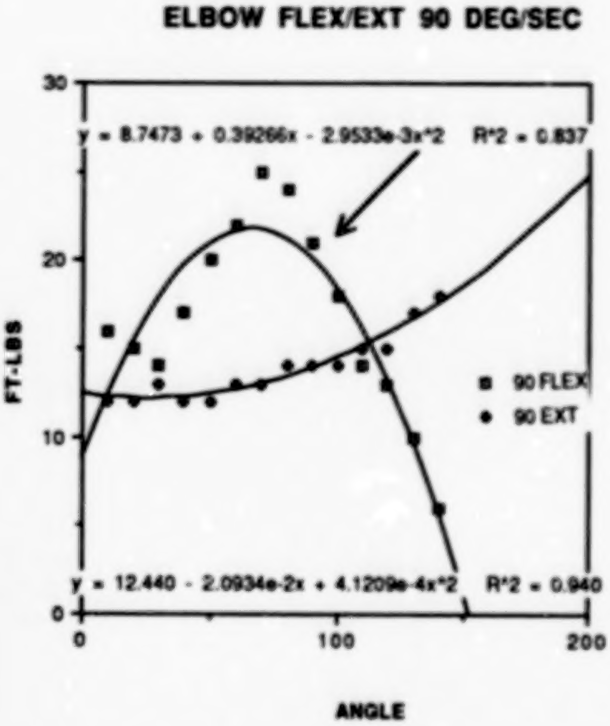

Figure 5. Raw data and regression equations for elbow flexion and extension at 90^0/sec.

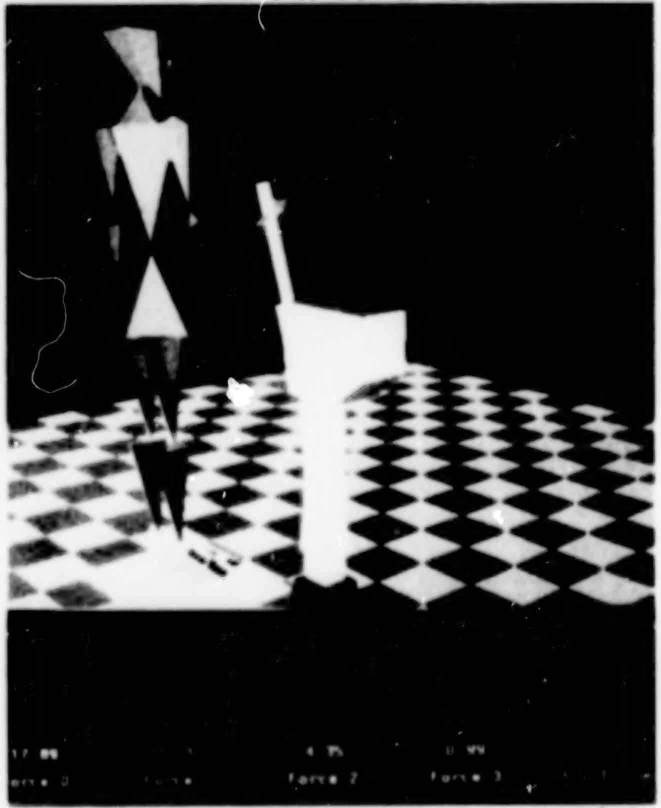

Figure 6. Body model exerting force on ratchet wrench. Joint forces and effective force at wrench are displayed as bar graphs beneath the picture.

RECOVERY FROM AN ANOMALOUS THRUSTER INPUT DURING A SIMULATED DOCKING MANEUVER

Adam R. Brody
Sterling Software
MS 262-2
NASA Ames Research Center
Moffett Field, CA. 94035-1000

Stephen R. Ellis
MS 262-2
NASA Ames Research Center
Moffett Field, CA. 94035-1000

ABSTRACT

An experiment was performed in the Space Station Proximity Operations Simulator at the NASA Ames Research Center. Five test subjects were instructed to perform twenty simulated remote docking maneuvers of an orbital maneuvering vehicle (OMV) to the space station in which they were located. The OMV started from an initial range of 304.8 m (1000 ft) on the space station's negative velocity vector (-V-bar). Anomalous out-of-plane thruster firings of various magnitudes (simulating a faulty thruster) occurred at one of five ranges from the target. Initial velocity, range of anomalous burn, and magnitude of anomalous burn were the factors varied. In addition to whether the trial was successful, time and fuel to return to a nominal trajectory, total mission duration, total fuel consumption (Δv), and time histories of commanded burns were recorded. Analyses of the results added support to the hypothesis that slow approach velocities are not inherently safer than their more rapid counterparts. Naive subjects were capable of docking successfully at velocities faster than those prescribed by the "0.1% Rule" even when a simulated faulty thruster disturbed the nominal trajectory. Little to no justification for slow approach velocities remains from a human factors standpoint.

INTRODUCTION

The docking of two spacecraft is a complicated task whose failure could result in the loss of mission, vehicle, or crew. Spacecraft have typically been flown at small relative velocities in rendezvous and docking maneuvers both to increase safety margins in the event of an incorrect burn, and to minimize plume impingement and fuel consumption. Current astronauts are instructed in the use of a "0.1% rule" which suggests that the approach velocity be no greater than 0.1% of the range to the target. (At a range of 1000 ft, the approach velocity would be 1 ft/s. After 100 s, the vehicle would arrive at a range of 900 ft and the rate would be reduced to 0.9 ft/s.)[1] By decreasing the relative velocity with which one vehicle approaches another, demands upon reaction time are relaxed and workload is simultaneously (and proportionately) reduced as the number of required inputs per unit time decreases. However, surveys of aircraft and workload literature reveal that too low a workload may be just as dangerous as too high a workload.[2,3] Small approach velocities produce long mission durations where inactivity may lead to reduced attention, or sustained vigilance may lead to excessive fatigue. Long mission durations also may prove to be inordinately expensive in an operational space station era in terms of the time the crew are using to dock and not performing other duties. (However, fuel costs may obscure any such advantage for nominal missions.) Previous research revealed no statistically significant increase in failure rate with increased velocity; failure rate was more dependent upon a subject's risk profile than the velocity at which his/her docking maneuver began.[4, 5]

In general, very little human factors research in the area of piloting space maneuvers has been documented in the United States space program.[4-16] Analytical engineering tests have been used to generate rules of thumb and verify strategies from a systems point of view without regard to man-in-the-loop considerations. This study is part of a series seeking to rectify that situation and is directed toward developing a unified theory and comprehensive database for human performance aspects of spacecraft control.

Current and future work is concerned with determining the feasibility of expanding the operational performance envelope to include more rapid dockings at higher average velocities without increasing the probability of failure. The Soviets have also expressed a desire for manual control to "operate in [a] wider range."[17] Quicker dockings are important not only for increasing productivity but also for improving the likelihood of a successful rescue of a stranded crewperson or spacecraft low on consumables. In nominal missions, saving time at the expense of fuel may not be cost effective. However, contingencies may arise when the cost of time is extreme as in a rescue operation. One goal of this line of research is discovering the fastest safe docking times should rapid docking be required.

METHODS AND APPARATUS

The Space Station Proximity Operations Simulator at NASA Ames Research Center is a real-time flight simulator with which researchers have been studying docking maneuvers and other proximity operations for several years. It consists of three windows on which computer graphics images of stars and orbiting vehicles are presented, a 3-degree-of-freedom (DOF) hand controller, and other assorted controls and displays.[7, 14] The windows face the minus velocity vector (-V-bar) of a space station in a 270 nm orbit about the Earth. From this perspective, X is positive through the operator's back, Y is positive to the left, and Z is positive down.

Five test subjects (3 male, 2 female) each performed 20 simulated docking maneuvers commencing from 304.8 m (1000 ft) on the -V-bar. The trials began at one of five initial velocities: 0.3, 0.9, 1.9, 2.9, 3.6 m/s. A faulty thruster was simulated during each run by an anomalous out-of-plane burn of a preestablished magnitude at a preestablished range. The magnitude of the anomaly was one of five Δvs (0.0, 0.2, 0.5, 0.8, 1.0 m/s) and occurred at one of five ranges (20, 45, 85, 125, 150 m) from the target. A response surface methodology arrangement was used to reduce the total number of initial conditions from 5 x 5 x 5 = 125 to 20.[18] The subjects were cautioned to be wary of an unexpected incident but until the first trial containing an anomaly, did not know what form the anomaly would take. Each subject started from the following 20 initial conditions, but in different random orders.

Initial Velocity (m/s)	Range (m)	Magnitude (m/s)
1.9	85	.5
.9	45	.8
1.9	85	.5
1.9	20	.5
3.6	85	.5
.9	125	.8
.9	45	.2
2.9	45	.8
1.9	85	1.0
2.9	45	.2
2.9	125	.2
1.9	85	.5
1.9	85	.5
1.9	85	0.0
1.9	85	.5
1.9	150	.5
.3	85	.5
2.9	125	.8
1.9	85	.5
.9	125	.2

A successful docking was operationally defined as satisfying the following range and rate conditions upon contact with the space station. At a range of 2 m from the station's center of mass axial velocity must be no greater than 0.15 m/s, up/down and right/left range no greater than 0.23 m, and up/down and right/left velocity no greater 0.6 m/s.[19] In addition to whether the docking was successful, total mission duration, fuel consumption (measured in Δv), time out-of-plane ("awaytime"), out-of-plane fuel ("y delta V"), and temporal/spatial histories of pilot burns were recorded for each simulated mission. Also, two derived quantities known as "reserve time" and "radial delta V", were obtained by subtracting a reference time/fuel from the mission duration/fuel consumption values.[4-5]

RESULTS

Figure 1 shows the burn history versus range on the x-axis for a typical trial for one of the subjects. The initial velocity was 0.9 m/s, and an anomalous burn of 0.8 m/s occurred at an x-range of 125 m. For this trial, total mission duration was 498 s, total velocity increment (delta V) was 7.51 m/s, awaytime was 249 s and Y delta V was 1.88 m/s.

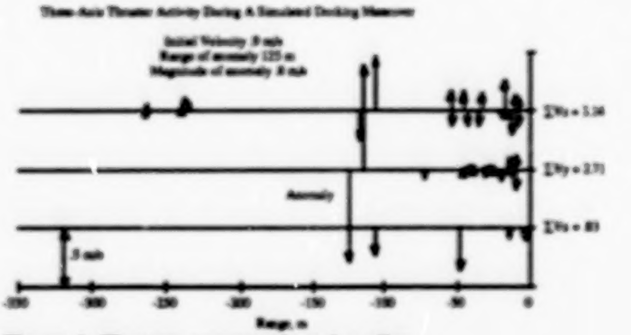

Figure 1: Thruster commands, naive pilot

Figure 2 shows an expert pilot's response to the same initial conditions. Mission duration, delta V, awaytime, and Y delta V quantities were all lower than the test subject's with values of 380 s, 4.92 m/s, 9 s, and 1.32 m/s respectively. The expert pilot's superior response is more likely due to several year's intensive experience with simulated spacecraft docking maneuvers than any innate ability.

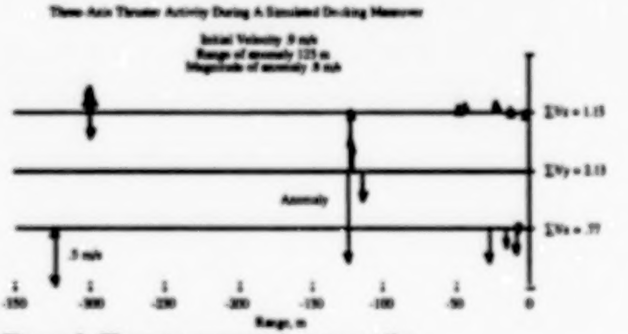

Figure 2: Thruster commands, expert pilot

While both trials were successful, the expert used fuel more effectively and efficiently as evidenced by the lower total velocity increment and by the smoother, and less active, burn history plots. He also recovered from the anomaly in under 4% of the test subject's time and then focused on slowing down the vehicle to satisfy the final docking conditions. Also, while mission duration generally varies inversely with fuel consumption (more fuel is required to travel faster and reduce time), the expert managed to reduce overall time without expending additional fuel by using every burn efficiently and minimizing pilot-induced oscillations.

Multiple regression analyses were performed on the data to establish the existence of any statistically significant effects. Analyses were performed not only on the whole data but also on the data after points outside the semiinterquartile range (outliers) had been removed, and after data associated with unsuccessful attempts were removed. Initial velocity, range, magnitude and trial were the independent variables analyzed in each case.

As in earlier studies[4-5], two variables, "reserve time" and "radial velocity increment", were derived from the mission duration and delta V data since increases in initial velocity generally "force" the mission duration to decrease and the fuel consumption to increase. Reserve time was calculated by dividing the initial range by the initial velocity and subtracting this value from the measured mission duration. In this way, the effect of the initial velocity is somewhat removed from the measurement and what is left is the time the test subject reserved for herself to accomplish the task successfully. The radial velocity increment values were obtained by subtracting the starting and stopping Δv and the Y delta V from the total delta V.

Two other variables were created to evaluate the final 3-axis range and rate parameters as something besides the binary successful/unsuccessful. "Squared" was computed by summing the squares of the terminal range and rate values along the three axes. "Abs" is the sum of the absolute differences between the actual terminal range and rate values and those required for a successful docking.

$$\text{squared} = Y^2 + Z^2 + \text{Xrate}^2 + \text{Yrate}^2 + \text{Zrate}^2$$

$$\text{abs} = -((\text{abs}(Y) - .23) + (\text{abs}(Z) - .23) + (\text{abs}(\text{Xrate}) - .15) + (\text{abs}(\text{Yrate}) - .06) + (\text{abs}(\text{Zrate}) - .06))$$

Since the inclusion of outlying data points greatly compressed most of the data, these points were removed and regression analyses were recalculated. Removing outlying data points served to reduce the variance of the data and increased the likelihood of statistical significance. A list of all statistically significant effects from response surface analysis appears in table 1.

Table 1: Significant Effects

Dependent Variable	Significant Factor(s)	t-statistic	p
Total Data			
Mission Duration	init. vel.	-5.43	< .001
Velocity Increment	trial	-2.78	.006
Y Vel. Inc.	trial	-3.18	.002
Z Vel. Inc.	trial	-2.77	.007
	init. vel.	-2.12	.036
Squared	init. vel.	-2.08	.040
Abs.	init. vel.	2.35	.021
Without Outliers			
Mission Duration	init. vel.	-5.59	< .001
	trial	2.55	.013
Velocity Increment	init. vel.	3.93	< .001
	magnitude	3.16	.002
Y Vel. Inc.	magnitude	5.04	< .001
Reserve Time	init. vel.	2.30	.024
	trial	2.53	.013
Squared	magnitude	2.01	.047
	trial	-2.43	.018
Abs.	trial	2.69	.009
Successful Runs			
Mission Duration	init. vel.	-3.27	.002
Velocity Increment	magnitude	2.41	.020
Y Vel. Inc.	magnitude	2.15	.036
	trial	-2.22	.031
Z Vel. Inc.	magnitude	2.49	.016
Awaytime	magnitude	2.24	.029

T-Tests were performed between data collected from successful docking missions and those collected from unsuccessful missions. The only variable for which there was a statistically significant difference was trial (4.20, p < .001) whose average was 12 for the successful missions and 8 for the unsuccessful.

DISCUSSION

As in earlier studies without anomalies, mission duration was inversely related to initial velocity.[4-5] This relationship is not surprising considering that the faster one travels, the less time a trip of a given distance will take. The fact that this relationship was preserved when the anomalous thruster firings were included means that subjects did not slow down from fast initial velocities in order to recover from the "accident." Starting off at a high velocity caused the shortest mission durations despite the occurrence of anything unusual. Apparently, plenty of time was available for recovery even at an initial velocity as high as 3.6 m/s.

Removing the outliers, thereby decreasing the variance of the data, revealed a practice effect: trial became a significant factor determining mission duration. Some practice effect was expected but the scatter of all the raw data points obscured it. Removing the data associated with the unsuccessful runs eliminated the practice effect while maintaining the velocity effect. Since practice both increased the likelihood of success and decreased the mission duration, removing the unsuccessful runs also eliminated the long duration runs thereby eliminating a perceived practice effect when the data from the unsuccessful runs were removed.

Vehicles should pay for accelerating to, and decelerating from, higher velocities with higher fuel consumption (Δv). In the former study, there was a direct linear relationship between velocity increment and initial velocity as intuition would suggest. However, in the current experiment, delta V was solely a function of trial indicating a practice effect. Apparently, the inclusion of the anomalies destroyed the effect of velocity on Δv.

Delta V data without outliers not only show a velocity effect, but also indicate an effect based upon the magnitude of the anomalous burn and omit an effect based upon experience. Clearing out the spurious data left two expected relationships: the velocity increment increased with initial velocity and with magnitude of the anomaly. Removing the data collected from the unsuccessful missions left only the magnitude effect.

Awaytime was correlated with magnitude. That is, the larger the magnitude of the out-of-plane burn, the longer it took to recover to the same plane as the space station. This effect disappeared when the outliers were removed but existed when only the unsuccessful data were removed. Since awaytime is bounded on the bottom by 0, removing the high, outlying data points eliminated any chance for the high awaytimes to be associated with the high magnitudes.

Y delta V, like total delta V exhibited a practice effect when all of the data were included and had only a magnitude effect when the outliers were removed. However, unlike total Δv, Y delta V had an effect of trial when the data collected from the unsuccessful missions were ignored. The trial effect is only evident when the outliers are included in the calculation.

Squared and abs both displayed a velocity effect when all of the data were used and neither showed any main effects when the unsuccessful data were removed. Squared had both a magnitude and a trial effect when the outlying data were removed while abs had only a trial effect.

T-tests revealed only one statistically significant difference between the data collected from successful missions and those from the unsuccessful: subjects were more likely to have a successful mission toward the end of their experimental session. Although both squared and abs were derived from the range and rate parameters on impact, neither parameter was significantly different when calculated from a successful mission or an unsuccessful one. While both values exhibited a velocity effect implying that velocity had some impact on the accuracy of the docking, this effect was not related to success at all. Velocity played no role in the success of the mission. In further corroboration, the t-test performed on velocity had a statistic of 0 with a p value of 1 indicating a 0% assurance that the populations are distinct.

CONCLUSIONS

As in earlier studies, researchers were unable to justify utilization of the 0.1% rule or any other flight profiles requiring an arbitrarily slow approach velocity from a human factors point of view. Not only did faster approach velocities fail to decrease safety during nominal operations, the presence of an anomalous thruster firing during the mission did not alter this result. Examination of human factors considerations allows the operational flight envelope of a vehicle docking to a space station, or any other object, to be expanded. This permits more rapid and lower duration missions.

While engineering considerations, such as fuel consumption (cost), overwhelmingly demonstrate the value of slow missions, should fuel be made from waste water[19] or some other source thereby decreasing its cost, a least time solution would become a least cost solution as well. Also, for a vehicle and/or pilot with 10 minutes worth of consumables remaining, a 60 minute docking maneuver is not very helpful. An understanding of the fastest safe docking technique will always be necessary for contingencies that will inevitably arise. Highly trained NASA pilot-astronauts with a mandatory minimum 1000 hours jet experience should have no trouble exceeding the performance values measured here. The safe operating envelope of space vehicles can now be expanded providing the ability to rescue a crewmember or vehicle low on consumables.

REFERENCES

1. NASA Lyndon B. Johnson Space Center Mission Operations Directorate Training Division Flight Training Branch, "Rendezvous/Proximity Operations Workbook," RNDZ 2102, 1985.
2. Wiener, E. L. "Computers in the Cockpit: But What About the Pilots?," SAE Technical Paper 831546, 1983.
3. Wiener, E. L. "Beyond the Sterile Cockpit," Human Factors, Vol. 27(1), February 1985, pp. 75-90.
4. Brody, A. R. "Spacecraft Flight Simulation: A Human Factors Investigation Into the Man-Machine Interface Between an Astronaut and a Spacecraft Performing Docking Maneuvers and Other Proximity Operations," MIT S. M. Thesis, April 1987. (see also NASA-CR-177502, 1988.)
5. Brody, A. R. "The Effect of Initial Velocity on Manually Controlled Remote Docking of an Orbital Maneuvering Vehicle to a Space Station," 27th Aerospace Sciences Meeting, AIAA 89-0400, January, 1989. (see also "Evaluation of the '0.1% Rule' for Docking Maneuvers," Journal of Spacecraft and Rockets, Vol. 27(1), January-February 1990, pp. 7-8.)
6. Brody, A. R. "EivaN: A Forward-Looking Interactive Orbital Trajectory Plotting Tool for Use with Proximity Operations (PROX OPS) and Other Maneuvers Description and User's Manual," NASA-CR-177490, 1988.
7. Brody, A. R., "Modifications to the NASA Ames Space Station Proximity Operations (PROX OPS) Simulator," NASA-CR-177510, 1988.
8. Brody, A. R., Ellis, S. R., Grunwald, A. and Haines, R. F., "An Evaluation of Interactive Displays for Trajectory Planning and Proximity Operations," Proceedings of the Digital Avionics Systems Conference, San Jose, CA, Vol. 2, October 1988, pp. 542-547.
9. Ellis, S. R., and Grunwald, A. J., "A Visualization Tool for Planning Orbital Maneuvers: Design Philosophy and Preliminary Results," Proceedings of the 23rd Annual Conference on Manual Control, Cambridge, MA, June 1988.
10. Grumman Aerospace Corporation, "OMV On-Orbit Simulations Using the Grumman LASS in June, 1985 final report (revision 1)," August 1985.
11. Grumman Aerospace Corporation, "Simulating On-Orbit Satellite Maintenance & Servicing Part I--executive summary," August 1985.
12. Grumman Space Systems, "RMS Docking/Tracking Operations and EVA Truss Structure Assembly Using Advanced Controls and Displays Technology," Report No. SA-MSET-FR-8701, March 1987.
13. Grunwald, A. J. and Ellis, S. R., "Interactive orbital proximity operations planning system," Proceedings of the 1988 IEEE International Conference on Systems, Man, and Cybernetics, Peking, China, IEEE CAT 88CH2556-9, 1305-13-12, 1988.
14. Lee, E., and Wu, A. "Space Station Proximity Operations Workstation Docking Simulation," Sterling Software TN-87-7104-519-13, 1987.
15. Levin, E., and Ward, J. "Manned Control of Orbital Rendezvous," Manned Space Stations Symposium, Los Angeles, CA, April 1960.
16. McCoy, W. K. J., and Frost, G. G. "Predictor Display Techniques for On-Board Trajectory Optimization of Rendezvous Maneuvers," AMRL-TR-66-60, 1966.
17. Hillyer, M. S., "Cosmonauts Have the Right Stuff, Too: A Conversation with Vladimir Dzhanibekov," Space World, September, 1986, pp. 17-20.
18. Clark, C., and R. C. Williges. "Response Surface Methodology Central-Composite Design Modifications for Human Performance Research," Human Factors, Vol. 15(4), August, 1973, pp. 295-310.
19. NASA Lyndon B. Johnson Space Center, Proceedings of the Rendezvous and Proximity Operations Workshop, 1985.
20. Larson, V. R., and S. A. Evans. "Propulsion for the Space Station," IAF-86-182, October 1986.

CONSIDERATIONS FOR HUMAN-MACHINE INTERFACES IN TELE-OPERATIONS

Curt Newport

Ocean Systems Engineering, Inc.
7700 Leesburg Pike, Suite 200
Falls Church, Virginia 22044

ABSTRACT

Numerous factors impact on the efficiency of tele-operative manipulative work. Generally, these are related to the physical environment of the tele-operator and how well he interfaces with robotic control consoles. The capabilities of the operator can be influenced by considerations such as temperature, eye strain, body fatigue, and boredom created by repetitive work tasks. In addition, the successful combination of man and machine will, in part, be determined by the configuration of the visual and physical interfaces available to the tele-operator. The design and operation of system components such as full-scale and "mini"-master manipulator controllers, servo joysticks, and video monitors will all have a direct impact on operational efficiency. As a result, the local environment and interaction of the operator with the robotic control console have a substantial effect on mission productivity.

INTRODUCTION

The telerobotics field is wide ranging and encompasses work in several disciplines. Some of the typical uses of telerobotics systems today are in underwater inspection and work operations, inspections of nuclear power plants, the operation of remotely piloted vehicles (airborne RPVs), and the disposal of unexploded ordnance. But of all the contemporary applications of telerobotics, the subsea field is certainly one of the most diverse uses of telerobotics technology. As a result, the subsea field offers one of the most varied databases of operational experience for study, regarding all aspects of operator interfacing with robotic hardware.

Underwater telerobots must be designed specifically with the environment in mind. Both in space and underwater, the challenges to the designer are significant if they are to provide equipment that can accomplish the desired remote task on a cost effective basis. It is also not surprising that the existing subsea operator interfaces look very similar to their proposed space counterparts, given the similarities of the design drivers for both environments.

The designer of telerobotics workstation interfaces for the space environment faces much the same problems as anyone developing equipment for the underwater environment. The consoles must be compact, and capable of supporting remote work on a 24 hour basis. In addition, the console interfaces must be compatible with the operator, so they can work for extended periods with minimal fatigue. Also, consoles designed for both environments must offer the capability of positioning the robotic work system and operating its manipulators. Consequently, an examination of the subsea robotic field can help pinpoint areas of concern with regard to operational environments and the interfaces between the teleoperator and the work system.

The human factors related to remote work tasks must also be considered. Robotic work systems are hardware designed to be operated by humans. As a rule, humans work more efficiently if the local environment is comfortable and free of distractions. The same will be true of space based teleoperations. Therefore, the human factors and lessons learned by the design and operation of subsea telerobotic control consoles are directly applicable to space robotic operations. Most subsea robotics workstations incorporate many of the basic functions required of both on-orbit and ground-based space robotic control stations.

PHYSICAL AND ENVIRONMENTAL FATIGUE FACTORS

The efficiency of the human-machine interface is determined by two factors: the operator's local environment and the compatibility of the workstation to operator interface.

The Teleoperator Environment

The teleoperator is affected by their local environment as is any individual attempting a task requiring high degrees of concentration. Factors such as the ambient temperature, noise levels, seating orientation, and the mental state of the individual will take on a more important role than in less demanding situations. In addition, the length of time that the operator is required to concentrate his attention on remote tasks will greatly influence the onset and degree of operator fatigue.

There are several ways a teleoperator is affected by the local environment. Some of these concerns relate to the actual physical environment, while others have to do with the nature of the remote work being attempted. Operational stress is generally created in situations where the work task is extremely difficult, whether it be because the robotic system is being operated outside of its capabilities or has experienced some type of failure. Typically, even if manipulators or related equipment are only partially operational, the job will continue because of cost or criticality concerns. This type of situation is very trying for the operator because they are attempting a task outside of the nominal method of operation. However even with a fully operational system, complex work tasks can take their toll on the operator due to the required amount of concentration. Consequently, the onset and level of operator fatigue is directly related to task complexity. Manipulator operators can "burn out" after only 30 minutes during difficult operations, whereas in other cases with less demanding tasks, they can function productively for several hours.

Eye strain is another problem with extended teleoperations. Usually, the degree to which this is a factor is related to the length of operations, and the size and quality of the video image. Fuzzy or partially out of focus pictures can be irritating to look at for any length of time. Also, the speed with which the camera focus motors operate can contribute to this problem by making it difficult for the operator to get a clear picture on the video monitor. In this type of situation, considerable time is wasted as the camera lens continually runs past the optimum focus point by either being too near or too far. Cameras fitted with zoom lenses are notorious for this focusing problem.

As with any work environment, the ambient temperature must be comfortable and within the proper range of humidity. This concern is not only for comfort because robotic system microprocessors (as with most electronic equipment), only operate within definite temperature ranges. Related equipment such as high voltage transformers can dissipate tremendous amounts of heat, sometimes in an area located near the operator. These factors must be taken into account when specifying environmental control units and ventilation requirements for the teleoperations area.

The lighting conditions in the operations area is also a concern. Improperly placed or excessively intense lighting can cause glare on the video monitors making them difficult to see. All too often, personnel not directly connected with the job can frustrate and distract the operator by switching on nearby lights at the worst time. For example, the writer was trying to follow a lift line with a Remotely Operated Vehicle (ROV), during a deepwater operation under low visibility conditions. An individual opened the door to the control van (where the workstation was located), spilling bright ambient light onto the pilot's video monitor. The teleoperator immediately lost sight of the line and much time was wasted surfacing the vehicle and starting all over again.

In addition, excessive noise affects operator productivity. Occasionally, minimal consideration is given to the type of ancillary equipment operating near the control console. A high ambient noise environment enhances fatigue and also places unreasonable demands on the communications system.

Physical Factors

The physical interfaces between the operator and console also influence the practicality of doing remote work. All too often, the designers of robotic work consoles will not consider the physical movements required by the teleoperator to control remote vehicles and manipulators. The operations console must be looked at as the physical link between the operator and the robotic system; i.e., the path through which all of the operator's senses must receive visual and physical feedback from the robotic system, and the point of physical contact by which they direct the movement of the remote work system. This link, if flawed in any way, will degrade the ability of the teleoperator to communicate with the robotic system.

Body, joint, and hand fatigue is caused in several ways. First of all, any extended operations with large scale master arms (over 45 minutes), can result in arm fatigue. During the use of a master controller, the operator's arm muscles are constantly in contraction and extension as they attempt to position the slave arm. This, in itself, is not a serious problem. However, the level of concentration required during the task is passed down to the operator's arm, inducing a higher level of muscle tenseness than would normally be present. As indicated above, this is greatly influenced by the amount of visual concentration required to do the task. Generally, the problem manifests itself in the form of a very tight grip on the hand grip of the master arm. Like general operator fatigue, arm fatigue is directly driven by the difficulty of the remote task. Extended operations with miniature joystick controllers is also a problem. Hand fatigue is quite common during long term use of small proportional controllers (similar to the ones used in "Pong" games).

Body fatigue is created by the operator's seating position at the control console. Unfortunately, little thought is normally put into the design of operator's seating configuration and the amount of leg room available. Regardless of the type of restraint in use, for the operator to concentrate their attention on the job at hand, they must be comfortable and have room to stretch. However, extended zero-G operations will be a new application for teleoperator seating/restraint concepts.

Finally, long term repetitive teleoperations work, as a rule, can be somewhat boring. Once the initial fascination of the operation wears off, operator boredom will normally speed up the onset of fatigue, with the result that teleoperators can literally fall asleep at the console. This is particularly true during jobs where the work involves primarily supervision and little operator interaction with the equipment. The only way to combat the problem is to rotate operators on a frequent basis and vary their job requirements.

HUMAN-MACHINE INTERFACES

General Console Layouts

Telerobotic workstations come in a variety of configurations, but they all have a common purpose: to act as a two way conduit of operator inputs and robotic system feedback. Generally, the typical teleoperations console can come in two designs: a small portable workstation that is installed and used as needed, or a dedicated console that is permanently mounted in a specific operations area.

81

Portable Consoles

Portable consoles have been in use the subsea telerobotics field for over a decade and can range from small suitcase sized units to ones that are hand-held. The hand-held consoles normally encompass the basic system functions and are integrated with a separate video display. The larger portable consoles are similar, but usually contain the surface or upside system electronics. The primary problem with these types of consoles is that they must be set up before use and are very prone to damage if they are accidentally bumped in the process. Most of the internal electronics associated with these units are delicate and not capable of withstanding significant abuse. In addition, the time needed to prepare the robotic system for operation can consume valuable operations time. The other problem is that because of the console or controller's small size, some compromises are usually made with regard to the configuration of the robotic system functions. In other words, the quality of the operator interfaces can be degraded because of space or size limitations.

Dedicated Consoles

Dedicated consoles offer more flexibility, from the operational standpoint, because they have more console surface area onto which to mount the system functions; i.e., they can be optimized for the most compatible operator interface. The dedicated console will also make it possible to install "operator friendly" components such as larger video monitors (some dedicated to a single camera), larger sized hand controllers, and system diagnostics. In addition, since the consoles are permanently mounted in a specific location, they are not subject to any physical abuse, and enable the creation of a single-purpose area for teleoperations. However, the down side is that dedicated consoles require more IVA volume for installation and sometimes eliminate the possibility of using the area for other purposes.

Hand Controllers and Master Arms

Hand controllers are a direct physical interface point between the teleoperator and the workstation. Consequently, their design can have a significant impact on the overall compatibility of the control console. Large scale master controllers, as indicated earlier in this paper, contribute to operator arm fatigue during extended use. However, that is only one potential problem. While the large scale master does offer intuitive control and force reflective capabilities, they do require a large IVA work envelope for use. This can drive the interior design of the operations area in an undesirable way, in that it increases the free-volume requirements for the location. In addition, the masters can at times be delicate contraptions that are easily damaged, and require somewhat elaborate stowage schemes to keep them out of the operator's way when they are not in use. While master arm indexing can reduce the volume required for use, this feature can detract from the primary advantage to using a large scale master in the first place; that the master kinematically represents the current position of the slave manipulator.

"Mini" masters represent a departure from their large scale counterparts in that they offer a kinematic replication of the scale arm, albeit on a smaller scale. Like the larger masters, they are subject to breakage and stowage problems. Unfortunately, there are not yet any commercially available "mini" masters with force reflection.

"Bang-bang" rate controllers are limited in capability in that they can only be used with rate manipulators. However they are generally simple in construction, highly reliable and offer an extremely small IVA work envelope. Another advantage to rate controllers is that they give the operator the opportunity to do manipulative work on a part-task basis because the arm automatically freezes when the operator removes his hands from the controller. While the same could be said of large scale and "mini"master controllers, the rate controller offers this capability as an inherent function of its design.

Proportional joysticks can be used for end point control with resolved rate type manipulators. Depending upon their physical size and design, they are comfortable or fatiguing to use. Typically, these types of hand controllers are integrated with controls for ancillary functions such as camera pan, tilt, focus, and zoom. While this is a desirable feature, it can sometimes get out of hand. There are only so many functions an operator can memorize on one control stick, and while it is highly desirable to incorporate multiple functions on one controller, there should not be so many that the operator has trouble memorizing the individual functions, or can accidentally actuate a function during normal operations.

SPECIFIC RECOMMENDATIONS AND CONCLUSIONS

Environmental

There are several conclusions that can be derived from the information presented in this paper, but one is obvious: the local environment of the teleoperator has a significant and measurable effect on the efficiency of doing remote work tasks. As a result, steps must be taken to guarantee that the environment of the operations location is favorable to practical work.

Some of the recommendations that will aid in the above goal are as follows: While it seems like a logical concern, the temperature of the telerobotics operations area is a factor that is often overlooked. The operations location must be comfortable to the teleoperators or they will have difficulty concentrating on the job at hand. The amount of heat generated by control consoles themselves is sometimes minor, but related support equipment can radiate large amounts of energy (this is of particular concern if ventilation within the operations area is lacking). The designer must consider these facts when specifying the requirements for environmental control equipment. In addition, the expected environment of the exterior of the control area, must be considered with respect to any external influences (direct sunlight, radiation, etc.).

High noise levels in the operations area can also cause problems, especially with regard to communications. A high ambient noise level will drive headset needs in an undesirable manner. Communications headsets should be able to be selected on the basis of their comfort and clarity, not sound isolation properties. Finally, as with temperature, excessive sound levels will increase the onset of operator fatigue. Any equipment expected to generate high noise levels should be isolated from the teleoperations area, if possible.

Body and hand fatigue will become a significant negative influence during any extended teleoperations. But how much of a factor it becomes will be determined in part by the design of IVA restraints and hand interfaces. As a result, there are specific areas of concern that can be dealt with to reduce fatigue problems. First of all, hand controllers should incorporate some form of hand or forearm rest to help relieve operator muscle tension. For the proportional joystick, possibly some type of padded area (similar to an arm rest on a chair) that the operator can place his arm against would be beneficial. In the microgravity environment, it may be necessary to supply a flexible restraint to hold the arm against the rest during operations. Obviously, a force reflective system will demand some form of restraint if the teleoperator is to have any hope of "feeling" mechanical feedback generated by the master arm.

Operator restraints should be highly adjustable, with regard to their orientation with the control console, and general configuration. The restraint should be flexible enough to fit a wide range of operations personnel (this is especially true during any operations involving force reflection, since the operator will measure the physical feedback while using the restraint as a stop). In addition, there should be sufficient IVA free volume surrounding the operator restraint to allow for body flexing (especially the legs) during extended IVA operations.

Operational stress will be a driving force behind the onset of operator fatigue during teleoperations. This stress can manifest itself in several ways but primarily, it will be related to task difficulty. Highly complex manipulative operations, especially those that involve work on the borderline of system capabilities, will be extremely fatiguing to operations personnel. For example, if a manipulator has an end point positioning accuracy of plus or minus 1", and the arm is being used to assemble components that have .90" clearance around them, then clearly, it is going to be a difficult time for the arm operator (especially if the components have been designed without alignment guides). Consequently, in these types of situations the operators should be changed out on a frequent basis.

The number of degrees of freedom the operator is required to operate can also influence operational stress levels. Typically, pilots of subsea robotics systems have been able to do simultaneous operations such as combined vehicle and manipulator operations at mid-water. However, such accomplishments were normally under good conditions using only 3 - 4 DOF arms. This maximum DOF issue is one that requires further study.

Job stress is also related to how well the robotic system is operating. Equipment that experiences excessive down time will frustrate teleoperations personnel because they will spend more time repairing the equipment than operating it.

The quality and type of video monitors impact productivity by contributing to operator eye strain. Individuals doing teleoperations do not just "look" at video monitors, but must examine and understand the visual information on the screen. Trying to do this with a degraded video image is difficult, at best. Some basic suggestions are that video monitors used for teleoperations should be at least 9" in size, and incorporate standard controls for brightness, contrast, and sharpness. In addition, the IVA work environment should offer indirect lighting of variable intensity. The distance from the video displays to the operator's eyes, as a general guideline, should be no less than about 3/4 arm length.

Physical Interfaces

Hand Controllers

The type of manipulative operation and design of the manipulator system should be the determining factors with regard to the configuration of arm controllers. While large scale master arm controllers can be very beneficial to teleoperations, they will cause arm fatigue if used for extended periods. Steps should be taken to ensure the availability of sufficient operations personnel for an acceptable rotation schedule during extended or complex manipulative work tasks. In addition, any full-scale masters installed in a robotic workstation should be capable of stowage during periods of non-use.

Proportional hand controllers should be sized in relation to expected task duration. Generally, if sufficient IVA console space is available, medium sized joysticks (that can be grasped by the entire hand), should be employed.

The designer should strive to make the hand controllers reflect the physical configuration of the manipulator system. In other words, the arm controllers should be referenced to the video monitor screen as a representation of how the subsystems are physically related at the worksite. The most important aspect is the video camera to end effector relationship. If the robotic system is configured with the video camera in the middle of two manipulators, then the two arm controllers at the workstation should be mounted on either side of the video monitor. The work station should represent the remote work system as much as is practical.

Standardization of teleoperator interfaces will aid operational efficiency by reducing learning requirements between different robotic systems. There are several ways that standardization can be applied to physical interfaces, but the most obvious solution, such as using identical controllers for several applications, is not necessarily the best; operator interfaces do not have to look alike to be standardized!

There are a multitude of telerobotic vehicles in use today in the subsea field, and outside of the individual manufacturers, there is little or no standardization. But what has been learned in the past decade of teleoperations is that standardization is more related to method of operation than appearance.

Some underwater remote vehicles are controlled by two joysticks while others can be driven with one. It all depends upon how the control subsystems are configured and the preferences of the manufacturer (some seem to prefer a one over a two stick arrangement). Field personnel who take over control of a vehicle with no prior experience on a particular system can usually learn the functions fairly quickly, especially if the operator is highly experienced. However, standardization of the operator interfaces would certainly reduce the amount of time it takes to learn a particular robotic system.

Robotic system controls should be standardized with respect to function and mode of operation. The key is to guarantee that identical physical movements are required of the operator to achieve a particular result. A standard typewriter is an excellent analogy. There are many varieties of typewriters, but in most designs, the keys (the separate letters, that is), are always in the same location. The typist can then learn one interface pattern, then have the ability to use all typewriters. The reason this is so important is that the teleoperator references all of their resultant actions (the physical movements they see on the video monitor) to specific movements at the workstation. The operator knows that if he moves a control in a certain direction, he will see a corresponding result on the video screen. This results in a "learned relationship" between action and reaction. This relationship is what is learned by the operator, not the shape, size, or color of the hand controller. As a result, systems that operate outside of this database of information have to be relearned all over again so the operator can develop a new action/reaction relationship. This process wastes time. Hence, the relative dynamic relationship between the operator and the controller is what should be standardized, not the physical design of the controller.

Control Consoles

Telerobotic workstations should be configured to act as the operator's reference point to the robotic system. First of all, if possible, there should be a dedicated video monitor for each camera. This will enable the teleoperator to instantly view the entire visual range surrounding the telerobot, without confusion as to what camera they are viewing. Of course, given the space limitations on-orbit, this may be impractical. A compromise would be to use video multiplexing so that the teleoperator can examine multiple video images on one video monitor. The goal should be to make sure the teleoperator knows which video image is being generated by what camera.

The mechanical orientation of manipulator controls should mimic the configuration of the telerobot as much as is feasible. For example, if the robotic system has two arms, then there should be two separate controllers instead of one controller with a selection switch.

Camera pan and tilt controls should also follow the same practice; i.e., there should be a separate controller for each camera. Ideally, pan and tilt controls should be incorporated into hand controllers so the teleoperator can operate the manipulator and camera controls without diverting their attention from the video monitor.

System functions should be unique and configured based upon their function. For example, the switches used to turn lights off and on should be of a different design than the ones that control system power. Ideally, the console should not need labels on all of the controls for the operator to know their functions. Overall, a customized function layout will reduce errors and enhance compatibility. The console should be ergometric so that the operator can easily reach all of the system's functions without constant body movements. This feature will reduce body fatigue.

In general, the concept behind a telerobotic console should be to design for functionality, compatibility, and practicality. The foremost thought that should be behind the design of the console is that the workstation is the teleoperator's hands and eyes at the worksite.

Portable workstations that have to be set up or installed before use should be avoided, if it is at all possible. The types of compromises made in portable designs are sufficient to render them undesirable for extended teleoperations use. A far better arrangement is the design of a workstation permanently installed into a "teleoperations work area". This will enable the teleoperator to do the job at hand in the most compatible environment possible. However, in situations where it is absolutely impossible to create a dedicated area, such as in the Orbiter's aft flight deck, then any portable workstations should be highly adjustable, with regard to the installation point and mounting angle, so the teleoperator can customize the operator to workstation interface.

HUMAN FACTORS PROGRAMMATICS

(No papers presented at this session)

87

HUMAN FACTORS TECHNOLOGY TRANSFER PANEL

(No papers presented at this session)

HUMAN COMPUTER INTERACTION

89

THE USE OF ANALYTICAL MODELS IN HUMAN-COMPUTER INTERFACE DESIGN

Leo Gugerty

Lockheed Engineering and Sciences Company

INTRODUCTION

Researchers in the human-computer interaction (HCI) field commonly advise interface designers to "know the user". Various approaches are currently used to get information about the user into the hands (and mind) of the designer. One approach is to use design guidelines (e.g., NASA/Johnson Space Center, 1988), which can incorporate knowledge of human psychological strengths and weaknesses and make it accessible to designers. However, guidelines give only overview information. They do not help the designer to configure the interface for a specific task and specific users (Gould & Lewis, 1985).

Another way to know the user is to conduct usability tests (Gould & Lewis, 1985). This involves building prototype interfaces as early as possible in the design process, observing typical users as they work with the prototype, and fixing any observed problems during the next iteration of the design. While effective in making the designer aware of user needs, usability testing adds a significant amount of time to the design of user interfaces.

Recently, a large number of HCI researchers have investigated another way to know the user -- building **analytical models** of the user, which are often implemented as computer models. These models simulate the cognitive processes and task knowledge of the user in ways that allow a researcher or designer to estimate various aspects of an interface's usability, such as when user errors are likely to occur. This information can lead to design improvements. Analytical models can supplement design guidelines by providing designers rigorous ways of analyzing the information-processing requirements of specific tasks (i.e., task analysis). These models offer the potential of improving early designs and replacing some of the early phases of usability testing, thus reducing the cost of interface design.

This paper will describe some of the many analytical models that are currently being developed and evaluate the usefulness of analytical models for human-computer interface design. The paper is intended for researchers who are interested in applying models to design and for interface designers. This is a summary of an extensive literature review paper on the use of analytical models in design that is being conducted at the Johnson Space Center's Human-Computer Interaction Laboratory.

The question of whether analytical models can really help interface designers is currently receiving much attention in the field of human-computer interaction. Advocates of model-based design claim that our knowledge of cognitive psychology is becoming sophisticated enough to allow analytical models of the user to play a useful role in interface design (Kieras, 1988; Butler, Bennett, Polson, & Karat, 1989). Modeling proponents suggest that models could be used during interface design in two important ways:

1. Models can help designers conduct a rigorous task analysis, which in turn may help generate design ideas. A number of analytical models (e.g., the GOMS model, Card, Moran, & Newell, 1983) involve specifying the goals, actions, and information requirements of the user's

task. Research suggests that these task analyses can help designers generate effective design ideas.

2. After interface designs have been generated, models can help evaluate their effectiveness. A human-factors psychologist or engineer could work with a designer to build a computer model of how a user would interact with a new interface. This model could be run with various input conditions to predict how long the user will take to perform tasks using the interface, and likely sources of user errors.

The benefits of analytical models are by no means universally accepted in the HCI community. Many HCI researchers and practitioners have questioned the usefulness of models for interface design. Whiteside and Wixon (1987) claim that current models are only applicable to the specific task and context for which they were developed and cannot be applied to new interfaces. Others (e.g., Curtis, Krasner, & Iscoe, 1988; Rossen, Maas, and Kellog,1988) suggest that models may not fit in with the needs of design organizations or with the intuitive thinking and informal planning that designers sometimes use.

This paper will focus on computational analytical models, such as the GOMS model, rather than less formal, verbal models, because the more exact predictions and task descriptions of computational models may be useful to designers. The literature review paper that is summarized here evaluated a number of models in detail, focusing on the empirical evidence for the validity of the models. Empirical validation is important because, without it, models will not have the credibility to be accepted by design organizations. This paper will briefly describe two analytical models in order to illustrate important conclusions from the literature review. Following this, the paper will discuss some of the practical requirements for using analytical models in complex design organizations such as NASA.

EMPIRICAL EVALUATION OF ILLUSTRATIVE MODELS

GOMS Model

The GOMS model was developed as an engineering model to be used by HCI designers, and it has received much more empirical testing than any other analytical model of HCI tasks. Many of the issues concerning the use of GOMS models in design are relevant to other analytical models as well.

GOMS models are applicable to routine cognitive skills. They are best suited for tasks where users make few errors. More open-ended tasks that involve extensive problem solving and frequent user errors (e.g., troubleshooting) are not good candidates for GOMS modeling.

GOMS stands for goals, operators, methods, and selection rules, the four elements of the model. GOMS models are hierarchical. The assumption is that at the highest level, people's behavior on a routine computer task can be described by a hierarchy of goals and subgoals. At the most detailed level, behavior is described by operators, which can be physical (such as typing) or mental (such as comparing two words). Operators that are often used together as a unit are built up into methods. For example, one might have a standard method of deleting text in a text editor. Sometimes more than one method can meet a goal, and selection rules are used to choose among them.

GOMS models can help an interface designer get a qualitative understanding of the goal structure and information requirements of a task (i.e., a task analysis). In addition, Kieras and Polson (1985) developed a formal implementation of GOMS models -- Cognitive Complexity Theory (CCT) -- that allows designers to make quantitative statements about users' errors, learning time, and performance time for particular interfaces. In CCT, GOMS models are represented as production systems. In a production system the parts of a GOMS model are represented by a series of if-then rules (production rules) that can be run as a computer simulation model. A number of quantitative metrics can be derived from a CCT production system that, according to proponents of CCT, can be used to predict users' performance on a task (Kieras, 1988; Olson & Olson, in press). For example, task learning time, task performance time, and the number of user errors can be predicted.

To date, GOMS models have not been used to help design a commercial interface. Most empirical studies of GOMS models have been evaluations of existing interfaces that were designed without using GOMS. For example, Bovair, Kieras, and Polson (in press) evaluated GOMS estimates of task performance time for existing interfaces. Using a text editing task, they found that the number of production-system cycles and of certain complex operators (such as looking at the text manuscript) could match performance time fairly well, explaining about 80% of the variability of users' performance times across editing tasks.

It is important to point out that in studies like this, data (such as errors and the time to learn and perform tasks) are collected from users of an interface, and statistical techniques (such as regression) are used to determine whether the GOMS predictions match the data. In these studies, GOMS models are not used to make *a priori* predictions of user performance. Rather, the models' estimates of user performance are statistically compared to the empirical data to see how much of the variability in users' performance data can be explained by the model. Although some researchers suggest that GOMS models can be used to make a priori predictions of user performance (Olson & Olson, in press), this has not been done successfully to date.

In addition to evaluations of existing interfaces, a few studies have looked at how GOMS models can be used to generate ideas for redesigning interfaces. These studies take advantage of the fact that GOMS models provide a detailed task analysis (i.e., a representation of the goals, subgoals, and procedural steps) required to perform a task. Elkerton & Palmiter (1989) used a GOMS model of the knowledge required for Hypercard authoring tasks to design a menu-based Hypercard help system that allowed faster information retrieval and was liked better than the original help system. This study is important because it shows that GOMS models can be used for more than post-hoc evaluation of existing designs. In this study, the task analyses provided by GOMS models were used to generate computer-related artifacts (in this case, procedural instructions). In addition, these artifacts were generated fairly directly from the task analyses, without extensive interpretation or "judgment calls".

To summarize the empirical evaluation of GOMS models, models developed for a single, existing interface can be used in a *post-hoc*, quantitative fashion to explain performance time, learning time, and number of errors with that interface. No one has yet tested whether GOMS models can make accurate quantitative performance predictions for an interface that is still in design. However, encouraging progress has been made in using the task analyses provided by a GOMS model to help generate effective instructions that can be incorporated in help systems and user manuals.

Tullis' Model

The next model to be described has a much narrower range of application than GOMS models and focuses on general psychological processes rather than task analysis. Perhaps because of these differences, this model, developed by Tullis (1984), is better than GOMS at making *a priori* predictions of user performance. Tullis' model focuses on aspects of a display, such as display density, that affect how well people can find information in the display. It emphasizes general processes, such as perceptual grouping, that affect display perception regardless of the content of the display. The effects of task knowledge on display perception (e.g., effects of user expertise) are not considered. Tullis' model is applicable only to alphanumeric displays that make no use of color or highlighting. The model has been applied to simple search tasks involving displays for airline and motel reservations, and for aerospace and military applications (Tullis, 1984).

Based on a literature review, Tullis hypothesized that five factors would affect the usability of alphanumeric displays: overall density, local density, the number and size of the perceptual groups, and layout complexity. He developed operational definitions so that quantitative values could be calculated for each factor, given a display layout as input. Then, he conducted an experiment in which subjects searched for information in displays and rated the usefulness of the displays. Regression analyses showed that the five factors could explain subjects' search times and subjective ratings fairly well.

Tullis implemented his regression model in the Display Analysis Program (Tullis, 1986). This program accepts a display layout as input. It outputs quantitative estimates of overall density, local density, number of perceptual groups, and average group size. It also provides graphical output describing the display density analysis and the perceptual groups. Finally, it predicts average search time and subjective ratings for the display.

Tullis (1984) then used his model to predict search times and subjective ratings for a second experiment, using different subjects and displays than the experiment that was used to develop the regression equations. The predicted search times and subjective ratings matched the actual times and ratings fairly well, with a correlation of about 0.64 (r^2) for each variable. The model correctly predicted the displays with the best search time and rating. Tullis' model was also able to predict search times from three previous studies in the literature ($r^2 > 0.63$ in each study) (Tullis, 1984). However, when Tullis' model was tested on tasks more complex than simple display search, it did not predict subjects' performance well (Schwartz, 1988).

To summarize, Tullis' model is applicable within a limited domain -- inexperienced users performing simple search tasks involving alphanumeric displays. Within this domain, however, the model's performance is impressive. Tullis has taken the step that GOMS users have neglected and used his model to predict performance for displays and subjects different from the ones on which the model was developed. The model was able to predict well in these cases. One disadvantage of Tullis' model is that it neglects cognitive factors affecting display perception, such as the effect of a user's task knowledge.

Conclusion: Empirical Evaluation of Analytical Models

Earlier in the paper, it was suggested that analytical models could be used in interface design in two ways. The first of these involves using models early in the design process to conduct rigorous task analyses, which are then used to generate ideas for preliminary designs (e.g., menu structures) The second potential use of models occurs later in the design process, after preliminary designs have been developed. In this case models are used to evaluate designs by making quantitative predictions about expected user performance given a particular design.

The empirical evidence considered in the literature review, and summarized here, suggests that, except for one model with a narrow range of application, there is no empirical evidence that analytical models can predict user performance on a new interface. There is some encouraging evidence that analytic models used for task analysis can help in the process of generating designs; however, this conclusion is based on only a few studies. The review of the empirical evidence suggests, then, that future research aimed at demonstrating model-based improvements in interfaces should focus on three areas:

- Replicating and extending the studies of model-based interface redesign (e.g., Elkerton & Palmiter 1989).
- Demonstrating model-based interface design for a new interface.
- Demonstrating the predictive use of models to evaluate preliminary designs

Based on the empirical evidence to date, the first two of these would be the most promising avenues of research.

What are some possible reasons for the failure of models to accurately predict performance with a new interface? It may be that critics such as Whiteside and Wixon (1987) are correct in that people's procedures, goals, and cognitive operators are too context-specific to allow prediction in a context as different as a new interface. A large body of research in cognitive psychology suggests that expert's performance in a particular domain is largely dependent on domain-specific knowledge, as opposed to general-purpose cognitive skills (Chi, Glaser, & Rees, 1982; Glaser, 1984). And models such as GOMS focus primarily on the task-specific knowledge of experienced users. It is interesting that the model that was able to predict user performance on a slightly different interface (Tullis') is not a task analytic model. Tullis' model focuses on general perceptual abilities. This suggests that in order to predict performance for new interfaces, task analytic models must include more explicit representation of how general purpose cognitive characteristics (such as working memory limitations) affect user performance.

An addition should be made to the above list of research areas. This suggestion is based on the fact that there are no empirically validated models that can describe HCI tasks involving higher-level cognitive processes such as problem solving. However, space-related computer systems are rapidly becoming intelligent enough to assist people in complex tasks such as medical diagnosis and scientific research, which involve more complex cognition. Models are currently being developed with the goal of describing these more complex tasks in a way that is useful to interface designers. An example is the Programmable User Models (PUMs) (Young & Whittington, 1990). However, most of these models have not been empirically validated.

A fourth area of further research, then, is:

- Developing and testing models of complex HCI tasks involving high-level cognitive processes.

USING MODELS IN DESIGN ORGANIZATIONS

So far, this paper has focused on whether analytical models can improve interface designs. However, even if models were conclusively demonstrated to improve interfaces, this would still not ensure their use by design organizations such as NASA. What is needed is evidence for the usefulness as well as the validity of models. That is, it must be shown that models can meet the needs of individual designers (e.g., preferred design methods), and of design organizations (e.g., cost, scheduling, and personnel constraints).

With respect to individual designers, an understanding of the various ways that designers generate, develop, and evaluate ideas is needed. Analytical models would be provided to designers as detailed procedures or as software tools. The principle of considering the cognitive and motivational processes of users applies to model developers just as it does to the designers of other software tools. In short, designers are users too. Therefore, if model developers want their models to be used in actual design projects, they must either construct their models to fit in with the preferred design processes of designers or provide ways of training designers to use the models.

But decisions regarding the commercial use of models are made by managers, not by individual designers. Therefore, models also must be shown to meet the multi-faceted needs of design organizations, for example, cost, schedule, and personnel requirements. This section will discuss the problems that must be overcome before analytical models are accepted by designers and their work organizations.

Needs of Individual Designers

Two studies conducted by Curtis and his colleagues showed that major difficulties in software design are caused by a lack of application-domain knowledge on the part of designers. (Curtis, et al., 1988; Guindon, Krasner, & Curtis, 1987). The analogous problem in the case of interface design would be a lack of knowledge of the user's task. When Rosson, et al. (1988) interviewed interface designers about the techniques they used to generate design ideas, they found that the most frequently mentioned techniques (about 30%) were for analyzing the user's task. Most of this task analysis involved informal techniques, such as interviewing users or generating a task scenario.

These findings present both an opportunity and an obstacle to the use of models by interface designers. First, since designers often lack knowledge of the user's task and spend a large amount of effort getting it, they might see the usefulness of task analytic models such as GOMS. The potential obstacle is that designers may prefer to stick with their informal techniques, instead of the more rigorous task analytic models. Rosson et al. suggest that tools to aid in idea generation should primarily support designers' informal techniques. Lewis, Polson, Wharton, and Rieman (1990) offer an interesting way of combining formal modeling with a technique currently used by software designers -- design walkthroughs. They developed a formal model of initial learning and problem solving in HCI tasks, and then derived from the model a set of structured questions (a cognitive walkthrough) that can be used to evaluate the usability of an interface.

This discussion presents only an example of the kind of issues that need to be considered regarding the needs of individual designers. Further research is needed on the cognitive and motivational processes of designers and what these processes suggest about the design of analytic models.

Needs of Design Organizations

The Curtis, et al. (1988) study mentioned above also considered the organizational aspects of software design. In addition, Grudin and Poltrock (1989) conducted an extensive interview study of the organizational factors affecting interface design. Some of the findings of these studies that relate to the use of analytical models are discussed below.

An important characteristic of many computer-system design organizations is complexity. Many groups may contribute to a final design product: interface and system designers, human factors personnel, training developers, technical writers, and users (e.g., astronauts). Curtis, et al. (1988) noted a wide variety of communications problems that resulted because of this organizational complexity. One such problem arises when groups interpret shared information differently because of differences in background knowledge. This could easily cause problems, for example, if the people in an organization who are experienced with modeling (e.g., a designer or human factors expert) have to communicate the results of a modeling analysis to a project manager. A possible solution to this problem of misinterpretation is for model developers to make the structure and outputs of their models as clear as possible.

In addition to communication problems, another problem arising from the variety of roles in design organizations has to do with personnel and training. A manager considering the use of models on a design project faces a number of questions along these lines. Can existing personnel do the modeling (e.g., designers or human factors personnel)? How much training will they require? If new personnel must be hired, what kinds of background must they have? Model developers must have answers to these questions.

One answer comes from the work of Kieras (1988). He has developed and published a procedure for building GOMS models. Informal testing showed that computer science undergraduates could use this procedure to generate GOMS models and make usability predictions "with reasonable facility". More than this is necessary, however. Validation studies must be done to test whether the personnel that would use models in design organizations can build models that make the same kinds of predictions as the experts who initially developed the model. These studies should also document the kind of training necessary to achieve these ends.

In addition to complexity, other characteristics of design organizations that affect their openness to modeling are strict project scheduling and a concern with monetary costs. Detailed estimates are needed of the time and money costs of using analytical models in commercial design.

CONCLUSION - THE USE OF ANALYTICAL MODELS IN INTERFACE DESIGN

Can the use of analytical models be recommended to interface designers? Based on the empirical research summarized here, the answer is: Not at this time. There are too many unanswered questions concerning the validity of models and their ability to meet the practical needs of design organizations. However, some of the research described here suggests that models can be of practical use to designers in the near future. Of special interest is the research that used models as task analytic tools to generate interface design ideas (e.g., Elkerton & Palmiter, 1989).

This paper has suggested research and development that is necessary in order for analytical models to be accepted by complex design organizations. These suggestions are summarized in Table 1. It seems that the empirical research on analytical models gives good reason to pursue the research and development goals outlined here.

ANALYTICAL MODELS AND SPACE-RELATED INTERFACE DESIGN

So far, this paper has provided a general analysis of the use of analytical models in human-computer interface design. How much of this analysis is applicable to the design of space-related interfaces? The Human-Computer Interaction Laboratory (HCIL) at the Johnson Space Center is currently conducting preliminary task analyses for the tasks required on a long-duration space mission, such as a mission to Mars (Gugerty & Murthy, in preparation). This work suggests that the range of tasks on such a mission is quite broad -- ranging from reading to controlling complex equipment to conducting scientific research. The possible information technologies for long-term missions are also quite diverse, for example, workstations for supervisory control, graphics workstations for scientific research, computer-supported group meetings, medical expert systems, and virtual workstations for telerobotic control. It seems that space-related tasks are diverse enough to span almost the entire range of human-computer interaction tasks. Therefore, the general analysis of this paper will be applicable to space-related tasks in most cases.

One project in the JSC HCIL is focusing on the use of analytical models in designing medical decision support systems for space crews. This project is following up on the work of Elkerton and Palmiter (1989), in which GOMS was used as a task analytic model to help generate interface design ideas. One medical task that space crew members will face is learning or relearning medical procedures from computer displays. This project will test whether building GOMS models of medical procedures can help interface designers build better interfaces for displaying this procedural information. The GOMS approach will be compared with other methods of task analysis, including psychological scaling techniques such as the Pathfinder algorithm (McDonald & Schvaneveldt, 1988).

Table 1
Methods of Increasing the Use of Analytical Models in Interface Design

Demonstrate Design Improvements:

- Validate model-based interface redesign.
- Validate model-based interface design.
- Validate predictive use of models to evaluate preliminary designs.
- Develop and validate models of complex HCI tasks involving high-level cognitive processes.

Meet the needs of individual designers:

- Study the design methods and cognitive processes of individual designers.
- Change the models and/or develop training materials to ensure that models fit in with designers methods and cognitive processes.

Meet the needs of design organizations:

- Make models' structure & outputs easily interpretable.
- Develop means of training designers to use models. Validate that this training works and document the costs of training.
- Document the time and monetary costs of using models.

REFERENCES

Bovair, S., Kieras, D. E., & Polson, P. G., The acquisition and performance of text editing skill: A production system analysis, *Human Computer Interaction*, in press.

Butler, K, Bennett, J., Polson, P., & Karat, J., Report on the workshop on analytical models,*SIGCHI Bulletin*, 20, 4, 1989, pp. 63-79.

Card, S. K., Moran, T., & Newell, A.,*The psychology of human-computer interaction*, Lawrence Erlbaum Associates, Hillsdale, NJ, 1983.

Chi, M. T. H., Glaser, R., & Rees, E., Expertise in problem solving, in R. J. Sternberg (Ed.), *Advances in the psychology of human intelligence* (Vol. 1), Lawrence Erlbaum Associates, Hillsdale, NJ, 1982.

Curtis, B., Krasner, H., & Iscoe, N., A field study of the software design process for large systems,*Communications of the ACM,* 31,11, 1988, pp.1268-1287.

Elkerton, J. & Palmiter, S., Designing help systems using the GOMS model: An information retrieval evaluation, *Proceedings of the Human-Factors Society 33rd Annual Meeting*, Santa Monica, CA,1989.

Glaser, R., Education and thinking: The role of knowledge, *American Psychologist*, 39, 2, 1984, pp. 93-104.

Gould, J. D. & Lewis, C. H., Designing for usability and what designers think,*Communications of the ACM*, 28, 3, 1985, pp. 300-311.

Grudin, J. & Poltrock, S. E., User interface design in large corporations: Coordination and communication across disciplines, in K. Bice & C Lewis (Eds.), *Proceedings of the CHI 89 Conference on Human Factors in Computing. Systems* , Association for Computing Machinery, New York, NY 1989.

Gugerty, L. J. & Murthy, P. (in preparation), Using task analysis to guide information-technology development for future space missions, Paper to be presented at the AIAA Space Programs and Technologies Conference, September, 1990.

Guindon, R., Krasner, H., & Curtis, B., Breakdowns and processes during the early activities of software design by professionals, in G. M Olson, S. Sheppard, & E. Soloway (Eds.), *Empirical studies of programmers: Second workshop*, Ablex Publishing Corp., Norwood, NJ, 1987.

Kieras, D. E., Towards a practical GOMS model methodology for user interface design, in M. Helander (Ed.), *Handbook of human-computer interaction,* Elsevier Science Publishers, Amsterdam,1988.

Kieras, D. E. & Polson, P G., An approach to the formal analysis of user complexity, *International Journal of Man-Machine Studies,* 22, 1985, pp. 365-394.

Lewis, C., Polson, P., Wharton, C., & Rieman, J., Testing a walkthrough methodology for theory-based design of walk-up-and-use interfaces, in J. C. Chew & J. Whiteside (Eds.), *Proceedings of the CHI 90 Conference on Human Factors in Computing. Systems* , Association for Computing Machinery, New York, NY,1990.

McDonald, J. E. & Schvaneveldt, R. W., The application of user knowledge to interface design, in R. Guindon (Ed.), *Cognitive science and its applications for human-computer interaction.*, Lawrence Erlbaum Associates, Hillsdale, NJ, 1988.

NASA/Johnson Space Center, Space Station Freedom Program human-computer interface guide (USE 1000, Version 2.1), Johnson Space Center, Houston, TX,1988.

Olson, J. R. & Olson, G. M., The growth of cognitive modeling in human-computer interaction since GOMS, *Human-Computer Interaction*, in press.

Poltrock, S. E., Innovation in user interface development: Obstacles and opportunities, in K. Bice & C Lewis (Eds.), *Proceedings of the CHI 89 Conference on Human Factors in Computing. Systems*, Association for Computing Machinery, New York, NY,1989.

Rosson, M. B., Maass, S., & Kellogg, W. A., The designer as user: Building requirements for design tools from design practice, *Communications of the ACM*, 31, 11, 1988, pp. 1288-1299.

Schwartz, D. R., The impact of task characteristics on display format effects, *Proceedings of the Human Factors Society - 32nd Annual Meeting.*, Human Factors Society, Santa Monica, CA,1988.

Tullis, T. S., Predicting the usability of alphanumeric displays., Doctoral Dissertation, Rice University, The Report Store, Lawrence, Kansas, 1984.

Tullis, T. S., A system for evaluating screen formats, *Proceedings of the Human-Factors Society 30th Annual Meeting.*, Human Factors Society, Santa Monica, CA, 1986.

Whiteside, J. & Wixon, D., Discussion: Improving human-computer interaction - A quest for cognitive science, in J. M. Carroll (Ed.), *Interfacing thought: Cognitive aspects of human-computer interaction.*, MIT Press, Cambridge, MA, 1987.

Young, R. M. & Whittington, J., Using a knowledge analysis to predict conceptual errors in text-editor usage, in J. C. Chew & J. Whiteside (Eds.), *Proceedings of the CHI 90 Conference on Human Factors in Computing. Systems*, Association for Computing Machinery, New York, NY, 1990.

MICROGRAVITY CURSOR CONTROL DEVICE EVALUATION FOR SPACE STATION FREEDOM WORKSTATIONS

Susan Adam, Kritina Holden, Douglas Gillan
Lockheed Engineering and Sciences Company
and
Marianne Rudisill
NASA/Johnson Space Center

ABSTRACT

Computer Workstations will control Space Station Freedom systems and payloads. These microgravity workstations will use direct manipulation as the primary interface. They significantly reduce the number of finite actions required to operate a computer over that for a command-line interface, thus reducing errors and overall task completion times. This research addresses direct manipulation interface (cursor-control device) usability in microgravity. The data discussed are from KC-135 flights and an STS-29 (shuttle) Detailed Test Objective (DTO). Three commercially-available devices: an optical mouse, a trackball and a post-mouse, were chosen to begin investigating the best characteristics required for an optimal microgravity device. A text editing task was performed aboard the KC-135 flights. This included pointing and dragging movements over a variety of angles and distances. Detailed error and completion time data from this task, as well as crew comments from the DTO, provided us with information regarding cursor control shape, selection button arrangement, sensitivity, selection modes, and considerations for future research.

INTRODUCTION

The Man-Systems Division at NASA-Johnson Space Center (JSC) has an active research program pursuing answers to questions about Human Computer Interaction (HCI). This research is currently being applied to the design of the Space Station Freedom (SSF) Workstations, as well as for the modification of the Space Shuttle computer interface for compatibility with the station. Shuttle experience shows that in 0-g, keyboard entry of command line input proves to be a less than optimal means of HCI. Because each astronaut aboard the SSF will have to spend much of his/her day interacting with a computer workstation, it is mandatory that the interface maximizes the productive use of this valuable time. A direct manipulation interface has been determined to be the best choice in microgravity because it reduces the number of finite actions required to operate a computer, thus reducing opportunities for error and overall time to complete a task. One-g research in the Human-Computer Interaction Laboratory (HCIL) has concentrated on human performance modeling with cursor control devices (e.g., Gillan, Holden, Adam, Rudisill & Magee, 1990).

The current research addresses the usability of cursor control devices in microgravity aboard the KC-135 and as part of a DTO aboard the STS-29 shuttle flight. Due to the limited availability of such flights, a representative subset of available devices had to be selected for evaluation. Devices which require minimum "real estate" for operation and allow highly accurate input are desirable for use in the space station task environment. A survey of current research shows that touch screens and light pens provide for faster performance than with a trackball or mouse; however, they are less accurate due to parallax problems, obstruction caused by placing the hand in front of the screen, and the large resolution required for touch activation. Touch technology is not recommended for use under demanding conditions or intensive use and where high resolution is required (Whitfield, Ball & Bird 1983; Beringer & Peterson, 1985). The trackball and mouse allow for the greatest accuracy, with moderate speed, of commercially-available off-the-shelf (COTS) products (Brown, 1989). Also, a post-mouse device called the Felix™ was selected because it is about the size of a standard trackball, it allows absolute cursor positioning by movement of its post/entry button within a one inch square.

KC-135 EVALUATIONS

The Reduced Gravity Program at NASA-JSC owns and operates an experimental aircraft, the KC-135, which simulates a "weightless" environment similar to the environment of space flight for test and training purposes. The specially-modified turbojet transport flies a parabolic arc to produce short periods of 0-g lasting an average of 23 seconds (Williams, 1987) surrounded by a 2-g pull-up and a pull-out. A flight consists of 40 parabolas.

In designing the task to be performed aboard the aircraft, consideration was given to produce a short, repeatable, though realistic task. These characteristics were especially important because: 1) It is not possible to sustain perfect 0-g throughout the 23 seconds; 2) The operators require a few seconds to physiologically adjust from the 2-g pull-up to the free-floating condition; 3) Operator discomfort /illness is not uncommon and often causes the loss of the data from a few parabolas. A text editing task was considered to be realistic because it will be necessary aboard the space station, it requires a great deal of cursor movement and control, and represents a task requiring high accuracy. Text editing incorporates the three basic cursor control actions, pointing, dragging, and clicking. It was also determined that the task could be completed approximately three times per parabola.

The common features of the two KC-135 experiments will be presented here. Additional details will be given in the Procedures and Results & Discussion sections specific to each experiment.

METHOD

Subjects

Two subjects were used in each experiment. All were employed by Lockheed Engineering and Sciences Company (LESC). All were experienced Macintosh and mouse users.

Apparatus, Stimuli, and Data Recording

Both experiments were conducted using a standard Macintosh Plus with 1.0 MB of memory and an external disk drive. The four control devices evaluated were a Macintosh mechanical mouse, an A Plus™ Optical Mouse with a reflective pad, a Turbo Mouse™ trackball and a Felix™ post-mouse. The computer was mounted on an aluminum stand which provided a worksurface for the use of the cursor control devices. The trackball, Felix™ and mouse pads were restrained with velcro. Foot and waist restraints were used to secure the subject while performing the task. In practice trials aboard the aircraft, it became apparent that during microgravity the ball of a Macintosh mechanical mouse floated into the housing, making it unusable. The control/display ratio for the optical mouse and trackball was set to the second slowest setting for mouse sensitivity on the Macintosh control panel. The Felix™ required that the tablet (or very slow) setting was used.

The Apple software product, Hypercard™, was used for presentation of the text editing task. The stimuli included: 1) a two-line block of text with a portion underlined (5, 14 and 26 characters i.e., 1.4, 3.0, and 5.7 cm. respectively); 2) a Select button which varied in location among the four corners of the display screen; 3) a NEXT button for user selection of the next trial screen (see Figure 1). The text block was located to produce three different pointing distances with respect to each Select button. Each of the 36 conditions (three text selection lengths x three pointing distances x four pointing angles) was presented in a randomized order as a block of trials. Each flight was composed of four sets of ten parabolas.

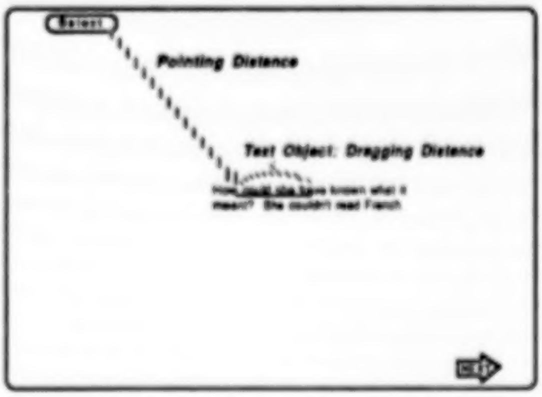
Pointing Distance
Text Object: Dragging Distance
How could she have known what it meant? She couldn't read French

Figure 1. Elements of the basic display

A macro-recording program, Automac III™ (Genesis Software), was used to record a time stamp and cursor location every time the cursor control device select button was depressed and every tick (one sixtieth of a second) while it was depressed.

KC-135 EXPERIMENT 1

Procedure

Two subjects used each device twice during four testing sessions which were held for pretest, flight, and posttest conditions. Sessions (1) and (2) each consisted of one block of 36 text selection trials using one device. Sessions (3) and (4) were composed of two blocks of 36 trials, each performed with a different device. The pre- and posttest sessions were held over three consecutive days because session (1) & (2) were combined. The flight sessions were held over four consecutive days, where sessions (1) & (2) consisted of only two parabolas rather than four.

Results & Discussion

The trials in which subjects made incorrect selections were eliminated for the examination of movement times. With each device pointing times by pointing distances were similar across all gravity conditions. Dragging times for each of the drag distances were also similar across gravity conditions. However, it is apparent that learning occurred due to the decrease in overall selection times from pretest to postest sessions. The learning effect appeared to continue across the flight conditions except that for the longest drag target, 26 characters (5.7 cm), selection times,

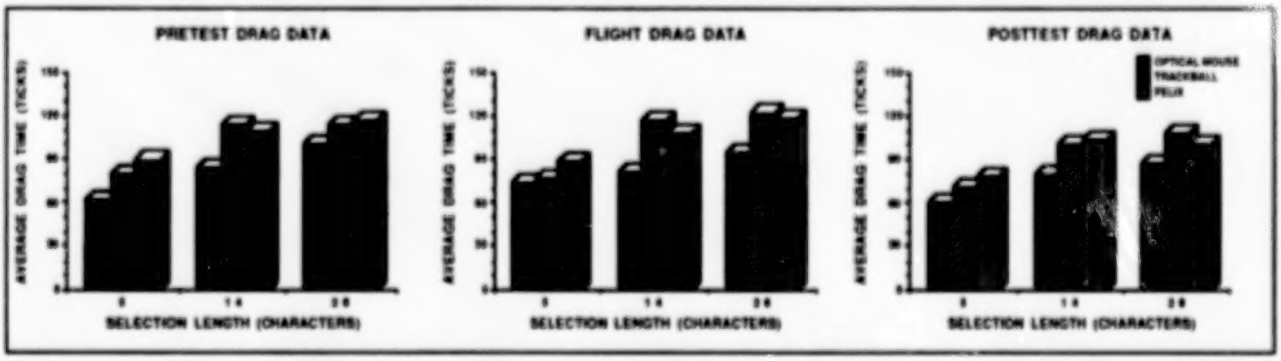

Figure 2. Drag times by selection length and device for Experiment 1

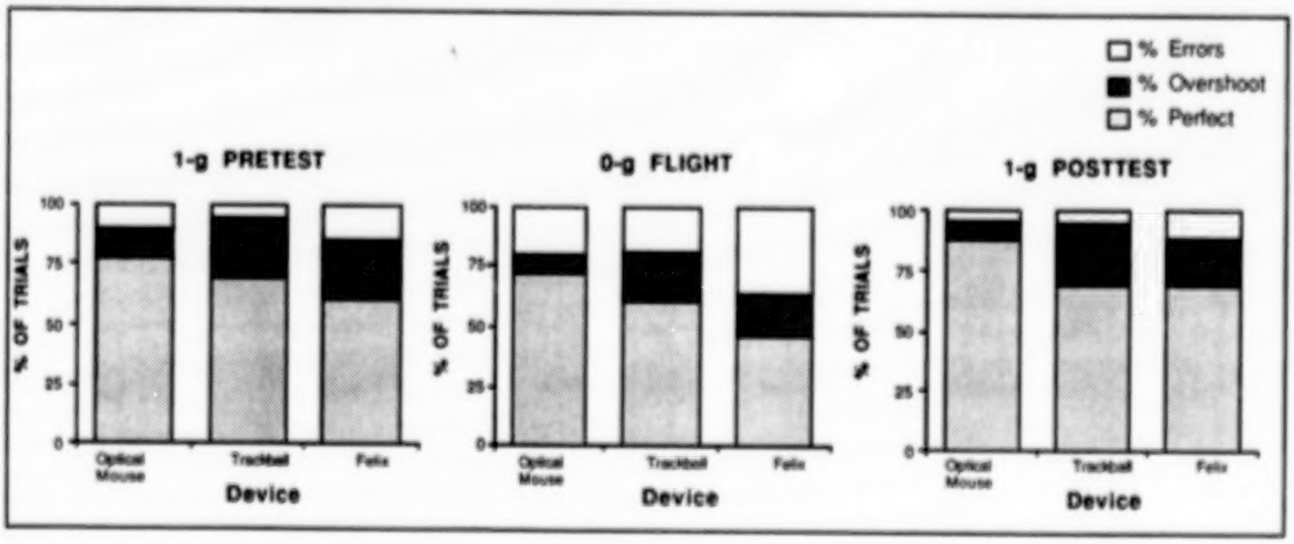

Figure 3. Error distribution across test conditions for Experiment 1

collapsed across devices, were 8.7% slower in 0-g than the average of the 1-g trials. While there was not a significant effect for device used, in both the pointing and dragging portions of the tasks for pretest, flight, and posttest conditions, the optical mouse was fastest (see Figure 2).

The error data presented in Figure 3 shows the percentage of trials where the subject's selection resulted in an (1) Error: the subject made errors resulting in an incorrect selection, (2) Overshoot: subject moved the cursor from the leftmost character of the underlined area (+/-.5 character) beyond the end of the underlined area, but then moved back to the end of the underlined area (+/-.5 character) before releasing the mouse button, and (3) Perfect selection: where the subject made a perfect selection (+/-.5 character) at each end of the underlined area. More errors occurred in flight than in pre- or posttest. The greater percentage of overshoots with the trackball and the Felix™ may contribute to the somewhat longer pointing and dragging times.

STS-29 DTO

The cursor control device evaluation flew as a part of an engineering evaluation of a portable computer to be used as a Payload General Support Computer (PGSC) aboard the shuttle.

Subjects

The participants were the astronauts on the STS-29 Shuttle crew. Each was familiarized with the task before flight but was otherwise unfamiliar with the mouse or trackball.

Apparatus

The evaluation was performed using a GRiD 1536™ Personal Computer with a 10 in. diagonal blue LCD screen. The cursor control devices evaluated were the MSC Technologies™ optical mouse with reflective pad and a PC-TRAC™ trackball. Velcro was fastened to the back of the reflective pad and trackball so that they could be affixed to the cabin wall or the crewmember's pant leg (thigh).

Procedure

The crew was instructed on how to set up the computer and cursor control devices. The evaluation consisted of subjective comments on a questionnaire after attempting specific point, click and drag movements on displays from existing software for the Shuttle Flight Data File. The questionnaire asked the crew to describe: (1) their body position while using the device, (2) ease of use for each of the devices with the point, click and drag movements, and (3) suggestions for modifications to the devices.

Results & Discussion

In all test cases the crewmembers were free floating while using the devices.

The mouse was given a rating of 1 on a scale of 10, were 10 indicates an excellent device. It was considered very difficult to use aboard the shuttle without a specially designed work surface. The crew described it as "requiring three hands" to operate. The trackball was rated a 7 on the same 10 point scale. It was used as a restraint by the crew in that they could keep themselves from floating away while using the device by holding on to the device itself. This method of use suggests that the input or click buttons, located on the top face of the device with the ball, should be located above rather than below the ball. This allows for the user to grasp the trackball with the thumb and ring finger while using the index and middle fingers to manipulate the ball and buttons.

The crew also suggested the incorporation of a toggle mode for selection. This would allow the user to click at the beginning of the text to be selected, thus triggering a selection mode, then move the ball and click at the end to complete the selection. Currently the drag mode of selection requires the user to hold down the selection button while using the ball to move the cursor to the end of the selection area. Holding down a button while moving the ball can be difficult, even in 1-g, depending on the relative locations of the button and ball.

KC-135 EXPERIMENT 2

Procedure

This experiment compared the use of the toggle selection mode suggested by the STS-29 crew with the typical Macintosh drag selection mode. The trackball and the optical mouse were used in each mode.

Two subjects practiced with each device in each selection mode to steady state performance prior to pretest data collection. Pretest and posttest data collection sessions were held for four days. Each day each subject completed eight blocks of trials (i.e., two blocks with each device in each selection mode).

Four flight sessions were planned but one was lost due to computer problems. The design allowed for each subject to perform two blocks of trials using each device in one selection mode per flight. On day two each subject would use the selection mode they had not used the day before. Similarly, on day three they switched modes again. Because during the last day no data was collected, each device x mode condition was performed twice by one subject and only once by the other. A General Linear Model (GLM) statistical analysis showed the subject effect was not significant.

Results & Discussion

Contrary to the expectation that the toggle selection mode would provide faster performance, the drag mode proved to be significantly faster as collapsed across all other testing conditions ($p < 0.05$). Selection times were not significantly different, though the mouse was consistently faster in both drag and toggle modes than the trackball (see Figure 4).

CONCLUSION

Direct manipulation performance is somewhat slower and more error prone in microgravity than in 1-g, even with sufficient restraint mechanisms. Longer selections, greater than 5 cm, are most affected by microgravity. Fifteen-inch diagonal displays have been baselined for use aboard Space Station Freedom. This current data shows that either the interface must be designed to minimize large selections or cursor controllers must be further researched to improve performance and accuracy.

The mouse has consistently provided for faster text selection than the trackball or post-mouse. The European Space Agency (ESA) has also independently arrived at this same conclusion (Gale, 1989). However, the mouse requires greater real estate for operation (i.e., the footprint of the control device) and requires more elaborate restraint than does the trackball. However, by increasing the gain (the control/display ratio) the footprint of the mouse can be substantially reduced. The trackball allows for one-handed use and serves as its own restraint for the resolution of input forces in microgravity. More research needs to be conducted which considers modifications to the trackball to improve its performance. Incorporation of the toggle mode of selection was such an attempt. One-g research is planned to evaluate the placement of selection buttons on the trackball.

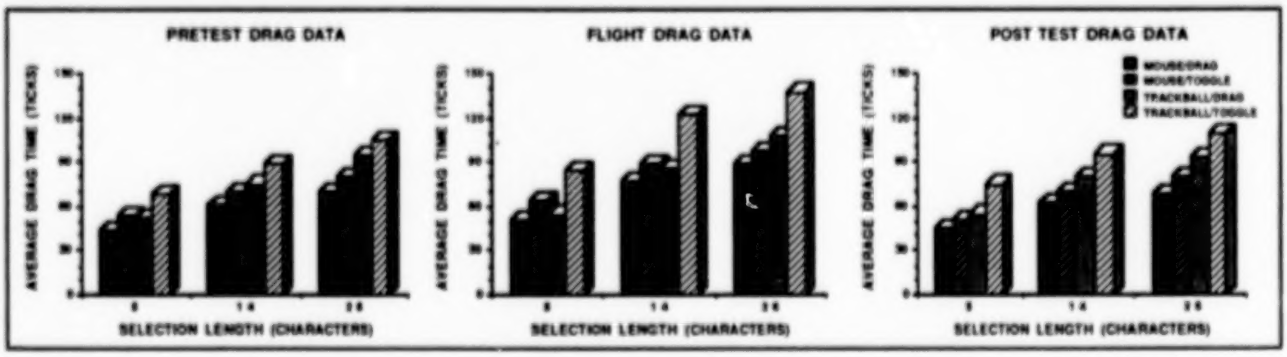

Figure 4. Drag times by selection length and device for Experiment 2

A DTO planned to fly aboard STS-41 in October 1990 will compare the 1.3 in. trackball built into a Macintosh portable with a new version of the Felix™. The new Felix™ is expected to be less sensitive than the original Felix™ used in Experiment 1.

A KC-135 flight planned for November 1990, will evaluate various restraint mechanisms for use with each of the two cursor control devices McDonnell Douglas Space Systems Company (MDSSC) has tentatively baselined for the space station workstation. These devices are a standard type trackball as well as a 1.5 in. joystick mounted thumb-ball/trackball. These designs will be further refined and evaluated aboard a DTO planned for May 1991.

Variations of the control/display ratio, variable gain designs, as well as double-click speeds will be further researched to define appropriate ranges for use in 0-g. Such controls will be user selectable aboard the space station for whatever device is chosen. Practice to steady state performance in 0-g is unfortunately impossible until the station is in place. It would be difficult and unwise to absolutely predefine these settings for all users.

ACKNOWLEDGEMENTS

Support for this investigation was provided by the National Aeronautics and Space Administration through Contract NAS9-17900 to Lockheed Engineering and Sciences Company.

REFERENCES

Beringer, D. B. & Peterson J. G. (1985). Underlying behavioral parameters of the operation of touch-input devices: Biases, models and feedback. *Human Factors, 27(4)*, 445-458.

Brown, C. M. (1989). *Human-computer interaction design guidelines*. New Jersey: Ablex.

[illegible], F C. T. (1989). *Report on the parabolic flight testing of pointing devices*. (Approval pending- ESA Tech. Report WGSG/90005/TG.) Noordwijk, The Netherlands: ESTEC-WGSG.

Gillan, D.J., Holden, K., Adam, S., Rudisill, M., & Magee L. (1990). How does Fitt's law fit pointing and dragging?. In J. Carrasco Chew & J. Whiteside (Eds.), *CHI'90 Conference Proceedings--Human Factor's in Computing systems: Empowering People* (pp. 227-234). New York: ACM Press.

Whitfield, D., Ball, R. G., & Bird, J. M. (1983). Some comparisons of on-display and off-display touch input devices interaction with computer generated displays. *Ergonomics, 27(11)*, 1033-1053.

Williams, R.K. (1987). *JSC reduced gravity program user's guide*. (NASA Tech. Report JSC - 22803). Houston, Texas: NASA Lyndon B. Johnson Space Center.

DEVELOPING THE HUMAN-COMPUTER INTERFACE FOR SPACE STATION FREEDOM

Kritina L. Holden
Lockheed Engineering and Sciences Company
2400 Nasa Rd1, MC-C95
Houston, TX 77058-3711

ABSTRACT

The Human-Computer Interaction Laboratory (HCIL) at Johnson Space Center (JSC), Houston is tasked with being responsible for defining the global Human-Computer Interface (HCI) for Space Station Freedom. This responsibility entails the early definition of hardware and software capabilities to support the HCI, definition of requirements for display developers and the identification of stylistic guidelines as well. The charter of the HCIL is uniquely defined in that it supports the applied development work necessary for designing the interface as well as applied research that is necessary for influencing design decisions. For the past two years, the HCIL has been heavily involved in prototyping and prototype reviews in support of the definition phase of the Freedom program. On Space Station, crewmembers will be interacting with multi-monitor workstations where interaction with several displays at one time will be common. The HCIL has conducted several experiments to begin to address design issues for this complex system. Experiments have dealt with the design of ON/OFF indicators, the movement of the cursor across multiple monitors, and the importance of various windowing capabilities for users performing multiple tasks simultaneously.

INTRODUCTION

Space Station Freedom, scheduled to be completed in the late-1990s, will be equipped with one of the largest and most sophisticated computer systems ever placed in orbit. Freedom's network of computers will control and monitor thousands of automated systems as well as provide an interface to the crew for the command and control of many additional functions.

The importance of the Human-Computer Interface (HCI) for Space Station Freedom cannot be underestimated; astronauts will come to depend on the HCI for all aspects of Space Station life including controlling the onboard environment and life support, the conduct of experiments, communication with earth and emergency procedures. In fact, the core HCI must be in place by First Element Launch, since the computer system will actually guide the assembly of Freedom.

104

The level of automated monitoring onboard is consistent with a typical process control environment such as that found in a nuclear power plant; however, Freedom's onboard environment is unique in that the computer system will provide extensive interactive capabilities as well. In fact, the interface will be primarily a direct manipulation interface where crewmembers can use a cursor control device to manipulate real objects (e.g., pumps) by pointing and clicking. A command language will be available (User Interface Language (UIL)), but the majority of a crewmembers work will be accomplished using direct manipulation. The complexity and flexibility of a direct manipulation interface, in combination with the process control aspects of the environment, constitute an interesting challenge for HCI designers.

SPACE STATION FREEDOM DATA MANAGEMENT SYSTEM

Space Station Freedom's computer system, called the Data Management System (DMS), is a complex distributed system composed of nine workstations, each having separate processors, connected via a state-of-the-art fiber optics network. The architecture of the component systems is similar to an IBM PS/2 Model 80 workstation, providing capabilities such as multitasking, color and gray scale, windowing and onscreen video.

PHASED HCI DEVELOPMENT PROCESS FOR FREEDOM

The process of designing an HCI for such a large, complex system must involve a phased plan with Human Factors input throughout planning, development and production. The team of HCI specialists at the Human-Computer Interaction Laboratory (HCIL) at Johnson Space Center (JSC), Houston has been tasked with providing that Human Factors input to ensure that Space Station Freedom has a safe and usable HCI.

HCI development for Space Station has been divided into three phases:
(1) Hardware and Software architecture and requirements definition
(2) Interface development and review
(3) Integration and testing.

The bulk of the HCI work has been completed as part of Phase 1, the Requirements Definition phase. Phase 1 is coming to a close and preparations are being made to move into formal review and usability testing that will occur in Phase 2. Actual development of hardware and software for Space Station Freedom is beginning now.

CONSISTENCY IN DESIGN

One of the primary concerns of Space Station HCI developers is the need for consistency throughout the hundreds of displays that will be available for viewing onboard. There are two primary means for achieving this consistency: (1) the development of interface requirements and standards documents in combination with a Review board to ensure strict compliance, and (2) the development and mandated use of a display builder toolkit (software) that will enforce standards and requirements by making available only acceptable display options. For example, the display builder toolkit will provide one standard shape for a momentary software button. This is the only shape that will be available to the developer. Likewise, the palette of colors provided will contain only sanctioned colors.

The goal of the HCI development team during Phase 1 has been to ensure that all of the hardware and software requirements necessary for providing a safe and usable HCI are in place and officially baselined. To accomplish this task, it was necessary to identify as many design issues and problems as possible within a limited amount of time.

The most effective technique for quickly identifying interface issues is rapid prototype iteration. Once issues have been demonstrated via a prototype, design decisions can be made or applied research can be performed if necessary to select a particular design.

ROLE OF PROTOTYPING IN SPACE STATION FREEDOM HCI DESIGN

Prototyping in the HCI domain differs somewhat from that done in other disciplines. In industrial settings, the term "prototype" usually implies that there is an end product that will be built. In HCI design, often times the end product is merely a display concept or idea for a method of interaction. In fact, many of the prototypes created in the HCIL do not necessarily reflect detailed technical information, but demonstrate display concepts and methods of interaction. Often times a display containing realistic technical details is not necessary to demonstrate a single concept, and thus it is most time efficient to prototype only to the level of realism necessary for the particular goal. When required, the prototypes progress into more mature phases to include interactive capabilities, realistic technical details and possibly connection to a database or network simulating realistic data.

PROTOTYPING TOOLS

Prototyping often begins as paper and pencil sketches of system components and relationships. Once enough basic information is available, a working prototype is put together using a tool such as Hypercard® (Apple) or Supercard® (Silicon Beach). These tools are excellent for rapid, interactive highly graphical prototyping. Much of the prototyping can be done without programming. When programming is necessary, English-like languages are available with these tools (Hypertalk® and Supertalk® respectively) so that HCI designers who are not programmers, can, without much difficulty, build an interactive prototype. If capabilities are needed that are beyond those available in Hypercard and Supercard (e.g. more speed, flexibility and connectivity), the prototypes are recreated on more sophisticated tools such as Dataviews (V.I. Software) or Scientific Software Intercomp's Advanced Man-Machine Interface (SAMMI).

THE DEVELOPMENT OF GUIDELINES, REQUIREMENTS AND STANDARDS

Initial development work on the HCI began approximately three years ago, before the prime Space Station contract had been awarded. The HCIL was tasked with providing an HCI guidelines document for Space Station Freedom. In order to accomplish this task, a set of representative Space Station tasks was selected for task analysis and prototyping. Performing task analyses for tasks and systems whose designs had often not been completed was quite a challenge. Nevertheless, a set of concept prototypes based on the task analyses was created to address global HCI issues. Prototyping was accomplished on a Macintosh using Hypercard® software. Creating these prototypes proved to be very beneficial in raising technical issues and testing out design ideas. It provided a starting point for identifying the kinds of concerns and issues that needed to be addressed in an HCI guidelines document. The final product (Space Station Freedom Program Human-Computer Interface Guide Ver 2.1; USE 1000) was completed in May, 1988 and has been distributed throughout the Space Station Freedom program and world-wide for use in interface design.

Following the award of the Space Station prime contract to McDonnell Douglas Space Systems Company (MDSSC), the need arose to develop hardware and software requirements and HCI style standards. Once again, a cycle of prototype generation and review proved to be very successful for identifying necessary hardware and software capabilities and issues needing more work. To ensure that all pertinent technical and experiential viewpoints were represented in the HCI design solutions for Freedom, an HCI team was formed consisting of representatives from the HCIL, MDSSC, Huntington Beach, CA (prime contractor), Mission Operations Directorate (MOD) , JSC, Houston and the Astronaut Space Station Support office, JSC, Houston. MDSSC created an interface prototype and sent it to the team at JSC for review and comment. The group at JSC independently and collectively reviewed the prototype, compiling a list of suggested changes and issues needing resolution. Every two weeks a teleconference was held so that all HCI team members could discuss the prototype and the suggestions. HCI team members worked together on almost a daily basis by phone or in person to continue refining the requirements definition. Once again, the use of prototyping for identification of software and hardware requirements and identification of major design issues

107

was very effective and time efficient. It became clear through prototyping that issues such as how a crewmember navigates within a very large hierarchical system displayed on three physical monitors are very important and are much more complex than they appear on the surface. As major issues were identified, each was approached individually as a new concept to be prototyped. Three documents are the products of the HCI team's Phase 1 work: (1) detailed requirements for the DMS User Support Environment (software requirements), (2) HCI standards (design/style standards) and (3) display examples (onboard).

THE ROLE OF RESEARCH IN HCI DESIGN

Throughout all of the various prototyping efforts undertaken in the HCIL, design reviews have identified problems and issues needing empirical resolution. The unique charter of the HCIL is such that facilities and personnel are available to do on-the-spot applied research to answer design questions. Because the HCIL performs phased prototyping, questions raised early in the prototype can be resolved prior to the completion of the prototype. Two examples of applied research performed for the express purpose of design resolution are studies dealing with (1) indicators and (2) multiscreen Issues.

ON/OFF Indicator Study

A fairly early prototype of the Power System for Space Station Freedom employed the use of many ON/OFF indicators. These indicators were not controls, but were status indicators for various components of the system. The display technique used to denote the active state of an indicator was reverse video, which is a commonly used equivalent code for a hardware light. Many direct manipulation interfaces that employ the use of selections or mode indicators, use reverse video to denote the active or selected state. During a preliminary design review of the interface, several reviewers commented that the active state as coded, was ambiguous. In other words, it was not clear whether a series of indicators read "ON" or "OFF". Although the majority of reviewers reported that the coding was clear, the possible serious impact of ambiguous coding led to the decision to perform a study. The study evaluated confusability and response time for subjects reporting the state of an ON/OFF indicator within a display similar to that in the Power system prototype. Several proposed designs were compared, including reverse video, check mark, reverse video with check mark, color (cyan) and bold frame. Half of the trials were shown on a black background and half were shown on a white background. The effects of background color and indicator type were not significant for the response time measure. The effects of background color and indicator type on response classification (i.e. whether subjects

108

responded "ON" or "OFF") were not significant. Thus, it appears that while a few persons may have trouble distinguishing the active state when coded with reverse video, empirical tests do not indicate that this is a general problem. This result enabled the HCI team to proceed ahead with using reverse video for coding, while remaining aware that a consistent method of coding active states will be necessary to help users generalize among displays. The results are currently being written up as a NASA Technical Report.

Multiscreen Studies

Space Station Freedom will provide a workstation to crewmembers that is equipped with three physical display devices/monitors. The workstations will include one keyboard, one cursor control device and one cursor. This configuration has raised several major issues centering around how crewmembers will interact with multiscreen systems.

During the prototype review cycle, the issue of how a crewmember would move the one cursor among three monitors was raised. Several methods were proposed: (1) continuous cursor movement (i.e., one virtual display surface where the cursor flows smoothly among monitors), (2) a direct, single action method of moving the cursor among the monitors, such as with fixed function keystrokes, clicks on a software button or the depression of a programmable display pushbutton (3) a cyclic method involving the cycling of the cursor in a predetermined (e.g., counter-clockwise) direction by means of repeated fixed function keystrokes, repeated clicks on a software button, repeated depression of a programmable display pushbutton or the repeated double clicking of the selection button on a cursor control device. The HCIL has designed an experiment to compare these seven separate methods. Subjects will use each of these methods to perform tasks requiring keyboard entry or tasks requiring control device entry. Each method of cursor movement has advantages and disadvantages. The primary purpose of the empirical study will be to determine which cursor movement methods are the least disruptive to the primary task at hand. The study will be completed this summer and written up as a NASA Technical Report. Preliminary review by several astronauts reveals a preference for the direct address fixed function key method where a function key is associated with a particular monitor. Astronauts expressed an interest in the continuous flow method, but there were many concerns about accidental movement of the cursor and subsequent unintended clicks or typing within the wrong monitor.

Additional work is ongoing in the area of user multitasking. One of the first experiments deals with the importance of windowing capabilities for a user performing one, two or four simultaneous tasks. This experiment will be conducted on a single monitor as well as a multi-monitor system and the results will be formally written up at completion.

CONCLUSIONS

Developing the HCI for Space Station Freedom is a challenging task and one that requires the coordinated efforts of many organizations. The HCIL is completing it's role as the lead during the architecture and requirements definition phase. As we move toward actual design, the HCIL will take on a new role to: (1) ensure that completed interfaces are compliant with the Standards document and (2) conduct usability testing to ensure that the interfaces are safe, usable and technically and operationally correct. As new issues arise in development, the HCIL will continue to use rapid prototyping as a means of quickly demonstrating several alternate design solutions and will conduct research as necessary to select the best design solutions. The work ahead will take several years to complete and there are many issues yet to be solved. The early human factors input provided by the HCIL at JSC is helping to ensure that crewmembers onboard will be able to do their jobs safely, comfortably and with ease as they interface with the computer system onboard Space Station Freedom.

SPACECRAFT CREW PROCEDURES FROM PAPER TO COMPUTERS

Michael O'Neal and Meera Manahan
Lockheed Engineering and Sciences Company
2400 NASA Road 1, MS C95
Houston, TX 77058

ABSTRACT

Many of the tasks the crew of a spacecraft must perform during a mission are recorded as crew procedures - step-by-step instructions describing how to perform the tasks. Currently, these crew procedures are created and carried into space in large paper notebooks. In the future, however, these procedures will be authored, edited, and performed using computer-based systems. This paper describes a research project that uses human factors and computer systems knowledge to explore and help guide the design and creation of an effective Human-Computer Interface (HCI) for spacecraft crew procedures; this HCI is an important component in an effective computer-based procedure system. By having a computer system behind the user interface it is possible to have increased procedure automation, related system monitoring, and personalized annotation and help facilities. The research project includes the development of computer-based procedure system HCI prototypes and a testbed for experiments that measure the effectiveness of HCI alternatives in order to make design recommendations; the testbed will include a system for procedure authoring, editing, training, and execution. Progress on developing HCI prototypes for a middeck experiment performed on Space Shuttle mission STS-34 and for upcoming medical experiments are discussed. The status of the experimental testbed is also discussed. Future implications and issues of computer-based procedure systems will be discussed including the effect on users' cognitive workload, system versus user task allocation, and system adaptability to changing procedural environments.

INTRODUCTION

Large volumes of paper are launched with each Space Shuttle mission that contain step-by-step instructions for various activities that are to be performed by the crew during the mission. These instructions include normal operational procedures and malfunction or contingency procedures and are collectively known as the Flight Data File, or FDF. An example of nominal procedures would be those used in the deployment of a satellite from the Space Shuttle; a malfunction procedure would describe actions to be taken if a specific problem developed during the deployment.

A new Flight Data File and associated system is being created for Space Station *Freedom.* The system will be called the Space Station Flight Data File, or SFDF. NASA has determined that the SFDF will be computer-based rather than paper-based for reasons including the following:

- The long duration of the Space Station program precludes one-time launch of all crew procedures.
- Repeated launch of crew procedure segments is not cost effective, since each pound of launch weight costs approximately $20,000.
- Large amounts of manual effort are required to create, edit, and maintain paper-based crew procedures.
- Changes made after procedure printing require annotation of each individual copy, a time-consuming and error-prone process.
- The time involved in implementing and delivering approved Space Station crew

procedure changes or updates in a paper-based system would be significant, including scheduling of resources on a Space Shuttle flight.

The main components of interest in a Human-Computer Interface (HCI) include the information available on the screen at any given time, how to change the quantity or content of the information present on the screen, how the information is organized, and how the user interacts with the displayed information. Designing an effective HCI is an important step in developing a viable computer-based crew procedure system for reasons including the following:

- An effective HCI will allow faster, more accurate crew interaction with spacecraft crew procedure systems.
- The HCI will facilitate the crew's monitoring of other spacecraft computer systems while performing crew procedures.
- The HCI will allow the crew to easily verify procedure steps performed by the computer system as procedure automation increases.
- A context- and user-sensitive help and annotation system within the HCI will allow the user to rapidly and efficiently access this type of information while performing the procedures.
- The effective HCI will provide rapid, easy access to required supporting information such as procedure reference items.
- The development of a standard HCI across all crew procedures will lessen the amount of cross-training required for different types of procedures and will thus lessen the amount of errors made during procedures.

The research project described in this paper uses human factors and computer systems knowledge to explore and help guide the design and creation of an effective HCI for computer-based spacecraft crew procedure systems. The research project includes the development of computer-based procedure system HCI prototypes and a testbed including a system for procedure authoring, editing, training, and execution to be used for experiments that measure the effectiveness of HCI alternatives in order to make design recommendations.

CREW PROCEDURE TASKS AND USERS

Many different tasks are required to create and maintain a spacecraft crew procedure system. Procedures must be created by personnel familiar with the tasks in question and by procedure authors and editors. The crew responsible for performing the procedures must be trained in how to use the procedures. Training crew personnel to be familiar with off-nominal procedures is also required so the procedures can be used quickly and effectively if needed during a mission. The actual performance of the procedure during the mission is an important task, including assistance and adaptation to changing conditions if necessary. If a procedure is used repeatedly during one or more missions, changes to the procedure may be required to correct inefficiencies or errors, and current versions of such procedures must be maintained and distributed to all appropriate personnel.

Personnel groups responsible for specific crew procedure tasks represent different user groups of the crew procedure system. Procedure authors create the procedures, assuring that they correctly describe the work to be performed and that they conform to a standard procedural format (e.g. FDF or SFDF); they are also involved in scheduling procedures during a mission to create mission plans and crew member short-term plans. Authors may also work with individual payload specialists or experimental scientists. Trainers review the procedures with the crew members who will perform the tasks; comments or problems with procedure details or clarity are reported to procedure authors or editors for correction. Crew members are involved with actual procedure performance, training, and correction or editing if required. Mission control personnel assist in scheduling procedures, working with the crew during the mission, and in monitoring the mission plan and short-term plans. Experimental investigators and payload specialists are involved in creation and execution of those procedures relevant to their experiment or payload. Procedure editors are also responsible for updating and distributing required procedure changes found during training or execution.

An effective computer-based procedure system, and an effective HCI to this system, must take into account the full range of tasks and users of the procedure system. In particular, a common interface that can be created by authors and used by trainers, crew members, and mission control personnel will contribute to faster, more accurate interaction with crew procedures.

PROJECT GOALS

The ultimate goal of the current research is to create HCI design guidelines that can be used for spacecraft crew procedures and other computer systems that display procedural information to procedure users. These guidelines should lead to faster, more accurate user interaction with procedural information on a computer.

The first step in the project is a review of available literature on computer presentation of procedural material and the evaluation of the current paper-based FDF procedure system for Space Shuttle. With this information, key issues are identified and their role in the research outlined. Using background information and human factors and computer system knowledge, alternative interfaces are created via prototypes. These prototypes are then evaluated by the various users of crew procedures listed above. Experiments are then performed using different presentation and interaction techniques; these experiments provide specific data on the relative speed and accuracy of procedure tasks using different interfaces. Comments from prototypes and results and conclusions from interface experiments are then compiled into human-computer interface guidelines for presentation and interaction with spacecraft crew procedures.

CREW PROCEDURE ISSUES

There are both advantages and disadvantages of moving from a paper-based to a computer-based crew procedure system. The current research project addresses these issues as they relate to the human-computer interface of the system. Advantages of using a computer will be utilized while disadvantages will be addressed and minimized.

Computer Advantages

Having a computer system behind the interface to a crew procedure system offers many advantages. By monitoring related onboard systems, the computer system can automatically perform many procedure steps that require simple status verification (e.g. "Check that switch F6 is ON"), thus reducing the time required to perform the procedure. A training mode is now feasible so that the crew member can practice using the procedure in exactly its final form with the exception that system actions are not actually performed; training and execution modes for the same procedure will increase the effectiveness of training. Personal annotation files can be attached to each procedure, thus allowing each crew member to create and refer to individual notes during both training and execution of procedures; these notes will be available whenever and wherever the crew member uses the procedure. The computer-based procedure system can coordinate with other spacecraft computer systems, providing easier transitions to and from other systems. The computer-based help system can adapt to both the user of the procedure and the context in which the procedure is being performed. The amount of detail (i.e. the prompt level) of the procedure can change for different users and situations. Finally, expert systems can be integrated into the procedure system, thus providing a more intelligent interface to crew procedures.

Computer Disadvantages

When procedural information is presented on a computer screen, the context of the information presented typically seems more limited than with a page of paper, although the actual amount of information present on a computer screen may or may not be smaller. There is less context information on where the current screen of information fits into the overall system; in a book, the location of the page in the overall book is an example of available context data. This issue will be addressed in the HCI to the computer-based system by generating and evaluating ideas to provide additional context information (e.g. screen number, screen position in overall outline, etc.).

In a complex computer system such as the onboard Data Management System (DMS) for Space Station *Freedom*, many levels of subsystems are present. The inability to rapidly navigate among the systems and subsystems can be a serious detriment to overall performance. This issue will be addressed in the HCI to the computer-based system by generating and evaluating ideas to provide information on current position within the system hierarchy and to provide tools to rapidly and directly move between subsystems either during or after a computer task.

RESEARCH FOUNDATIONS

Initially, a review of NASA literature on computer presentation of procedural information was completed. Information on work performed at MITRE for the Procedure Formatting System (PFS) project was reviewed and prototypes were viewed (Johns 1987 and 1988, Kelly 1988). Previous research in the Human-Computer Interaction Laboratory (HCIL) of the NASA Johnson Space Center was reviewed, and results from experiments on procedure context and format (Desaulniers, Gillan, and Rudisill 1988 and 1989) will be incorporated into the current research project. Coordination is in progress with the Mission Operations Directorate (MOD) at the NASA Johnson Space Center, as described below.

PROJECT STATUS

Current Project Prototypes

Prototype development is in progress for two Space Shuttle experiments. The procedures were selected for prototyping due to their similarity to typical research that will be conducted on Space Station *Freedom* since Space Station procedures are not yet available. The two prototypes will also use different HCI approaches.

The first system is a computer-based prototype of a middeck experiment, Polymer Morphology (PM), that was performed on Space Shuttle mission STS-34. The PM experiment consists of four procedures (setup, sequence initiation, sample check, and stowage) and six procedure reference items (interconnection overview, keystroke definitions, window definitions, notebook, sequences, and worksheets). The prototype is created within the framework of the Space Station basic screen layout being developed by the NASA/McDonnell Douglas HCI development team. Included in this prototype is an initial version of an Interface Navigation Tool developed at the HCIL that is currently being reviewed by the HCI team. Initial versions of the six reference items have been created. Development of the interface for the four procedures is in progress.

The second system is a computer-based prototype of an expert system for medical experiments to be performed on two upcoming Space Shuttle missions. The system, Principal Investigator in a Box, or [PI], will include an expert system. The motivation for this medical expert system is to provide the capability to perform medical experiments with minimum ground control or support. A separate HCIL research project is in progress to study the interface as it relates to the expert system, and this research will be coordinated with the current research which examines the same interface from the viewpoint of presentation of the procedures. The [PI] interface is being modified for the Space Station basic screen layout and will be evaluated as an alternative HCI design for crew procedures.

Current Project Experiments

As discussed above, the current procedures research will include the performance of experiments to gather specific data to support HCI guidelines for computer presentation of procedures. These experiments will begin as specific questions arise from the creation and analysis of HCI prototypes. The experiments will use subjective comments and speed and accuracy measurements to provide data for comparing different HCI alternatives. The experimental testbed will include a system for procedure authoring, editing, training, and execution that will allow HCI alternatives to be easily generated and compared.

COOPERATIVE WORK

In addition to continuing work with the MITRE PFS system, two cooperative projects with the NASA Johnson Space Center Mission Operations Directorate (MOD) are in the planning stages. Research will be performed in the HCIL to assist MOD in creating procedure standards for SFDF. Studies and experiments will be performed to provide human factors input into the standards created. Also, procedure authoring and execution software being developed within MOD will be evaluated from a human factors and HCI perspective.

FUTURE RESEARCH ISSUES

The current research project will continue to explore human factors issues relevant to the interface to electronic spacecraft crew procedures. The effect on the cognitive workload of the procedure users will be examined, with the goal of reducing this workload through automation. The allocation of procedure tasks between the user and the computer system will also be examined. Creating an interface that is adaptable to changing environments will be explored, including the method and user aids available during interruption and resumption of procedures. Research will also be performed on the use of the same computer interface during both training and execution of procedures.

CONCLUSION

Spacecraft crew procedures are increasingly being computerized, as in NASA's Space Station *Freedom* program. The human interface to these computer-based crew procedure systems is an important component, and research into improving the interface will provide faster and more accurate human interaction with the computer. The current research project uses prototypes and experiments to explore and help guide the design and creation of the human-computer interface for spacecraft crew procedure systems such as the Space Station. Prototype and experiment development is currently in progress. Issues relevant to human interaction with procedures will continue to be researched within the HCIL and in cooperation with other crew procedures researchers and developers.

LIST OF ACRONYMS

DMS	Data Management System onboard Space Station Freedom
FDF	Flight Data File (Space Shuttle)
HCI	Human-Computer Interface
HCIL	Human-Computer Interaction Laboratory
MOD	Mission Operations Directorate
PFS	Procedure Formatting System from MITRE
PM	Polymer Morphology experiment of STS-34
SFDF	Space Station Flight Data File

ACKNOWLEDGEMENTS

This research was funded by the National Aeronautics and Space Administration, Office of Aeronautics and Exploration Technology, through contract NAS9-17900 to Lockheed Engineering and Sciences Company. The research was performed at the Johnson Space Center Human-Computer Interaction Laboratory.

REFERENCES

Desaulniers, D. R., Gillan, D. J., and Rudisill, M. (1988). *The Effects of Format in Computer-Based Procedure Displays.* NASA Technical Report. Houston, Texas:

Lockheed Engineering and Sciences Company.

Desaulniers, D. R., Gillan, D. J., and Rudisill, M. (1989). *The Effects of Context in Computer-Based Procedure Displays.* NASA Technical Report. Houston, Texas: Lockheed Engineering and Sciences Company.

Desaulniers, D. R., Gillan, D. J., and Rudisill, M. (1988). *A Comparison of Flowchart and Prose Formats for the Presentation of Computer-Based Procedural Information.* NASA Technical Report. Houston, Texas: Lockheed Engineering and Sciences Company.

Johns, G. J. (1987). *Flight Data File for the Space Station, Volume I, Baseline Definition, and Volume II, Baseline Functional Requirements.* (MITRE Report No. MTR10019). Houston, Texas: The MITRE Corporation.

Johns, G. J. (1988). *Dynamic Display of Crew Procedures for Space Station, Volume I, Baseline Definition, and Volume II, Functional Requirements.* (MITRE Report No. MTR-88D033). McLean, Virginia: The MITRE Corporation.

Kelly, C. M. (1988). *Conceptual Definition for a Flight Data File Automated Control and Tracking System.* (MITRE Report No. MTR-88D0017). McLean, Virginia: The MITRE Corporation.

NASA/JOHNSON SPACE CENTER HUMAN-COMPUTER INTERACTION LABORATORY

Marianne Rudisill
NASA/Johnson Space Center

(Paper not provided at publication date)

117

CREW SYSTEM DYNAMICS

118

CREWS AND TEAMS IN THE FUTURE: A VISION OF COMMAND AND CONTROL

Lorraine Duffy
USAF Human Resources Laboratory

(Paper not provided at publication date)

CREW COORDINATION IN TRADITIONAL AND AUTOMATED COCKPITS

Thomas R. Chidester
NASA/Ames Research Center

(Paper not provided at publication date)

ELECTRONIC COLLABORATION: SOME EFFECTS OF TELECOMMUNICATION MEDIA AND MACHINE INTELLIGENCE ON TEAM PERFORMANCE

A. Rodney Wellens
Department of Psychology
University of Miami
Coral Gables, Florida 33124

ABSTRACT

Both NASA and DoD have had a long standing interest in teamwork, distributed decision making and automation. While research on these topics has often been pursued independently, it is becoming increasingly clear that the integration of social, cognitive and human engineering principles will be necessary to meet the challenges of highly sophisticated scientific and military programs of the future. Images of human/intelligent-machine electronic collaboration were drawn from NASA and Air Force reports as well as from other sources. Areas of common concern were highlighted. The report ends with a description of the author's research program testing a "psychological distancing" model of electronic media effects and human/expert system collaboration.

INTRODUCTION

Corporate as well as military decision makers have become increasingly dependent upon electronic media for information gathering and transmission. Groups whose members are separated by geographic barriers would find it difficult to function effectively without using telecommunication networks to coordinate their activities. Likewise, decision makers have also become increasingly dependent upon electronic machine aides for integrating and displaying complex data. Without the use of computers, many military, industrial and scientific projects would simply come to a halt.

Concern for the speedy integration of electronic media, remote sensing and computing led the National Science Foundation (NSF) to recently initiate a program dealing with "coordination theory and technology." According to one NSF report calling for the establishment of a "National Collaboratory," (Lederberg & Uncapher,1989), some of the most pressing challenges facing the United States and the world can only be met through remote interaction with instruments, colleagues and data. The term "electronic collaboration" used in the title of the present report was chosen to reflect this general idea. Specifically, *electronic collaboration involves linking two or more intelligent entities via electronic media to facilitate coordination and cooperation in performing a joint task.* The "intelligent entities" included in this definition can be humans, intelligent machines, or a combination of the two.

The relevance of "electronic collaboration" to the Air Force/NASA Space Operations, Applications and Research (S.O.A.R.) conference will be made evident by pursuing three primary themes:

1. NASA and the Air Force have areas of common concern regarding human-intelligent machine interaction
2. Communication between humans over electronic media can be used as a model for studying human-intelligent machine interactions.
3. The social psychological study of human-to-human and human-machine interactions can contribute to the development of future NASA and Air Force systems.

AREAS OF COMMON CONCERN

Interacting with Intelligent Machines. During the summer of 1983, NASA sponsored a summer workshop, managed by Ames Research Center, entitled "Autonomy and the Human Element in Space." The workshop brought together a group of 18 university professors from institutions throughout the United States, representing such fields as physics, psychology, chemical and industrial engineering, urban ecology and environmental planning, business and management, anthropology, and computer sciences. The purpose of the 10 week workshop was to study "autonomy" in space and it's role in an evolving, permanent extra-terrestrial human presence. The Office of Aeronautics and Space Technology (OAST) wanted to collect ideas about the relationship of humans and intelligent machines within the context of a future space station. The ambiguity in the title of the workshop, however, lead to more ideas than had originally been anticipated. For the engineers in the group, autonomy clearly meant "automation"; the social scientists in the group interpreted autonomy in terms of the relative "freedom" of the crew; the management professors saw autonomy in terms of the location of organizational "control". In their final report (Johnson, Bershader & Leifer, 1985), the group settled on a three dimensional model of autonomy that incorporated all of these ideas. Thus, the group reviewed the literature regarding the partioning of tasks between humans and machines (automation). They looked at situations involving humans managing machines and machines directing human activity (locus of control). They also looked at the relative merits of ground-based versus station-based control of operations (locale of control) and the communication systems needed to support both.

Jumping ahead five years, a recent international conference, co-sponsored by the U.S. Air Force, entitled, "The Human-Electronic Crew: Can They Work Together?" reflects current thinking regarding the cockpit of the future. A sampling of topics discussed at the conference (Emerson, Reising, Taylor & Reinecke, 1989) included:

1. Implications for the design process of the human electronic crew concept
2. Trust and awareness in human-electronic crew teamwork
3. Pilot vehicle interface management
4. Getting ready to team with an electronic copilot
5. Levels of autonomy in a tactical electronic crewmember
6. The pilots associate: Today tomorrow

As these conference topics suggest, many of the issues studied by the NASA group regarding the collaboration of intelligent machines with humans in a space station context are now being address by the Air Force within the context of highly automated aircraft. How should tasks be allocated between humans and machines? When should an intelligent machine be allowed to "take over" the controls of an aircraft? How can trust be established between humans and intelligent machines?

Coping with the Information Glut. On yet another front, a recent article in *Science* magazine (Waldrop, 1990), was entitled, "Learning to Drink from a Fire Hose." The analogy of drinking from a fire hose has been used by human factors specialists describing the condition of a fighter pilot attempting to monitor all the displays that have been provided within sophisticated fighter aircraft. The phrase also appears appropriate for describing the condition of command post personnel who must monitor and integrate vast amounts of intelligence and sensor data or for describing mission control console operators who must similarly monitor multiple system functions in order to insure a safe and successful space flight mission. Interestingly, the *Science* article dealt with none of these situations, but described instead the plight of earth bound scientists attempting to cope with the ever increasing amounts of data from large interdisciplinary projects such as global change, biomedical research and astronomy. As the complexity of our machines and organizations increases we are faced with an increasing glut of information that often needs to be processed in real time. How can this be accomplished?

THE TEAM APPROACH: ELECTRONIC COLLABORATION BETWEEN PEOPLE AND MACHINES

When task demands exceed the capabilities of a single individual, one approach to getting the job done has been to divide the task among several individuals to form a team. This is the basic idea behind the multiperson airline crew, shuttle crew or command post team. Each person specializes in a particular subtask, attends to information relevant to that subtask and communicates with other team members as needed to maintain coordination. The performance of the team would be expected to vary as a function of the individual team members' capabilities, the quality of the information they receive and the degree of coordination among team members. Coordination and cooperation is facilitated by appropriate communication between team members.

There has been an extensive body of research developed dealing with groups and teams (Steiner, 1972; Dyer, 1984; McGrath, 1984). However, this research has traditionally studied groups in face-to-face settings. There has been relatively little work done on groups whose members are geographically dispersed and must depend upon electronic media to function effectively (Short, Williams & Christie, 1976; Johansen, Vallee & Spangler, 1979). Virtually unstudied are groups whose members include one or more intelligent machines that can automatically respond to events without human intervention (Wellens & McNeese, 1987).

Electronic Media. In order to provide a framework within which to study the effects of electronic telecommunication media upon group processes, Wellens (1986) reviewed the telecommunications literature and proposed a "psychological distancing" model of telecommunication effects. The model predicts increased feelings of psychological closeness (and thus, increased liking, cohesion and cooperation) between individuals as the communication bandwidth (defined in terms of the amount and kind of information exchanged) linking them increases. Thus, an information lean medium like electronic mail would engender more feelings of remoteness between tele-interactants than would an information rich medium like two-way television.

Electronic Partners. The concept of an intelligent machine partner has recently come into vogue both within the military and civilian communities. An early example was the robot *R2D2* from the *Star Wars* film series who projected a friendly image of an intelligent machine assistant. Interestingly, the image of this fictional robot was used as an unofficial mascot within both the NASA and Air Force-sponsored workshops previously cited. In a more recent promotional video, Apple Computer Company introduced the idea of the "Knowledge Navigator" (see Brower, 1988). In the video a professor interacted with an artificially intelligent humanoid that appeared on a computer screen. This "user agent" helped the professor with phone messages, lecture notes and communication with a colleague over a video telephone. Within a few months of the video's release, an enterprising software company introduced an animated "talking head" that looked like the bow-tied character depicted in the Apple video (see 31 Jan 1989 MacWeek). Similar fictionalized characters have appeared for public consumption in popular television programs (e.g., *Max Headroom*).

The appeal of an intelligent machine assistant appears to center upon the desired ability to quickly assemble information and respond autonomously when needed while remaining subservient and self-sacrificing toward humans. While reality has not quite caught up with fiction, several projects are attempting to close the gap. For example, the idea of "knowbots" (autonomous software modules) that inhabit computer networks to aid human users has been seriously proposed and is in the early stages of development (Waldrop, 1990). Similarly, the "pilot's associate" research and development program (Small, Lizza & Zenyuh, 1989), funded in part by DARPA, is an ongoing project with a projected completion date of 1992. The objective of both programs is to develop one or more artificially intelligent agents that will be able to collect and integrate large amounts of information in real time. The "knowbots" will fuse and present data in interpretable formats for human users while the pilot's associate will go one step further by potentially taking over certain aspects of mission planning and flight control in future fighter aircraft.

With these and other projects expanding the boundaries of artificial intelligence, Wellens and McNeese (1987) recently called for research into the "social psychology" of intelligent machines. The interaction of humans with artificially intelligent machines was seen as a new form of dynamic social interaction. These authors recommended an interdisciplinary approach for understanding the impact of machine intelligence upon human cognitive, emotional and behavioral functioning that would take a social psychological perspective.

AN INTEGRATIVE RESEARCH APPROACH

In an attempt to assess the utility of applying social psychological principles to the study of human-intelligent machine interactions, the present author availed himself of a unique opportunity to pursue a collaborative research project as an AFOSR/URRP Visiting Scientist at the Armstrong Aerospace Medical Research Laboratory (AAMRL), Wright-Patterson Air Force Base, Ohio. The results of this two-year effort are contained within a recently released report entitled "Assessing Multi-Person and Person-Machine Distributed Decision Making Using an Extended Psychological Distancing Model" (Wellens, 1990). The report relates findings associated with human-to-human tele-interaction with human-machine interaction. This was accomplished within a research paradigm that capitalized upon the natural filtering that occurs when humans communicate with each other over telecommunication devices. Within a telecommunications context messages can be digitized, quantified and potentially duplicated by computer. As the bandwidth used to connect humans decreases and the data processing capabilities of machines increases, the distinction between human and machine messaging becomes increasingly blurred. (See Brody, 1983, for advances in teleconferencing bandwidth compression techniques and Bolt, 1980, for advances in expanding human-machine interfacing.) By extending the "psychological distancing" model described earlier in this report to include both human-to-human and human-machine interactions predictions were made regarding the effects of bandwidth expansion or compression upon group functioning. Thus, as the communication bandwidth between intelligent entities was increased it was anticipated that information would flow more easily, increased trust and liking would develop and collaborative performance would increase. These ideas were empirically tested within a specially designed media laboratory developed within the C^3 Operator Performance Engineering (COPE) project at AAMRL.

Two experiments were conducted that systematically varied the kind of telecommunication channels used to link human or machine "analysts" engaged in a situation assessment and resource allocation task (see Wellens & Ergener, 1988, for a complete description of the task). The workstation used by subjects who participated in the experiments consisted of a color television monitor equipped with a touch screen and placed adjacent to a table-top communication console. The console contained a two-way television monitor connected to an adjacent control room that allowed either (1) full motion color television images accompanied by voice communication (2) voice only communication or (3) electronic mail messages to be passed between pairs of collaborating team members.

Within the first experiment 40 pairs of human subjects were randomly assigned to one of the three communication situations described above or to a no communication control condition. Records were kept of all messages exchanged between partners as well as their overall performance on the task. Post experimental questionnaires were used to measure subjects' impressions of their partners, their level of situation awareness during the task and their satisfaction with the communication channels provided. Results generally supported the psychological distancing model in that the number of words exchanged between individuals significantly increased with communication bandwidth as did subjects' impressions of felt teamness, trust and liking. Unexpectedly, situation assessment information increased only slightly as communication bandwidth increased and actually decreased for some subjects as the communication demands of the task competed for attention. While subjects' satisfaction with the communication link increased with manipulated bandwidth, their overall performance on the task increased only slightly.

Within the second experiment the same workstation arrangement was used to connect human analysts with an "electronic partner." The electronic partner was an expert system equipped with a messaging system that displayed either a "talking head" capable of delivering self-initiated voice messages that were accompanied by an animated computer-generated face or sent written messages via an electronic mail system. Eighteen subjects were exposed to each of the two messaging conditions described as well as a no communication control condition while participating in a variation of the situation assessment and resource allocation problem used in the first experiment. Results showed increased ratings of trust, liking and teamness between the no communication control condition and the two messaging conditions. However, no significant differences were found between the two messaging conditions. This same pattern of results was found for the performance and situation awareness measures. Apparently, the content of the expert system's messages, which did not vary between the talking head and electronic mail conditions, was sufficient for subjects to coordinate their actions relative to their resource allocation responsibilities. Subjects reported liking the voice aspect of the talking head condition in that they could listen to messages without having to look away from their primary task monitors. Conversely, the written messages were seen as more easily understood, but required looking away from their primary task monitors to read.

The results of these two experiments suggest that providing even a minimal communication link between humans or between humans and intelligent machines will tend to increase felt teamness, cooperation and performance. A present, however, increasing the bandwidth beyond that which is minimally necessary for task accomplishment increases performance only marginally. When there is some "depth" to the intelligent entities being connected (as is the case with most human subjects), increasing bandwidth generally leads to increased communication activity which may in turn lead to increased trust and cohesion. However, the time taken away from primary duties to engage in conversation may temporarily reduce attention toward other task responsibilities.

Contrasting human-to-human interactions with human-machine collaboration painted a somewhat different picture. The expert system used in the present experiment mechanically issued messages when they were required by the task, but was otherwise a "dull" partner. Until intelligent machines acquire more "depth" and improve their "social skills," it is unlikely that humans will take the time to "chat" with them, especially when they are under pressure to perform well on other aspects of a task. For now it would appear that having task information presented in an easily understood fashion is more important than having it delivered by a humanoid persona.

SUMMARY AND CONCLUSIONS

This report began by pointing out that the Air Force and NASA have both had interests in human-intelligent machine interaction, decision making and team performance. Images of "electronic partners" who could work collaboratively with humans to reduce information overload and improve task performance were drawn from science fiction themes as well as from ongoing research programs. A research approach was described that used a telecommunications context to study both human-to-human and human-machine interaction. Predictions based on a psychological distancing model of telecommunications effects were supported when humans were linked electronically to other humans. Reported feelings of teamness, liking and trust increased as the bandwidth of communication increased. However, predictions regarding improved group situation awareness and team performance received only partial support. For humans linked electronically to a message generating expert system, it was found that increasing the bandwidth of communication beyond that minimally needed for successful task accomplishment had little effect. However, feelings of teamness, liking and trust, as well as task performance were all significantly higher in the two communication conditions examined than when no messages were sent by the expert system.

By taking a social psychological perspective when studying human-machine interaction, investigators must not only view the interactive role of intelligent machines in a new light, but also rethink assumptions regarding human-to-human collaboration. When attempting to optimize human-to-human collaboration via telecommunication interfacing one quickly discovers what is essential for successful task accomplishment and what additional factors influence group cohesiveness. As computer power increases and advances are made in providing expert systems with more "social skills," informed decisions will need to be made regarding the degree of bonding desired between humans and their electronic partners. It is hoped that the ideas presented in this report will be useful in making these decisions.

ACKNOWLEDGMENTS

The author wishes to thank the Air Force Office of Scientific Research, University Resident Research Program, for sponsoring the research described in this report. Thanks are also extended to the Armstrong Aerospace Medical Research Laboratory, Human Engineering Division, for hosting the project over its two year duration. The author would also like to acknowledge the help of Mr. Mike McNeese in locating reports dealing with the Pilot's Associate program and sharing his insights into collaborative problem solving processes.

REFERENCES

Bolt, R. (1980). Put-that-there: Voice and gesture at the graphics interface. *Proceedings of the SIGGRAPH '80 Conference, Computer Graphics,* 14 (3), 262-270.

Brody, H. (1983). Reach out and see someone. *High Technology,* 3 (8), 53-59.

Brower, E. (1988). Knowledge navigator draws fire: Viewers react to Apple video. *MacWeek,* 6 December, p. 3.

Dyer, J. (1984). Team research and team training: A state-of-the-art review. In F.A. Muckler (Ed.), *Human Factors Review.* Santa Monica, CA: The Human Factors Society, Inc.

Emerson, J., Reising, J., Taylor, R. M., & Reinecke, M. (1989). *The human-electronic crew: Can they work together?* WRDC-TR-89-7008, Conference Proceedings, Ingolstadt, Federal Republic of Germany, 18-22 September, 1988.

Johansen, R., Vallee, J., & Spangler, K. (1979). *Electronic meetings: Technical alternatives and social choices.* Reading, Mass.: Addison-Wesley Publishing.

Johnson, R. D., Bershader, D., & Leifer, L. (1985). *Autonomy and the human element in space.* Final Report of the 1983 NASA/ASEE Summer Faculty Workshop, Stanford University, 20 June - 26 August, 1983.

Lederberg, J. & Uncapher, K. (1989). *Towards a national collaboratory: Report of an Invitational Workshop.* Rockefeller University, 13-15 March, 1989.

McGrath, J. E. (1984). *Groups: Interaction and performance.* Englewood Cliffs, N.J.: Prentice-Hall, Inc.

Short, J., Williams, E., & Christie, B. (1976). *The social psychology of telecommunications.* New York: John Wiley & Sons.

Small, R. L., Lizza, C. S., & Zenyuh, J. P. (1989). The pilot's associate: Today and tomorrow. In J. Emerson, et al. (Eds.). *The human-electronic crew: Can they work together?* WRDC-TR-89-7008, Conference Proceedings, Ingolstadt, Federal Republic of Germany, 18-22 September, 1988, pp. 133-138.

Steiner, I. D. (1972). *Group process and productivity.* New York: Academic Press.

Waldrop, M. M. (1990). Learning to drink from a fire hose. *Science,* 248, 674-675.

Wellens, A. R. (1990). *Assessing multi-person and person-machine distributed decision making using an extended psychological distancing model.* AAMRL-TR-90-006, Final Report, AFOSR University Residence Research Program, Wright-Patterson Air Force Base, Ohio, 16 July 1987 - 15 July 1989.

Wellens, A. R. (1986). Use of a psychological distancing model to assess differences in telecommunication media. In L. Parker & C. Olgren (eds.) *Teleconferencing and electronic media,* Vol. V, pp. 347-361. Madison, Wisconsin: Center for Interactive Programs.

Wellens, A. R. & Ergener (1988). The C.I.T.I.E.S. game: A computer-based situation assessment task for studying distributed decision making. *Simulation and Games,* 19, 304-327.

Wellens, A. R. & McNeese, M. D. (1987). A research agenda for the social psychology of intelligent machines. *Proceedings of the IEEE National Aerospace and Electronic Conference,* 4, 944-950.

BRIEF BIOGRAPHICAL SKETCH

Dr. A. Rodney Wellens received his Ph.D. degree from Vanderbilt University in Experimental Social Psychology in 1972. Dr. Wellens is currently Professor of Psychology and Communications and Associate Chairman of the Department of Psychology at the University of Miami, Coral Gables, Florida. Dr. Wellens directs the Interactive Television Laboratory for the Study of Social Interaction at the University of Miami where he has co-developed several video and computer based devices for studying interpersonal and human-machine interaction.

Dr. Wellens recently completed a two year appointment as a Visiting Scientist at the Armstrong Aerospace Medical Research Laboratory, Human Engineering Division, Wright-Patterson Air Force Base, Ohio. Dr. Wellens was also one of 18 Faculty Fellows who participated in a NASA sponsored workshop held at Stanford University that dealt with space station issues. Dr. Wellens' presentation at the 1990 S.O.A.R Conference drew upon his experiences with the Air Force and NASA.

ISSUES ON COMBINING HUMAN AND NON-HUMAN INTELLIGENCE

Irving C. Statler
NASA Ames Research Center
N239-1
Moffett Field, CA 94035

Mary M. Connors
NASA Ames Research Center
N262-5
Moffett Field, CA 94035

Introduction

For the foreseeable future, there will be very few activities or missions that will be accomplished entirely by non-human, totally autonomous systems. Human intelligence and the ability it confers to exercise judgment and, thus, deal with unexpected situations will warrant the services of human members in future systems. The number of autonomous systems working in conjunction with, or in support of, human crews has been growing rapidly and can be expected to grow at an even faster rate in the future. We are faced with the problem of designing systems in which a machine intelligence and a human intelligence can work together as partners. This may be more difficult than designing a fully automatic, unmanned system. Unfortunately, we have little appreciation of either the potential or the limitations of close working relationships between humans and intelligent machines, or of how these interactions affect relations with other crew members or total crew performance.

The purpose of this paper is to call attention to some of the issues confronting the designer of a system that combines human and non-human intelligence. We do not know how to design a non-human intelligence in such a way that it will fit naturally into a human organization. Our concern is that, without adequate understanding and consideration of the behavioral and psychological limitations and requirements of the human member(s) of the system, the introduction of artificial intelligence (AI) subsystems can exacerbate operational problems. We have seen that, when these technologies are not properly applied, an overall degradation of performance at the system level can occur. Only by understanding how human and automated systems work together can we be sure that the problems introduced by automation are not more serious than the problems solved.

Background

Our experience with automation in space is still quite limited. However, there are examples from aircraft operations to illustrate the point that the implementation of engineering "solutions" may prove inadequate when human behavior is involved. A number of incidents (Connors 1989, Wiener & Nagel 1988) have raised questions about our ability to combine humans and automation into effective teams. Although we will be referring here primarily to examples from aircraft cockpits, the problems of man-machine integration in complex systems are ubiquitous. It is easy to strike out "cockpit" and fill in "air traffic control center", "submarine", "nuclear power plant", "launch control center", "space station", or "Mars vehicle". For many years, we have been able to rely on the adaptability of the human to take maximum advantage of each new technology. In the current environments of data-display that missions have required and computers have enabled, our man-machine systems are capable of saturating the human component with the sheer number of displays to be read, controls to be engaged, and decisions to be made. Nevertheless, we continue to depend on the human pilot to assess the situation instantaneously, to make the "right" decision, and to initiate the appropriate action. Many of us believe that, in the realm of both military aircraft and space systems, we are close to the practical limitations of human sensory and cognitive capabilities.

For example, over the years, electro-mechanical instruments, switches, and buttons have propagated wildly in the cockpit, filling all the available space. When the designer of the modern fighter aircraft cockpit was faced with the dilemma of reduced display space in the smaller cockpits along with the need for still more information to be displayed to the pilot, his solution was to replace task-specific displays and controls with multi-purpose displays and multi-function controls. Although this solution addresses the narrowly-defined display problem, it does not solve the operational problem, since modern computers that are brought aboard to drive these displays are capable of presenting far more data than a human can possibly access and assimilate in real time.

The F-18 aircraft has one of the more advanced cockpits and is a good example of the problem of data overload. This cockpit has three cathode-ray tubes and a head-up display. There are 675 acronyms and 177 symbols that can appear in four different sizes on any of the three cathode ray tubes. There are 73 threat, warning, and caution indicators, 59 indicator lights, and 6 warning tones (no messages, just tones), 10 multi-function switches on the throttle, 7 on the stick, 19 controls on the panel underneath the head-up display, and 20 controls around the periphery of each of the three cathode-ray tubes, each of which has a multi-switch capability. Most of the data displayed requires that the pilot's foveal vision be engaged (while peripheral vision, utilized in earlier displays, is largely ignored.) Every piece of information that is available to the pilot for multi-purpose display requires an additional control to access that information. This imposes a memory load on the crew who must remember how to access the desired information and how to perform the required control function. Often, these controls must be found and actuated by touch while the pilot is visually engaged elsewhere, sometimes during moments of extreme physical and mental stress. Since not all of the information about his aircraft can be displayed to the pilot at all times, there has evolved a proliferation of warning and alerting systems. These systems remind pilots to take actions, call attention to deviations from expected ranges, suggest or demand an action, warn of unacceptable configurations, and even take action on their own.

One of our favorite examples of where the engineering solution to a problem seems to disregard basic human-factors principles is the helmet-mounted display for the US Army's attack helicopter called the Apache. When a military helicopter is operating nap of the earth at night or in adverse weather, the pilot desperately needs help. He must be able to see something of the outside world. There is an infrared sensor, called a FLIR, in the nose of the helicopter that provides a display in the cockpit. There is also a computer on board that generates symbologies both for flight-control information and for weapons-control information. There are 19 such symbols in three different formats, depending on the flight phase. For the pilot of this aircraft, all of this (the FLIR image with superimposed flight- control symbologies and weapon-control symbologies) is presented on a two and a half centimeter monocle over his right eye. At the same time, his left eye is expected to take care of the contextual scene and the instrument panel.

We must also keep in mind that equipment intended to enhance human capability can actually encumber it by exacting a physiological toll that, in turn, compromises performance. The tendency to attach devices to the head is of particular concern, often leading to a loss of head mobility and fatigue. We have found some equipment of this type to cause both physiological and psychological problems in our military pilots. For example, some current helmet-mounted displays provide different and potentially disorienting visual images to the two eyes.

The typical military or civil pilot today must integrate enormous amounts of data from many dissimilar sources, sometimes under great time pressure. In our attempts to maximize the number of physical channels available for transferring these data, we have introduced voice and other aural displays. However, the addition of secondary modalities does not double the human's information processing capability; indeed it may even impede it by distracting the operator at a critical time. In fact, the operator may not even be aware of additional information because humans, under certain conditions, tend to narrow their attention. The problem may be further exacerbated by the human tendency in stressful situations to see what he expects to see and to hear what he expects to hear. Both the civil and the military sectors provide examples of where warning signals have been ignored due to the human tendency, when under stress, to selective attention.

The main point we wish to make is that humans, although highly adaptable, are not unlimited in their ability to accommodate to demanding task environments. In some of our more complex cockpits, the human may no longer be able to "take up the slack". In addition, the electronic systems we are now providing to aid the pilot may not be helping at all, and may actually be complicating his job. He is confronted with too much data and in formats that may not be conducive to rapid interpretation. It is useless to continue providing more data if the operator is unable to use it, since it is relevant information, not data, that is needed if the operator is to make good decisions.

In the past, when similar situations have been encountered, we have typically solved the problem by putting more men on the job. There are many situations in which this solution is impractical, and so it is tempting to look to artificial intelligence (AI) as a way of augmenting human capabilities. Presumably, with AI, one could fuse sensor outputs, integrate data, present only what was needed when it was needed, and assist the pilot in making decisions.

In keeping with this view, there have been proposals for military aircraft with one human pilot and several electronic crew members. Artificial intelligence, decision-support systems, knowledge-based systems, and expert systems became the buzz words of the eighties. However, although there has been a great deal of casual talk about the role that machine intelligence might play, the problem of developing the essential symbiotic relation between human and non-human intelligence has been examined only cursorily. We really do not understand what it takes to satisfy human needs, and it appears that even if we did, we do not yet know how to build it.

The Problem

Knowledge-based and expert systems have found some limited application in the control of physical plants, manufacturing processes, and quality control. However, they have yet to find a role in circumstances that cannot be described with mathematical algorithms or logical rules. But, not all knowledge is susceptible to logic.

There exist many potential applications for knowledge-based systems. Unfortunately, there are several fundamental things that we still do not know how to do. Following are just a few:

1. how to develop the complete knowledge base (or even know when or if it is complete,) particularly if it does not lend itself to logical rules;
2. how to have an expert system learn from experience by changing its rules;
3. how to enable the system to make complex decisions in real time during unexpected situations;
4. how to assure compatibility with the human operator's perceptions of the situation and acceptability by the operator of recommended solutions; and
5. how to validate the "sanity" of the system.

As AI grows and progresses, we can expect some advances in knowledge and understanding of these areas. However, automated systems will remain limited by the assumptions that created them, i.e., they will always to "blind" to conditions that were not explicitly or implicitly included in their design (Winograd and Flores, 1987).

Also, while computers can, after a fashion, think and learn, they do not think or learn as humans do. Consequently, if computational systems should take over decision-making chores, the human operator may find himself at odds either with what the computer is doing or the way in which it is doing it.

The rationale behind the introduction of automation has been the desire to enhance total system capabilities while maintaining operator workload at acceptable levels, thereby minimizing the possibility of human error. However, as more and more physical control activities have been successfully automated, they have been replaced by mental activities on the part of the human operator. Our experience with automation indicates that its introduction usually relocates and changes the nature and consequences of human error, rather than removing it.

The negative reactions and incident reports that NASA is beginning to receive regarding the electronic crew member in the glass cockpit of our modern civil transports support our concern. The glass cockpit has been criticized for its failure to reduce mental workload. Pilots believe that automatic devices demand constant attention and each device creates its own demands on the pilot's time. Automation tends to isolate the flight crew from the state of the aircraft and the modern pilot can feel not only left out of the loop, but externally controlled. Recent accidents suggest that excessive automation tends to lower the level of vigilance of human operators. Moreover, automation frequently addresses short-term, subsystem solutions, rather than total system performance. For instance, there is often inadequate feedback and interaction with the human controller (Norman 1990). Consider, for example, the system that corrects for a fault without notifying its human partner. In one incident, a race car equipped with the latest automatic compensation for brake failures suffered a failure in one brake. The system automatically compensated, just as it was designed to do. Shortly after, a second brake failed, and, due to the increased loading, the third-brake failure quickly followed the second. But, the automatic compensation system had done its job so well that it was not until the fourth brake failed that the driver realized he had a problem. This is an example of a faulty design philosophy that has as its goal to show the operator only what he needs to know when (someone else determines) he needs to know it.

In an analogy with the artificial heart program, the introduction of AI in a given system can fail (and has failed) because we do not understand the reaction mechanisms of the human. An AI subsystem must be designed to sing and dance gracefully with the human crew as well as with the energy sources that power it and the environment in which it must operate.

Therefore, the total system design must take into account the capabilities, limitations, and needs of the human component. We do this already with respect to human physiological constraints, but now we must take into account cognitive, motivational, and other psychological needs. We will continue to rely on the human in the vehicle for creativity and innovation in coping with the unexpected. In our future space systems, these humans will be better trained and more knowledgeable than ever before; but they remain humans whose tolerance for vibration, heat, hypoxia, and G-forces has not changed; whose visual perception and information-processing capacity are still limited; and whose decision-making ability remains susceptible to fatigue, illusions, biases and stress.

The design of the equipment intended to improve total system performance must consider the full impact it has on human behavior and on the human's ability to perform the role expected of him. This requires consideration of such things as the effects on humans of being "in the loop" or "out of the loop", the nature of trust between humans and machines, the ability of the machine to communicate the reasons for its actions to the satisfaction of the human operator, the ability of the machine to respond to the human's "what if I did it this way?" queries (Galdes and Smith, 1990) and the fact that the human needs to feel that he or she is ultimately in control. How can we be certain that any data display will be clear and unambiguous in all situations, so as to ensure the correct interpretation by the human for fast and accurate reaction in the rare critical situation? How do we keep the human well informed without annoying him? If the machine carries out all the routine tasks, how is the human to be kept in a state of alertness in which he or she is capable of performing adequately if the machine should fail? Many decisions regarding whether or not to manually override an automatic system will need to be made during critical phases of missions. Given the demands of these phases, does the automated system provide a net benefit to the crew? Can the workload required of the human crew during these periods be kept within acceptable limits?

Involving the human in the decision-making process provides a essential layer of checks and balances to make up for the shortcomings of the non-human intelligence. However, there is no point in extolling and relying on the real or imagined virtues of human creativity and innovation if the human doesn't know when to take control, or if the system design is such that the human is unable to be creative or innovative in the actions which the system allows him to initiate.

Often the problem of the human-machine interaction is considered to be merely one of interface design. This viewpoint is a dangerous oversimplification. It is like suggesting that human communication can be explained on the basis of word recognition. System functionality depends on characteristics of the communicating systems that extend well beyond issues of the operator interface. AI is going to be used to support dynamic interactive tasks in which the human mind is an important and active component of the total system. Designing tools for this kind of complex cognitive-psychological activity goes well beyond the issue of display and control interfaces. It can no longer be viewed as a process of designing a machine to do something, and then designing the information displays and controls which enable the operator to guide the machine. A system's usability is determined by the details of a given design and not just by its interface style.

Approach: The Crew System

The introduction of the concept of artificial intelligence to work with the human requires that we begin to think, not in terms of a human operating a machine as we have in the past, but in terms of communication between intelligent agents. The problem of designing a system that produces a symbiotic integration of the powers of the human brain and computers is incredibly complex and difficult. It is not simply a question of the proper allocation of functions between man and machine, nor should the human and the machines be considered in competition for duties. Rather it is essential that the human and the machine are explicitly considered as parts of a larger functioning system. The human may no longer be the sole supplier, as in the past, of the initiative, the direction, the integration, and the standards. For instance, it may be that the safest and most efficient system will be one that incorporates considerable duplication or interchangeability of functions among its human and non-human crew members and thus benefits from the strengths of both. A joint cognitive system implies a productive relationship between the knowledge of the machine and that of the human in which the different points of view are integrated in the decision process.

In a previous paper, one of us used the term "crew system" to describe all active, intelligent flight participants, whether human or artificial. Dr. Malin at JSC has proposed the idea of making humans and computers "team players". The implication of these terms is that the human(s) and the machine(s) must be considered as forming a partnership, sharing all the responsibilities and authorities in a concept of cooperation rather than one of human or machine control. The close coupling of humans and machines requires us to view their interactions as a total system design problem; i.e., a crew that is composed of both human and non-human intelligence.

One requirement of this integrated-design concept is for training and support to help humans cope with the new electronic environment. A second, and more pressing requirement, is to learn to design machine components for compatibility with real human behavior and with full recognition that human beings experience fluctuating motivation and attention and also make errors.

System design geared to blending human and automated systems must take into account all levels of human activity from the most basic perceptual response, through man-machine interface, and up to and including full integration into the relevant environment. For a human to perform a particular task, he must be able to translate his psychological representations of the system state, his goals, and his intentions into physical actions. To interpret the outcome of his actions, the human must be able to perceive the resulting system state and relate those perceptions to his psychological representations. We must understand how people recognize patterns, integrate information, add their own previous knowledge and value structure and come up with intelligent, appropriate decisions under difficult circumstances. A problem will ensue if the non-human intelligence negatively interferes with any part of this fundamental process (Norman 1987).

The need for considering design from the aspect of a crew system also introduces concerns related to small group and organizational science. We need to expand our view of system requirements to include information processing and motivation of multiple agents in organizations. When we introduce a non-human intelligence into the crew, the entire interactional structure of the crew changes. At these higher levels of integration, the results of NASA's extensive research in group dynamics pertaining to flight crews of long-haul civil air transports are particularly relevant. For example, in human groups it has been found that junior members are often reluctant to question the actions of the senior member even in critical situations. Similarly, automated systems that are perceived as highly reliable or having a high level of authority have produced an unwillingness on the part of the human to question and override. The quality of interpersonal interactions and coordination among the members of a crew in terms of their behavior and communications has been shown to be a fundamental factor in the performance of that crew and its susceptibility to errors. For human crews, this problem is a matter of selection, training, and organizational management; for the non-human member, it is a matter of design; for the entire system, all these factors, along with integrating procedures, must be included.

As yet, the human factors community has been unable to consolidate its empirical data into design methods and principles to guide the design process. The demands for performance-enhancing human/automation systems exceed our present understanding of the science. There are too many uncertainties in what principles are relevant to what tasks; empirical emphasis tends to be placed upon isolated properties of individual processes; and even well-established phenomena developed in laboratory settings often have very different levels of influence when imbedded in more complex tasks.

Since comprehensive design guidelines have been unavailable, system developers have attempted to assess the qualities of systems composed of AI and human components in a post facto manner. Thusfar, the index of acceptability has tended to be that the AI system has reached operational status. This is an unacceptable validation procedure and begs the question of total system capability. New indices of quality and acceptability are needed and even basis assumptions should to be re-examined.

In considering what might happen in combining human intelligence and artificial intelligence, one might postulate four major outcomes: (1) performance (in terms of effectiveness, efficiency, cost, etc.) is equal to that of the human crew alone;

(2) performance is equal to that of the automated system; (3) performance is less than that of the human crew or of the automated system alone, and (4) performance is better than either system alone. In general, only the fourth outcome (improved system performance) justifies the investment required for combined systems. The task then becomes finding practical methods and appropriate metrics for assessing the level of performance and the facility with which the human and the machine cooperate to solve unexpected problems. This task represents a substantial challenge to both the AI and the human factors communities.

A paper presently in preparation by one of the authors (Connors and Harrison, 1990) outlines research issues that are likely to be important in combining human and non-human intelligence. As this paper points out, one way to begin to understand the possibilities of integrated systems is to fully understand the failures that occur in present systems. A useful approach is to analyze the specifics of how human error changes (if at all) in the presence of automated systems. It is not enough, however, to examine error events in terms of number, severity, point in the mission, and the like. Critical information may be lost if one fails to examine error (or other measurable change) in terms of the human functions impacted (i.e., perception, recognition, attention, memory, information processing, coordination, and the like.) All opportunities, whether in simulation, field studies, or actual operations need to be utilized to begin to appreciate the dynamics of human behavior in human/automated settings. Cumulatively, our experience base could help focus future research and, eventually, to establish selection, training, procedural and design criteria.

Conclusion

Currently, systems are being planned based on exceedingly generous estimates of the human's capabilities for processing information and of the artificial intelligence capabilities for making sound decisions that are accepted by the human. In other words, we are busy building solutions when we do not yet fully understand the problem. Without an understanding of how to combine human and non-human intelligence effectively, we shall be unable to implement rational designs for our future space systems. The issues we have raised here, and others, need to be examined when considering the potential of these systems. The need for an effective marriage of human and non-human intelligence will increase greatly with the advent of Space Station Freedom and with the subsequent, more distant, missions. Life in these space vehicles is likely to mimic life in other isolated and confined settings, i.e., marked by fatigue, moodiness, disturbed sleep, sensory deprivation, reduced motivation, and loneliness (Connors, Harrison and Akins, 1985; Harrison and Connors, 1984). All of these will tend to exacerbate the physical problems that the space crews will endure. Yet, the crew must not only survive, but display a high level of productivity. In the longer-durations space missions of the future, the use of automation and the discharge of responsibilities by human and non-human crewmembers will be essential to the conduct of the mission as well as to the health and welfare of the crew.

While we stress, as we do here, the problem of data and activity overload, we should keep in mind that, during some phases of long-duration spaceflight, the opposite problem may occur. Boredom during long and uneventful phases of flight could lead to loss of productivity and it may be necessary to design into these system a level of crew workload that is not only sufficiently restricted to be manageable, but also sufficiently large and engaging to offset boredom and ennui (Statler and Billings, 1989).

One day, some believe, the intelligence of a computer may rival that of the human brain. One day, we may learn how to couple human brains and computing machines in new and productive partnerships. For now, however, we must rely predominantly on human intelligence, judgement, flexibility, creativity and imagination in dealing with unexpected events; while relying heavily on machine intelligence for the logic, speed, persistence, consistency and exactitude it possesses.

Our task for the near future is to begin the process of building towards symbiosis and improved system performance, avoiding on the way, the pitfalls that could lead to precipitous system failure.

References

Connors, Mary M. (1989) Crew System Dynamics: Combining Humans and Automation Presented at the 19th Intersociety Conference on Environmental Systems, 24-26 July 1989, San Diego. SAE Technical Paper Series 891530; 1989 Transactions in press.

Connors, Mary M. and Harrison, Albert A. (1990) Combining Humans, Automation and Telecommunications in Space-Analog Environments. Paper in preparation.

Connors, Mary M., Harrison, Albert A. and Akins, Faren F. (1985) *Living Aloft*: Human Requirements for Extended Spaceflight. NASA SP-483.

Galdes, D. and Smith, P., Ohio State U., personal communication, March, 1990.

Harrison, Albert A. and Connors, Mary M. (1984) Groups in Exotic Environments. *Advances in Experimental Social Psychology*, *18*, L. Berkowitz , (ed), Academic Press, pp. 50-87.

Norman, Donald A. (1987) Cognitive Engineering-Cognitive Science. Chapter 12 in J.M. Carroll (ed) Interfacing Thought. Cambridge, Mass: A Bradford Book, The MIT Press.

Norman, Donald A. (1990) The Problem with Automation: Inappropriate Feedback and Interaction, Not "Over-automation". Phil. Trans. R. Soc. Lond. B 000, 000-000.

Statler, Irving C. and Billings, Charles E. (1989) Maintaining Human Productivity During Mars Transit. Presented at the 19th Intersociety Conference on Environmental Systems, 24-26 July 1989, San Diego. SAE Technical Paper Series 891435.

Wiener, Earl L. and Nagel, David C. (eds.) (1988) Human Factors in Aviation San Diego: Academic Press, Inc.

Winograd, Terry and Fernando, Flores (1987) Understanding Computers and Cognition. Addison-Wesley Publishing Co.

r' 134

LIFE SCIENCES

MEDICAL OPERATIONS SUPPORT

(No papers submitted)

ENVIRONMENTAL FACTORS

(No papers submitted)

GENERAL BIOMEDICAL

(No papers submitted)

PROGRAMMATIC OVERVIEW

(No papers presented at this session)

DECOMPRESSION SICKNESS

INTENSITY OF EXERCISE AND LIKELIHOOD OF DECOMPRESSION SICKNESS

J. M. Waligora, D. J. Horrigan, and K. V. Kumar
NASA/Johnson Space Center

(Paper not provided at publication date)

141

SELECTION OF AN EMERGENCY BACKUP PRESSURE FOR AN 8.3 psi SPACE SUIT

D. J. Horrigan and J. M. Waligora
NASA/Johnson Space Center
J. Conkin
KRUG International

(Paper not provided at publication date)

ANALYSIS OF DOPPLER ULTRASOUND BUBBLE DETECTION DATA BY MEANS OF THE TIME/INTENSITY INTEGRAL

M. R. Powell
NASA/Johnson Space Center

(Paper not provided at publication date)

ANALYSIS OF THE INDIVIDUAL RISK OF ALTITUDE DECOMPRESSION SICKNESS UNDER REPEATED EXPOSURES

K. Vasantha Kumar, M.D.*
James M. Waligora, M.S.
David J. Horrigan, M.S.
John H. Gilbert, Ph.D.

National Research Council*/ Space Biomedical Research Institute, Environmental Physiology Group, Mail Code SD5, NASA Johnson Space Center, Houston, Texas, 77058.

ABSTRACT: In a case-control study, we examined the risk of Decompression Sickness (DCS) in individual subjects with higher number of exposures. Of 126 subjects (mean [SD]) of age 31.2 (7.2) years, body mass index 16.0 (4.2) and 2.7 (2.5) exposures each, 42 (33%) showed one or more episode of DCS. Examination of exposure-DCS relationship by odds ratio (OR) showed a linear relationship ($r=0.98$). The risk of DCS, when number of exposures >3, was 3.7 times (95% confidence interval 1.8,8.7) greater than ≤ 3 exposures in the individual. Stratification analyses showed that sex, tissue ratio (360-min half-time) and presence of Doppler microbubbles were confounders of this risk. Higher number of exposures increased the risk of DCS in our analysis.

INTRODUCTION : Decompression Sickness (DCS) is the result of a series of pathophysiological processes to acute changes in ambient pressure. There is considerable evidence that some individuals are more susceptible than others ("resistant") to DCS. Further, some authors believe that there is adaptation to DCS stress with repeated exposures.

The problem is twofold: First, what is the risk of DCS in individuals who are exposed many number of times compared to individuals with one or two exposures? Second, what is the risk of DCS in individuals on subsequent exposures? The latter is the question of adaptation or acclimatization and has been investigated by many.

In this paper, we analyze the risk of DCS in individuals with higher number of exposures in the various experiments conducted at NASA Johnson Space Center, Houston, TX, involving simulated extravehicular activities (EVA).

METHODS AND RESULTS :

Information on 126 healthy, individuals (101 males, 25 females), who participated in a total of 345 exposures to reduced pressure were collected. The exposures involved both direct and staged decompression profiles. The individuals exercised at altitude simulating extravehicular activities (6). They were also monitored for the presence of circulating microbubbles (CMB) by a precordial Doppler monitor. The exposure pressure and pre-breathe times were expressed as a 360-minute half-time tissue ratio (TR) (2). All exposures were for a period of 3 to 6 h at altitude. Further details on these profiles may be obtained elsewhere (2,6).Subjects were also required to rate their activities on a scale of 1-10, for assessment of fitness levels. Individual baseline characteristics were as below (mean[SD]):

Age	31.2 (7.2) yrs
Body mass index	16.0 (4.2)
No. of exposures	2.7 (2.5)
Tissue Ratio (360-minute)	1.5 (0.2)

Symptoms occurred in 56/345 (16%) of these exposures, of which only 4% (2/56) were severe or Type II DCS, the rest being pain-only bends. Forty-two individuals presented the 56 episodes of symptoms as below:

Once = 30 (71%)
Twice = 10 (24%)
Thrice = 2 (5%)

Distribution of cases (mean[SD]) with and without any symptom occurrence is given in Table I.

The number of exposures in individuals with and without symptoms was significantly different (Table I). Hence, we divided the entire group based on ≤3 and >3 exposures (Table II).

Table I. Distribution of cases

	No symptoms (n=84)	Symptoms (n=42)	
Age-years	30.5 (0.8)	32.5 (1.1)	
BMI	15.7 (0.5)	16.5 (0.6)	
TR	1.5 (0.1	1.6 (0.1)	*
No. of exposures	2.3 (0.3)	3.6 (0.4)	*
No. runs with CMB	0.6 (0.1)	2.1 (0.2)	*
Sex			
Male	61	40	*
Female	23	2	
Fitness scores			
≤5	48	19	
>5	36	23	

BMI=body mass index; * $p<0.05$

Table II. Subgroup on Exposure

	≤3 exp (n=100)	>3 exp (n=26)	
Age-yrs	31.3 (0.7)	30.6 (1.3)	
BMI	15.7 (0.4)	17.0 (0.6)	
TR	1.5 (0.1)	1.5 (0.1)	
No. of exposures	1.7 (0.8)	6.9 (2.7)	*
No. of runs with CMB	0.8 (0.0)	2.5 (0.4)	*
Sex			
Male	75	26	*
Female	25	0	
Fitness scores			
≤5	51	16	
>5	49	10	

* $p<0.05$

We calculated the odds ratio (OR) or cross-product ratio as a measure of relative risk of symptoms with higher exposure numbers in individuals (3). The results are given in Fig. 1.

Compared to occurrence of symptoms in individuals with single hypobaric exposure, there was greater risk of DCS in individuals with higher number of exposures. This increase in risk was linear (r=0.98). However, these findings were limited by the sample size, hence the wide confidence intervals (CI).

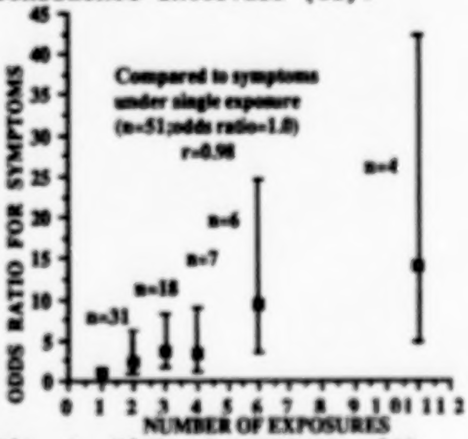

Fig. 1. **Risk of symptoms with increased exposures**

The overall OR for symptoms when the number of exposures were >3, compared to ⩽3 in the individual is given in Table III.

Table III. Individual risk with higher exposures.

	No DCS	DCS	OR
⩽3 exposures	73	27	1.0
>3 exposures	11	15	3.7 (1.8,8.7)

OR=odds ratio; 95% confidence intervals in parentheses.

We also examined the baseline differences (Table II) on the individual exposure information (⩽ and >3 exposures) by stratification analyses and Mantel-Haenszel statistics (3). The results are in Table IV.

Table IV. Stratification Analysis

	No DCS	DCS	OR	OR-MH
1. Sex				
Male :				
⩽3 exp	50	25	1.0	
>3 exp	11	15	2.7	
Female:				
⩽3 exp	23	2	1.0	
>3 exp	0	0	-	2.7 * (0.9,7.5)
2. No. of runs with CMB				
once :				
⩽3 exp	68	11	1.0	
>3 exp	7	2	1.8	
> once:				
⩽3 exp	5	16	1.0	
>3 exp	4	13	1.0	1.3 (0.01,137.5)
3. TR				
⩽1.5 :				
⩽3 exp	43	4	1.0	
>3 exp	8	5	6.7	
>1.5 :				
⩽3 exp	30	23	1.0	
>3 exp	3	10	4.4	5.2 * (1.8,14.7)

OR=odds ratio; OR-MH=odds ratio by Mantel-Haenszel statistic; 95% confidence intervals in parentheses; TR=360-minute half-time tissue ratio; * chi-square p<0.05.

DISCUSSION:

The results of the analyses showed that individuals with >3 exposures were 3.7 times more at risk for DCS, compared to individuals with ⩽3 exposures.

Bason et al. observed increased incidence (up to 12-fold) of DCS in the inside observers, compared to hypobaric chamber trainees (1). They attributed that this greater risk resulted from the higher number of exposures in the observers. Similar examination by Piwinski et al. on USAF data showed that the inside technicians showed a 4.6 times increased risk of DCS (maximum of 41 exposures), compared to students (5). They observed that in addition to the lower number of exposures, trainees were younger in age.

In repeated exposures, Malconian et al. observed that the period of exposure to altitude was also an important factor increasing the risk of DCS in observers (4). All the above studies, however examined only the overall risk and not the individual risk with increased exposures.

In our analysis, we looked at the risk of DCS in a group of healthy individuals who participated in the simulated EVA profiles. Although sex and TR showed higher risk of DCS in individuals with >3 exposures (Table IV), 95% confidence intervals of the crude OR were wide and sample size limited. However, we did not look into the possible effects of interval between exposures and no multivariate analyses were undertaken. More data is being accumulated to include these analyses.

SUMMARY:

Individuals with >3 exposures were at 3.7 times greater risk of DCS in our analysis. Sex, TR and number of runs with Doppler detectable microbbubbles were confounders of this risk. Number of exposures in the individual appears to be an independent risk factor for DCS.

REFERENCES:

1. Bason R, Pheeny H, Dully FE. Incidence of Decompression Sickness in Navy low-pressure chambers. Aviat. Space Environ. Med. 1976;47:995-7.

2. Conkin J, Edwards BF, Waligora JM, Horrigan DJ. Empirical model for use in designing decompression procedures for space operations. Springfield,VA: NTIS, 1987. NASA Tech memo TM100456.

3. Hennekens CH, Buring JE. Epidemiology in medicine. Boston: Little,Brown and Co., 1987.

4. Malconian MK, Rock P, Devine J, et al. Operation Everest II: altitude decompression sickness during repeated altitude exposure. Aviat. Space Environ. Med. 1987;58:679-82.

5. Piwinski S, Cassingham R, Mills J, et al. Decompression sickness incidence over 63 month of hypobaric chamber operation. Aviat. Space Environ. Med. 1986; 57:1097-101.

6. Waligora JM, Horrigan DJ, Conkin J, et al. Verification of an altitude decompression prevention protocol for shuttle operations utilizing a 10.2 psi pressure stage. Springfield,VA: NTIS 1984. NASA Tech Memo 58259.

SPACE ADAPTATION SYNDROME I - SENSORY PATHOLOGY

(No papers submitted)

SPACE ADAPTATION SYNDROME II – CARDIOVASCULAR AND EXERCISE PHYSIOLOGY

(No papers submitted)

149

ENVIRONMENTAL INTERACTIONS

SPACE PLASMA INTERACTIONS I

151

SPACECRAFT AND SURFACE INTERFERENCE

Willie Mackey
NASA/Lewis Research Center

(Paper not provided at publication date)

SPACE STATION FREEDOM AND ITS PLASMA ENVIRONMENT

Frederick P. Blau

(Paper not provided at publication date)

SSF SOLAR ARRAY PLASMA TESTS

Marian Felder

(Paper not provided at publication date)

154

APPLICATION OF ENGINEERING TOOLS TO SPACECRAFT POLAR AURAL CHARGING

N. John Stevens
TRW Space and Technology Group

(Paper not provided at publication date)

MAGNETOPLASMA SHEATH WAVES ON A CONDUCTING TETHER IN THE IONOSPHERE, WITH APPLICATIONS TO EMI PROPAGATION ON LARGE SPACE STRUCTURES

K.G. Balmain, Department of Electrical Engineering, University of Toronto,
Toronto, Canada, M5S 1A4
H.G. James, Communications Research Centre, Ottawa, Canada
C.C. Bantin, University of Toronto, Toronto, Canada

ABSTRACT

Electromagnetic waves called "sheath waves" can propagate with low attenuation in the ion sheath, a region of low electron density that separates any conducting surface from an ionized-gas plasma in which it is immersed. Cold-plasma theory predicts propagation in a passband from zero frequency up to $1/\sqrt{2}$ times the electron plasma frequency for isotropic plasmas and up to $1/\sqrt{2}$ times the upper hybrid frequency for anisotropic plasmas permeated by a magnetic field in the direction of propagation. A recent space experiment has confirmed sheath-wave propagation on a kilometer-long insulated wire in the ionosphere, oriented parallel to the earth's magnetic field. This space-tether experiment, OEDIPUS-A, showed a sheath-wave passband up to about 2 MHz and a phase velocity somewhat slower than the velocity of light in a vacuum, and also demonstrated both ease of wave excitation and low attenuation. The evidence suggests that, on any large structure in low earth orbit, transient or continuous-wave electromagnetic interference, once generated, could propagate over the structure via sheath waves, producing unwanted signal levels much higher than in the absence of the ambient plasma medium. Consequently there is a need for a review of both EMI/EMC standards and ground test procedures as they apply to large structures in low earth orbit.

INTRODUCTION

An ionized gas plasma in contact with a solid surface is not homogeneous near the surface. Rather, it is inhomogeneous, forming a thin layer which contains ions from the plasma but very few electrons, so it is known as the "ion sheath". At the frequencies of interest, the ions are massive enough to be almost immobile, so it is the electrons that govern sheath behavior. Because the sheath is electron-depleted, to a first approximation it may be regarded as a vacuum gap. If the solid surface in question is a metal, then the picture that emerges is that of a vacuum gap separating a good conductor from a plasma which is also a conductor, albeit a very complex one. It is plausible that a vacuum gap between these two conductors can act as a guiding channel for an electromagnetic wave, and indeed this is known to be the case, the waves being called "sheath waves".

Early theoretical studies of sheath waves on a cylindrical conductor were done by *Seshadri* [1965], and by *Miller* [1968] who analyzed the case with a static magnetic field parallel to the conductor axis. Experimental studies were included in the papers by *Ishizone et al.* [1969, 1970a, 1970b], *Lassudrie-Duchesne et al.* [1973], *Meyer et al.* [1974], *Marec* [1970, 1974] and *Marec and Mourier* [1970, 1972]. Recently, *Laurin et al.* [1989] analyzed sheath-wave propagation over a planar surface, propagating in a direction parallel to the ambient static magnetic field, and they compared their analysis with laboratory experimental results for a thin wire in a magnetized plasma. Their conclusion was that sheath waves propagate in a frequency range from zero to $1/\sqrt{2}$ times the upper hybrid frequency, at least for the special case of wave propagation parallel to the magnetic field. Moreover they concluded that the waves propagate with a phase velocity that is slower than the velocity of light in a vacuum and approaches a nearly constant value at low frequencies (i.e. it is nearly dispersionless). Propagation in isotropic (unmagnetized) plasma is similar, with the plasma frequency f_p replacing the upper-hybrid frequency f_u, where $f_u^2 = f_p^2 + f_c^2$ and f_c is the electron cyclotron frequency.

THE "OEDIPUS-A" ROCKET EXPERIMENT

This project involved an ionospheric rocket which was launched in January 1989 from Andoya, Norway. It was separated into two parts early in its flight, the two parts remaining connected by a thin, insulated wire (or "tether") that unreeled from a spool in the rocket nose section, reaching a maximum wire length of 985 m near apogee. During the flight, the tether orientation stayed within 5° of being parallel with the earth's magnetic field. A stepped-frequency transmitter with an output level of 50 Vrms and covering the range 50 kHz - 5 MHz was located in the nose section and a synchronized receiver was located in the tail section. There were several experiments on board, the one of primary interest in this paper having the configuration shown in Figure 1, the purpose being to measure the transmission of signals end-to-end along the tether. The particulars of the tether are shown in Figure 2, in which it can be seen that the tether unreeled steadily, reaching maximum extension midway during the flight.

Figure 3 is a gray-scale representation of received signal strength as a function of both frequency and elapsed time during the flight. The dominant feature is a strong passband from zero frequency up to a sharp cutoff frequency between about 1.7 and 2.3 MHz. Above the cutoff frequency is a strong stopband extending upward to a frequency between 3 and 4 MHz where there is a return to fairly strong signal levels. As an aid to interpretation, Figure 3 includes a graph of plasma frequency f_p (taken from delayed-pulse measurement data supplied by one of the authors, H.G.J.) along with a graph of cyclotron frequency f_c . Also included are graphs of upper-hybrid frequency f_u and sheath-wave cutoff frequency $f_s = 1/\sqrt{2}\, f_u$, as well as harmonics of the cyclotron frequency.

The theoretical sheath-wave cutoff frequency f_c is about 30% higher than the measured cutoff frequency. This may be due to the expected high attenuation of sheath waves just below the cutoff frequency. Above the cutoff frequency is the stopband which extends upward to the upper-hybrid frequency f_c , as predicted by cold-plasma theory.

Within the low-frequency passband and for the earlier part of the flight, some very faint curved lines can be seen. These are enhanced by adjusting the gray-scale and are shown much more clearly in Figure 4. It is postulated that they are resonances occurring whenever the tether length is a multiple of a sheath-wave half-wavelength. Based on this postulate, contours for different sheath-wave phase velocities (refractive indices or wavenumbers) were drawn until a reasonable fit was obtained as shown, which is for a constant refractive index of 1.7 : this indicates that a relatively non-dispersive slow wave exists on the tether, in agreement with the sheath-wave postulate. The resonances are clearly visible at all frequencies up to the cyclotron frequency f_c , above which only faint indications of resonances can be seen and only up to an elapsed time of about 260 seconds. It will require further study to determine whether or not the rapidly rising attenuation (with increasing frequency) as predicted by *Laurin et al.* [1989] is sufficient to explain the disappearance of the resonances at or just above f_c for the greater part of the flight duration.

As an aside, it is interesting to note that dipole-to-dipole transmission experiments (with one dipole on the nose section and one on the tail section) produced gray-scale plots similar to Figures 3 and 4. In particular, the tether-length resonances were clearly visible even though the tether was not connected either to the transmitter or the receiver. This indicates that there was strong excitation of sheath waves in a situation where it was not intended.

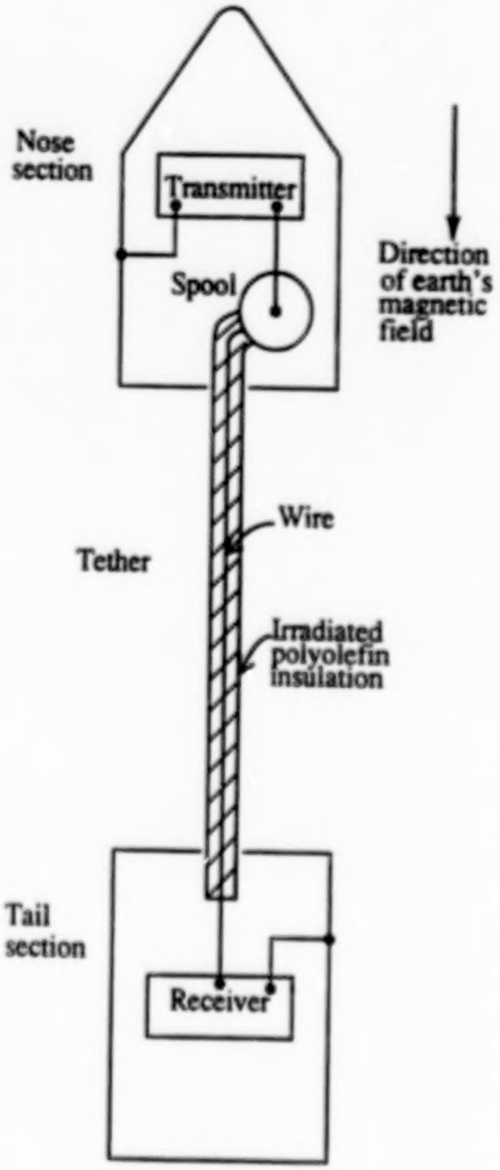
Nose section
Transmitter
Spool
Direction of earth's magnetic field
Wire
Tether
Irradiated polyolefin insulation
Tail section
Receiver

Figure 1. Diagram of the "OEDIPUS A" rocket experiment configuration used for the study of sheath waves.

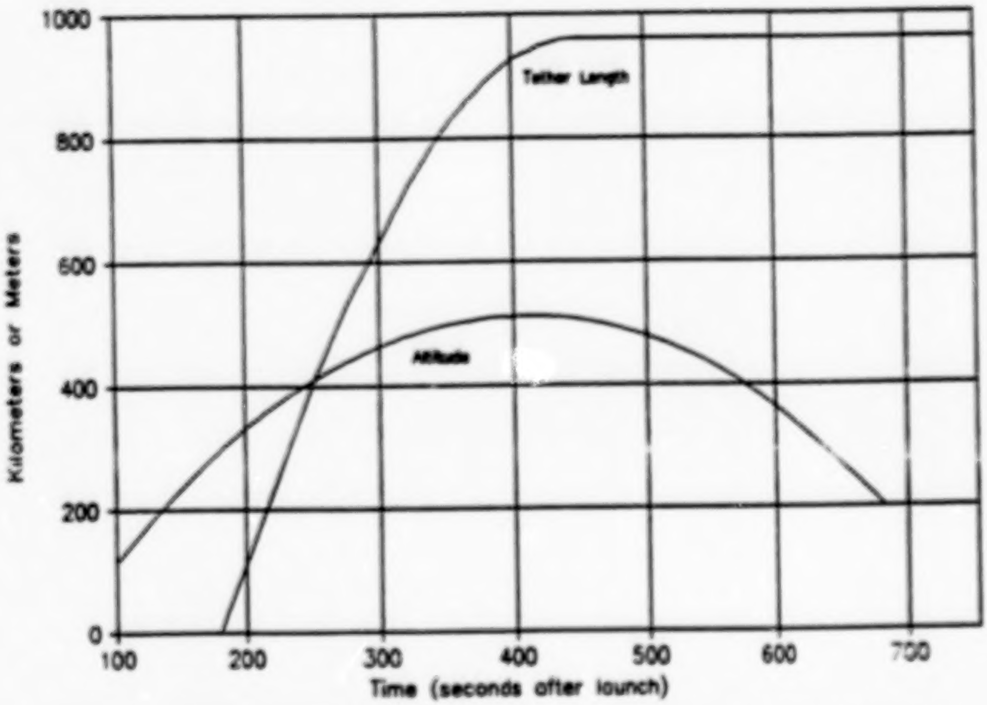

Figure 2. Tether length and altitude as functions of elapsed time. Tether wire length: 1300 meters; tether wire: No. 24 AWG, 19 strands of No. 36 copper, diameter 0.020"; tether wire coating: irradiated polyolefin, diameter 0.057", $\epsilon_r = 2.32$; wire resistance: < 100 ohms over 1300 meters; spool-to-chassis resistance: $> 3 \times 10^{14}$ ohms; contact: slip ring; braking: constant-torque of 6.5 oz-in.

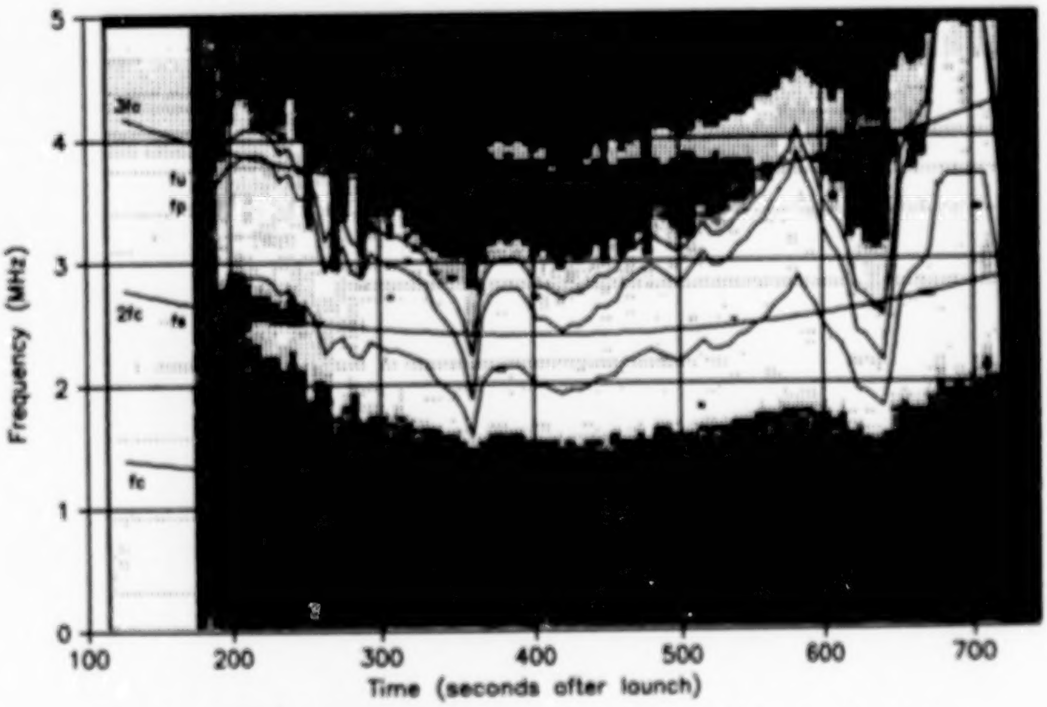

Figure 3. Received signal strength (darker gray scale means higher signal level) showing the cyclotron frequency f_c and its harmonics, the plasma frequency f_p, the upper-hybrid frequency f_u, and the nominal sheath-wave cutoff frequency $f_s = f_u / \sqrt{2}$.

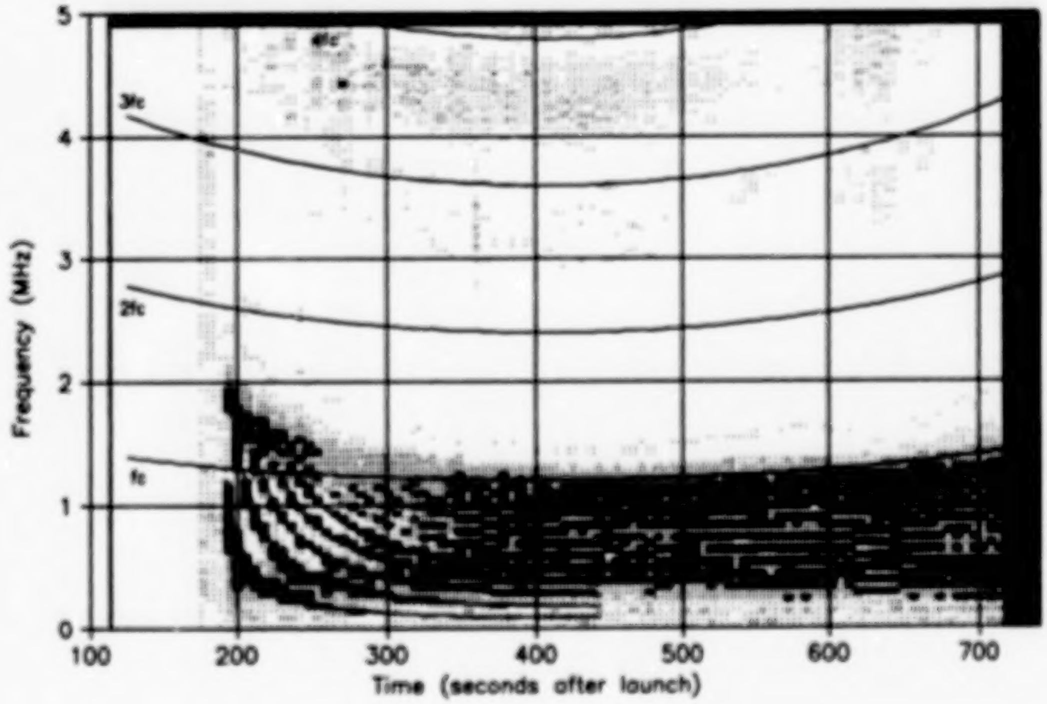

Figure 4. Received signal strength with gray-scale adjusted to show tether-length resonances. Lines show where tether is a multiple of a half wavelength long, assuming a wavenumber of 1.7.

Figure 5 shows received amplitude plotted against frequency at four different times during the flight. The features already discussed are evident, but most prominent is the high level of the low-frequency passband and the depth of the stopband, the difference in levels being of the order of 70 dB.

A particularly interesting feature visible in Figs. 3, 4 and 5 is the association of gray-scale boundaries with the harmonics of the cyclotron frequency. This suggests that cyclotron-harmonic waves which propagate *across* the magnetic field play a part in sheath-wave attenuation, say by carrying energy away from the tether (a suggestion made by one of the authors, H.G.J.). There are two implications, the first that this is a "leaky wave" phenomenon (and that the tether has become a leaky-wave antenna), and the second that kinetic theory will be required to explain fully the phenomenon of sheath waves.

Highly simplified theory may still be helpful, however, especially in view of the scarcity of theoretical developments adequate for the computation of fields due to given sources in finite-temperature anisotropic plasmas. Consider isotropic, cold plasma : existing thin-wire computer programs for lossy media can be adapted readily to cover this case, for example the program developed by *Richmond* [1974] and improved by *Tilston and Balmain* [1990]. This program can model isotropic cold plasma and a vacuum-gap sheath surrounding any interconnected network of thin wires. Its utility in application to anisotropic plasma will always be limited but, for the case of a wire parallel to the magnetic field, the strong radial electric field is always perpendicular to the magnetic field. This means that the perpendicular permittivity will predominate, with its zero at the upper-hybrid frequency rather than at the plasma frequency as would be the case with no magnetic field. This suggests that isotropic cold-plasma theory could be useful as a rough first approximation provided that the numerical value of the upper-hybrid frequency is substituted for the plasma frequency. The result of doing this is shown in Figure 6 in which the sheath-wave refractive indices deduced from measured resonances (ranging from 1.20 to 1.75) are bracketed by theoretical values computed by selecting two isotropic plasma frequencies spanning the range of upper hybrid frequencies in the experiment.

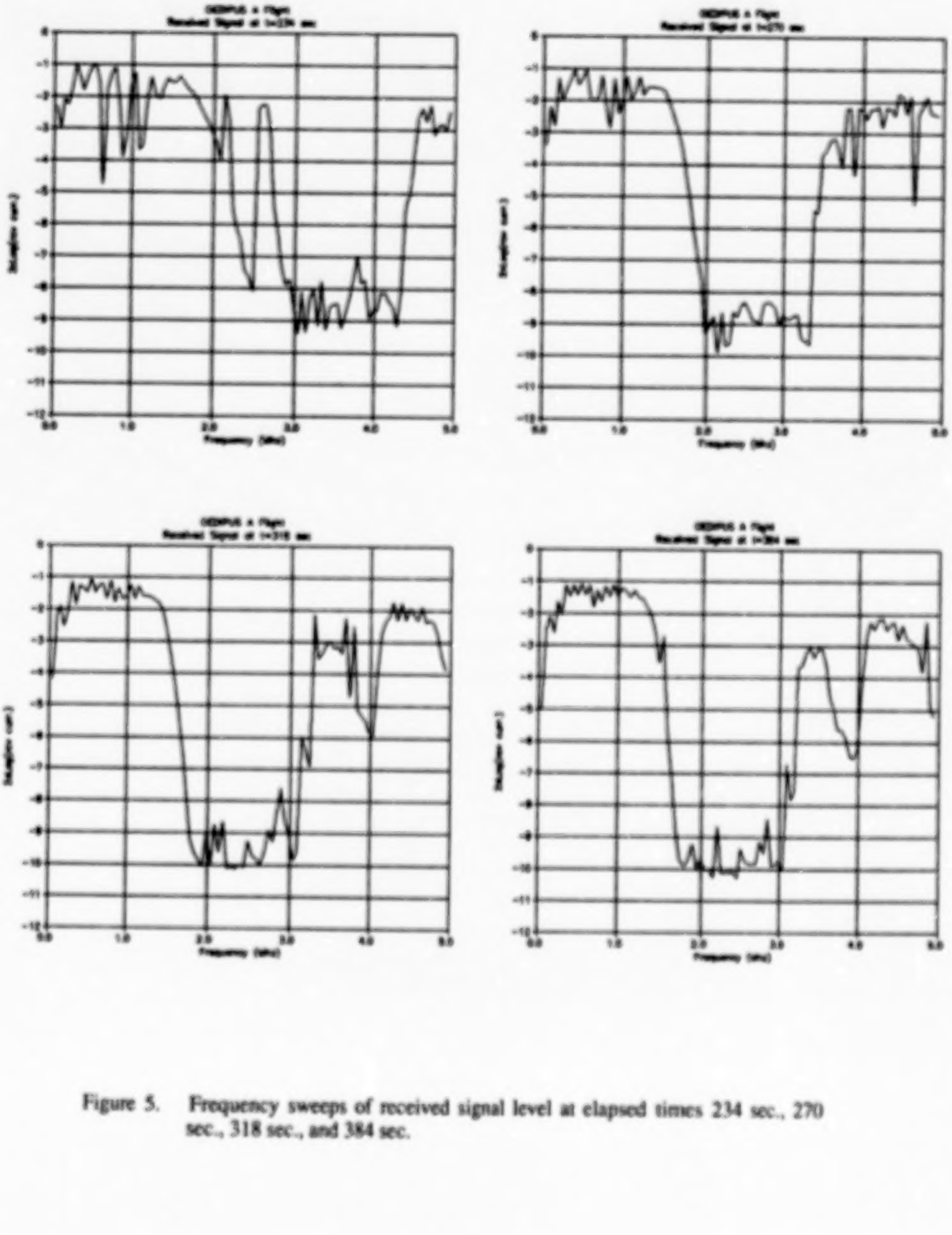

Figure 5. Frequency sweeps of received signal level at elapsed times 234 sec., 270 sec., 318 sec., and 384 sec.

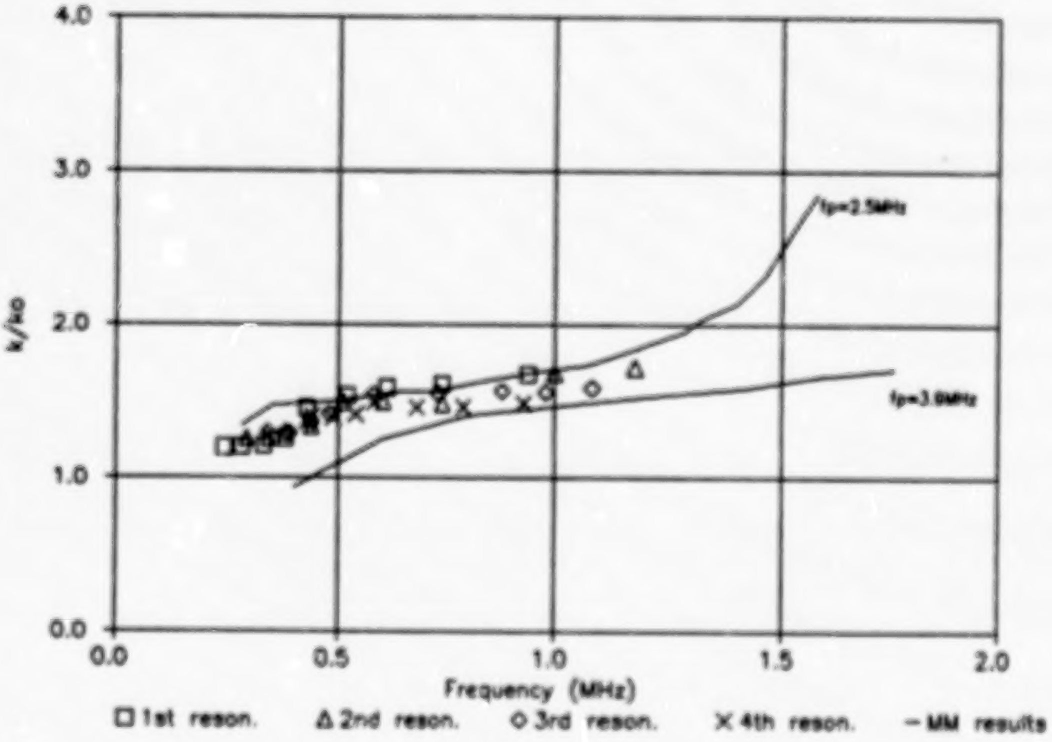

Figure 6. Wavenumbers derived from various resonances, together with moment-method calculations of wavenumbers in isotropic plasma, using two different values of plasma frequency intended to span the actual experimental values of upper hybrid frequency. The assumed sheath radius is 2.5 cm.

The use of gridded end-plates to represent the rocket nose and tail in this cold-plasma numerical calculation enables a calculation of typical transmitted signal level along with a free-space comparison as shown in Figure 7. The low-frequency passband and the transition to a deep stopband around 70 dB lower are clearly evident, along with tether-length resonances. The calculated cutoff frequency f_s at 2.6 MHz is clearly too high (compared with the measured value of 1.8 MHz at an elapsed time of 590 sec.). Nevertheless, the calculations up to 1 MHz or somewhat higher still are the best available theoretical results that include approximate representations of the rocket nose and tail sections. In particular, the comparative plasma-with-sheath and free-space calculations deserve attention. With the sheath, the signal level in the plasma is 30 dB to 60 dB higher than in free space, at frequencies below 1 MHz. It is this strong coupling that has implications for EMI/EMC on large structures such as the Space Station. Without the sheath, Figure 7 shows essentially no coupling, as expected.

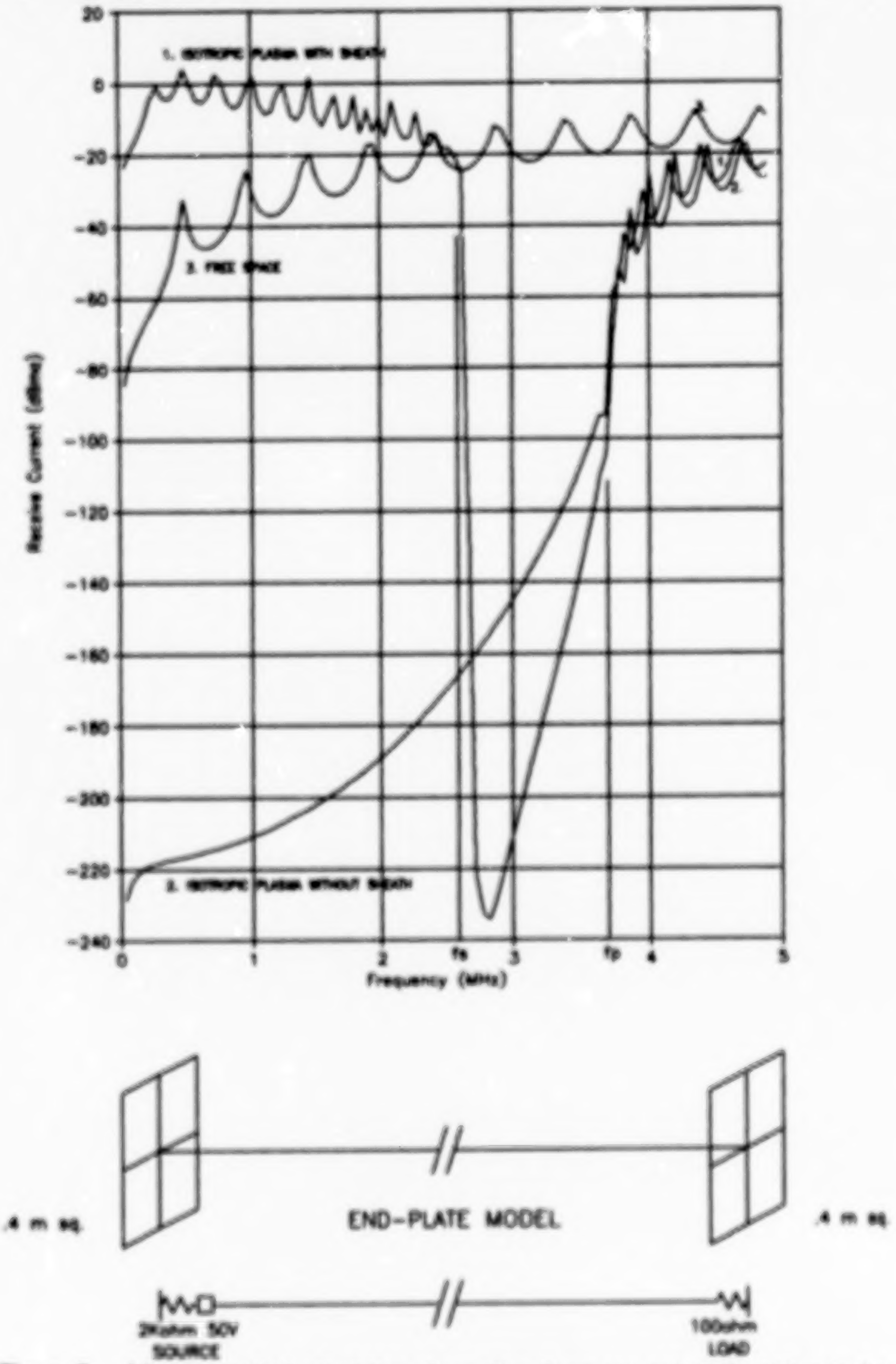

Figure 7. Moment-method calculation of coupling from one end of the tether to the other, for both free space and plasma environments, the latter for two conditions, with no sheath and with a 2.5 cm diameter sheath. The tether length is 300 m.

The coupling factor is potentially important because EMI/EMC standards and test methods are based on the assumption of a free-space environment. Therefore a source of interference at one point on the Space Station will couple to a susceptible instrument at a distant point much more strongly than might be anticipated, implying that tighter standards would be needed either for emission or immunity, for interference with significant spectral content below about 1.5 MHz. The above computations using a computer program valid for isotropic dielectric media suggest that such programs could be useful in getting a first estimate of interference levels.

Another relevant aspect of EMI/EMC is ground test procedure for emission or susceptibility. Putting a large part of the Space Station in a plasma chamber is clearly out of the question when it comes to deciding whether a given unit emits excessive unwanted radiation. Because at low frequencies the plasma can be regarded as a conductor and because it is separated from any surface by the sheath region which is a few centimeters thick, it is postulated that a first-order laboratory equivalent model would consist of a wire mesh completely surrounding the part of the Space Station under test and separated from it by a few centimeters. To represent the cutoff frequency and the stopband, it is postulated that the wire mesh could be segmented and the segments separated by appropriately synthesized lumped-element networks, as shown in Figure 8. If the equivalence of this wire-mesh configuration could be established, then relevant emission and susceptibility test methods and standards could be derived.

CONCLUSIONS

The OEDIPUS-A ionospheric rocket flight involving radio transmission along a conducting tether parallel to the earth's magnetic field has established the existence in the ionosphere of sheath waves on the wire and revealed some of their properties, including passbands, stopbands and phase velocities. The existence of tether-length-dependent resonances shows that the sheath waves can propagate with little attenuation, especially at frequencies below the electron cyclotron frequency. Existing cold-plasma theory explains in part the properties of the sheath waves but kinetic theory analysis ultimately will be needed for in-depth understanding.

The ease of coupling between widely separated parts of a long structure in the ionospheric plasma has implications for EMI/EMC standards applicable to systems on the Space Station. Some EMI/EMC calculations probably can be done with sufficient accuracy using existing computer programs valid for isotropic, lossy dielectrics. Ground test for EMI/EMC compliance may be possible using a modified wire mesh envelope to represent the sheath-plasma boundary.

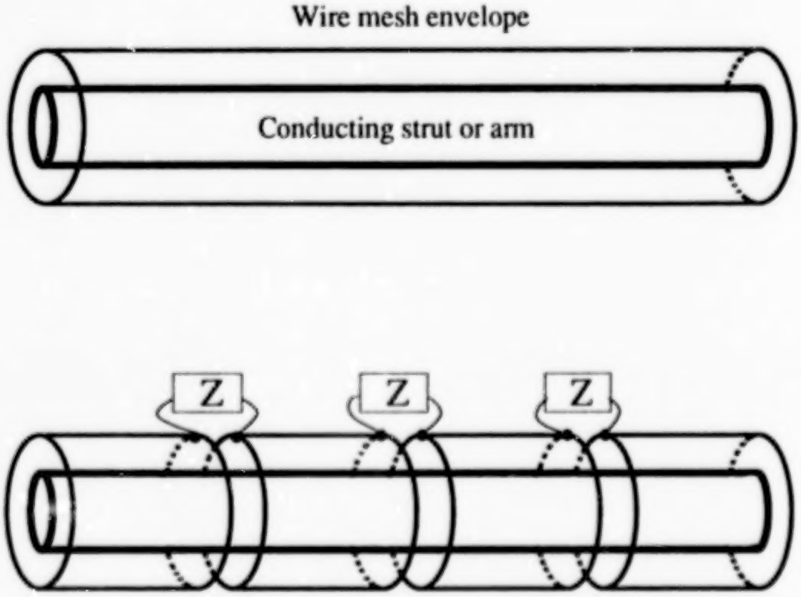

Figure 8. Proposed ground-test configuration with a wire mesh representing the sheath edge and the plasma beyond it. The lower part of the figure shows how synthesized impedance loading of the mesh might be employed to improve simulation in the vicinity of the primary stopband.

ACKNOWLEDGMENTS

The authors are indebted to Dr. Guy Hulbert of York University, Toronto, for providing pre-processed OEDIPUS flight data. This work was supported by the National Research Council of Canada, by the Natural Sciences and Engineering Research Council of Canada, and by the Ontario Institute for Space and Terrestrial Science.

REFERENCES

Ishizone, T., Adachi, S., Taira, K., Mushiake, Y., and Miyazaki, K., "Measurement of Antenna Current Distribution in an Anisotropic Plasma," IEEE TRANS. ANTENNAS PROPAG., Vol. AP-17, No. 5, 1969, pp. 678-679.

Ishizone, T., Adachi, S., and Mushiake, Y., "Electromagnetic Wave Propagation along a Conducting Wire in a General Magnetoplasma," PROC. IEEE, Vol. 58, No. 11, 1970a, pp. 1843-1844.

Ishizone, T., Adachi, S., and Mushiake, Y., "Measurement of the Phase Constant along a Conducting Wire in a Magnetoplasma," PROC. IEEE, Vol. 58, No. 11, 1970b, pp. 1852-1854.

Lassudrie-Duchesne, P., Dubost, G., et Terret, C., "Mesure de la Distribution de Courant à la Surface d'un Doublet Immergé dans un Plasma Chaud Isotrope," C.R. ACAD. SC. PARIS, t. 276, série B, 1973, 207-210 pp.

Laurin, J.-J., Morin, G.A., and Balmain, K.G., "Sheath Wave Propagation in a Magnetoplasma," RADIO SCI., Vol. 24, No. 3, 1989, pp. 289-300.

Marec, J.L.E., "Propagation d'ondes Electrostatiques dans les Gaines au Voisinage d'un Conducteur," Thèse de Doctorat 3rd Cycle, 99 pp., Fac. des Sci. de Paris, Paris, Nov. 1970.

Marec, J.L.E., "Ondes de Gaine, Amortissements Non Collisionnels," Thèse de Doctorat Es-Sciences, Univ. de Paris, 1974.

Marec, J., and Mourier, G., "Sur la Propagation des Ondes de Surface et la Nature des Résonances Electrostatiques de Gaine," C.R. ACAD. SC. PARIS, t. 271, Série B, 1970, 367-370 pp.

Marec, J., and Mourier, G., "Sur l'Admittance d'Entrée d'une Antenne Plane Immergée dans un Plasma," C.R. ACAD. SC. PARIS, t. 274, Série B, 1972, 471-474 pp.

Meyer, P., Vernet, N., and Lassudrie-Duchesne, P., "Theoretical and Experimental Study of the Effect of the Sheath on an Antenna Immersed in a Warm Isotropic Plasma," J. APPL. PHYS., Vol. 45, No. 2, 1974, pp. 700-706.

Miller, E.K., "Characteristic Waves on an Infinite Cylindrical Antenna in a Plasma Medium," RADIO SCI., Vol. 3, No. 12, 1968, pp. 1175-1178.

Seshadri, S.R., "Propagation Coefficient for the Current Distribution along a Cylindrical Antenna Immersed in a Warm Plasma," PROC. IEEE, Vol. 112, No. 5, 1965, pp. 877-882.

THE SOLAR ARRAY MODULE PLASMA INTERACTIONS EXPERIMENT (SAMPIE)

A Shuttle-based Plasma Interactions Experiment

Dr. G. Barry Hillard
Project Scientist
Sverdrup Technology Inc.
2001 Aerospace Parkway
Book Park, Ohio 44142

ABSTRACT

The SAMPIE flight experiment, tentatively scheduled to fly on the OAET-1 shuttle mission in mid 1992, will investigate plasma interactions of high voltage space power systems. Solar cells representing a number of technologies will be biased to high voltage to study both negative potential arcing and positive potential current collection characteristics. Additionally, several idealized metal/insulator mockups will be flown to study the basic nature of these interactions. Originally proposed as a collaboration with the European Space Agency (ESA), SAMPIE is now primarily a NASA effort with the possibility of limited involvement by ESA. This paper briefly describes the rationale for a space experiment as well as the measurements to be made and the significance of the expected results. The current design status of flight hardware is presented.

INTRODUCTION

Traditionally, space power systems have operated at low voltages and have not suffered from the effects of plasma interactions. High power systems now being developed for space applications will operate at high end-to-end voltages in order to minimize array current. The emergence of such systems is motivated primarily by a desire to save weight. Since the resistance of the necessary cabling is a strongly decreasing function of mass per unit length and since cable losses are proportional to current squared, it is desirable to operate at high voltages and low currents. A further consideration is the reduced effect of magnetic interactions (torque and drag) that will follow from low current operation.

While high voltage systems are obviously desirable from the standpoint of the power system designer, they suffer the drawback of interacting with the ionospheric plasma (Grier and Stevens, 1978 and Grier, 1983) in two different ways. Conducting surfaces which are at a high negative bias with respect to the plasma undergo arcing which causes current disruptions, significant electromagnetic interference (EMI), and large discontinuous changes in the array potential. For arrays using traditional silver-coated interconnects, a threshold potential for arcing of about -230 volts relative to the plasma is believed (Ferguson, 1986) to exist. There are theoretical reasons (Jongeward et. al., 1985) and limited ground test results (Snyder, 1986) to believe that different metals will arc at different thresholds. Since new solar cell designs are emerging using copper traces, it is important to determine arcing

165

thresholds, arc rates, and arc strengths for a variety of materials exposed to space plasma.

For solar arrays or other surfaces which are biased positive with respect to the plasma, a second effect occurs. Such surfaces collect electron current from the plasma resulting in a parasitic loss to the power system. Since the mass of electrons is much less than ions, the magnitude of current collection is much greater for surfaces with positive bias. At bias potentials greater than about 200 volts, sheath formation causes the entire surrounding surface, normally an insulator, to behave as if it were a conductor. This effect, called "snapover", results in large current collection even from a very small exposed area. In addition to producing a power loss, this current will significantly effect the potentials at which different parts of the array will "float". Depending on the way the power system is grounded, this in turn will effect the equilibrium potentials of various spacecraft surfaces with respect to the plasma.

Two previous flight experiments involving standard silicon arrays, PIX I and PIX II (Grier and Stevens, 1978 and Grier, 1983), have shown many differences between ground tests and behavior in space. For arcing, arc rates in space were quite different and generally larger than in ground tests. For parasitic current collection, the current versus bias voltage curves obtained in space not only differed radically from the ground tests but differed depending on whether the data was taken with the array exposed to spacecraft ram or wake. It is necessary, therefore, that the behavior of various solar cell technologies be established with a suitable in-space test.

In this paper, we have only briefly reviewed the background and justification for SAMPIE since this has been presented previously (Ferguson, to be published). We will present the current status of the design and a discussion of the selected experiments to be done.

OBJECTIVES

There are six basic objectives of the SAMPIE experiment:

1. For a selected number of solar cell technologies, determine the arcing threshold as well as arc rates and strengths.

2. For these solar cells, determine the plasma current collection characteristics.

3. Propose, demonstrate in ground tests, and fly an arc mitigation strategy, i.e. modifications to standard interconnect design which may significantly improve the arcing threshold.

4. Design simple metal/insulator mockups to allow the dependance of current collection on exposed area to be studied with all other relevant parameters controlled.

5. Design a simple arcing experiment to test the dependance of arcing threshold, arc rates, and arc strengths on the choice of metal.

6. Measure a basic set of plasma parameters to permit data reduction and analysis.

APPROACH

SAMPIE will consist of a metal box with an experiment plate fixed to the top surface. It will mount directly to the Hitchhiker-M carrier and will have a suitable adapter to permit either top or side mounting. A power supply will bias the solar cell samples and other experiments to DC voltages as high as +700 volts and -700 volts with respect to shuttle ground. When biased negative, suitable instruments will detect the occurrence of arcing and measure the arc rate as a function of bias voltage. For both polarities of applied bias, measurements will be made of parasitic current collection versus voltage. Other instruments will measure the degree of solar insolation, plasma electron density and temperature, and monitor the potential of the shuttle with respect to the plasma. Shuttle operations logs will be relied upon for detailed information about the orientation of the experiment with respect to the vehicle's velocity vector as well as times and conditions of thruster firings.

A simplified description of the experiment is to bias one solar cell sample to a particular voltage for a preset time while measuring arcing and current collection data. A set of plasma diagnostics is then taken and the procedure is repeated at the other bias voltages until all measurements have been made. Vehicle orientation is critical since ram and wake effects are known to be significant. SAMPIE will request control of the orbiter orientation such that one entire set of measurements is made with the payload bay held in the ram direction and a second set with the bay in the wake.

DESIGN STATUS

Since SAMPIE was originally designed to be deployed on a 15 meter collapsible tube mast of ESA design (Ferguson, to be published), it has been severely constrained in mass. As a result, although the current baseline is for direct mounting to the Hitchhiker carrier, the package remains quite compact. Figure 1 shows several views of the basic package. The top mounted experiment plate overhangs the box on three sides, allowing the langmuir probe to be attached on the back.

Figure 2 shows the proposed layout of the experiment plate. For solar cells, a baseline for comparison is provided by including a small 9-cell coupon of standard technology silicon 2 cm by 2 cm cells. This is the technology that has been used exclusively in the U.S. space program to date. It was flown on PIX I and PIX II as well as being the subject of extensive ground based testing and will provide a basis for continuity with past results. A 4-cell coupon of 8 cm by 8 cm space station cells, having copper interconnects in the back will allow a test of this technology. A 12-cell coupon of 2 cm by 4 cm APSA cells will test the behavior of this relatively new, very thin (60 micron) technology.

A breakdown test will explore the hypothesis that negative potential arcing is a special case of the classical vacuum arc (Hillard, to be published). With geometry and test conditions controlled, only the composition of the metal varies. To study snapover, we include 6 1 cm diameter copper disks covered with 5 mil kapton. Each has a pinhole in the center with hole sizes tentatively chosen as .1 mm, .3 mm, .5 mm, .7 mm. 1 mm, and 1.5 mm. The resulting family of current versus applied bias curves will be compared with predictions of NASCAP/LEO and other theoretical treatments.

A number of arc suppression techniques are under investigation as part of our ground based testing. These all follow from the work of Katz et. al. on the SPEAR program which showed that inbound ions striking the junction of insulator, metal, and plasma, sometimes called the triple point, resulted in secondary emission and arcing. A bushing employing a set of guard rings (Katz and Cooper) to collect inbound ions was able to prevent arcing in the SPEAR tests. Figure 3 shows three possible ways to exploit this finding.

Figure 3a shows the basic model of a solar cell biased to a high negative potential in a plasma environment. Inbound ions are free to strike the triple points, producing secondary electron emission which leads to breakdown. Figure 3b shows a straightforward attempt to collect inbound ions before they reach the triple points by using a small conducting rod which protrudes from each interconnect. In figure 3c, a conducting dielectric, possibly ITO, covers the critical junctions. Figure 3d shows that simply extending the coverslides to the maximum consistent with mechanical constraints may be sufficient to control the flow on inbound ions.

All of these techniques will be pursued in the ground based phase of the project. If successful, one or more of them will be flown.

SUMMARY

The SAMPIE flight experiment is the first space power system - plasma interaction experiment since PIX II and is by far the most ambitious to date. In addition to testing two emerging solar cell technologies, it will explore the viability of several arc suppression techniques. Using controlled experiments, it will provide basic data on arcing and current collection which can be compared to existing theories. SAMPIE will be designed and built in a highly modular way that will have easy reflight capability in mind. To this end, it can serve as a test-bed for future solar cell technologies.

REFERENCES

Ferguson, D.C. 1986, "The Voltage Threshold for Arcing for Solar cells in LEO - Flight and Ground Test Results", NASA TM-87259.

Ferguson, D.C. "SAMPIE - A Shuttle-bases Solar Array Arcing Experiment", to be published in the proceedings of "Spacecraft Charging Technology Conference, Montery CA, 31 October - 3 November 1989

Grier, N.T. 1983, "Plasma Interaction Experiment II (PIX II): Laboratory and Flight Results", Spacecraft Environmental Interactions Technology 1983, NASA CP-2359, pp. 333-347

Grier, N.T. and Stevens, N.J. 1978, "Plasma Interaction Experiment (PIX) Flight Results", Spacecraft Charging Technology 1978, NASA CP-2071, pp. 295-314

Hillard, G.B., "Negative Potential Arcing: Current and Planned Research at LeRC", to be published in the proceedings of "Spacecraft Charging Technology Conference, Montery CA, 31 October - 3 November 1989

Jongeward, G.A. et. al. 1985, "The Role of Unneutralized Surface Ions in Negative Potential Arcing", IEEE Trans. Nucl. Sci., vol. NS-32, no. 6, Dec., pp 4087-4091

Katz and Cooper, U.S. patent 4835841

Snyder, D.B. 1986, Private Communication

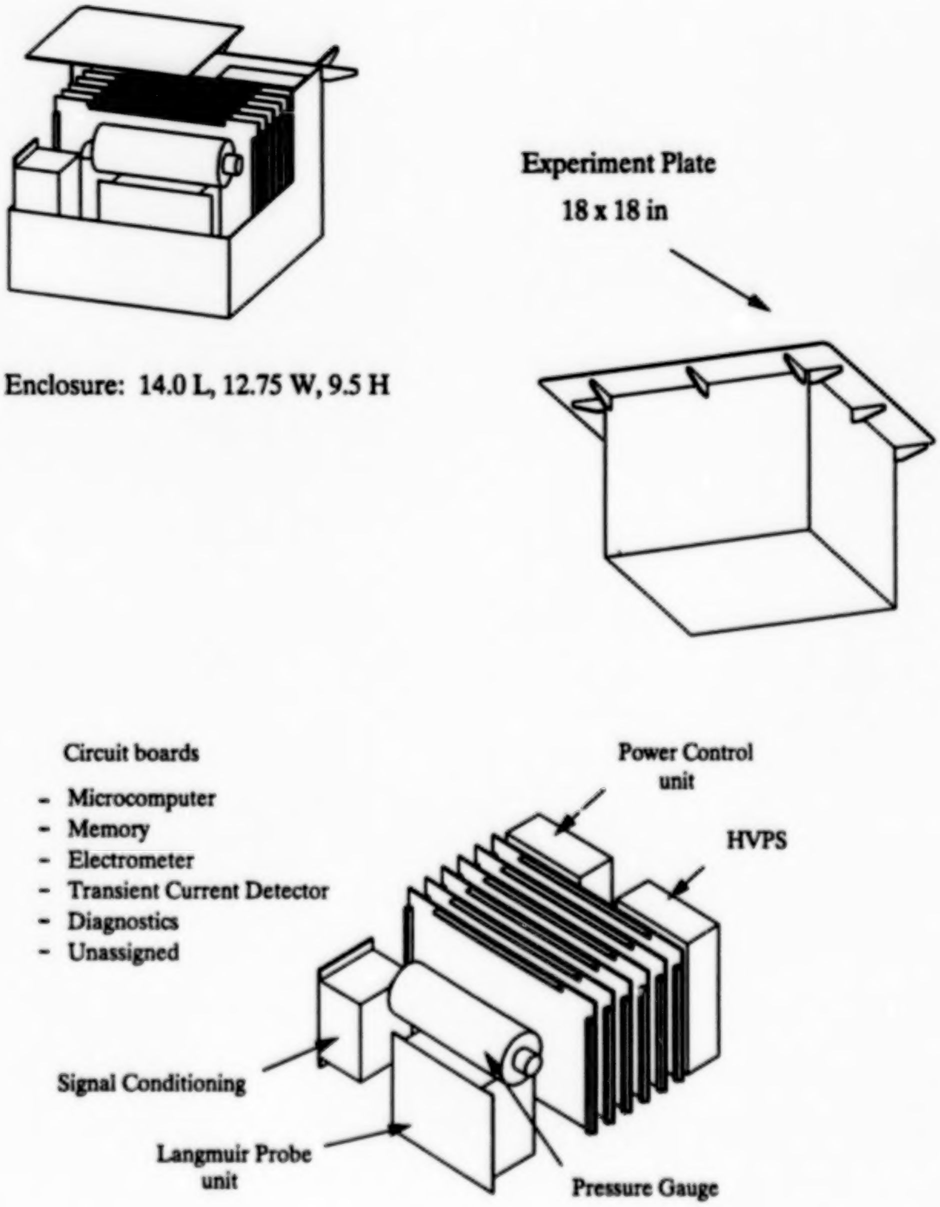
Experiment Plate
18 x 18 in
Enclosure: 14.0 L, 12.75 W, 9.5 H
Circuit boards
- Microcomputer
- Memory
- Electrometer
- Transient Current Detector
- Diagnostics
- Unassigned
Power Control unit
HVPS
Signal Conditioning
Langmuir Probe unit
Pressure Gauge

Figure 1 - Current design of experiment package

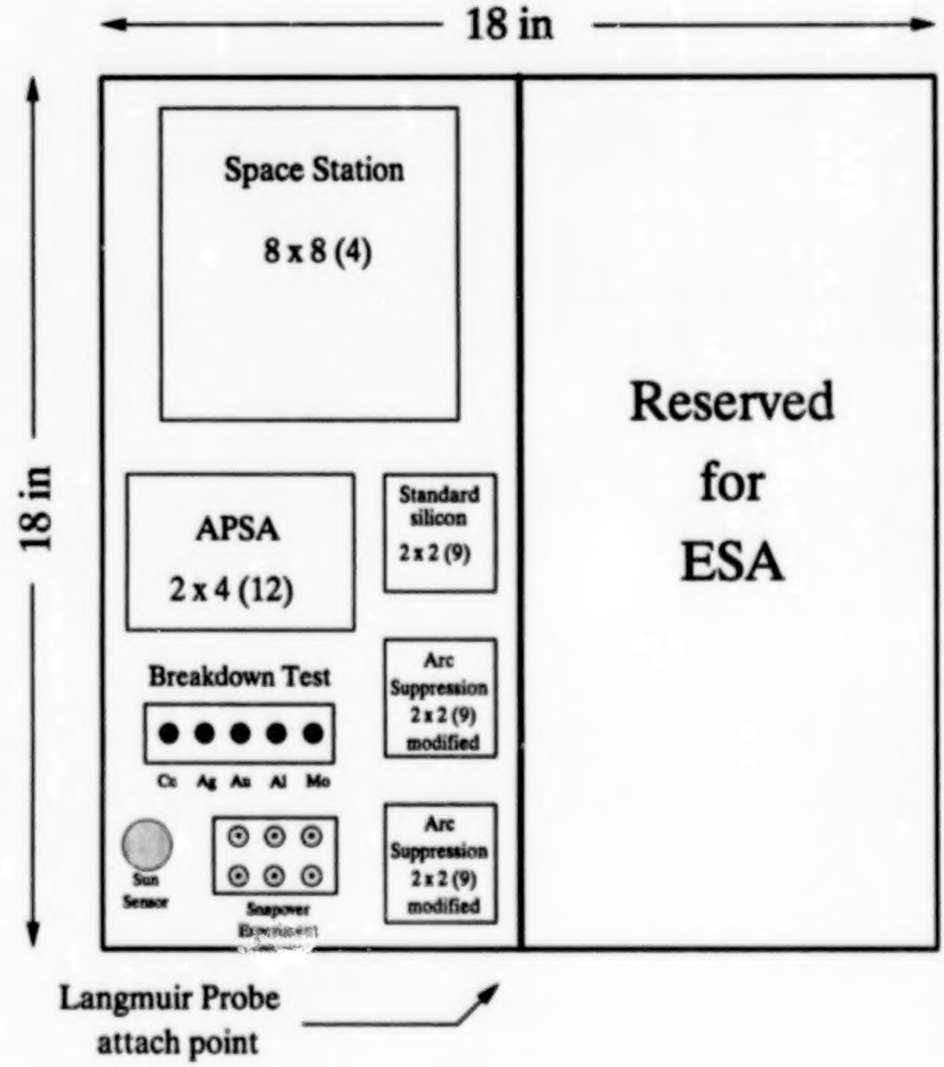
18 in
18 in
Space Station
8 x 8 (4)
APSA
2 x 4 (12)
Standard silicon
2 x 2 (9)
Breakdown Test
Cu
Ag
Au
Al
Mo
Arc Suppression
2 x 2 (9)
modified
Arc Suppression
2 x 2 (9)
modified
Sun Sensor
Snapover Experiment
Reserved for ESA
Langmuir Probe attach point

Figure 2 - layout of experiment plate
(solar cell dimensions in cm)

171

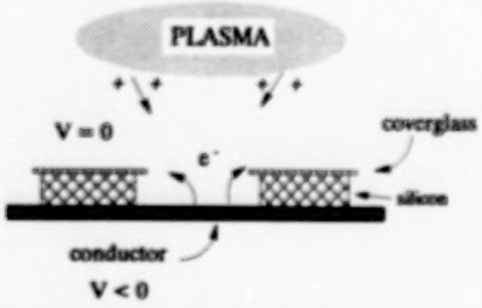
PLASMA
+
+
+
+
V = 0
e⁻
coverglass
silicon
conductor
V < 0

Figure 3a - schematic representation of standard solar cell model

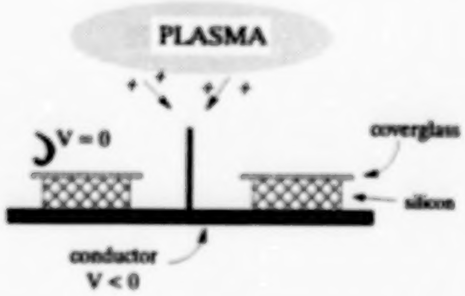
PLASMA
+
+
+
+
V = 0
coverglass
silicon
conductor
V < 0

Figure 3b - schematic representation of possible "lightning rod" modification

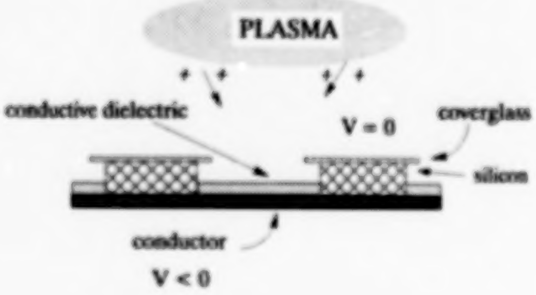
PLASMA
+
+
+
+
conductive dielectric
V = 0
coverglass
silicon
conductor
V < 0

Figure 3c - schematic representation of possible "dielectric coating" modification

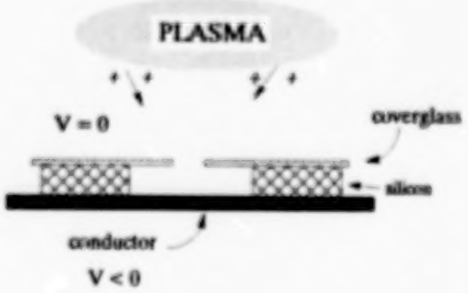
PLASMA
+
+
+
+
V = 0
coverglass
silicon
conductor
V < 0

Figure 3d - schematic representation of possible "extended coverglass" modification

SPACE PLASMA INTERACTIONS II

ELECTROSTATIC DISCHARGES ON SPACECRAFT

D. Allred

(Paper not provided at publication date)

COMPUTER MODELS OF PLASMA INTERACTIONS BETWEEN SPACECRAFT AND THE IONOSPHERE

Ira Katz, M. J. Mandell, and J. R. Lilley
S-Cubed Division of Maxwell Laboratories, Inc.
J. C. Roche
NASA/Lewis Research Center
David L. Cooke
Hanscom Air Force Base

(Paper not provided at publication date)

A FLUID MODEL APPROACH TO SPACECRAFT CHARGING

Russell Cottam

(Paper not provided at publication date)

176

PLASMA EFFECTS ON THE SPACECRAFT CHARGING, ETC.

David L. Cooke
Hanscom Air Force Base

(Paper not provided at publication date)

177

ENVIRONET: AN ONLINE ENVIRONMENTAL INTERACTIONS RESOURCE

Michael Lauriente

NASA Goddard Space Flight Center, Greenbelt, MD 20771

ABSTRACT

EnviroNET is a centralized depository for technical information on environmentally induced interactions likely to be encountered by spacecraft in both low-altitude and high-altitude (including geosynchronous) orbits. It provides a user-friendly, menu-driven format on networks that are connected globally and is available twenty-four hours a day - every day. The service pools space data collected over the years by NASA, USAF, other government research facilities, industry, universities, and the European Space Agency. This information, updated regularly, contains text, tables, and over one hundred high resolution figures and graphs based on empirical data. These graphics can be accessed while still in the chapters, making it easy to flip from text to graphics and back. Interactive graphics programs are also available on space debris, the neutral atmosphere, magnetic field, and ionosphere. EnviroNET can help designers meet tough environmental flight criteria before committing to flight hardware built for experiments, instrumentation, or payloads to the launch site. A test bed for developing an expert system for diagnosing environmentally induced anomalies for spacecraft has been in progress in cooperation with the USAF. An agreement has also been made with the USAF to use EnviroNET as a test bed for proposed standard atmosphere models by the AIAA Atmospheric Standards Committee.

BACKGROUND

EnviroNET was initiated at the request of NASA headquarters to provide a centralized depository of design guidelines for use by the space community with access capability. This action was prompted by the need for a detailed description of the environmental interactions with Shuttle and its payloads. The extreme complexity and size of the Shuttle made it very difficult to characterize these environments by direct computation

In the fall of 1982, NASA conducted its first Shuttle Environment Workshop to determine what had been learned from these measurements[1]. This led to environmental concerns voiced and a need for up-to-date information, on a continuing basis. To address the issues, NASA's Office of Space Science and Applications (OSSA) requested that a focal point be established for this environmental information, and that the activity be coordinated with other NASA centers, government agencies, and the user community. Goddard Space Flight Center (GSFC) was asked to lead this Agency-wide effort. It also suggested that the data obtained from this activity be put into an electronic database which could be accessed by any interested user from its work place. A second workshop was held where the concept for the current EnviroNET information resource was organized[2]

What has evolved is a user-friendly; menu-driven space environment information service[3]. Utilizing the global network of the Space Physics Analysis Network (SPAN)[4] this service is available to the space community, nationwide, as well as internationally. It is also useful to designers of equipment for low and high altitude satellites—including geosynchronous spacecraft. It is available twenty-four hours a day..every day. The system incorporates a combination of expository text and numerical tables amounting to about 2 million characters (bytes), plus Fortran programs that model several natural environments.

BROWSE

The main-menu system, which controls the EnviroNET activity on the MicroVAX II, allows one to run BROWSE, the principal retrieval program. With BROWSE, data files can be accessed, graphics and text downloaded, mail sent to the system manager, bulletin board notices read, the models run, or the system exited. Simple command choices allow one to page through the EnviroNET database sequentially, or jump to points of interest. BROWSE does require a VT100-compatible terminal or emulation. Three menus are available: Main Topics, Data and Table of Contents/Index. One can move among the three menus to any part of the database, or back to the EnviroNET main menu with a single keystroke. As you BROWSE about the database and change menus, the information on the terminal screen will change, but the basic layout of the screen will remain the same. The text is under continuous review by technical subpanels (each corresponding to the subject areas of the database) of experts who correct and augment the database to keep it accurate and current.

A partial list of the current topics contained in EnviroNET is shown in Fig. 1. The topics of primary interest to this session are the chapters on the Natural Environment and Surface Interactions, and the interactive graphics facility. The chairman of the subpanel on Surface Interactions Henry Garrett gave two papers at the SOAR '89. They were on the environmental interactions on space robotics and the Space Station[5,6].

- **Introduction**
- **Thermal and Humidity**
- **Vibration and Acoustics**
- **Electromagnetic Interference**
- **Loads and Low Frequency Dynamics**
- **Microbial and Toxic Contaminants**
- **Molecular Contamination**
- **Natural Environment**
- **Orbiter Motion**
- **Particulate Environment**
- **Surface Interactions**
- **Interactive Graphics Facility**

Fig. 1 Current Topics

ENVIRONET'S INTERACTIVE GRAPHICS AND MODELING

Use of models have been simplified by to providing tabular outputs to the screen or to files and for plotting the resultant models. Orbit dosage programs are designed to allow the user to analyze the radiation dosage for a given orbital configuration or to predict densities and temperatures encountered along a given orbit. Computer models are being expanded beyond the current models (thermosphere, ionosphere, energetic particles, magnetic field) to include gravity, radiation, meteoroids, the increasingly important space debris, and spacecraft anomalies.

The scope of the interactive models is shown in Fig. 2. The models include neutral atmosphere density and temperature, ionosphere, electron temperature and density, the magnetic field vector, and energetic particle or radiation flux. These models are based on data from satellites which orbit the earth in the thermospheric and exospheric regions of the atmosphere.

The implementation of on-line simplified computational models in the EnviroNET database has been strongly recommended by many EnviroNET users. A review of published prediction models indicates that selective computational models can be sufficiently simplified to meet the user-friendly requirement of the EnviroNET database user. Environet models provide a readily accessible method to do quick accurate calculations. These models encompass many important environments for engineers. A user-friendly informative interface is standard on all models. All models have a pop-up help window which give more information on inputs, outputs and caveats. Fig. 3 is an example of a model help window for the International Geomagnetic Reference Field model[7].

Mass Sprectrometer Incoherent Scatter (MSIS)*
Marshall Engineering Thermosphere (MET)*
International Reference Ionosphere (IRI)*
Cosmic Ray Effects on Microelectronics (CREME)
Energetic Particles*
Radiation Belts
Solar Flux
International Geomagnetic Reference Field (IGRF)*
Orbital Debris*
Maragram*

***Suitable for orbit integration**

Fig. 2 Scope of Interactive Models

Fig. 3 Help window from the IRI model

The orbital debris model provides essential data needed for risk assessment. The model is a widely used one of the current and future debris environment. The model permits order-of-magnitude estimates of collision probabilities. Fig. 4 is an example of a user friendly model for space debris[8]. The input parameters are on the left and input ranges on the right. After the computer is asked to run the model with keyed in values, the output then appears on the split screen on the bottom.

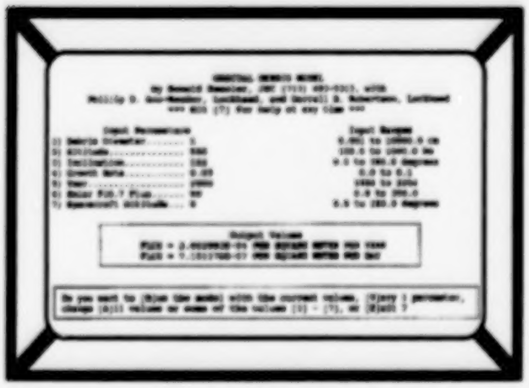

Fig. 4 User-friendly space debris model

The interactive graphics system permits plotting from common graphics terminals and emulators (Tektronics). The system allows plotting of output versus any input parameter. Graphs are generated using interactive data language (IDL), a commonly used commercial package as shown in Fig. 5. The real time graphing can do "What if...." scenarios.

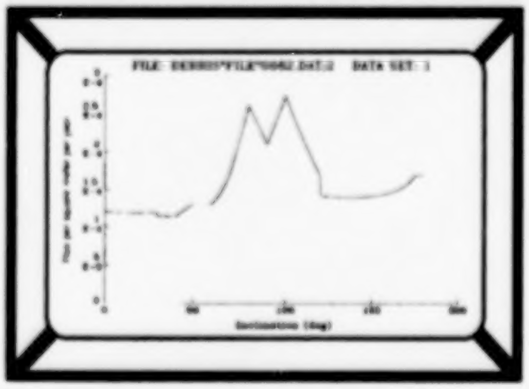

Fig. 5 Plot from the output of space debris model

Fig. 6 is an example of a user-friendly model for the 1986 Mass Spectrometer Incoherent Scatter (MSIS)-86 Model⁹. It is a standard empirical neutral atmosphere model. User-friendly output of temperatures and densities of atmosphere components including atomic oxygen are possible. As shown below, calculations of mission fluences of atmospheric species when integrated over an orbit model are easy. Such information would be valuable for drag calculations or calculating oxygen erosion.

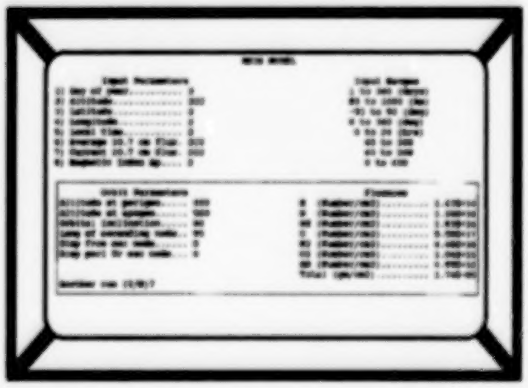

Fig. 6 MSIS model output showing orbital fluence of species

Environmental scientists may now map space atmospheres in spatial dimensions. Affordable tools now make it feasible to gain access to the scientific data which we have expressed in FORTRAN-compiled information. The CISC and VMS combination of c programming are used to deliver solutions to computational intense graphical applications. Fig. 7 is an example of a surface plot superimposed over a topographic plot from the output of the MSIS-86 model. The F 107=90, F 107 average=90. Day of the year is along the x-axis, latitude along the y-axis, and density along the z-axis.

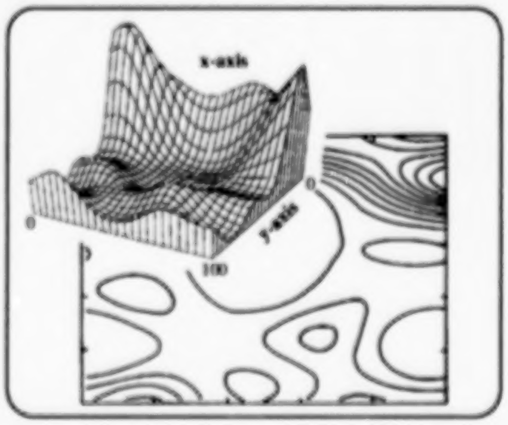

Fig. 7 Sample output plot produced from MSIS-86 model Altitude=900km; Local time =12:00; Longitude=15°; F107=90; Mean F107=90; x axis is day of year(1-365); Y-axis is Latitude(-90-90); z-axis is density of atomic oxygen;

SPACECRAFT ANOMALIES EXPERT SYSTEM

Through the years, a host of information related to spacecraft anomalies have been accumulated. This information is principally located in the chapters on the natural environment and surface interactions. We are coordinating with all the agencies working in this area to help us develop an online facility to diagnose anomalies. In this category, Koons and Gorney, who have been working on an expert system to address anomalies due to surface charging, bulk charging, single event effects and total radiation dosage have agreed to share their experience with us. We also have the assistance of NASA which publishes an annual anomalies report on its satellites. Lastly there is NOAA with its online reporting system. Expert systems provide an effective method of saving corporate knowledge. They also allow computers to sift through large amounts of data and pinpoint significant parts. Fig. 8 shows the expert system interface. Heuristics are used for predictions instead of algorithms. Approximate reasoning and inference are used to attack problems not rigidly defined.

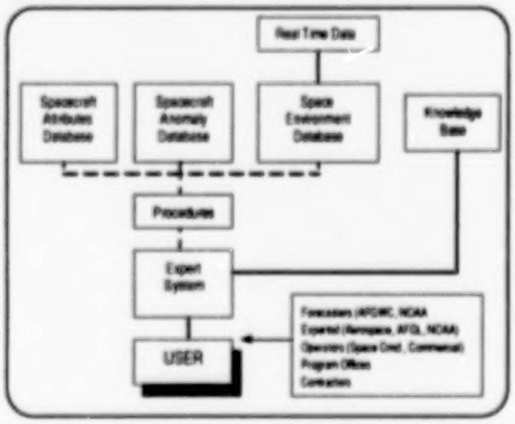
Real Time Data
Spacecraft Attributes Database
Spacecraft Anomaly Database
Space Environment Database
Knowledge Base
Procedures
Expert System
USER
Forecasters (AFGWC, NOAA)
Experts (Aerospace, AFGL, NOAA)
Operators (Space Cmd., Commercial)
Program Offices
Contractors

Fig. 8 Expert system interface

The Spacecraft Anomalies Expert System is a tool to diagnose causes of environmentally induced anomalies. It is also effective as a learning tool on environments. Modular systems allows expansion of satellite, technology, and past environmental conditions databases. The prototype program was developed by Aerospace Corp.

SPACE ENVIRONMENT STANDARDS

This continuing effort is ideally suitable to link the scientific community with users. By presenting our developments at national meetings and participating in committee meetings on standards it is anticipated that a contribution to development of space environment standards will be achieved. At the invitation of Dr. Al Rubin, chairman of the AIAA Atmospheric Standards, a presentation was made on January 8, 1990. It was suggested that EnviroNET be used as a mechanism for proposed standards because of the linkage to the space community through the Space Physics Analysis Network.

TELESCIENCE TESTBED

EnviroNET is ideally suited for investigators to cooperate from their "remote" home laboratories and computers with their colleagues by computer networking. This is an expansion of the concept started with the Atmosphere Explorer and Dynamics Explorer programs when many scientists were connected over dedicated phone lines to a central "remote" computer site containing their data and computer programs. With the advent of SPAN, the remote Dynamics Explorer scientists can communicate with one another directly and offload calculations and data analysis to their home systems, thereby improving productivity with simultaneous analysis on remote, distributed computer systems. EnviroNET is being upgraded to permit the users to conduct teleanalysis, i.e., perform analyses using Space Shuttle/Space Station environment data and the models on computers at remote institutions. EnviroNET has always drawn on the NASA centers, other government laboratories, industry, and universities for help. The academic community is especially involved because it provides important opportunities for testing and evaluating new ideas, techniques and concepts before they have reached the state of maturity considered by contractors and project mangers suitable for implementation. A testbed program like EnviroNET provides a valuable way of training graduate students who represent the future scientists and engineers of the nation, and who need to be at the cutting edge of technology to ensure our economic survival.

UPDATING ENVIRONET

EnviroNET is a living document. One of the driving forces for having an "electronic handbook" was to compress the time for communicating important information. Although the National Security Council's Interagency Report On Orbital Debris[10] was issued a few weeks before the NASA/DOD Orbital Debris Conference[11], we were able to have the complete report online in time for the meeting. Robinson's Spacecraft Environmental Anomalies Handbook sponsored by the Air Force[12] will soon be online.

Workshops conducted periodically are issued as informal documents for the purpose of feedback of information essential to the improvement of the services to users. As an example, at the mini-workshop held by the Natural Environment Panel, recommendations were made to add models that will generate energetic electron and proton environment values for a point in space, calculate orbital integrations of particle fluence, provide magnetic field traces and calculate ionospheric parameters. Now featuring interactive graphics software, the system will eventually simplify space environment mission analysis.

Last year a mini-workshop was held on environmentally induced spacecraft anomalies. In addition to NASA, the meeting was supported by the National Oceanic and Atmospheric Administration, TRW Inc., U.S. Air Force Systems Command, Global Weather Central Environmental Technical Applications Center, and Air Weather Service. Koons and Gorney described a spacecraft anomaly expert system, Elsen reported on Goddard spacecraft anomalies, Robinson presented material on single-event upsets, Heckman and Allen reported NOAA spacecraft anomaly data, and Wilson and Scro reported on the Air Force spacecraft anomalies database. This meeting was followed by a special session on environmentally induced spacecraft anomalies chaired jointly by the Air Force and NASA at the AIAA January meeting in Reno[13]. The session was expanded to include a description of the Goddard's trapped radiation facility and a paper by Garrett and Whittlesey on Anomalies on TDRSS.

CONCLUSION

EnviroNET is an operational system available to the scientists, engineers, satellite operators and users concerned with space environments who have access to a terminal or dial-up port. It is a tail node on SPAN accessible directly or through the national networks via NPSS. The EnviroNET staff welcomes comments and suggestions for how to improve this service. To summarize, the benefits to using EnviroNET include:

1) Validated NASA environmental information and interactive space models

2) Facilitating analysis of the natural space environment for missions

ACKNOWLEDGMENTS

The information on modeling was contributed by D. Bilitza, J. Green, A. Hedin, and J. Vette of NASA/GSFC. The author acknowledges indirect but valuable contributions gained from the shuttle Environment Working Group through many telecons, meetings, and general exchange of unpublished information. Funding was provided by NASA Headquarters, the Geophysical Laboratory (GL) Space Systems Environmental Interaction Technology Office, and by the U.S. Air Force Systems Command, Space Systems Division

REFERENCES

1. Proceedings: The Shuttle Environment Workshop. Prepared for NASA by Systematics Corp., Contract NAS5-27326, Feb. 1983.

2. Wilkerson, Thomas D., Michael Lauriente, and Gerald W. Sharp. Space Shuttle Environment. Library of Congress Catalog No.: 85-81606, ISB No-939204-28-2

3. The EnviroNET Users Guide. Code 410.1, NASA/GSFC, Greenbelt, MD 20770

4. Green, James L. The Space Physics Analysis Network. Computer Physics Communication 49, pp. 205-213, North-Holland, Amsterdam, 1988.

5. Henry B. Garrett, Space Environments And Their Effects On Space Automation And Robotics, SOAR 89.

6. G.B. Murphy, H.B. Garrett, Interactions Between The Space Station And The Environment , SOAR 89.

7. Peddie, N.W., International Geomagnetic Reference Field; the third generation, J. Geomagn. Geoelectr. 34, 309-326, 1982.

8. Kessler, D.J., Phillip D. Anz-Meador, and Robert C. Reynolds, Orbital Debris Environment for Spacecraft Designed to Operate in Low Earth Orbit, NASA TM-100471, 1989.

9. Hedin, Alan E. The MSIS-86 Thermospheric Model, J. Geophys. Res., vol. 92, pp. 4648-4662, 1987.

10. Report on Orbital Debris by Interagency Group (SPACE) for National Security Council, Washington, D.C. February 1989.

11. AIAA/NASA/DOD Orbital Debris Conference: Technical Issues & Future Directions, April 16-19, 1990, Baltimore, MD

12. Paul A. Robinson, Spacecraft Environmental Anomalies Handbook, August 1, 1989, NTIS.

13. 28th Aerospace Sciences Meeting, Reno, Nevada, January 8-11, 1990

A. Vampola, Tutorial on Spacecraft Environmental Interactions Anomalies, CP AIAA 90-0172.

D. Wilkinson, NOAA's Spacecraft Anomaly Data Base, CP AIAA 90-0173.

P. Robinson, Anomalies Due to Single-Event Upsets, CP AIAA 90-0174.

D. Gorney and H. Koons, Spacecraft Anomaly Expert System, CP AIAA 90-0175.

J. Gaffey and D. Bilitza, Trapped Radiation Model Facility, CP AIAA 90-0176.

H. Garrett and A. Whittlesey, Environmentally Induced Spacecraft Anomalies on TDRSS, CP AIAA 90-0178.

SPACECRAFT CONTAMINATION

PHOTOMETRIC ANALYSIS OF A SPACE SHUTTLE WATER VENTING

R. A. Viereck, E. Murad, and C. P. Pike,
Geophysics Laboratory, Space Physics Division, Hanscom AFB, MA 01731
I. L. Kofsky, C. A. Trowbridge, and D. L. A. Rall,
PhotoMetrics, Inc., Woburn, MA 01801
A. Satayesh,
Radex, Inc., Bedford, MA 01730
A. Berk and J. B. Elgin,
Spectral Sciences, Inc., Burlington, MA 01803

ABSTRACT

A photometric-photogrammetric analysis of intensified-video images from AMOS and onboard Shuttle Orbiter "*Discovery*" of a sunlit venting of supply water has shown that the 1½ mm-diameter liquid stream breaks up within ~1 m to form ice/snow particles of two characteristic sizes, much as was observed in earlier space-tank simulations. Discrete droplets produced by the flash evaporation are the principal feature in the photographs of the wake trail taken from the bay and crew cabin; these particles have an "average" diameter comparable with that of the initial continuous flow. Unresolved submicron ice droplets formed by recondensation when the evaporated water gas overexpands dominate the images of the ~2½ km of trail detectable by the groundbased tracking telescope-camera; these particles sublimate at rates that we modeled from the decrease in visible radiance of the trail by applying energy balance arguments for spherical Rayleigh-Mie scatterers/radiators in low earth orbit that undergo the (small) surface roughening seen in laboratory experiments. The angular spreads of the two types of ice particle are the same within observational error, and the kinetic energy imparted by the boiling-explosion of the superheated (in vacuum) quasi-cylindrical water stream is about an order of magnitude less than the injection energy.

INTRODUCTION

We present here a preliminary interpretation of a recent experiment conducted on Space Shuttle *Discovery* (mission STS 29-orbit 49, 16 Mar 1989) in which a stream of liquid supply water (1) was vented into space at twilight. The data consist of video images of the sunlight-scattering water/ice-particle cloud that formed, taken by visible light-sensitive intensified cameras both onboard the spacecraft and at the AMOS ground station near the trajectory's nadir. This experiment was undertaken to study the phenomenology of water columns injected into the low earth-orbital environment, and to provide information about the lifetime of ice particles that may recontact Space Shuttle several orbits later (2). The findings about the composition of the cloud have relevance to ionospheric plasma depletion experiments (3) and to the dynamics of the interaction of orbiting spacecraft with the environment (1).

EXPERIMENTAL

Pure and largely gas-free liquid water produced in the vehicle's fuel cells was forced out through a 0.14-cm diameter nozzle, which was heated to ~70° C to prevent its blockage by icing; 19.4 g/s was vented within a few degrees of the wake direction. The experiment was planned so that the spacecraft would be directly solar illuminated just before dawn, while the atmosphere below ~100 km altitude remained in the hard earth's shadow. *Discovery* was in a southwest-to-northeast circular orbit at 329 km that passed almost directly over AMOS (the Air Force Maui Optical Station), which is atop 3.0 km high Mt. Haleakala, HI (21° N - 204°E). The radiance distributions of the water trail were measured for about 2 min in three projections: to a closed circuit zoom television camera in the open bay just forward of the spacecraft's tail, 18 m from the nozzle; to a similar camera handheld to point out of a crew cabin window a few m forward of and above the nozzle; and to the ground station, where an ISIT low-light-level video camera with 55 cm-diameter objective lens, 0.4° by 0.3° field of view, and S-20 spectral response (FWHM 0.4-0.65 μm) precisely tracked the spacecraft. Examples of the imagery from the three intensified electronic cameras are in Figure 1.

Discovery came into direct sunlight at 62° elevation southwest of the ground station, and the water trail remained above background until it moved to about 5° in the northeast. The solar scatter angles, aspect angles to the

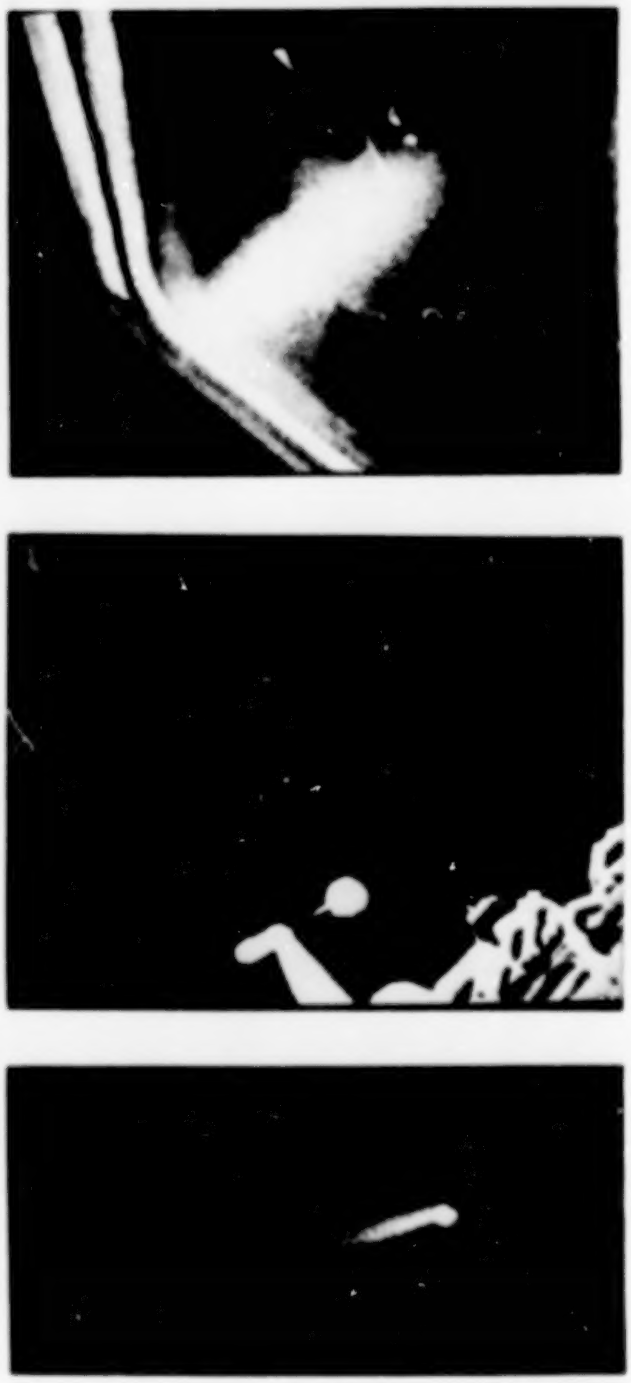

Figure 1. Views of the sunlit water/ice particle trail from onboard *Discovery* (a and b) and from AMOS with a 0.37°-wide field (c). a) is a projection to crew cabin window W1 and b) is a view from the zoom camera mounted just forward of the vertical stabilizer. In c) the solar-scatter angle is 48°, and the equivalent stellar magnitude of Orbiter (whose bloomed image is at the head of the water trail) is + 3.6.

trail's symmetry axis, zenith angles, and slant range to AMOS are in Figure 2. Both onboard cameras could view the essentially-backlit water cloud (the rising sun being toward the northeast) beyond about 5 m from the ejection nozzle. The bay camera, whose maximum field of view encompassed most of the detectable length of the trail, was at times pointed in azimuth to include its vanishing point. The groundbased camera's projected field varied between about 1¼ times (at culmination) and 5 times (near the horizon) the maximum above-threshold longitudinal extent of the optically thin sunlight-scattering volume.

DATA

The video images represent a series of illumination/viewing conditions of a time-stationary physical phenomenon. We analyzed radiometrically the AMOS scene at zenith angle 61° and azimuth 70° (Figure 1c), in which the high differential cross-section for forward scattering of sunlight (scattering angle 48°) and moderately elongated sight path (angle to long axis of cloud 33½°) resulted in the best video signal/noise ratios. *Discovery*, whose visual magnitude at this range (640 km) is about +3½, appears as a strongly bloomed, photocurrent-saturated feature at the head of the quasiconical extended water-containing volume. Figure 3 plots the relative brightnesses along the long axis of this trail (the instrumental baseline is subtracted, and a linear dependence of photocurrent on cathode irradiance characteristic of is its assumed), and these brightnesses summed over pixels along lines transverse to this direction. (This latter, rapidly decreasing quantity is the sterance per unit longitudinal path.)

The two onboard cameras show principally a flow of densely-packed discrete particles, with a relatively broad size distribution indicated by the variability of the video photocurrents from particles at sensibly the same range. This cloud diverges at about the same angle as the trail in the AMOS images (see Figure 1), and its "edge" projects back to an apex within a meter from the nozzle. We measured the longitudinal velocity as 23 m/s ±30% by following individual strong sunlight-scatterers in successive video frames, finding the variation among particles to be less than the precision of this measurement. The mean cross-track speed in the essentially-perpendicular view directions to the two onboard cameras can be seen to be about ¼ this axial speed, which indicates that the transverse momentum imparted to these particles is small compared with their wake-directed momentum. Many of these particles flicker, with characteristic periods near ½ s, and are therefore more likely tumbling ice/snow crystallites than spheres; indeed, erratic droplet shapes as well as a broad "size" distribution have been observed in a laboratory simulation of the venting of water into near-space (4).

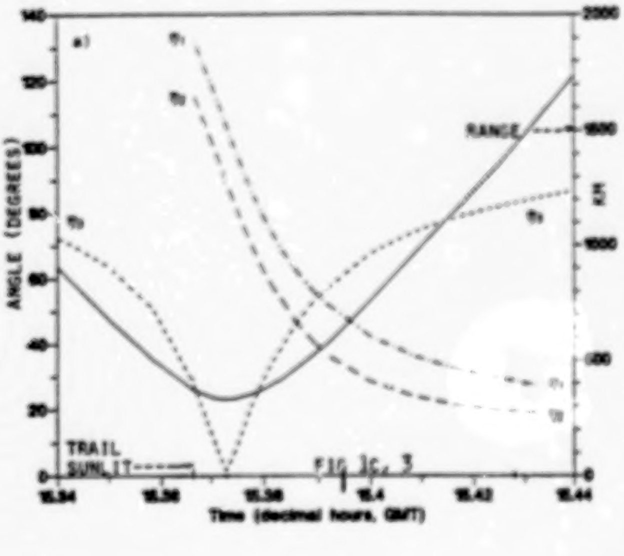

Figure 2. Solar scatter angle (η_1), aspect angle to the trail axis (η_2), zenith angle of *Discovery* and the trail (η_3), and slant range to *Discovery* from AMOS (solid line) during the water venting.

Approximately 100 of these large particles per m path can be resolved in the video frames from *Discovery's* camera. This number would be expected from the laboratory finding (4-7) that the mean diameters of the explosion-product ice particles are comparable with the diameter of the ejection nozzle.

INTERPRETATION

We interpret the discrete sunlight scatterers seen by *Discovery's* onboard cameras to be the product of the cavitational bursting of initially-coherent water streams in vacuum, which results from the rapid formation of bubbles ("steam") in the superheated liquid (4-8). A cloud of much smaller (tenths-micron diameter) particles that has also been identified in laboratory tank experiments is not unambiguously detectable against these bloomed images of the close-lying large droplets. This second component of the flow is formed by recondensation of water molecules that had been evaporated from the original and flash-exploded stream after this gas becomes overexpanded. On the basis of the following observations, we judge these much smaller particles to be responsible for the major fraction of the radiances of the trail that were measured by the groundbased camera (Figure 1c).

[1] Thermodynamic arguments (3) show that most (~70%) of the water mass remains in the large ice particles, while a laboratory simulation (6) indicated that the small recondensate particles contain less than 2%. We applied standard light scattering theory for 0.2 μm and 0.7 mm radius ice, finding that despite the great differences in both the fraction of initial water in and the absolute scattering amplitudes of the two populations, the much larger number of small particles results in considerably more visible radiance over the length of water trail detectable by the AMOS camera. (That is, the particles whose circumference is comparable with the photon wavelength have higher scattering "efficiency".)

[2] The surface brightnesses of the trail measured from the ground exhibit a very weak dependence on the solar-scatter angle, which is a behavior characteristic of Rayleigh rather than geometric scattering (particle large compared with the photon wavelength). Specifically, the fractional increase in the axial brightnesses beyond about 1 km from the nozzle, corrected for sight path length, remains small as the sunlight scattering angle decreases from 107° (when the trail was at AMOS zenith) to 48° (to which Figure 3 refers). This small change is consistent with the differential cross-sections of submicron particles, while in contrast scattering of visible light per unit solid angle from mm spherical ice drops would increase by about a factor 50 over this range of angles.

[3] The dependence of axial and crosswise-integrated radiance of the optically thin trail on distance from *Discovery* (Figure 3) is consistent with a simple model of the energy balance of the smaller ice particles. We applied standard Mie radiation theory with the known dependence of the real and imaginary components of the index of refraction of ice on wavelength to calculate the sublimation rate of smooth spheres in vacuum, taking into account the energy they absorb from earthshine and the incident solar flux and the energy they lose by thermal emission and sublimation. (Collisional heating and recondensation can be readily shown to be negligible.) The equilibrium 166K temperature is reached within less than a second after the particles form.

Since the emissivity of weakly-absorbing spheres is proportional to their radius r when r is less than ~1 μm, their radiance decreases exponentially with time, or distance x from the spacecraft. That is, r of submicron particles with axial velocity v (which we took as the velocity of the large particles, in view of the similar cone angles) varies as exp [-ax/v], where a (= 0.004 s^{-1} for smooth spheres) is the fractional loss rate due to sublimation. Thus the scattering in the "geometric" particle size range, which we take to be where the cross-section at fixed angle varies with r^2, would exhibit an exp [-2ax/v] dependence. In contrast scattering in the Rayleigh size range, where the cross-section varies as $r^2 \cdot r^4 = r^6$, would vary as exp[-6ax/v]. The "break" near x=1400 m in Figure 3 is due to the transitioning of the radius of the subliming particles from the geometric to the Rayleigh-scatter regime. (The familiar Mie oscillations in this transition region are

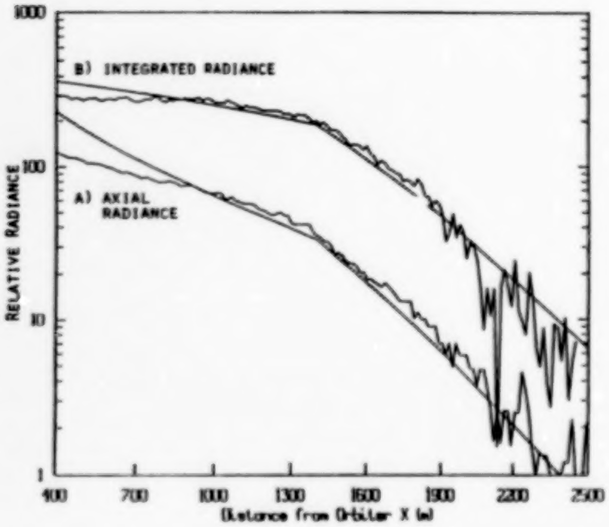

Figure 3. a) Relative radiance along the line of maximum brightness extending out from *Discovery* in the AMOS image (Figure 1 c), with background subtracted (and a linear relationship between the video photocurrent and scene radiance assumed). b) Radiances summed along lines transverse to this long axis. The data are contaminated by video blooming from *Discovery's* image when x≲500m.

largely washed out by the polychromatic sunlight illumination.)

Figure 3 indicates that the radiances measured from AMOS can be described by geometric scattering over the first ~1400 m and by Rayleigh scattering over the remaining ~1000 m (beyond which the trail's brightnesses fall below the camera's threshold), when a small correction for the progressive roughening of the particles is included in the calculation. The correction assumes a linear increase in sublimation rate with time, so that the radius decreases about as exp $[-ax/v-bx^2/v^2]$. That somewhat-larger ice droplets in vacuum indeed develop irregular surfaces that lead to more rapid sublimation was observed in laboratory experiments in which the chamber walls were held at low temperatures (9). The roughening required to achieve the fit of the data shown to an energy-balance model that includes this effect increases the rate of decay of mean radius by sublimation from the submicron particles by up to only a factor 2, which is in general agreement with the laboratory findings. The small downward curvature of the radiances in the two scattering regimes is also predicted by the progressively-increasing surface roughness that we assumed.

These calculations also showed that sublimation would result in a virtually negligible decrease in the sunlight-scattering cross-sections of one-mm ice droplets over the ~100-sec length (2½ km/23 ms^{-1} in the spacecraft's frame of reference) of the visible trail. The substantial measured decrease in total sterance per unit longitudinal path shown in Figure 3 and a calculation of the absolute mean radiances from solar scatter with the observed 100 such particles per m path, both further show that these much larger ice droplets could be responsible for only a minor fraction of the optical signal at AMOS.

The transition to Rayleigh scattering near x = 1.4 km indicates that the mean particle radius at this distance from *Discovery's* nozzle is between 0.1 and 0.3 μm. Our sublimation model gives an estimate of the mean initial radius as 0.3 ± 0.15 μm. The corresponding radius inferred in a space-simulation chamber (6), in which the water stream had 1.6 mm diameter, 20°C temperature, and a somewhat higher total flow rate, was 0.08 ± 0.03 μm.

CONCLUSION

The cloud of discrete particles that results when mm-diameter continuous water streams are vented into the low earth-orbital environment is found to have three components. Macroscopic (from laboratory observations, also mm-diameter) ice/snow particles are created by the explosive bursting of the supersaturated high-vapor pressure liquid, producing irradiances that were readily detectable in the images from the intensified video cameras onboard *Discovery*. The narrow cone angle in which these particles appear indicates that this flash evaporation imparts relatively little momentum compared with the longitudinal momentum of these particles. Much smaller droplets that theory indicates result from condensation of gaseous water produce radiances that dominate the images from the much more distant groundbased ISIT telescope-camera, in a volume with essentially the same angular spread as the large particles. The ~25% water gas, which is not detectable by either type of camera, is evolved from vaporization and sublimation of the liquid and solid (3, 7, 8). We have estimated the mean diameter of the submicron particles from an analysis of the dependence shown in Figure 3 of the relative brightnesses from scattering of sunlight at visible (S-20 photocathode response) wavelengths on distance into the wake of the spacecraft. The surface roughening that has been reported from laboratory experiments is interpreted as accelerating the sublimation rates of these small particles by factors up to about 2.

188

ACKNOWLEDGEMENTS

The success of this experiment is due to the support provided by a number of USAF, NASA, and AMOS personnel. We thank especially D. J. Knecht, J. P. Bagian, J. F. Buchli, Lt T. Hols, L. Dungan, J. Baird, Maj E. Imker, G. Ashley, and L. Twist.

REFERENCES

1. Pickett, J. S., D'Angelo, N., and Kurth, W. S., Plasma Density Fluctuations Observed During Space Shuttle Orbiter Water Releases, J. GEOPHYS. RES., 94, 12081-12086, 1989.

2. Fowler, M. E., Leger, L.J., Donahoo, M. E., and Maley, D. D., Contamination of Spacecraft by Recontact of Dumped Liquids, Third Annual Workshop on Space Operations and Robotics (SOAR 89), NASA Conf. Pub. 3059, p. 99, 1989.

3. Bernhardt, P. A., A Critical Comparison of Ionospheric Depletion Chemicals, J. GEOPHYS. RES., 92, 4617-4628, 1987.

4. Kassal, T. L., Scattering Properties of Ice Particles Formed by Release of H_2O in Vacuum, J. SPACECRAFT ROCKETS, 11, 54-55, 1974.

5. Curry, B. P., Bryson, R. J., Seibner, B. L., and Jones, J. H. Selected Results from an Experiment on Venting an H_2O Jet into a High Vacuum, Technical Report AEDC-TR-84-28, January 1985.

6. Curry, B. P., Bryson, R. J., Seibner, B. L., and Kiech, E. L., Additional Results from an Experiment Venting an H_2O Jet into a High Vacuum, Technical Report AEDC-TR-85-3, June 1985.

7. Fuchs, H., and Legge, H., Flow of a Water Jet Into Vacuum, ACTA ASTRONAUTICA, 6, 1213-1226, 1979.

8. Muntz, E. P., and Orme, M., Characteristics, Control, and Uses of Liquid Streams in Space, AIAA J., 25, 746-756, 1987.

9. Patashnick, H., and Rupprecht, G., Sublimation of Ice Particles in Space, Technical Report ED-2002-1654, March 1973.

A COMPARISON OF SHUTTLE ENGINE FIRINGS IN SPACE TO CODE PREDICTIONS

J. B. Elgin
Spectral Sciences Incorporated

(Paper not provided at publication date)

190

INFRARED BACKGROUND SIGNATURE SURVEY: A REVIEW OF AF SCIENCE OBJECTIVES AND A HARDWARE DESCRIPTION

Capt. Al J. Locker III, E. Murad, and R. A. Viereck
Geophysics Laboratory
Hanscom Air Force Base

(Paper not provided at publication date)

THE SHUTTLE INFRARED TEST EXPERIMENT

B. D. Green, D. Trembley, G. Sacco, H. Cohen, W. Lynch, J. Werner, J. Baker,
and A. Woodman
Physical Sciences Incorporated

(Paper not provided at publication date)

THE ENVIRONMENT WORKBENCH
A DESIGN TOOL FOR SPACE STATION FREEDOM

Gary A. Jongeward, Robert A. Kuharski, Thomas V. Rankin, and Katherine G. Wilcox
Maxwell Laboratories, Inc., S-CUBED Division
P. O. Box 1620, La Jolla, California 92038-1620

James C. Roche
NASA/Lewis Research Center
21000 Brookpark Road, Cleveland, Ohio 44135

INTRODUCTION

The Environment WorkBench (EWB) is being developed for NASA by S-CUBED to provide a standard tool that can be used by the Space Station Freedom (SSF) design and user community for requirements verification. The desktop tool will predict and analyze the interactions of SSF with its natural and self-generated environments. The project is funded by Space Station (SSE) and managed by NASA/Lewis Research Center. In this paper, we briefly review the EWB's design and capabilities. We then show calculations using a prototype EWB of the on-orbit floating potentials and contaminant environment of SSF. We examine both the positive and negative grounding configurations for the solar arrays to demonstrate the capability of the EWB to provide quick estimates of environments, interactions, and system effects.

THE ENVIRONMENT WORKBENCH

The design of the EWB is based on the Environment Power System Analysis Tool (EPSAT) developed by S-CUBED for NASA and SDIO. EPSAT integrates into one modern screen-oriented desktop tool the environment and analysis modules needed to design and perform system studies on power systems. For the EWB, the environment and interaction modules are being replaced with modules containing Space-Station-approved models. The architecture of the EWB is shown below in Figure 1. The user interface is isolated from the calculation modules, allowing sophisticated display capabilities to be standardized. The calculational portion of the tool is designed to allow modules containing physics models to be "plugged" into software expansion slots similar to a bus on a PC. The process controller then coordinates all input/output (I/O) from the individual modules and data bases. This structure provides flexibility and expandability. When new modeling capabilities are needed, the necessary modules are "plugged" and automatically work with all the other physics modules and the display module.

The environment and interaction modules to be incorporated into the EWB are called out in SSF 30425 and are listed in Figure 2. The SSF document also details the specifics of the

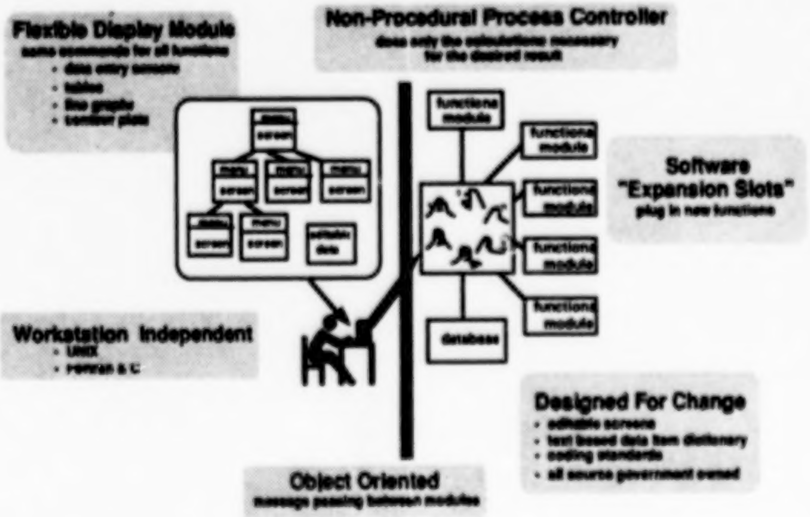
Flexible Display Module
same commands for all functions
• data entry screens
• tables
• line graphs
• contour plots
Non-Procedural Process Controller
does only the calculations necessary
for the desired result
menu
screen
editable data
functional module
database
Software
"Expansion Slots"
plug in new functions
Workstation Independent
• UNIX
• Fortran & C
Designed For Change
• editable screens
• text based data item dictionary
• coding standards
• all source government owned
Object Oriented
message passing between modules

Figure 1. The architecture of the EWB. The display module presents information to the user on screens or in tables and graphs. The software bus integrates the calculational modules and handles all data storage and I/O from the modules.

- Neutral Atmosphere
- Plasma
  - Ionospheric plasma
  - Auroral Plasma
  - Geosynchronous Plasma
- Penetrating Charged Particles
  - Magnetospheric
  - Trapped Radiation
  - Cosmic Rays
- Electromagnetic Radiation
  - Galactic Radiation Noise
  - Solar EM Noise
  - Natural Environment EMR
  - Man-made Noise
- Meteor and Debris
  - Meteoroids
  - Debris
- Earth's Magnetic Field
- Gravitational Field
- Induced Environmental Effects
  - Plasma Wake
  - Neutral Wake
  - Glow
  - Charging
  - Contamination
  - EMR from Power
  - Induced Perturbations
  - V x B
  - Plasma Currents
  - Drag
  - Torques
  - Radiation Dose
  - Meteor and Debris Impacts
  - Surface Degradation

Figure 2. Environment and interaction models to be incorporated into the EWB.

models as currently conceived. However, as discussed above, the modular design of the EWB will facilitate modifications, extensions, and replacements as needed.

SPACE STATION FREEDOM CALCULATIONS

In this section, we present prototype EWB calculations of the $\mathbf{v} \times \mathbf{B}$-induced potentials, floating potentials, and contaminant environment about SSF. The prototype EWB is an extension of EPSAT and forms the basis of the EWB. These calculations show that, for the negative ground configuration of the solar arrays, the truss structure will float more than 100 volts negative. During these conditions, thruster firings can ground the structure significantly, increasing the current through the structure.

In the calculations below, a 28° inclination 300 kilometer orbit is used. Figure 3 shows a plot of the north, east, and down components of the Earth's magnetic field as a function of mission time for this orbit. The plot extends for approximately one orbit. The magnetic field module contains the IGRF-87 model of the earth's magnetic field. The orientation of SSF on its orbit has the cabin facilities in the gravity gradient direction and the truss structure normal to the orbit plane. In this orientation, the down component of the magnetic field induces the potential gradient along the 130 meter truss structure. As seen in Figure 3, the down component changes sign between the northern and southern magnetic hemisphere and ranges to almost 0.3 Gauss.

The induced $\mathbf{v} \times \mathbf{B}$ potential across the entire truss structure is shown below in Figure 4. The potential is given as a function of mission time for an entire day (86,400 seconds). The potential is not periodic with orbit due to the rotation of the earth. The sign of the potential changes with that of the down component of the magnetic field (see figure 3). The maximum potentials of +33 volts and -32 volts occur when SSF is nearest to the magnetic poles.

Floating potential calculations were performed for the two grounding schemes of the solar arrays. The results are shown in Figures 5 and 6. For both cases, the 130m × 5m × 5m truss structure was assumed to be solid and conductive. The solar arrays were assumed to generate 150 volts continuously. (Shadowing by the earth was ignored.) Solar array plasma current collection is taken as the sum of the collection by the individual solar cells. Each solar cell is assigned a voltage depending on its position in the array and the array ground potential. The plasma current collection by an individual cell is dependent on the array and cell design and must be parametrically defined. We use the form shown in Figure 7,

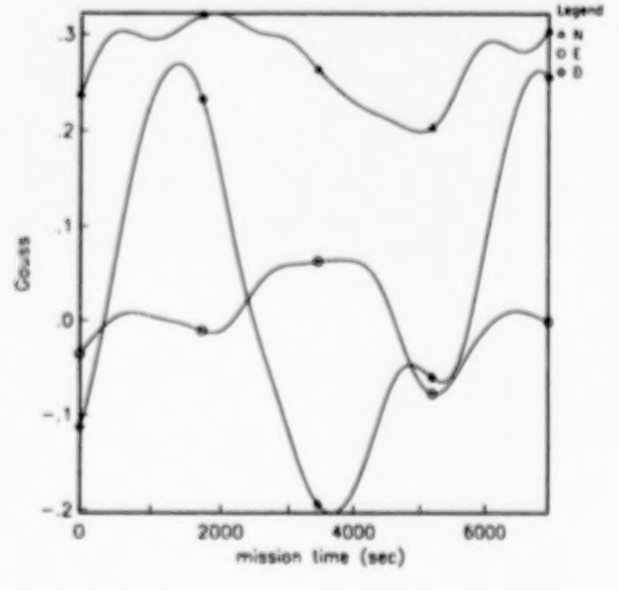

Figure 3. The north (N), east (E), and down (D) components of the Earth's magnetic field for one orbit. The magnetic field values are not periodic with each orbit due to the revolution of the Earth.

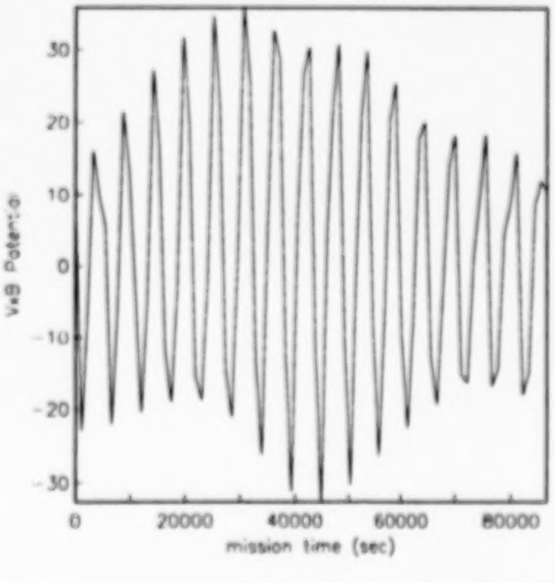

Figure 4. The potential induced across the truss of SSF by its motion through the Earth's magnetic field. The cyclic motion is due to the orbit around the earth, and the envelope is due to the earth's rotation.

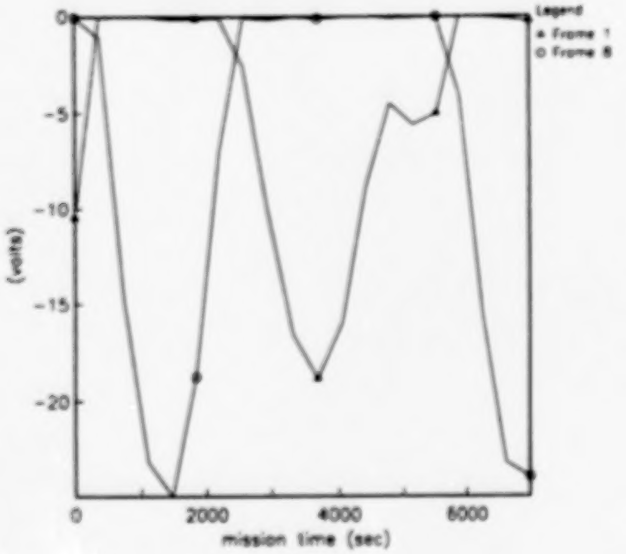

Figure 5. Floating potential of the truss for the positive ground configuration. The two curves show the potentials with respect to plasma ground of the two ends of the truss.

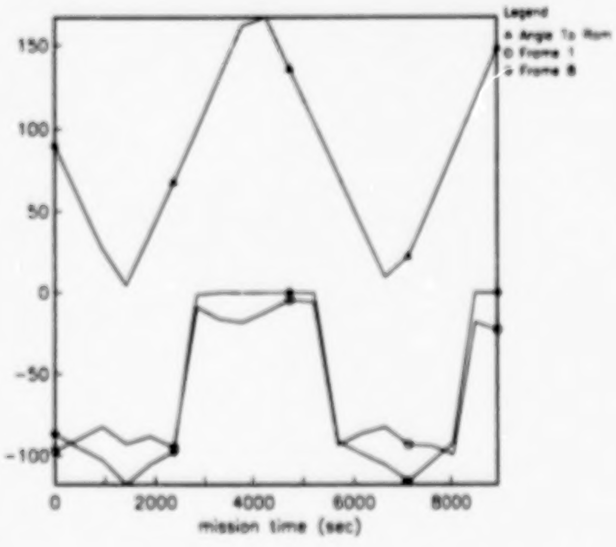

Figure 6. Floating potential of the truss for the negative ground configuration. The two lower curves show the potentials with respect to plasma ground of the two ends of the truss. The top curve shows the orientation of the solar arrays with respect to the ram.

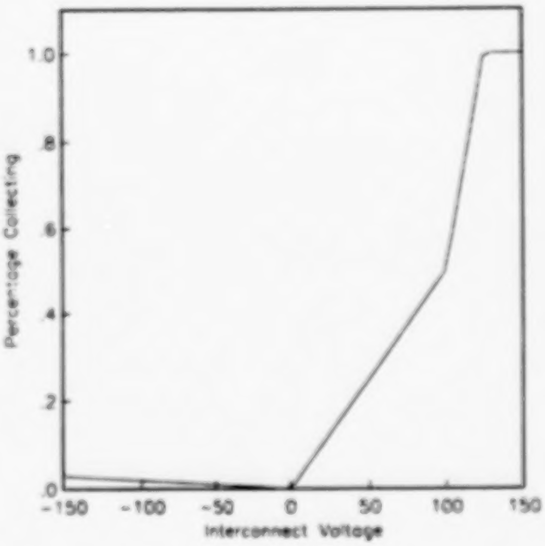

Figure 7. Parametrized collection efficiency of a single solar cell used in the floating potential calculations. The plasma current collected is the incident plasma current onto the cell surface multiplied by the collection efficiency.

which allows for different ion and electron collection efficiencies and secondary electron and snapover effects. The specific values used in these calculations were chosen to reproduce the collection efficiencies of NASCAP/LEO simulations of the SSF solar cells.

The SSF floating potential as a function of mission time is shown in Figure 5 for the solar array positive ground configuration. At each mission point, the EWB uses the IRI-86 plasma density module to compute the plasma density appropriate for the location and local time. The floating potential module then determines the potential that must be added to each component to produce zero net plasma current to the system. The two curves shown in Figure 5 are the potentials with respect to plasma ground of the two ends of the truss. As seen, the potential stays within **v** × **B**•**L** of plasma ground. The most positive part of the solar array is near plasma ground, and the most negative portions are 150 volts negative.

The negative ground configuration is shown below in Figure 6. The difference is dramatic. The truss floats between 100 and 130 volts negative depending on the **v** × **B**•**L** potential. When the truss is floating at 130 volts negative, over 1 ampere is flowing through the structure. Figure 6 also shows the angle of the solar arrays with respect to the ram. During part of the orbit, the solar arrays do not face into the ram plasma and cannot collect current. For these times, the floating potential falls to low values similar to the positive ground configuration.

The final EWB calculations show the effect of firing a 10 lb. thruster. As shown in Figures 8a and 8b, the density near the thruster is high enough to cause a Paschen breakdown (~ 0.2 Torr-cm). This is confirmed in Figure 9, which shows a plot of the pressure and the Paschen breakdown pressure threshold as a function of distance along the truss. Near the location of the thruster (120 m), the pressure threshold is exceeded. In this region, it is possible to have Paschen breakdown given high enough voltage. However, if breakdown does occur, it will tend to extinguish itself because the rest of the plasma circuit (truss, solar arrays, etc.) cannot collect enough current to sustain the arc. The system will be driven more positive, increasing the current to the arrays.

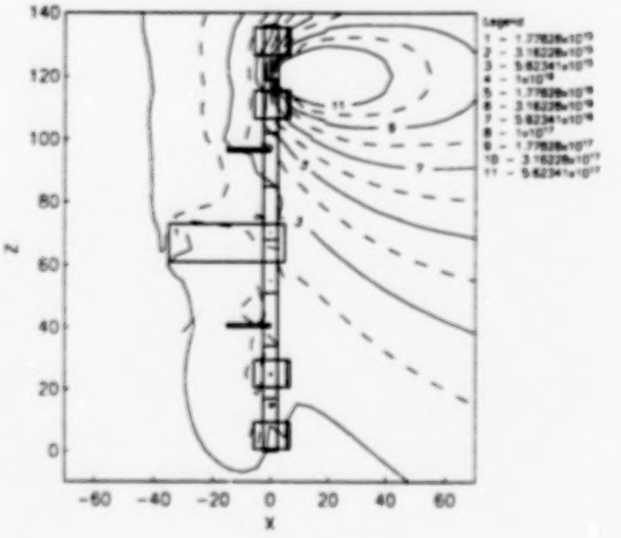

(a)

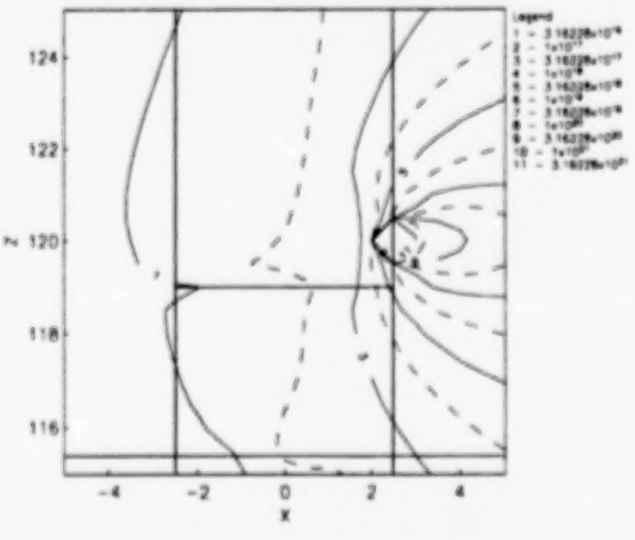

(b)

Figure 8. (a) Total neutral density near SSF during operation of a 10 lb. thruster located at 120 m up the truss. The calculation includes the ambient neutrals and accommodated thruster neutrals. (b) Blowup of the thruster region.

SUMMARY

The Environment WorkBench is being developed to provide Space Station designers and users with a tool to determine interactions of Space Station Freedom with its natural and self-generated environments. The EWB will integrate into one desktop tool the environment and interaction models needed to perform system analysis and requirements verification. As demonstrated by the prototype calculations presented here, having environment and interaction models integrated into one tool allows the user to analyze quickly and reliably system performance of configurations and to determine if requirements are being met.

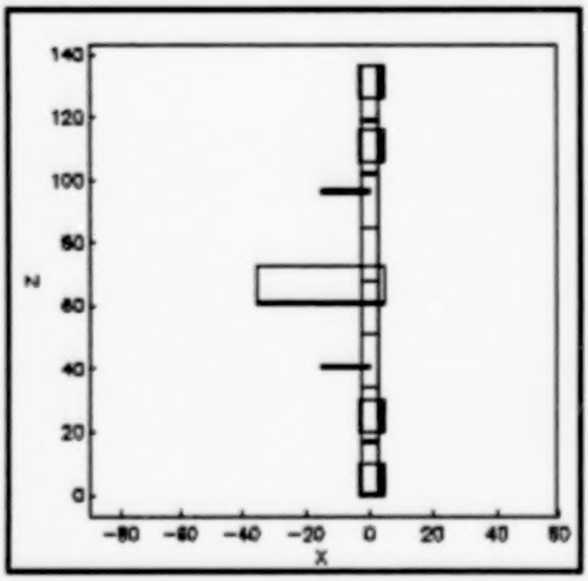

Figure 9. (a) Profile of the EWB space station model. The thruster is located at 120 m. (b) Neutral pressure and Paschen breakdown pressure threshold as a function of distance along truss. Near the thruster, the breakdown pressure is exceeded.

ACKNOWLEDGEMENT

EPSAT is supported by the NASA Lewis Research Center, Cleveland, Ohio, under Contract NAS3-25347.

196

SPACE ENVIRONMENTAL EFFECTS PROGRAM

Wayne E. Ward
Wright Research and Development Center

(Paper not provided at publication date)

FINDINGS OF THE JOINT WORKSHOP ON
EVALUATION OF IMPACTS OF
SPACE STATION FREEDOM GROUND CONFIGURATIONS

Dale C. Ferguson and David B. Snyder, NASA Lewis Research Center,
Cleveland, Ohio, 44135, USA,
Ralph Carruth, NASA Marshall Space Flight Center,
Huntsville, Alabama, 35812, USA

ABSTRACT

A workshop to consider the effects of the various proposed SSF grounding schemes was held at NASA Lewis Research Center May 22-24, 1990. Experts from the plasma interactions community evaluated the impacts of environmental interactions on SSF under each of the proposed grounding schemes. The grounding scheme chosen for the Space Station Freedom (SSF) power system was found to have serious implications for SSF design. Interactions of the SSF power system and structure with the low Earth orbit (LEO) plasma differ significantly between different proposed grounding schemes. Environmental constraints will require modification of current SSF designs under any grounding scheme. Maintaining the present, negative grounding scheme compromises SSF safety, structural integrity, and electromagnetic compatibility, and will increase contamination rates over alternative grounding schemes. One alternative, positive grounding of the array, requires redesign of the primary power system in Work Package Four. Floating the array reduces the number of circuit changes to Work Package Four but adds new hardware. Maintaining the current design will affect all Work Packages. However, no impacts were identified on Work Packages One, Two or Three by positively grounding or floating the array, with the possible exception of extra corona protection in multi-wire connectors.

INTRODUCTION:

Interactions of spacecraft with the natural environment have been of concern ever since the Gemini space program. Since that time, much has been learned of spacecraft/environment interactions, especially as new technology has been developed and flown.

Space Station Freedom (SSF) represents a significant increase in spacecraft size and power levels. Old rules of thumb must be re-examined and their validity retested before applying them to the new technology. In the 1980's, with the advent of the STS, efforts were begun to understand how large spacecraft interact with the ionospheric plasma. By 1986, recommendations were made to ground SSF to the positive side of its arrays. Many engineers in Work Package 4 used a positively grounded array as a baseline at a time when the primary power distribution system was AC. In 1989, when the primary power changed to a DC distribution system, power system designers assumed a negatively grounded system. However, the plasma interactions community raised concerns about this grounding scheme in meetings of the Space Station Plasma Interactions and Effects Working Group, through a change request proposal to change the grounding scheme to a positive ground, and through letters and conversations with SSF personnel.

On May 22-24, 1990, experts on the Low Earth Orbit (LEO) environment plasma interactions met with engineers from the major Space Station Freedom contractors, and representatives of NASA management to evaluate the impacts of the different proposed power system grounding schemes for Space Station Freedom. It was known that the interactions of SSF with the ambient LEO environment would be quite different for the different grounding schemes. The impacts of these interactions on the safety, weight, feasibility, operating requirements, maintenance and reliability or risk of SSF were in need of evaluation to support an imminent decision on the SSF grounding scheme. The results reported here are the result of that evaluation process. An attempt has been made to bring to bear all known engineering and physical facts about interactions with the LEO environment to evaluate the impacts of all the proposed grounding schemes. An effort has been made to be as quantitative as possible. It is hoped that this report will be a first step in the necessary evaluation of the environmental issues regarding SSF grounding.

The first day of the Workshop was devoted to presentations about what we can expect in the way of grounding-related SSF environmental interactions, how they may be estimated, and what kinds of answers need to be obtained. Ground rules for the next day's calculation sessions and the basic premises of the Workshop were presented. These basic premises are repeated below:

o SSF operations and designs can be optimized by including considerations of physical processes of environmental interactions.

o In LEO, current balance will be satisfied - positive and negative collected currents must balance.

o The grounding configuration chosen for the Space Station will influence all systems.

o Our understandings of the laws of physics (models, theories, equations, empirical guidelines) are sufficient that some predictions of the interactions and their impacts may be made.

o No one wants a SSF that won't work well.

On the following day, the Workshop split up into four working groups, The FLOATING POTENTIALS AND GROUND CURRENTS WORKING GROUP, the ATOMIC OXYGEN, SPUTTERING, MATERIALS DEGRADATION AND CONTAMINATION WORKING GROUP, the CORONA, ARCING, AND INSULATION WORKING GROUP, and the ARC RATES AND EFFECTS, EMI, AND KAPTON PYROLIZATION WORKING GROUP. Much of the following is the result of their calculations and estimates.

SPACECRAFT/PLASMA INTERACTIONS:

The ionosphere in LEO is a conductive plasma. Any spacecraft placed in this environment will come to an equilibrium potential relative to the plasma such that no net current is collected. If the spacecraft has a distributed voltage (driven, perhaps, by an illuminated solar array) which permits currents to be collected from the plasma, then part of the spacecraft will be positive relative to the plasma potential ("zero volts"), collecting electrons, and the rest will be negative relative to the plasma, collecting ions. The electrons are very light, mobile, and easily collected. The ions are massive, slower moving, and difficult to collect. Therefore, the total spacecraft voltage relative to the plasma will be such that most of its area will be negative of the plasma potential and only a small part will be positive. Figure 1 illustrates these points. It also shows that if a spacecraft structure is grounded to the positive side of the solar array then it will be near zero volts because its surface area adds to the surface area which can collect electrons. If the spacecraft is grounded to the negative side of the solar array it will be driven negative by most of the array-generated voltage. Many experiments on the Space Shuttle and free-flying LEO spacecraft have shown these concepts to be sound.

In the past, these effects have been seen on spacecraft in LEO conditions, but the voltages and spacecraft sizes were such that they only had to be considered in correcting and interpreting results of scientific experiments. However, the physical size and voltage level of the SSF power system require that plasma effects be considered in the design.

BASIC ASSUMPTIONS ABOUT THE SSF POWER SYSTEM:

The objective of this workshop was to investigate the consequences of various grounding schemes. In order to justify the practicality of the grounding configurations chosen for evaluation, some features of the power distribution system were noted. Details of the power system are discussed in reference 1.

With this background three possible grounding configurations were identified. Additional configurations may be identified but their consequences are covered in this set, and they give rise to additional levels of impracticality.

The first configuration identified has the array grounded with the primary power distribution on its negative side and the secondary power distribution also grounded on the negative side. This is the concept currently being used to design the power distribution system (Fig. 2).

The second configuration is to ground the array and the primary power system positive, and ground the secondary power distribution negative. The ground reference would change sign across the transformer in the DDCUs (DC to DC Converter Units). The primary power distribution system would have positive referenced circuitry (Fig. 3).

The third configuration would float the solar arrays and negatively ground both the primary and secondary power distribution systems. For this configuration a DDCU would have to be added outside the alpha joint, either in the DCSU (DC Switching Unit) or just after the SSU (Sequential Shunt Unit). This may require an additional DDCU for each solar array mast. Such a DDCU would have different requirements than the DDCUs which convert to the secondary power system and, in general, will not have interchangeable parts. This would permit most of the power distribution circuitry to have a negative ground. But the SSU and some support circuitry might need to be grounded separately and electrically isolated from the rest of the system (Fig. 4).

PLASMA/SSF GROUNDING:

If the structure is grounded to the negative side of the array, the structure/array will float nearly the entire array voltage negative in the daytime (about -150 to -130 V negative of the ionospheric plasma). This is to balance the positive ion collection by the structure and array with the electrons collected by the array (Figure 2). At night, when no voltage is generated by the array, the structure will be near plasma potential.

With the structure grounded to the positive side of the array, the positive structure is electron collecting, while nearly the entire array must be ion collecting to balance this (Figure 3). As a result the structure is only slightly positive relative to the plasma. However, the negative side of the array now floats nearly 160 V negative relative to plasma.

A floating array would permit the array to float relative to plasma, and permit the structure to float near plasma potential (Figure 4). This option combines some environment interactions advantages with a slightly reduced arc probability due to the slightly more positive floating array.

IDENTIFIED IMPACTS OF GROUNDING SCHEMES ON SSF:

Grounding configurations considered in this effort were:

1. Solar arrays (SA), primary power distribution (PC), and secondary power distribution (SC) all grounded negative.
2. SA and PC grounded positive and SC grounded negative.
3. SA floating, but both PC and SC grounded negative.

Some of the relevant effects of these configurations are presented in matrix form in Table I. This table gives both advantageous and disadvantageous impacts. Additional details of the impacts, the methods used to quantify and evaluate them, and detailed recommendations on implementing the different grounding schemes can be found in reference 1.

SUMMARY:

There are technical problems with all grounding designs which will affect SSF's costs and/or schedule. They arise for a variety of reasons, involving design changes to accommodate identified deficiencies in the current design or to accommodate the alternative grounding schemes.

Present design (Negative Ground):

The present design grounds all systems negative, and ties the ground to the negative side of the array. This will cause SSF ground and structure to float 130 to 150 V below plasma. Safety concerns are raised because of the 140 V difference between SSF and free flying bodies such as the docking of Shuttle or astronauts on EVA. Interlock mechanisms will need to be incorporated to prevent thruster firings or venting events while these other bodies are connected to or touching SSF because such events will cause currents through the spacecraft body or the Extravehicular Mobility Unit (EMU) of about 10 amps. Alternatively, active charge control systems (hollow cathodes or other plasma contactors) could be used to limit potentials. However, these will increase the plasma density around the entire SSF and will exacerbate other interactions (such as array current collection).

Arcs will occur on the structure. The present anodized surface will break down under the electric field imposed on it. Arcs will be triggered by micrometeoroid impacts, but their characteristics are unknown. Arcs analogous to solar array arcs may occur on the structure.

The SSF structure design will need to be re-evaluated. Erosion rates are increased because of sputtering by ions accelerated by the -140 V structure potential to holes in the anodization caused by dielectric breakdown or debris impacts. This will compromise the structural integrity of the trusses in from five to thirteen years.

Large currents that violate present EMI requirements will occur. In addition to the solar array related currents, a current of about one Amp DC is expected because of leakage currents through the structure anodization. This will increase over the lifetime of SSF. Voltage transients of 160 V and current transients of about 10 Amps are expected during thruster firings. During arcs, similar voltage swings and transient currents up to 100 Amps may occur. Additional shielding may be required on equipment.

Finally, contamination rates on Solar Arrays, Thermal Coating, and Optics will be increased because of the increased sputtering of the structure.

Positive ground:

In order to ground the solar array and primary power distribution positively while maintaining negative ground on the secondary power system, Work Package Four will have to redesign the primary power distribution system. Either NPN technology will have to be replaced with PNP technology or circuits will need to be more complicated. Also the DDCUs will need minor modifications for their insulation to survive increased corona occurrence, as will multi- wire connectors. Solar array arcs have a slightly higher risk of occurring because of the -160 V maximum negative potential rather than the -140 Volts on the negative grounded system. The sputtering problem on the solar arrays will be slightly increased.

Floating:

In order to float the array, new hardware will be needed. New additional DDCUs will be required. These DDCUs will not be parts-compatible with the other DDCUs because they must tolerate higher voltages, higher power levels, and higher corona levels.

Summary of impacts:

Environmental constraints require modification of present SSF designs. Maintaining the current grounding scheme compromises Safety, Structural Integrity, Electromagnetic Compatibility, and will increase contamination rates. Positive grounding of the array requires reworking of the primary power system, which impacts Work Package Four. Floating the array reduces the number of circuit changes to Work Package Four but adds new hardware.

TABLE I. PRIMARY POWER GROUNDING CONFIGURATION ASSESSMENT

IMPACTS CONFIGURATION	ADVANTAGEOUS IMPACT	DISADVANTAGEOUS IMPACT
Modules/Truss grounded to negative end of solar array (current design approach - see Fig. 2)	• -140 V vs -160 V max potential on solar array with respect to plasma (a minimal advantage)	• All Work Packages impacted by plasma effects • Safety (EVA/Docking) compromised by induced voltages and 10 amp current through EMU vents • Thermal control materials must be re-evaluated, redesigned or substituted • Truss structure seriously questionable in 5-13 years • Large plasma-induced currents and voltages to be accommodated • Contamination increased by sputtering • Conducted EMI requirement not met
Modules/Truss grounded to positive end of solar array (see Fig. 3)	• Module/Truss voltage near plasma potential eliminates structural sputtering, insulation req. • Thermal coatings: no change • Minimum plasma/structure current • No new EVA/Docking safety problems • Keeps impacts & redesign issues in a single Work Package	• 260 V vs 160 V maximum DC potential in power connectors to DDCU • Redesign of DC-DC Converters required • Corona design requirements increased in DDCU • Redesign of primary power control circuitry
Modules/Truss floating with respect to solar array (see Fig. 4)	Same as above	• Corona design requirements slightly increased in new, additional DDCU • Design new DDCU (160 V to 180 V) • Redesign of solar panel power control circuits

Maintaining the current negative ground design will affect all Work Packages. However, no impacts were identified on Work Packages One, Two or Three by positively grounding or floating the array, with the possible exception of increased corona protection in multi-wire connectors.

REFERENCES:

1. Ferguson, D.C., Snyder, D.B., and Carruth, R., *Report of the Joint Workshop of the Space Station Freedom Plasma Interactions and Effects Working Group, the Space Station Freedom Plasma Working Group, and the Space Station Freedom EMI/EMC and Electromagnetic Effects Working Group on Evaluation of Impacts of Space Station Freedom Grounding Configurations, May 22-24, 1990*, in publication.

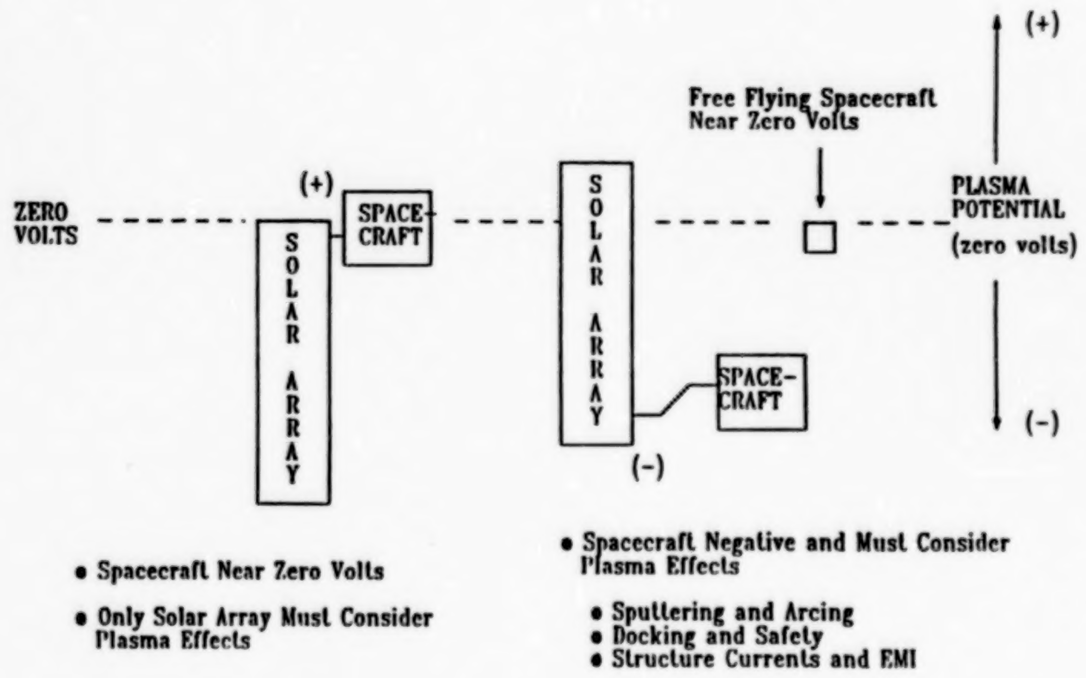
(+)
Free Flying Spacecraft Near Zero Volts
ZERO VOLTS
(+)
SPACE-CRAFT
SOLAR ARRAY
SOLAR ARRAY
PLASMA POTENTIAL (zero volts)
SPACE-CRAFT
(-)
(-)
• Spacecraft Near Zero Volts
• Only Solar Array Must Consider Plasma Effects
• Spacecraft Negative and Must Consider Plasma Effects
• Sputtering and Arcing
• Docking and Safety
• Structure Currents and EMI

Figure 1. How a spacecraft with High Voltage Solar Arrays floats in the plasma.

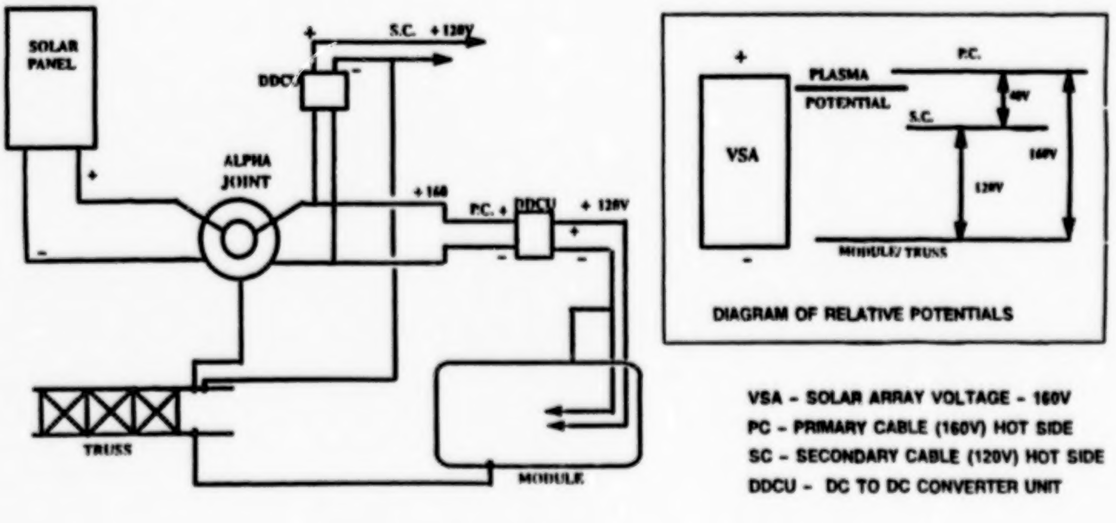
SOLAR PANEL
DDCU
S.C. +120V
ALPHA JOINT
+160
P.C. +
DDCU
+120V
TRUSS
MODULE
+
-
PLASMA POTENTIAL
P.C.
S.C.
40V
160V
120V
VSA
MODULE/TRUSS
DIAGRAM OF RELATIVE POTENTIALS
VSA - SOLAR ARRAY VOLTAGE - 160V
PC - PRIMARY CABLE (160V) HOT SIDE
SC - SECONDARY CABLE (120V) HOT SIDE
DDCU - DC TO DC CONVERTER UNIT

Figure 2. The presently baselined SSF Negative Ground Configuration.

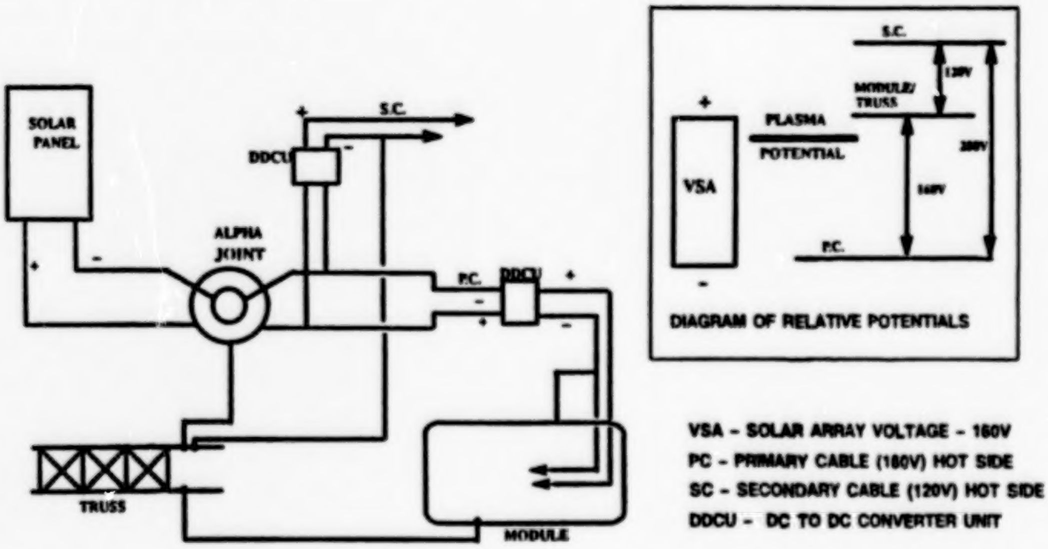
SOLAR PANEL
+
-
ALPHA JOINT
DDCU
+
S.C.
-
P.C.
DDCU
+
-
+
-
TRUSS
MODULE
S.C.
120V
MODULE/ TRUSS
280V
+
PLASMA
POTENTIAL
VSA
160V
P.C.
-
DIAGRAM OF RELATIVE POTENTIALS

VSA - SOLAR ARRAY VOLTAGE - 160V
PC - PRIMARY CABLE (160V) HOT SIDE
SC - SECONDARY CABLE (120V) HOT SIDE
DDCU - DC TO DC CONVERTER UNIT

Figure 3. A Positively Grounded Solar Array with Negatively Grounded Secondary.

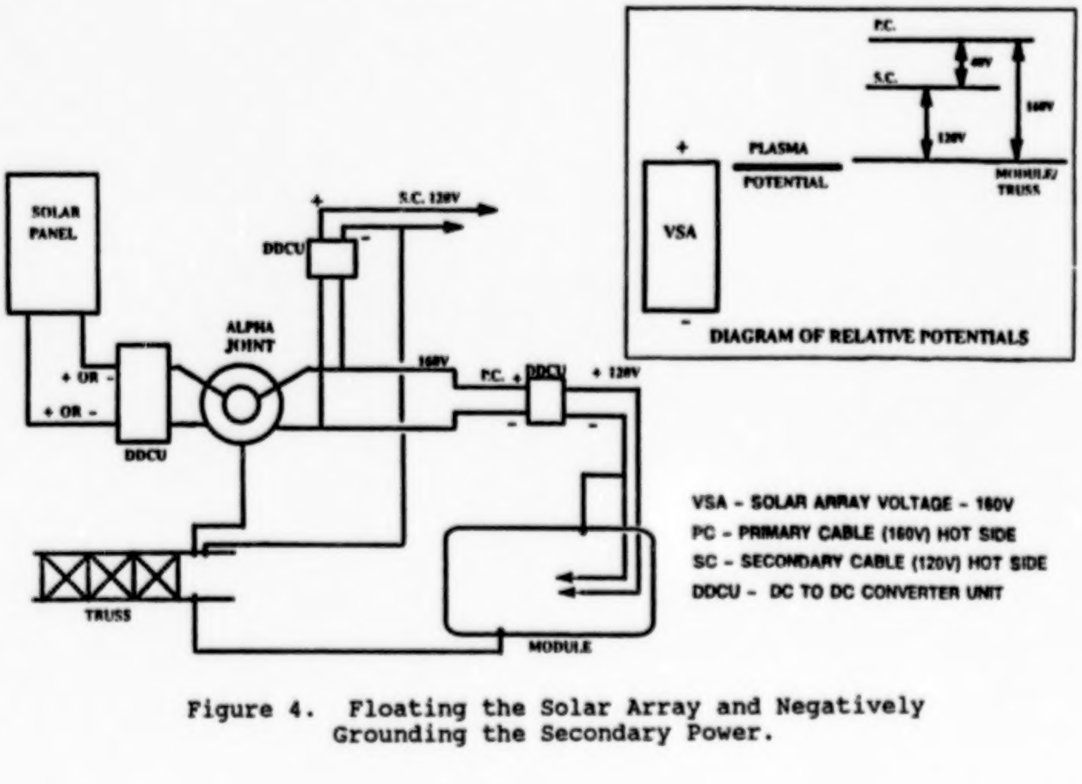
P.C.
40V
S.C.
160V
120V
+
PLASMA
POTENTIAL
MODULE/ TRUSS
VSA
-
DIAGRAM OF RELATIVE POTENTIALS
SOLAR PANEL
+ OR -
+ OR -
DDCU
ALPHA JOINT
DDCU
+
S.C. 120V
-
160V
P.C.
+
DDCU
+ 120V
-
-
TRUSS
MODULE

VSA - SOLAR ARRAY VOLTAGE - 160V
PC - PRIMARY CABLE (160V) HOT SIDE
SC - SECONDARY CABLE (120V) HOT SIDE
DDCU - DC TO DC CONVERTER UNIT

Figure 4. Floating the Solar Array and Negatively Grounding the Secondary Power.

DEBRIS

SMALL SATELLITE DEBRIS CATALOG MAINTENANCE ISSUES

Major Phoebe A. Jackson
Headquarters United States Space Command
Deputy Directorate for Space Control
Peterson AFB, CO 80914-5003

ABSTRACT

The United States Space Command (USSPACECOM) is a Unified Command of the Department of Defense with headquarters at Peterson Air Force Base, Colorado Springs, CO. One of the tasks of USSPACECOM is to detect, track, identify, and maintain a catalog of all man-made objects in Earth orbit. This task we call space surveillance. The most important tool for space surveillance is the satellite catalog. The purpose of this paper is threefold. First, to identify why the command does the job of satellite catalog maintenance. Second, to describe what a satellite catalog is. Third, and finally, to identify small satellite debris catalog maintenance issues. This paper's underlying rationale is to describe our catalog maintenance services so that the members of the community can use them with assurance.

USSPACECOM OVERVIEW

USSPACECOM is a warfighting command. It is authorized to employ forces in support of its missions. USSPACECOM exercises combatant command of its assigned space forces by assigning tasks, designating objectives, and providing direction. A summary of the USSPACECOM mission, taken from the Unified Command Plan, is presented below:

- Space operations to include space control and space support.
- Integrated warning for North American Aerospace Defense Command and other Unified and Specified Commands.
- Planning for eventual operation of the Ballistic Missile Defense system.

Space surveillance is important to all three USPACECOM missions. However, it is actually a subtask of the space operations mission called space control.

Space control is USSPACECOM's warfighting mission. Space control is analogous to sea control. Its goal is to achieve superiority in those areas of space vital to U.S. national interest. Through the space control function, USSPACECOM ensures access to space, tracks objects in space, protects U.S. and allied space-related assets, and when directed, negates hostile space-related forces.

USSPACECOM SURVEILLANCE MISSION

Space surveillance is the fundamental task. It includes detecting objects as they enter space, detecting events caused by objects in space as they occur, and confirming that an object has departed space. Space surveillance is thus essential to control of space. Without accurate surveillance, efforts at assessment and warning, protection, and negation would be futile.

Space surveillance tasking is directed by the USSPACECOM Space Surveillance Center (SSC). The SSC performs space surveillance using both a space-based constellation of geosychronous launch detection sensors and a ground-based network of tracking sensors. The SSC uses this set of sensors to detect and track launches when they enter space. Once the launch is tracked, the SSC can enter information about the launch into the SSC satellite catalog.

To summarize, USSPACECOM maintains the SSC satellite catalog because it is essential to space control operations. Actually, the principle of maintaining it is simple. The SSC tasks the space surveillance network to use the satellite catalog to track satellites. The SSC then takes the observations and updates the satellite catalog. (See Figure 1) However, the actual processes for maintaining the catalog are not so simple. Thus, this paper will next describe what the satellite catalog is and then how things get into it.

WHAT A SATELLITE CATALOG IS.

"Every State launching an object into space is required to maintain a registry" (Convention on Registration of Objects Launched into Outer Space, 1975). Further, every State is required to provide to the Secretary-General of the United Nations the following information, as soon after launch as practicable.

> Name of launching State (or States), designator of the space object, date and location of launch, basic orbital parameters (nodal period, inclination, apogee, and perigee) and general function of the space object.

The SSC Satellite Catalog contains not only this registry information, but other operationally useful information, as well. In general, the SSC catalog is used in two forms. The first form is the registry. The second one is a data base of current orbital parameters on every object for which the SSC can maintain data. A set of orbital paramenters for an object is called an "element set". Thus, this second catalog is called the SSC element set catalog. The discussion that follows will consider the following three questions. First, what kind of information is kept in the registry? Second, what does the element set catalog contain? And, three, how do objects get into the catalog?

SSC REGISTRY CATALOG

The registry catalog maintains the following kinds of information on each object:

The SSC number, satellite common name, international designator, owner source, launch date, launch site, and decay date (when appropriate).

The SSC number is assigned sequentially by the SSC as objects of the launch attain orbit and have a current element set. For example, the oldest object in orbit is satellite number 0005, Vanguard 1, a payload, launched from Air Force Eastern Test Range on March 17, 1958.

The satellite common name, launch site, and launch date is as stated by the owner when the launch is announced.

The international designator is assigned based on rules in COSPAR Information Bulletin No 9, July 1962.

The international designator contains year of launch and number of the launch that year, on a worldwide basis. The final suffix uniquely and sequentially defines each object put in orbit by that launch.

The SSC uses the following conventions to assign object suffixes. The suffix "A" is always reserved for the primary object of a launch. Then, suffixes are assigned by a combination of availability of element sets and importance of the object, usually payload, rocket body, and then debris. (See Figure 2)

The summary of basic orbital parameters on each object is current as of the date that the catalog was generated. These basic orbital parameters are taken from the SSC satellite element set data base.

SSC ELEMENT SET CATALOG

The most commonly available satellite element set catalog contains "two-card" element sets: This form of satellite element set is described in two 69-character data lines. It is a mean, general perturbations element set using modified Keplerian elements, including; epoch time, drag terms, inclination, right ascension of the ascending node, eccentricity, argument of perigee, mean anomaly, and mean motion in revolutions per day. This mean two-card element set is used with our ephermeris prediction package to generate predictions on the satellite's location. A mean orbit is the mathematically smoothed description of the orbit. An osculating orbit represents the actual orbit of the satellite as it is acted on by natural forces.

Table I provides a summary of objects in the SSC Element Sets Catalog as of 05 June 1990

	PAYLOADS	ROCKET BODIES	DEBRIS
OBJECTS	1666	989	3515

Table I. Summary of Object Types in the SSC Catalog

The structure and content of the SSC satellite catalog is significant to the user. Note that the catalog includes both registry and satellite element set information. We protect the distribution of our catalog because sometimes we have information on a launch that may not be confirmed by the satellite owner. We respect the confidentiality of a satellite owner's decision to not release this information.

HOW THINGS GET INTO THE CATALOG?

The most essential step in space surveillance is to detect man-made objects during launch, before they enter space. This is the most common way that objects are found and entered into the satellite catalog.

Space launches are initially detected before they enter space by the Defense Support Program (DSP), a constellation of satellites in geosynchronous orbit.

With initial launch detection information, the ground-based sensor network is directed by the SSC to locate the new launch and all of its pieces. The sensor tracking data is then used to update the SSC element set data base (Figure 1). When the element sets are associated with the launch event, the launched objects are cataloged. Technically, SSC may have an element set, but no registration information on an object to enter it into the catalog. As of 05 June 1990, there were 370 element sets with no registration information.

Today, twenty-six sensor systems make up the USSPACECOM space surveillance network. Figure 4 depicts the low-altitude coverage provided by our space surveillance sensors at 100nm above the Earth. The dashed line shows a typical Soviet satellite orbit trace for a launch from the Soviet Union.

Another significant way for objects to enter the catalog is when a satellite breaks up into many smaller pieces. When an object breaks up, the cloud of pieces is often found by the large search patterns maintained by certain ground-based sensors. Sensors such as NAVSPASUR, Eglin, and Cavalier keep large search fences up at all times. Administratively, the largest piece of the breakup maintains the satellite catalog name given when the object was initially correlated to a launch. The rest of the pieces are cataloged with new international designator suffixes, beginning from the last cataloged piece of the launch.

Satellites no longer in space are logged in the satellite catalog as "decayed". A decayed satellite is one which reenters the earth's atmosphere; thus, it is no longer in orbit.

Presently, man-made objects reenter from orbit on the average of more than one per day. Of these, over 95% are so small that they break up and burn up in the earth's atmosphere. Those that might survive reentry are monitored in a program called Tracking and Impact Prediction (TIP).

Many factors make it difficult to precisely predict where and when a satellite will decay. There are two important factors to mention. The first one is the fact of atmospheric reentry: the combination of atmospheric drag and unique physical characteristic of the object significantly influences both the speed and course of an object's decay. The second part is that our sensor network, due to sensor coverage limits, cannot maintain continuous track on such objects during their decay phase. Thus, depending on the time of the last track (from just now to three hours ago) the ground area of the reentry prediction could be from 100 to 1000 miles long. Historically, 95 out of 100 objects have decayed within the predicted "confidence window", which has an error of plus or minus 20% of the time from the last observation to the predicted decay time.

SMALL DEBRIS MAINTENANCE ISSUES

Presently, USSPACECOM does not track and maintain orbit predictions on small debris (objects less than 10 cm). However, if USSPACECOM is going to maintain small debris there are three issues that must be addressed. Each of these issues are stated below.

One: All satellite element sets are not alike.

Two: Definition of a Tracking Observation.

Three: Size of Small Debris Tracking Requirement.

ALL SATELLITE ELEMENT SETS AREN'T ALIKE

Actually, the SSC uses several forms of element sets. The first one described was the SSC two-card element set. This form is an analytically derived mean element set. The other common SSC element set is a numerically derived special perturbations vector, or "XYZ" vector. This vector is an osculating representation of an object's orbit. For a visual representation of "mean" versus "osculating" see Figure 3. It is very important to note that these two kinds of element sets cannot directly replace one another.

This issue gets even more complex. Depending on the application, different descriptions of the forces on an orbiting object are included in the element set. For example, near-earth perturbations are different from those experienced in deep space. Near-earth orbits have more atmospheric drag effects than geosynchronous deep-space orbits. Therefore, depending on the requirements of their satellite orbits, other agencies have developed their own element set forms. For example, SSC routinely provides vectors in forms used by Onizuka AFB, CA and NASA Goddard, MD for satellite control. SSC also services six other user coordinate systems in non-real time. Note that this also means that an SSC vector cannot directly replace an Onizuka or NASA vector.

The bottom line to you, as a user, is that any element set is not necessarily equivalent to any other element set. Fortunately, we can provide both element sets and look angle prediction software to authorized agencies.

DEFINITION OF A TRACKING OBSERVATION

There are actually three problems within this issue. The first one is called observation "correlation". The second is definition of how many observation constitute a track. And the third is how many site tracks are needed to define the first SSC element set, called "Element Set 1".

OBSERVATION CORRELATION:

The SSC satellite element set data base provides the location of all trackable objects in orbit around the earth. This data base is used to generate predicted look angle data for comparison to actual track data. If tracking data compares very closely, then the object is identified as a "correlated" object. If the object does not correlate, then it is an "uncorrelated target (UCT)". If all objects in earth orbit have current element sets (and thus are correlated), then a UCT is probably tied to a significant space event. Thus, another good reason for maintaining the satellite catalog is to allow our sensor network to detect new uncorrelated objects rapidly and easily.

Our experience is that failure to use identical correlation procedures both at the SSC and at the sensors can have a measurable impact on the SSC computational process.

DEFINITION OF THE TERM "TRACK".

While a track may contain one observation, it generally contains several observations taken during a length of time. For example, from our historic experience in tracking UCTs, we know that a roughly five minute long track on a near-earth object from a single site will produce an element set good for several revolutions. After that time, new observations are needed. Given that this 5 minute track length on a 90 minute orbit provides a basic element set, our rule of thumb is that the initial track length on a UCT must be at least 5.5% of the orbit period. This rule provides the appropriate track length as a function of period in Table II below.

OBJECT PERIOD (Minutes)	TRACK LENGTH (Minutes)
90	5
100	5.6
250	13.9
300	16.6
500	27.8
800	44.4

TABLE II. Track Length as a Function of Object Period

NUMBERS OF SITE TRACKS IN ELEMENT SET 1.

Once a good track length is obtained, then a certain dispersion of site traking observations is required in order to define the element set parameters. Practically, this is stated in the following rules for SSC Element Set One:

> Observations from any three sensors which track the object.
>
> Two sensor's obervations at least one-half revolution apart.
>
> Same sensor's observations on separate revolutions.

Once Element Set 1 is established, the element set can be maintained with a relatively small sample of tracking observations gathered periodically.

In summary, generation of an element set on any object that the SSC will maintain requires not one observation, but several sets of tracking observations. The tracking length will also be a function of the object's orbit period. Note that element set generation is not element set maintenance.

SIZE OF A SMALL DEBRIS TRACKING REQUIREMENT

The size of this requirement; that is, how many additional objects need to be tracked is important. For example, if the catalog doubles, we have problems that can be resolved by upgrading equipment. If however, the catalog increases ten-fold, we probably need a great deal more computer and communication capacity and more sensors. In other words, there is a significant cost factor.

SSC SPACE SURVEILLANCE NETWORK

The network used by the SSC uses several types of sensors including mechanical tracking radars, phased array radars, and tracking telescopes. (Table II lists our ground-based sensor capabilities.) The capability of sensors to track is a fixed function of their total sensor tracking opportunities.

For example, mechanical tracking radars generally have only one tracking beam. Also, they generally do not have the inherent capability to track objects smaller than 10 cm. The exception is Haystack. In addition, these sensors have no extra time to track other objects such as small debris. They are primarily used to track high priority objects as payloads and rocket bodies. Thus, these sensors have limited tracking opportunities to track small space debris.

The phased arrays functionally have more than one tracking beam and thus inherently could be used to track more objects. However, only a few have the inherent capability to support tracking objects less than 10 cm. The sensors that could support include the radars at Cavalier and Eglin.

The tracking telescopes also functionally have a single object tracking capability. Depending on refelectivity of the object and site weather, telescopes can track small debris. However, in reality, they have little time to track other objects such as small debris. They are primarily used to track deep space objects and perform periodic deep space searches. Indeed, the command has further requirements for two more deep space tracking sensors.

The bottom line is this. If the catalog doubles, there are few sensors that will have available tracking opportunities to handle this. One would expect that the phased arrays of the existing SSC network should be able to handle it. However, if the catalog increases on the order of tenfold, then new tracking sensors will probably be required.

SPACE SURVEILLANCE COMPUTATIONAL CAPACITY

Now, the computational capacity concern. The current SSC satellite element set data base includes nearly 7,000 objects in earth orbit. The present SSC system (427M) processes approximately 40,000 observations per day. The new SPADOC 4B, due in summer 1991, will not be able to provide significant support to 427M for catalog maintenance. SPADOC 4C, due in mid 1995, is intended to greatly improve catalog maintenance capabilities. It is planned currently to process about 150,000 observations per day.

Satellite element sets are maintained by a process called "differential correction". Fundamentally, this process starts with a site observation and a predicted observation from the current SSC element set. These two positions are compared and the error, or residual, is used to generate a correction to the current element set. Practically, this process "iterates" until the corrected element set fits the site observations on the object. The daily network differential correction process requires a fast scientific computer, not a data base configured computer.

As the numbers of objects increase in the data base, then the need for more speed and/or distributed scientific computer power rises in the SSC.

The loads on the communications system connecting the SSC and the sensors is routinely quite high. Double the size of the catalog and the communications system may not be able to pass the amount of observations required to maintain that doubled satellite catalog. The communications pipes may not be large enough to handle that flow.

The bottom line for computers and communications lines is that we may be able to handle a doubling of the satellite catalog. If larger numbers of objects must be maintained, more scientific computer power and larger communications pipes most probably must be obtained.

CONCLUSION

USSPACECOM has the mission to detect, track, identify, and maintain a catalog of all man-made objects in earth orbit. However, there is currently no military requirement to track small debris, and we do not have, nor are we developing the capability to do so. Most of our sensors are not capable of tracking small debris. Our computational resources and communications lines may functionally handle the problem, but more capacity is probably required. Based on national needs and other important factors, if it is decided to require USSPACECOM to track small debris, then funds must be applied to improve USSPACECOM resources.

RADAR SENSORS

SYSTEM	LOCATION	SENSOR TYPE	RANGE (KM)	SMALL DEBRIS CAPABILITY
ALCOR	Kwajalein Atoll	C Band	5555 KM	
ALTAIR	Kwajalein Atoll	UHF/VHF	40000 KM	
FPQ-14	Antiqua lls	C Band	2300 KM	
FPQ-15	Ascension lls	C Band	1600 KM	
FPS-92	Clear, AK	UFH	5555 KM	
HAYSTACK	Millstone Hill, MA	X Band	35000 KM	X
COBRA DANE	Shemya lls	L Band	5555 KM	
FPS-85	Eglin, FL	UHF	5555 KM	X
FPS-49	Fylingdales, England	UHF	5555 KM	
NAVSPASUR	Dahlgren, VA	Continuous Wave	8100 KM	
FPQ-14	Kaena Point, HI	C Band	1800 KM	
MILLSTONE	Millstone Hill, MA	L Band	35000 KM	
FPS-79	Pirinclik, Turkey	UHF	4300 KM	
PAVE PAWS	Cape Cod, MA Beale, CA Robins, GA Eldorado, TX	UHF	5555 KM	
PARCS	Cavalier, ND	UHF	3200 KM	X
SAIPAN	Saipan lls	C Band	2500 KM	
SPAR	Thule AFB, Greenland	UHF	5555 KM	

ELECTRO-OPTICAL SENSORS

SYSTEM	LOCATION	SENSOR TYPE	RANGE (KM)	SMALL DEBRIS CAPABILITY
AMOS	Maui, HI	Visible, LWIR	35000 KM	
GEODSS	Socorro, NM Taegu, Korea Maui, HI Diego Garcia	Visible	35000 KM	X
MOTIF	Maui, HI	Visible, LWIR	35000 KM	
SITU	St Margarets Canada	Visible	35000 KM	

TABLE III. Space Surveillance Sensor Capabilities

210

BIBLIOGRAPHY

1. Aerospace Defense Command, Office of Astrodynamics, Aerospace Defense Center, Project SPACETRACK, "Models for Propagation of NORAD Element Sets", SPACETRACK Report No. 3, December 1980.

2. Cook, David, Major, O.M.M., "Satellite Data bases: The Future of the Catalog", 5 April 1988.

3. Cook, David, Major, O.M.M., "The SMART Catalog", undated, Paper AAS 87-450.

4. Headquarters Air Force Space Command, Directorate of Operations Analysis. Deputy Chief of Staff Operations, "Proposed Astrodynamic Standards (Original Version)", Technical Note 88-02, 29 February 1988.

5. Headquarters North American Aerospace Defense Command (NORAD). SPADOC Computational Center (SSC) Computer Program Product Specification. Mathmatical Foundation for SSC Astrodynamic Theory. NORAD Technical Publication SCC 088, 06 April 1982.

6. Headquarters United States Space Command, "Doctrine for Space Control Forces", USSPACECOM Pamphlet 2-1, 19 March 1990.

7. Headquarters United States Space Command. Space Surveillance Network Data User Support. USSPACECOM Regulation 55-6, 06 November 1986.

8. Jackson, Phoebe, Major, USAF, "Space Surveillance Catalog Maintenance", AIAA 90-1339, 16 April 1990.

9. United Nations, "COSPAR Guide to Rocket and Satellite Information and Data Exchange" COSPAR Information Bulletin No 9, July 1967, Special Edition.

10. US Senate Staff Report, "Convention on Registration of Objects Launched into Outer Space: Analysis and Background Data", US GPO Washington, 1975.

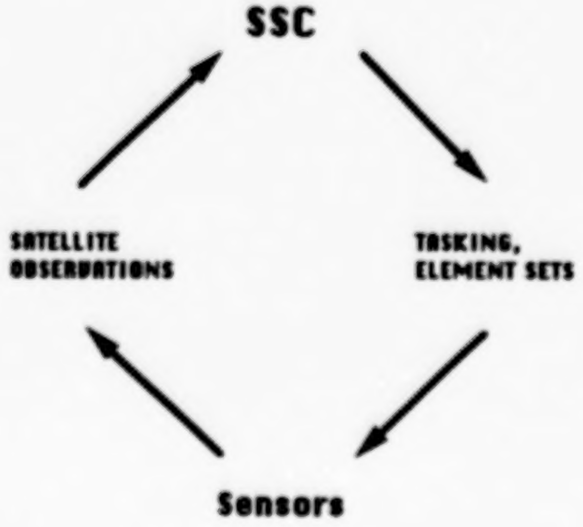
SSC
SATELLITE OBSERVATIONS
TASKING, ELEMENT SETS
Sensors

FIGURE 1. Space Surveillance Satellite Catalog Maintenance

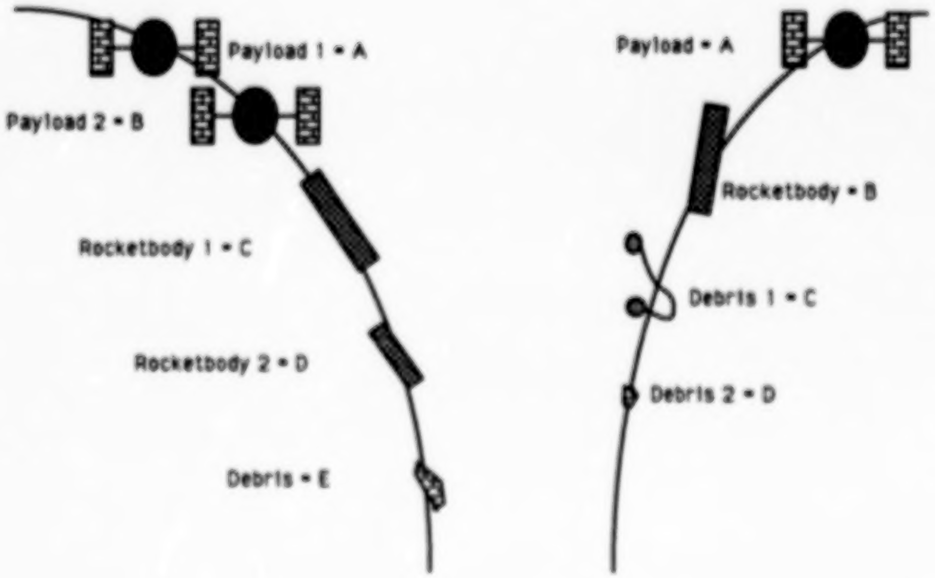
Payload 1 = A
Payload 2 = B
Rocketbody 1 = C
Rocketbody 2 = D
Debris = E
Payload = A
Rocketbody = B
Debris 1 = C
Debris 2 = D

FIGURE 2. Precedence for Assigning International Designators

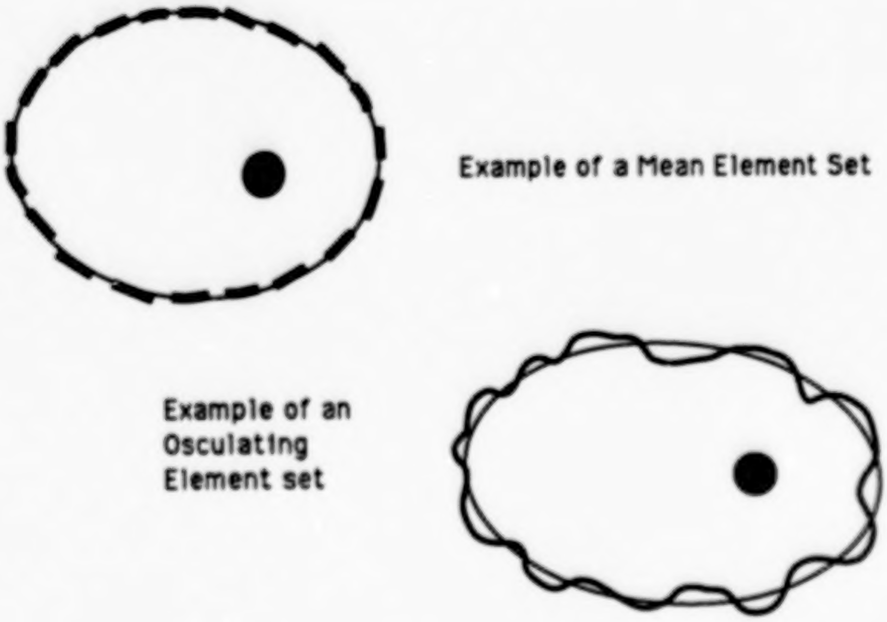
Example of a Mean Element Set
Example of an
Osculating
Element set

FIGURE 3. Distinction between Mean and Osculating Orbits

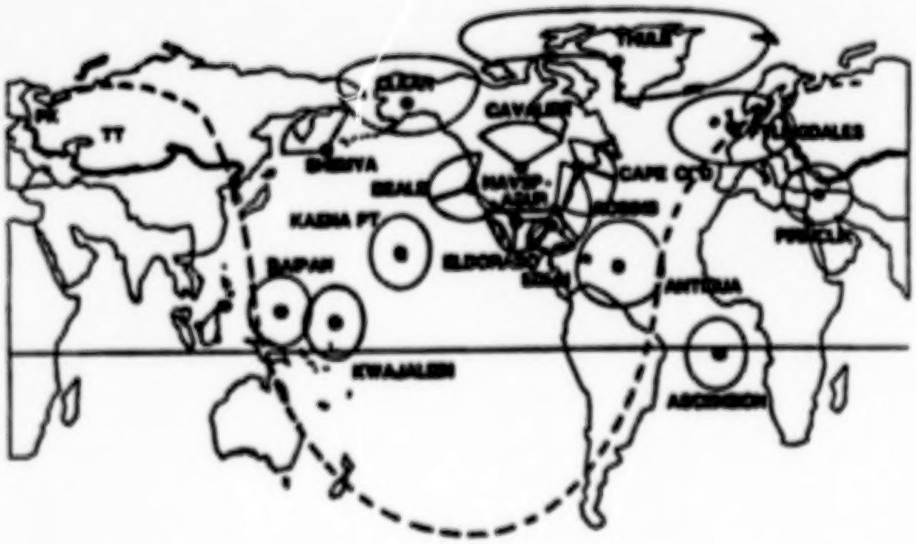
THULE
CLEAR
CAVALIER
FYLINGDALES
PK
TT
SHEMYA
BEALE
NAVSPASUR
CAPE COD
KAENA PT
PIRINCLIK
SAIPAN
ELDORADO
ANTIGUA
KWAJALEIN
ASCENSION

FIGURE 4. Low Altitude Ground-based Space Surveillance

LEO DEBRIS EFFECTS ON THE OPTICAL PROPERTIES OF MIRRORED SURFACES

Carl Maag
SAIC

(Paper not provided at publication date)

214

THE IMPORTANCE OF MOMENTUM TRANSFER IN COLLISION-INDUCED BREAKUPS IN LOW EARTH ORBIT

Robert C. Reynolds and Brian J. Lillie

INTRODUCTION

Although there is adequate information on larger objects in low Earth orbit, specifically those objects larger than about 10 cm in diameter, there is little direct information on objects from this size down to 1 millimeter. Yet this is the size regime where objects acting as projectiles represent the ability to seriously damage or destroy a functioning spacecraft if they collide with it. Since there is poor data in this size regime, this population component must be inferred from the creation of larger fragments in observed breakups. Of the three commonly attributed causes of breakup, low- or high-intensity explosions and collisions /1/, only collisions, with a power law distribution in fragment size, represents the potential for a significant source of millimeter and centimeter debris.

The observed consequences of known collisional breakups in orbit indicates no significant momentum transfer in the resulting debris cloud. The position taken in this paper is that this is an observational selection effect, that what is seen in these events is an explosion-like breakup of the target structure arising from shock waves introduced into the structure by the collision, but one that occurs significantly after the collision processes are completed; the collision cloud, in which there is momentum transfer, consists of small, unobserved fragments. Preliminary computations of the contribution of one known collisional breakup, Solwind at 500 km in 1985, and Cosmos 1275 at 950 km in 1981, assume no momentum transfer on breakup and indicate that these 2 events are the dominant contributors to the current millimeter and centimeter population. A different story would emerge if momentum transfer was taken into account.

The establishment of the role of momentum transfer in collisional processes will become more critical in the future, as collisions become more frequent. Also, kinetic energy anti-satellite (ASAT) weapons tests and usage, which might be anticipated, need to be understood in the role they will play in the state of the environment.

DISCUSSION

Observation of On-Orbit Collisional Breakups

There are 2 cases in which collisional breakups have occurred in orbit under known conditions. The first of these was the test of a hovering ASAT vehicle by the United States in 1985 using as a target Solwind, a science satellite. This breakup occurred at an altitude of 525 km, and the resulting debris cloud was well observed. The second was the designed impact of the upper stage and the science payload in the Delta 180 flight. Again, the debris clouds resulting from this test were well observed.

The most significant feature in both tests was that the debris clouds, a single cloud for Solwind, and two clouds for Delta 180, showed little evidence of momentum transfer occurring during the collision process/2,3/. The center of mass for the Solwind cloud was that of the satellite had it not encountered the ASAT vehicle; for the Delta 180 experiment, there were 2 debris clouds, one moving in the orbit of each vehicle. Instruments that were able to observe smaller fragments found more indication of momentum transfer than those seeing only the largest objects.

These observed results appear to oppose what seems to be intuitively obvious, that there must be momentum transfer in a collisional process. This can be viewed as demonstrating the special characteristics of hypervelocity impact processes. In laboratory tests of small projectiles at small targets, an exiting debris plume is observed if the projectile is large enough to penetrate through the target. This debris plume shows a mixture of target and projectile material where there has been momentum coupling, but consists entirely of very small particles. Scaling the interacting particles to sizes of objects in orbit, but moving the impact 100's of kilometers away would lead to a debris cloud that would be difficult to detect.

These data can be combined into a single model for collisional breakup of objects in orbit if the collisional process is viewed as directly involving only the material in the line of flight of the impacting projectile. It is this material which is subject to momentum exchange and fragment creation following the power law size distribution characterizing collisional impacts. The impact, because it is occurring at speeds higher than the sound speed in the target structure, deposits significant energy, but little momentum, in the form of shock waves propagating through the structure. The energy of these shock waves yields the catastrophic fragmentation of the entire structure that was observed in Solwind.

Because the source of breakup energy is being supplied by shock waves, it might be expected that the size distribution of this second cloud would resemble that of a high- intensity explosion, and because little momentum was transferred into these shock waves, the resulting breakup would have the motion of the unperturbed structure motion as its center of mass motion.

Model for Momentum Transfer

The model for momentum transfer is summarized in Figures 1 and 2. First of all, a spacecraft can be viewed as consisting of several weakly connected components, called elements, as shown in Figure 1. In this figure, a generic spacecraft consists of 4 elements: a main body, 2 solar panels, and an antenna. If the line of flight of debris hitting the spacecraft does not go through 2 or more elements, which it generally will not, only a single element would need to be considered in the collision process. In contrast to connections between elements, which are relatively weak, the connections within an element are strong and an element can be viewed as a single cohesive object. Within the element, the material in the target structure is viewed as having 2 components, the material in the line of flight of the projectile, denoted as the column mass, and material out of the line of flight, called the residual mass. This type of model has been suggested by Chobotov and co-workers /4/. The column mass participates in the creation of collisional debris - it plus the projectile mass yield a debris cloud having size and velocity distribution characteristics of collisional processes. If the residual mass is large enough, that material remains intact; if not, it breaks up in a size and velocity distribution characteristic of an explosion event /5/.

When hypervelocity impact occurs, a cone of ejecta, consisting of both projectile and target material, emerges from the impact site. If there is a void on the back side of the first surface in the target, as there is for a Hubble shield and for fuel tanks on spent stages, the debris cloud expands as it propagates and spreads over a larger area on the second surface it encounters. However, if there is material behind the front surface, it might be expected that this material will collimate the debris cloud, since there is no significant source of energy to cause it to expand. In effect, for filled volumes, the geometry for propagation of hypervelocity fragments is similar to that for subsonic propagation. The coupling between the collisionally involved material and the rest of the structure comes from the edge effects, where very large impulsive loads transform into shearing, with little momentum transfer. Because this coupling involves area to mass effects, laboratory tests on scale models will have to be interpreted with care.

Within the columnar mass and the projectile, the interaction is taken to be completely inelastic, so that the consequent mass forms a single debris cloud moving with a center of mass characterized by the center of mass of the projectile plus the column mass.

The residual mass plus any appendages will remain after the collision, but will experience shock waves propagated by the initial impact. These shock waves will transform into stress waves at free surfaces, and at all changes in material conditions. Links between other elements and that directly involved in the collision will be relatively weak, and will be the most easily broken. In fact, compared to the connection strengths within these other elements, it might be expected that very little shock is propagated into these elements and that they retain their integrity, either associated with the affected structure or appearing as large debris objects emerging from the collision.

Within the element directly involved with the collision there will be much stronger bonding between the components, so there will be much more damage caused by the shock waves. Rather than viewing the consequences of impact in terms of shock waves in this structure, it is easier to picture the fragmentation of this structure as occurring from a large amount of energy being released within the structure, as would occur in an explosion.

This leads to the picture in Figure 2 of two types of clouds - one characterized by collision processes and the other by explosion processes. This is an adequate picture for the impact of objects of significantly different size. If the objects are of comparable size, since off-center collisions are most likely to occur, the overlap masses will become the column masses, and the non-overlap masses will become the residual mass. In this case there would be two explosion clouds created, one from each of the residual masses, as well as a collision cloud. This case has been discussed by Chobotov and co-workers /4/.

Velocity Space Representation of Breakup Clouds

The velocity space representation provides a singularly simple means of representing the intact objects before collision, and the debris cloud(s) after collision. If the coordinate axes in this space are taken to be Z-axis radial velocity, X-axis the in- plane horizontal velocity, and Y-axis cross-range horizontal velocity, kinematically interesting characteristics can be expressed in terms of conic surfaces. At a given altitude, the surfaces of constant perigee altitude will be hyperboloids of revolution about the Z-axis and will have the functional form

$$v_H^2\left(\frac{r_P+r_0}{2\mu}\left(\frac{r_0}{r_P}\right)\right)-v_Z^2\left(\frac{r_0\,r_P}{2\mu(r_0-r_P)}\right)=1 \qquad (1)$$

where

v_H = horizontal velocity = sqrt(v_x^2 + v_y^2)
v_Z = radial velocity
r_P = perigee radius = perigee altitude + radius of Earth
r_0 = radius distance of reference point
μ = gravitational constant * mass of Earth

The associated surfaces of constant apogee altitude in this space are ellipses, which have the functional form

$$v_H^2\left(\frac{r_A+r_0}{2\mu}\left(\frac{r_0}{r_A}\right)\right)+v_Z^2\left(\frac{r_0\,r_A}{2\mu(r_A-r_0)}\right)=1 \qquad (2)$$

where

r_A = apogee radius

Figure 3 presents a 2-dimensional cross-section of this space, with the radial velocity plotted on the vertical axis, and the horizontal velocity plotted on the horizontal axis. The space is symmetric about both the horizontal and vertical axes, so only one quadrant is shown. The altitude is 500 km. A hyperbolae opening to the right represent families of orbits having common perigee altitude, as labeled on each curve. The ellipses opening to the left are the lines of constant apogee, also labeled on each curve. The zero energy surface, marking the limit of bound orbits is the circle of radius 10.8 km/sec. The point representing a circular orbit at 500 km is indicated by the "x" at a horizontal velocity of 7.626 km/sec.

As the perigee altitude approaches 500 km (from below), the hyperbola representing orbits of that altitude become more elongated along the horizontal axis; the horizontal axis to the right of the circular orbit velocity represents orbits having perigee of 500 km. Similarly, the horizontal axis to the left of the circular orbit velocity represent orbits having apogee of 500 km.

It is obvious from this figure that there is a compression in the hyperbolae along the horizontal axis, indicating that a small reduction in the horizontal velocity for an object in circular orbit will significantly reduce the perigee altitude of the resulting orbit. A debris cloud, which forms a volume in this space, will consist of objects with orbits of lower perigee altitude, and hence reduced lifetime, if the center of mass for the cloud can be moved to the left.

The explosive breakup of a single object in orbit will retain the orbit of that object for its center of mass. That is, for an explosive breakup spherically symmetric in the co-moving frame of the exploding object, the breakup cloud will form a spherical volume in velocity space centered on the velocity of that object.

However, the picture will be different for collisionally induced breakups. Momentum exchange in a collisionally induced debris cloud will have the center of mass of the interacting material as its center, or the velocity of the intact object as its center for the explosion component of the breakup. Specifically, for the 4 cases in Figure 2, there will be:

Case 1: the single object in the center of mass orbit

Case 2: an explosion cloud and a collision cloud, both centered on the center of mass velocity

Case 3: a single large object moving in its original orbit, and a debris cloud centered on the center of mass velocity for the directly involved collisional material

Case 4: an explosion debris cloud centered on the velocity of the large object and a debris cloud centered on the center of mass velocity of the directly involved collisional material.

The effect of momentum transfer in the collisional clouds is important because the center of mass velocity will be less than the circular orbit velocity, if neither of the initial velocities exceeds the circular orbit velocity. That means that in velocity space the center of the clouds will move toward the Z axis, and the fragments in the cloud will therefore have lower perigee altitudes than they would had momentum exchange not been accounted for.

Looking at a debris cloud in velocity space, it is possible in a very straightforward way to determine the amount of material that re-enters almost immediately by calculating the volume of that cloud (in velocity space) having orbits inside a hyperboloid of low perigee altitude. An altitude of 200 km will be used in this paper. The volume will depend on the center of mass velocity for the cloud and on the characteristic velocity perturbations for the cloud particles.

Figure 4 presents the cross-section of a spherical debris cloud, showing velocity intervals of 200 m/sec up to 1 km/sec and centered on the circular orbit velocity. The shaded region represents the orbits that are reentering, where it must be noted that the full 3 dimensional space must be shown to measure the actual volume. The percentage of orbits reentering as a function of center of mass velocity is shown in Figure 5.

While the figures show how to represent the volume of the debris cloud in velocity space, the density distribution of fragments in this volume is the real quantity of interest. It is this density times the related volume that will characterize the number of objects reentering, or populating short- or long-life orbits. To calculate this density distribution, N(v,d), the velocity distribution integrated over size must be established for the debris cloud.

This joint size and velocity distribution will be assumed to be separable and of form

$$N(v,d)=K_d\begin{cases}V/V_0 & 0.1V_0\le V\le V_0\\ \dfrac{1.3-V/V_0}{0.3} & V_0\le V\le 1.3V_0\end{cases}\tag{3}$$

as suggested by Kessler (/6/), where the K_d is evaluated from the size distribution. Integrating over all velocities leads to

$$N(d)=0.645\ K_d V_0\tag{4}$$

However, the expression for N(d) is (/7/)

$$N(d)=bAm^{-(b+1)}\tag{5}$$

to give a value to K_d of

$$K_d=\frac{bAm^{-(b+1)}}{0.645\ v_0}\tag{6}$$

To convert from mass to size, the relationship

$$m=\frac{\pi d^3\rho}{6}$$

will be used, leaving K_d defined as

$$K_d=\frac{bA}{0.645}\left(\frac{\pi\rho}{6}\right)^{-(b+1)}\frac{d^{-3(b+1)}}{V_0\ (d)}\tag{7}$$

leading finally to a joint distribution function given by

$$N(v,d)=\frac{bA}{0.645}\left(\frac{\pi\rho}{6}\right)^{-(b+1)}\frac{d^{-3(b+1)}}{V_0\ (d)}\begin{cases}V/V_0 & 0.1V_0\le V\le V_0\\ \dfrac{1.3-V/V_0}{0.3} & V_0\le V\le 1.3V_0\end{cases}\tag{8}$$

The peak in the velocity distribution, denoted as v_0, is itself a function of size. In this paper, the size/velocity relationship derived by Su (/8/) is assumed. It is of form

$$\log_{10}V_0=\begin{cases}0.875-0.676\ (\log(d/d_m))^2 & d\ge d_m\\ 0.875 & d\le d_m\end{cases}\tag{9}$$

where

$d_m = 9.9083\text{X}10^{-8} m_p^{1/3} v_p^{2/3}$ (m)
m_p = projectile mass (kg)
v_p = impact velocity (km/s)

This function is plotted in Figure 6 for $m_p = 15kg$ and $v_p = 10km/s$. A line of constant velocity in this diagram will map onto a spherical surface in velocity space, when the center of the sphere is taken to be the velocity of the center of mass for the cloud. The relative contribution of different sizes of objects at a given breakup velocity v_1, i.e. the density distribution along a horizontal strip of Figure 6, can be seen in plots of $N(v_1,d)$.

For purposes of illustration throughout the rest of the paper, $d_m = 1.26X10^{-6}$ meters and $b = 0.7496$ will be assumed. Figure 7 presents plots for v_1 = 50m/s, 300m/s, and 1km/s, where the curves have been normalized by dividing out the constant (size independent) part of K_d. This makes sense because only relative contributions are used in the following discussion. The 50m/s curve characterizes the largest objects in the breakup, the 300m/s velocity the centimeter fragments, and the 1km/s velocity the millimeter fragments.

To calculate the number of objects as a function of velocity only, $N(v_1)$, the joint distribution function must be integrated over size, thus

$$N(v_1) = \int_{D_{min}}^{D_{max}} N(v_1, x)\, dx \qquad (10)$$

where the upper and lower integration limits are functions of v_1. They are determined as follows:

(1) the lower limit is the diameter $D_{min}(v_1)$ having a v_0 satisfying $0.1 \cdot v_0 = v_1$, and

(2) the upper limit is the diameter $D_{max}(v_1)$ having a v_0 satisfying $1.3 \cdot v_0 = v_1$

Since the primary concern is for debris fragments that can seriously damage a spacecraft, D_{min} is taken to be no smaller than 1mm.

Performing the integral expressed in Equation 10 leads to the density distribution within the cloud. A plot of $N(v_1)$, using the same normalization as for Figure 7, is provided in Figure 8 for three cases - of 10cm and larger, 1cm and larger, and 1mm and larger debris clouds. Using this density distribution, the percentage of reentering objects is shown in Figure 9 for these three cloud components.

It only remains to relate the center of mass velocities, as derived from conservation of momentum, to the velocities shown on the abscissa of Figures 5, 8, and 9. This will be done for two cases in the following sections.

Case: Collision Induced by a Zero Velocity Projectile

For this case the collision is induced by a projectile near apogee in a ballistic orbit, so that the impact speed is the orbital speed of the target object. This is the type of ASAT test conducted against the Solwind satellite. It is the simplest case for calculating momentum transfer, as the results can be characterized by the single parameter of ratio of the projectile mass, m_p, to the column mass, m_c. The center of mass velocity as a function of these quantities is given by

$$V_{cm} = \frac{M_c}{M_c + M_p} V_0 = \frac{1}{1 + X_0} V_0 \qquad (11)$$

where

$x_0 = m_p / m_c$

The ratio $m_c/(m_p + m_c)$ is plotted as a function of mass ratio, m_p/m_c, in Figure 10. The percentage of mass to re-enter as a function of mass ratio is provided in Figure 11.

Case: Collision Induced by a Projectile in Circular Orbit

The case of 2 objects in circular orbit colliding presents a more complex problem since the solutions depend on both mass ratio and encounter angle. The center of mass velocity, expressed in terms of these quantities, is

$$a_0 = \frac{1}{1 + X_0} (1 + 2 X_0 C_\theta + X_0^2)^{1/2} \qquad (12)$$

where

$C_x = Cos(x)$
$a_0 = v_{cm} / v_0$

The greatest complication is that the collision speed, which enters the velocity distribution as seen in Equation 9, depends on this encounter angle through the simple relation

$$V_p = \sqrt{2}\, V_\theta \, (1 - C_\theta)^{1/2} \qquad (13)$$

This has the effect of varying the distribution as shown in Figure 8 as a function of θ. For the volume of the cloud in velocity space that lies in the reentry region, as opposed to the number of reentering objects, this complication does not arise, and a plot such as Figure 12 can be used to characterize surfaces of constant ratio between the center of mass velocity and the orbital speed. The line of fixed a_0 corresponds to a single point on the horizontal axis of Figure 5; if the velocity distribution was not a function of θ, such a line would also correspond to a single point on the horizontal axis of Figure 9.

CONCLUSIONS

A two component collisional breakup process has been suggested to provide a mechanism for distinguishing between material directly involved in the collision process, and that material in the same structure only indirectly involved. Only the indirectly affected material forming an explosion-type of cloud has been observed in on-orbit tests, since this cloud contains the larger objects. Momentum transfer only involves the directly involved material, which is characterized by the column mass in the target. This model provides a method for identifying the mass involved in the collisional component of the resulting debris cloud.

Momentum transfer in the collisional component of a collisional breakup can lead to significant reduction in the amount of debris scattered into long-life orbits. Two cases were used to demonstrate the technique for determining center of mass velocities.

The major deficiency in the current work is that the effect of relative velocity, which is a parameter of the collisional debris velocity distribution, is not considered. Also, the suggested model decoupling the directly involved target mass from the residual mass can be better documented relative to hypervelocity impact tests and modeling than has been done in this paper. Both considerations are currently being addressed.

ACKNOWLEDGMENTS

The authors wish to thank Val Chobotov and David Spencer for review comments on this paper, and to Glenn Kempf for help in developing software and producing figures for the paper.

REFERENCES

1. Badhwar, G.D., Potter, A.E., Anz-Meador, P.D., and Reynolds, R.C.. Characteristics of Satellite Breakups from Radar Cross- Section and Plane Change Angle. Journal of Spacecraft and Rockets,

2. Reynolds, R.C. and Mazade, A.V. Interim Report: Hypervelocity Breakup of a Spacecraft in Low Earth Orbit (U). Lockheed Engineering and Management Services Report to NASA/JSC.

3. Anz-Meador, P.D., Talent, D.L., and Rast, R.H. Hazard Analysis for the Break-up of Satellites 16937 & 16938. NASA/JSC Report #22471 (U), Lockheed Engineering and Management Services Report #23613, 1987.

4. Chobotov, V.A., Spencer, D.B., Schmitt, D.L., Gupta, R.P., Hopkins, R.G., and Knapp, D.T. Dynamics of Debris Motion and the Collision Hazard to Spacecraft Resulting from an Orbital Breakup. Aerospace Corp. Report SD-TR-88-96, 1988.

5. Chobotov, V.A. and Spencer, D.B. Debris Evolution and Lifetime Following an Orbital Breakup. AIAA-90-0085 presented at the 28th Aerospace Sciences Meeting, January, 1990, Reno, NV.

6. Kessler, D.J. Private Communication.

7. Bess, T.D. Mass Distribution of Orbiting Man-Made Space Debris. NASA Report L-10477, 1975.

8. Su, S.Y. On the Velocity Distribution of Collisional Fragments in the New Ejecta Model and Its Effect on the Future Space Environment. Lockheed Engineering and Management Services Co. Internal Report, 1985.

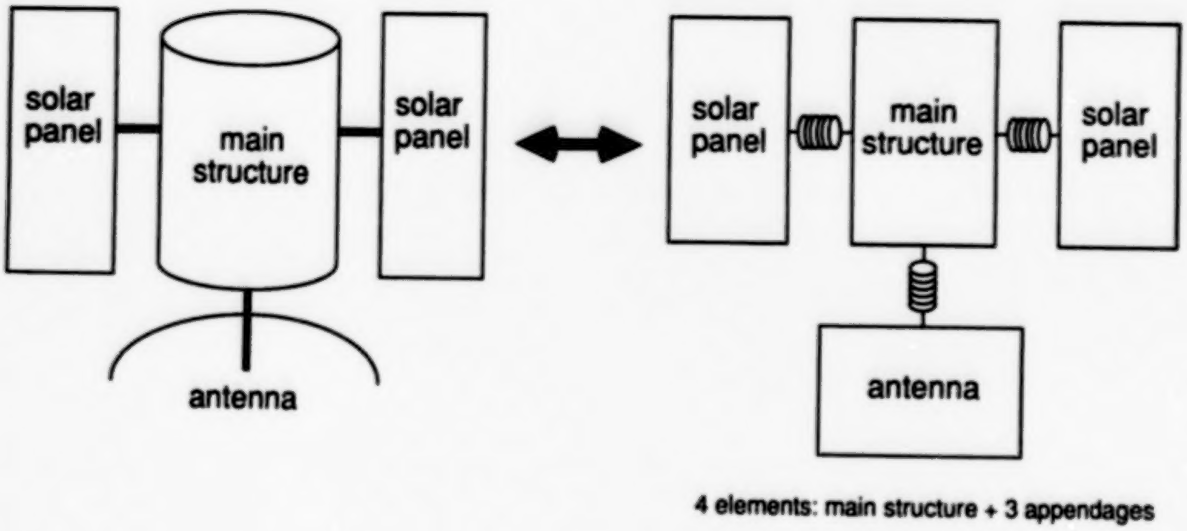
solar panel
main structure
solar panel
antenna
solar panel
main structure
solar panel
antenna
4 elements: main structure + 3 appendages

FIGURE 1. Element Diagram for Spacecraft

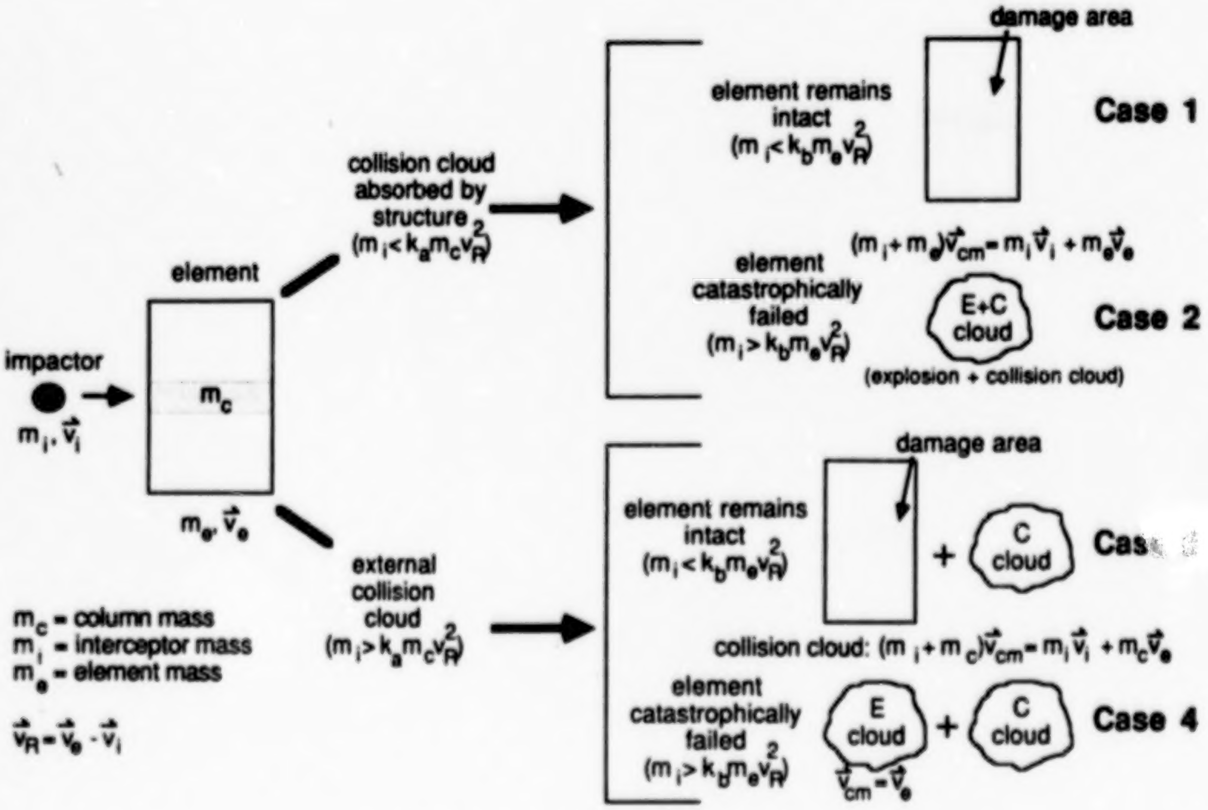
damage area
element remains intact
$(m_i < k_b m_e v_R^2)$
Case 1
collision cloud absorbed by structure
$(m_i < k_a m_c v_R^2)$
$(m_i + m_e)\vec{v}_{cm} = m_i\vec{v}_i + m_e\vec{v}_e$
element
element catastrophically failed
$(m_i > k_b m_e v_R^2)$
E+C cloud
Case 2
(explosion + collision cloud)
impactor
m_c
$m_i, \vec{v}_i$
$m_e, \vec{v}_e$
damage area
element remains intact
$(m_i < k_b m_e v_R^2)$
C cloud
Cas
external collision cloud
$(m_i > k_a m_c v_R^2)$
m_c = column mass
m_i = interceptor mass
m_e = element mass
$\vec{v}_R = \vec{v}_e - \vec{v}_i$
collision cloud: $(m_i + m_c)\vec{v}_{cm} = m_i\vec{v}_i + m_c\vec{v}_e$
element catastrophically failed
$(m_i > k_b m_e v_R^2)$
E cloud
C cloud
Case 4
$\vec{v}_{cm} = \vec{v}_e$

FIGURE 2. Diagram for Treating Collisional Interaction

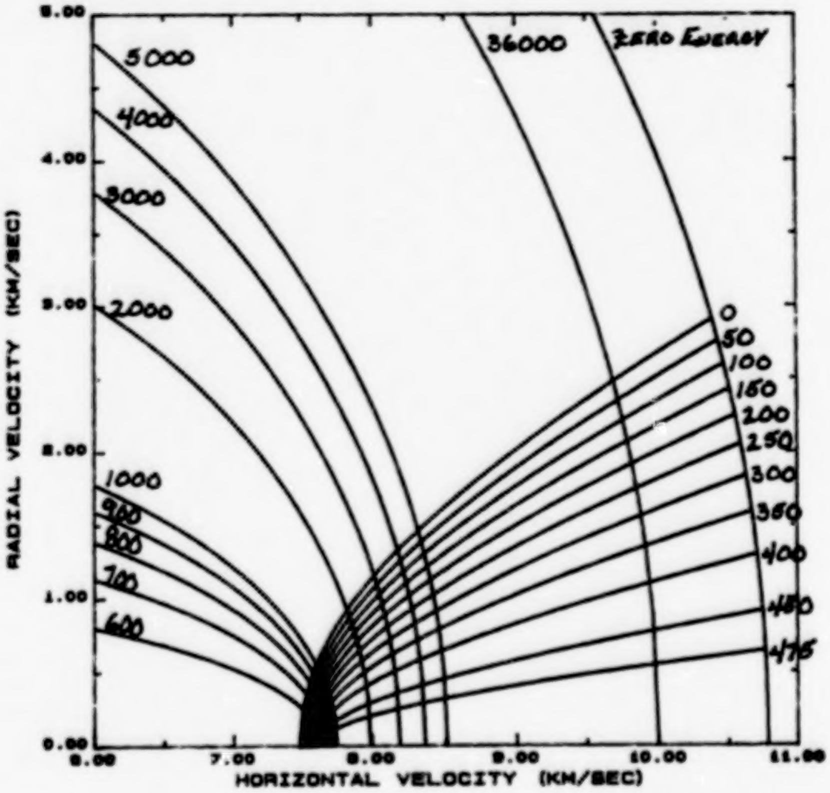

FIGURE 3. Velocity Space Diagram for Altitude 500 Km.

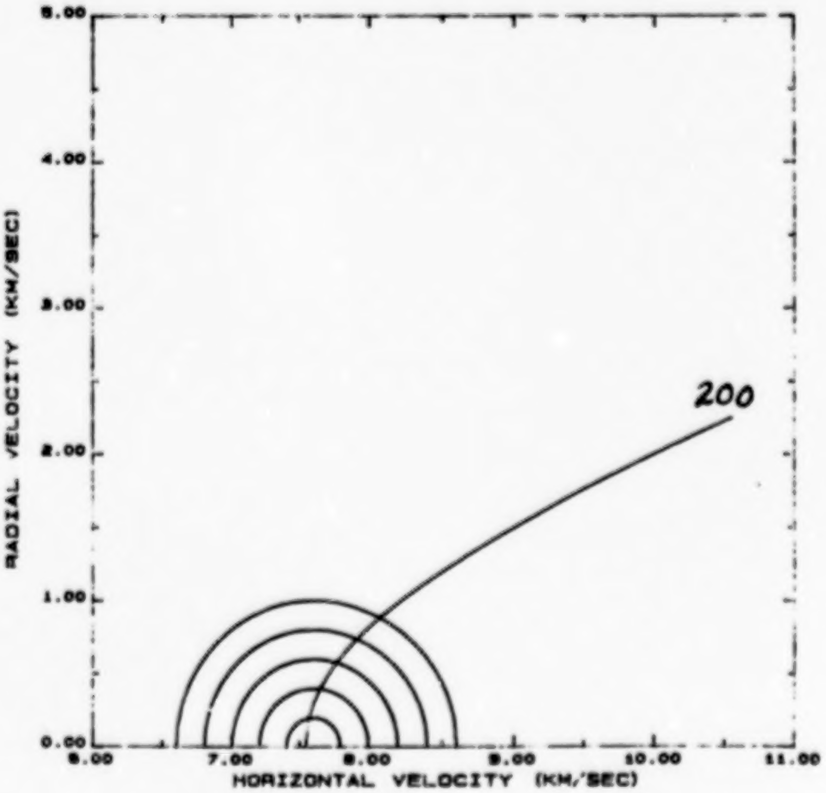

FIGURE 4. Velocity Space Diagram for Altitude 500 Km - cloud included and shaded region showing reentry orbits

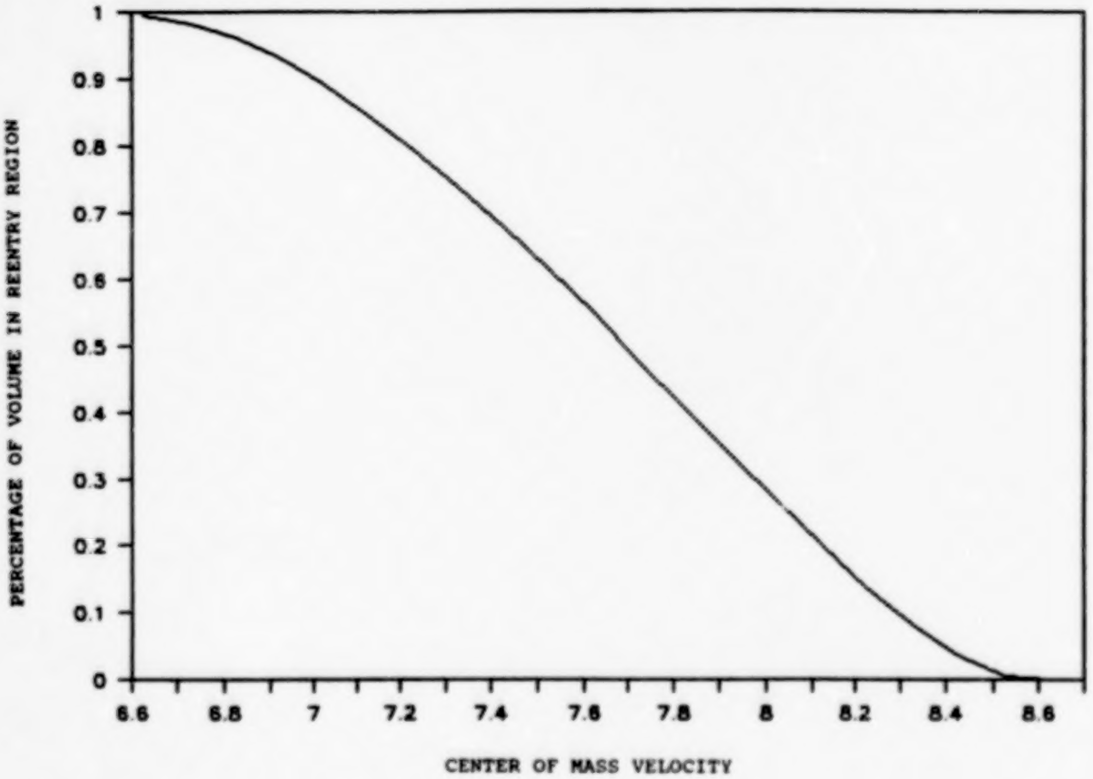

FIGURE 5. Percentage of Velocity Space Cloud Volume in the Reentry Region vs. Center of Mass Speed. Alt = 500 km.

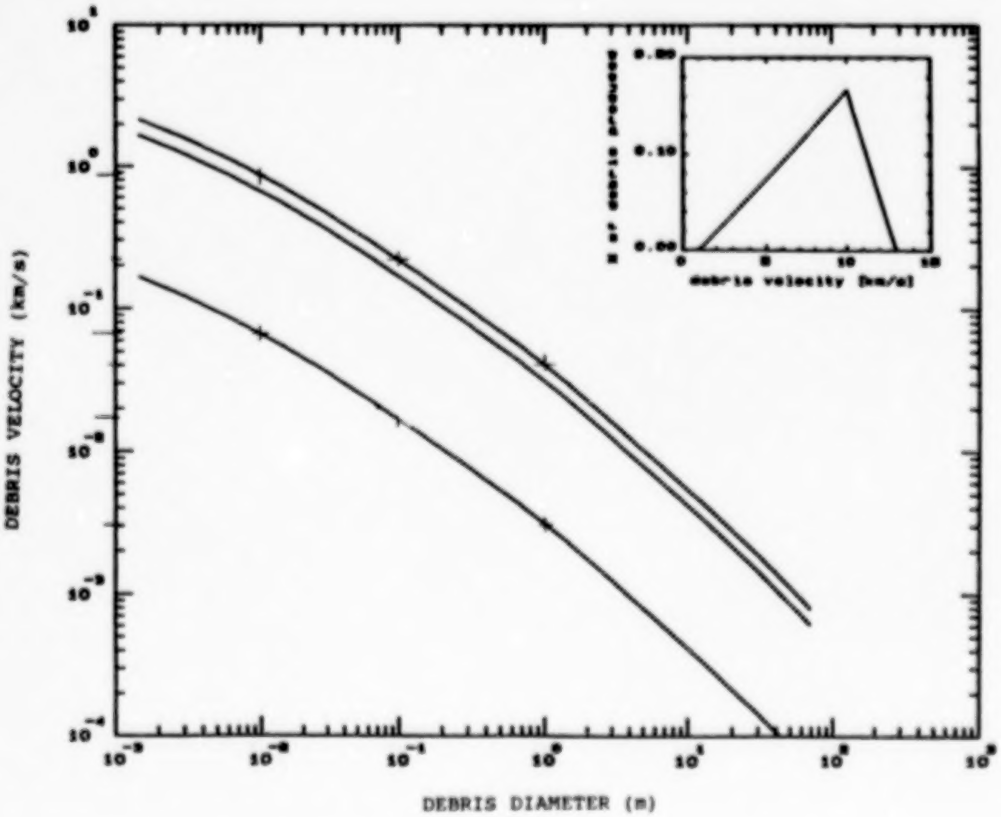

FIGURE 6. Breakup Velocity vs. Size Distribution for Projectile Mass of 15kg and Impact Velocity of 10km/s. (from /6/)

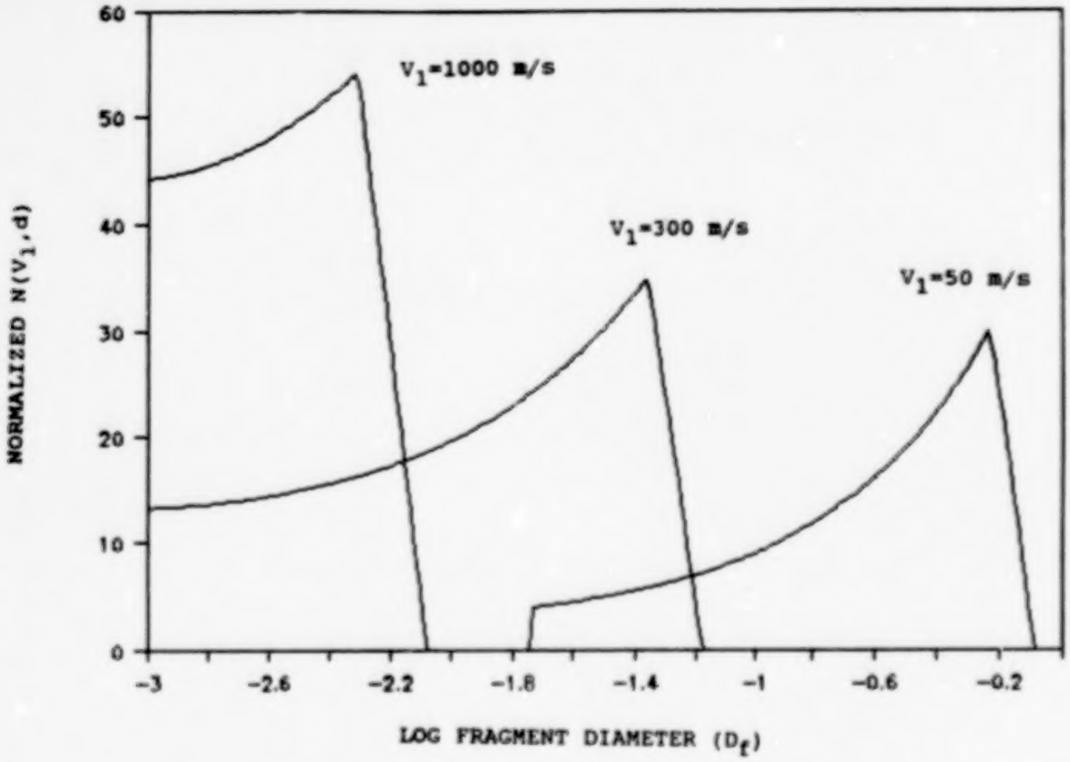

FIGURE 7. Size Composition of Debris Cloud Components for Breakup Velocities of 50, 300, 1000 m/s Using the Reference Velocity and Size Distributions.

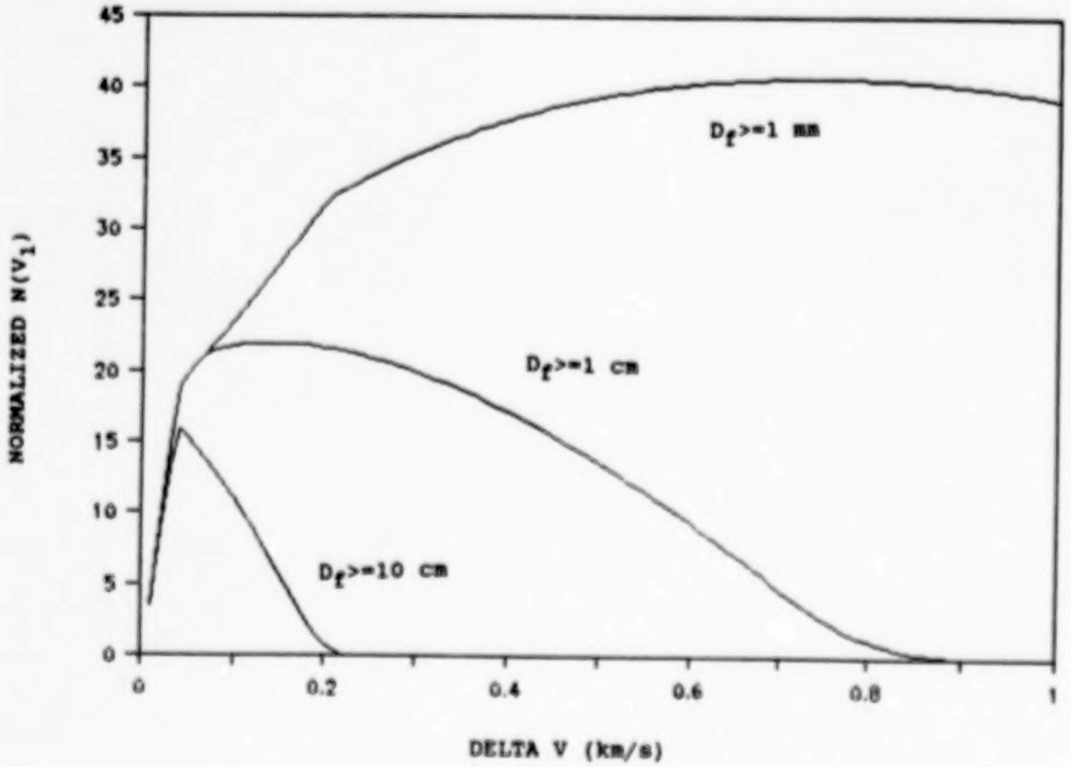

FIGURE 8. Velocity Distribution for the Debris Cloud Fragments Larger Than 10cm, 1cm, and 1mm.

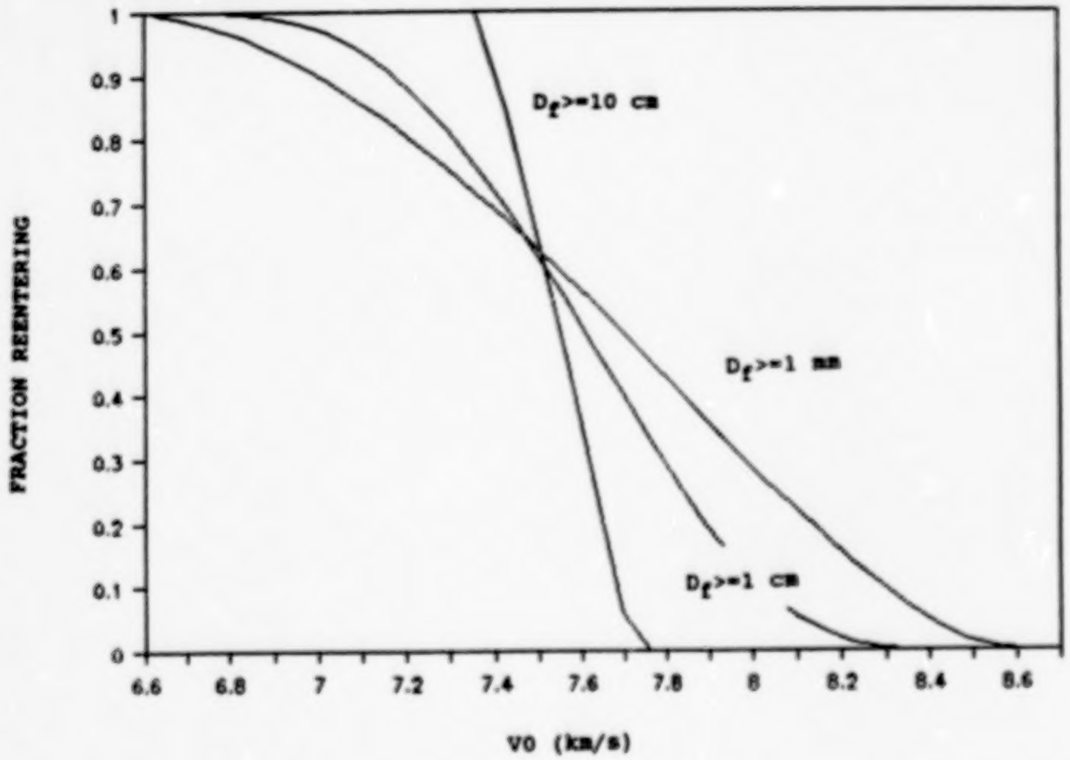

FIGURE 9. Percentage of Objects Reentering vs. Center of Mass Speed Using Reference Velocity Distribution. Alt = 500 km.

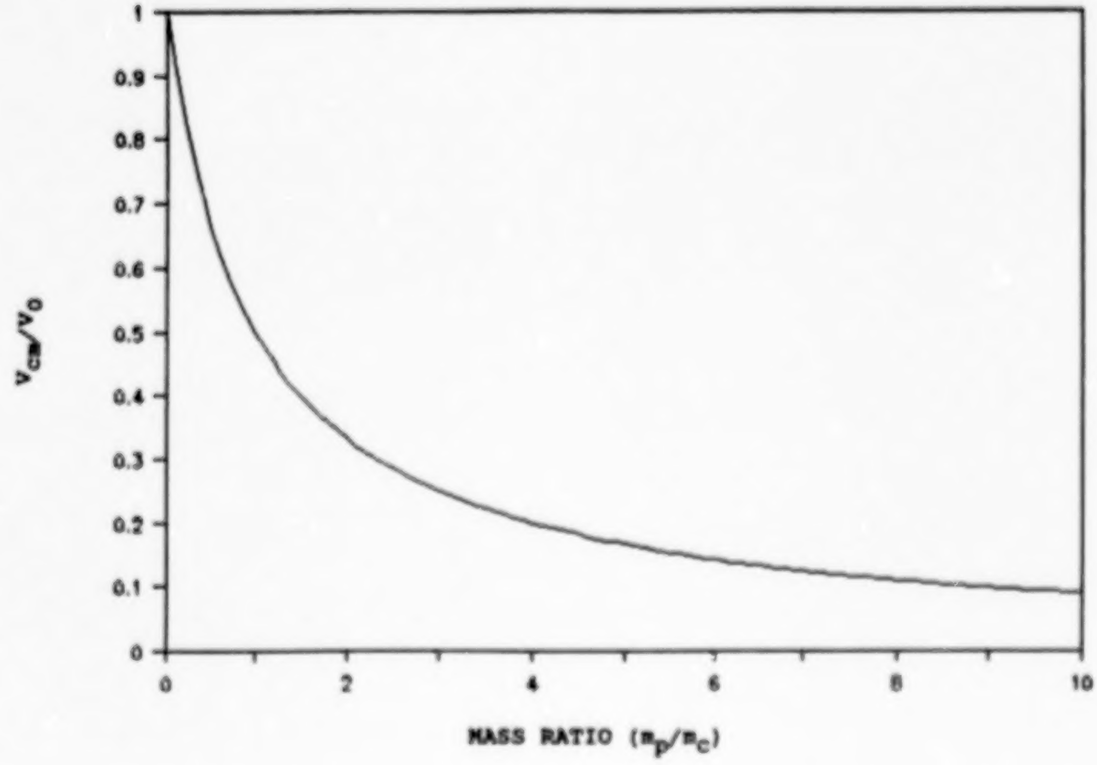

FIGURE 10. Hovering ASAT - Fraction of Circular Orbit Speed as a Function of Mass Ratio

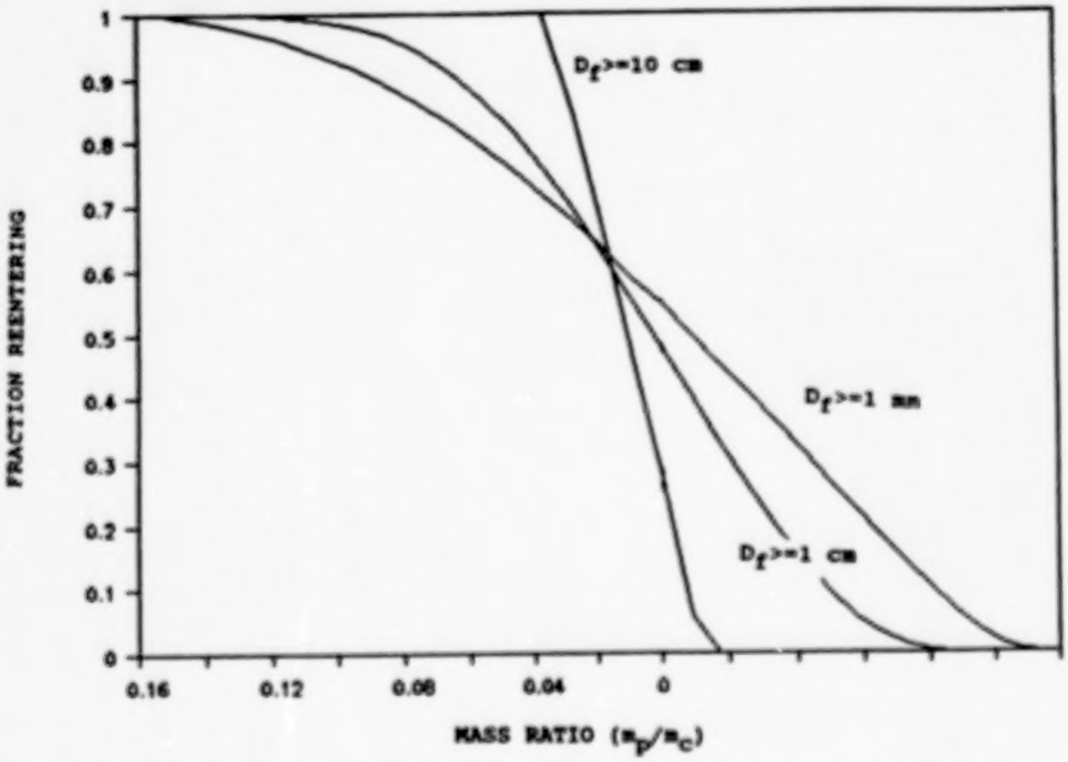

FIGURE 11. Hovering ASAT - % of Objects to Re-enter as a Function of Mass Ratio. Alt = 500 km.

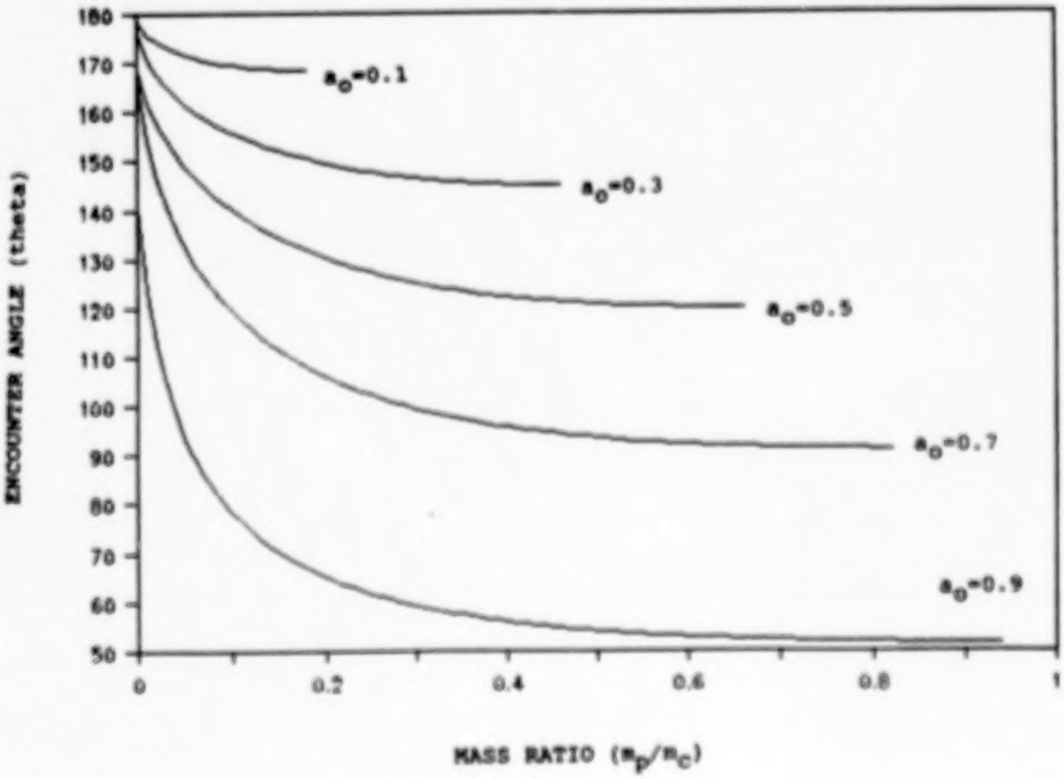

FIGURE 12. Co-Orbiting ASAT - Contours of Constant Center of Mass Velocity as a Function of Encounter Angle and Mass Ratio.

NAVSPASUR ORBITAL PROCESSING FOR SATELLITE BREAK-UP EVENTS

Paul W. Schumacher, Jr.
Analysis and Software Department
U. S. Naval Space Surveillance Center
Dahlgren, VA 22448

ABSTRACT

Satellite break-ups via explosion or collision can instantly increase the trackable orbiting population by up to several hundred objects, temporarily perturbing the routine space surveillance operations at U. S. Space Command (USSPACECOM) and the Naval Space Surveillance Center (NAVSPASUR). This paper is a survey of some of the procedures and techniques used by NAVSPASUR to respond to such events. First, the overall data flow at NAVSPASUR is described, highlighting the places at which human analysts may intervene with special processing. So-called manual intervention is required in a variety of non-nominal situations, including break-ups. Second, a description is given of some of the orbital analysis and other software tools available to NAVSPASUR analysts. These tools have been developed in-house over the past thirty years and can be employed in a highly flexible manner. The basic design philosophy for these tools has been to implement simple concepts as efficiently as possible and to allow the analyst maximum use of his personal expertise. Finally, several historical break-up scenarios are discussed briefly. These scenarios provide examples of the types of questions that are fairly easy to answer in the present operational environment, as well as examples of questions that are very difficult to answer.

INTRODUCTION

NAVSPASUR has conducted space surveillance operations for almost 30 years. The primary product of such work is a satellite database containing orbital element sets and associated observations for all trackable objects. Many military, scientific and engineering enterprises depend on the accuracy and timeliness of this database. Although most of the satellite cataloging operation is completely automated, a variety of situations can occur in which a human analyst must intervene with special procedures. A break-up event is just such a case. Historically, NAVSPASUR has been quite successful in deriving orbital elements from observations of new debris fragments, even when the event involves several hundred trackable objects. This fact has come into special prominence since 1985 when NAVSPASUR was designated as Alternate Space Surveillance Center (ASSC), back-up to the Space Surveillance Center (SSC) operated by USSPACECOM at Cheyenne Mountain AFB. A dozen major break-ups have occurred since then [1]. Currently, NAVSPASUR provides identifications for almost all of the unassociated observations reported to the SSC by the worldwide surveillance network.

NAVSPASUR contributes two main resources to the space surveillance effort. The first is the NAVSPASUR "fence", a radar interferometer deployed on a great circle coast-to-coast across the southern United States, which provides unusually wide geographical and altitudinal coverage. It is an all-weather, dedicated space surveillance instrument that does not have to be "tasked" (scheduled in advance for aiming) as do tracking radars. Rather, 3 transmitters provide a continuous-wave fan beam in the great-circle plane. Satellites penetrating the beam reflect signals to one or more of 6 receiver sites. At each receiver site, signal phases and amplitudes are measured on arrays of antenna elements and this data is relayed in real time to Dahlgren for processing. The second main resource is less tangible, namely, human expertise. NAVSPASUR employs civilian orbital analysts for operational work and requires them to have at least 6 years' experience. There are several staff members with over 20 years' experience. The result is that the analysts' subjective judgment becomes well tuned to the problems of orbital element maintenance. In the present system, human expertise is indispensible, especially for infrequent but stressing situations such as break-ups.

NAVSPASUR DATA FLOW

In order to understand the special processing needed for break-up analysis, it is necessary to understand something of the routine processing that occurs in maintaining the satellite catalog. NAVSPASUR is continually receiving a mixture of observations and element sets from the SSC and other surveillance network sensors, besides raw data from the fence (Fig. 1).

OBSERVATION & ELEMENT DATA FLOW

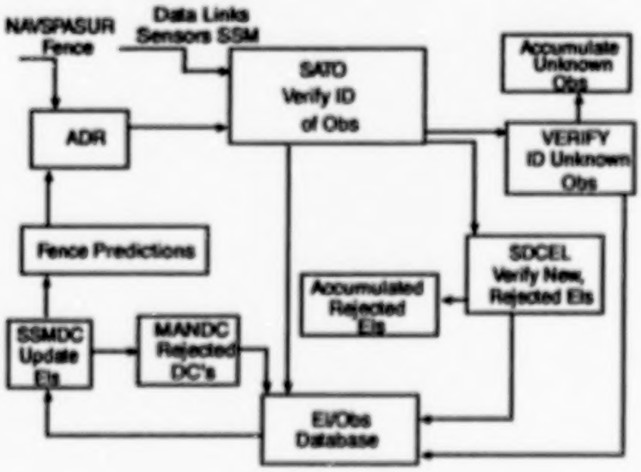

FIGURE 1

ADR is the real-time program which reads the incoming fence data and converts the phase measurements into direction cosines as seen from each receiver site. Doppler measurements are also extracted from the raw data. ADR attempts to associate these single-station sightings with known orbits based on comparisons with a time-ordered list of predicted time, cosine and Doppler values for fence crossings of known satellites. These predicted values will have been computed from the most recent element set on file for each satellite, as described later. In case the sighting cannot be associated within nominal tolerances, ADR performs a triangulation of time-correlated single-station sightings to arrive at a position estimate for the object. Various other programs will use this position in a more refined attempt at association, but in a non-real-time manner.

SATO is really a set of programs which are cued every 15 minutes to add incoming element sets and observations to the database. Unassociated observations and tracks are written to a holding file. Elements that are new or out of tolerance with the existing sets are written to another holding file.

SDCEL is executed once each day to re-examine incoming element sets rejected by SATO. A more thorough comparison with existing sets is made and those sets still rejected are saved for review by analysts.

VERIFY also is executed once each day to re-examine the unassociated tracks rejected by SATO. If, after more extensive checking, the track still cannot be associated with a known orbit, it is saved for analyst review.

SSMDC attempts a batch least-squares differential correction of each element set in the database using the associated observations, if new observations have become available since the last epoch. The new epoch is placed at the time of the last observation. The fit interval is chosen by an empirical formula containing the satellite's mean motion and rate of change of mean motion (the latter is mainly a decay effect). If the fit interval has fewer than 5 observations, or if new elements change by more than prescribed tolerances from the earlier values, or if the residuals in the fit are too high, the orbit is declared "not fit" and is noted for attention by analysts. However, SSMDC is able to fit about 98.5% of the database automatically under routine conditions; that is, of 6500 orbits, only about 100 will need further work by the analysts.

Finally, another set of programs uses the updated orbital elements to produce a time-ordered list of all predicted fence penetrations for the next 24 hours.

SOFTWARE TOOLS

Observations that cannot be associated with known orbits by VERIFY must be associated by the analysts. Likewise, incoming element sets that were rejected by SDCEL (for any of a variety of reasons) can be entered into the database only under direct analyst supervision. Moreover, there are always a few correctly associated observations that still do not produce an acceptable differential correction in SSMDC. These cases also require analyst attention. There are tools designed to aid in all these processes (Fig. 2).

General UCT Processing

The abbreviation "UCT" stands for "uncorrelated target", that is, an unassociated observation or track. The initial association attempt can fail for a variety of reasons, even for well known objects, and, in fact, about 94% of all UCTs turn out to be finally associated with some already-cataloged orbit [1].

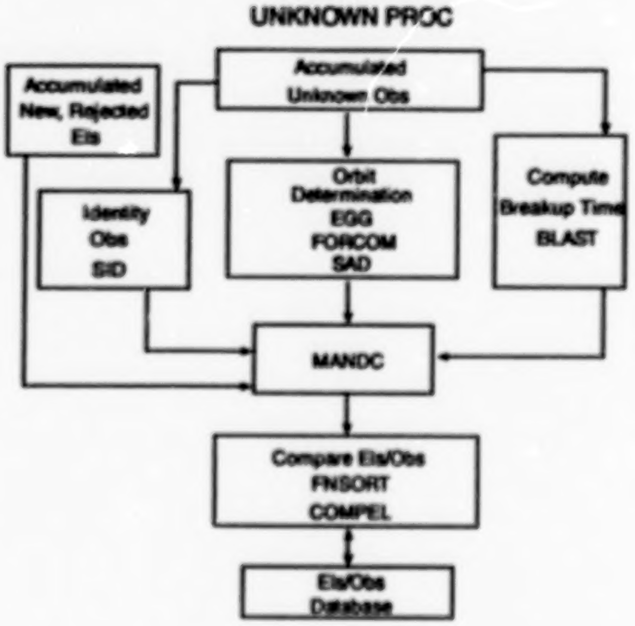
UNKNOWN PROC
Accumulated Unknown Obs
Accumulated New, Rejected Els
Identify Obs SID
Orbit Determination EGG FORCOM SAD
Compute Breakup Time BLAST
MANDC
Compare Els/Obs FNSORT COMPEL
Els/Obs Database

FIGURE 2

Hence, one should try to associate a UCT with an existing element set before assuming that a new orbit has appeared. If only a few observations or tracks are to be considered, the analyst can address them essentially one by one. There are several programs designed to operate on this category of problems.

SID seeks to associate observations and tracks with known orbits through a systematic relaxation of tolerances. Here, the analyst's knowledge of such things as lunar/solar effects, decay behavior and maneuvers is used to compensate for the incomplete representation of these effects in the orbital model.

FORCOM and EGG produce an element set from a single track and attempt to associate other tracks to this candidate orbit.

FNSORT compares each element set from FORCOM and EGG to the catalog to see if it matches an existing set (perhaps locating a "lost" satellite) or if it is an entirely new orbit.

COMPEL helps insure close correlation between the satellite databases at NAVSPASUR and at the SSC. Elements sets generated at the two centers are compared and and a list is generated of those orbits for which NAVSPASUR has a more recent epoch. Occasionally, NAVSPASUR has a current epoch for a satellite reported by the SSC as "lost". (By convention, a satellite is "lost" if it has had no observations associated to its orbit for a specific time span: 5 days for near-Earth objects or 30 days for deep-space objects.)

MANDC (Manual Differential Correction) allows the analyst complete control of the fitting process. This program is identical in concept with a program of the same name used at the SSC. The user may specify the fit interval, the tolerance used to accept observations, and the starting value of any element. Any subset of an element set can be corrected, and the user can reject observations at will.

COMBO (Computation Of Miss Between Orbits) is also conceptually identical to a program of the same name used at the SSC. It computes the times and locations of local minima in the distance between any two specified satellites in a given time span. A straightforward option allows a list of satellites to be compared against another list. The method uses analytic procedures to identify the distance minima that are less than a specified value, and then numerical integration is used to compute these close encounters as accurately as possible. The SSC version of the method has been described in the open literature [8]. In either version, the program can require long execution times, so some analyst discretion is needed to employ it effectively.

Break-up Processing

When a break-up occurs, one is faced with a large number of UCTs plus actual new orbits. The analyst workload always tends to go up geometrically with the number of UCTs because, in order to determine the orbits, observations have to be associated between successive passes of the debris cloud through the fence or other sensor coverage. The above programs by themselves would not be adequate for this task, but special software has been devised to help the analyst sift through the vast number of possible association combinations that must be checked.

SAD (Search and Determine) operates on an analyst-specified subset of the whole UCT list [2,3]. The analyst may suspect, based on his experience and intuition, that some particular observations all belong to the same break-up. SAD selects pairs of positions and computes candidate orbits by solving the secular-perturbed Lambert boundary-value problem for each pair. The size of the family of candidate orbits is constrained by user-specified limits on inclination, period and eccentricity. The analyst may also enforce an a-priori decay rate on the orbits. For each candidate orbit, the full orbit model is used to try to associate other observations with the candidate, based on position tolerances in radial, transverse and normal directions. If enough associations are found, the orbit is refined via differential correction. The fit statistics are compared with previous differential corrections for the family and the best orbits are saved. When no more observations can be associated, another pair of positions is selected and the whole process is repeated. When all pairs of observations have been checked, the analyst has a list of element sets with which to begin MANDC processing. The list is likely to contain many spurious orbits, but an experienced analyst will be able to "separate the wheat from the chaff" in a reasonable amount of time. Of course, the running time of SAD is potentially very long and the analyst must exercise discretion in presenting data to this program. Besides time span and element value limits, the user can select association tolerances and the number of associations which must be found before a differential correction will be performed. One more option, crucially important, will be discussed below after a different program has been described.

BLAST attempts to solve the special problem of locating when and where the break-up occurred, assuming an instantaneous event [3]. A list of candidate element sets is used to calculate the position on each orbit at equal time increments (initially 7 minutes) using the full orbit model. Conjunctions in these ephemerides are detected and recorded for analyst review. Presumably, the positions will show definite clustering near the actual break-up location, even given the inaccuracies in the element sets. It is quite common for several candidate "blast points" to appear, and the analyst must choose between them on statistical grounds and based on a-priori information.

Once the blast point is known, that time and position can be used to constrain the selection of orbits on which the remaining unassociated observations are assumed to lie. An additional option in SAD is to force the blast point to be always one of the pair of positions to be processed. This is the crucial step in sorting out the whole mass of unassociated observations; not only is the SAD processing time drastically reduced, but also the results generally contain fewer spurious orbits. The new SAD orbits can be used to refine the estimate of the blast point in another run of BLAST, which in turn increases the efficiency of subsequent SAD searches. The temptation in this type of processing is always to try to determine the blast point too soon, that is, before enough data is available. If an inaccurate blast point is adopted then the subsequent searches may go astray. SAD might appear to be confirming this wrong point when, in fact, the fits are not nearly as good as they would be if the correct point were being used.

EXAMPLE BREAK-UP EVENTS

It is difficult to classify any given break-up as "typical", either in terms of orbital behavior or processing sequence. However, several examples will illustrate the degree of success which can be achieved in the current system.

The first example illustrates the simplest type of break-up, one in which only a few small pieces appear singly over an extended period of time and depart from the parent body at low relative velocity [1]. TIROS N, a fourth generation Television and Infrared Observation Programs satellite, was launched on 13 October 1978 into a sun-synchronous orbit at 99 degrees inclination. The altitude of 451 x 460 nautical miles gave the satellite a long orbital lifetime estimated at 350 years, and the payload remained active until 1 November 1980. Seven years later, NAVSPASUR analysts discovered and cataloged two small debris pieces which were shown to have originated recently from TIROS N. Break-ups at this altitude, whatever the piece count, have intrinsic interest because they contribute to the growing problem of long-lived orbital debris. Analysis showed the first piece to have separated at 1658UT on 28 September 1987 and the second at 2107UT on 4 October 1987. High probability attaches to these times, and hence to the corresponding locations, because of the simplicity of the scenario. Only one orbit at a time had to be identified, and the low-eccentricity, low-decay orbits could be propagated quite accurately.

The second example is more complicated [1]. Cosmos 1823, a second generation geodetic satellite, broke up on 17 December 1987. The satellite had been in an orbit of 73.6 degrees inclination at an altitude of 785 x 823 nautical miles, so again much of the debris would become part of the permanent orbiting population. The event aroused extra interest because this type of satellite has not been prone to break up. COMBO analysis demonstrated that the original satellite had experienced no conjunctions as close as 25 nautical miles to any known orbiting object. The first observations were made by the PARCS phased array at Cavalier, North Dakota. 22 pieces were detected between 2105UT and 2115UT. Two hours later, the cloud passed through the NAVSPASUR fence. 36 pieces were detected between 2305UT and 2319UT. On 18 December, after additional observations had become available, NAVSPASUR analysts were able to generate 10 element sets and a blast point. The main debris piece was identified by determining which orbit was most similar to the parent orbit. This identification, supported by a high observation count, allowed the SSC to renumber the main debris piece to the parent number. Over the next several weeks, NAVSPASUR analysts continued to discover additional pieces associated with this break-up. By 7 January 1988, a total of 175 element sets had been sent to the SSC, and of these, 33 had been cataloged. The main complication in this scenario was the large number of objects. The orbits were mostly low-decay and so could be propagated accurately, while the pieces persisted long enough that many observations could be taken and reliable orbits computed.

The third example indicates that low-altitude break-ups can be more difficult to assess operationally than higher-altitude events [3]. Cosmos 1405 had been deployed originally in an orbit of 65 degrees at an altitude of 168 x 181 nautical miles, but broke up on 20 December 1983. From later analysis, the event was believed to have occurred at 1214UT at 23.7 degrees S latitude, 44.9 degrees E longitude, 182 nautical miles altitude, with a standard deviation of 3.5 nautical miles. The first NAVSPASUR observations were not made until more than 7 hours later. 67 pieces later associated with this event were detected between 1929UT and 1936UT, spread geographically between longitudes 102 degrees and 95 degrees W and altitudes 133 and 233 nautical miles. In one 2-minute period, at least 20 objects were detected, however. This tight clustering meant that NAVSPASUR analysts had to wait until the cloud had passed through the fence for the third time, late on 21 December, before before meaningful element sets could be generated. Time had to be allowed for the cloud to disperse sufficiently so that new observations could begin to be associated correctly with previous observations. By then, though, the analysis proved to be difficult for a different reason. All the pieces were in high-decay orbits. The orbit model could not propagate the orbits as accurately as for higher-altitude events, and pieces were already beginning to reenter, eliminating opportunities for further observations. Moreover, the differential decay rates among pieces were rather high, amounting (in-track) to 30 seconds in a 12-hour prediction and apparently due to different pieces having different area-to-mass ratios. Therefore, not only were predicted fence crossing times uncertain, the predicted order of pieces passing through the fence also was unreliable. Only 24 element sets were produced, and some of these are likely to have been spurious. In the end, BLAST produced several candidiate event locations. The accepted time-and-location quoted above was selected based on its marginally higher statistical weight and the fact that no element sets were rejected in this solution. The solution also happened to be near the middle of the various candidate solutions. By two weeks after the event, the number of UCTs that could be associated with the break-up had dwindled to 1 or 2 per day, and all the cataloged pieces were being seen regularly. Without the complications due to high decay, an event of this magnitude would probably have ceased to be an operational problem within one week, even using only NAVSPASUR fence data [3].

The final example is, to date, unique in NAVSPASUR records of break-up processing [4,5,6]. Three satellites were involved in the analysis, and at the time some suspicion was raised that an inadvertent on-orbit collision had occurred. Before it broke up, Cosmos 1646 had been deployed in an orbit of 65 degrees inclination at an altitude of 216 x 234 nautical miles. The accepted time and location of break-up were determined by NAVSPASUR analysts to be 0131UT on 20 November 1987 at 64.9 degrees N latitude, 60.3 degrees W longitude. Early piece counts were about 50, while later estimates ranged up to 150. On 21 November, TVSAT-1, key payload in a cooperative European venture, was launched due east from Kourou, French Guiana, aboard the Ariane V20 vehicle. 3rd stage injection into geosynchronous transfer orbit commenced at 0235UT and payload separation occurred on schedule at 0238UT. 30 seconds later, the payload and the spent 3rd stage crossed the Cosmos 1646 orbit plane near the west coast of Africa at approximately the altitude of the debris. At about 0244UT it was discovered that one of the solar panels on the payload had failed to extend. Between 0530UT and 0726UT the 3rd stage was tracked from Kwajalein (by ALTAIR) and observed to have an anomalous low thrust. Launch plans had called for the 3rd stage to remain in orbit, but instead the low thrust caused reentry on the first revolution at about 1249UT. The coincidence of these two malfunctions led debris scientists at NASA/Johnson Space Center to speculate that collisions with small particles, even millimeter-scale ones, from the Cosmos break-up could have punctured the pressurized 3rd stage and damaged the solar panel. (The relative velocity was about 9 km/sec.) NAVSPASUR was asked to investigate the orbital conjunction. COMBO analysis indicated that TVSAT-1 did indeed penetrate the debris cloud but had approached no closer than 103 nautical miles to any of the known pieces. Some uncertainity attaches to this figure because of fairly high decay in the debris orbits. Meanwhile, contractor analysts at NASA/JSC pursued a parallel study. They used NAVSPASUR element sets because the accepted time and location of the break-up had been based on NAVSPASUR calculations. However, not having access to the NAVSPASUR orbit model, they attempted to recreate the scenario using the SSC orbit model. It was found that the latter model would not propagate the NAVSPASUR element sets backwards to a close conjunction at the accepted time of break-up, making any forward calculation of conjunction with TVSAT-1 highly dubious. In retrospect, this failure is not too surprising because the two models differ markedly in their decay terms. When SSC-generated elements were used, a fairly close conjunction with the 3rd stage could be calculated, which showed the stage somewhat below and behind the known debris pieces rather than among them. Either COMBO result could be used to argue for taking the collision risk seriously, but, of course, the actual verdict on collision is at most a weak "not proven". At NAVSPASUR the collision hypothesis is considered very unlikely in view of the fact that the payload was later reported to be functioning normally, while the Ariane itself has not had a trouble-free history.

It is easy to see that early prediction of accurate conjunctions between debris and other satellites will become essential in future space operations. In this connection, the prediction incompatibility between NAVSPASUR and the SSC evidenced in the TVSAT-1 example is certainly of operational concern; however, it is a well known problem [7]. Various work-around procedures have been used for more than a decade, though not always with complete success. The apparently obvious remedy of adopting a common orbit model turns out to create other operational difficulties which are beyond the scope of this discussion, and in any case a common model is only part of the answer. Currently, Air Force Space Command (Directorate of Operations) is taking the lead in developing comprehensive operational standards for astrodynamics, and NAVSPASUR has developed an element conversion procedure that partly compensates for the orbit model incompatibilities.

SUMMARY AND CONCLUSION

Using a variety of special software tools and drawing on a wealth of in-house expertise, NAVSPASUR analysts have been quite successful in deriving orbital elements for trackable debris fragments from break-ups. In the present system, reliable figures can almost always be given for the time and location of a break-up within one day of the event and sometimes sooner. Within a week, most of the observations due to a high-altitude break-up can be associated with element sets. For low-altitude events, the association may take longer because of the complications introduced by high decay.

In the present surveillance network, of which NAVSPASUR is a part, it is difficult to calculate event time and location within, say, 1 or 2 time periods of revolution of the debris cloud by the orbital mechanics techniques outlined here. The cloud must have dispersed sufficiently for correct associations of observations to be possible, and sufficient numbers of observations on each piece must be available to estimate the orbits. Moreover, since initial debris orbits are known with relatively poor accuracy, conjunctions with other satellites of interest cannot always be accurately predicted. As a result, the collision risk from even the trackable debris can be only poorly known in the current system until well after the break-up occurs.

ACKNOWLEDGMENTS

The author is especially indebted to the NAVSPASUR staff members who produced Reference 1. Several of the program descriptions, as well as the first two break-up examples, follow that report.

REFERENCES

1. Knowles, S.; Melson C.; Jenkins E.; Perini, D.; "Uncorrelated Target (UCT) / Breakup Processing at NAVSPASUR", NAVSPASUR internal report, 15 Feb 1990.

2. Lipp, F.; "SAD Program Description", NAVSPASUR internal memo, July 1988.

3. Lipp, F.; "Separation of Objects from Cosmos 1405", NAVSPASUR Technical Note No. 1-84, 4 Apr 1984.

4. anon.; "The TVSAT-1 Rocket Body Cosmos 1646 Space Anomaly", NAVSPASUR internal report, 25 Jan 1988.

5. Kessler, D.; "Cosmos 1646 Fragmentation and Ariane V20 Launch", NASA/JSC internal memo, 28 Apr 1988.

6. Rast, R.; "Ariane V20 Anomaly", Lockheed Services Co. internal memo, Houston, TX, 31 Mar 1988 (attachment to Ref. 5 above).

7. Schumacher, P.; "Future Developments in Operational General Perturbation Theories: a NAVSPASUR Perspective", NAVSPASUR internal report, 5 Apr 1989.

8. Hoots, Felix R.; Crawford, Linda L.; Roehrich, Ronald L.; "An Analytic Method to Determine Future Close Aproaches Between Satellites", Celestial Mechanics, vol. 33, 1984, pp. 143-158.

ATOMIC OXYGEN INTERACTION WITH MATERIALS

ATOMIC OXYGEN INTERACTION WITH SOLAR ARRAY BLANKETS AT PROTECTIVE COATING DEFECT SITES

Bruce A. Banks, Bruce M. Auer, and Sharon K. Rutledge
National Aeronautics and Space Administration
Lewis Research Center
Cleveland, Ohio 44135

Carol M. Hill
Case Western Reserve University

ABSTRACT

Atomic oxygen in the low-earth-orbital environment will oxidize SiOx protected polyimide Kapton solar array blankets at sites which are not protected such as pin windows or scratches in the protective coatings. The magnitude and shape of the atomic oxygen undercutting which occurs at these sites is dependent upon the exposure environment details such as arrival direction and reaction probability. The geometry of atomic oxygen undercutting at defect sites exposed to atomic oxygen in plasma ashers was used to develop a Monte Carlo model to simulate atomic oxygen erosion processes at defect sites in protected Kapton. Comparisons of Monte Carlo predictions and experimental results are presented for plasma asher atomic oxygen exposures for large and small defects as well as for protective coatings on one or both sides of Kapton. The model is used to predict in-space exposure results at defect sites for both directed and sweeping atomic oxygen exposure. A comparison of surface textures predicted by the Monte Carlo model and those experimentally observed from both directed space ram and laboratory plasma asher atomic oxygen exposure indicate substantial agreement.

INTRODUCTION

The prime material being considered for construction of the Space Station Freedom solar array blanket is polyimide Kapton (ref. 1). This material has been shown to be vulnerable to oxidation by low-earth-orbital atomic oxygen thus indicating a need for its protection or replacement with a suitable alternative material (ref. 2). Because atomic oxygen durable substitutes for Kapton have not yet been demonstrated to be fully acceptable, 1300Å thick SiOx (where x = 1.9-2.0) sputter deposited coatings are to be used to protect a two-layer polyimide blanket with coatings on either side of each sheet of each one-mil (0.025 millimeter) thick Kapton H polyimide blanket as shown in figure 1. The mechanical ability of the array blanket to provide support for the solar cells and the flexible printed circuitry is highly dependent upon the atomic oxygen durability of the SiOx protected Kapton. Defects in the protective coatings can exist because of particulate contaminates, surface irregularities, abrasion during handling and processing, and micrometeoroid and debris impacts. Portions of the solar facing side of the array blanket (between the cells) and all of the anti-solar side of the array blanket are exposed to sweeping atomic oxygen attack. Recent atomic oxygen durability evaluations of 1300Å thick SiOx sputter deposited coatings on each side of Kapton H blankets indicate that scratch defects as opposed to pin windows represent the most serious threat to high fluence solar array blanket durability. Figure 2 is a photograph of a sample of such a material after exposure to an effective fluence of 1.28 x 10^{22} atoms per cm^2 on each side of the SiOx coated 1 mil (0.025 millimeter) thick Kapton H. As can be seen by Figure 2, significant oxidation has occurred along scratched defect sites.

Efforts to model the atomic oxygen undercutting which occurs at scratched defect sites have resulted in a Monte Carlo model which is capable of simulating the effects of plasma asher, directed space ram, and sweeping space ram attack at scratch defect sites (ref. 3). The Monte Carlo model predicts undercutting shapes at defect sites by statistical ray tracing techniques. The model operates on the following assumptions:

- Two dimensional scratch or crack defects.
- Atomic oxygen reaction probability with Kapton H is proportional to $E^{.68}$ where E is the impact energy.
- Reaction probabilities:
  - a) 0.138 for space (for first impact).
  - b) 0.0098 for space (for

    second and subsequent impacts).
  c) 0.0098 for plasma ashers.
- Reaction probability decreases for grazing incidence and is proportional $(\cos \theta)^{1/2}$ where θ is the angle between the surface normal and the impact direction.
- Atomic oxygen thermally accommodates with surfaces impacted.
- Atomic oxygen remains atomic after impacting protective coatings.
- Unreacted atomic oxygen leaves surfaces in a cosine distribution.

This technique was used to predict the shape of atomic oxygen undercutting geometries which are presented in reference 3. Recent scanning electron microscopy investigations at defect sites indicate that the undercut profiles experimentally observed from plasma asher exposures are not as accurately predicted by the Monte Carlo model as is desired. This paper more closely examines the details of the undercut sites and utilizes that information to refine the Monte Carlo model and predict laboratory and space atomic oxygen undercutting profiles.

APPARATUS AND PROCEDURE

Atomic oxygen exposure at defect sites is accomplished by use of 13.56 MHz RF plasma ashers operated on air and a directed atomic oxygen ion beam using a gridless (end Hall) ion source operated on oxygen. Details of the atomic oxygen exposure apparatus are given in references 1, 4, and 5. The directed oxygen ion beam was capable of directed ram oxygen attack as well as sweeping ram attack.

Samples exposed in the plasma asher were examined by scanning electron microscopy to document the shape and size of scratch and pin window defects. Aluminum adhesive tape used for scanning microscopy sample grounding was applied to the surface of the sample. This tape was then peeled off which removed the SiOx coatings from the underlying Kapton where undercutting had occurred. As a result, a clear view of the undercut patterns was observed in subsequent scanning microscopy inspections. The shape of these undercut profiles was used as a guide to modify the Monte Carlo assumptions to allow a better match between theory and experiment.

Alterations to the assumptions of the Monte Carlo calculation were evaluated and compared with experimentally observed plasma asher results as well as knowledge of directed and sweeping beam results to produce a predictive model which more accurately agrees with observed experimental results. Modifications to the initial assumptions included consideration of the following items:

- Higher atomic oxygen reaction probability at the SiOx Kapton interface than in the bulk.
- A finite probability of recombination of atomic oxygen upon each impact.
- Specular as opposed to diffused scattering off the SiOx surfaces.
- A higher initial impact reaction probability than subsequent impact reaction probabilities for Kapton in plasma ashers.

RESULTS AND DISCUSSION

Although previous examination of the shape of atomic oxygen undercutting of Kapton at defect sites was greatly limited because remnants of the protective coating blocked inspection of the undercut cavity below the protective coatings, tape peeling allowed full inspection of defect sites. Figure 3a and 3b compare plasma ashed SiOx coated Kapton prior to and after tape peeling. Many atomic oxygen defect sites can be clearly identified after tape peeling which are marginally or not at all evident prior to tape peeling. Figure 4a and 4b compare the more microscopic details of a defected area prior to and after tape peeling. As can be seen in figure 4a, the defect on the left has a central pin window approximately 1.5 micrometers in diameter. The SiOx coating has spontaneously peeled away from the defect after the conclusion of plasma ashing. This observation can be concluded by a comparison of the resulting axisymmetric undercut profile and the unpeeled defect protective coating geometry. The defect on the right in figure 4a and 4b has a diameter that must be substantially less than one micron in diameter. By comparison of these two defects and numerous others, a conclusion was drawn that defects whose width-to-coating-thickness ratio greatly exceed one, produce double dimpled cavities as shown on the left in figure 4b; whereas those whose width-to-coating-thickness ratio is less than or equal to one, produce a single dimpled cavity which is rather conical in shape. These results appeared to be consistent whether the defect is a pin window, a crack, or a scratch. In addition, the angle between the polyimide Kapton and the oxidized surface plane at the perimeter of the defect was not 90° as was previously predicted by the Monte Carlo model. Alterations in the Monte Carlo assumptions were evaluated to see if different modeling assumptions would produce either the double dimpled defect cavity shape or the more conical cavity as opposed to a hemispherical cavity. Alteration of the Monte Carlo model to assume specular scattering of atomic oxygen off the bottom of the protective coating was found not to cause any measurable change in the profile of the undercut defect. A model alteration which included a finite probability of atomic oxygen recombination upon each impact, similarly did not yield undercut profiles which agreed with experimental results. However, if one assumes that the probability of atomic oxygen reaction with the Kapton at the SiOx interface is greater than that of the bulk Kapton, then a more conical undercut cavity is predicted at its outer edges. Figure 5 is a plot of the undercut angle resulting from various interface reaction probabilities. Assuming that the bulk reaction probability is 0.0098, based on experimental plasma asher observation, an interface reaction probability of 0.049 (5 x bulk reaction probability) was selected for the Monte Carlo model improving assumption. The double dimple feature observed for large width-to-coating-thickness defects was found to be produced if one assumed the initial impact reaction probability for plasma ashers was larger than the subsequent thermally accommodated impact reaction probabilities. Based on trials of various initial impact reaction probabilities, an initial impact reaction probability of 0.0392 (4 x reaction probability for the second and subsequent impacts) for plasma ashers was selected to produce erosion predictions which were in reasonable agreement with experimentally observed results in plasma ashers.

Rationale for the reasonableness of these two model change assumptions have not been fully developed. However, it is quite conceivable that the atomic oxygen reaction probability at the polyimide SiOx interface is in fact different than the bulk due to details of the interface chemistry either resulting from the Kapton fabrication or the sputter deposition of the SiOx coating. The higher initial impact reaction probability for plasma ashers is quite possible because of the mix of many stable states and ions at higher than thermal temperatures in the plasma asher discharge. This may produce reaction probabilities which exceed those which would be projected based on the room temperature energy alone. The higher initial impact reaction probability was assumed only for the plasma asher environment and not for the more energetic 4.5 ev space atomic oxygen. A summary of the revised Monte Carlo assumptions is given in table 1.

Figure 6 compares the predicted Monte Carlo undercutting profiles for large crack-width-to-coating-thickness defects and small crack-width-to-coating-thickness defects. As can be seen from figure 4b, the experimentally observed undercutting profile of the wide defect is in reasonable agreement with the Monte Carlo predicted profile. Figure 7 is a scanning electron photomicrograph of a plasma ashed undercut defect site for a narrow width-to-coating-thickness ratio defect. As can be seen, it also compares favorably with the predicted results shown in figure 6. A comparison of the Monte Carlo predicted and experimentally observed undercutting profile for plasma ashed polyimide Kapton which has protective coatings on both surfaces and a defect on the top surface only is shown in figure 8. As can be seen by comparing figures 8a and 8b, the predicted camphored walls of the undercut polyimide Kapton is in reasonable agreement with experimentally observed results. Based on comparisons between pin window and scratch defects from plasma asher experiments, the undercut profiles of each appear to have the same general shape. Thus the two-dimensional results of the Monte Carlo prediction are relevant to the three-dimensional pin window defect profiles.

The higher initial impact reaction probability of space ram atomic oxygen interaction causes a considerable drilling effect as shown in figure 9 for normal incident atomic oxygen because of the higher interface reaction probability. There is also a small but noticeable flaring to the undercut profile at the SiOx interface. Figure 10 compares the results of a wide defect exposed to fluence levels which produce the same depth of erosion for both plasma asher and normal incident space ram atomic oxygen attack. As can be seen, the surface morphology of a plasma asher is rather smooth compared to the space ram exposed surfaces. These results are very consistent with experimentally observed plasma asher and space exposure results. The predicted undercut Kapton profile for scratch or crack defects exposed to space sweeping ram atomic oxygen exposure as would occur on Space Station Freedom photovoltaic arrays is shown in figure 11 for polyimide Kapton protected on one surface and figure 12 for polyimide Kapton protected on two surfaces. As can be seen in figure 12, scattered atomic oxygen widens the undercut region well beyond the defect site.

SUMMARY

Tape peeling of plasma ashed SiOx coated polyimide Kapton provides a clear view of defect undercutting profiles by scanning electron microscopy. The undercutting profiles have a conical shape for defects whose width-to-coating-thickness ratio is less than or equal to one, and have a double dimple shape for defects whose width-to-coating-thickness ratio greatly exceeds one. The undercutting profile experimentally observed is more conical

236

than the hemispherical undercutting that previous Monte Carlo modeling had predicted. Monte Carlo modeling provides a good fit to experimental results if the initial impact reaction probability in plasma ashers is 4 times the subsequent impact reaction probability and the probability of interface reaction for plasma ashers in space is 5 times the bulk reaction probability. Observed surface textures produced by plasma ashers and normal incident space ram are in good agreement with resulting Monte Carlo predictions. Sweeping ram exposure to polyimide Kapton protected on the top and bottom surfaces is expected to produce wide undercutting due to scattered atomic oxygen.

REFERENCES

1. S.K. Rutledge and J.A. Mihelcic, "Undercutting of Defects in Thin Film Protective Coatings on Polymer Surfaces Exposed to Atomic Oxygen," (NASA TM #101986), paper presented at the 16th International Conference on Metallurgical Coatings sponsored by the American Vacuum Society, San Diego, California, April 17-21, 1989.

2. B.A. Banks et.al., "Ion Beam Sputter-Deposited Thin Film Coatings for Protection of Spacecraft Polymers in low earth orbit," (NASA TM #87051), paper presented at the 23rd Aerospace Sciences Meeting sponsored by the American Institute of Aeronautics and Astronautics, Reno, Nevada, January 14-17, 1985.

3. B.A. Banks, S.K. Rutledge, B.A. Auer, and F. DiFilippo, "Atomic Oxygen Undercutting of Defects on SiOx Protected Polyimide Solar Array Blankets," paper presented at the Materials Degradation in Low Earth Orbit Symposium of the 119th TMS Annual Meeting and Exhibit, Anaheim, California, February 18-22, 1990.

4. B.A. Banks, et.al., "The NASA Atomic Oxygen Effects Test Program," paper presented at the 15th Space Simulation Conference, Williamsburg, Virginia, October 31-November 3, 1988.

5. B.A. Banks, et.al., "Simulation of the Low Earth Orbital Atomic Oxygen Interaction with Materials by Means of an Oxygen Ion Beam." (NASA TM #101971), paper presented at the 18th Annual Symposium on Applied Vacuum Science and Technology conducted by the American Vacuum Society, Clearwater Beach, Florida, February 6-8, 1989.

TABLES

Table I - Monte Carlo Model Assumptions with Modification to Produce Agreement with Plasma Asher Results.

ASSUMPTIONS:

- 2D model simulates scratch or crack defect
- Reaction probability α (energy)$^{[illegible]}$
  - 0.138 for space (1st impact)
  - 0.0098 for space (≥ 2nd impact)
  - 0.0392 for plasma ashers (1st impact)
  - 0.0098 for plasma asher (≥ 2nd impact)
  - 0.0490 for plasma asher and space at Kapton/protective coating interface
- Reaction probability decreases for grazing incidence α $(\cos\theta)^{1/2}$

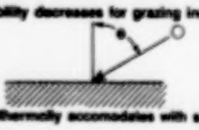

- Atomic oxygen thermally accomodates with surfaces impacted
- Atomic oxygen remains atomic after impacting protective coating
- Unreacted atomic oxygen leaves surfaces in a cosine distribution

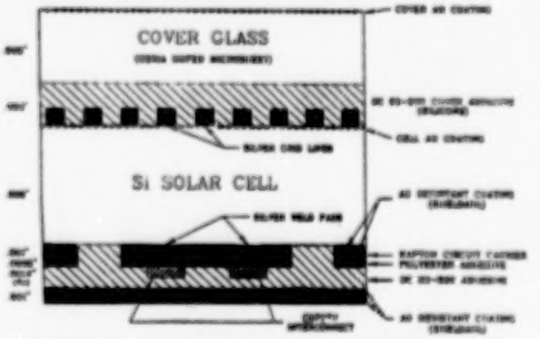

Figure 1 - Cross Section of Space Station Freedom Photovoltaic Array.

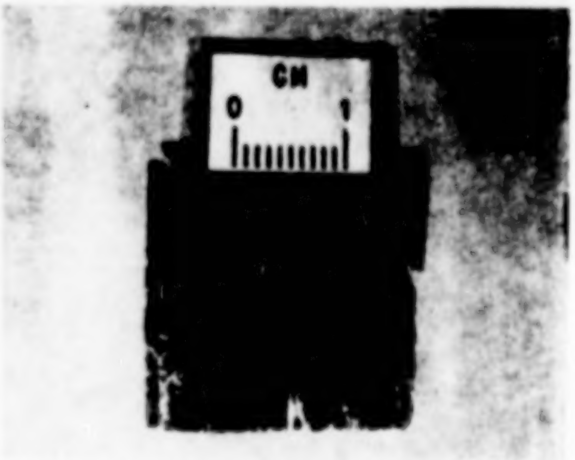

Figure 2 - Kapton H Protected on Both Sides with 1300Å Thick SiOx coatings After Plasma Ashing to a Fluence of 1.28 x 10^{22} atoms per cm^2 on each side.

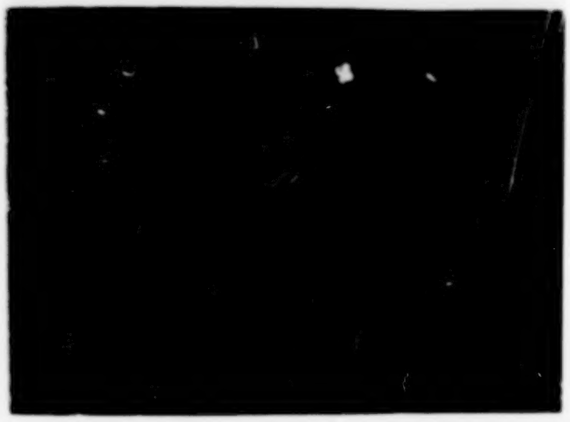

(a) Before Tape Peeling.

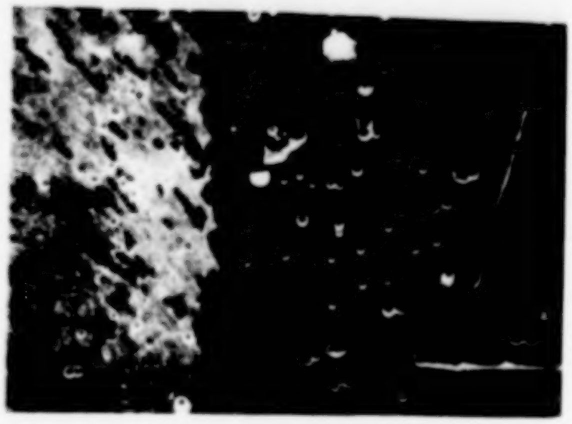

(b) After Tape Peeling.

Figure 3 - SiOx Coated Kapton H after Plasma Asher Exposure to a Fluence of 4.45 x 10^{20} atoms per cm^2.

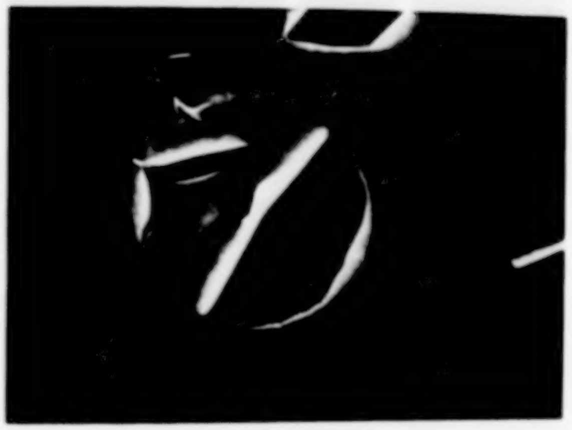

(a) Before Tape Peeling.

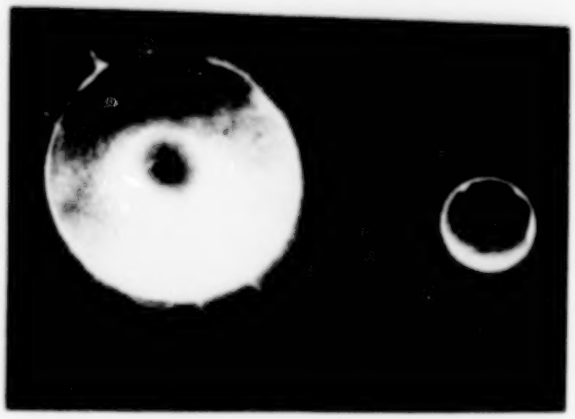

(b) After Tape Peeling.

Figure 4 - Comparison of Two Defects in Protected Kapton after Plasma Asher Exposure to a Fluence of 4.45 x 10^{20} atoms per cm^2.

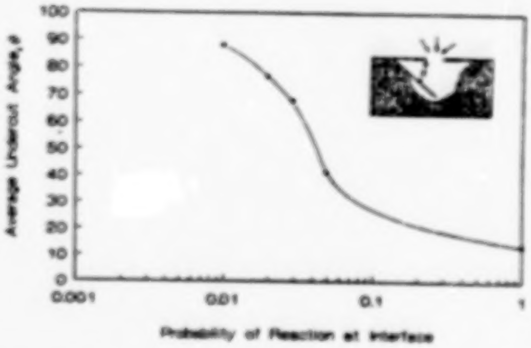

Figure 5 - Atomic Oxygen Undercut Angle at Kapton Interface Dependence Upon Interface Reaction Probability.

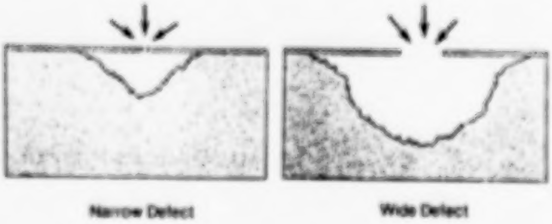

Figure 6 - Monte Carlo Plasma Asher Undercutting Defect Profiles Comparing Large and Small Defect Width-to-Coating-Thickness Ratios.

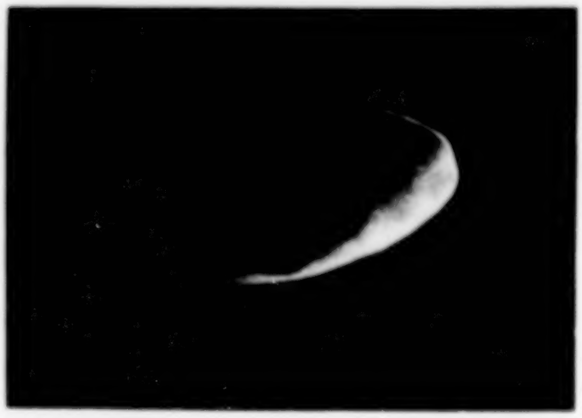

Figure 7 - Scanning Electron Photomicrograph of Plasma Ashed (to a fluence of 1.28 x 10^{22} atoms/cm^2) and Tape Peeled Defects on 1300Å SiOx Coated Kapton with a Small Defect-Width-to-Coating Thickness Ratio.

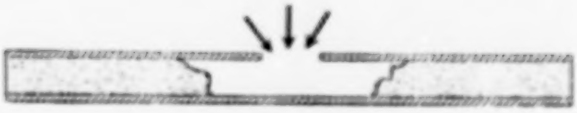

(a) Monte Carlo Prediction for Crack in Top Surface Defect.

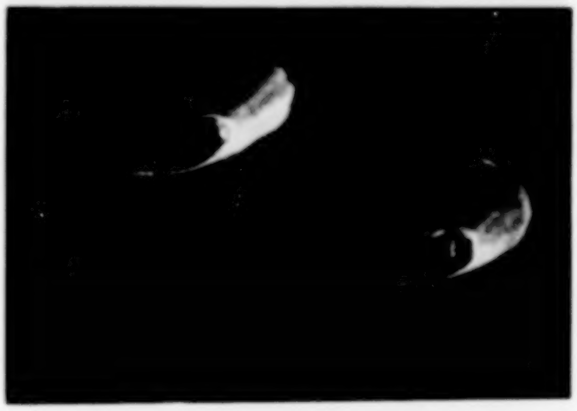

(b) Plasma Asher Experimentally Observed Results for Pin Window Defect.

Figure 8 - Comparison of Monte Carlo Predicted and Experimentally Observed (after plasma ashing to a fluence of 1.28 x 10^{22} atoms/cm^2) Atomic Oxygen Undercutting Profiles for Polyimide Kapton Protected (1300Å SiOx) on Both Top and Bottom Surface with a Defect in the Top Surface Only.

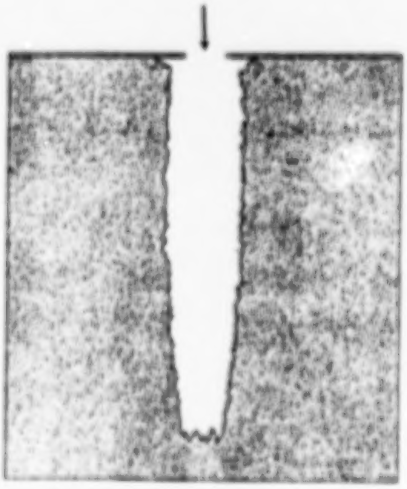

Figure 9 - Normal Incident Space Ram Atomic Oxygen Monte Carlo Prediction for Defect on Kapton Protected on One Surface.

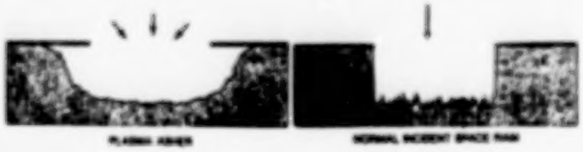

Figure 10 - Comparison of Monte Carlo Predicted Surface Profile for Equal Depth Erosion Plasma Asher and Normal Incidence Space Ram Atomic Oxygen Exposure of a Wide Defect.

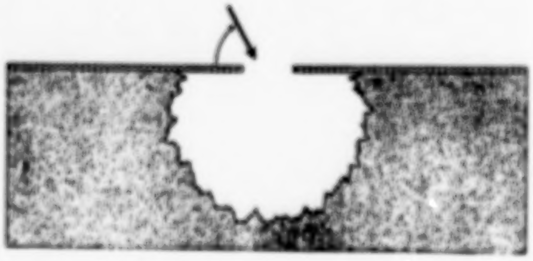

Figure 11 - Sweeping Ram Atomic Oxygen Monte Carlo Prediction for Defect on Kapton Protected on One Surface.

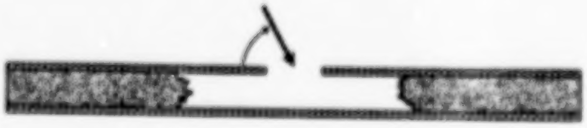

Figure 12 - Sweeping Ram Atomic Oxygen Monte Carlo Prediction for Defect on Kapton Protected on Top and Bottom Surfaces.

FAST OXYGEN ATOM ENVIRONMENTAL INTERACTIONS WITH LEO SPACECRAFT

G. E. Caledonia and R. H. Krech
Physical Sciences Incorporated

(Paper not provided at publication date)

241

ATOMIC OXYGEN BEAM SOURCE FOR EROSION SIMULATION

J. W. Cuthbertson, W. D. Langer, and R. W. Motley
Princeton Plasma Physics Laboratory

P.O. Box 451, Princeton, NJ 08543

J.A. Vaughn

NASA Marshall Space Flight Center

ABSTRACT

We describe a device for the production of low energy (3-10 eV) neutral atomic beams for surface modification studies, which reproduces the flux of atomic oxygen in low Earth orbit. The beam is produced by the acceleration of plasma ions onto a negatively biased plate of high-Z metal; the ions are neutralized and reflected by the surface, retaining some fraction of their incident kinetic energy, forming a beam of atoms. The plasma is generated by a coaxial RF exciter which produces a magnetically-confined (4 kG) plasma column. At the end of the column ions fall through the sheath to the plate, whose bias relative to the plasma can be varied to adjust the beam energy. The source provides a neutral flux $\approx 5 \times 10^{16}/\mathrm{cm}^2\mathrm{s}$ at a distance of 9 cm and a fluence $\approx 10^{20}/\mathrm{cm}^2$ in five hours. The composition and energy of inert gas beams has been diagnosed using a mass spectrometer/energy analyzer. The energy spectra of the beams demonstrate energies in the range 5–15 eV, and qualitatively show expected dependences upon incident and reflecting atom species and potential drop. Samples of carbon film, carbon-based paint, Kapton, mylar, and teflon exposed to atomic O beams show erosion quite similar to that observed in orbit on the Space Shuttle.

INTRODUCTION

In low Earth orbit, about 150-300 km altitude, the atmosphere consists primarily of atomic oxygen and molecular nitrogen. The surface of an orbiting spacecraft collides with these species with high relative velocity—the O atoms carry about 5 eV kinetic energy in the spacecraft frame. Spacecraft surfaces are thus exposed to a flux of highly reactive energetic O, ranging from 10^{13} to $10^{16}/\mathrm{cm}^2$ s, depending upon altitude. Observed effects of this bombardment include the production of an optical glow in front of ramming surfaces (the "spacecraft glow" phenomenon[1]) and the erosion of exposed surface materials.

Structures intended to remain in service in low orbit for many years, such as the Space Station, must employ protective surface materials and coatings which can withstand this chemically active flux. Thus there is a need for a source of "superthermal" (4–20 eV) neutral beams to study in the laboratory the effects of the energetic neutral bombardment, and for accelerated testing of candidate materials and coatings, simulating years of on-orbit exposure within a few days.

The need for laboratory facilities for studying the interaction of superthermal (5 eV) atomic oxygen with materials, including its role in the degradation of spacecraft surface materials and in the spacecraft glow phenomenon, has led to the development over the past several years of several new systems using different methods to achieve high fluxes of energetic oxygen atoms.

Besides their application to spacecraft environmental effects, these oxygen beam sources (and low energy neutral beam sources in general) are useful tools for many other purposes. Likely research "spinoffs" for these atomic beam techniques include: beam-surface interactions, atomic scattering, gas phase "hot atom" chemical reactions, and materials processing and surface modification technologies, such as semiconductor etching. Many of these processes have not been well studied at these energies because high flux sources have not been available—older methods of producing neutral beams (such as thermal effusion as in chemical molecular beam experiments, or acceleration and charge exchange neutralization of ion beams) do not work well in this energy range.

We will describe the operating principles and characterization of a system for the production of high-flux low-energy neutral beams which is based on a coaxial RF plasma source and utilizes a biased metal surface for the acceleration and neutralization of plasma ions. In this paper we emphasize the characterization of the beam energy and tests of the principles on which beam production is based. In an accompanying paper[2] results are presented from experiments to measure the beam flux and from material exposures performed to evaluate the beam's reproduction of effects due to exposure in orbit. The beam facility, developed at Princeton under contract for Marshall Space Flight Center, has proven successful in meeting the requirements for simulating the orbital interaction of atomic oxygen with materials, and shows promise for other technological applications. The beam source is capable of sustained production of high flux beams of essentially 100% atomic O.

PRINCIPLES OF OPERATION

The method we have used for producing a low energy neutral beam utilizes a metal surface in contact with a magnetically confined plasma to accelerate and neutralize plasma ions. The metal plate is biased negative with respect to the plasma potential, and plasma ions are accelerated onto the surface, attaining an energy determined by the bias voltage. The ions are neutralized by picking up an electron from the negatively charged metal, and undergo collisions with the atoms of the solid surface. If the metal atoms are much more massive than the ions, the incident particles are mostly reflected back from the surface, retaining a large fraction of their incident kinetic energy, thus forming a beam of superthermal neutrals of adjustable energy.

The interaction of the plasma ions with the metal surface is itself a process of fundamental interest. These interactions are not well studied experimentally in the energy range below 100 eV, due to lack of sources and diagnostics. Such processes are important in various technological areas, for example, in the edge regions of fusion plasma devices where the plasma interacts with material surfaces. The characteristics of the reflected neutrals produced in our beam source can yield significant new experimental data on these interactions and provide a test of theoretical models used to describe them. Calculations have been made with TRIM (TRansport of Ions in Matter), a Monte Carlo code used to model the interaction of a particle with a solid surface[3,4], in order to predict the reflection efficiency and energy spectrum for various incident ions and surfaces. The TRIM code follows the trajectory of each incident particle, calculating the effect of each successive collision with the atoms of the solid, and also models the effect of energy loss to electrons and of surface binding forces on the incident particle. The surface binding forces are modeled as a planar attractive potential directed toward the surface, which can only approximate the complex interaction with the atoms of the surface; thus the model's predictions are less certain for species which may tend to bind strongly (e.g. oxygen) than for those which interact more weakly (noble gases).

The reflection efficiency and energy spectrum of the reflected beam depend upon the exact species of the incident particles and surface atoms, their relative masses and the strength of binding forces acting between them, and upon the condition of the surface with respect to roughness and impurities. In general the TRIM calculations predict that for a large enough mass ratio, low energy (5-100 eV) ions are reflected fairly efficiently as neutral atoms, with the energy spectra peaked around a particular fraction of the incident energy, having a characteristic spread of a few eV. The larger the mass ratio between incident and surface atoms, the larger is the fraction of incident energy at which the peak in the reflected spectrum occurs. The expected angular distribution of the reflected beam is roughly a cosine distribution about the normal to the surface. Figure 1 shows an example of the energy spectrum of the reflected neutrals as predicted by the TRIM code for oxygen incident on molybdenum (a reflecting surface frequently used in our erosion experiments). Note that the spectrum is fairly peaked at around 6 eV, with a spread of a few eV.

Figure 2 shows the predicted reflection efficiency for oxygen atoms incident on molybdenum over the energy range 10-50 eV. Also shown is the fraction of the incident energy at which the peak of the reflected energy spectrum occurs for particles reflected into the solid angle range from 25-45° from the surface normal (±10° from our usual experimental viewing angle). Over a wide range of incident energies the reflection efficiency is around 60% and the ratio of the reflected energy peak to the incident energy is 0.40-0.50. For example, at 30 eV incident energy $E_{ref}/E_{inc} = 0.46$; this value from TRIM calculations can be compared with the energy retained upon a reflection due to a single elastic collision at 35° from the incident path, which for these masses would be

$$E_{ref}/E_{inc} = [m_1^2 + m_2^2 + 2m_1 m_2 \cos\theta_{CM}]/(m_1 + m_2)^2 = 0.54$$

SYSTEM DESIGN AND OPERATION

Figure 3 shows a cross-sectional view of our low energy neutral beam apparatus. It has two basic parts: a plasma chamber containing a coaxial plasma source and the neutralizing plate, and an experimental 'target'

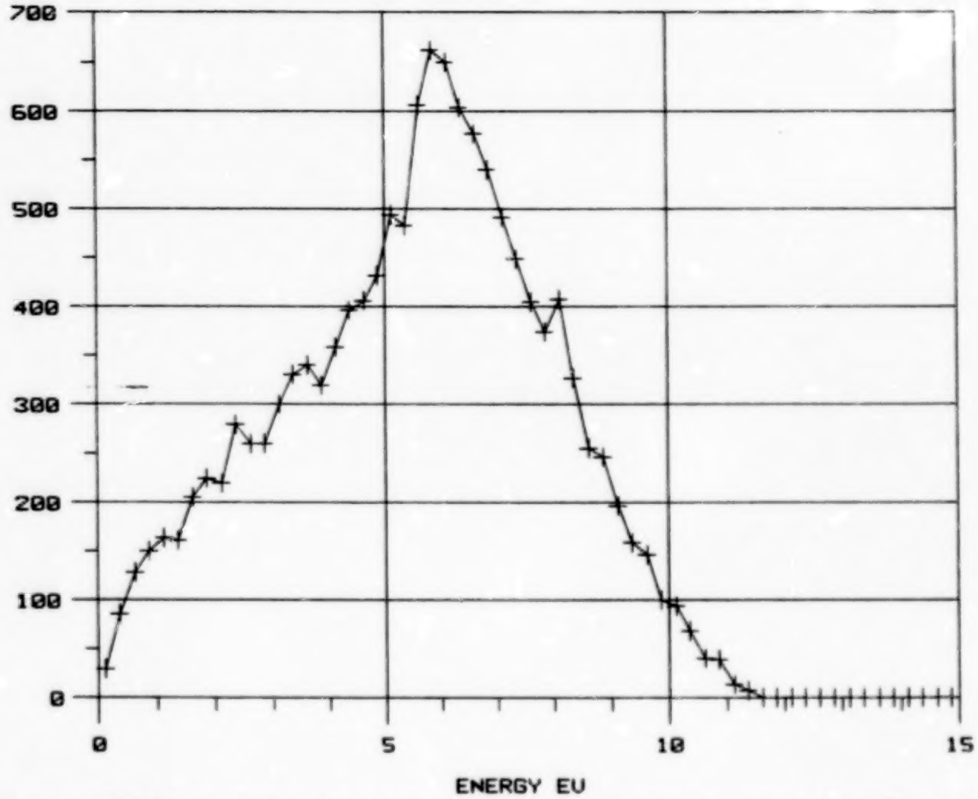

Figure 1: TRIM calculations for the reflected energy spectrum of oxygen atoms reflected from a molybdenum surface for an incident energy of 15 eV, for all reflection angles (0-90° from normal). The calculation used an attractive potential of 2 eV to model the binding forces between the oxygen and surface molybdenum atoms.

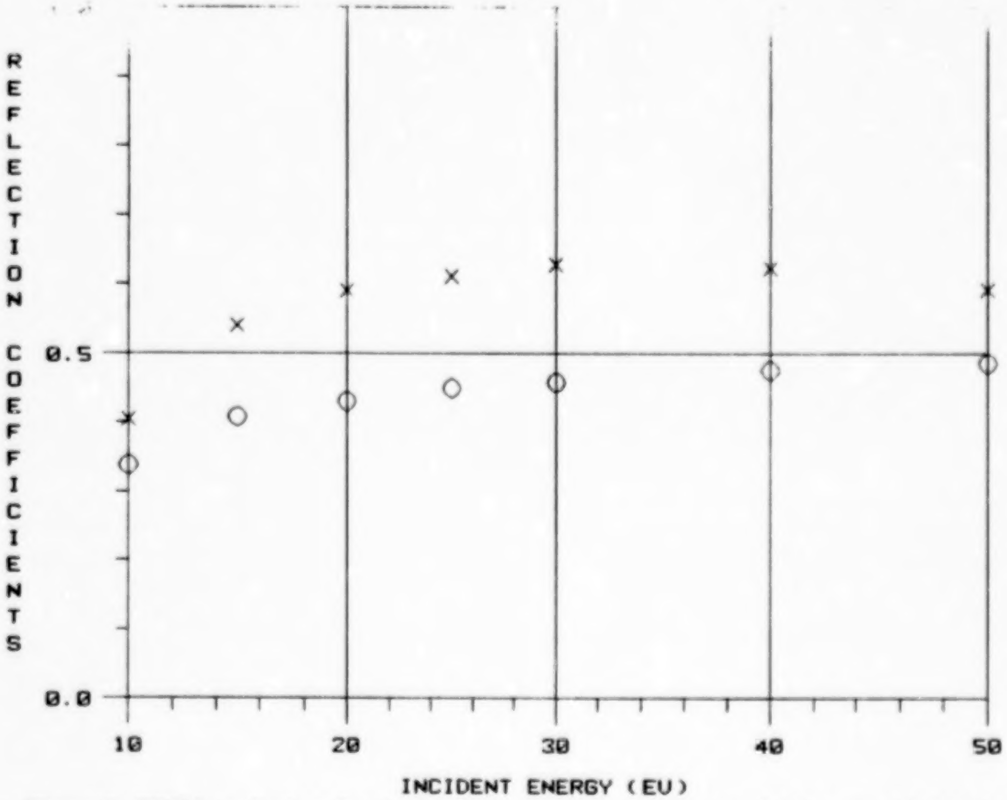

Figure 2: TRIM predictions for the reflection of oxygen ions from molybdenum with 10-50 eV incident energy. Crosses show the reflection efficiency; circles show the energy at which the peak of the reflected energy spectrum occurs for reflection angles 35 ± 10° as a fraction of the incident energy.

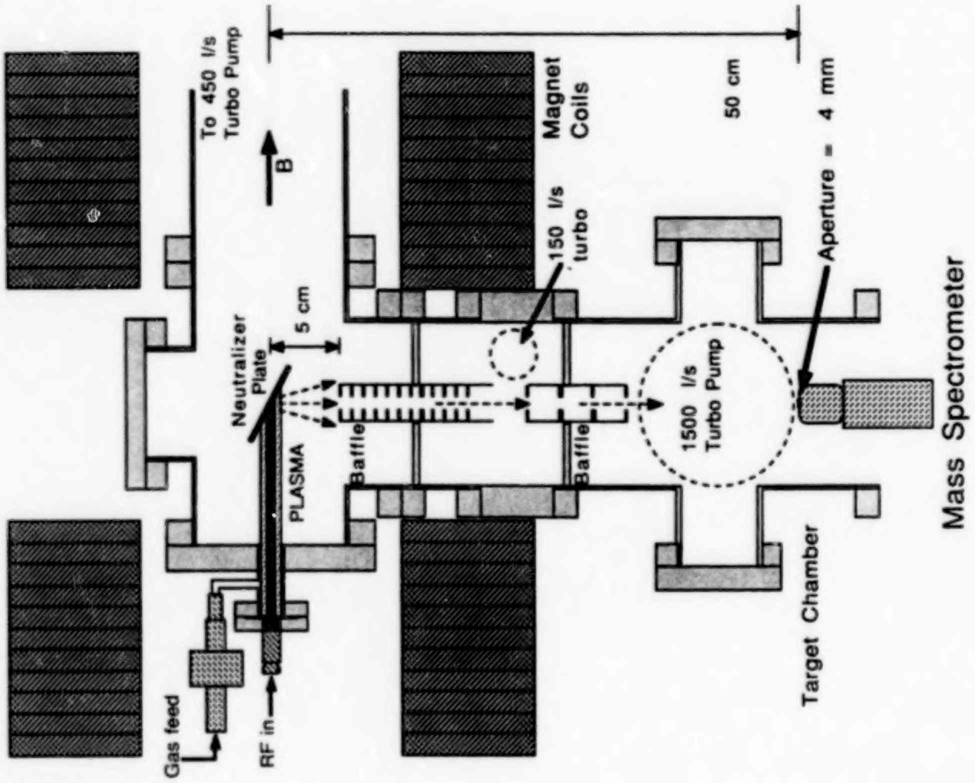

Figure 3: Cross-section view of the Princeton Low Energy Neutral Beam facility, as configured for beam energy measurements.

chamber oriented perpendicularly.

In order to produce pure oxygen plasmas, we use an RF driven plasma source, thus avoiding the problems associated with hot filaments and cathodes that limit the oxygen content of simple arc and glow discharges. Our system is based on a magnetically confined coaxial plasma source of the type developed by Motley and co-workers[5]. The source is driven by 1 kW microwave power at 2.45 GHz applied to a center conductor coaxial with an Inconel outer cylinder, which acts as a quarter-wave antenna. The RF propagates through the plasma as lower hybrid waves. The plasma source produces an intense plasma column of about 1 cm radius. The Inconel outer conductor and the back side of the ceramic seal are water cooled.

The magnetic field in the plasma source is produced by two sets of 11 water-cooled coils arranged in a Helmholtz-like configuration. A current of 440 A is passed through the coils, yielding an axial field of 4 kG.

Plasma particles travel along the field lines from the coaxial source to the neutralizer in a well-confined cylindrical column. The neutralizing surface is provided by a thin plate of metal mounted on a copper block which can be water- or air-cooled and which can also be heated to a few hundred degrees C by means of an internal heating element for purposes of outgassing. The surface materials used most often have been molybdenum and tantalum, chosen for their high atomic mass, resistance to reaction with oxygen, and low sputtering (platinum and gold surfaces have also been used).

The plate can be rotated to any angle with respect to the B field, and is usually oriented at about 55°. Because the potential drop across the sheath to the plate is large compared to the ion thermal kinetic energy, the ions impinge on the surface at nearly normal incidence. The reflected neutral beam is directed across the magnetic field, and thus the field keeps charged particles away from the beam target area. Because the plasma column striking the neutralizer is small in radial extent the neutral source is well defined and tightly focused. The neutralizer can be biased from -50 to +15 V relative to ground (positive bias limited by the electron current drawn); combined with the positive plasma space potential this gives incident ion energies from about 10 to 60 eV. The ion current to the neutralizer plate is measured from the voltage drop across a 1 Ω resistance in the power supply circuit using an oscilloscope.

Both parts of the vacuum vessel are composed of 6 inch diameter cylindrical stainless steel sections. Two baffled gas chokes may be installed in the target chamber, creating two stages of differential pumping. The high vacuum stage is connected to a 1500 l/s turbo pump. During beam production, operating pressure is a few mTorr in the plasma chamber, but can be held to a few times 10^{-7} Torr in the experimental chamber with the differential pumping. To reduce the danger of pumping pure oxygen, we bleed nitrogen into the backing pump at a nitrogen/oxygen ratio about 2:1.

For measurement of the properties of the plasma the system is equipped with two electrostatic probes, one a single Langmuir probe and the other an electron emitting hot probe. Each probe can be independently moved radially and axially through nearly the entire length of the plasma column; the probes have been used to measure the plasma density and electron temperature and the plasma space potential. The hot probe is especially useful for directly measuring the plasma potential, but has a limited range of densities over which it can operate. A monochromator spectrograph has also been used to measure the plasma emission spectrum, viewing the plasma column through a quartz window in the plasma chamber (not shown). Plasma emission spectra show virtually complete dissociation in oxygen plasma: the ions are O^+ rather than O_2^+. This is crucial since we desire a beam of atomic O.

The system can achieve a sustained ion current to the plate of 4 A in O^+ or Ar^+. Using the predicted reflection efficiency for O reflected from Mo this gives:

$$\text{O flux} > 5 \times 10^{16} cm^{-2} s^{-1}$$

at the usual target position about 9 cm from the neutralizer.

The system is operated in a pulsed mode, with pulse lengths of a few msec. Duty cycles of up to 10% have been achieved sustainably, limited by heating of the coaxial exciter center conductor. The system operates reliably in 100% oxygen plasmas over the long run times (several hours) needed to achieve high fluence ($10^{20} cm^{-2}$) exposures.

The damaging effects of atomic oxygen on system components have been small. The stainless steel center conductor of the coaxial is corroded visibly, but is robust enough to survive more than 100 hours plasma operation; no limit to survival time has been reached for any other system component.

NEUTRAL BEAM MEASUREMENTS

Measurements of the absolute neutral atom flux for atomic oxygen beams have been made in collaboration with the Physical Science Branch of the Materials Laboratory at Marshall Space Flight Center and are reported in a separate paper in these proceedings [2]. These measurements were made using catalytic probes [6] which measure the heat produced by the recombination of oxygen atoms striking a catalytic silver oxide surface. These measurements support the predicted flux levels to within the experimental error (about a factor of two). The measurements also confirm the expected variation of the flux as the inverse square of the distance from the neutralizer. Measurements of the angular distribution of the beam flux from the relative erosion rates of polyethylene targets exposed simultaneously in the target chamber are also reported in Vaughn et al.

In this paper we report the results of direct measurements of neutral beam energy spectra which have been made using an energy analyzing quadrupole mass spectrometer (VG model SXP-500) installed as in Fig. 3. Neutral particles enter this instrument through a 4 mm aperture and pass through an "ion source" region where a small fraction of them are ionized by electron impact. The ions then pass into a cylindrical mirror analyzer (CMA), which uses electrostatic focusing to allow only ions with a certain desired energy to pass through. The energy spectrum of incoming particles is obtained by scanning the energy at which ions can pass through the CMA. Ions then enter an electric quadrupole mass filter which will allow only ions of a particular q/m ratio to pass through. These ions are then detected by a channeltron electron multiplier.

The likelihood of an incoming particle's detection is determined by the probability of ionization upon passing through the ionizing region; this is proportional to the time spent in the region, and thus inversely proportional to the velocity. Therefore, the signal due to the thermal neutral gas (background from the gas feed to the plasma source) is much larger than the signal from the superthermal neutral beam (detected at 50 cm from the neutralizer), even with the background pressure in the spectrometer chamber kept quite low by differential pumping. Because of this effect and the instrumental broadening of the thermal gas energy spectrum, the tail of the apparent thermal distribution obscures the low energy end of the spectrum of the reflected beam. This imposes a low energy limit to observation of the spectrum of 2-3 eV.

Argon rather than oxygen atom beams have been used to perform most of the energy spectrum measurements for the source, for three reasons. First, argon has a high cross-section for electron-impact ionization. Second, being more massive than oxygen, argon has a lower velocity at a given energy, thus a longer residence time in the ionizing region of the spectrometer. These two effects make the quadrupole much more sensitive to argon than to oxygen. In addition, for molecular gases, dissociation of thermal background molecules in the ionizer creates atoms with a few eV energy (Franck-Condon dissociation energy). The signal from these energetic atoms can

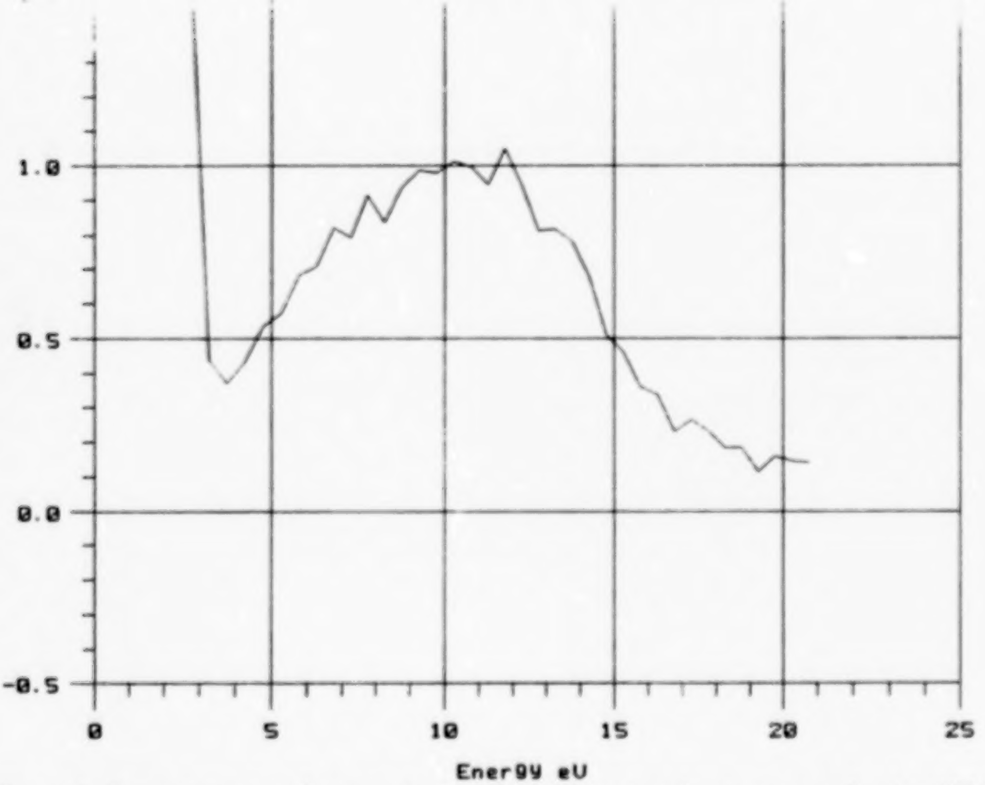

Figure 4: Energy spectrum for argon beam reflected from tantalum as measured using CMA energy analyzer. Instrumentally broadened signal from backgroung thermal gas obscures low energy end of beam spectrum. Data shown averaged to same energy resolution as numerical prediction (Figure 5).

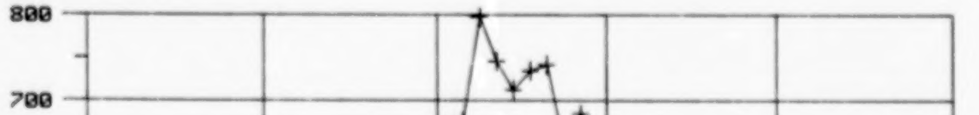

Figure 5: TRIM calculations for the reflected energy spectrum of argon atoms reflected from a tantalum surface for an incident energy of 30 eV, for all angles of reflection.

swamp the signal from the much less efficiently ionized superthermal neutral beam atoms in the affected energy range.

Figure 4 shows an example of the energy spectrum for an argon beam reflected from a clean (outgassed) tantalum surface. The peak energy is 10–12 eV with a spread (HWHM) of 4–5 eV. This spectrum can be compared with TRIM code results (Figure 5), which show a quite similar peak energy and energy spread. Energy spectra with characteristics like those of Fig. 4 are obtained during the first several minutes of beam production, after which the peak energy begins to shift downward, falling to about 7 eV for Ar on Ta after about 30–40 minutes of beam production. We believe the time variaton is caused by gas loading of the reflecting surface, as discussed below.

Evidence for the effect of the plate bias (i.e. accelerating potential across the sheath) on the energy is shown in Figure 6 for argon incident on molybdenum. A change in the sheath potential, measured with a Langmuir probe, from 40 to 10 Volts shifts the peak from about 8 to 5 eV, demonstrating the ability to control the energy of the beam.

In experiments performed with other plasma species and reflecting materials, we have seen qualitatively the expected variation in the beam energies depending upon the atomic masses of the incident and surface species, at least for those species for which we have collected significant data (for some cases examined, the data were not clear enough to characterize the spectrum). For example, the reflected energy spectrum for argon incident on molybdenum occurs at lower energies than for Ar incident on tantalum at comparable incident ion energy, demonstrating the dependence on target mass. Also, the reflected energy spectrum of Krypton incident on Ta falls at lower energies than that for Ar on Ta at comparable energy, demonstrating the expected dependence on incident ion mass

However, as mentioned above a complication arises from the contamination of the surface by atoms of the plasma species. TRIM predicts that at sufficient impact energies some incident particles will be implanted in the surface material rather than reflected; the residence time for such implanted particles in the metal is unknown. In addition, surface adsorption may also occur, especially for chemically reactive species. Incident particles which collide with implanted or adsorbed atoms of the same mass will lose more of their kinetic energy than if colliding

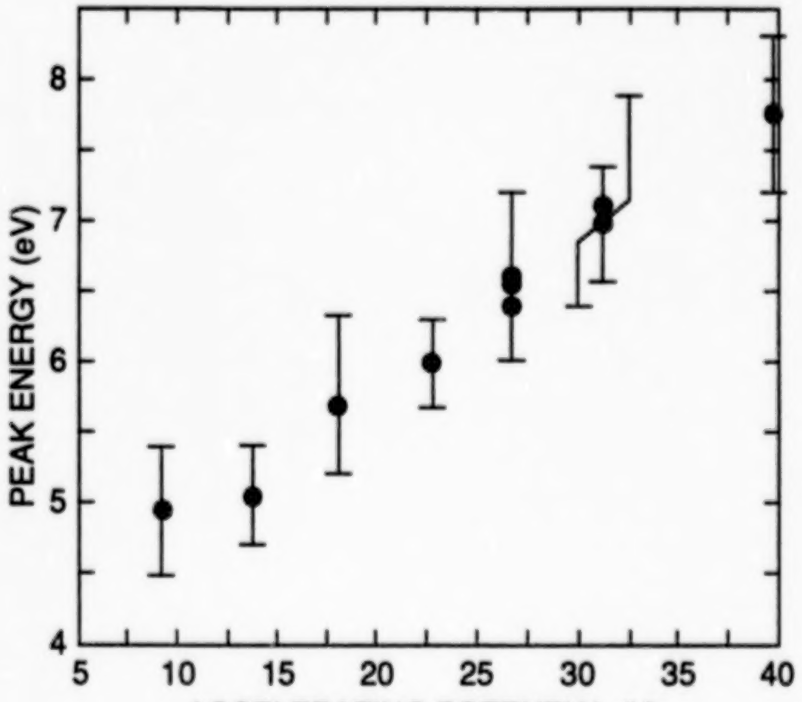

Figure 6: Location of the peak in the energy spectrum for argon beams reflected from a molybdenum surface, as a function of the incident energy of the ions (determined by the potential drop across the sheath to the reflecting surface). Error bars indicate the approximate uncertainty determining the peak from the mass spectrometer data; since the peaks are relatively broad and flat, determining the exact position of the maximum is somewhat uncertain.

only with the heavy metal atoms; this will result in a reflected beam of lower energy neutrals. Beginning with an outgassed reflecting surface, it has been observed that the energy spectrum of the neutral beam shifts to lower energies over the course of several minutes of operation. The spectrum can be shifted back to higher energies by outgassing the neutralizing surface. Thus the reflected energy spectrum from the interaction of an ion species with a homogeneous metal surface will be different from the spectrum seen in practical, prolonged steady beam production.

The unknown degree of occupation of the surface material by oxygen atoms makes it difficult to predict from theory exactly what the beam energy spectrum will be for long-time oxygen beam exposures. Direct measurements of the oxygen beam energy spectrum during steady-state beam production are necessary, and this is now one of the principal issues that need to be resolved.

CONCLUSIONS AND FUTURE WORK

The neutral beam source described here produces atomic beams with energy spectra that have been directly measured (for inert gas beams) to be in the desired energy range (about 4–15 eV), with an adjustable peak energy and a spectrum width of a few eV. Some qualitative features of the reflection of low energy inert gas atoms from surfaces have been observed from the measurements to date, and are in rough agreement with the numerical simulations from theory. It is clear, however, from the behavior over time of the observed spectra that surface loading of the reflecting material by the working gas ions plays a large role in the reflection physics. To explore this further we have added heating coils to the mounting of the neutralizing plate so that we can either heat cycle the plate between spectral measurements, or raise the plate to such a temperature that the gas atoms are expelled at the same rate they arrive so that suface conditions are stable.

Additionally, we intend to increase the duty cycle of the source above 10% by actively cooling the center conductor, and to reduce the O_2 pressure in the spectrometer chamber to permit the measurement of atomic oxygen beam spectra. The presence of O beams at high flux levels has already been conclusively demonstrated by other measurements (including direct flux measurements with catalytic probes, and erosion of exposed materials[2]), and the beam source has proven a useful simulation of the atomic oxygen bombardment in orbit, but the energy spectrum remains to be determined.

ACKNOWLEDGEMENTS

This work was supported by NASA under contract No. H83097B. We wish to thank Roger Linton, Ralph Carruth, and Ann Whitaker of the Materials Laboratory at Marshall Space Flight Center for their support of these experiments. We also thank David Ruzic of U. of Illinois for assistance with TRIM calculations, and acknowledge the Max-Planck-Institut für Plasmaphysik for permission to use the TRIM code.

REFERENCES

1. Torr, M.R. "Optical Emissions Induced by Spacecraft-Atmosphere Interactions." *Geophys. Res. Lett.* 10, 114, 1983.
2. Vaughn, A.J., R.C. Linton, M.R. Carruth, A.F. Whitaker, J.W. Cuthbertson, W.D. Langer, and R.W. Motley, 'Characterization of a 5 eV Neutral Atomic Oxygen Beam Facility", Proc. of Space Operations, Applications and Research Symposium, Albuquerque NM, 1990.
3. Eckstein, W. and J.P. Biersack, "Reflection of Low-Energy Hydrogen from Solids," *Appl. Phys. A* 38, 123, 1985.
4. Ruzic, D.N. and H.K. Chiu, "Modeling of Particle-Surface Reflections Including Surface Roughness Characterized by Fractal Geometry", *J. Nucl. Mater.* 162–164, 904, 1989.
5. Motley, R.W., S. Bernabei, and W.M. Hooke, "Coaxial lower hybrid plasma source," *Rev. Sci. Instrum.* 50, 1586, 1979.
6. Carruth, M.R., Jr., R.F. DeHaye, J.K. Norwood, and A.F. Whitaker, "Method for Determination of Neutral Atomic Oxygen Flux," *Rev. Sci. Instrum.* 61, 1211, 1990.

ATOMIC OXYGEN AND ULTRAVIOLET RADIATION EFFECTS ON SPACECRAFT THERMAL CONTROL COATINGS

H. G. Lee, K. S. Simpson, and C. A. Smith
McDonnell Douglas Space Systems Company

(Paper not provided at publication date)

250

LABORATORY INVESTIGATION OF VISIBLE SHUTTLE GLOW MECHANISMS

A. Leone, G.R. Swenson
Lockheed Research and Development Division

G.E. Caledonia, K.W. Holtzclaw
Physical Sciences Inc.

ABSTRACT

Laboratory experiments designed to uncover mechanistic information about the spectral and spatial characteristics of shuttle glow were conducted. The luminescence was created when a pulse of O atoms traveling at orbital velocities was directed toward NO molecules previously adsorbed to aluminum, nickel, and Z306 Chemglaze (a common baffle black) coated surfaces held at various temperatures.

Spectral and spatial measurements were made using a CCD imaging spectrometer. This instrument is identical to the one used in flight studies except for the substitution of a CCD array rather than photographic film at the focal plane. Corroborative spectral information was recorded in separate measurements using a scanning monochromator and gated photomultiplier arrangement. The surface mediated laboratory luminescence was found to be spectrally similar to space borne observations of the visible shuttle glow phenomena and to the red of the gas phase recombination previously reported at thermal energies and observed at orbital energies in the present work. Relative intensities above the three materials studied were found to be within a factor of two at liquid nitrogen temperatures. Spectral observations above the aluminum and chemglaze samples were similar but nickel was consistently shifted further to the red by approximately 30 nanometers. The intensity above a given surface was found to vary inversely with temperature increasing an order of magnitude as the temperature was dropped from ambient to liquid nitrogen (presumably due to enhanced NO accomadation).

The e-folding distance at several temperatures was calculated from images of the surface glow using the Photometrics image processing capability of the imaging spectrometer. The e-folding distance was not altered as a function of incoming O beam velocity (over the range 6-10 km/s tested). Plots of the projected e-fold distance versus the square root of temperature were linear implying a thermalization of the exiting species. These results coupled with the apparent need to utilize chemical energy in the removal of product species bound to the surface (as evidenced by the spectral shift observed in the heterogenous recombination spectra as a function of distance from the interaction plate and concomitant increase in lifetime) led to an assumption of Maxwellian exit speeds. The consequence of such spatial spatial measurements at 93 K leads to a computed average excited state lifetime on the order of 180 μseconds. These observations provide direct evidence that the visible Shuttle glow results from recombination of oxygen atoms and surface bound NO.

Introduction

The visible glow above shuttle surfaces subjected to impact by energetic atmospheric species was first observed during the STS-3 Mission (Banks et al., 1983). Starting with the next mission Mende and coworkers undertook a series of systematic photographic observations which characterized the glow phenomenon (Mende et al., 1983a, b, 1984a, b, 1985, 1986, 1988; Swenson et al, 1985). The glow was present only above surfaces subjected to the direct impact of the residual atmosphere, suggesting that kinetic energy played a role (Mende et al., 1988, Slanger, 1987). Spectrally resolved observations revealed the glow as a broad band emission peaking at 680 nm. Because of the similarity of the spectrum to that of the NO_2 gas phase recombination, heterogeneous recombination mechanisms involving atomic oxygen and NO at shuttle surfaces were postulated as the source of the glow (Swenson et al., 1985; Kofsky and Barrett, 1986). The glow brightness was inferred to vary inversely with temperature based on modeling of orbiter surface temperatures and NO surface residence times (Swenson et al., 1986).

Recently two laboratory studies (Arnold and Coleman, 1988, Orient et. al.,1990) of the surface mediated recombination of NO_2 using high velocity CW atomic oxygen beams have attempted to simulate the observed glow. Comparisons between their observations and results obtained in the present pulsed study reveal mechanistic features of the proposed luminescence processes.

Space borne measurements also revealed a characteristic spatial extent of the observed luminescence. The glow thickness is a result of the convolution of excited state lifetimes and the distribution of exit velocites of the emitting species from the interaction surface. Since the exact nature of the NO_2 formation mechanism is still debated, questions of recoil energy, thermalization, and excited state lifetime are still open to speculation. To further complicate matters the excited state lifetimes reported in the literature range from 1µs measured by Sackett and Yardley (1971) to 170-260 µs reported by Donnelly and Kaufman (1977). Variations between the lifetimes of NO_2 have been attributed to mixing of the $^2B_1$ and $^2B_2$ states or explained in terms of one or more of these excited state variably coupled to the high vibrational levels of the $^2A_1$ ground state (Douglas 1966, Paulsen 1970, Alder- Golden 1989) yielding a wide range of values. Considerable variation in lifetimes based solely upon emission criterion have also been reported. The common assumption of a 70 µ sec. lifetime qouted in the analysis of flight data forces an emitter velocity greater than the spacecraft surface temperature would provide and hence has generated a discussion of the possible transfer of ram energy.

An Ely-Rideal recombination process in which an incoming O atom pulls off a surface bound NO to form the excited state species might transfer some of the ram kinetic energy to the NO_2 product in an amount reduced by small losses to the surface. However, ejection of an excited NO_2 molecule with thermalized kinetic energy is expected if NO_2 is formed via the Langmuir-Hinselwood surface migration processes.

This report describes direct laboratory tests of these mechanistic tenants. Good agreement with spectra observed in orbit both in terms of spectral distribution and observed temperature scaling were observed. In addition, the results of this study suggest that thermalization even at high O atom velocities common to the ram interactions of the shuttle is likely, but cannot rule out a Rideal interaction hypothesis.

Experimental

Atomic oxygen with a velocity of 8 km/s was produced in a large vacuum chamber via a pulsed laser discharge technique (Krech and Caledonia, 1986) and was directed onto targets located 85 cm down stream from the O-atom source. The apparatus has been described in greater detail previously (Caledonia, 1989; Holtzclaw et al., 1990). Six by six inch targets of aluminum, nickel and Z306 Chem-glaze paint were mounted on a reservoir which could be filled with liquid nitrogen. Target temperature was monitored with a copper-constantan thermocouple probe calibrated by immersion into water/ice, dry ice/ethanol, and liquid nitrogen baths.

The surfaces were selectively doped prior to oxygen exposure with a purified pulse of NO. Residual non adsorbed gas was removed from the chamber during a pump out interval prior to O atom interaction. NO (stated purity >98.5 percent) was first passed through an Ascarite column to remove residual NO_2 prior to sample dosing. Dosing was performed with a small solenoid valve (General Valve series 9) placed directly in front of the target. NO flow was monitored with a mass flow meter and was typically 0.007 standard cc's per pulse. A pulse of NO was delivered to the target prior to every O-atom pulse. The NO mass flow rate was specified such that less than one monolayer of NO impinged the target with each pulse. The relatively high vapor pressure of NO, even at 77 K, precluded the buildup of a thick NO film on the target surfaces. A sufficient delay (~1s) between the NO and O-atom pulses was used to insure that all NO was evacuated from the chamber before the next oxygen atom pulse ($p < 10^{-5}$ torr). This precaution is important since gas phase reactions of O and NO could produce interfering emissions (Fontijn, 1964). Typical fast O-atom fluence levels for these tests were 1×10^{14} cm^{-2} per pulse.

Spectral and spatial information was taken using a CCD imaging spectrometer designed at Lockheed that has been used to photographically record the glow observed above the space shuttle in low Earth orbit. The instrument as employed in these experiments is identical to that used for the orbital studies (Swenson et al., 1985) except that an unintensified 378 x 576-line CCD array in a Photometrics model 3000 camera was substituted for the photographic film. The instrument has provision for removing the slit and grating from the optical axis wherein the instrument is an imager.

Spatial image measurements were performed upon surfaces at room temperature and when cooled to liquid nitrogen temperature. In addition, images were gathered of the interaction plume as a function of O atom velocity from 5km/s-10km/s. The inside of the chamber was blackened to minimize reflections which might obstruct the image. The instrument processor permitted real time display, background subtraction, and image analysis during these experiments.

With the the slit and grating inserted into the optical path, the instrument is a spectrometer with y axis wavelength dispersion (spectral resolution ~7 nm) as a function of the x (distance) axis of the array. Confirming spectral information was recorded in separate measurements using a scanning monochromator and photomultiplier tube where the signal processing was performed with a gated photon counter. The spectral resolution of the monochromator was 2.7 nm.

The relative spectral response of the CCD imaging spectrometer was determined using an NBS referenced quartz halogen lamp. Wavelength position and spectral resolution were determined using Hg and Ne line sources. The spectral response of the monochromator was determined by viewing the gas phase reaction of O and NO in a flow tube. This reaction has long been used as a secondary standard for spectral calibrations in the visible region of the spectrum (Fontijn, 1964).

Spectral Results :

An image of the surface glow above an NO-doped Z306 Chemglaze coated foil held at ~93 K taken with the imaging spectrometer is shown in Figure 1. The oxygen atom beam enters from the left and envelops the whole of the target. A separate nozzle also to the left is used to inject NO on the surface. This image was integrated over ~100 pulses of the beam. The black strip in the center of the image demarks the slit position. As mentioned above, when the slit and grating are inserted into the optical path, the instrument is a spectrometer with wavelength dispersion along the y axis of the array as a function of x distance from the target plate as shown in the inset of the figure.

The spectral distribution of the glow observed under these conditions was measured in separate tests using either the scanning monochromator or the CCD array-spectrometer. These observations are contrasted in Figure 2 with spectra measured from the Space Shuttle. All spectra have been smoothed for ease of comparison. The shuttle data (Mende et al., 1988) was taken with an imaging spectrometer similar to that used in the laboratory, but using film rather than a CCD array (Swenson et al., 1985). Intensities were obtained from densitometry traces and corrected for window transmission and film response. The laboratory spectra are in reasonable agreement with the observed Shuttle glow. The monochromator data displays a similar onset and the imaging spectrometer exhibits a similar spectral shape. Spectra obtained with the imaging spectrometer were found to fall symmetrically within the respective spectral envelope measured with the monochromator with similar wavelength maxima. The variation between the scanning monochromator and the imaging spectrometer spectra could be the result of calibration uncertainties; as described in the previous section the calibration procedures employed for the two diagnostics were quite distinct. The differences observed between laboratory and Shuttle glows may be within the cumulative experimental uncertainties in both the laboratory and flight data correction procedures. All three spectra suspected to result from surface mediation are significantly shifted from the gas phase three body NO_2 recombination spectra also shown in Figure 2. The magnitude of the observed shifts are in line with typical surface physisorption energies. In fact, the spectral shift of ~80 nm between the gas/gas and surface mediated spectra obtained in this work is thought to be the result of surface bond energy expended in the removal of NO_2^* from the target.

Measurements were performed in the absence of a target to examine the luminescence resulting from the NO gas phase collisions with the O beam employed in the present study. The gas phase luminescence is blue shifted relative to the surface glow described above, peaking at ~625 nm as in thermal recombination. Note that the mechanism producing the gas phase luminescence observed in this work has not been identified. NO recombination with collisionally slowed oxygen atoms or fast atom interactions with NO dimers may occur. The NO-NO dimer bond energy is only on the order of 0.06 eV.

Since the targets were limited to approximately monolayer coverage of NO, any material dependence observed will reflect differences in material adsorption properties relating to the heterogeneous recombination process. Luminescence measurements were performed on NO-doped cooled targets of Z306, nickel and aluminum. In all cases the observed intensities were similar in magnitude (factor of two, we did not evaluate the variability in adsorbed NO amongst these materials). The spectral distributions for the three materials are quite similar with the exception that the spectra on nickel appears red-shifted by approximately 30 nanometers. The delineation of any material dependencies will require careful acquisition of a larger database than provided to date.

A similar set of measurements were made for room temperature targets of Z306 and aluminum. All other experimental conditions were held the same. For these cases the surface glow was spectrally similar to that observed on the cooled samples but the intensity levels were down by an order of magnitude. This inverse temperature dependence may reflect the fact that more NO can be accommodated on surfaces as they are cooled. Swenson et al. (1986) have analyzed Shuttle glow data from various missions and show that the glow intensity drops approximately an order of magnitude as the surface temperature is decreased from room temperature to 173 K. Laboratory measurements at additional temperatures would elucidate the exact nature of this correlation of intensity as a function of temperature.

Spatial Results :

Images of the luminescent plumes created by the interaction of a pulse of O atoms with previously NO doped surfaces were recorded utilizing the CCD imaging spectrometer. A background subtraction provided difference images. Exposures integrating 100 such pulsed events were taken using a 35 mm lens at various surface temperatues. The overlpot on the 93 K image shown in Figure 1 displays the intensity drop off of the glow from the surface using the Photometrics image processing capability. The plot shows the relative intensity of a set of row elements selected from the image matrix array versus pixel location. As mentioned above, the black rows in the center of the image correspond to the position of the interchangeable slit which was removed during image measurements. An image of the NO nozzle provided a reticle to benchmark the spatial length represented by each pixel number. A narrow band of rows were selected symmetric about this vacant slit position for analysis. A uniform field correction on the order of 10 percent at the periphery was made by imaging a large uniformly illuminated diffuse plate.

Figure 3 shows a corrected intensity plot as a function of position in centimeters from the surface (derived from the image shown earlier in Figure 1) which is approximately linear when ploted on a logarithmic scale (see inset). Similar plots of pairs of such central row regions for a given image taken symmetrically about the slit region were found to be virtually identical.

Image data taken as a function of temperature and incoming O beam velocity were similarly analyzed. A few images were clearly obstructed by scattering but most displayed an exponential decay in intensity with distance from the interaction surface. The e-folding distance (distance over which the intensity drops to 1/e of the intial value) was calculated for each experimental condition. This parameter is of interest since the number of molecules in the excited state decays exponentially as exp $(-t/\tau)$. Multiplying the top and bottom of this exponent by the mean molecular speed characteristic of the product exit velocity distribution yields the expression exp $(-d/v\tau)$. Hence the e-fold (e^{-1}) distance d can be equated to the molecular velocity v times the average lifetime τ of the excited molecules.

No change in this e-folding distance (measured at 93 K) was observed as a function of initial O beam energy over the velocity range from 6 to 10 km/s tested. Thus increasing the translational energy of the incoming species within this range does not seem to impart any additional exit energy to the products formed by surface interaction. However, this result alone does not distinguish between a Langmuir Hinselwood or Rideal mechanism.

The calculated e-folding distances as a function of the square root of the plate temperature (in K) are plotted in Figure 3. The e folding distance increases in rough proportion to a square root dependence of the surface temperature. A linear fit is provided for comparison. Such behavior indicates that the interactions at the surface are thermalized and products are most likely ejected with root mean squared exit velocities determined by the surface temperature in a Maxwellian fashion ie. $v = \sqrt{3RT/M}$.

The low number densities of interacting species suggest a collisionless analysis regime with long mean free path. If the species are thermalized as they react at the surface and no elastic energy or momentum is imparted to the exiting products, then the assumption of a Lambertian directional distribution of these exiting species with Maxwellian speeds can be invoked. Under such an assumption no influence due to incoming beam profile is expected since no translational energy is transfered. As seen in Figure 1, the glow thickness is not uniform but diminishes at the edges since the interaction plate is of finite (6 inches in length) dimension. A flattened maximum spatial extent region above and below the slit position was found in each plume image distant enough from the edge to receive symmetrical contributions of the exiting species. A narrow set of rows within this region were selected to plot the intensity drop off as a function of position described above. The e-fold lengths described above are then projections along the line of sight of the distance these product molecular emitter species travel during their excited state lifetime. The average distance an emitter species travels in contributing to a line of sight pixel can be found by dividing the projected distance by the cosine of the half angle of 30° which demarks the solid angle into which half of these contibuters are dispersed in accordance with a Lambert cosine distribution. The average molecular distance associated with the e-fold parameter at 93 K was determined to be 4.2 centimeters. A value between the root mean squared speed of 225 m/s or the most probable speed of 183 m/s indicative of the Maxwell distribution curve at 93 K can serve as an estimate of the exit speed. The lifetime of the excited state can be determined as the ratio of this characteristic glow thickness parameter divided by the assumed exit velocity. A lifetime of the excited species on the order of 185-225 μsec results from such a calculation.

Spectra as a function of position from the plate are obtained by selecting column elements from the inset array shown in Figure 1 at various x distances from the plate. A spectral red shift on the order of 30 nm. is observed in spectra 1.3 cm. removed from the plate as compared to that observed on the surface. A progressive red shifting is observed for spectral slices as a function of distance from the plate. Species with longer lifetimes are responsible for the spectral emission at incremental distances from the interaction surface. These observations are consistent with the loss of energy required for these relatively longer lived species to overcome physisorption bonds to remove these product species from the surface. Surface bound emitters not having expended such energy are relatively shorter lived and their higher energy emission is peaked to the blue. The lifetimes of NO_2^* have been shown to depend upon excitation energy (Donnelly and Kaufman,1978; Alder-Golden, 1989). The higher energy excitation is associated with a shorter lived species and vice versa.

Discussion

The laboratory glow data are in quite reasonable spectral agreement with Shuttle glow observations and also exhibit a similar inverse temperature dependence. These observations provide strong evidence that the Shuttle glow results from recombination of oxygen atoms and surface bound NO. The NO_2^* recombination spectra created by a laboratory pulse of atomic oxygen traveling at orbital velocities was shown to be red-shifted from the gas phase interaction because of surface mediation. Only small variations in spectra and intensity were observed from material to material.

As mentioned above, two recent laboratory studies (Arnold and Coleman, 1988, Orient et. al.,1990) of the surface mediated recombination of NO_2 using high velocity CW atomic oxygen beams have attempted to simulate the observed glow. The first of these (Arnold and Coleman, 1988) directed a supersonic (1.4 km/s) beam containing oxygen atoms and an effussive NO beam at a nickel surface. The observed luminescence was observed to peak at 830 nm, well to the red of both the flight measurements of Shuttle glow and spectra obtained in the present pulsed study on nickel surfaces. A velocity effect may be indicated by this comparison, altough such a dramatic shift to the red may also be related to the alternate removal of a more tightly bound surface O atom by NO. In addition, the presence of excited oxygen molecules can also produce an NO_2 spectra to the red of that created by O + NO (Kenner and Ogryzlo 1984). More recently, (Orient et. al. 1990) directed an 8 km/s O beam and a jet of NO onto a MgF_2 surface. Their observations include a broad visible emission spectra peaked at 625nm which is similar to that observed in the present study when the gas pulses were allowed to interact prior to dopant isolation in the presence of a surface. Their light collection technique is not capable of spatial differentiation of the glows created as done in the present study.

It should be noted that the fast atom source used in these studies is not composed entirely of ground state oxygen atoms. Oxygen molecules are present at a concentration <20 percent and the metastable O(1D) density in the beam has not been measured. Although the concentration of this latter species is estimated to be low, based upon quenching rate constants for O(1D) by O and O_2 (Davidson et al, 1976) its potential contribution to the observed luminescence cannot be ascertained. This species is of course also present in the ambient atmosphere and its reactivity should be investigated independently.

Recently, a discussion of lifetimes and recoil energies involved in reconciling the flight data for various mechanisms proposed was provided by Slanger. Slanger suggests that translational energies in the 0.3 -1 eV range with radiative lifetimes between 100-200 µs are most compatible with existing evidence. Our measurements appear to be consistent with these predictions. No difference in e-fold was found by varying the impinging O atom velocity but a direct measure of product exit velocities was not undertaken. The possibility of a momentum exchange contribution which does not vary with the velocity of the incoming species is possible, but the energy lost to the surface which manifests itself as a spectral shift must be considered. The red shift in the NO_2 spectrum has been thought to indicate that internal chemical energy is needed to break the surface bond and that O atom collisional energy is not efficient in removing the product species from the surface. A red shift similar to the flight results was observed in these heterogeneous O + NO laboratory experiments.

It should be noted that exit velocities for erosion glows (Holtzclaw et.al. 1990) using a similar beam source were measured to be 1.3 km/s. Erosion glow processes result from quite different mechanisms in which a material's chemical bond is broken. If exit velocities of this magnitude (1 Km/s) are shown to be involved, the above mentioned calculated lifetimes would be reduced on the order of less than 35 µseconds. The present results argue against other than thermalized velocities and direct time of flight measurements of the product exit velocities in these surface mediated O + NO recombination studies are planned.

Acknowledgments : This work was funded under a Lockheed Independent Research and Development Program

REFERENCES

Alder-Golden,S.M., The NO + O and NO + O_3 Reactions, J. Chem. Phys., **9 3**, 684-697 1989.

Arnold, G.S. and Coleman, D.J., Surface Mediated Radical Recombination Luminescence: O+NO+Ni, J. Chem. Phys. **8 8**, 7147, 1988.

Banks, P.M., Williamson, P.R., and Raitt, W.J., Space Shuttle Glow Observations, Geophys. Res. Lett. **1 0**, 118, 1983.

Caledonia, G.E., Krech, R.H., and Green, B.D., A High Flux Source of Energetic Atoms for Material Degradation Studies, AIAA J. **2 5**, 59, 1987.

Caledonia, G.E., Laboratory Simulations of Energetic Atom Interactions Occurring in Low Earth Orbit, in Rarefied Gas Dynamics: Space Related Studies, Vol. 116 of Progress in Astrunautics and Aeronautics, AIAA, Washington, DC, pp. 129-142, 1989.

Davidson, J.A., Sadowski, C.M., Schiff, H.I., Streit, G.E., Howard, C.J., Jennings, D.A., and Schmeltekopf, A.L., Absolute Rate Constant Determinations for the Deactivation of O(1D) by Time Resolved Decay O(1D) > O(3P) Emission, J. Chem. Phys. **6 4**, 57, 1976.

Donnelly V.M., Kaufman F., Fluorescence lifetime studies of NO_2 I. Excitation of the perturbed $^2B_2$ state near 600nm. J. Chem. Phys. **6 6**, 4100-4110, 1977.

Donnelly V.M., Kaufman F., Fluorescence lifetime studies of NO_2 II. Dependence of the perturbed $^2B_2$ state on excitation energy. J. Chem. Phys. **6 9**, 1456-1460, 1978.

Douglas, A.E., Anomalously Long Radiative Lifetimes of Molecular Excited States J. Chem. Phys. **4 5**, 1007, 1966.

Fontijn, A., Meyer, C.B., and Schiff, H.I., Absolute Quantum Yield Measurements of the NO-O Reaction and its use as a Standard for Chemiluminescent Reactions, J. Chem. Phys., **4 0**, pp. 64-70, 1964.

Holtzclaw, K.W., Fraser, M.E., and Gelb, A., Infrared Emission from the Reaction of High Velocity Atomic Oxygen with Graphite and Polyethylene, in press, J. Geophys. Res., 1990.

Kenner, R.D., Ogryzlo, E.A., Orange chemiluminescence from NO_2 , J. Chem. Phys. **8 0**, 1-6, 1984.

Kofsky, I.L. and Barrett, J.L., Spacecraft Glows from Surface-Catalyzed Reactions, Planet. Space Sci. **3 4**, 665, 1986.

Mende, S.B., Garriott, D.K., and Banks, P.M., Observations of Optical Emissions on STS-4, Geophys. Res. Lett. **1 0**, 122, 1983a.

Mende, S.B., Vehicle Glow, AIAA-83-2607-CP, presented at Shuttle Environment and Operations Meeting, Washington, DC, 1983b.

Mende, S.B., Nobles, R., Banks, P.M., Garriott, D.K., and Hoffman, J., Measurement of Vehicle Glow and Space Shuttle, J. Spacecraft Rochets **2 1**, 374, 1984a.

Mende S.B., Banks, P.M., and Klingelsmith, III, D.A., Observation of Orbiting Vehicle Induced Luminosities on the STS-8 Mission, Geophys. Res. Lett. **1 1**, 527, 1984b.

Mende, S.B. and Swenson, G.R., Vehicle Glow Measurements on the Space Shuttle, AIAA-85-0909, presented at AIAA 20th Thermophysics Conference, Virginia, 1985.

Mende, S.B., Swenson, G.R., Clifton, K.S., Gause, R., Leger, L., and Garriott, O.K., Space Vehicle Glow Measurements on STS41D, J. Spacecraft **2 3**, 189, 1986.

Mende, S.B., Swenson, G.R., and Llewellyn, E.J., Adv. Space Res. **8** (1), 229, 1988.

Orient, O. J., Chutjian A, Murad E., Recombination reactions of 5 eV O (^{3} P) atoms on a MgF_2 surface. Phys. Rev. A, Rapid Comm. **4 1**, 4106-4108 (1990).

Paulsen, D.E., Sheridan, W.F., Huffman, R.E., Thermal and recombination emission of NO_2 J. Chem. Phys. **5 3**, 647-658 (1970).

Sackett, P.B., Yardley, J.T. Chem.Phys. Lett. **9** 61d2 (1971).

Slanger, T.G., Deductions from Space Shuttle Glow Photographs, Geophys. Res. Lett. **1 3**, 431, 1986.

Swenson, G.R., Mende, S.B., and Clifton, K.S., Ram Vehicle Glow Spectrum: Implication of NO2 Recombination Continuum, Geophys. Res. Lett. **1 2**, 97, 1985.

Swenson, G.R., Mende, S.B., and Llewellyn, E.J., The Effect of Temperature on Shuttle Glow, Nature **3 2 3**, 519, 1986.

257

Figure 1

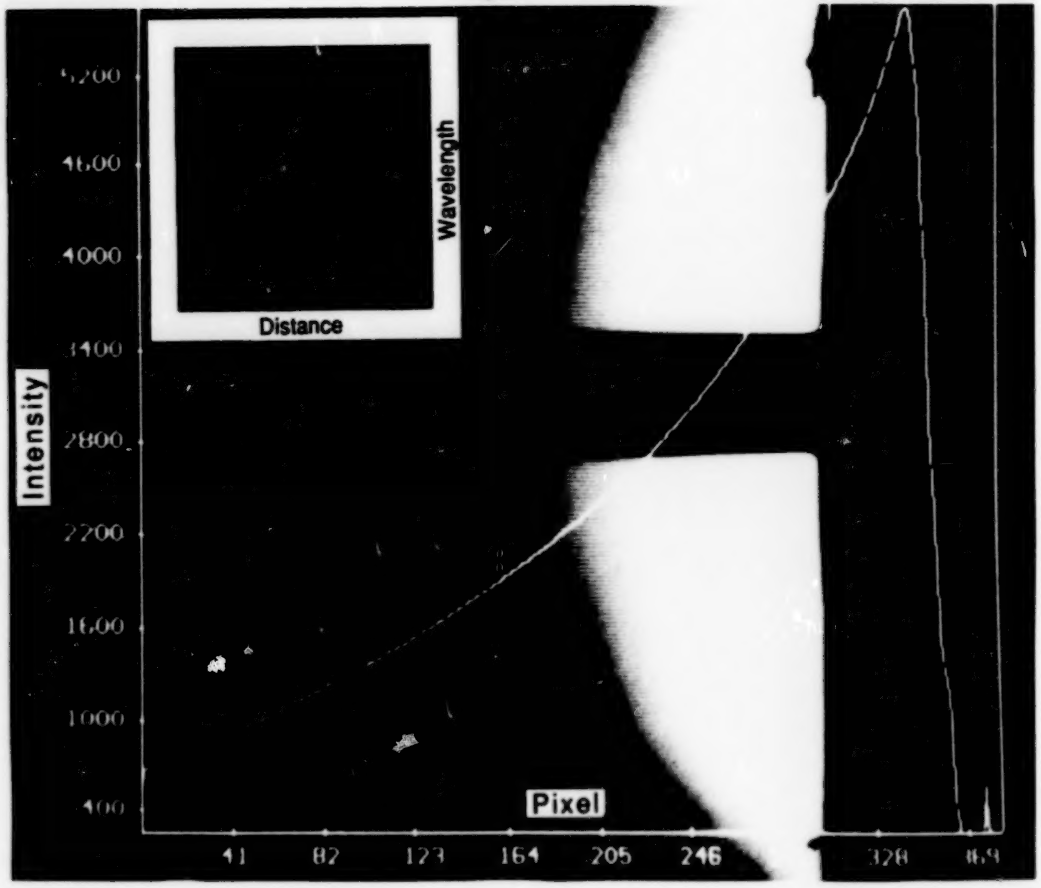

Figure 2

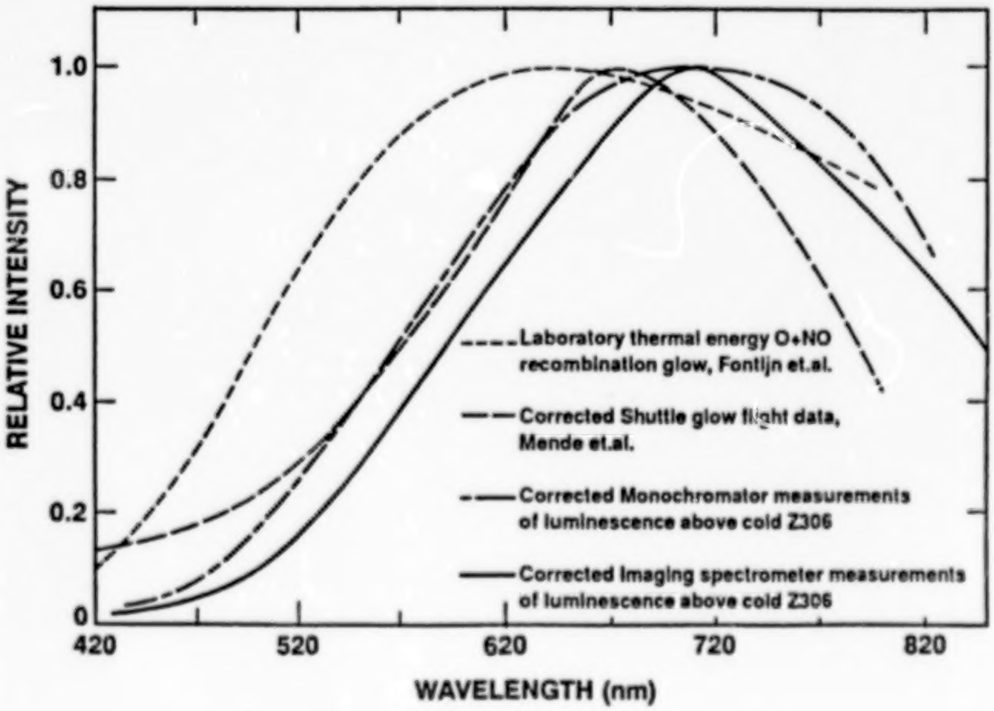

Figure 3

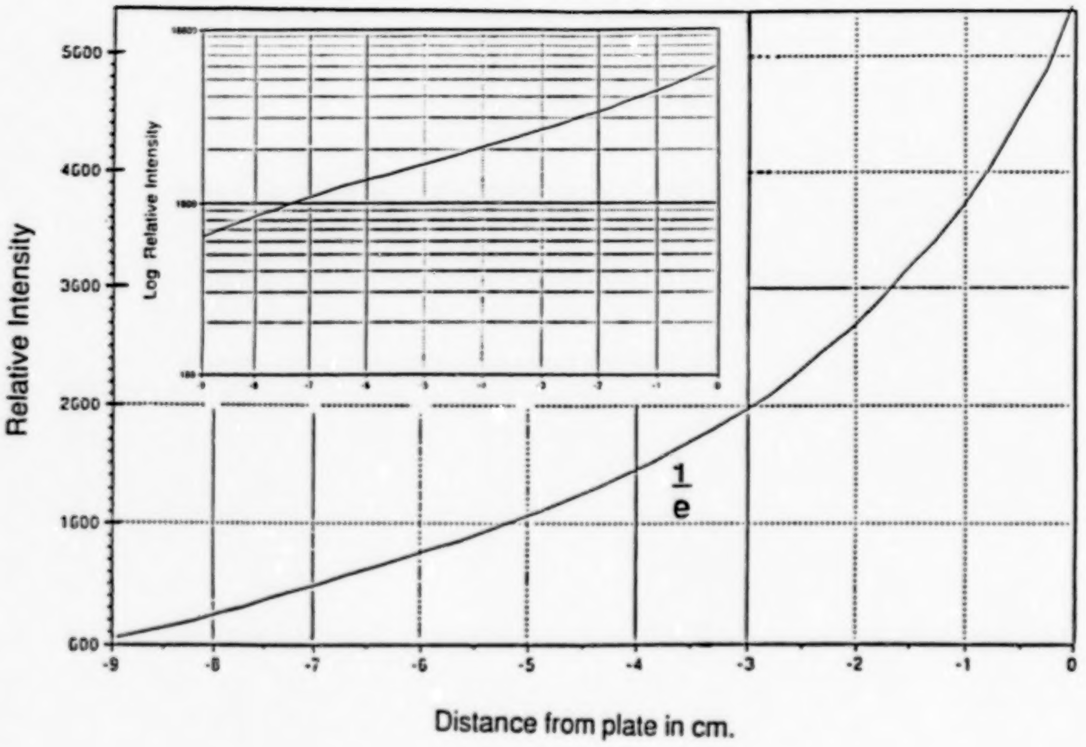

Figure 4

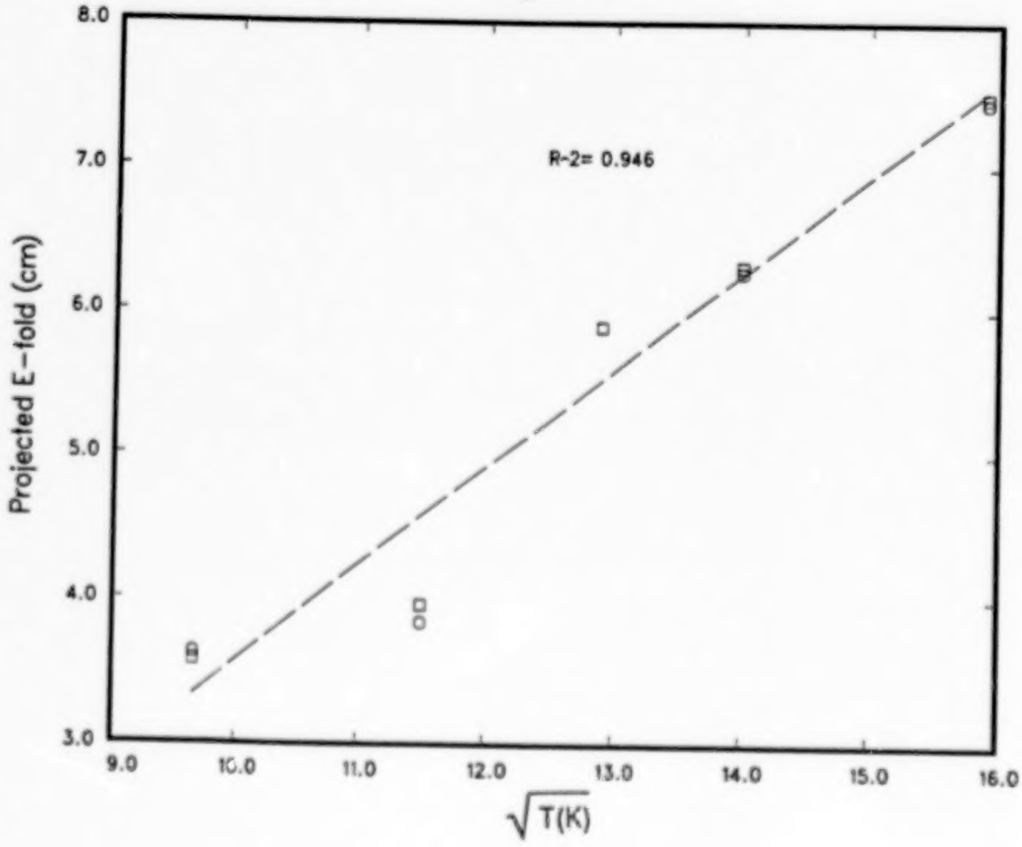

KINEMATICS OF ATOMIC OXYGEN-CARBON REACTIONS

W. C. Neely and T. Scrapchansky
Space Power Institute
Auburn University

(Paper not provided at publication date)

260

ATOMIC INTERACTION WITH MATERIALS

261

ATOMIC OXYGEN RESISTANT POLYMER FOR SPACE STATION SOLAR ARRAY APPLICATIONS

B. C. Petrie and H. Takeo
Lockheed Missile and Space Company
B. Sater
NASA/Lewis Research Center

(Paper not provided at publication date)

THE EFFECT OF ATOMIC OXYGEN ON POLYSILOXANE-POLYIMIDE FOR SPACECRAFT APPLICATIONS IN LOW EARTH ORBIT

Sharon K. Rutledge
NASA Lewis Research Center
Cleveland, Ohio

Jill M. Cooper and Raymond M. Olle
Cleveland State University
Cleveland, Ohio

ABSTRACT

Polysiloxane-polyimide films are of interest as a replacement for polyimide Kapton in the Space Station Freedom solar array blanket. The blanket provides the structural support for the solar cells as well as providing transport of heat away from the back of the cells. Polyimide Kapton would be an ideal material to use, however, its high rate of degradation due to attack by atomic oxygen in low Earth orbit, at the altitudes Space Station Freedom will fly, is of such magnitude that if left unprotected, the blanket will undergo structural failure in much less than the desired 15 year operating life. Polysiloxane-polyimide is of interest as a replacement material because it should form its own protective silicon dioxide coating upon exposure to atomic oxygen. This paper presents mass, optical and photomicrographic data obtained in the evaluation of the durability of polysiloxane-polyimide to an atomic oxygen environment.

INTRODUCTION

The Space Station Freedom solar array is being designed to provide the primary power for the first phase of the station (1). Polyimide Kapton (DuPont) was the material originally selected for the structural support of the solar cells for the flexible array. Its light weight, flexibility, strength and IR transparency made it an ideal material for this application. However, it is readily oxidized by atomic oxygen in the low Earth orbital (LEO) environment (2,3,4).

Single, neutral oxygen atoms in the ground state are the most predominant species in LEO between altitudes of 180 and 650 km (5). As spacecraft pass through the atmosphere at these altitudes, they collide with the oxygen atoms with an equivalent energy ranging from 3.3 to 5.5 eV (6). This is energetic enough to break many chemical bonds and allow the highly reactive atomic oxygen to oxidize many organic and some metallic materials (3). When atomic oxygen reacts with polymers it forms gaseous oxidation products (primarily CO) which results in material losses that can hinder system performance (7). The Space Station Freedom solar array is designed for a 15 year operating life in LEO, however, the oxidation rate of this material is great enough that structural failure of the blanket would occur in much less than 15 years. The current Space Station Freedom design utilizes a sputter deposited SiO_x (where x=1.9 to 2.0) for atomic oxygen protection.

A modified Kapton manufactured by DuPont designated as AOR (atomic oxygen resistant) Kapton has been proposed as a back up material for the Space Station Freedom solar array design. It is a polysiloxane-polyimide solid solution. Results of the testing of this material for atomic oxygen resistance is presented in this paper.

APPARATUS AND PROCEDURE

AOR Kapton

The AOR Kapton was manufactured by DuPont in an experimental batch process. It is a homogeneous dimethylpolysiloxane-polyimide film cast from a solution mixture. The dimethylpolysiloxane is added to the polyimide in an attempt to make the material resistant to attack by atomic oxygen since polysiloxane is a metal oxide former. Metal oxides are highly resistant to attack by atomic oxygen (3). The material lot # was RM449AAA. The material was received in 5 sheets from different portions of the processed roll. Four 2.54 x 2.54 cm atomic oxygen exposure samples were taken from each sheet in order to test for process uniformity. Since past testing of a different version of AOR Kapton (93-1) exhibited non-uniformity between the air and roll processing sides of the sheet, the four samples tested were sandwich samples with identical surfaces exposed to atomic oxygen (8). Acrylic adhesive from 3M was used to bond two adjacent sections of the sheet together that the samples were cut from. Two samples were prepared with the air sides out, and 2 with the roll side out on each sheet. In this manner, the durability to atomic oxygen could be determined separately for each side. Additional atomic oxygen exposure samples were prepared from sheet #3 as well as scanning electron microscope (SEM) samples (1.27 x 1.27 cm) and single thickness optical specimens. The optical specimens could not be sandwiched because the adhesive in the center would interfere with the measurement. Therefore, during atomic oxygen exposure only one side of the sample was exposed (air side) by placing the sample on top of a glass slide with the edges held down in close contact to the slide with a thick glass ring.

Atomic Oxygen Durability Testing

A plasma asher (SPI Plasma Prep II) was used to evaluate the atomic oxygen durability of the AOR Kapton. It uses a 13.56 MHz RF discharge to create an air plasma of oxygen and nitrogen ions and atoms in various energy states in a glass sample chamber kept at 80-100 mTorr. The nitrogen species have been shown to be relatively unreactive with polyimide in previous experiments (9). The species in the plasma impact surfaces placed in the plasma at thermal energies which is much lower than the energy in space but still energetic enough for chemical reactions to occur. The arrival at the surface is also omnidirectional while the arrival in space is more directed but sweeping, due to the rotation of the solar array to track the sun. The arrival flux (atoms striking/cm^2 of surface every second) is much greater than that in space. The combination of directionality and higher flux make the asher a more severe environment than space, but it can provide a qualitative indication of survivability since materials which survive in the asher also survive in LEO.

The atomic oxygen testing was performed in three different plasma ashers. The samples with the roll side out were placed in a separate asher for testing than those with the air side out because of observed contamination from the roll side of DuPont 93-1 that coated the polyimide Kapton HN witness coupon. All AOR roll position uniformity tests for a particular side were performed in the same asher. Exposure of additional mass loss coupons, optical, and SEM samples from sheet #3 of the roll were exposed in the third asher. All testing was performed with a polyimide Kapton witness coupon in the asher during testing. The mass loss of polyimide Kapton is well characterized in space and was used to correlate the different ashers as well as determine the effective atomic oxygen fluence (atoms striking during exposure/cm^2 of surface) in space that the asher exposure represented.

The AOR Kapton and polyimide Kapton witness coupons were dehydrated in a vacuum (30-50 mTorr) for at least 48 hours prior to the initial mass measurement of the sample and atomic oxygen exposure. This procedure was used to eliminate any errors in mass measurement due to water vapor from the atmosphere absorbing or desorbing from the polyimide. Although the effect of humidity on polyimide Kapton is quite large, AOR Kapton did not show any noticeable mass change due to humidity; however, it was dehydrated along with the polyimide Kapton so that both would be exposed to the same conditions. After atomic oxygen exposure, the Kapton was removed from vacuum and quickly weighed on a Sartorius microbalance to achieve an accurate mass value. The AOR was also weighed on the same balance.

Since three different ashers with glass racks supporting samples at two levels were used for sample exposure, it was important to determine the effect of the power level, intensity of the plasma, and the position in the asher on the atomic oxygen arrival flux. Since the plasma intensity is difficult to quantify, a solar cell connected to a current meter was placed against the asher glass to provide a relative intensity scale. Polyimide Kapton was used as a measure of the effective flux in the asher. Figure 1 contains a plot of the effective asher flux as a function of the power level meter reading. Each level indicated represents the multiple of 20 watts with 5 representing the full power of 100 watts according to the manufacturer. Test results indicate that the flux is independent of the power level for different tuned plasma intensities. Figure 2 indicates that the flux appears to be highly dependent on the intensity of the plasma and also shows its independence from the power level. As a result of these tests, the ashers were adjusted to roughly the same visual intensity during exposure of the AOR

Kapton. In each asher, the flux can also be dependent upon the position of the material in the asher. Flux is most likely highly dependent upon the amount of material placed in the asher since it changes the path of gas flow in the asher. Samples on a double rack fully loaded in the asher exhibit the flux arrivals shown in Figure 3. To determine the difference in arrival on the top and bottom of the samples, polyimide Kapton was used which had one side coated with silicon dioxide which could act as a barrier against atomic oxygen. The duration of the exposure was kept short in order to minimize any significant losses by undercutting of defects on the coated side. In general, the flux was more uniformly distributed on the bottom rack than on the top. On the bottom rack, the direction the Kapton faced did not seem to make a significant difference, however on the top rack, the Kapton facing up had a significantly larger flux. This is believed to be due to the proximity of the glass rack on the top level with respect to the gas inlet tube. The Kapton facing down had fluxes much closer to those on the bottom rack. Flux on the bottom rack appeared to decrease the farther the samples were from the roughing pump vent. Mass loss specimens were kept on the bottom rack for testing where possible and towards the back of the asher. Kapton witness coupons were placed in close proximity to the samples with a witness on each level so that flux variations and variations between ashers could be taken into account.

Durability Characterization

Durability to atomic oxygen was determined primarily through mass loss measurements and visual observation. Scanning electron microscopy using a JOEL 840 scanning electron microscope was used to document the visual changes occurring on the sample surface at different atomic oxygen fluence intervals. Total transmittance and reflectance measurements of the AOR Kapton representing different fluence intervals was taken with a Perkin Elmer Lambda 9 UV-VIS-NIR spectrophotometer with an integrating sphere attachment.

RESULTS AND DISCUSSION

Mass loss per area as a function of fluence was measured for AOR Kapton from each of the 5 sheets from the batch roll. Figure 4 contains the plots of this data for the air and roll sides. The data with the "*" by the number in the legend represents an adjacent piece from the same sheet which was included for improvement of test data reliability. The data indicates that the air and roll sides lose mass at very close to the same rate. The roll side may be slightly higher but is within the error of the mass measurement. The roll also shows a high degree of uniformity over the five sheets. The long term ashing test data in Figure 5 also agrees with that in Figure 4. Initially, the positional testing was to be used to determine uniformity of the roll only, with longer term ashing determining the durability. However, the AOR samples began to crack and split at a fluence of approximately 7×10^{21} atoms/cm^2 and fell apart completely at 9.5×10^{21} atoms/cm^2. One estimate for the total fluence that the SS Freedom solar array will encounter is 2×10^{22} atoms/cm^2 which is about twice the fluence experienced by the AOR when it structurally failed. The mass loss rate in comparison to Kapton is relatively constant for most of the exposure and is between 10 and 17 percent of that for unprotected Kapton HN. The AOR does provide an improvement over polyimide Kapton but still not enough to fulfill the SS Freedom life requirements.

Figure 6 contains a photograph of the optical samples that were exposed in the asher. Each sample represents a different atomic oxygen fluence level. The spots on the surface were believed to be caused by the remnants of a Si containing roll processing release agent which formed a thin film protective coating on the AOR Kapton. The unexposed sample has a barely visible spot of the release agent on its surface as well. The release agent coated areas offer limited protection due to the number of defects in the coating which increases with exposure. The samples which received roll side exposure were a slightly darker tan color overall in appearance with dark tan spots, while the air side was uniformly light tan with orange spots. The spots on the roll side behaved more like the overall AOR sample. In all other respects, both sides reacted the same. Eventually, the AOR begins to split and areas that were coated with release agent actually fall out as the AOR around them oxidizes through. The highest fluence sample in this photograph was too fragile to make an optical measurement on. The sample crumbled at the lower edge when trying to move it with tweezers. As exposure progressed, the once transparent surface became increasingly opaque as can be seen from the plot of transmittance as a function of wavelength at different fluence levels in Figure 7. The reflectance of the surface increased initially with fluence and then leveled off so that the net result was a slight increase in solar absorptance as shown in Figure 8.

Scanning electron photomicrographs of the AOR Kapton as a function of fluence are shown in Figure 9. The AOR Kapton at a fluence of 1.75×10^{21} atoms/cm^2 (Figure 9a) shows two areas with release agent surrounded by AOR Kapton. Initially, there is some cracking of the AOR but the majority of the cracking is centered around the release agent coated areas. With increasing fluence, cracking of the AOR becomes widespread until finally at 9.48×10^{21} atoms/cm^2, the majority of the AOR Kapton has lifted off of the surface leaving only a thin layer of AOR Kapton sections clinging to the adhesive used to bond the two sheets together. Figure 10 contains closeups of the AOR Kapton and release agent coated areas. Overall cracking of the AOR appears to occur quickly since full cracking was observed at 5.14×10^{21} atoms/cm^2. This represented a crack length per unit area increase from approximately 50 cm/cm^2 to nearly 120 cm/cm^2. Cracking of the release agent appeared to progress more linearly. A closeup of the AOR Kapton shows that the protection is particulate in nature. The surface exposed at the maximum test fluence still has particles clinging to the adhesive in a few locations but the matrix material is noticeably absent.

CONCLUSIONS

The experimental AOR Kapton evaluated for atomic oxygen resistance was found to exhibit a mass loss between 10 and 17% that of unprotected Kapton HN in the plasma asher. This is a significant improvement over polyimide Kapton, however the material does degrade and eventually structurally fails between 7 and 10×10^{21} atoms/cm^2 with a random atomic oxygen arrival. In space, the arrival of atomic oxygen is more directed and sweeping than in the asher so that the particulate sites of protection may provide more shielding of the matrix material allowing it to survive longer. However, this material is unlikely to meet the SS Freedom array lifetime without a thin film protective coating on the surface. A metal oxide coating would greatly improve the life of this material and the AOR Kapton underneath would add a backup safety factor to the coating since it is more durable than standard polyimide Kapton. A metal oxide coated AOR Kapton array blanket may be a viable solar array backup material for Space Station Freedom.

REFERENCES

1. Baraona, C.R., "The Space Station Power System," NASA TM-88847, Fifth Conference on Photovoltaic Generators in Space, Noordwijk, Netherlands, 1986.

2. Banks, B.A. et al., "Protection of Solar Array Blankets from Attack by Low Earth Orbital Atomic Oxygen," ISSN:0160-8371, Proceedings of the 18th Photovoltaic Specialists Conference, Los Vegas, Nevada, October 21-25, 1985.

3. Banks, B.A. and Rutledge, S.K., "Low Earth Orbital Atomic Oxygen Simulation for Materials Durability Evaluation,"Proceedings of the 4th International Symposium on Spacecraft in the Space Environment, Toulouse, France, Sept. 6-9, 1988.

4. Leger, L.J. and Visentine, J.T., "A Consideration of Atomic Oxygen Interactions with the Space Station," Journal of Spacecraft and Rockets, 23 (5) (1986), 505-511.

5. United States Committee on Extension to the Standard Atmosphere, U.S. Standard Atmosphere, 1976, U.S. Government Printing Office, Washington D.C., 1976.

6. DiFilippo, F., unpublished calculations, Case Western Reserve University, Cleveland, OH, 1989.

7. Golub, M.A., et al., "ESCA Study of Kapton Exposed to Atomic Oxygen in Low Earth Orbit or Downstream from a Radio Frequency Oxygen Plasma," Polymer Communications, 29, October, 1988.

8. Rutledge, S.K. and Mihelcic, J.A., "The Effect of Atomic Oxygen on Altered and Coated Kapton SUrfaces for Spacecraft Applications in Low Earth Orbit," Annual Meeting of TMS, Symposium on Materials Degradation in Low Earth Orbit, Anahiem, CA, 1990.

9. Rutledge, S.K., et al., "An Evaluation of Candidate Oxidation Resistant Materials for Space Applications in LEO," Workshop on Atomic Oxygen Effects, Pasadena, CA, 1986.

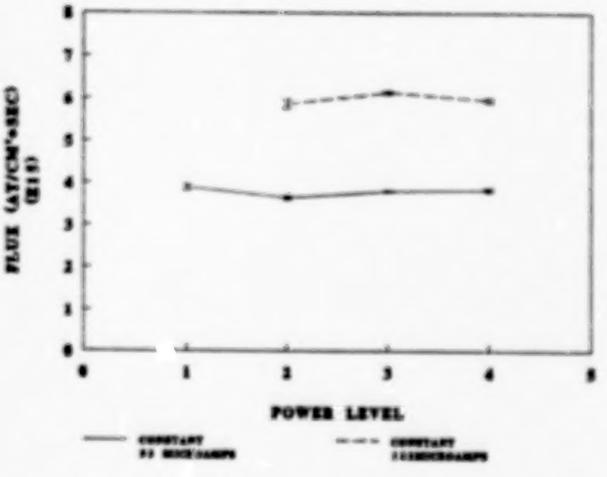

Figure 1 - Flux in the plasma asher as a function of the power level at constant plasma intensities.

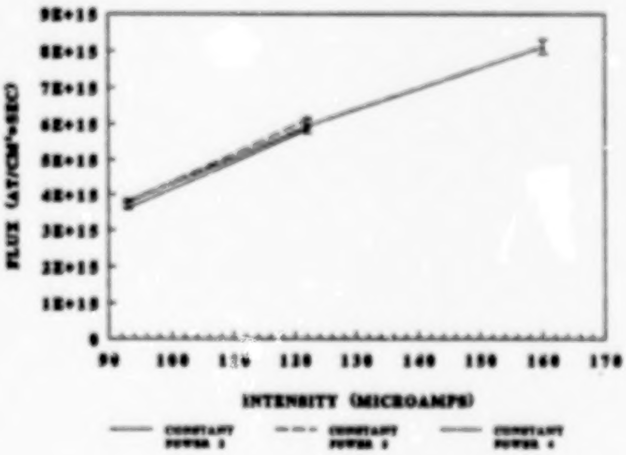

Figure 2 - Flux in the plasma asher as a function of plasma intensity at constant power levels.

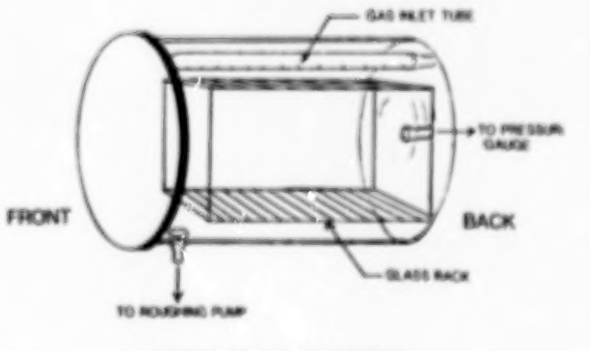
GAS INLET TUBE
TO PRESSURE GAUGE
FRONT
BACK
GLASS RACK
TO ROUGHING PUMP

ASHER GLASS CHAMBER

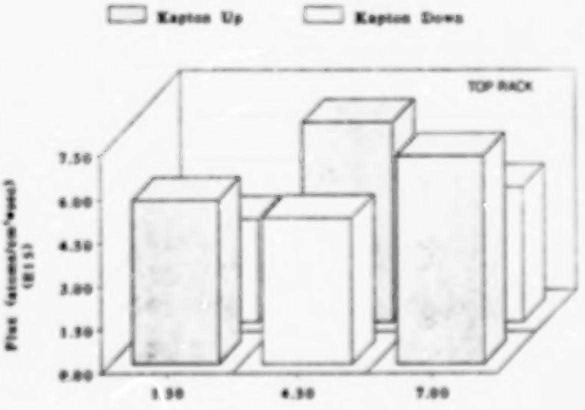

a. Asher top rack

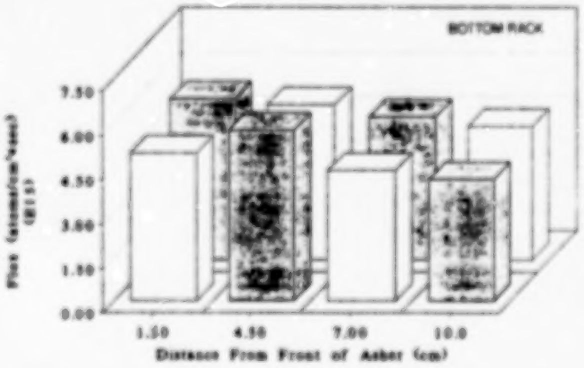

b. Asher bottom rack

Figure 3 - Flux as a function of position in the plasma asher.

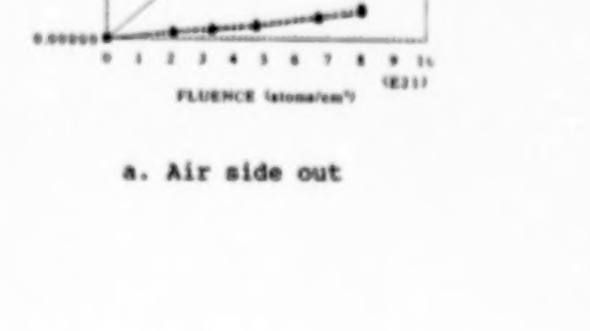

a. Air side out

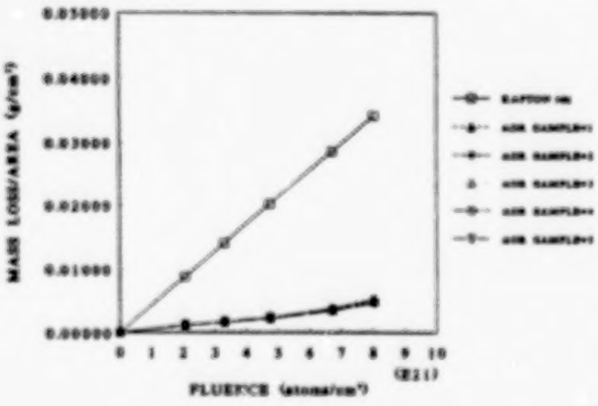

b. Air side out

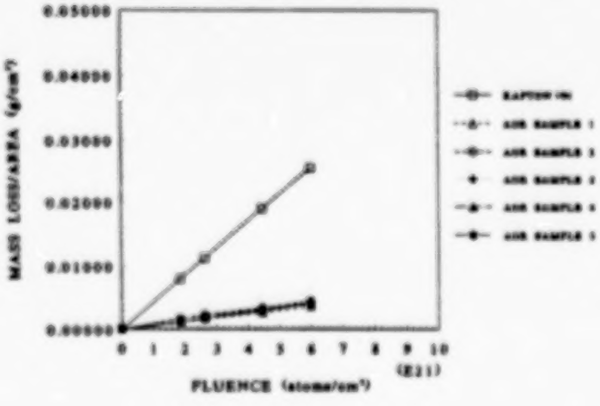

c. Roll side out

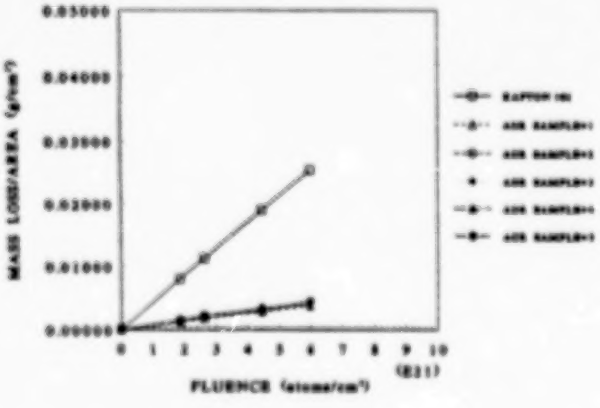

d. Roll side out

Figure 4 - Mass loss per area as a function of atomic oxygen exposure for air and roll side samples from different sheets of Kapton AOR.

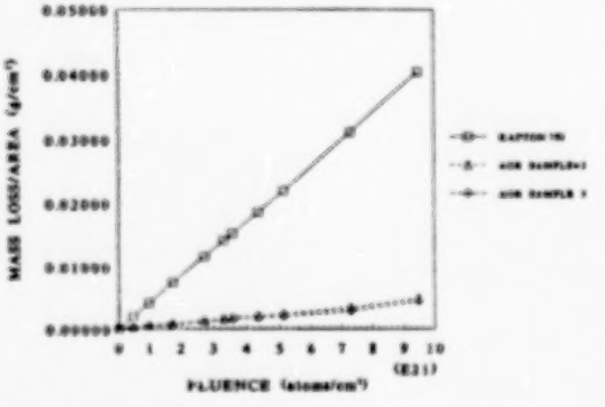

a. Air side out

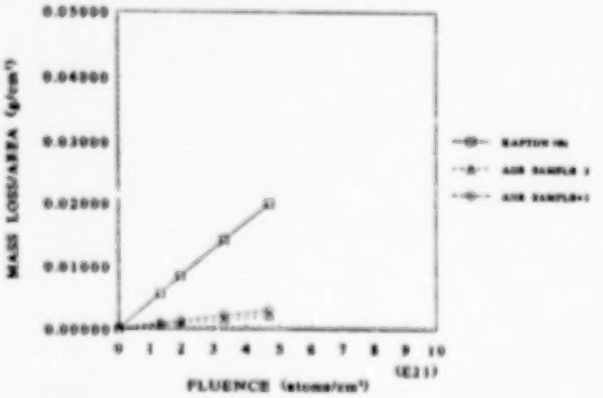

b. Roll side out

Figure 5 - Long term atomic oxygen exposure of AOR Kapton from sheet 3.

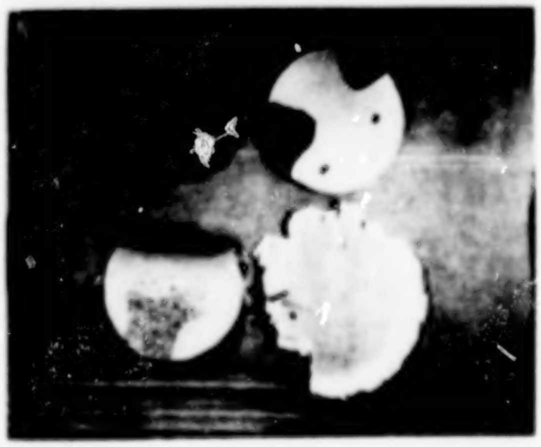

Figure 6 - Photograph of AOR Kapton optical samples exposed to various fluence levels; top left: 0 atoms/cm^2, top right: 1.75x10^{21} atoms/cm^2, bottom left: 5.14x10^{21} atoms/cm^2, and bottom right: 7.31x10^{21} atoms/cm^2.

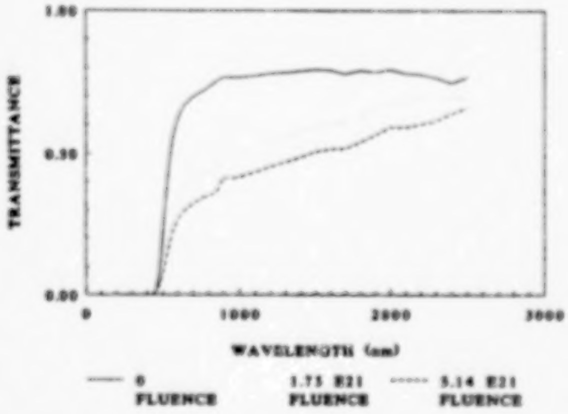

Figure 7 - Total transmittance of AOR Kapton from sheet 3 as a function of atomic oxygen exposure.

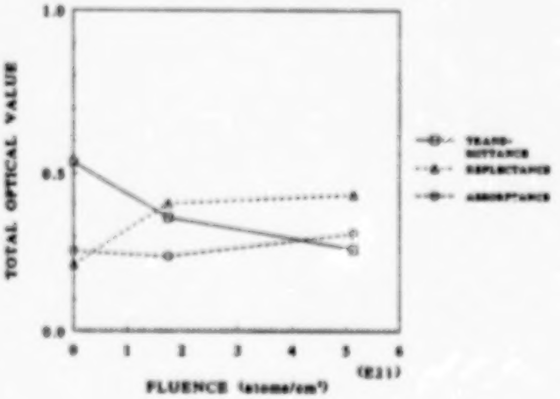

Figure 8 - Optical properties of AOR Kapton from sheet 3 as a function of atomic oxygen exposure.

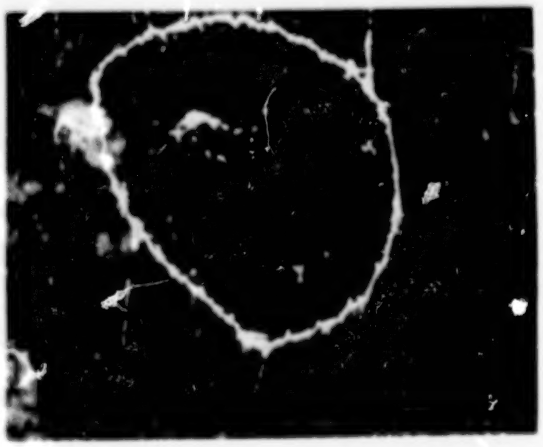

a. 1.75×10^{21} atoms/cm^2

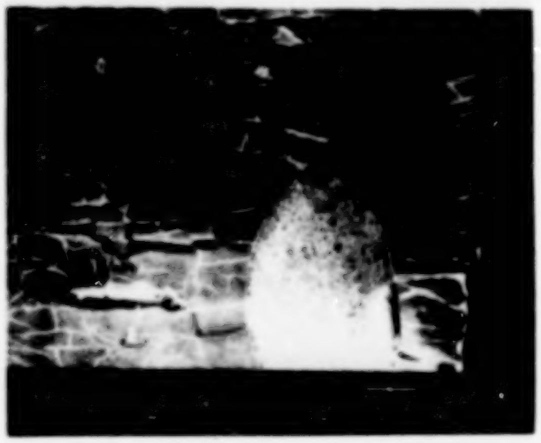

b. 5.14×10^{21} atoms/cm^2

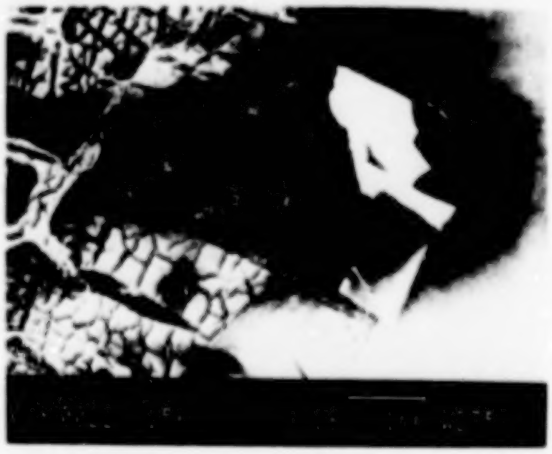

c. 9.48×10^{21} atoms/cm^2

Figure 9 - Scanning electron photomicrographs of AOR Kapton from sheet 3 (air side out) as a function of atomic oxygen exposure.

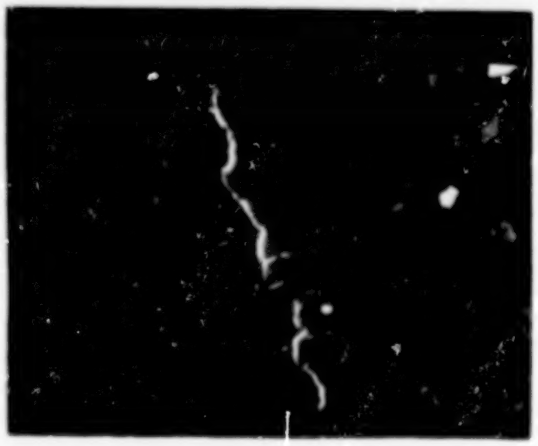

a. 0 atoms/cm^2

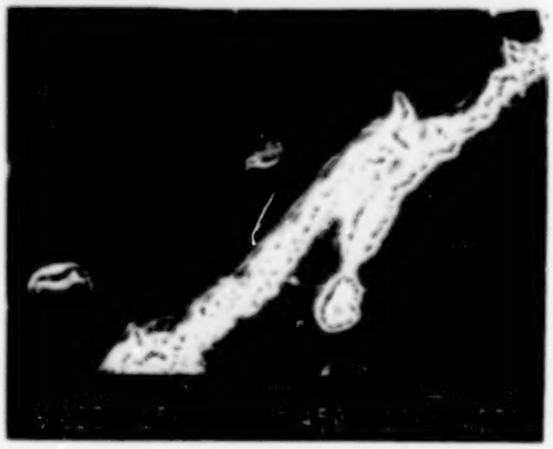

b. 1.75×10^{21} atoms/cm^2

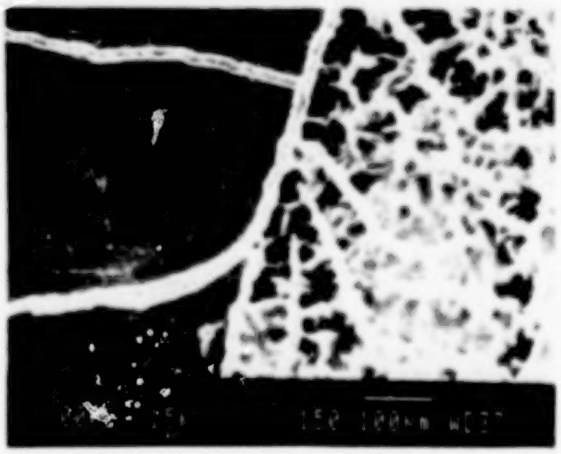

c. 5.14×10^{21} atoms/cm^2

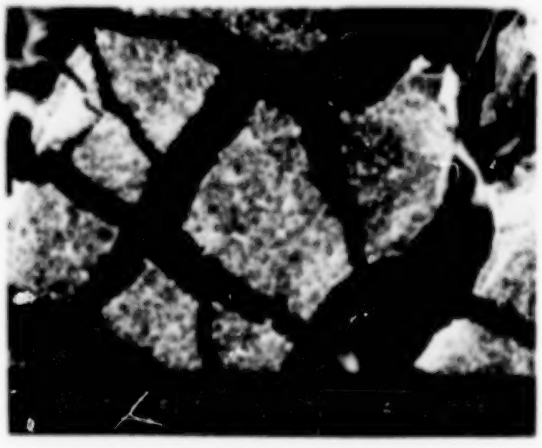

d. 9.48×10^{21} atoms/cm^2

Figure 10 - Scanning electron photomicrographs of AOR Kapton from sheet 3 (air side out) as a function of atomic oxygen exposure.

a. 1.75×10^{21} atoms/cm^2

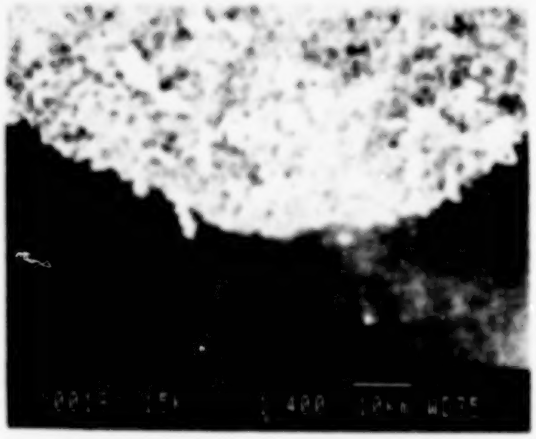

b. 9.48×10^{21} atoms/cm^2

Figure 11 - Scanning electron photomicrographs of AOR Kapton from sheet 3 (air side out) showing particulate nature of the protection.

PRELIMINARY OBSERVATIONS ON THE LDEF/UTIAS COMPOSITE MATERIALS EXPERIMENT AND SIMULATOR RESULTS ON PROTECTIVE COATINGS

R. C. Tennyson, W. D. Morison, J. S. Hansen, W. E. R. Davies, and J. Unger
University of Toronto
M. R. Wertheimer
Ecole Polytechnique
D. G. Zimcik
Canadian Space Agency

(Paper not provided at publication date)

271

CHARACTERIZATION OF A 5-EV NEUTRAL ATOMIC OXYGEN BEAM FACILITY

J. A. Vaughn, R. C. Linton, M. R. Carruth, Jr., and A. F. Whitaker
NASA/Marshall Space Flight Center
Huntsville, AL 35812

and

J. W. Cuthbertson, W. D. Langer, and R. W. Motley
Princeton Plasma Physics Laboratory
Princeton, NJ 08453

ABSTRACT

An experimental effort to characterize an existing 5-eV neutral atomic oxygen beam facility being developed at Princeton Plasma Physics Laboratory (PPPL) will be described. This characterization effort includes atomic oxygen flux and flux distribution measurements using a catalytic probe, energy determination using a commercially designed quadrapole mass spectrometer (QMS), and the exposure of oxygen-sensitive materials in this beam facility. Also, comparisons were drawn between the reaction efficiencies of the materials exposed in this facility, the reaction efficiencies of materials exposed in plasma ashers, and the reaction efficiencies previously estimated from space flight experiments. The results of this study show that the beam facility at PPPL is capable of producing a directional beam of neutral atomic oxygen atoms with the needed flux and energy to simulate low Earth orbit (LEO) conditions for real time accelerated testing. The flux distribution in this facility is uniform to ±6% of the peak flux over a beam diameter of 6 cm.

INTRODUCTION

The recent return of the Long Duration Exposure Facility (LDEF) provided startling evidence of how volatile the LEO environment is on materials. One of the most material destructive constituents in the LEO environment is atomic oxygen which oxidizes many metals and erodes the surface of many polymers. Considering the expense and logistical demands of doing flight experiments, such as LDEF, for investigating a materials susceptibility to atomic oxygen, the need for a ground-based facility capable of simulating the LEO atomic oxygen environment exists. The requirements of a facility capable of simulating LEO atomic oxygen conditions are: (1) the beam facility must be able to produce a high energy, directional beam of atomic oxygen atoms (i.e., the atom would have an energy equal to the mass of the atomic oxygen atom times the orbital velocity of the spacecraft of 5 eV for atomic oxygen atoms); and (2) the beam facility should produce a flux of atomic oxygen compatible with LEO mission-integrated flux in a reasonable test period (i.e., at least a flux in the range of 10^{14} to 10^{16} atoms/cm^2•s).

The 5-eV neutral atomic oxygen beam facility discussed in this paper was developed at PPPL under contract with NASA/Marshall Space Flight Center (MSFC). This neutral beam system is capable of producing atomic oxygen atoms with a flux of 10^{15} to 10^{16} atoms/cm^2•s and an energy of 4 to 20 eV which meets the previously stated requirements. Also, the facility has features which make it possible to study the combined effects of UV and other LEO environmental concerns on materials.

The results of this study include a direct measurement of the atomic oxygen flux in this beam facility using a catalytic probe similar to the one described by Carruth et al. [1] and a measurement of the flux uniformity by evaluation of material erosion at discrete intervals across the beam diameter. Reaction efficiencies from materials exposed in this facility and the reaction efficiencies of materials exposed in ground-based plasma ashers are compared to the published reaction efficiencies of materials exposed during the STS-8 and STS-41G missions. This comparison includes graphic evidence of the enhanced simulation of the surface morphology effects of LEO atomic oxygen with a directional beam then with plasma ashers. Scanning electron microscope (SEM) photographs will be shown to demonstrate how this beam facility closely reproduces the surface morphology of materials that have been exposed to atomic oxygen during flight experiments. The SEM photos of the flight and PPPL neutral atom beam facility exposed materials will be compared to materials exposed in plasma ashers at MSFC.

ATOMIC OXYGEN BEAM FACILITY

The PPPL atomic oxygen beam facility produces a low energy neutral atomic oxygen beam by placing a metal plate in contact with a magnetically confined (3 to 4 kG) oxygen plasma. The oxygen plasma is produced by a radio frequency (RF)-driven lower hybrid source [2] which operates on molecular oxygen gas. A magnetron supplies 1 kW of power at an RF frequency of 2.45 GHz to the center pin to break down the gas. The RF frequency of this facility produces a plasma with complete dissociation of the molecular oxygen gas [3]. Because of the intense heat built up on the center pin, the plasma source is currently pulsed at a 5% to 15% duty cycle over a few milliseconds. Cycling the plasma source in this manner enables the beam source to operate in oxygen for over 100 hours per pin. The plasma is confined by a magnetic field (3 to 4 kG) which produces an intense plasma column about 1 cm in diameter. Because of the tightly confined plasma column, the neutral atom distribution beyond the neutralizer plate is well collimated. The metal neutralizer plate is biased negative of plasma potential, and plasma ions are accelerated toward the surface of the plate by an energy determined by the potential difference between plasma potential and the plate bias. The ions impact and are reflected from the neutralizer plate picking up an electron in the process. The reflection is designed to be an inelastic reflection causing the atoms to lose a fraction of their energy. The fraction of energy retained by each atom depends primarily on the ratio of the particle mass to the neutralizer plate atomic mass. Because the energy of each particle depends on plasma potential and not all ions exit at the same potential, not all ions will be reflected at the same energy, producing a small spread in energy.

The lower hybrid plasma source is capable of supplying 4 amps of atomic oxygen ions to the neutralizer plate per pulse producing an estimated flux of $>5x10^{16}$ atoms/cm^{2}*s atomic oxygen atoms 10 cm from the neutralizer plate. The average integrated flux over the entire duty cycle is $1x10^{15}$ to $7x10^{15}$ atoms/cm^{2}*s at this same axial position. The limiting factor in the flux level for this beam facility is the duty cycle of the plasma source.

ATOMIC OXYGEN BEAM FACILITY DIAGNOSTICS

Energy Diagnostics

A commercially designed energy-analyzing QMS was used to detect the energy of the neutral atoms in this facility. The QMS is a standard QMS with a cylindrical mirror energy analyzer downstream of the quadrapole rods. With this instrument, a neutral beam entering the ionizing chamber can be scanned measuring both the energy spectrum of a particle at a single mass or the mass spectrum at a single energy. Special pumping stages were designed to incorporate the QMS in the neutral beam facility to minimize scattering of the incoming high energy atomic oxygen atoms and reduce the production of energetic atomic oxygen atoms (Franck-Condon atoms) created by the dissociation of molecular oxygen in the ionizing region of the QMS.

The energy measurements to date have been limited to monatomic gases such as argon and krypton. These measurements were compared to calculations using the TRIM model [3]. The beam energy and energy spread with these measurements agreed well with the TRIM calculations. The atomic oxygen energies presented in this paper have been estimated from the plasma potential, the neutralizer bias, and using conservation of momentum results from argon and krypton gases. Attempts to measure molecular gases like nitrogen and oxygen have been unsuccessful to date because of complicating effects caused by the dissociation of the thermal background molecules in the QMS ionizing section. A further reduction in background pressure is being considered to eliminate the background molecules.

Atomic Oxygen Flux Diagnostics

A special catalytic probe for monitoring the atomic oxygen flux was designed for use in this neutral beam facility. The catalytic probe was modeled after the one used by Carruth et al. [1] in a conventional plasma asher. The catalytic probe uses silver oxide as the catalyst to produce an increase in temperature caused by the recombination of atomic oxygen atoms on the surface of the catalyst. Since the inelastic collisions of the high energy neutral atoms with the catalytic probe also cause the probe to heat up, a method to account for this heating was devised. The catalytic probe designed for this facility consisted of two thin (approximately 1-mm thick) circular glass substrates with a type k thermocouple attached to the back. One probe was coated with 1,000 angstroms of silver and oxidized in an oxygen plasma atmosphere, while the other probe was left uncoated. The silver oxide probe was used as the active probe to measure the flux of atomic oxygen atoms in the facility, and the plain glass probe was used as a dummy probe to monitor the increase in the catalytic probe temperature due to the atomic oxygen atoms impacting on the catalytic probe surface. A separate thermocouple was placed near the chamber wall to measure the ambient temperature.

A simple first-order model was developed to make flux calculations from the recorded temperature data. The model assumes that both the catalytic probe and the dummy probe radiate their heat to the surrounding environment, and that conduction and convection heat losses were negligible. Because the thermocouple wire is the only heat conductive path possible and the wire is very thin, the assumption is correct to a first order approximation. The model also takes into account the energy of atomic oxygen recombination on the catalyst (5.2 eV per every two atoms [4]) and the fact that only a fraction of incoming atoms recombine on the surface of the probe (i.e. recombination coefficient).

A literature search shows that the value of the recombination coefficient used in previous work ranged from 0.25 to 1 [1]. Carruth et al. [1] assumed that the recombination coefficient for atomic oxygen on silver oxide was near unity for the work they did in an oxygen plasma asher knowing that some inaccuracy may exist. Because the inelastic collisions of the incoming atomic oxygen atoms with the silver oxide surface scatters a fraction of the atoms away, the recombination coefficient in the work in this paper was assumed to be 0.5. This assumption is inherently uncertain to within a factor of two because of the uncertainty in the scattering efficiency of the atomic oxygen atoms during the collision. However, data will be presented comparing the flux computed from catalytic probe temperature data and flux data from ion current measurements. Also, data showing the error in the recorded flux measurements caused by varying the recombination coefficient from 0.25 to 0.75 will be shown.

Below is the final result of the model. Equation (1) was used to make the atomic oxygen flux calculations for this particular study.

$$\text{flux} = \frac{1.4\text{x}10^7}{n}\left[e_p\,(T^4{}_p - T^4{}_w) - \frac{A_{gp}e_{gp}}{A_p}\,(T^4{}_{gp} - T^4{}_w)\right] \tag{1}$$

In equation (1) the constant ($1.4\text{x}10^7$) takes into account the 5.2-eV energy per every two atoms of recombination and converting the flux into the correct units of atoms/cm^2*s. The values of the emissivity and the area of both the active probe and the glass probe are listed as e_p, A_p and e_{gp}, A_{gp}, respectively. The silver oxide probe emissivity was 0.85, and the glass probe emissivity ranged from 0.7 to 0.8. The area of both probes was the same. Finally, n represents the recombination coefficient.

MATERIAL EXPOSURE PROCEDURE

Samples exposed to the atomic oxygen neutral beam were placed in an aluminum sample holder and insulated from the metal to keep them from being heated as the aluminum increased in temperature during operation of the plasma source. A type K thermocouple was placed in contact with the rear surface of the specimen for continuous monitoring. The samples were placed in the PPPL neutral beam facility at a location 8 to 10 cm downstream of the neutralizer plate.

The atomic oxygen beam was turned on when a pressure of 10^{-6} torr was reached inside the vacuum vessel. The samples were exposed to an atomic oxygen flux of $1\text{x}10^{15}$ to $7\text{x}10^{15}$ atoms/cm^2*s for 1 to 12 hours, depending on the desired fluence. The temperature was recorded as well as the ion current to the neutralizer plate at intervals during the exposure process. The ion current was measured by biasing the neutralizer sufficiently negative to repel all electrons from reaching the plate. This process lasted only a few seconds to minimize the effect on the samples.

The flux of atomic oxygen atoms arriving at the surface of the sample was calculated using a $1/R^2$ dependence (the $1/R^2$ dependence was measured and the data is shown in Fig. 3 of this paper). Equation (2) was used to calculate the atomic oxygen flux using the measured ion current data.

$$\text{flux} = \frac{J_n\ DC}{q\pi\ z^2}\,K \quad . \tag{2}$$

In this equation, J_n is the ion current hitting the neutralizer plate, DC is the duty cycle, q is the electronic charge, z is the axial distance from the neutralizer, and K is a constant. The factor K takes into account scattering of the neutral atoms due to collisions with molecules, the cosine distribution of the atoms leaving the plate, and the efficiency of the neutralizer plate to produce neutral atoms. This factor was calculated to be 0.5 based on available data.

NEUTRAL BEAM DIAGNOSTIC RESULTS

Beam Energy Data

Preliminary energy results using krypton reflecting off a tantalum neutralizer plate are shown in Fig. 1. The voltage bias (V_n) on the tantalum neutralizer plate for this set of data was -10 V. Figure 1 is a plot of QMS intensity as a function of beam energy. This QMS neutral beam profile shows that the krypton neutral beam has a peak energy of 7 eV and beam energy spread defined by the full-width-half-maximum (FWHM) of ±3 eV. The large signal in the few eV range, which is typical of all profiles taken in the PPPL neutral beam facility, is caused by the background pressure. The beam energy profile shown in Fig. 1 is typical of all QMS profiles taken with argon and krypton. Future work in this area will concentrate on producing reliable energy measurements of atomic oxygen by reducing the background pressure.

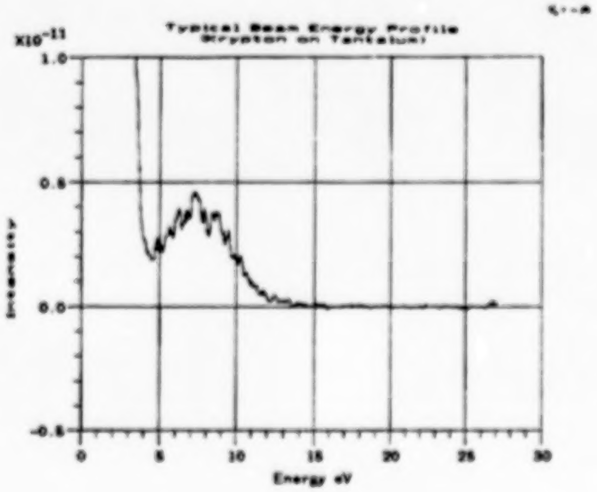

Figure 1 - Typical QMS Neutral Beam Energy Profile (Krypton on Tantalum Neutralizer Plate)

Atomic Oxygen Flux Results

Measurement of the flux and the flux distribution of the neutral atomic oxygen beam has shown much consistency. The flux level has been detected using the catalytic probe described earlier and verified from mass loss data of high density polyethylene (HDPE) exposed for a known period of time. Figure 2 shows the flux calculated using the temperature measured by the catalytic probes at various times over an 80-minute test period. The squared symbols indicate the atomic oxygen flux computed using equation (1), and the dashed line shows the atomic oxygen flux computed by measuring the ion current impinging on the neutralizer plate. The flux computed from catalytic probe temperature measurements agree well with the flux computed from the ion current measurements. The rise in the flux level at 42 minutes was caused by an increase in the duty cycle of the plasma source. The increase in the duty cycle was done deliberately to demonstrate the ability of the catalytic probe to adjust its temperature with a change in the level of atomic oxygen flux in the vacuum chamber. It should be noted that because the catalytic probe does not cool down quickly, all tests were done by starting at the lowest atomic oxygen flux level and working toward the highest in order to get a response in a reasonable amount of time. The error bars associated with computed flux from the catalytic probe temperature data signify the amount of uncertainty induced by varying the recombination coefficient (n in equation (2)) from 25% to 75% and by taking into account the uncertainty involved in the emissivity of both the glass and catalytic probes. Samples of HDPE were exposed to the same conditions as those data in Fig. 1. HDPE was used to make flux calculations based on the mass loss data because HDPE is not hydroscopic. The results of mass loss data similarly indicate the flux varied from $1.5x10^{15}$ and $4x10^{15}$ atoms/cm^2*s at the 5% duty cycle.

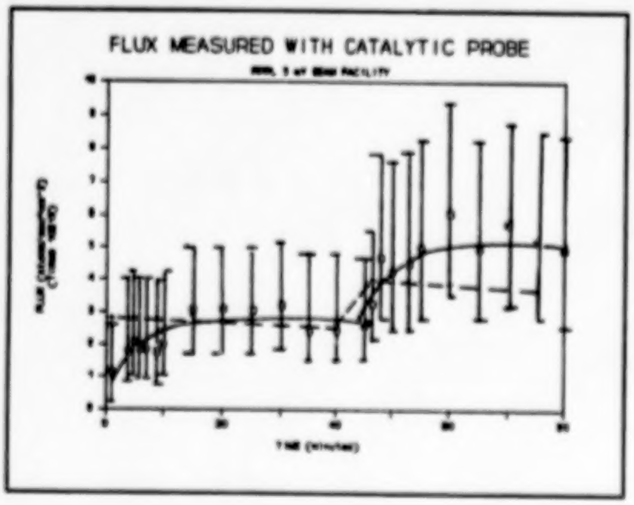

Figure 2 - Flux of Atomic Oxygen Atoms Measured With a Catalytic Probe

Figure 3 shows the atomic oxygen flux computed from catalytic probe temperature measurements made at three axial positions in the vacuum chamber. These measurements were made to demonstrate the $1/R^2$ dependence of the atomic oxygen flux in this chamber. The line in Fig. 3 represents the $1/R^2$ dependence line which was computed knowing the flux of atomic oxygen atoms just leaving the surface of the neutralizer plate and correcting the flux at incremental axial positions. The data points in Fig. 3 were computed from the mean catalytic probe temperature measured over a 15-minute period. The error bars indicate the spread in the flux computations caused by the variation in the measured temperature data. This figure indicates that the atomic oxygen flux closely follows the prescribed $1/R^2$ distribution.

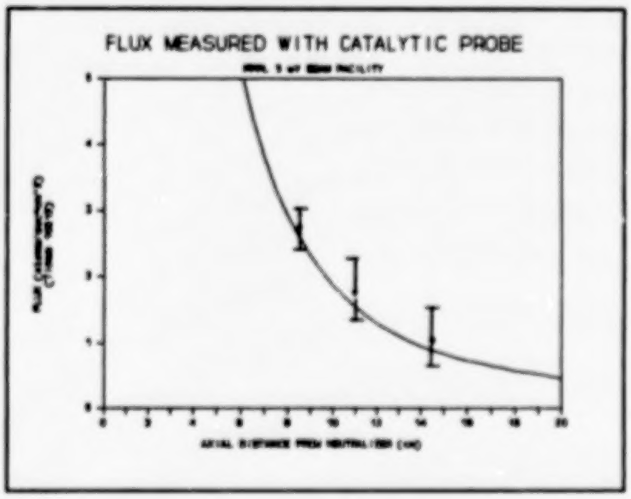

Figure 3 - Dependence of Atomic Oxygen Flux on Axial Distance

The flux uniformity in the sample exposure region was also measured from the mass loss data of 1.5 mil HDPE spaced equally across the specimen exposure plane. The flux calculations were made using the published reaction efficiency for polyethylene of $3.7x10^{-24}$ cm^3/atom [5]. The results of the flux distribution in the PPPL beam facility are shown in Fig. 4. The angle of the neutralizer plate was set to provide the highest flux down the center (or 0 cm radial distance) of the specimen exposure plane. The angle of the neutralizer was set at 35 degrees from the center of the sample region to the normal of the neutralizer plate. The square data points are the flux data computed from the measured mass loss of each polyethylene sample, and the inverse triangular symbols are for the flux data computed from the ion current data and corrected for the $1/R^2$ dependence from the center of the neutralizer plate. In this case, the flux computed from the mass loss data is four times higher than that indicated by the ion current measurements. The discrepancy in the data is not known at this time, but there is evidence that indicates the reaction efficiency may depend on the energy of incident atoms [6]. The higher energy atoms in the PPPL facility, with a higher reaction

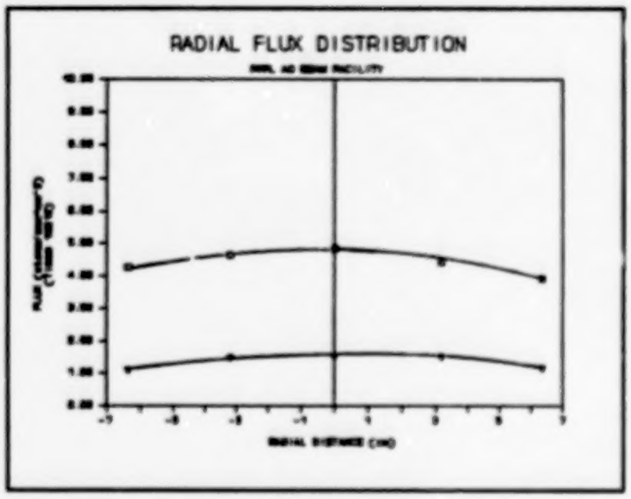

Figure 4 - Atomic Oxygen Flux Distribution in PPPL Beam Facility

efficiency, would lower the calculated flux. However, from a relative perspective, it is important to notice that the peak in both curves occurs at the center of the vacuum chamber, and the flux decreases 11% over a 13-cm beam diameter with the plate positioned at this angle. A question arose during these tests as to the extent the uniformity would be affected by a rotation in the plate. This question was addressed in a second 1.5-mil HDPE sample exposure. The same procedure was followed, except the plate was rotated 20 degrees from the first position (i.e., the normal of the plate was 55 degrees from the horizontal axis down the center of the sample chamber). Figure 5 shows the atomic oxygen flux distribution in the sample chamber measured from this test. It should be noted that the energy was intentionally reduced closer to 5 eV during this test to get the data in better agreement. The peak atomic oxygen flux in this case has shifted from the center of the vacuum vessel toward the right side of the vacuum chamber, but the uniformity has not changed. The atomic oxygen flux still decreases 6% 3.2 cm from the location of the peak atomic oxygen flux.

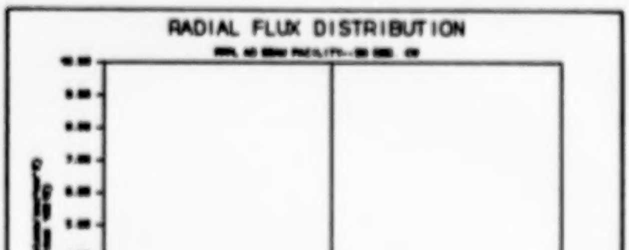

Figure 5 - Atomic Oxygen Flux Distribution in PPPL Beam Facility

Atomic Oxygen Beam Directionality

In order to examine the directionality versus the randomness of the atomic oxygen beam at the test sample location, experiments were conducted to address this question. Polycarbonate (LEXAN) samples were spaced evenly across the specimen exposure plane and exposed to a known fluence of atomic oxygen. Polycarbonate was chosen for this test because its crystalline structure preferentially etches under the attack of atomic oxygen [9]. The samples were covered with a transparent (90%) nickel mesh screen to protect a portion of the sample from atomic oxygen atoms. If the beam is directional, then the samples should be etched in the unprotected area producing a checkerboard pattern that has near vertical, uniform edges. If the beam is random, the checkerboard pattern will still be observed, but the face of the raised edges will not be vertical and uniform.

Figure 6 is an SEM photograph of the polycarbonate surface. The surface features shown in this photograph are typical of all the samples exposed in the beam. In Fig. 6, the light-colored area is the area attacked by the atomic oxygen, and the dark-colored area was protected by the screen. The SEM photograph shows that a distinct checkerboard pattern was etched in the polycarbonate sample by the atomic oxygen beam. One interesting characteristic of this photo which confirms the beam directionality is the sharp, square corners observed. A measure of the atomic oxygen erosion depth, and how straight and uniform the atomic oxygen eroded the polycarbonate, is shown in Fig. 7. The data shown in Fig. 7 were taken using a Dektak II surface profilometer, by scanning across one individual square. Fig. 7a is a scan across one of the squares etched in the polycarbonate samples, and

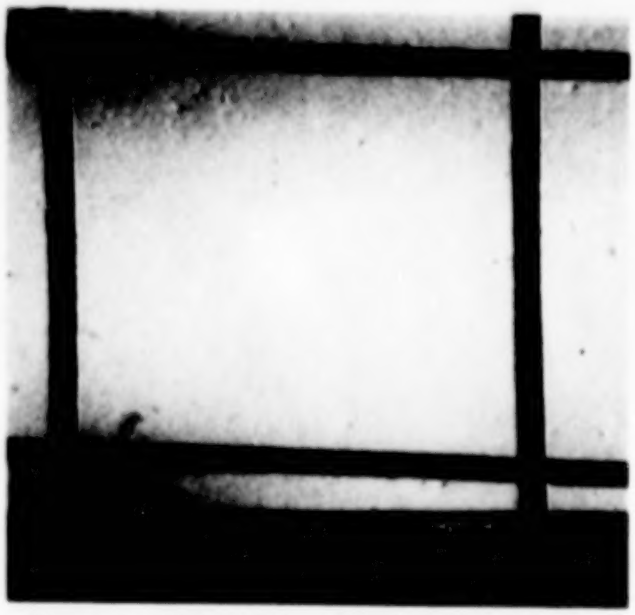

Figure 6 - SEM of Polycarbonate Covered With Nickel Screen Exposed in PPPL Neutral Beam Facility

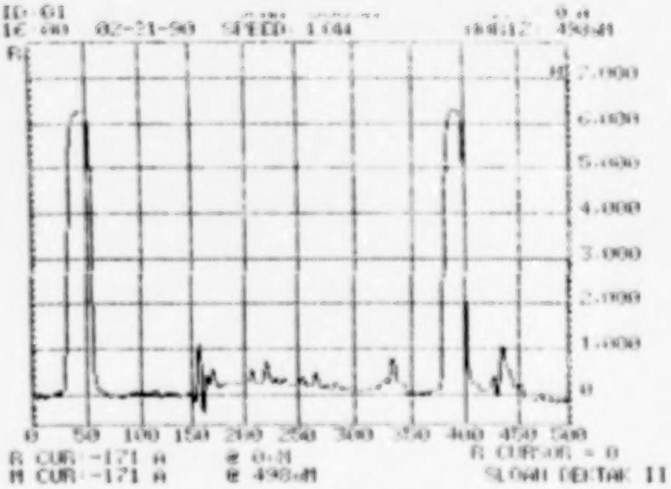

7(a)

Rotated 90°

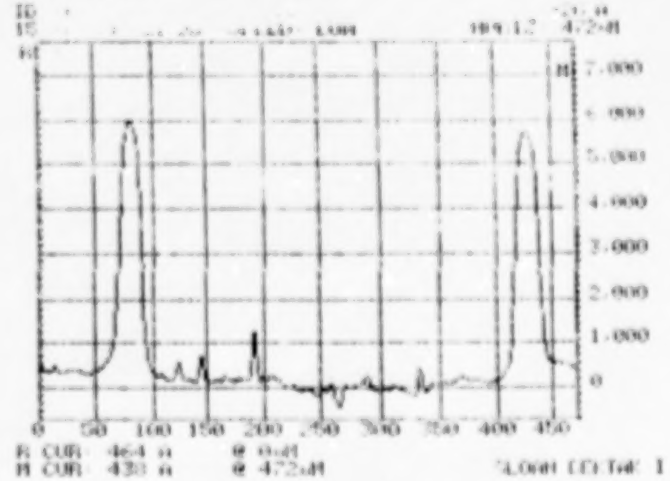

7(b)

Figure 7 - Polycarbonate Depth Profile

Fig. 7b is the same etched square rotated 90 degrees. These data indicate that the atomic oxygen etched the polycarbonate to a depth of 6,000 angstroms, and these traces show the precise, sharp edge between the unexposed and exposed polycarbonate. Comparing the distance between the two raised edges of each profile shows the etched area to be close to a perfect square. These data provide evidence that the neutral beam in this facility is likely directional.

COMPARISON OF VARIOUS ATOMIC OXYGEN EXPOSED MATERIALS

The effectiveness of this neutral beam facility in simulating the LEO atomic oxygen environment can be judged by comparing the results of material tests done in this facility to space flight material tests. The data compiled to make this comparison are shown in Table I. The data presented in this table were taken from various flight experiments [5,7,8] flown on STS-8 and STS-41G, the results of material tests done in the PPPL neutral beam facility, and material tests done in plasma ashers at MSFC. The data from which these results were compiled are for the same sample temperature. The results of this comparison show the reaction efficiency of the PPPL neutral beam facility to accurately reproduce the data from flight results. It should be noted that a large error was induced in the reaction efficiency of the kapton sample because of the hydroscopic nature of the sample and poor control over mass measurements to determine mass loss.

Table I - Reaction Efficiency of Atomic Oxygen (AO) Exposed Materials
(Reaction Efficiencies in units of cm^3/atoms)

	Kapton-H 2 mil	Black Kapton	Lexan 5 mil	HDPE 1.5 mil
Space (STS-8 & STS-41G)	* $3x10^{-24}$	+ $8x10^{-24}$	** $6x10^{-24}$	* $4x10^{-24}$
PPPL 5eV AO Beam	$11x10^{-24}$	$8x10^{-24}$	$5x10^{-24}$	$4x10^{-24}$
MSFC Plasma Asher	$4x10^{-26}$	$6x10^{-26}$	$5x10^{-26}$	$2x10^{-25}$

*[5] Visentine
+[8] Whitaker et al.
**[7] Gregory et al.

The reaction efficiency calculated from mass loss data of plasma asher exposed materials at MSFC differs from both space flight determined reaction efficiencies and PPPL determined reaction efficiencies. Two possible explanations have been identified as to the large discrepancy. The first suggests that the reaction efficiency of polymer materials is dependent upon the energy of the incoming atom. Secondly, the flux used to compute the above reaction efficiencies was $1x10^{18}$ atoms/cm^2•s which was measured by Carruth [2] using a catalytic probe. However, attempts to reproduce the flux measurements using HDPE indicate a flux two orders of magnitude different.

A final comparison of the surface morphology of materials exposed to the different atomic oxygen simulation techniques can be made from SEM photographs. Figure 8 is an SEM photograph of the surface of silver covered with 5 mils of FEP Teflon (Ag/FEP) exposed to a fluence of $1x10^{20}$ atoms/cm^2 in the PPPL neutral beam facility, and Fig. 9 is an SEM of similar material taken from the covering on The Transverse, Flat-Plate Heat Pipe Experiment (S1005) aboard LDEF. Comparing both Figs. 8 and 9 it is difficult to tell them apart at first glance. The slight difference observed in aspect ratio (ratio of height of peak to diameter of the base of peak) may be due to the difference in energy or dose of atomic oxygen (LDEF fluence was $9x10^{21}$ atoms/cm^2). In contrast,

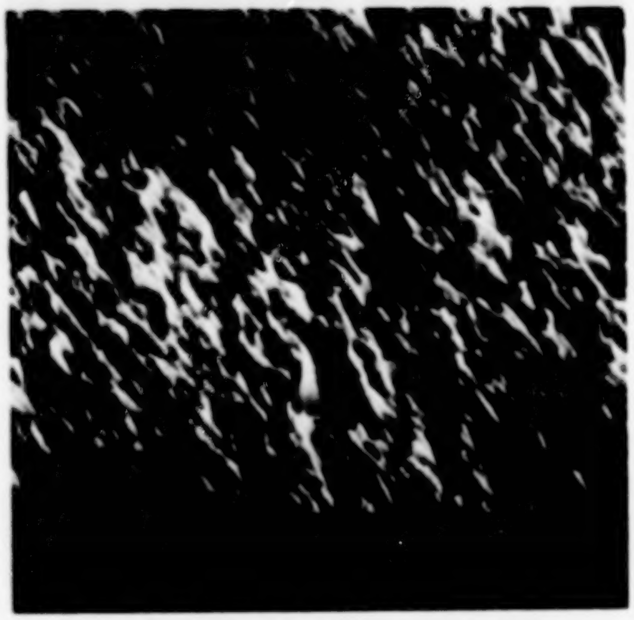

Figure 8 - SEM of Ag/FEP Exposed in PPPL Neutral Beam Facility (5k X)

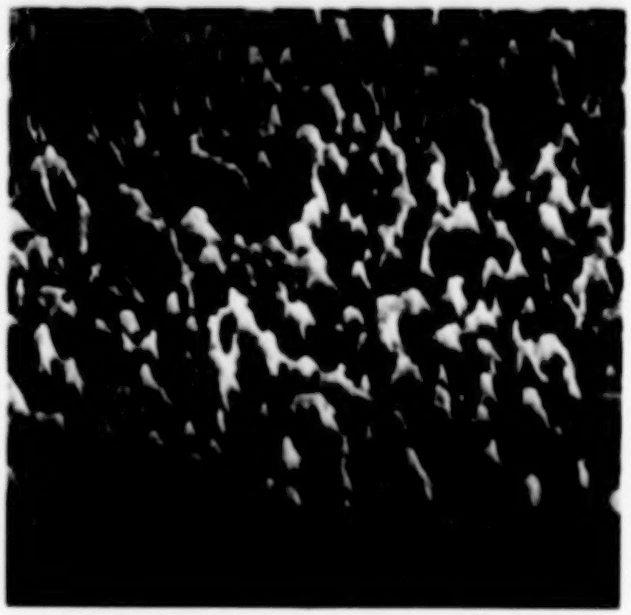

Figure 9 - SEM of Ag/FEP Exposed in Space Aboard LDEF (5k X)

Fig. 10 shows an SEM of the surface of Ag/FEP exposed in the MSFC plasma asher to a fluence of $1x10^{20}$ atoms/cm^2. The surface of the sample exposed in the plasma asher does not show the spiked nature seen in the other two SEM photographs. Overall, from the evidence provided, the PPPL neutral beam facility provides a better simulation to the LEO environment than the plasma asher.

CONCLUSIONS

The high energy atomic oxygen beam facility developed at PPPL is capable of simulating an LEO environment better than an ordinary plasma asher.

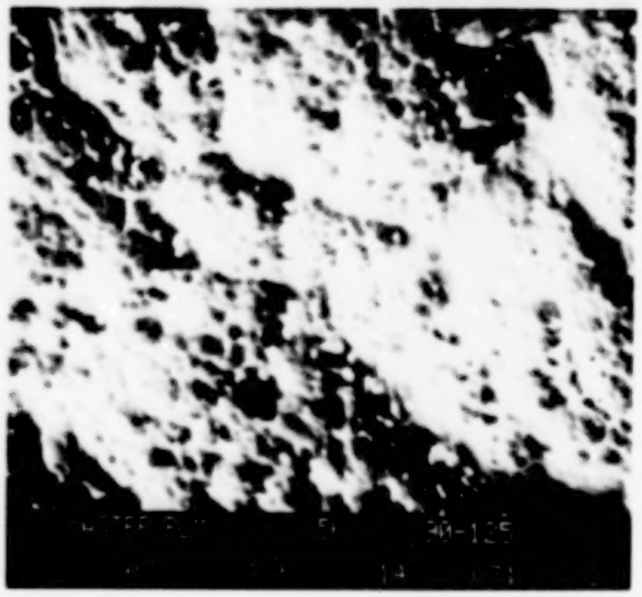

Figure 10 - SEM of Ag/FEP Exposed in Plasma Asher at MSFC

The reaction efficiency of materials exposed in this facility compares quite well to those exposed during flight experiments aboard STS-8 and STS-41G.

The high energy atomic oxygen beam source developed at PPPL is capable of producing atomic oxygen flux levels of $1x10^{15}$ atoms/cm^2•s and greater. These flux levels have been verified using both the catalytic probe and material mass loss data. The flux uniformity at the specimen exposure plane decreases 11% over a 13-cm diameter beam. While the flux distribution is not effected by rotating the neutralizer plate, the peak flux can be displaced from the centerline axis of the specimen exposure plane by this rotation.

The beam energy measurements, made with the QMS using argon and krypton reflecting off either tantalum or molybdenum neutralizer plates, show the facility does produce neutral beams with an energy range of 4 to 20 eV. Attempts to measure the energy of an atomic oxygen neutral beam have not been successful to date because of the creation of energetic particles produced during the dissociation of molecular oxygen in the ionizing region of the QMS. Further reductions in background pressure are needed to measure atomic oxygen atoms.

ACKNOWLEDGMENT

We would like to thank Mr. James Coston for his expertise in producing our SEM photographs of the samples, Mr. John Reynolds for assistance with the QMS, and Mr. James Owens and Mr. David Shular for access to the Ag/FEP from The Transverse, Flat-Plate Heat Pipe Experiment.

278

REFERENCES

1. Carruth, M. R., Jr., DeHaye, R. F., Norwood, J. K., and Whitaker, A. F., "Method for Determination of Neutral Atomic Oxygen Flux," Review of Scientific Instruments, Vol. 61, pp. 1211-1216, April, 1990.

2. Motley, R. W., Bernabei, S., and Hooke, W. M., "Coaxial Lower Hybrid Plasma Source," Review Scientific Inst., Vol. 50, pp. 1586, 1979.

3. Cuthbertson, J. W., Langer, W. D., and Motley, R. W., "Atomic Oxygen Beam Source for Erosion Simulation," presented at 19th Annual TMS Meeting, Anaheim, CA, February 18-22, 1990.

4. West, R. C., ed., "CRC Handbook of Physics and Chemistry," (CRC, West Palm Beach, FL, 1978).

5. Visentine, J. T., "Atomic Oxygen Effects Experiments: Current Status and Future Directions," NASA TM-100459, 1988.

6. Banks, B. A., "Simulation of the Low Earth Orbit Atomic Oxygen Interaction with Material by Means of an Oxygen Ion Beam," NASA TM-101971, 1989.

7. Gregory, J. C., and Peters, P. N., "The Reaction of 5 eV Oxygen Atoms With Polymeric and Carbon Surfaces in Earth Orbit," NASA TM-100459, 1988.

8. Whitaker, A. F., and Little, S. A., Unpublished results from STS-8 flight experiment.

Ground and Space Based Optical Analysis of Materials Degradation in Low-Earth-Orbit

John A. Woollam, Ron Synowicki, Jeffrey S. Hale, Jane Peterkin,
Hassanayn Machlab and Bhola N. De

Center for Microelectronic and Optical Materials Research, and
Department of Electrical Engineering, University of Nebraska,
Lincoln, NE; and: Blaine Johs, J A Woollam Co., Lincoln, NE

There is strong interest in being able to accurately and sensitively monitor materials degradation in both ground-based and space-based environments. In this paper we review two optical techniques for sensitive degradation monitoring, namely spectroscopic ellipsometry and photothermal spectroscopy. These techniques complement each other in that ellipsometry is sensitive to atomically thin surface and sub-surface changes, and photothermal spectroscopy is sensitive to local defects, pin-holes, subsurface defects, and delaminations. Our progress in applying these spectroscopies (both ex situ and in situ) to atomic oxygen degradation of space materials is reviewed.

Introduction:

Quantitative evaluation of material degradation rates and mechanisms is important for design of future long term space missions. Certain techniques for evaluation of materials on earth after space exposure are effective but can't be adopted for use in space. Examples are electron microscopy and weight loss. The purpose of this paper is to briefly review two optical techniques that are effective diagnostic instruments on earth but can also be potentially adapted for in situ space monitoring.

We have successfully applied spectroscopic ellipsometry to several space materials systems, including reflector materials, after exposure to a series of pure oxygen plasma ashings. These experiments yield information on changes in thicknesses of thin films of both metals and dielectrics as well as information on microstructural damage due to oxygen exposure. More recently we've developed in situ spectroscopic ellipsometry on vacuum chambers. This involves getting polarized light beams through stress free windows. The hardware for ellipsometry is now light weight, compact and reliable. Adaptation entirely to a vacuum environment is promising, and will be highly desirable for potential real time materials degradation measurements on space missions.

Photothermal spectroscopy has been developed for general material defect analysis, but until now has not been used for atomic oxygen degraded materials. Much of the hardware for this technique is similar to that used for ellipsometry and can thus be thought of as a related technology. An important difference from ellipsometry is that photothermal measurements involve thermal waves, and are highly effective in locating pinholes, delaminations, and sub-surface defects.

Several examples of applications of both spectroscopies to space materials degradation studies will be given.

Simplified Theory of Ellipsometry

The complete details of the theory are algebraically messy and won't be repeated here. In short, linearly polarized light having in-plane (p-polarized) and out-of-plane (s-polarized) light vector components is incident on a material under study. The reflected ray is elliptically polarized, and the ellipticity and orientations of the ellipse are determined using a second (rotating) polarizer. The simplest geometry is shown in Figure 1 for a material with no surface roughness and no films. The incoming light beam makes an angle of incidence of ϕ to the sample normal, and incident and reflected beams define the plane of incidence. Real materials are more complicated, and ellipsometry can be used to determine layer thicknesses, surface and interfacial roughnesses, and alloy fractions in complicated materials systems.

In our system the initial polarizer is at a fixed azimuth and a second polarizer (analyzer) is rotated. The relative (not absolute) intensity of light as a function of analyzer azimuth is measured. Figure 2 shows a system we call VASE (for Variable

Angle Spectroscopic Ellipsometry). Under computer control are the wavelength of light, polarizer and analyzer azimuths, a shutter and filter, and the angle of incidence. The system is fast, and data at a large number of angles of incidence and wavelengths can be taken.

For in situ applications (including potential space flights) ellipsometers are remarkably compact. Figure 3 shows a schematic of an ellipsometer recently adapted for vacuum systems.

Measured is the complex reflectance ratio $\rho = \tan\psi \exp(j\Delta) = Rp/Rs$ where Rp and Rs are the complex Fresnel Reflection coefficients for p- and s- polarization vector components. These coefficients contain information of interest about the material, such as layer thicknesses, alloy fractions, void fractions, and general optical constants.

The analysis procedure is to calculate ρ based on an assumed structure for the material and to compare the experimental and calculated ρ. A regression analysis is done to minimize the differences between experimental and calculated ρ, where the variables are the unknown materials parameters such as layer thicknesses.

There are two important caveats in ellipsometric analysis. The first is that the sensitivity to measurement of a system variable depends strongly on angle of incidence and wavelength as a result of the spectral dependence of the optical constants of solids. This means that the user must have both angle of incidence and wavelength under control in order to gain proper sensitivity.

Secondly, parameters are often correlated, meaning the value found for one layer thickness depends on the value found for another. To avoid or minimize correlation the user can select a proper number of measurements at the best angle and wavelength conditions. Often even this is not enough and the user needs to know when variables are correlated. Commercial systems with one wavelength and limited angle of incidence selection generally meet neither the sensitivity, nor the correlation criteria.

Thus we are strong proponents of a full VASE analysis, with ability to calculate sensitivities and correlations.

Thus when done properly ellipsometry can be an extremely sensitive tool. It can be performed in a wide variety of ambient conditions, including a wide range of pressures and temperatures, and can even be performed in an aqueous environment. It is also completely non-destructive. (Even electron beams in SEMs damage surfaces). The experiments can be performed remotely, and real time operation in space is a realistic possibility.

Simplified Theory of Photothermal Spectroscopy

Photothermal spectroscopy can be performed in several modes. In this paper we discuss the version known as photothermal beam deflection spectroscopy, which is a sensitive non-contacting and non-destructive evaluation technique. It has a number of applications including thermal imaging of defects, optical absorption coefficient, film thickness, and thermal diffusivity measurements. The spectroscopy is especially useful for imaging subsurface defects, not normally visible, such as delaminations and subsurface damage.

Figure 4 shows the experimental apparatus layout. The sample is mounted on a computer controlled x-y translation stage, and one light beam "skims" just above the surface of the sample. A second beam is directed perpendicular to the sample and is chopped at a controlled (variable) frequency. Absorption of this radiation causes periodic heating of the sample at the chopped frequency. Heating causes a periodic index of refraction gradient resulting in a small but measurable deflection of the sensing ("skimming") beam. The deflection is detected with a position sensitive solid state detector using a lock-in-amplifier.

Example Ellipsometry Applications to Space Materials

Atomic oxygen is known to enlarge pinholes and erode materials even beneath a coating. In addition it can cause uniform oxidation over larger areas, and uniform erosion of materials including metals and carbonaceous materials. A major purpose of ellipsometric analysis of space materials is to detect and follow (with monolayer sensitivity) changes in surfaces, interfaces, and films after exposure to atomic oxygen for even very short times. Thus it is sensitive to degradation very early in a mission.

Figure 5 shows the thickening of an oxide, and simultaneously the thinning of a silver metal film monitored by ellipsometry. Note the very fine scale of error bars for measurement. Figure 6 similarly shows the formation of aluminum oxide from an aluminum reflector exposed to atomic oxygen.

Examples of Photothermal Imaging

Figure 7 shows a photothermal image over the surface of a silicon semiconductor wafer showing the edge of a film having 1000 Angstroms thick tin oxide covering 400 Angstroms thick silver which was deposited on the wafer.

Figure 8 shows the photothermal image of a pulsed laser evaporated "strip" of copper removed from a substrate. The removal was not "clean", and residual metal was left in central regions, but the spectra are dominated by excess metal piled up at the edges of the "strip".

Figure 9 shows a photothermal image of a defect hole in a film of 300 Angstroms of silver on 25 Angstroms of aluminum on a silicon wafer. The hole is approximately 1000 microns wide. Figure 10 shows that the hole has widened and eroded after 3 hours of ashing to 1300 microns width.

We are in the early stages of applying photothermal imaging to space coatings, and the resolution and scale of data presented above will likely improve dramatically in the near future. It will be especially useful for quantitatively detecting film undercutting and delamination due to atomic oxygen.

* Research supported by NASA Lewis Grant NAG-3-95.

Bibliography:

Ellipsometry

(1) B.N. De, Y. Zhao, P.G. Snyder, J.A. Woollam, T.J. Coutts, X. Li, "Effects of Oxygen "Ashing" on Indium Tin Oxide Thin Films", Proceedings of ICMC89, Thin Solid Films, (1989), 39/40, 647 (1989).

(2) B.N. De, J.A. Woollam, "Ellipsometric Study of Al_2O_3/Ag/Si and SiO_2/Ag/Quartz Ashed in an Oxygen Plasma", J. of Appl. Phys., 66(11), 5602 (1989).

(3) J.A. Woollam, P.G. Snyder, "Fundamentals and Applications of Variable Angle Spectroscopic Ellipsometry (VASE)", Proceedings of EMRS Symp. C (1989), Materials Science and Engineering B5, 279 (1990).

Photothermal Imaging

(1) L.D. Favro, P.K. Kuo, R.L. Thomas, "Thermal Wave Techniques for Imaging and Characterization of Materials", Review of Progress in Quantitative Nondestructive Evaluation, Vol. 6A. Edited by Donald O. Thompson and Dale E. Chimenti (Plenum Publishing Corp., 1987).

(2) G.C. Wetsel Jr., F.A. McDonald, "Subsurface-structure determination using photothermal laser-beam deflection", Appl. Phys. Lett. 41(10), 926-928, (1982).

(3) G.C. Wetsel Jr., F.A. McDonald, "Resolution and definition in photothermal imaging", J. Appl. Phys. 56(11), 3081-3085, (1984).

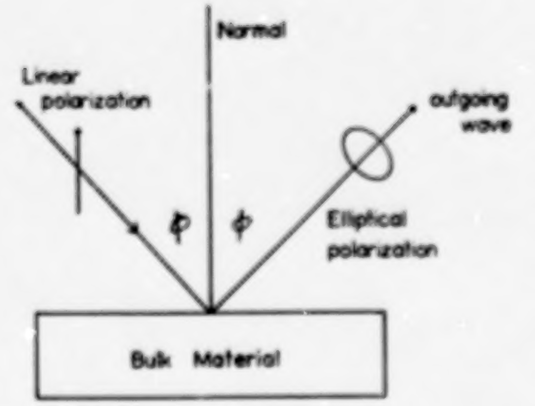
Normal
Linear polarization
outgoing wave
ϕ
ϕ
Elliptical polarization
Bulk Material

Figure 1
Ambient-bulk model for ellipsometric analysis

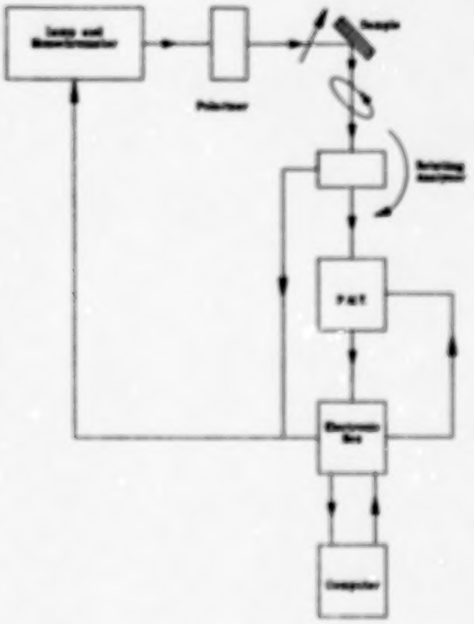
Lamp and Monochromator
Sample
Polarizer
Rotating Analyzer
PMT
Electronics Box
Computer

Figure 2
Schematic diagram of a variable angle spectroscopic ellipsometer (VASE)

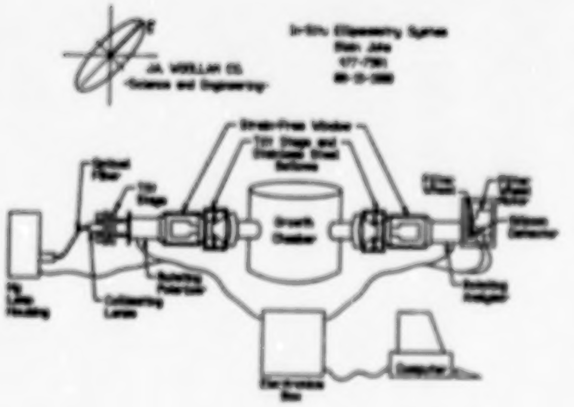
J.A. WOOLLAM CO.
Strain-Free Window
Growth Chamber
Computer
Electronics Box

Figure 3
Schematic of in situ ellipsometer

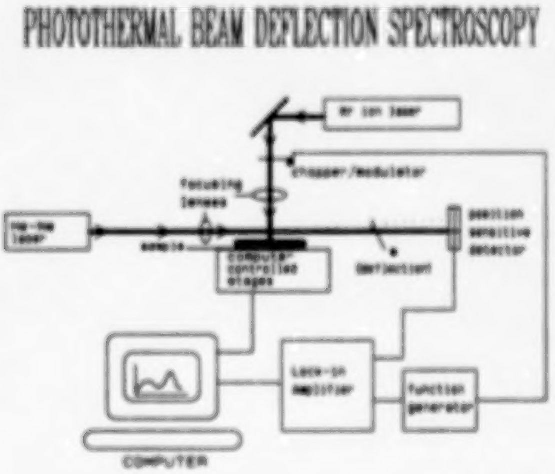
PHOTOTHERMAL BEAM DEFLECTION SPECTROSCOPY
Ar ion laser
chopper/modulator
focusing lenses
He-Ne laser
sample
computer controlled stages
Deflection
position sensitive detector
Lock-in amplifier
function generator
COMPUTER

Figure 4
Schematic of photothermal beam deflection spectrometer

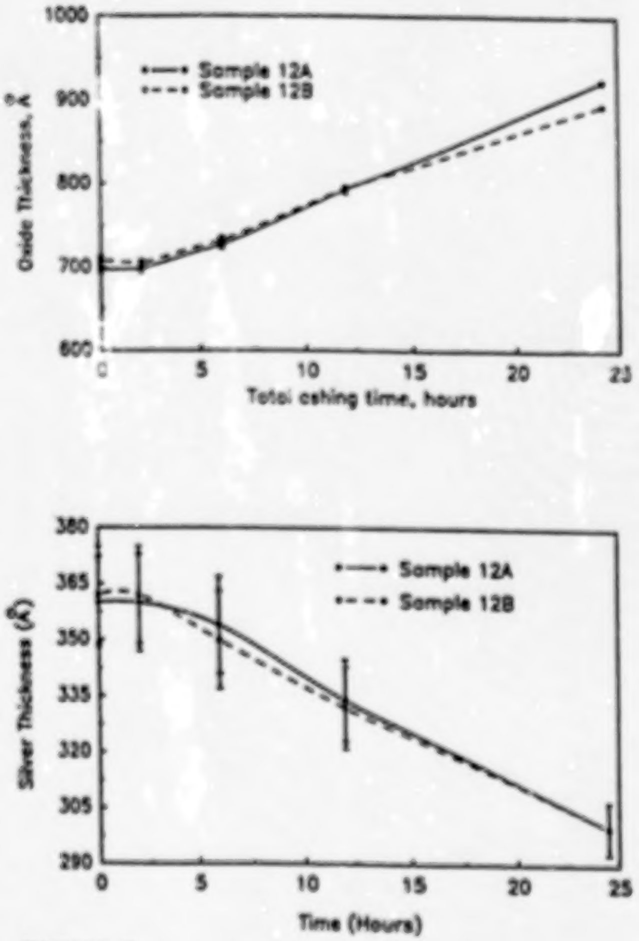

Figure 5
Thicknesses of SiO2 and silver films as a function of ashing time determined simultaneouly in one sample using ellipsometry

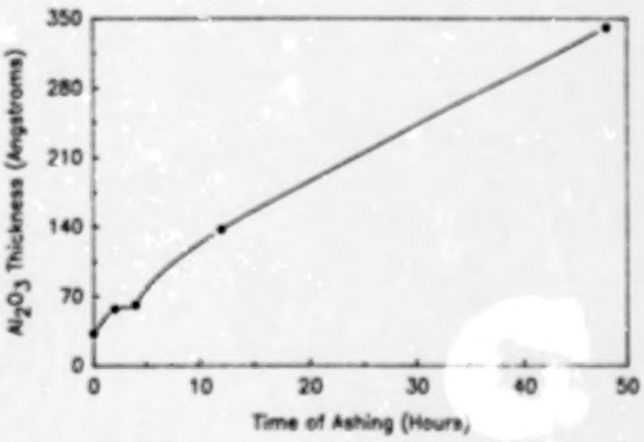

Figure 6
Thickening of Al203 on aluminum due to ashing, monitored ellipsometrically

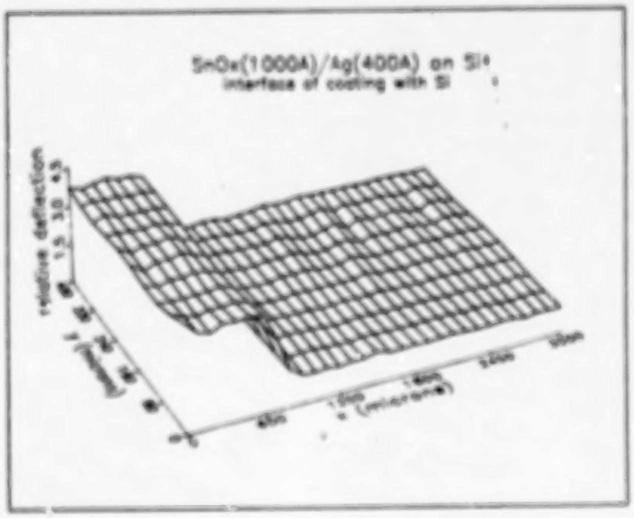

Figure 7
Photothermal image of edge of a film of tin oxide on silver on silicon

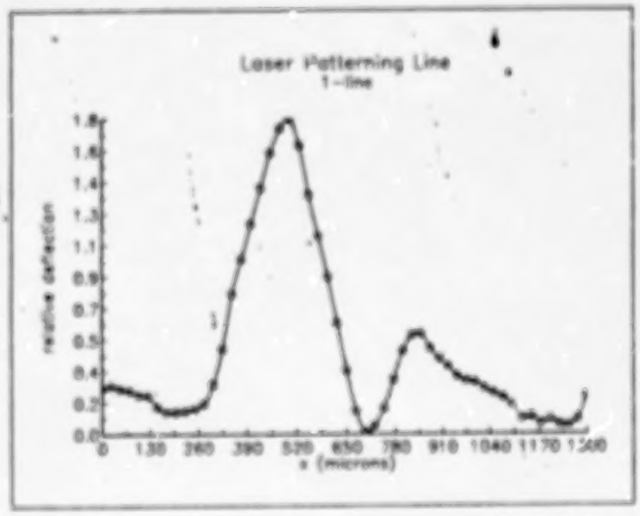

Figure 8
Photothermal image of removal of copper in a strip geometry (using laser ablation)

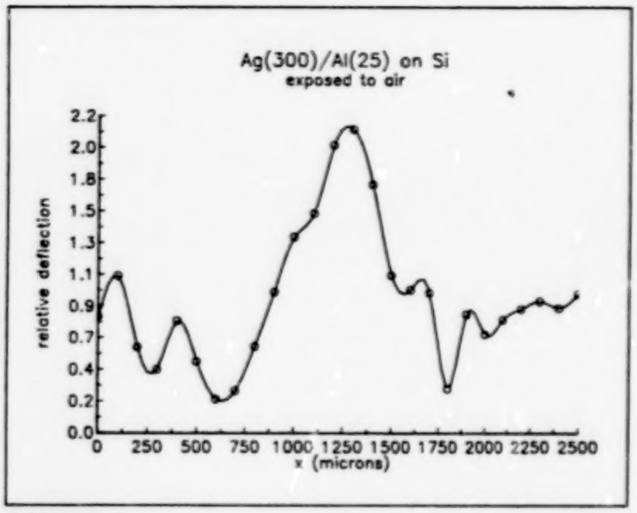

Figure 9
Photothermal image of a defect hole in a film on a silicon wafer substrate

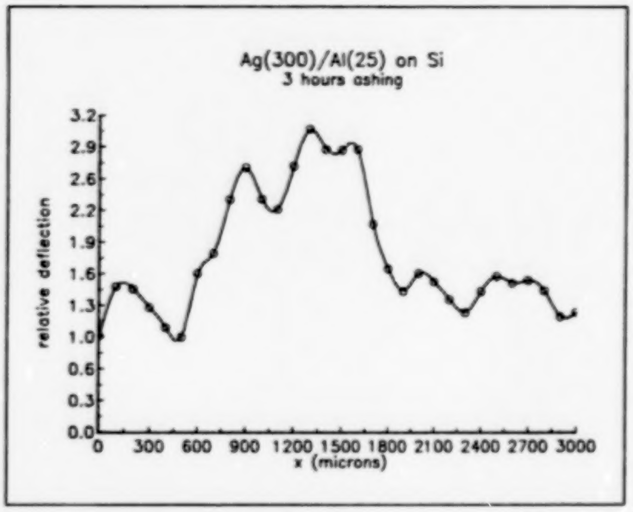

Figure 10
Photothermal image of hole from Figure 9 sample after 3 hour exposure to oxygen ashing

THE TRANSITION OF GROUND-BASED SPACE ENVIRONMENTAL EFFECTS TESTING TO THE SPACE ENVIRONMENT

by

Stephen V. Zaat, Glen A. Schaefer and John F. Wallace
NASA Center for the Commercial Development of Space
Case Western Reserve University
Cleveland, Ohio

Introduction

The goal of the Space Flight Program at the Center for the Commercial Development of Space—Materials for Space Structures located at Case Western Reserve University is to provide environmentally stable structural materials to support the continued humanization and commercialization of the space frontier. Information on environmental stability will be obtained through space exposure, evaluation, documentation and subsequent return to the supplier of the candidate material for internal investigation. This program provides engineering and scientific service to space systems development firms and also exposes CCDS-developed candidate materials to space environments representative of in-flight conditions.

The maintenance of a technological edge in space for the National Aeronautics and Space Administration suggests the immediate search for space materials that maintain their structural integrity and remain environmentally stable. The materials being considered for long-lived space structures are complex, high strength/weight ratio composites. In order for these new candidate materials to qualify for use in space structures, they must undergo strenuous testing to determine their reliability and stability when subjected to the space environment. Ultraviolet radiation, atomic oxygen, debris/micrometeoroids, charged particle radiation, and thermal fatigue all influence the design of space structural materials as shown in Figure 1.[1-3] The investigation of these environmental interactions is key to the purpose of this Center, one of the sixteen Centers established and sponsored by NASA.

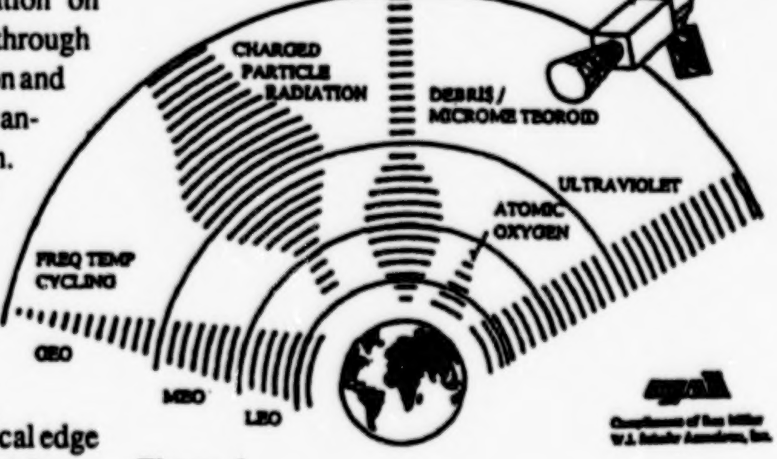

W.J. Schafer Associates, Inc.

Figure 1

Space Flight Program

Materials produced by CCDS projects will be verified for space environment stability by testing on future space flights beginning in April 1991 and continuing through 2005. Currently, no terrestrial capability exists that precisely reproduces the environment in which these materials must function. This Space Flight Program concentrates on using existing and planned

Space Transportation Systems to facilitate exposure of materials while, at the same time, reducing costs. The Space Flight Program intends to build on the completed experiments of Long Duration Exposure Facility (LDEF) and Evaluation of Oxygen Interactions with Materials (EOIM) through the development of materials exposure fixtures which will provide for *in-situ* data generation. Thus, the search for the information necessary to ascertain which materials will be suitable for space applications stretches into the next century. These advanced materials investigations will allow the development of special application engineered materials.

The Space Flight Program at this CCDS consists of three distinct phases. Phase I focuses on program planning and program development under the auspices of active Center sponsors from Industry, Academia and Government. The Phase I flight requests consist of essentially three passive payloads currently scheduled in 1991. Data from these flight related activities will be used to:

1. Expand the existing space materials data base
2. Establish a service related endeavor with functional/operational parameters
3. Verify standards for materials degradation
4. Calibrate and perform functional checks of required special nondestructive test equipment

The flight projects identified by the Center under Phase I development are termed Limited Duration space environment Candidate Materials Exposure (LDCE) experiments.

As the CCDS flight activities grow, the need for *in-situ* data generation also grows. Phase II flights address this need. During Phase II, the CCDS will expand the number of tests conducted to expose materials to the space environment, and undertake the analysis of those test results. Four extended duration payloads will be flown during Phase II under three distinct modes. One scheduled via the STS carries the designation CMSE/E, and one representing an expansion of CMSE/E is designated CMSE-1; one scheduled on Wake Shield carries the designation MATLAB-1; and one scheduled on the Office of Commercial Programs free flyer "COMET" is designated MATLAB-2. Data from these flights will be used to:

1. Expand the technology base for increased operations
2. Refine sensor performance

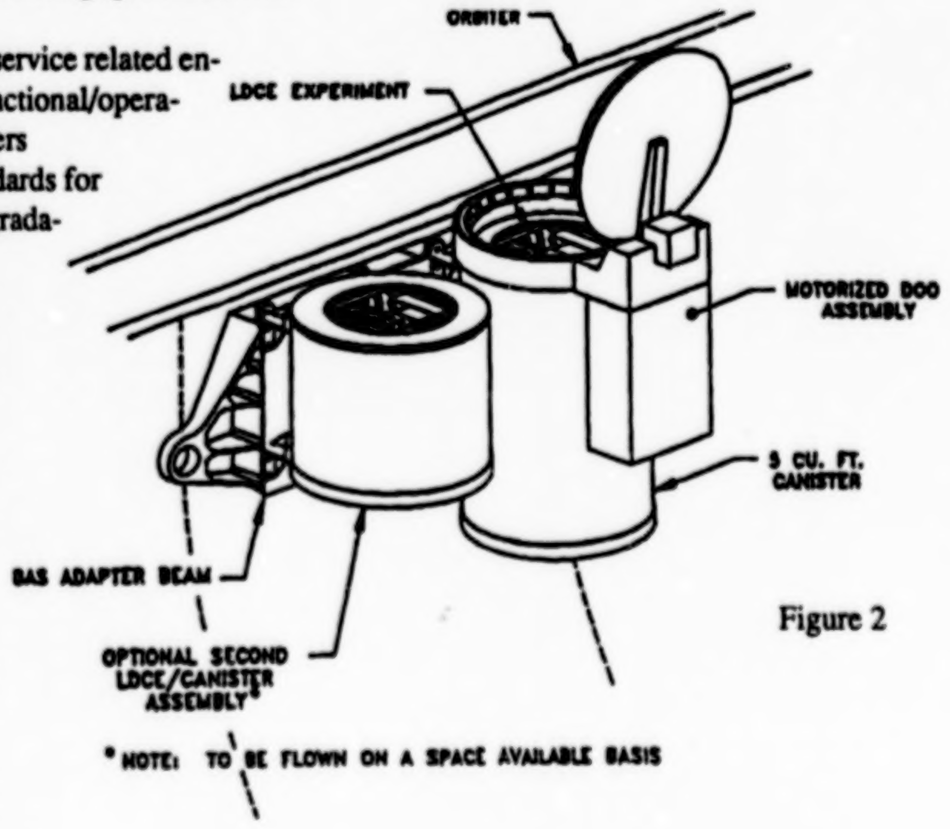
ORBITER
LDCE EXPERIMENT
MOTORIZED DOO ASSEMBLY
5 CU. FT. CANISTER
GAS ADAPTER BEAM
OPTIONAL SECOND LDCE/CANISTER ASSEMBLY*
* NOTE: TO BE FLOWN ON A SPACE AVAILABLE BASIS

Figure 2

3. Evolve advanced materials with smart structure integration modules for space or terrestrial use

The three Phase II flights are scheduled to begin in December 1991 and to end in 1993.

This CCDS plans additional, long duration exposure facilities during Phase III of this program. These payloads contain experiments designed to be conducted in space on existing or planned structures/platforms. This phase also includes the use of the planned Space Station as a materials exposure and evaluation facility. Flight requests submitted to the NASA Office of Commercial Programs for Phase III were deferred pending successful integration during Phase I. However, the CCDS will continue to concentrate on project definition and industrial sponsorship.

Space Flight Payloads

PHASE I Limited Duration space environment Candidate materials Exposure (LDCE)

The three LDCE payloads utilize a complex autonomous payload (CAP) container with a motorized door assembly (MDA) mounted in the Orbiter (Figure 2)[4]. The LDCE payload fixture is a 19.65 inch diameter disc with a 15.34 inch diameter midsection to which the candidate materials are attached and exposed when the MDA is opened (Figure 3). This configuration meets the immediate requirements of this Center and current industry backlog. The interim objective is to perform atomic oxygen durability verifications using this passive fixture arrangement. Preflight and post-flight sample surface analysis in addition to carefully controlled sample mass determinations will provide insight to the atomic oxygen influence on surface recession or growth.

Passive materials exposure experiments constitute the LDCE-1, LDCE-2 and LDCE-3 payloads and consequently have a very limited operation scenario. The intended operation steps to support these experiments are:

1. Step one, Attitude requirement - The payload bay faces forward so an ambient atomic oxygen beam is presented to the material surface areas. The exposure surfaces are perpendicular to the Orbiters operational velocity vector (-Zvv).

2. Step two, MDA operation - Once the Orbiter orientation is obtained, the MDA is opened for LDCE-1 and LDCE-3. LDCE-2 is mounted without a MDA.

3. Step three, Materials exposure - The ambient atomic oxygen interaction is required for 40 hours.

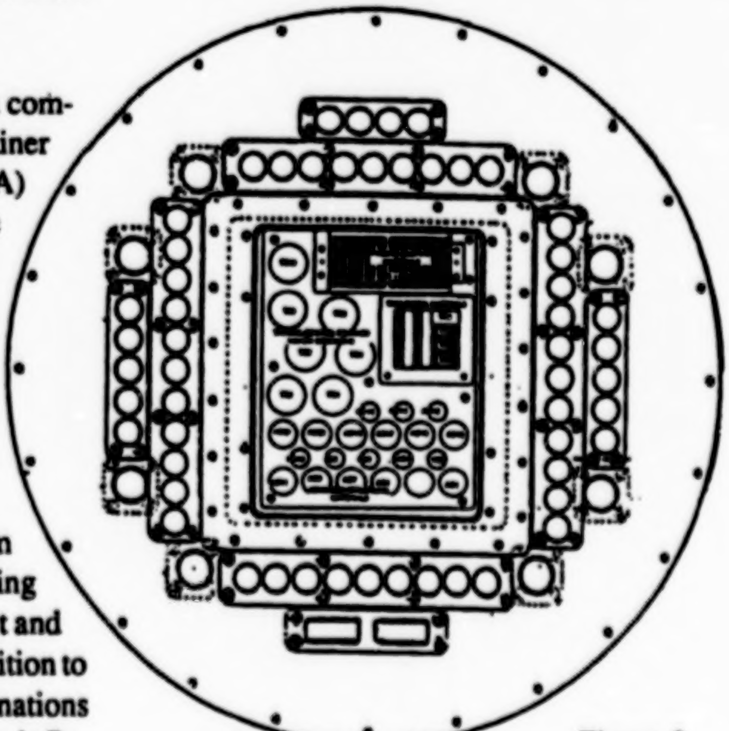

Figure 3

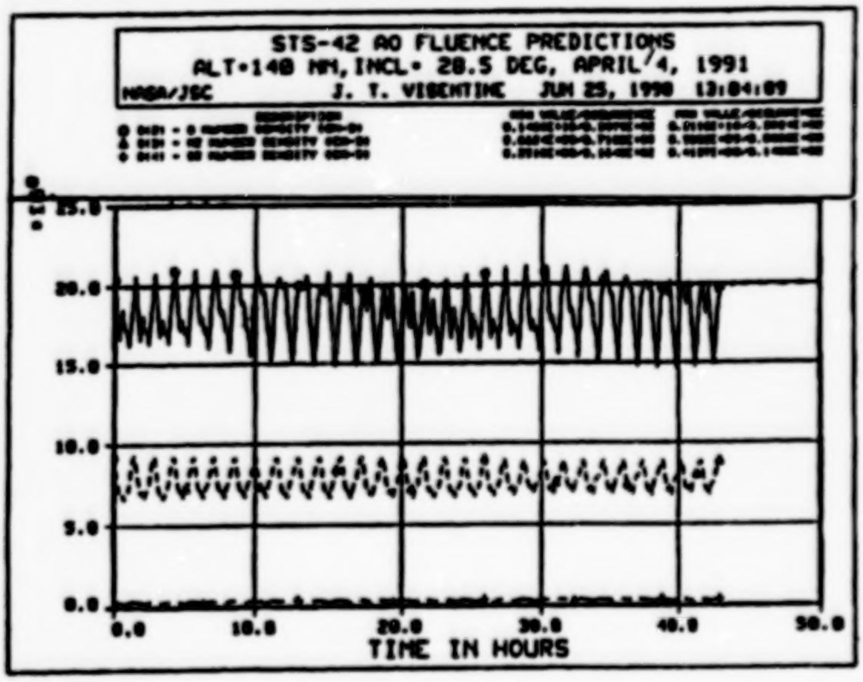

Figure 4

4. Step four, MDA operation - Before repositioning the Orbiter, the MDA is closed.

NASA will supply an Orbiter altitude between 120-180 n. miles and an Orbiter orientation [payload bay facing forward (-Zvv)] for ground simulation experiments.

One such ground simulation study involves the calculation of the total atomic oxygen fluence the samples received. The Johnson Space Flight Center computed the atomic oxygen species predicted from STS-42 flight geometry using the MSIS86 atomic oxygen fluence calculation program (Figure 4)[5]. The STS-42 flight sequence scheduled for April 1991 tentatively carries the LDCE-1 and LDCE-2 payloads. Several well characterized passive atomic oxygen fluence dosimeters are included in each of the LDCE series experiments.

Following the determination of post flight exposure from the Mission Elapsed Time documentation, an update of MS1S86 fluence calculation will further define this elusive variable. This active participation and coordination with various NASA installations further enhances the materials data base generated by Center research.

PHASE II Increasing Space Activities

Candidate Materials Sample Exposure (CMSE) - CMSE/E

From a materials' perspective, the flight of EOIM-III in December 1991 will provide benchmark data for LEO environment operations. NASA centers (JSC, GSFC, MSFC, LaRC, JPL and LeRC) and selected Space Station contractors have contributed experiments toward EOIM-III success. One experiment in particular, an ion-neutral mass spectrometer, will have significant influence on quantifying LEO species. The CMSE/E payload incorporates active/passive samples for a proposed baseline correlation with experiments being performed on EOIM-III. The active box incorporated in CMSE/E and correlated with advanced EOIM-III hardware becomes an integral portion of all Phase II experiments for this Center (CMSE and MATLAB payloads). The active box transmits data accumulated from sample changes due to strain, temperature, resistance, photo-intensity and frequency. Fixtures and active box configurations are compatible with the LDCE series hardware by making CMSE/E a cost effective, upgraded follow-on configuration. This design allows for baseline data correlation, determination of coupled environmental factors, and *in-situ* sensor module evaluation and calibration. The CMSE/E payload will aid in the understanding of the mechanisms and processes of atomic oxygen.

CMSE-1

Capitalizing on the success of LDCE and CMSE/E, CMSE-1 utilizes the same calibrated box (or boxes) but increases the number of samples in the payload. A CMSE Experiment Support Assembly (Figure 5), remote from the CAP, will expose additional active/passive samples. The Shuttle manipulator arm lifts the Experiment Support Assembly from the cargo bay and orients the assembly for the LEO exposure.

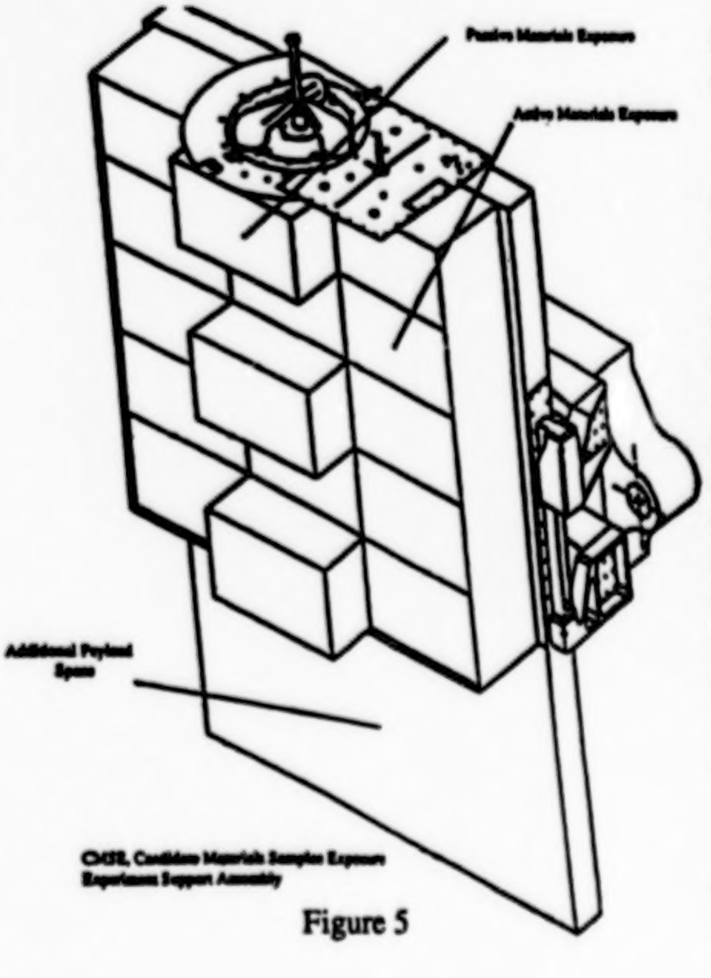
Passive Materials Exposure
Active Materials Exposure
Additional Payload Space
CMSE, Candidate Materials Samples Exposure Experiment Support Assembly

Figure 5

MatLab-1 and MatLab-2

The MatLab payloads augment the CMSE/E and CMSE-1 experiments through changes in LEO positioning. The proven hardware of the MatLab-1 fixture will be located on the forward, high pressure side (atomic oxygen ram) of Wake Shield. Additional plasma diagnostics experiments incorporated into Wake Shield hardware will enhance data reliability and provide further insight into the LEO environment.

MatLab-2 will occupy space on the NASA Commercial Programs "COMET" payload. This "free flyer" will extend the payload exposure duration for additional LEO characterization.

PHASE III Future Projects - Space Station Freedom

Long Duration Space Environment exposure (LDSE)

The LDSE proposal utilizes portions of the space station as an orbiting platform for long term space materials exposure. This payload is scheduled as part of the Space Station Freedom and will support long term materials exposure for several decades beginning in 1996. The payload will incorporate several exposure surfaces capable of supporting numerous materials samples in locations which will render maximum exposure to targeted LEO environments. This flight project will require frequent on-site servicing by the Space Transportation System(STS) to start six months after the placement of the first fixture and once every six months thereafter.

Space Materials Evaluation Facility (SMEF)

The SMEF proposal will be a working part of the Space Station in the year 2000. The facility is dedicated to the processing, preparation and on-site materials analysis of space environment exposed materials. SMEF will have the capacity to monitor materials environmental control measures, perform materials properties experiments on microgravity processed materials and conduct failure analyses in support of Space Station servicing requirements. Housed in a SpaceHab Space Station Support Module, SMEF is planned as a full service, lightweight and compact materials science laboratory. The evolution of Space Station clearly supports establishing this service oriented development effort.

Future Projects - Space Exploration

Lunar Surface Candidate materials Exposure (LSCE)

This flight project includes the placement of an active materials exposure fixture on the lunar surface and the return of a structurally complex element of a previous lunar mission in the year 2010. The planned active materials exposure fixture will telecommunicate materials stability data to the SMEF or Earth.

Deep Space Candidate materials Exposure (DSCE)

This DSCE project will be required to support the future humanization of space by 1996. This flight test project is planned to evolve as flights of opportunity. The flight materials instrumentation package involved with this project will monitor and report materials stability in unknown environments.

Summary

Current flight payloads identified in Phase I and Phase II of the Space Flight Program are summarized in Figure 6. The graph indicates available space on appropriate exposure experiments. The Center actively seeks co-sponsorship proposals from firms or agencies actively participating in "leading edge" materials technologies. Through this mechanism, the concept of "commercial" participation expands.

Advanced space structural materials require exposure testing in the space environment. The NASA-CCDS — Materials for Space Structures at Case Western Reserve University has identified this necessity and has proposed a Space Flight Program to affect a gradual, ordered, cost-effective way for Industry, Academia and Government to access space for materials evaluation. Low-cost participation in the space environment will commercialize the endeavor and allow a cost-effective way for Industry, Academia and Government to access space for materials evaluation. The Space Flight Program will aid the commercial transition from the decade of the 1990's into the 21st Century.

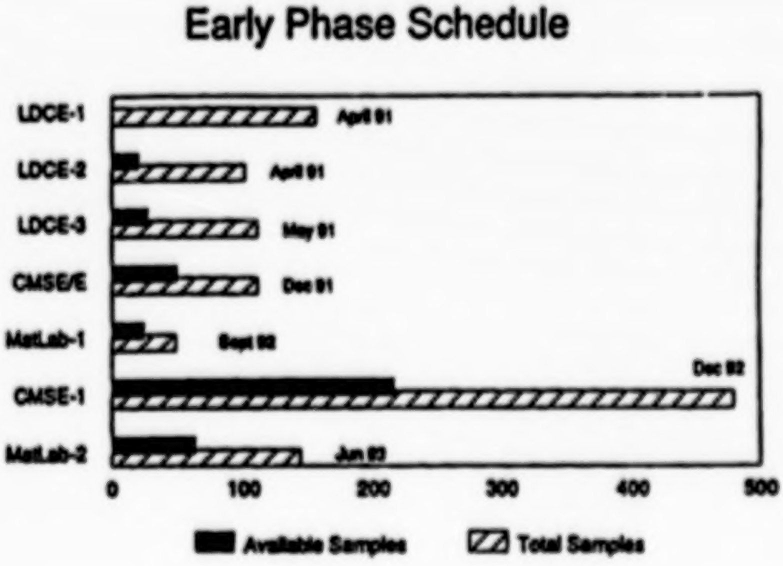

Figure 6

Information as of June 1, 1990

References

1. Haffner, J.W., "Environmental Effects on Spacecraft Materials," NASA/SDIO Space Environmental Effects on Material Workshop, NASA Conference Publication 3035, Part 1, 1989.

2. Hutton, Donald E., "Shuttle Glow," Scientific American Volume 78, No. 2, March -April 1990.

3. Courtesy of Rex J. Miller, W.J. Schafer Associates, Inc.

4. Stepp, Robert, Customer Support Manager-Hitchhiker Project, Goddard Space Flight Center, 1989.

5. Visentine, J.T. and Leger, L.J., "Material Interactions with the Low Earth Orbital Environment: Accurate Reaction Rate Measurements," AIAA Shuttle Environment and Operations I Conference, Houston, TX, November 13-15, 1985.

AUTHOR INDEX

Adam, Susan 582
Adler, Richard M. 324
Aitken, Donald J. 484
Albery, W. B. 536
Allen, Bradley P. 456
Allred, D. 664
Andary, J. 151
Atkinson, David J. 244
Auer, Bruce M. 726

Bailey, Robert W. 2
Balmain, K. G. 646
Baker, Carolyn G. 347
Baker, J. 683
Banks, Bruce A. 726
Bantin, C. C. 646
Barnes, John 44
Bartholomew, Maureen O'Brien 194
Bedard Jr., Roger J. 78
Bejczy, A. K. 23
Belkin, Brenda L. 405
Beller 323
Berk, A. 676
Biefeld, Eric W. 268
Bierschwale, John M. 172
179
Blau, Frederick P. 643
Brody, Adam R. 557
Brown, D. 134
Brown Jr., H. Benjamin 91
Bryan, Thomas C. 126
Bryant, Keith 172
Bushman, J. B. 499

Caledonia, G. E. 733
743
Carnes, James R. 338
Carroll, John D. 126
Carruth Jr., M. Ralph 689
764
Case, C. M. 392
Chelette, T. L. 536
Chen, Guanrong 201
Chidester, Thomas R. 605
Chiu, Stephen 440
Chiu, Sujeet 441
Choi, T. 226
Cleghorn, Timothy F. 113
Cohen, H. 683
Conkin, J. 631
Connors, Mary M. 612
Cook, Richard L. 543
Cooke, David L. 665
667
Cooper, Jill M. 755
Cooper, Lynne P. 268
Cottman, Bruce H. 324
Cottam, Russell 666
Cox, B. 134
Craig, F. G. 392
Cuthbertson, J. W. 734
764
Cutts, D. E. 392

Davies, W. E. R. 763
Davis, William S. 275
De, Bhola N. 772
Delingette, H. 226
DeLuise, M. 226
Dewberry, Brandon S. 338
Dewitt, J. Russell 9
Donnell, Brian L. 464
Doyle, Richard 344
Duffie, Neil A. 53
104
170
Duffy, Lorraine 604

Elgin, J. B. 676
681
Ellis, Stephen R. 557
Engrand, Peter A. 331

Felder, Marian 644
Fennel, T. R. 392
Ferguson, Dale C. 689
Fleming, J. L. 430
Fleming, Terence F. 179
Fox, Barry R. 279
Fridge III, Ernest M. 477

Friedman, Mark B. 91
Funk, Ken 508
Fussell, L. R. 397

Gabrielian, Armen 368
Gale, Karen L. 53
104
Gargan, Robert 290
Garin, John 172
Geddes, Norman D. 521
528
Gierow, Paul A. 126
Gilbert, John H. 633
Gillan, Douglas 582
Goodwin, M. A. 397
Granaas, Michael M. 529
Green, B. D. 683
Greenhut, Darlene D. 285
Greiner, Helen 84
Gugerty, Leo 574

Hadaller 323
Halbfinger, Eliezer, M. 280
Hale, Jeffrey S. 772
Hall, David K. 355
Hammen, David G. 347
Hansen, J. S. 763
Hartman, Wayne 259
Hasselman, Timothy K. 442
Hebert, M. 226
Heindel, Troy A. 236
Hill, Carol M. 726
Hillard, G. Barry 655
Hiltz, M. 134
Holden, Kritina L. 582
588
Holtzclaw, K. W. 743
Horrigan, D. J. 630
631
633
Hoshstrasser, Belinda H. 528
Howie, Michael B. 543
Hsin, Y. 226
Hughes, Peter M. 493

Ikeuchi, K. 226
Ince, Ilhan 172

Jackson, Phoebe A. 696
James, H. G. 646
James, Mark L. 244
Johnson, Debra Steele 418
Johnson, Earl 317
Jones, P. M. 499
Jongeward, Gary A. 684

Kan, Edwin P. 143
Kanade, Takeo 91
Katz, Ira 665
Kelly, Christine M. 347
Kofsky, I. L. 676
Konkel, Carl R. 9
Krech, R. H. 733
Krishen, Angele 542
Krishen, Kumar 207
Krotkov, Eric 96
Krupp, Joseph C. 296
Kuharski, Robert A. 684
Kumar, K. Vasantha 630
633

Landauer, C. 415
Langer, W. D. 734
764
Lau, Sonie 469
Lauriente, Michael 668
Lavery, David 78
Leahy Jr., M. B. 67
Lee, H. G. 742
Lee, S. Daniel 375
456
Leone, A. 743
Levin, Barry E. 304
Lilley, J. R. 665
Lillie, Brian J. 776
Lindell, R. 414
Linton, R. C. 764
Locker III, Al J. 682
Lollar, Louis F. 355
Lynch, W. 683

Maag, Carl 705
Machlab, Hassanayn 772
Mackey, Willie 642
Maida, James 552
Manahan, Meera 595

Mandell, M. J. 665
Margolis, Steven 367
Marsh, Christopher A. 347
Martin, R. Gaius 244
Marzwell, Neville I. 143
McColligan, Elizabeth 543
McFarland, Robert Z. 236
Miller, Chris A. 528
Miller, David P. 362
Miller, Ross 481
Mitchell, Christine M. 490
499
522
Mitchell, Tami 331
Morison, W. D. 763
Motley, R. W. 734
Mullins, Barry 346
Murad, E. 676
682
Motley, R. W. 764

Nader, Blair A. 207
Nagel, Arthur 345
Neely, W. C. 752
Newport, Curt 561
Nieten, Joseph L. 424
Nussman, Dale A. 167

O'Neal, Michael 595
Olle, Raymond M. 755

Palmer, J. R. 392
Pandya, Abhilash 552
Parrish, Joseph C. 184
Peterkin, Jane 772
Peters, H. L. 397
Petrie, B. C. 754
Pike, C. P. 676
Pitman, Charles L. 477
Potter, Scott S. 547
Powell, M. R. 632
Powers, Allen K. 9
Pushkin, Kachroo 542

Quinn, Todd M. 383
Quiocho, Leslie J. 2

Rall, D. L. A. 676
Rankin, Thomas V. 684
Rasmussen, Arthur N. 236
Regian, J. Wesley 429
527
Repperger, D. W. 536
Reynolds, Robert C. 706
Ricci 323
Riley, Gary 464
Roche, James C. 665
684
Ross, Timothy J. 442
Rubin, K. S. 499
Rudisill, Marianne 601
Rutledge, Sharon K. 726
755

Sacco, G. 683
Sampaio, Carlos E. 172
179
Satayesh, A. 676
Sater, B. 754
Schaefer, Glen A. 778
Schultz, R. D. 397
449
Schumacher Jr., Paul W. 718
Scrapchansky, T. 752
Seraphine, Kathleen M. 424
Shahinpoor, Mo 15
159
Shalin, Valerie L. 528
Shute, Valerie J. 431
Simmons, Reid 96
Simpson, K. S. 742
Smith, Barry D. 280
Smith, Bradford 159
Smith, C. A. 742
Snyder, David B. 689
Spidaliere, P. 151
Sredinski, Victoria E. 529
Statler, Irving C. 612
Stengel, Robert F. 405
Sternberg, Stanley R. 113
Stevens, N. John 645
Stobie, Iain 449
Stuart, Mark A. 172
179
Swenson, G. R. 743
Synowicki, Ron 772

Szakaly, Z. F. 30
Szatkowski, G. P. 304

Takeo, H. 754
Tennyson, R. C. 763
Tran, Doan Minh 194
Trembley, D. 683
Trowbridge, C. A. 676

Unger, J. 763

Vaughn, J. A. 734
764
Veerasamy, Sam 120
Viereck, R. A. 676
682

Waligora, J. M. 630
631
633
Walker, Michael W. 59
Wallace, John F. 778
Walls, Bryan 355
Walters, Jerry L. 383
Ward, Wayne E. 688
Wee, Liang-Boon 59
Wellens, A. Rodney 606
Werner, J. 683
Wertheimer, M. R. 763
Whitaker, A. F. 764
Wiker, Steven F. 53
104
Wilcox, Katherine G. 684
Wilkinson, John 317
Williams II, Robert L. 23
Woodman, A. 683
Woods, David D. 543
547
Woolford, Barbara 552
Wright, H. G. 484

Yan, Jerry C. 469
Yen, Thomas Y. 104

Zaat, Stephen V. 778
Zik, John J. 53
Zimcik, D. G. 763
Zweben, Monte 290

REPORT DOCUMENTATION PAGE

1. Report No. NASA CP-3103, Vol. II	2. Government Accession No.	3. Recipient's Catalog No.

4. Title and Subtitle
Fourth Annual Workshop on Space Operations Applications and Research (SOAR '90)

5. Report Date
January 1991

6. Performing Organization Code
PT4

7. Author(s)
Robert T. Savely, Editor

8. Performing Organization Report No.
S-618

9. Performing Organization Name and Address
Lyndon B. Johnson Space Center
Houston, TX 77058

10. Work Unit No.

11. Contract or Grant No.

12. Sponsoring Agency Name and Address
National Aeronautics and Space Administration
Washington, D.C. 20546
U.S. Air Force, Washington, D.C. 23304
University of New Mexico, Albuquerque, NM 87131

13. Type of Report and Period Covered
Conference Publication

14. Sponsoring Agency Code

15. Supplementary Notes

16. Abstrart

The papers presented at the Space Operations, Applications and Research (SOAR) Symposium, hosted by the Air Force Space Technology Center and held at Albuquerque, New Mexico, on June 26-28, 1990, are documented in these proceedings. Over 150 technical papers were presented at the Symposium, which was jointly sponsored by the Air Force and NASA Johnson Space Center. the technical areas included were: Automation and Robotics, Environmental Interactions, Human Factors, Intelligent Systems, and Life Sciences. NASA and Air Force programmatic overviews and panel sessions were also held in each technical area. These proceedings, along with the comments by technical area coordinators and session chairmen, will be used by the Space Operation Technology Subcommittee (SOTS) of the Air Force Systems Command and NASA Space Technology Interdependency Group (STIG) to assess the status of the technology, as well as the joint projects/activities in various technical areas. The Symposium proceedings include papers presented by experts from NASA, the Air Force, universities, and industries in various disciplines.

287

17. Key Words (Suggested by Author(s))
Life Sciences, Knowledge Acquisition, Biofilm Compass, Sharp/Robotic, Debris, Ultraviolet Radiation, CLIPS, Photometric, Neural Network, Space Station Freedom, Fuzzy Logic, Diagnostics/Algorithm, Microbiology, Ellipsometric, Biomedical

18. Distribution Statement
Unclassified - Unlimited
Subject Category: 59

19. Security Classification (of this report)	20. Security Classification (of this page)	21. No. of pages	22. Price
Unclassified	Unclassified	304	A14

*For sale by the National Technical Information Service, Springfield, Virginia 22161